



**U.S. Department
of Transportation**

**Pipeline and
Hazardous Materials
Safety Administration**

Failure Investigation Report

**Plains Pipeline, LP, Line 901
Crude Oil Release, May 19, 2015
Santa Barbara County, California**

May 2016

Plains Pipeline, LP - Failure Investigation Report
Santa Barbara County, California Crude Oil Release - May 19, 2015

Table of Contents

Executive Summary..... 3

Final Report Methodology..... 4

Facility Background 4

Events Immediately Prior to and During the Crude Oil Release..... 6

Plains’ Field Response and National Response Center Notifications 7

PHMSA’s Corrective Action Order 9

Pipeline Alignment 9

 Las Flores Station to Gaviota Station Line 901 Elevation Description 9

 Gaviota to Pentland Station Line 903 Elevation Description 10

Post-Incident Investigation Results 11

 Metallurgical Evaluation of Failed Pipe 11

 In-Line Inspection Survey Review 12

 Number of Anomalies 13

 Cathodic Protection Findings..... 13

 Spill Volume Estimate from Plains’ Third-Party Consultant 13

Investigation Findings and Conclusions..... 14

 Proximate or Direct Cause 14

 Contributory Causes..... 14

PHMSA Post-Incident Action Chronology 18

Appendices 20

Executive Summary

At approximately 10:55 a.m. Pacific Daylight Time (PDT) on May 19, 2015, the Plains Pipeline, LP (Plains), Line 901 pipeline in Santa Barbara County, CA, ruptured, resulting in the release of approximately 2,934 barrels (bbl) of heavy crude oil.ⁱ An estimated 500 bbl of crude oil entered the Pacific Ocean. Line 901 is a 24-inch diameter buried, insulated pipeline which extends approximately 10.7 miles in length and transports heated crude oil from Exxon Mobil's storage tanks in Las Flores Canyon westward to Plains' Gaviota Pumping Station. On May 21, 2015, the Pipeline and Hazardous Materials Safety Administration (PHMSA), a regulatory agency within the U.S. Department of Transportation, issued a Corrective Action Order (CAO) that required the operator to shut down Line 901. Concurrent with the issuance and implementation of the CAO, PHMSA conducted an investigation to identify causal factors that contributed to the occurrence and size of the crude oil release. As the failure investigation progressed, the CAO was amended to address additional safety concerns that were identified. On June 18, 2015, Line 901 was purged and filled with inert nitrogen to enhance safety during the investigation and development of a remedial action plan.ⁱⁱ No fatalities or injuries occurred as a result of this rupture and release. The spill resulted in substantial damage to natural habitats and wildlife.

PHMSA's findings indicate that the proximate or direct cause of the Line 901 failure was external corrosion that thinned the pipe wall to a level where it ruptured suddenly and released heavy crude oil. PHMSA's investigation identified numerous contributory causes of the rupture, including:

- 1) Ineffective protection against external corrosion of the pipeline
 - The condition of the pipeline's coating and insulation system fostered an environment that led to the external corrosion.
 - The pipeline's cathodic protection (CP) system was not effective in preventing corrosion from occurring beneath the pipeline's coating/insulation system.
- 2) Failure by Plains to detect and mitigate the corrosion
 - The in-line inspection (ILI) tool and subsequent analysis of ILI data did not characterize the extent and depth of the external corrosion accurately.
- 3) Lack of timely detection of and response to the rupture
 - The pipeline supervisory control and data acquisition (SCADA) system did not have safety-related alarms established at values sufficient to alert the control room staff to the release at this location.
 - Control room staff did not detect the abnormal conditions in regards to the release as they occurred. This resulted in a delayed shutdown of the pipeline.
 - The pipeline controller restarted the Line 901 pipeline after the release occurred.
 - The pipeline's leak detection system lacked instrumentation and associated calculations to monitor line pack (the total volume of liquid present in a pipeline section) along all portions of the pipeline when it was operating or shut down.
 - Control room staff training lacked formalized and succinct requirements, including emergency shutdown and leak detection system functions such as

alarms.

The consequences of the spill were additionally aggravated by an oil spill response plan that did not identify the culvert near the release site as a spill pathway to the Pacific Ocean.

This report contains factual information and analysis regarding the events leading up to the release, information collected during PHMSA's failure investigation to date, and the technical analysis of that information known at the time of the completion of this report. PHMSA used this information to mandate remedial measures on Line 901, Line 903, and associated stations and tankage. PHMSA will also use the information to determine whether violations of the federal pipeline safety regulations occurred.

Final Report Methodology

PHMSA conducted relevant interviews, gathered and reviewed numerous historical documents and available records, and performed a thorough review of the Plains Control Room in Midland, TX. An ILI subject matter expert (SME) was hired to review the raw magnetic flux leakage (MFL) data and final vendor reports from the MFL surveys, and evaluated Plains actions as a result of their review of the vendor reports. PHMSA issued a CAO which in part instructed Plains to have the failed pipe examined by a PHMSA-approved metallurgical laboratory and to have a root cause failure analysis (RCFA) performed by a third party independent consultant.

The factual evidence reviewed includes: the Plains Integrity Management Plan (IMP), CP records, ILI reports, anomaly dig information, SCADA event and alarm logs, pressure and flow trends, procedures and reports obtained from the pipeline operator and PHMSA SMEs.

The arrangement of this report provides a general description of the pipeline system, the events that occurred on the day of the release, and acts or omissions of the operator that led to this failure and release of crude oil. Specific evidence is supplied and pertinent statements from each report are excerpted where appropriate.

Facility Background

Plains transports crude oil produced in federal and state waters off the coast of Santa Barbara, CA to inland refineries. Plains' pipeline is composed of two major pipeline sections: (1) Line 901, and (2) Line 903. Lines 901 and 903 were constructed in the late 1980s, hydrostatically tested in 1990, and went into crude oil service in 1992 and 1991, respectively. The pipelines are coated with coal tar urethane and covered with foam insulation which in turn is covered by a tape wrap over the insulation. Shrink wrap sleeves, which provide a barrier between the steel pipeline and soil for corrosion prevention, are present at all of the pipeline joints on Line 901 and multiple locations on Line 903. The pipelines carry high viscosity crude oil at a temperature of approximately 135 degrees Fahrenheit to facilitate transport. Lines 901 and 903 are controlled from the Plains Control Room's (PCR) California console in Midland, TX.

(1) Line 901 is a 24-inch diameter pipeline that extends approximately 10.7 miles in length from the Las Flores Pump Station to the Gaviota Pump Station; and (2) Line 903 is a 30-inch diameter pipeline that extends approximately 128 miles in length from the Gaviota Pump Station to the Emidio Pump Station, with intermediate stations at Sisquoc Mile Post (MP) 38.5 and Pentland (MP 114.57). There is a delivery point into Line 901 from Venoco's Line 96 located approximately 2 miles downstream of the Las Flores Station. All of Line 901 crude oil throughput enters Line 903. Line 901 was manufactured of low carbon steel by Nippon Steel

Plains Pipeline, LP - Failure Investigation Report

Santa Barbara County, California Crude Oil Release - May 19, 2015

in Japan in 1986. Line 901's pipe specifications are API 5L, Grade X-65 pipe, 0.344-inch wall thickness, with a high frequency-electric resistance welded (HF-ERW) long seam. The line was hydrotested to 1,686 pounds per square inch gauge (psig) on November 25, 1990.

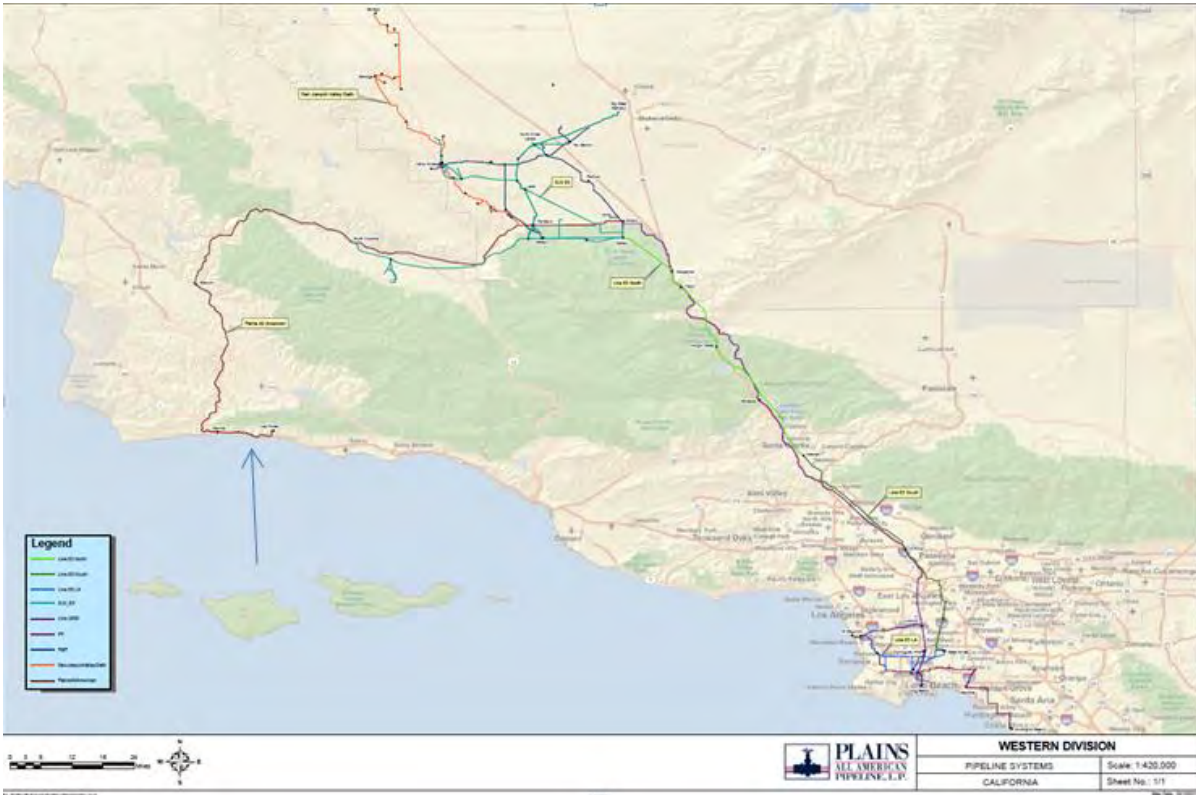


Figure 1. Map of Plains' Western Division Pipelines. The arrow points to the approximate release site on Line 901.

At Sisquoc Station, crude oil can be pumped to one of two locations: a nearby refinery via a 12-inch diameter pipeline operated by Phillips 66, or continue down Line 903 to Pentland Station. There are additional crude oil lines coming in and out of Pentland Station with numerous tanks at that station used to blend different crude oils for delivery further downstream. At Emidio Station crude oil is delivered to above-ground storage tanks for future delivery to Los Angeles refineries in a separate pipeline system.

Prior to the May 19, 2015 release, there had been four small releases meeting PHMSA reportable criteria at pump stations on Lines 901 and 903. No releases were reported to PHMSA on the pipelines outside of pump stations prior to 2015. The operator reported maximum operating pressure (MOP) of Line 901 is 1,341 psig.

At the time of the spill, Plains All American Pipeline (PAAPL) operated Line 901 and Line 903 under a Federal Energy Regulatory Commission (FERC) certificate of economic regulatory jurisdiction that was issued in 1987. Plains Pipeline, LP, is a subsidiary of PAAPL. Based on the FERC filing, Lines 901 and 903 were classified as interstate pipelines, pursuant to 49 U.S.C. § 60101(7), as facilities used to transport hazardous liquid in interstate or foreign commerce, and as such, were regulated by PHMSA as interstate pipelines. Plains cancelled the FERC certificates for Lines 901 and 903 on February 12, 2016 and April 29, 2016,

respectively, stating that the transportation service was no longer available in interstate commerce. Line 903 from Gaviota to Sisquoc to Pentland Stations was purged with nitrogen in accordance with Amendment No. 2 to the CAO, and remains shut down between these stations. The Pentland to Emidio segment of Line 903 is active and operating intermittently at low pressures. This section of pipe between Pentland and Emidio is not directly connected to the Gaviota to Pentland segment and is used to transport crude product from breakout tanks in Pentland Station.

Events Immediately Prior to and During the Crude Oil Release

On the morning of May 19, 2015, Lines 901 and 903 were transporting crude oil with a flow rate setpoint of 1,240 bbl per hour (BPH) leaving the Las Flores Station, and the discharge pressure was approximately 575 psig. Pumps were operating at the Las Flores Station on Line 901 and Sisquoc Station on Line 903. A Plains instrumentation and electrical technician was dispatched that morning to disconnect and remove a motor from a non-operational pump at the Sisquoc Station. While the technician was performing his work, the operational pump (Pump 401) at the Sisquoc Station was shut down unintentionally (i.e., “uncommanded”). When Pump 401 on Line 903 stopped operating, the pressure in Line 901 increased. The pressure rose to a maximum of 696 psig at the Las Flores Station discharge. The controller shut down the pump at Las Flores Station and the pressure remained at 677 psig. Approximately four minutes later, the pump at Las Flores Station was restarted. At approximately 10:55 a.m. PDT, the flow rate at Las Flores Station climbed from zero to 2,042 BPH. Concurrently, the line pressure rose to a high of 721 psig, then dropped to 199 psig, and then slightly increased to approximately 210 psig until the Las Flores pump was shut down a second and final time. Generally, a sudden increase in flow rate accompanied by a decrease in pressure is indicative of a release. PHMSA has determined that Pump 401 going offline in an “uncommanded” manner on the morning of May 19, 2015, was an abnormal event, but that this in itself should not have caused Line 901 to rupture.

PHMSA performed a detailed review of the SCADA event and alarm logs, and pressure and flow records. The review indicated that there was information reported by the SCADA system that indicated a release had occurred by approximately 10:58 a.m., and an alarm was generated on low pressure. The alarm was not set at an appropriate value. The alarm also did not have a major priority/severity or safety-related alarm status. The controller did not recognize the information he received as indicative of an abnormal operation. Evidence indicates that the controller was focused on the events at Sisquoc Station (i.e., restarting the Sisquoc pump that had gone down once uncommanded, and a second time on high case temperature along with other duties).ⁱⁱⁱ

Due to the Sisquoc Station maintenance activity resulting in an unplanned pump shutdown, the controller anticipated alarms would be activated from the pipeline leak monitoring (PLM) system. According to interviews and a review of the alarm log, the PLM inhibit was requested by the controller to the step-up shift supervisor between 11:15 and 11:22 a.m.^{iv} The step-up shift supervisor then inhibited (shut off) the PLM system alarms.^v Also, during this time, the controller started an investigation of the SCADA data in an attempt to understand the operational abnormalities that were occurring. After attempting to restart the Sisquoc pump twice, the controller shut down the pipeline. PHMSA requested the operator review the flow imbalance calculations and provide a time when the PLM system would have generated an alarm if not inhibited, and it was determined that alarms would have been generated

Plains Pipeline, LP - Failure Investigation Report

Santa Barbara County, California Crude Oil Release - May 19, 2015

approximately two minutes before the controller shut down the pipeline.^{vi}

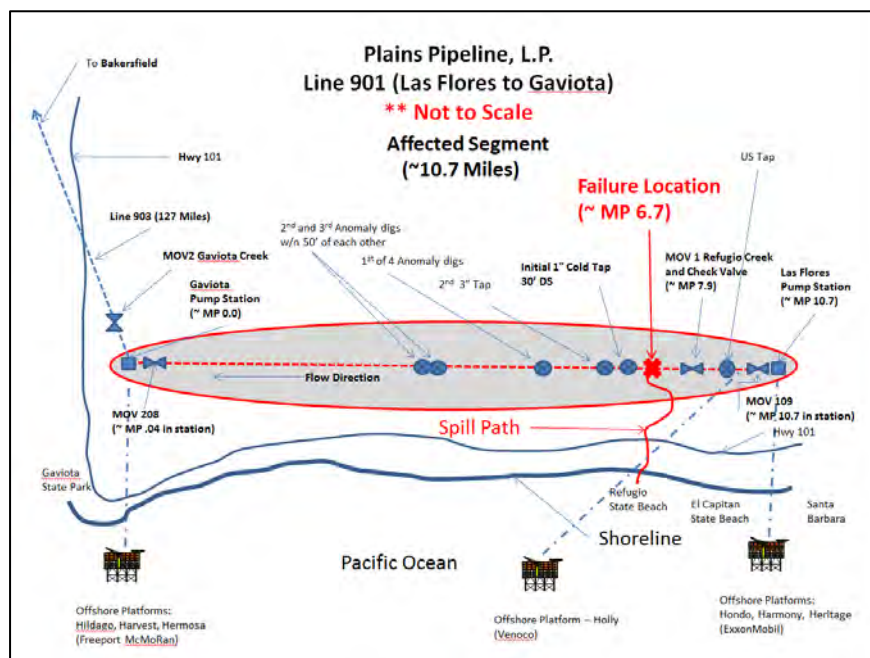


Figure 2. Schematic of Plains Pipeline, LP, Line 901 and spill path.

Plains' Field Response and National Response Center Notifications

The following is a timeline of Plains and emergency responder activities conducted immediately prior to locating the leak site:^{vii}

- At 11:42 a.m. a call reporting a petroleum smell was received at Santa Barbara Fire Department (SBFD) Station 18. Engine 18 left the station to investigate the odor complaint near Refugio State Beach.
- At approximately 12:15 p.m., prior to a scheduled tabletop spill drill required by federal regulations 49 C.F.R. §194, the pre-drill meeting was completed and adjourned. A representative from the Santa Barbara Office of Emergency Management (SB-OEM) received a call from the SBFD reporting that there was oil on Refugio Beach. The SB-OEM representative and the Plains representatives left the spill drill and drove separately to Highway 101 at Refugio Beach.
- The Santa Barbara Dispatch notified the National Response Center (NRC #1116950) at 12:43 p.m. PDT of an unknown sheen in the ocean at Highway 101 and Refugio Beach.^{viii}
- At approximately 12:55 p.m., the two Plains representatives arrived at the south side of Highway 101 where the SBFD personnel were. They noted oil in the ocean but could not determine the source of the oil. One of the Plains representatives told the assembled group that he did not think the oil was coming from Line 901 because the pipeline is located on the other side of Highway 101, and there would be oil flowing across Highway 101 if Line 901 was leaking.

Plains Pipeline, LP - Failure Investigation Report

Santa Barbara County, California Crude Oil Release - May 19, 2015

- The Plains representatives drove to the company's pipeline right-of-way (ROW). At approximately 1:27 p.m., the Plains representatives located the leak site on the Plains ROW. They called the controller to report the leak and to tell the controller to leave Line 901 shut down and to close the Refugio gate valve. The Plains representatives used their cell phones to contact other Plains personnel, the landowner where the leak occurred, Plains' oil spill response contractors, and others. The Plains representatives noted that crude oil from the release site had entered a culvert that crosses under the Highway 101 and railroad tracks and discharges to Refugio Beach. The Plains representatives, along with Fire Department personnel, attempted to stop the flow of oil into the culvert. However, the culvert was too large to stop the flow with shovels, and sand bags were not readily available, so their immediate efforts were unsuccessful. At approximately 3:00 p.m., additional equipment and personnel arrived, the culvert was dammed and oil was prevented from entering the culvert.
- At 2:56 p.m., a representative from Plains called the NRC to report (NRC #1116972) the release of crude oil at 2:56 p.m. PDT. This report indicated that the release was at Latitude: 34° 27' 43" N; and Longitude: 120° 05' 24" W. This NRC report was made 89 minutes after the release site was found by Plains field personnel.^{ix}



Figure 3. Spill location relative to Refugio Beach in Santa Barbara County, CA. Photo: John L. Wiley <http://flickr.com/jw4pix>

Federal pipeline safety regulations, (49 C.F.R. § 195.52), require that the NRC be notified at the earliest practicable moment following discovery of a release of a hazardous liquid, including “[a]ny failure that resulted in pollution of any stream, river, lake, reservoir, or other similar body of water that violated applicable water quality stands, caused a discoloration of the surface of the water or adjoining shoreline, or deposited a sludge or emulsion beneath the surface of the water or upon adjoining shorelines.” On January 30, 2013, PHMSA issued an

Advisory Bulletin clarifying that this was to be interpreted as within one hour of discovery. Plains reported the rupture to the NRC approximately 89 minutes after discovery, thus notifying the NRC 29 minutes late.

The estimated costs reported by the operator as of December 23, 2015, were \$142,931,884. This figure includes all costs the operator spent as a result of this release through the date reported, including commodity lost, the operator's property damage and repairs, operator's emergency response, environmental remediation, and estimated other costs spent including government agency costs and media relations expenses.^x

PHMSA's Corrective Action Order

On May 21, 2015, PHMSA issued a CAO, CPF No. 5-2015-5011H, to Plains. The CAO required Plains to purge Line 901; review the pipeline's construction, operating, maintenance, and integrity management history; expedite the review of data from the May 5, 2015, ILI tool run; conduct metallurgical evaluation of the failed pipe; repair any integrity-threatening anomalies identified by the ILI survey; and conduct a root cause failure analysis. The CAO requires Plains to purge Line 901 and to keep Line 901 shut down until PHMSA approves the restart of the pipeline. Plains' Line 901 was purged and filled with an inert nitrogen gas on June 18, 2015.

On June 3, 2015, PHMSA issued Amendment No. 1 to the CAO. The amendment was issued to address preliminary findings from the early stages of PHMSA's investigation, and the possibility that the conditions on Line 901 also existed on Plains Line 903. The amendment to the CAO required Plains to conduct additional non-destructive testing of ILI anomalies on Lines 901 and 903; review the construction, operating, maintenance, integrity management, and ILI history of Line 903; and reduce the operating pressure of Line 903 to 80% of the highest pressure sustained for a continuous 8-hour period during the month before the May 19 failure. This pressure reduction was intended to enhance safety until all facets of the line's integrity could be evaluated.

On November 12, 2015, PHMSA issued Amendment No. 2 to the CAO. The amendment required Plains to empty and purge Line 903 between Gaviota and Pentland Stations and fill it with an inert gas. Line 903 was purged between Gaviota and Pentland Stations and filled with inert nitrogen. The complex purging operations began in December 2015, and were completed on April 18, 2016. Both Line 901 and the purged sections of Line 903 will remain shut down until all actions required by PHMSA's CAO and subsequent amendments have been completed. PHMSA may continue to issue additional amendments to the CAO as necessary.

Pipeline Alignment

Las Flores Station to Gaviota Station Line 901 Elevation Description

To fully understand the Line 901 release, it is vital to understand the elevation profile of Line 901 and Line 903 from the Las Flores Canyon to Pentland Station. Line 901 starts at the Las Flores Station at an elevation of approximately 180 feet. There are two large hills downstream of the originating pump station. The first hill has a peak elevation of approximately 740 feet and the second hill has an elevation of approximately 600 feet. The release occurred downstream of the second hill at an elevation of approximately 80 feet. Immediately downstream of the release point, the pipeline rises slightly and then runs relatively level approaching the Gaviota station. This fact is important because as soon as the pump at Las

Flores Pump Station was turned off the second time, the only crude oil that could be released was the height of oil in the pipeline above the release site and not the amount located between the two aforementioned hills.

Gaviota to Pentland Station Line 903 Elevation Description

Line 903 receives all of the crude oil delivered by Line 901. The line elevation at Gaviota is approximately 150 feet. The elevation at Sisquoc is approximately 880 feet. Downstream of Sisquoc, Line 903 rises to 2,420 feet and then to a height of approximately 2,750 feet and ultimately to an elevation of close to 3,000 feet before dropping into Pentland Station at an elevation of approximately 690 feet. Line 903 exhibits many of the same construction and operation conditions as Line 901 and was addressed by the amendments to the CAO. Pump 401 at Sisquoc Station has adequate capacity to push the oil up and over the downstream hills and into Pentland Station but only if it has full suction pressure and full flow coming into the pump. Because of the release, the pump could not push the oil over the downstream hills, and so the oil in the pump became hot and the pump shut down to prevent overheating.

Post-Incident Investigation Results

Metallurgical Evaluation of Failed Pipe

The failed pipe segment has been analyzed by third-party metallurgical experts, Det Norske Veritas (U.S.A.), Inc.'s (DNV-GL) in Dublin, OH. The failed pipe assessment and testing was witnessed by PHMSA, the California Department of Fish and Wildlife, and the U.S. Department of Justice.



Figure 4. The failed pipe and surrounding insulation and coating.



Figure 5. Pipe External Surface at the Line 901 failure site after cleaning.

Plains Pipeline, LP - Failure Investigation Report

Santa Barbara County, California Crude Oil Release - May 19, 2015

DNV-GL's draft report was completed and disseminated to Plains and PHMSA on August 6, 2015. The draft report was reviewed by PHMSA engineers, and a number of comments and clarification requests were made. DNV-GL reviewed the comments and revised the report. The Final Report was issued on September 18, 2015.

The Final Report provides a summary of findings, including the following excerpt:

“The results of the metallurgical analysis indicate that the leak occurred at an area of external corrosion that ultimately failed in ductile overload under the imposed operating pressure. The morphology of the external corrosion observed on the pipe section is consistent with corrosion under insulation facilitated by wet-dry cycling.”^{xi}

In-Line Inspection Survey Review

Plains conducted ILI surveys on Line 901 (10.7 miles in length) to assess the integrity of the pipeline in accordance with PHMSA regulations in 2007, 2012, and 2015. According to 49 C.F.R. § 195.452(j)(3), the pipeline is required to be surveyed at intervals commensurate with the pipeline's risk of integrity threats, but at least every 5 years. Plains changed Line 901 from a 5-year assessment cycle to a 3-year assessment cycle after the 2012 ILI survey.

The data collected during these surveys must be fully evaluated within 180 days of the ILI, and an operator must take action upon discovery of any “immediate repair conditions” as defined in 49 C.F.R. § 195.452(h) unless the operator can demonstrate that the 180-day period is impracticable.

The most recent ILI survey for Line 901 was completed on May 6, 2015. The 2015 ILI survey data for the first 2 miles of Line 901, as measured from the Las Flores Station, was found to be incomplete and not useable for ILI analysis. For the rest of the ILI survey, the correlation digs, which are used to gauge survey data accuracy in the ILI vendor's preliminary report, had not been finished at the time of the May 19, 2015 failure.

PHMSA's independent third-party ILI SME also performed an analysis of the data from past ILI surveys of Line 901. Preliminary data from the results of each of the ILI surveys are summarized below and show a growing number of corrosion anomalies on Line 901.

Plains Pipeline, LP - Failure Investigation Report
Santa Barbara County, California Crude Oil Release - May 19, 2015

Number of Anomalies

Metal loss	June 19, 2007	July 3, 2012	May 6, 2015
Greater than 80%	0	0	2
60-79%	2	5	12
40-59%	12	54	80

The May 6, 2015 ILI survey data and subsequent analysis by the ILI vendor predicted external corrosion at the failure site with an area of 5.38 inches by 5.45 inches, and a maximum depth of 47% of the original pipe wall thickness. After the failure, the DNV-GL metallurgical investigators physically measured external corrosion at the failure site to have a maximum depth of 89%.^{xiii} The dimensions of the corrosion feature were 12.1 inches axially by 7.4 inches in circumference. The maximum depth, as measured using laser scan data, was 0.318 inches or 89% of the measured wall thickness (0.359 inches).

The ILI summary report prepared by PHMSA’s SME also examined the “as-called” (ILI-predicted) versus as-found (field measured) lengths, widths and area for the excavated anomalies on Line 901. The report demonstrates that the lengths and widths of the anomalies were under-called (underestimated) in many cases, however many were also over-called. Plains submitted little documentation concerning their analysis of how the field measured anomalies compared to the ILI vendor analysis. Furthermore, Plains did not provide documentation showing that discrepancies between the originally reported anomaly sizes predicted by the ILI vendor and Plain’s actual field-measured sizing of the corrosion anomalies were subsequently discussed with the ILI vendor, as required by Plains’ IMP.^{xiii}

Cathodic Protection Findings

According to 49 C.F.R. § 195.563, CP is required under the federal Pipeline Safety Regulations to prevent external corrosion of buried pipelines. Historical CP records for line 901 have been reviewed and reveal protection levels that typically are sufficient to protect non-insulated, coated steel pipe. Line 901 and Line 903, however, are insulated. An increasing frequency and extent of corrosion anomalies were noted on both Lines 901 and 903 in ILI survey results, anomaly excavations, and repairs. PHMSA inspectors noted moisture entrained in the insulation at four excavations performed by Plains on Line 901 after the May 19 spill and prior to the PHMSA-mandated purging of the pipelines.

Spill Volume Estimate from Plains’ Third-Party Consultant

Plains initially estimated the volume of spilled crude oil to be approximately 2,400 bbl, of which 500 bbl was estimated to have reached the ocean. On August 4, 2015, Plains reported to the Unified Command that the 2,400 bbl release estimate was still accurate. However, after Plains completed the PHMSA-mandated purge, the company’s calculations indicated that up to 3,400 bbl had possibly been released from the pipeline. Plains notified the Unified Command

that RPS Knowledge Reservoir (RPS), a third-party investigator hired by Plains, was still trying to reconcile the difference.

On November 24, 2015, Plains informed PHMSA that RPS had completed their analysis regarding the release volume and produced a report of findings. RPS used the OLGA simulation software tool to model the behavioral dynamics of the pipeline prior to, during, and immediately after the May 19, 2015 leak. The report concluded that the discharge leak volume was 2,934 bbl. The RPS report was dated November 11, 2015. Plains has reported 1,100 bbl of crude oil have been recovered.

Investigation Findings and Conclusions

Line 901 pipeline ruptured at approximately 56% of the MOP. Although the operational events that occurred on the morning of the release were abnormal, this should not have caused the release if the pipeline's integrity had been maintained to federal standards.

Proximate or Direct Cause

PHMSA determined that the proximate or direct cause of the release was progressive external corrosion of the insulated, 24-inch diameter steel pipeline. The corrosion occurred under the pipeline's coating system, which consisted of a urethane coal tar coating applied directly to the bare pipe, covered by foam thermal insulation with an overlying Polyken tape wrap. Water has been noted in the foam insulation at a number of digs, indicating that the integrity of the coating system had been compromised. The external corrosion was facilitated by the environment's wet/dry cycling, as determined by the PHMSA-approved, third-party metallurgical laboratory. The release was a single event caused at an area where external corrosion had thinned the pipeline wall. There is no evidence that the pipeline leaked before the rupture. There was a telltale "fish mouth" (a split due to over-pressurization) at the release site indicating the line failed in a single event.

PHMSA's investigation identified numerous contributory causes of the rupture. The contributory causes can be grouped into three categories: 1) ineffective protection against external corrosion of the pipeline; 2) failure by Plains to detect and mitigate the corrosion; and 3) lack of timely detection of the rupture. Below is a summary of the key contributory causes:

Contributory Causes

- 1) Ineffective protection against external corrosion of the pipeline
 - Plains' CP system was ineffective in protecting thermally insulated underground pipeline systems from external corrosion. Industry practices recognize that an impressed current system like the one utilized on Line 901 cannot protect an insulated steel pipeline should the coating (tape wrap over insulation) become compromised. The external coating in the area of the rupture had allowed moisture to enter the insulation adjacent to the steel pipe.^{xiv} Corrosion under insulation (CUI) cannot be prevented on insulated lines where the coating system has been compromised.^{xv}
- 2) Failure by Plains to detect and mitigate external corrosion
 - Plains did not identify CUI as a risk-driving threat in their federally-mandated integrity management program (IMP).

Plains Pipeline, LP - Failure Investigation Report

Santa Barbara County, California Crude Oil Release - May 19, 2015

- Plains' did not fully implement their IMP.
 - Plains did not perform suitable analysis of the field measurements of the excavated corrosion anomalies that occurred after ILI surveys were completed in 2007 and 2012.
 - The data reported by the ILI vendor were inconsistent (and did not meet the published accuracy of the ILI tools of +/- 10%, 80% of the time for depth) when compared to the results of the field-measured corrosion anomalies.
 - Plains' as-found field measurements of corrosion anomalies were inconsistent with the as-called vendor-provided ILI data and analytical reports. ILI surveys conducted in 2007 and 2012 revealed inconsistencies in the character of the anomalies. In both of these cases, Plains did not consult the ILI vendor to help resolve the inconsistency.
 - Plains failed to follow written procedures directing the IMP group to perform appropriate statistical analysis after the anomaly dig reports were received from the field, and to discuss any inconsistencies with the ILI vendor.^{xvi}
 - Plains' Pipeline Integrity group created a unity plot for depth after the 2012 ILI survey and anomaly digs. There is no documentation detailing what was done with the information from the unity plot.
 - Plains incorrectly added the over-called anomalies in the close-out reports.
 - The close-out reports should have only reported the anomalies that were within the reported accuracy of the ILI tool. The reported tool accuracy is +/- 10 %, 80 % of the time. Adding the overcalled anomalies outside of the tool accuracy skews the data.
- Plains' Pipeline Integrity group was historically focused on pitting corrosion under "shrink sleeves" at the pipeline girth welds (circumferential welds to join pipe segments).
 - The release location was within 6 feet of a corrosion anomaly that was exposed and repaired after the 2012 ILI survey. There was evidence of corrosion and degraded coating systems between the 2012 repair site and the 2015 rupture site.
 - The anomaly that ruptured was called out by the ILI tool at 45% depth in 2012. Plains' IMP specified adding 10% to all anomalies (55% depth in this case) then "growing them" to predicted failure using an anticipated corrosion growth rate. This analysis would provide a predicted failure time. Plains did not excavate the anomaly that failed.

3) Lack of timely detection of and response to the rupture

- The controller did not have information communicated from the SCADA system in such a manner to be successful in detecting abnormal operations. The pipeline SCADA system did not have safety-related alarms on low pressure configured at the

correct value or priority to alert the control room staff of the rupture. When this alarm was provided to the controller, the discharge pressure at Las Flores was 199 psig but, within a minute, pressure elevated above 210 psig, the alarm status cleared, and the discharge pressure remained above 200 psig (approximately 210-211 psig) until the pipeline was purged. The pipeline was still leaking when the discharge pressure at Las Flores was above 200 psig, and continued to do so without additional alarm indications. When the pipeline was down, isolated but still leaking, the minimum pipeline discharge pressure at Las Flores remained at 210-211 psig. The low discharge pressure alarm setpoint value was not set properly as it should have been above 211 psig. This type of alarm should be identified as a high priority safety related alarm. While the controllers and shift supervisors can access historical trend data or continue to monitor a given pressure or flow, when the pipeline was ultimately shut down at 11:30 a.m., neither the controller nor step-up shift supervisor detected any drop of pressure at the specific failure location that would indicate that oil was being released.

- Neither the pipeline controller nor step-up shift supervisor detected the initial abnormal conditions as the release occurred. There was an indication of decreased pressure and increased flow between 10:53 and 10:58 a.m., which is consistent with a pipeline release. This resulted in a delayed shutdown of the pipeline. Adequate alarm setpoint values with correct priorities are essential to controller and shift supervisor recognition of abnormal operations, especially when many pipeline systems are operated from the same console.
- The pipeline controller restarted Line 901 after the release occurred.
- The pipeline leak detection system lacked instrumentation and associated calculations to monitor line pack.
 - The function of the PLM system was a simple line balance calculation based on flow meter values without line pack considerations. The PLM relies on comparing “meter in – meter out” calculations over time. This type of leak detection system without the use of safety-related, high-priority, low-pressure alarms does not provide the controller or shift supervisors with adequate information when the pipeline is down.
 - When the pipeline is not running, even if only due to scheduling and not required maintenance activities, flows will be close to zero and the imbalance calculation will provide little if any value as currently configured. Leak detection on a down pipeline requires a robust system of planned and accurate high-priority alarm types and alarm setpoint values in order for response to occur on critical low pressures.
 - The leak detection system for Lines 901 and 903 consists of two leak detection segments. Additional instrumentation such as pressure and temperature transmitters located at Refugio Gate and Cuyama valve settings (both transmitter types on each side of the valves) would allow additional information about the operating status of the pipeline to be presented and pack calculations pursued.
 - Plains utilizes the SimSuite application for other pipelines in the control

Plains Pipeline, LP - Failure Investigation Report

Santa Barbara County, California Crude Oil Release - May 19, 2015

center. This application does allow for pack calculations to be utilized in the leak detection system. According to information obtained during meetings with Plains hydraulic specialists, Lines 901 and 903 were pipeline systems with a low to medium priority defined for future modeling efforts compared to other assets in the Plains operations. The approach utilized by Plains for prioritizing which systems should be modeled first did not appear to take into account all appropriate consequence-based asset impacts (such as culverts providing a pathway to the ocean) associated with these two systems. Existing instrumentation and the need for added instrumentation would factor into this prioritization decision.

- Control room staff training lacked formalized and succinct requirements, including emergency shutdown and leak detection system functions such as alarms.
 - Interviews determined that the step-up shift supervisor and shift supervisor training lacked formalized and succinct requirements, including that for leak detection system functions such as “inhibit” options. The interviews determined that different shift supervisors performed PLM inhibit functions without contacting the console supervisor first as required by procedure.
 - Step-up and shift supervisor responsibilities include emergency shutdown of any pipeline. However, training does not cover a means by which to accomplish this for all relevant pipelines. A general emergency shutdown provision has not been programed for supervisory use on all systems.
- The oil spill response plan required by 49 C.F.R. §194 did not account for a culvert near the release site that traversed the Pacific Coast Highway and Amtrak railroad tracks. This culvert provided a quick flow path between the pipeline ROW and the Pacific Ocean, thereby allowing crude oil to flow easily towards Refugio State Beach and the ocean. The response plan did not have a response strategy that considered the presence of the culverts.

PHMSA Post-Incident Action Chronology

Following the May 19, 2015 Plains Pipeline, LP, Line 901 rupture in Santa Barbara County, CA, PHMSA took the following actions:

- On May 19, 2015, PHMSA deployed inspectors to investigate the Plains Pipeline LP Line 901 pipeline failure in Santa Barbara County, CA. PHMSA also provided information updates to the Unified Command (UC), US Coast Guard, the Federal on Scene Coordinator (FOSC), State Fish and Wildlife, and other agencies on site.
- On May 21, 2015:
 - PHMSA issued a Corrective Action Order (CAO), CPF No. 5-2015-5011H, to Plains Pipeline LP ordering it to suspend operations and to specific safety actions to further protect the public, property, and the environment from potential hazards associated with the recent failure. PHMSA staff reviewed the CAO with the operator and briefed the California State Attorney on the CAO and provided an overview of PHMSA's regulations.
 - PHMSA sent an inspector to Plains' control room in Midland, Texas to collect operational data and interview the control room operators on duty at the time of the incident and their supervisors. The inspector gathered any pertinent logs and information, including electronic copies of relevant data from the Supervisory Control and Data Acquisition (SCADA) system.
 - PHMSA staff worked with the operator to review their plan to expose the pipe and to cold tap it to ensure there was no pressure or crude left in the line at a low spot immediately downstream of the release point. The plan was signed off by the UC at approximately 5 pm PDT.
- On May 22, 2015:
 - PHMSA staff met with representatives from the Assistant U.S. Attorney, DOT Inspector General, EPA Criminal Investigation Division, California Attorney General, and others to brief them on PHMSA's process for securing and transporting the failed pipe to a metallurgical lab for evaluation.
 - PHMSA staff remained on the scene as the operator exposed, tapped, removed any remaining product, and excavated the pipeline downstream of the release site.
- On May 25, 2015:
 - PHMSA issued an approval letter for Plains to excavate, remove and secure the failed joint of pipe under the supervision of two DNV metallurgists (third party contractor) but requested that the coating and insulation not be touched until the failed pipe has been removed because the DNV personnel were interested in gathering available samples there as well.
 - A PHMSA inspector returned to Midland, TX to interview the controller and the Operations Control Center supervisor and to obtain any handwritten logs created by the controller on the morning of the release.
- On May 28, 2015:
 - A PHMSA investigator was on site when affected pipeline was removed, crated, and transported to secure location for metallurgical evaluation. PHMSA retained a third-party ILI expert to examine the 2012 and 2015 ILI runs. DNV personnel took soil and insulation samples.
- On June 3, 2015, PHMSA amended the CAO to address preliminary findings from the early stages of the investigation (Amendment No. 1). The amended CAO mandated

Plains Pipeline, LP - Failure Investigation Report

Santa Barbara County, California Crude Oil Release - May 19, 2015

additional safety requirements on Line 901 and expanded the scope of the CAO to include the 128-mile long Line 903, which is located downstream of Line 901. The amendment reduced the operating pressure of the Line 903 by 80% of the highest 8 hour continuous pressure between April 19, 2015 and May 19, 2015. On May 30, 2015, Plains voluntarily shutdown Line 903.

- On June 18, 2015, PHMSA staff monitored the Line 901 purge to ensure safety during the purging process. Plains completed the purge and injected inert gas in Line 901.
- On September 18, 2015, PHMSA received the DNV Final Mechanical and Metallurgical Report. PHMSA staff reviewed the document and provided comments.
- On November 12, 2015, PHMSA issued Amendment No. 2 to the CAO, which ordered Plains to purge and shutdown Line 903 from Gaviota to Pentland.
- On December 1, 2015, PHMSA staff monitored Plains moving Freeport McMoRan crude oil from their offshore platforms into Line 903 from Gaviota Station to Sisquoc Station. Movement of the Freeport McMoRan oil was completed on December 10, 2015.
- On December 4, 2015, PHMSA staff received the DNV Root Cause Failure Analysis Report. PHMSA reviewed and commented on the report.
- On December 14, 2015, PHMSA staff monitored the purge process on Line 903 from Gaviota Station to Sisquoc Station. The purge was completed on December 18, 2015 and the line was filled with inert gas.
- On February 17, 2016, PHMSA issued a Preliminary Factual Final Report.
- On April 2, 2016, PHMSA staff monitored the Line 903 Sisquoc to Pentland portion purge that was completed on April 18, 2016. Line 901 and 903 are shutdown, except for the Pentland to Emidio section of Line 903, which is not connected to 903 any longer.

Plains Pipeline, LP - Failure Investigation Report
Santa Barbara County, California Crude Oil Release - May 19, 2015

APPENDICES

- A. Investigation Summary Detail
- B. Supervisory Control and Data Acquisition (SCADA) Log Excerpts
- C. Pipeline Leak Monitoring Details
- D. Excerpts and Discussion of Plains Integrity Management Plan (IMP) Requirements
- E. Corrosion Control and Pipeline Conditions
- F. Industry Standards and General Requirements for In-Line Inspection
- G. In-Line Inspection Report
- H. PHMSA's Independent Analysis of In-Line Inspection Data
- I. Maps and Photographs
- J. National Response Center Report #1
- K. National Response Center Report #2
- L. Form PHMSA F 7000.1: Accident Report for Hazardous Liquid Pipeline Systems
- M. Det Norske Veritas (U.S.A.), Inc. (DNV GL): Line 901 Release (5/19/15) Mechanical and Metallurgical Testing
- N. Det Norske Veritas (U.S.A.), Inc. (DNV GL): Line 901 Release (5/19/15) Technical Root Cause Analysis
- O. NACE International: Effectiveness of Cathodic Protection on Thermally Insulated Underground Metallic Structures

ⁱ According to the *FRACTURE CONTROL TECHNOLOGY FOR NATURAL GAS PIPELINES CIRCA 2001* (the PRCI report superseding NG-18 Report 208): "The distinction between leak and rupture for the pipeline community is based on the size and configuration of the breach, not how it develops." Based on these calculations and visual observations, the length of the feature is consistent with a leak, arresting within the corrosion feature, and did not propagate outside of the feature into nominal wall-thickness pipe. According to the instructions for completing PHMSA Accident Form 7000-1, this type of accident would be classified as a rupture since PHMSA defines a "rupture" as a "loss of containment that immediately impairs the operation of the pipeline".

ⁱⁱ The remedial action plan requires: a) investigation and remediation of anomalies on Line 901 (including anomalies requiring repair per 49 C.F.R. § 195.452(h) and similar anomalies); b) analysis of field measurements taken from anomaly investigations; c) re-grade of previous in-line inspection (ILI) data from 2012 and 2015 ILI surveys using an expanded set of interaction criteria; d) additional integrity assessments using a circumferential magnetic flux leakage (MFL-C) ILI tool and integration of MFL-C ILI data with previous ILI survey results; e) investigation and remediation of anomalies that are identified in the MFL-C tool run (if any); f) based on information collected from remedial work plan and root cause analysis report released by Det Norske Veritas (U.S.A.), Inc., improving the integrity management program; and g) integrity studies to reduce spill volumes, including an emergency flow restriction device evaluation and a surge study. Completion of the remedial work plan is required prior to the PHMSA Western Region Director approving a restart plan and return to service for Line 901.

ⁱⁱⁱ High case temperature refers to the oil temperature inside the pump cavity. The case holds the pump impeller

Plains Pipeline, LP - Failure Investigation Report
Santa Barbara County, California Crude Oil Release - May 19, 2015

where oil passes through. This was a centrifugal pump that continues spinning whether there is product in the pump or not. When the rupture occurred, there was not enough pressure or flow rate to allow the pump to continue pumping the oil over the hills and into Pentland Station. Therefore, the oil that was in the pump remained in place and as the pump continued to spin, and temperature was reported to the SCADA system. If the pump reaches the high temperature setpoint, the pump shuts itself off to protect itself from burning up.

^{iv} The PCR utilizes two shift supervisors to cover the entire set of 22 consoles. The California Console is handled by shift supervisor B. The shift supervisor B position at the time of the failure was filled by a step-up shift supervisor. A step-up shift supervisor is a controller who is currently qualified on a specific console in the PCR and has received some informal training by working on shift with other shift supervisors. Step-up shift supervisors are used to cover the shift supervisor positions when additional personnel are needed due to illness, vacation, training, etc. Plains has indicated that two step-up shift supervisors are not allowed to be on duty at the same time so one shift supervisor is paired with a step-up shift supervisor when additional personnel is needed.

^v PLM is the SCADA vendor software tool that serves as the leak detection system for PCR.

^{vi} See Appendix B.

^{vii} SCADA Data/Plains Control Room time is local to the Central Time Zone. A two-hour time difference separates Central Time from Pacific Time, with Central Time falling two hours ahead. The release occurred in the Pacific Time Zone which is two (2) hours earlier. All times in this report have been adjusted to Pacific Time.

^{viii} See Appendix J.

^{ix} See Appendix K.

^x See Appendix L.

^{xi} See Appendix M.

^{xii} PHMSA has access to this data through a view-only web portal.

^{xiii} See Appendix G.

^{xiv} The inability of an impressed cathodic protection system to protect insulated pipelines was most recently reaffirmed in the National Association of Corrosion Engineers (NACE) Publication 10A392 (2006 Edition) – “Effectiveness of Cathodic Protection (CP) on Thermally Insulated Underground Metallic Structures.”

^{xv} See NACE Report at Appendix O, Background section stating that “[o]n most thermally insulated oil and gas transmission pipelines installed prior to 1980 to 1981, a shop mold-formed thermal insulation was placed directly over the bare steel pipe, with an outer jacket applied to moisture-proof the system. At the field joint, preformed insulation half shells were applied over the joint area to fit between the ends of the shop-applied insulation. After the insulation was fitted, a heat shrink sleeve or a tape wrap was applied over the insulation. When the integrity of the outer moisture barrier was compromised, the space, gap, or void between the edges of the preformed half shells and the shop-applied insulation allowed oxygenated water to diffuse to the bare steel beneath. Damage to the outer moisture barrier has also occurred remote from the joint, allowing oxygenated ground water ingress.

“Thermally insulated pipelines have experienced relatively aggressive corrosion, with some failures occurring within three years of service, although acceptable industry standards of CP had been applied and maintained shortly after line construction. The most predominant failures have been those occurring at joints; however, moisture has migrated along the pipeline steel surface to create electrochemical corrosion cells remote from the field joint, culminating in extensive replacements of substantial lengths of line. An article titled ‘Corrosion of Underground Insulated Pipelines’ supports this committee’s conclusions that sufficient CP current from an external source may not reach the insulated metallic surface in sufficient quantity to establish adequate corrosion control.”

^{xvi} See Appendix D.

Appendix A
Investigation Summary Detail

Appendix A: Investigation Summary Detail

DOT US Department of Transportation
PHMSA Pipelines and Hazardous Materials Safety Administration
OPS Office of Pipeline Safety
Western Region

Principal Investigator Peter J. Katchmar
Regional Accident Coordinator Peter J. Katchmar
Region Director Chris Hoidal
Date of Report 5/5/2016
Subject Failure Investigation Report – HL Santa Barbara County CA
Crude Oil Release

Operator, Location, & Consequences

Date of Failure 5/19/2015
Commodity Released Crude Oil
City/County & State Refugio State Beach, Santa Barbara County, CA
OpID & Operator Name 300 – Plains Pipeline, LP
Unit # & Unit Name 33175 - CSFM #1050A
SMART Activity # 150537
Milepost / Location MP 4.16
Type of Failure External Corrosion
Fatalities 0
Injuries 0
Description of area impacted Ranch land ¼ mile east of the Pacific Ocean, Refugio State Beach and the Pacific Ocean. Oil flowed to a water drainage culvert that ran under California State Highway 101 (Pacific Coast Highway) and the Amtrak Railroad embankment and into the Pacific Ocean.
Property Damage and Cleanup Cost \$ 142,931,884 (through December 23, 2015)

Appendix B

Supervisory Control and Data Acquisition (SCADA) Log Excerpts

Appendix B: Supervisory Control and Data Acquisition (SCADA) Log Excerpts

Listed below is a chronology of events, as obtained from the Plains Control Room (PCR) Supervisory Control and Data Acquisition (SCADA)¹ logs. The SCADA log records alarms and events that occur per pipeline system for each line operated from the console. Due to the significant volume of entries and information occurring at the time of this release, only those data points relevant to the CA30 system (901 and portions of 903) have been included

- At 10:42:06, Pump 401 at the Sisquoc Station shut down uncommanded due to maintenance activities.
- At 10:48:44, the Plains controller at the PCR issued a command to shut down Pump 102 at the Las Flores Station as the result of pump problems at Sisquoc.
- At 10:48:52, the SCADA system reported that the Pump 102 at Las Flores had successfully shut down.
- The discharge pressure at the Las Flores Station immediately prior to shutdown was recorded by the SCADA to have reached ~677 psig at a flow setpoint of ~1220 Barrels per Hour (BPH).
- At 10:49, Tech 2 called the controller and notified him that he could restart Pump 401 at Sisquoc Station.
- At 10:52:52, the controller issued a command to restart Pump102 at Las Flores PS.
- At 10:53:01, the SCADA system reported Pump 102 successfully started.
- Between 10:53 and 10:56 the Pressure and Flow Data from the SCADA indicated the discharge pressure at the Las Flores PS reached ~721 psig and the flow rate reached as high as ~2042 barrels per hour (BPH). Pressure and Flow Trends confirm that 10:55 is approximately when the release occurred.
- At 10:55:52, the controller commanded the Pump 401 at the Sisquoc Station to start.
- At 10:56:52, the SCADA system reported that Pump 401 at Sisquoc Station was running.
- At 10:57:59, the SCADA system reported the discharge pressure at the Las Flores Station dropped to 199 psig and the SCADA system reported a low pressure alarm to the controller.
- At 10:58:48 the discharge pressure rises to 210 psig. This automatically resets the low pressure alarm.
- At 10:58:58 the controller acknowledges the 210 psig discharge pressure notification.

¹ SCADA systems are used to remotely control and monitor pipeline operations.

- At 11:00:00 the SCADA system reported the flow rate was at 1458 BPH – (a soft high state)
- At 11:00:05 controller acknowledges the soft high flow rate.
- At 11:00:14 the SCADA system reported flow rate at Las Flores was 1254 BPH = Normal State.
- At 11:09:20, the SCADA System recorded that Sisquoc Pump 402 had a high case temperature. However, Sisquoc Pump 402 was not running.
- At 11:12, Venoco personnel called the controller and notified him they wanted to start a delivery into line 901 through their line 96. Venoco’s line 96 ties into line 901 about 2.83 miles downstream of the Las Flores Station between the two hills.
- At 11:14, controller called the I&E Tech at Sisquoc Station to tell him of the high temperature on Pump 402.
- At 11:15:14, the SCADA System recorded that Sisquoc Pump 401 shut down on High Temperature.
- At 11:15:48, Venoco started their pump to start a delivery into line 901.
- At 11:20, Venoco personnel called the Plains controller and told him the pressure in line 901 was too low to run their line 96 pump.
- At 11:20:12, Venoco turned off their pump and closed their valve.
- At 11:22:58, the SCADA log states “PLM inhibited.” The Pipeline Leak Monitoring System, or PLM, calculates the imbalance between volumetric meters along the pipeline.
- At 11:26:43, the controller issued a command to start Pump 401 at Sisquoc PS.
- At 11:27:50, the pump start command timed out. Pump 401 did not start.
- At 11:28:12 the controller again issued a command to start Pump 401 at Sisquoc PS.
- At 11:29:20, the pump start command timed out. Pump 401 did not start.
- At 11:29:56, the controller issued a stop command to the Pump 102 at Las Flores PS. **[2 minutes after the PLM would have alarmed according to the calculation presented in Appendix C.]**
- At 11:30:05, the SCADA system reports that Pump 102 at Las Flores PS is stopped. Mainline Valve 102B at Las Flores closes automatically upon Las Flores Pump 102 shutdown. The pressure at Las Flores is recorded by the SCADA to be between 211 and 213 psig.
- At 1:27, the PCR was notified of the line 901 release near Refugio Beach, approximately 4.16 miles from the Las Flores PS. The static pressure immediately downstream of the Las Flores PS is recorded by SCADA to be 211 psig.
- At 1:27:23, the controller at the PCR issues a command to close the Refugio Creek mainline valve. **[This and the following actions were in response to the controller being informed of oil on the ground at MP 4.16.]**

- At 1:28:31, the controller Issues Command to close Valve 108 at Las Flores PS.
- At 1:29:34, SCADA reports the mainline valve at Refugio Creek, approximately 2.83 miles downstream of the Las Flores PS and 1.2 miles upstream of the release site, had successfully closed.
- At 1:30:34, SCADA reports Las Flores PS Valve 108 successfully closed.
- Between 3:47:14 and 3:48:13, the controller issues commands to close valves 208A, 208 C, and 209A at Gaviota Station.
- Between 3:49:51 and 3:51:11, SCADA reports successful closure of valves 208A, 208C, and 209A at Gaviota PS.
- At 3:57:48, controller issues command to close valve 209B at Gaviota PS.

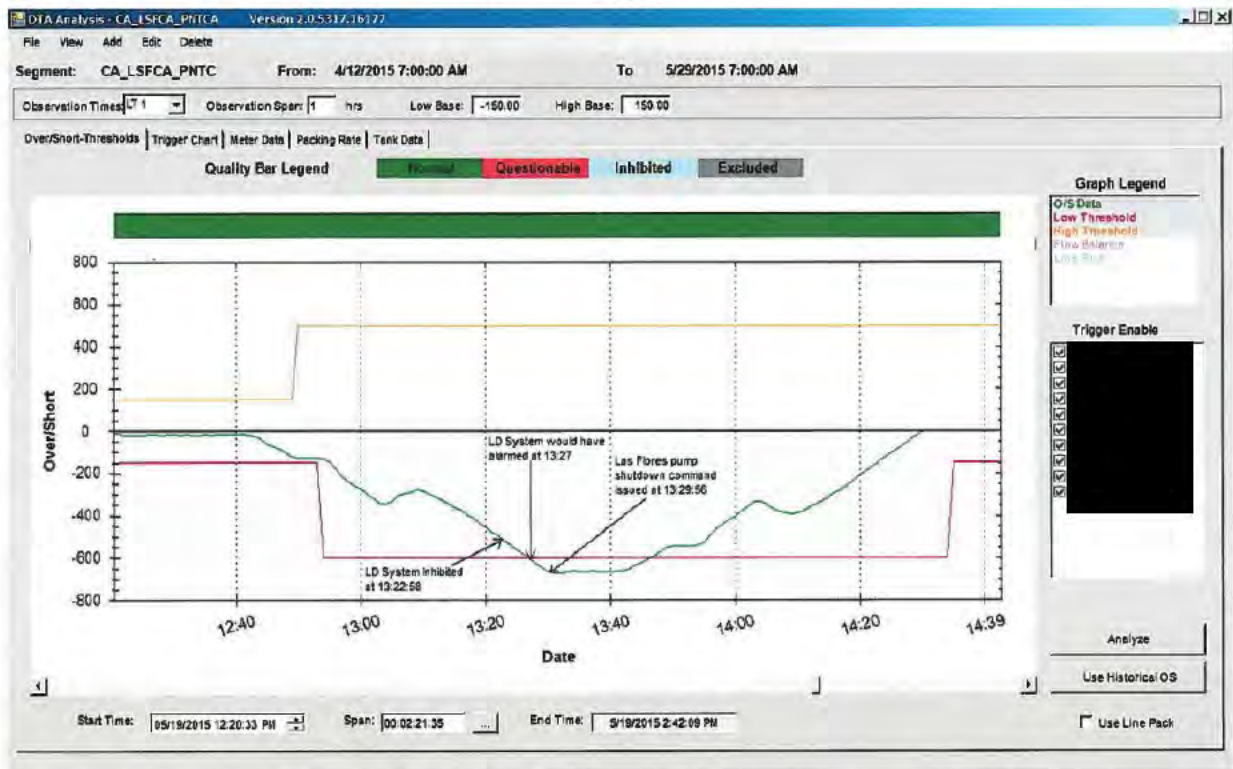
At 4:00:49, SCADA reports successful closure of Valve 209B at Gaviota PS and the pipeline remained down.

Appendix C

Pipeline Leak Monitoring Details

Appendix C: Pipeline Leak Monitoring Details

Plains submitted documentation showing the parameters of the PLM and extrapolated what would have occurred if the PLM system had not been inhibited. The submitted documentation shows that the PLM would have alarmed at approximately two minutes before the controller issued the command to shut down the pump at Las Flores PS at approximately 11:30am PDT. The graphical representation is shown on this page.



Graphical Representation of when the PLM System would have alarmed had it not been “inhibited”. Times in the graph and explanation are in Central Time. Pacific Time is two hours earlier.

Plains provided the following explanation along with the graphical representation above. It is quoted as all content is there. [A few changes were made for emphasis and readability that do not compromise the integrity of the explanation.]

“This is an explanation of how the program calculated the time when the PLM would have alarmed.”

- There are 5 meters that receive oil into the line 901/903 PLM. The SCADA tags are:

- [REDACTED]
- [REDACTED]
- [REDACTED]
- [REDACTED]
- [REDACTED]

- There are 6 meters that deliver oil out of the PLM. The SCADA tags are:

- [REDACTED]

Appendix D

Excerpts and Discussion of Plains Integrity Management Plan (IMP) Requirements

Appendix D: Excerpts and Discussion of Plains Integrity Management Plan (IMP) Requirements

Plains submitted a copy of their IMP dated, December 18, 2003. Applicable sections from that IMP are copied below.

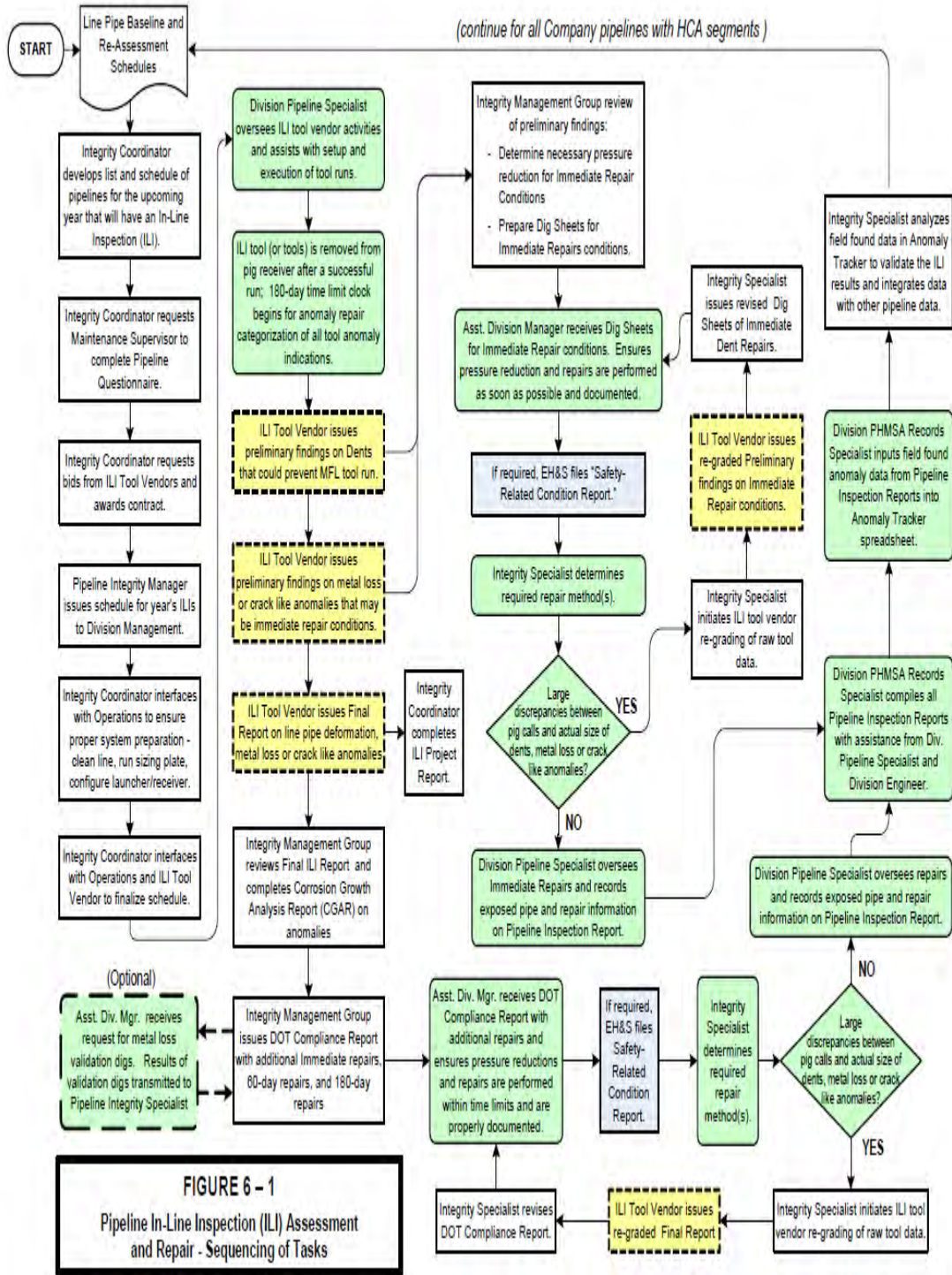
“Section 6.0 Procedures for Conducting Assessments and Processing Results

Rule 49 CFR §195.452 (f)(8) and (f)(4) requirements:

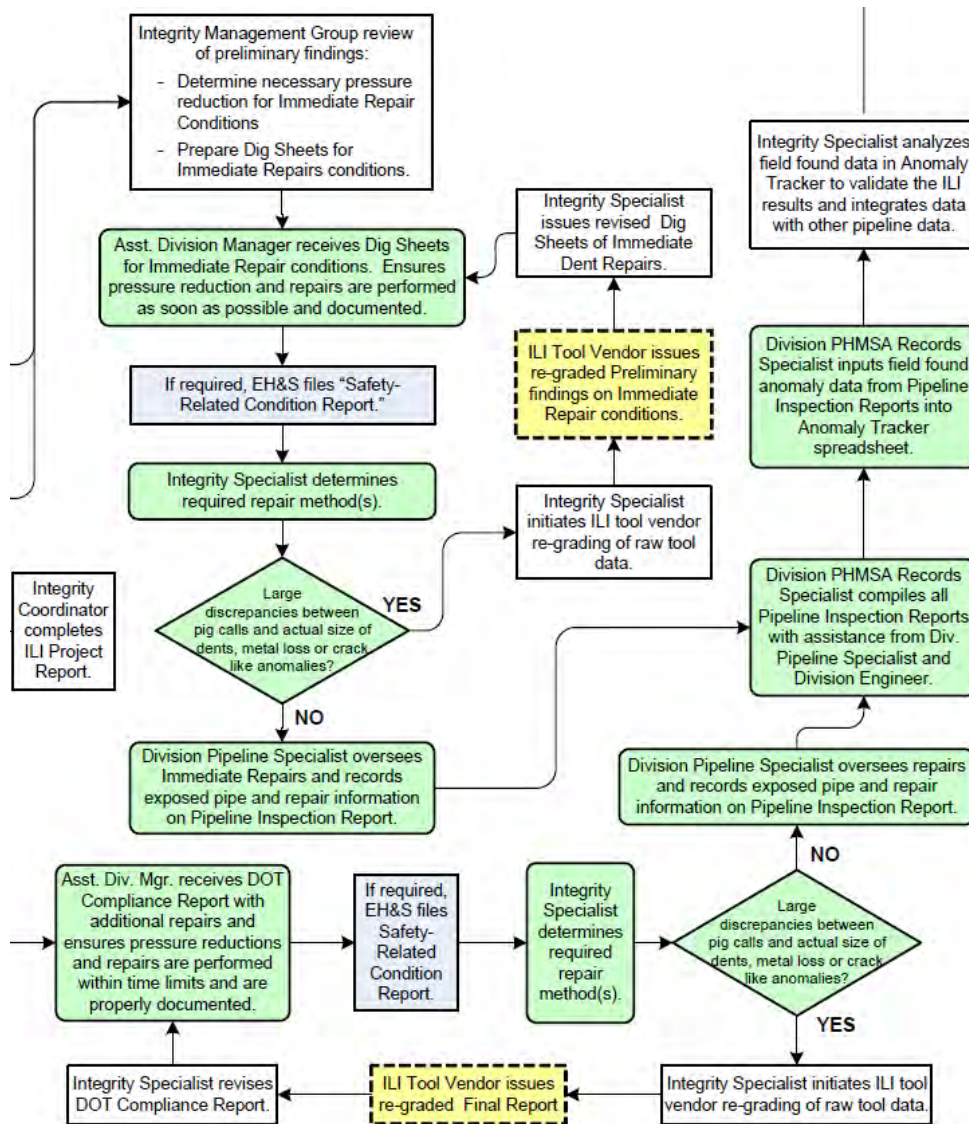
(f)(8) - A process for review of integrity assessment results and information analysis by a person qualified to evaluate the results and information.

(f)(4) Criteria for remedial actions to address integrity issues raised by the assessment methods and information analysis.”

On page 6-4 of the Plains’ IMP, there is a flowchart, “Figure 6-1 Pipeline In-Line Inspection (ILI) Assessment and Repair – Sequencing of Tasks.”



An enlarged portion of Figure 6-1, from the bottom right quadrant is copied below.



The two diamond shapes in the flowchart state the same decision point:

“Large discrepancy between pig calls and actual size of dents, metal loss or crack like anomalies?”

If “yes” the next box in both cases is:

“Integrity Specialist initiates ILI tool vendor re-grading of raw tool data.”

PHMSA requested all documentation between the Plains IMP Group and their ILI vendor with respect to their line 901 and 903 before March 19, 2015. PHMSA was provided access to three email strings between the vendor and Plains IMP Group. The first email string had to do with discrepancies noted by Plains IMP group for “clustering” on the Pentland to Emidio

segment on line 903.

The second and third email strings discuss an anomaly called out as a 66% wall loss by the vendor which was found to be 95% wall loss when excavated and measured in the field. This anomaly was on line 903 between the Gaviota PS and Sisquoc PS and was excavated after the 2013 ILI survey on that line segment. This event was described as a “close call” by the Plains representative. He asked the vendor what the cause of this under reporting might be. The ILI vendor responded:

“The anomaly in the 2008 run had a lower calculated wall loss of 28% (A neighboring anomaly had a wall loss of 32%, which ended up being assigned to the cluster) because the lower resolution DHD sensors capturing the signal as one anomaly with a wide profile, which resulted in a low wall loss calculation. For the 2013 run, although the tool captured a better profile, with two peaks at that same spot, the anomaly sized a bit wider, encompassing part of the neighboring peak (which had the lower amplitude), which resulted in the 66% wall loss. After adjusting the width to only account for the higher peak, the resulting wall loss was 76%.”

The vendor also requested additional dig results from this Gaviota to Sisquoc survey via email. Plains apparently sent them additional digs results at a later date via email attachment.

This interaction demonstrates that the ILI vendor is able to reanalyze data and did come closer to the actual anomaly depth. Even after re-analyzing the anomaly, the vendor still under-called the anomaly by 19%. This should have led to increased conversation.

When provided additional information from the operator, the vendor uses the “new” information to reanalyze the specific anomaly to better provide a more accurate characterization of the anomaly. Also, the vendor analyst requested additional data from the digs that were being performed.

Appendix E

Corrosion Control and Pipeline Conditions

Appendix E: Corrosion Control and Pipeline Conditions

Corrosion Control

All interstate pipelines regulated by PHMSA on which construction was begun after March 31, 1970 are required to be coated and cathodically protected. Cathodic protection (CP) is a process by which bare steel is protected from corrosion by introducing a small electric current from a rectifier through an anode bed into the earth and back to the rectifier through the pipe (the cathode). A pipe will corrode if steel is allowed to leave the pipe at bare spots called “holidays” in the coating. CP forces electricity toward the pipe at holidays which counters the corrosion process.

Pipeline Coatings

The first line of protection from pipeline corrosion is a good coating. Line 901 was installed with a coal tar urethane coating in intimate contact with the bare steel 24-inch pipe. Approximately 1.5-inches of urethane foam insulation were then sprayed onto the pipe over the coal tar urethane coating. The pipe was then finally wrapped with a polyethylene tape as a moisture barrier and to hold and protect the insulation on the pipe. The girth welds, where each joint of pipe is welded to the next joint, were coated with shrink sleeves which are made of a thermoplastic that shrinks when heat is applied with a torch which then adheres the sleeve tightly to the pipe.

CP on Line 901

Operators are required to install and monitor a CP system within a year of constructing a pipeline. This was done for Line 901. Periodic testing and evaluations are required to ensure the CP system is functioning properly. Bimonthly inspections of rectifiers and annual inspections of pipe-to-soil potentials at each test station along the pipeline are required and reports are kept. PHMSA reviewed CP reports for Line 901 with a focus on 2003 to the present. The operator conducted a close-interval-survey (CIS) in December 2008 and again in April 2015 on Line 901. A CIS is an effort where the operator reports an “on” potential and an “off” potential at approximate three-foot intervals. These reports showed that the CP system appeared to be working well and that the pipe-to-soil potentials were within accepted criteria. The CIS in 2008 showed that the polarized potential of the pipeline was generally around a volt (-1,000mV). In 2015, the polarized potential had moved in the more negative direction towards the maximum polarized potential of steel or ~1,200mV. The off readings in 2015 were generally more negative than -1,100mV.

There are two explanations for the movement of the polarized potential on Line 901. One would be that the operator turned up the output on the rectifiers that supply the current to the pipe or they installed additional rectifiers. The second would be that the operator removed some of the protected steel from the CP circuit.

PHMSA reviewed the rectifier inspections and found that they were not “turned up” during this time period. The rectifiers had generally consistent output. This meant that the only other possibility would be the removal of a significant amount of steel from the protected pipeline system.

PHMSA requested that the operator provide documentation of the amount of pipe removed

from the system between 2008 and 2015. Plains provided a statement to PHMSA indicating that between 2008 and 2015, approximately 2120 feet of 20-inch and 24-inch piping was disconnected from or removed from the cathodically protected pipeline system.

CP is Ineffective on Buried Insulated Pipelines

After the release, PHMSA personnel visited Plains offices in Houston, TX, to continue the investigation. During this first visit, one of the first questions concerned external corrosion and cathodic protection because this appeared to be the apparent cause of the release. Plains personnel showed PHMSA a Technical Committee Report from the National Association of Corrosion Engineers (NACE International), titled, “Effectiveness of Cathodic Protection (CP) on Thermally Insulated Underground Metallic Structures” - NACE International Publication 10A392 (2006 Edition) – originally prepared in 1992 by NACE Task Group (TG) T-10A-19, a component of Unit Committee T-10A on Cathodic Protection and was reaffirmed with editorial changes in 2006 by Specific Technology Group (STG) 35 on Pipelines, Tanks, and Well Casings. It is published by NACE under the auspices of STG 35.”

This report details the reasons that CP is not effective on buried insulated underground structures. In the “Background” section the report states,

“Thermally insulated pipelines have experienced relatively aggressive corrosion, with some failures occurring within three years of service, although acceptable industry standards of CP had been applied and maintained shortly after line construction. The most predominant failures have been those occurring at joints; however, moisture has migrated along the pipeline steel surface to create electrochemical corrosion cells remote from the field joint, culminating in extensive replacements of substantial lengths of line.”

Ultimately, it appears that moisture migrated along Line 901 to the lowest local elevation point and created an electrochemical corrosion cell approximately six (6) feet from the nearest girth weld.

Discussion of Corrosion Under Insulation (CUI)

On non-insulated buried pipelines, external corrosion is normally able to be mitigated by Cathodic Protection (CP). Generally, external corrosion cannot occur as long as CP current is getting onto the pipe. CP current creates an oxygen-free environment around the pipe which will stop the electrochemical process of corrosion, barring additional circumstances.

Where external corrosion does occur, current is allowed to get off the pipe and migrate into the surrounding soil. When this occurs, the current takes metal ions with it causing the wall loss or external corrosion. There is little to no “corrosion product” that remains at the pipe surface.

In a buried insulated line, the coatings and insulation do not allow the metal ions that result from the electrochemical process of corrosion to migrate away from the pipe surface. Thus, the “corrosion product” will remain close to the pipe and it will become dormant when the electrochemical process depletes all of the oxygen in the moisture. This is known as the dry cycle. When fresh “oxygenated” moisture infiltrates the coating and reaches the area of external corrosion on the pipe, the corrosion process reactivates and again continues until the oxygen is depleted. This is known as the wet cycle. This process is described in detail in the attached metallurgical report as Corrosion Under Insulation (CUI) facilitated by wet/dry cycling which was determined to be the actual cause of the wall thinning at the release site.

The metallurgical report contained descriptions of the “corrosion product” as being dense and

tightly adhered to the pipe. The structure of the “corrosion product” was alternating layers of magnetite and goethite; both have magnetic properties. Due to the composition and density, PHMSA requested additional testing to better quantify the parameters of density and magnetic permeability of the “corrosion product”. This was done and the results were presented in the final root cause failure analysis (RCFA) report also attached to this report. The results came back that the density of the “corrosion product” was 25% of steel and the magnetic permeability was 5% that of steel. While 5% magnetic permeability is small, the large volume of the corrosion product compared with that of the remaining pipe wall led, in part to the MFL tool’s inconsistent reporting. This phenomenon is discussed below and in more detail in the ILI SME Report.

Magnetic Flux Leakage (MFL) Technology and Under-Calling the Failed Anomaly

In simple terms, the MFL tools used are comprised of magnets that apply a magnetic flux into the pipe steel in the longitudinal direction. The amount of magnetic flux put into the pipe is calibrated to saturate the full wall thickness. There are numerous sensors placed circumferentially around the tool and central to the induced flux field so as to measure and record variances in the magnetic flux that remains in the pipe wall. Any volumetric metal loss that the magnetic field encounters will cause the magnetic flux to “leak” from the pipe wall. The amount of this leakage is then recorded by any number of the sensors in its proximity. When this data is processed, the leakage can be measured to infer the depth, length and width of the metal loss in the pipe wall. As discussed above, when external corrosion is allowed to leave the pipe and migrate into the surrounding soil, the anomaly that is left is usually only the remaining steel. Slight corrosion product might be discovered but not to the extent encountered under insulated coated buried pipe.

On coated, insulated and buried pipe, the “corrosion product” grows and remains in close proximity to the pipe steel. This is similar to the type of corrosion on vehicles, in which the corrosion under bubbled paint can be easily flaked off. The corrosion-related paint bubbling on vehicles is similar to what occurred on Line 901. There is a pinhole in the paint where oxygenated moisture can get in and allow the corrosion to occur. The remaining paint has enough integrity to keep the moisture in, which allows the corrosion to occur and corrosion product to grow. The corrosion product gets thicker and thicker until the paint fails entirely.

This is similar to the mechanism of CUI that occurred on Line 901. The following picture is excerpted from the metallurgical report.



This picture is excerpted from the final metallurgical report. “Figure 16. Photograph showing a piece of insulation removed from adjacent to the failure location; near 4:30 orientation.”

Appendix F

Industry Standards and General Requirements for In-Line Inspection

Appendix F: Industry Standards and General Requirements for In-Line Inspections

49 CFR Part 195.452(b)(6) requires that operators, “Follow recognized industry practices in carrying out this section, unless – (i) This section specifies otherwise; or (ii) The operator demonstrates that an alternative practice is supported by a reliable engineering evaluation and provides an equivalent level of public safety and environmental protection.” The following discusses the three current accepted industry standards for In-Line Inspections (ILI).

The American Petroleum Institute (API) developed “API Standard 1163, “In-line Inspection Systems Qualification Standard” in 2005. A portion of the forward states that this document, “...serves as an umbrella document to be used with and complement companion standards. NACE RP 0102 Standard Recommended Practice, In-Line Inspection of Pipelines; and ASNT ILI-PQ In-Line Inspection Personnel Qualification & Certification all have been developed enabling service providers and pipeline operators to provide rigorous processes that will consistently qualify the equipment, people, processes and software utilized in the in-line inspection industry.”

Section 1.2 Guiding Principles of API 1163 goes on to state, “Personnel and equipment used to perform in-line inspections and analyze the results shall be qualified according to this Standard and its companions, ASNT In-Line Personnel Qualification and Certification Standard No. ILL-PQ, and NACE Standard Recommended Practice In-Line Inspection of Pipelines RP0102. Combined, these three standards provide requirements and processes for the qualification of inline inspection systems, including the in-line inspection tools, their software, and the personnel to operate the systems and analyze the results. This Standard is an umbrella document covering all aspects of in-line inspection systems, incorporating the requirements of ASNT ILI-PQ and NACE RP 0102 by reference.

Section 9 System Results Verification and Section 9.2.4 – Verification Measurements requires in part, “When verification digs are performed, information from the measurements shall be given to the service provider to confirm and continuously refine the data analysis processes. The information to be collected from the verification measurements and given to the service provider shall be agreed upon by both the operator and the service provider and shall include the measurement techniques used and their accuracies. Information to be provided by the service provider to the operator should include the measurement threshold, reporting threshold, and interaction criteria, if any. Appendix D lists types of information that should be provided to the service provider. Any discrepancies between the reported inspection results and verification measurements that are outside of performance specifications shall be documented. The source of the discrepancies should be identified through discussions between the service provider and the operator and through analyses of essential variables, the dig verification process, and data analysis process. Based on the source and extent of the identified and analyzed discrepancies, one of the following courses of action may be taken: a. The inspection data may be reanalyzed taking into account the detailed correlations between anomaly characteristics and the inspection data. b. All or part of the inspection results may be invalidated. c. The performance specification may be revised for all or part of the inspection results.”

Generally, the pipeline operator will contract with an ILI vendor to provide an assessment of

their pipeline. It must be stated that even though MFL ILI devices are known as “Smart Pigs” they only report what they record. It is up to the pipeline operator to establish defined parameters for what they want the ILI vendor to do with the raw data. The operator, by contract, establishes operational parameters, sets interaction criteria, and must work intimately with the ILI vendor to obtain useable information about their pipeline system.

After a tool is removed from the pipeline, the vendor converts the raw data into useable, measurable data. They provide a final report to the operator that provides their best analysis of the data obtained from the tool within the operator’s defined parameters. It is then the operator’s responsibility to review the final report and create a dig list and perform the excavations. A vital step in the overall process is feedback to the vendor with respect to the accuracy of their tool calls.

Section “8.7 Correlation of ILI Reported Results with Field Measurements from Section 8: Data Analysis in the NACE Standard RP0102 – “In-Line Inspection of Pipelines” is excerpted below:

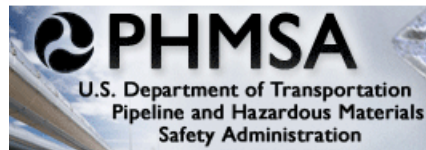
“8.7.1 An important part of “closing the loop” is the feedback of the field inspection results to the ILI service provider. Using this information, the ILI vendor can continuously improve the validity and accuracy of the data analysis.”

Appendix G
In-Line Inspection Report



In Line Inspection Review

For



NPS 24 Pipeline

**Plains All American Pipeline;
Line 901 – Las Flores to Gaviota**

Last Surveyed

May 6, 2015

Final Report March 4, 2016

**Contains Confidential Information Provided By
Plains All American Pipeline LP**

121 Lippincott St
Toronto, ON M5S 2P2
Canada

Cell: 289.259.6277
email: mlamontagne@pipe-life.com

Private and Confidential; Client/Attorney Privileged

Disclaimer

Lamontagne Pipeline Assessment Corporation is not responsible for errors in calculation as a result of third party inaccuracies in information provided by Plains All American Pipelines. The evaluations provided are estimates calculated on a best efforts basis. Oak Ridge National Laboratory and the Pipeline and Hazardous Materials Administration must be aware of the inaccuracies of in-line inspection tool data and their subsequent effect on data interpretation and evaluation and heed any suggested limitations provided in the following document. Lamontagne Pipeline Assessment Corporation is to be held wholly harmless as a result of any inaccuracies, misrepresentations, misinterpretations or anomalies not interpreted at all from the in-line inspection data or other consultant reports used to prepare this report.

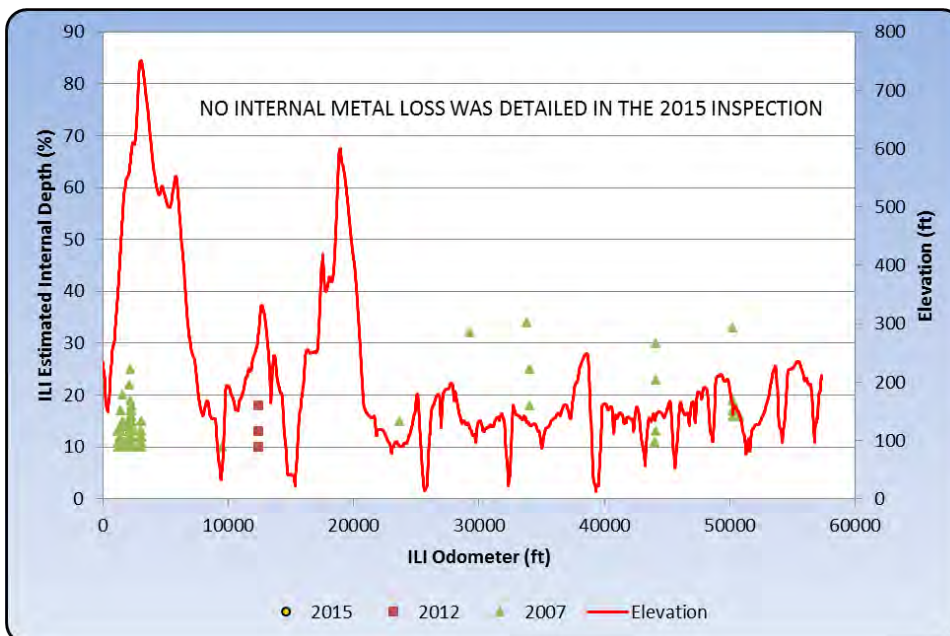
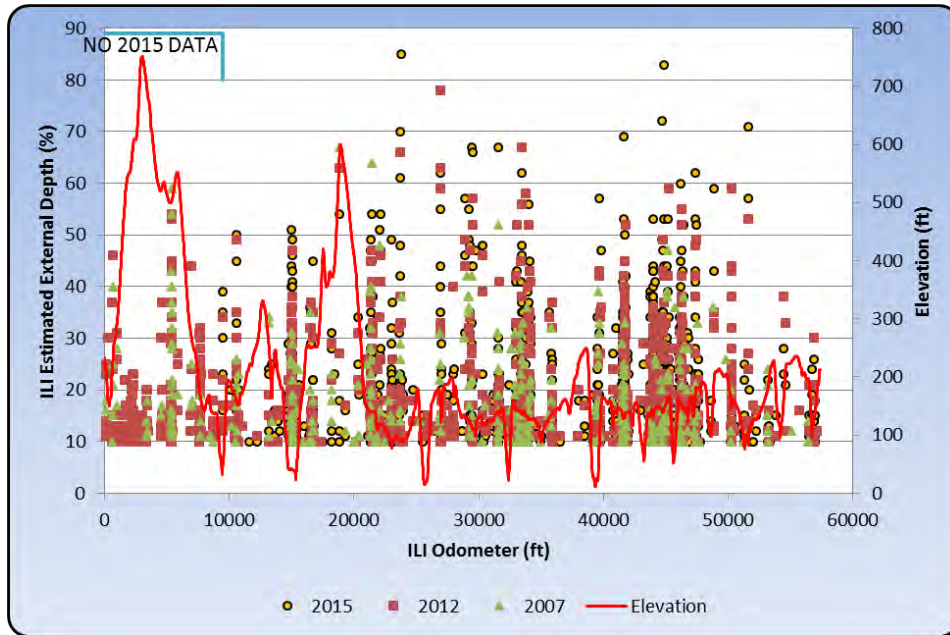
At no time should the data provided herein be used as reason to ignore, violate, or alter any law, regulation, or published industry standard. In no event shall Lamontagne Pipeline Assessment Corporation be liable for any special, incidental, indirect, or consequential damages whatsoever including, but not limited to damage to any reservoir or pipeline, pipeline failure, blowout, explosion, pollution (whether surface or subsurface), damages for loss of business profits, business interruption, loss of business information, or any other pecuniary loss arising out of the use of, or inability to use, the data provided herein.

The information contained in this document is CONFIDENTIAL information intended for the use of the individual or entity named herein. If the reader of this document is not the intended recipient, or the employee or agent responsible to deliver it to the intended recipient, you are hereby notified that any dissemination, distribution or copying of this document is strictly prohibited.

Contains Confidential Information Provided By Plains All American Pipeline LP

Executive Summary

An ILI review has been completed on the Plains All American Pipeline, 10.87 mile, 24” OD Line 901 - Las Flores to Gaviota based on the comparison of the June 19, 2007, July 3, 2012 and May 6, 2015 magnetic flux leakage (MFL) and associated deformation inspections. The focus of this report was to examine the veracity of the inspections and to estimate appropriate growth rates within the segment then apply those rates to the metal loss anomalies as delineated in the most recent 2015 MFL inspection. An excavation prioritization for the segment was then investigated. A discussion on the MFL characterization of the failed anomaly is also presented.



The in-line inspection results from the 2007, 2012, and 2015 MFL runs were examined. The vast majority of the corrosion is external and distributed throughout the length of the segment. The distribution of the external metal loss, in general terms, can be said to predominate in localized low elevations. Previous to the 2015 inspection, the majority of the internal anomalies were found in the first 3000'. This data was not collected in 2015. All three inspections were completed by Rosen USA with different tool designations and modifications employed for each run, either in hardware or software.

<i>Inspection</i>	<i># Ext. Metal Loss</i>	<i># Int. Metal Loss</i>	<i># Mill Metal Loss</i>	<i>Total Metal Loss</i>	<i>Metal Loss in First 9450'</i>	<i># Dents</i>	<i># Dents with Metal Loss or on Weld</i>
2007 MFL (≥10%)	386	237	88	711	277	0	0
2012 MFL (≥10%)	1578	6	2	1586	469	22	2 (repaired)
2015 MFL* (≥10%)	1747	0	21	1768	N/A	6	1 (repaired)

*First 9450' of 2015 data did not record metal loss

There is a trend indicating an increase in the number of metal loss anomalies greater than 10% depth. The 2007 inspection had an ID/OD discrimination fault defining many external anomalies as internal. This discrimination error would not compromise excavation prioritization.

An anomaly matching analysis was conducted between the 2007, 2012, and 2015 MFL inspections by aligning each of the runs by distance and orientation. The following table describes the number of metal loss anomalies that were aligned (considered the same anomaly) between particular inspections. The “percent possible” noted represents the percentage aligned of the maximum possible. It is intuitive that the greater the number of matches, the more informed is the determination of growth.

<i>ILI Runs Compared</i>	<i># of Matches for External Metal Loss</i>	<i># of Matches for Internal Metal Loss</i>	<i># of Matches for Mill Metal Loss</i>	<i>Total # Anomaly Matches (% of possible matches)</i>
2007-2012	488	1	2	491 (70%)
2007-2015*	306	0	12	318 (73%)
2012-2015*	802	0	18	820 (73%)

*Consideration given to missing data area

Corrosion growth rates were investigated by analyzing the growth of matched metal loss anomalies between the 2007, 2012, and 2015 MFL inspections. The best statistical fit came from the 2007 to 2015 comparison. A growth rate could only be established for external corrosion as no internal anomalies were delineated in the 2015 inspection and very few in 2012 as well. The corrosion rate for the external anomalies was calculated as the 99th percentile with a 95% confidence interval and was determined to be 0.0166 in/yr.

By applying this estimated growth rate to the anomalies delineated in the first 9450’ of the 2012 inspection and the 2015 data, a suggested excavation timeline based on a 50% depth limit and 139% MOP pressure limit was investigated. This is a conservative approach but is considered necessary as a result of the errant depth reported by the ILI at the failed defect.

Based on the above limits, and taking into account excavations already completed, the following excavation timeline for metal loss was delineated;

Dig Date	Anomalies 'Failing' 50% Depth Criteria	Number of Excavations
Jan-15	3	3
May-15	18	17
Nov-15	7	5
Jan-16	3	2
May-16	12	6
Jul-16	2	1
Nov-16	8	5
Jan-17	5	2
May-17	11	5
Jul-17	4	2
Nov-17	7	3
Jan-18	10	6
May-18	20	10
Jul-18	20	8
Nov-18	34	9

Based on the ILI sizing and these growth estimates, all of the anomalies will fail by the 50% depth criterion prior to being concerned with the burst pressure approaching 139% MOP.

The locations with the 2015 excavation timeline are,

GW	Dig Start	Dig End	Length	Dig Date	GW	Dig Start	Dig End	Length	Dig Date
260	636.44	636.47	0.03	Jan-15	9270/9280	33431.52	33460.75	29.23	May-15
1370	4608.59	4610.89	2.3	Jan-15	9280/9290	33469.53	33482.42	12.89	May-15
1570	5382.03	5382.84	0.81	Jan-15	9420	33999	34026.28	27.28	May-15
4150/4160/ 4160.01/4160.02	14945.13	14968.53	23.4	May-15	11060	39810.31			Nov-15
					12410/12420	44708.24	44725.74	17.5	May-15
4210/4220	15049.79	15076.28	26.49	Nov-15	12420/12430	44745.1	44774.5	29.4	Nov-15
4220/4230	15086.08	15106.27	20.19	May-15	12820/12830	46183.26	46208.59	25.33	May-15
6100/6110	22033.77	22035.46	1.69	May-15	12880	46415.43	46424.28	8.85	May-15
6350/6360	23006.72	23032.43	25.71	May-15	13200/13210	47373.47	47402.54	29.07	May-15
7990	29171.19	29171.21	0.02	May-15	13210	47412.91	47413.4	0.49	May-15
8060	29453.57	29471.01	17.44	May-15	13700	48882.16	48882.36	0.2	May-15
8140	29742.02			Nov-15					
8280/8290	30307.15	30333.12	25.97	May-15					
8640/8650	31555.39	31558.11	2.72	May-15					

The growth rates, excavations required and re-inspection frequency should be re-examined after every future in line inspection.

The depth sizing accuracy stated by Rosen is $\pm 10\%$ with 80% certainty for pitting and general corrosion. With respect to depth measured during excavations, the 2015 inspection was within $\pm 10\%$, 57% of the time, the 2012 inspection was within $\pm 10\%$, 58% of the time, and the 2007 inspection was within $\pm 10\%$, 33% of the time. If overcalled anomalies were considered (i.e. ILI depth $> 10\%$ over actual) then in all years the unities would be $\pm 10\%$, $> 70\%$ of the time. Likewise, employing API 1163, the tool performance was not within stated specifications.

The length and width dimensions of metal loss anomalies also play a key part in the sentencing of metal loss with respect to the remaining strength. The depth and axial length of metal loss are primary factors in the remaining strength evaluations, whilst the width estimates can affect the estimated depth of an anomaly during grading by the ILI vendor. Parameters that may affect the accuracy of the sizing estimate are the aspect ratio of the corrosion, corrosion geometry, corrosion complexity, defect spacing, tool velocity, and pipe line magnetic permeability amongst others. The length and width sizing specification given by Rosen is $\pm 0.59"$ for general corrosion and better for pitting.

The importance of interacting "boxes" appropriately to form "clusters" of an area as closely approximating the actual corrosion area dimensions cannot be emphasized enough. Plains specifies an interaction rule that is one of the most commonly employed throughout industry. But Plains requires that only metal loss with depths 15% or greater, are to be included for "clustering". This differs from the usual. Typically all ILI delineated corrosion is interacted to define "clusters". The vast majority of all excavated anomalies have been undercalled in length and to a lesser extent in width. A recommendation is provided to review and possibly alter the present interaction criteria for both the in-line inspection analysis and the field measurement process.

Deformation or dents were examined with consideration to depth, location to welds and their association to corrosion. The 2012 inspection delineated 1 dent on a weld that was subsequently repaired and the 2015 ILI reported 6 dents. In order to expedite the May 2015 deformation report after the rupture, Plains asked for the report with graded metal loss only. As a result, the report did not provide sizing of the dents. Consideration should be given to reviewing this further. For further delineation of possible dents with metal loss, ILI anomaly alignment was also completed between the 2007, 2012, and 2015 MFL and deformation runs. To which, no locations of a dent with metal loss were found.

The documented procedure used by Plains entitled "Procedure for the Assessment of In-Line Inspection Results; DOC NO: PAALP-INT-PRC-NJP- 001" was provided as part of the review process. The document outlines the steps Plains personnel are required to take following the receipt of preliminary and final ILI reports. According to this document they comply with the requirements of the Code of Federal Regulations 49 Part 195.452 with respect to addressing MFL detectable anomalies.

Besides the complex shape of the corrosion, it is surmised that the tightly adhered magnetically susceptible corrosion product may have had some influence in the MFL sizing of the failed anomaly. This segment should be re-inspected with an ultrasonic wall loss tool. The ultrasonic inspection will provide a measure of the remaining wall thickness and length without being influenced by the corrosion product and less by shape. A circumferential MFL may delineate the corrosion lengths more accurately but there is still the issue of depth determination by that magnetic tool.

Table of Contents

Executive Summary 2
 Introduction 7
 Results and Discussion..... 7
 Review of the Inspection Metal Loss Data 7
 In-Line Inspection Comparison and Growth Rate Estimation 11
 In-Line Inspection Tool Accuracy 13
 Plains Anomaly Mitigation Strategy 20
 ILI Details for the Failed Anomaly 22
 Future Anomaly Mitigation..... 28
 Deformation Discussion..... 29
 Discussion to Note 30
 Appendix A – ILI growth variance in depth between all inspections 31
 Appendix B – Individual Anomaly Excavation Timeline..... 33
 Appendix C – Full Excavation Timeline (30’ limit) 89

List of Tables

Table 1. Percentage of metal loss by depth under shrink sleeves. 10
 Table 2. In line inspection results..... 11
 Table 3. Anomaly matches between inspections. 11
 Table 4. Distribution of metal loss lengths for boxes and clusters..... 17
 Table 5. Distribution of metal loss widths for boxes and clusters. 17
 Table 6. Close-Out summary for the 2012 inspection of Las Flores to Gaviota..... 21
 Table 7. ILI reported dimensions of the failed area. 22
 Table 8. Estimated failure pressure from profile in Figure 18. 24
 Table 9. Magnetic properties of the pipeline steel and corrosion product (EWI). 27
 Table 10. Suggested excavation timeline..... 29
 Table 11. Suggested excavation locations..... 29
 Table 12. Dent summary from previous deformation inspections. 30

List of Figures

Figure 1. Distribution of external metal loss anomalies..... 8
 Figure 2. Distribution of internal metal loss anomalies. 8
 Figure 3. Distribution of external metal loss anomalies by clock position. 9
 Figure 4. Distribution of internal metal loss anomalies by clock position. 9
 Figure 5. Distance of metal loss to the nearest girth weld in 2012. 10
 Figure 6. Distribution of growth rates for matching metal loss. 12
 Figure 7. Probability plot of growth rates for a linear rate assumption..... 12
 Figure 8. Distribution of external growth by ILI depth variance. 13
 Figure 9. Unity plot for the 2015 MFL inspection. 13
 Figure 10. Unity plot for the 2012 MFL inspection. 14
 Figure 11. Unity plot for the 2007 MFL inspection. 14
 Figure 12. Interacted MFL metal loss in failed anomaly. 16
 Figure 13. ILI estimated length compared to field measured..... 18
 Figure 14. ILI estimated width compared to field measured. 18
 Figure 15. ILI estimated depth compared to field measured..... 19
 Figure 16. Metal loss area; ILI vs field measurement. 19
 Figure 17. C-Scans with boxes of the failed location as detailed by the 2007, 2012 and 2015 inspections 22
 Figure 18. The failed area, A) the Rosen 2015 A-Scan, B) the Laser Scan. 23
 Figure 19. Depth profile of failed anomaly (DNV)..... 24
 Figure 20. Tightly adhered corrosion product (Fig. 58 from metallurgical report). 26
 Figure 21. X-Ray Diffraction (XRD) of the corrosion product indicating layering of Magnetite and Goethite... 27
 Figure 22. Amplitude magnetic permeability of the pipeline steel and corrosion product (EWI). 27

Introduction

Data was provided by Plains All American Pipelines (Plains) for three magnetic flux leakage (MFL) and deformation in-line inspections (ILI) that have been conducted on the 10.87 mile, 24" OD Line 901 - Las Flores to Gaviota segment. This line is reported to transport crude oil at high temperatures (135°F+) and is comprised of 0.344" API5L X-65 HF-ERW and 0.500" API5L X-60 HF-ERW pipe. The inspection runs reviewed were all axially oriented magnetic flux leakage tools by ROSEN USA (Rosen). The inspections were conducted on June 19, 2007, July 3, 2012 and May 6, 2015. The 2007 inspection employed the CDG (corrosion detection and mapping tool) and EGP (Electronic Geometry Pig) in two separate runs. The 2012 and 2015 inspections used tools having both metal loss and geometry capabilities. The 2012 inspection utilized the CXG (corrosion detection and extended geometry) tool and the 2015 inspection was made using the A/XT (Axial extended geometry) tool.

The aim of this report is to review the findings of the in-line inspections with the focus on anomalies requiring excavation and further evaluation that may lead to repair. This report will review the caliper and corrosion inspections and recommended excavation evaluation for those anomalies to be examined in short order and based on an estimated growth rate applied to the 2012/2015 inspection to determine future excavation dates. The growth rates will be estimated based on the differences found by comparing the 2007 MFL inspection to the most recent 2012 and 2015 MFL inspections. There are also brief discussions on the Plains mitigation strategy and details surrounding the MFL interpretation of the failed anomaly.

Results and Discussion

Review of the Inspection Metal Loss Data

The service provider, Rosen, has stated within the 2007 and 2012 reports received by Plains that all data was accepted and used for evaluation purposes. The 2015 inspection data from ~ 9450' to the end of the inspection was accepted. At the time of the release Plains and Rosen were in discussions around scheduling a re-inspection of this segment to capture the initial 9450'.

The distribution of the metal loss anomalies is detailed in Figures 1 and 2. The vast majority of the corrosion is external and distributed throughout the length of the segment. The distribution of the external metal loss, in general terms, can be said to predominate in localized low elevations. The internal anomalies are seen primarily in the first 3000' and are most likely the result of the incline of the pipeline. There was no internal metal loss delineated in the 2015 inspection, which may be due to the data quality or classification, it also did not have any information on the first 9450' of pipe.

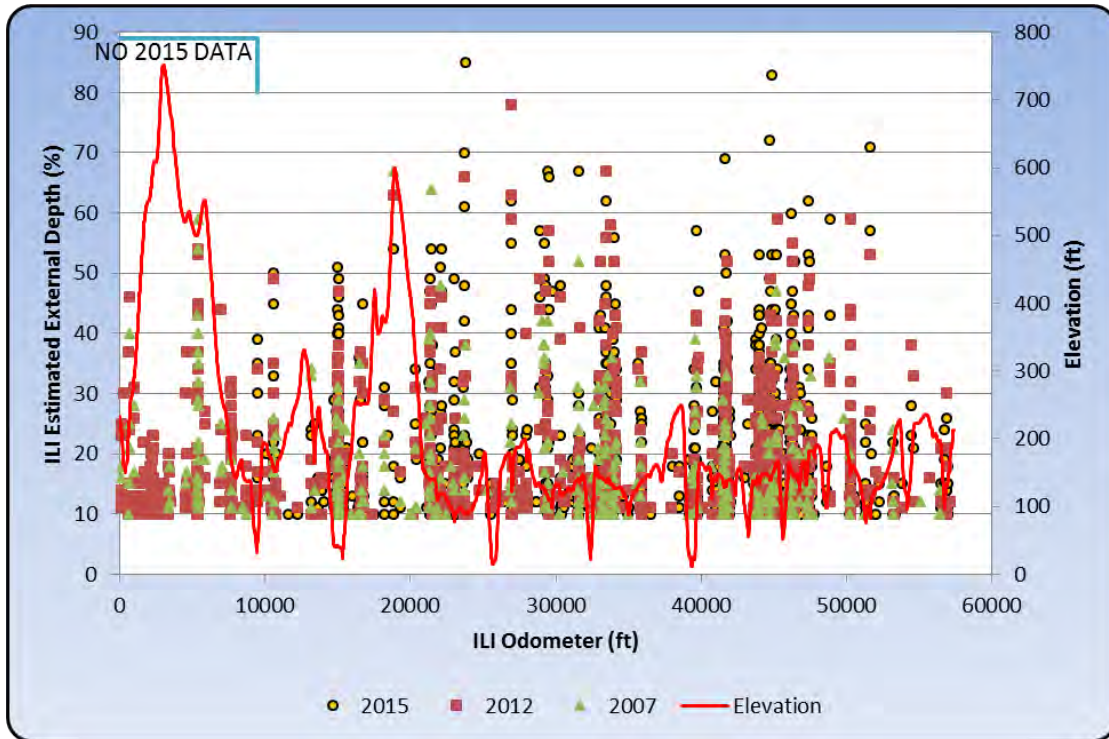


Figure 1. Distribution of external metal loss anomalies.

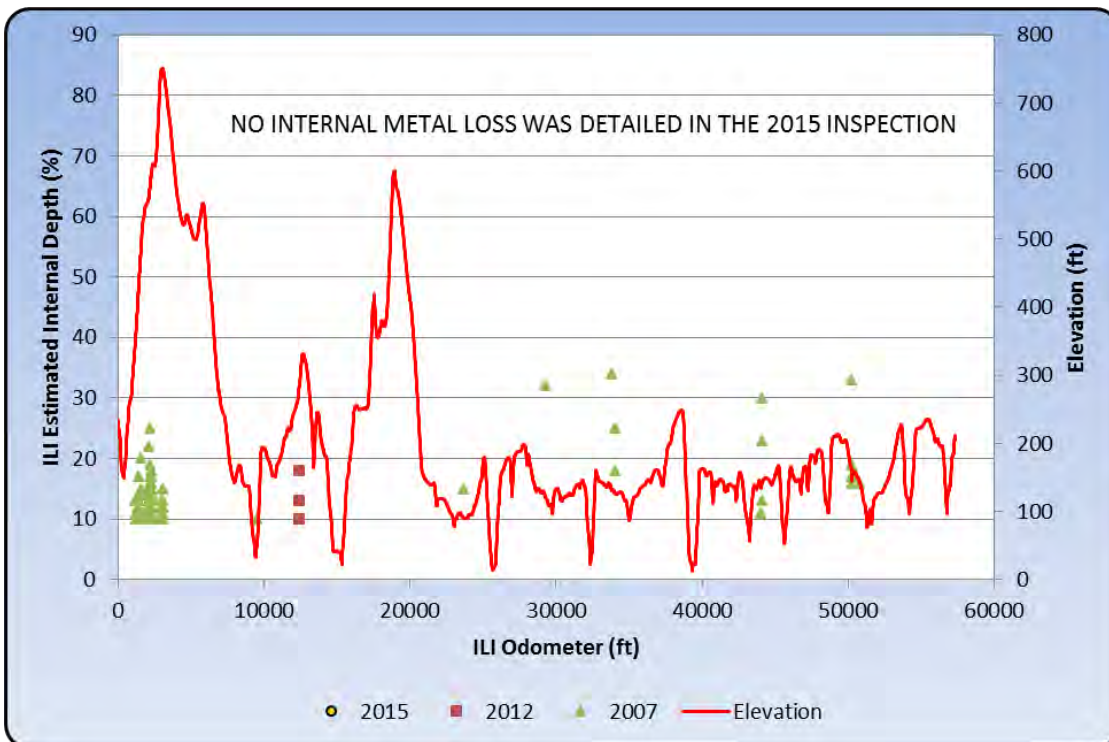


Figure 2. Distribution of internal metal loss anomalies.

A check of the distribution of the corrosion anomalies by clock position in Figures 3 and 4 showed some preference for external metal loss around 4:00 to 8:00 (bottom of pipe) but may be found in all orientations. The internal metal loss in the first 3000' can be found at any

orientation. The remainder of the internal metal loss is shown to be between the 4:00 to 8:00 (bottom of pipe) o'clock orientations. The internal anomalies identified in 2007 in the first 3000' may be external due to an ID/OD discrimination error.

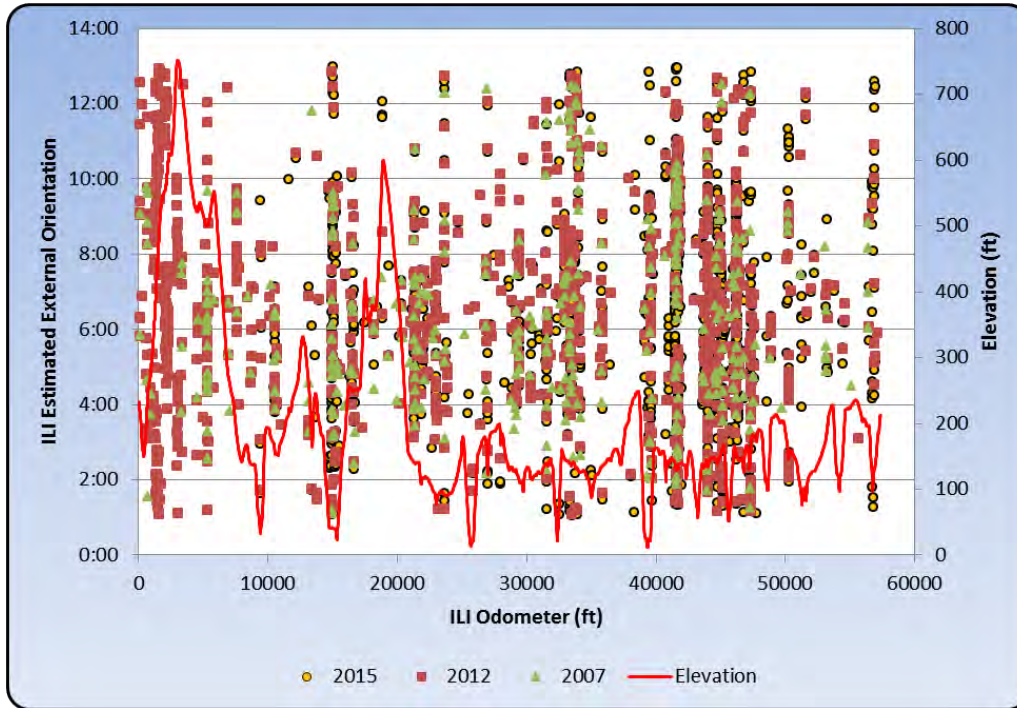


Figure 3. Distribution of external metal loss anomalies by clock position.

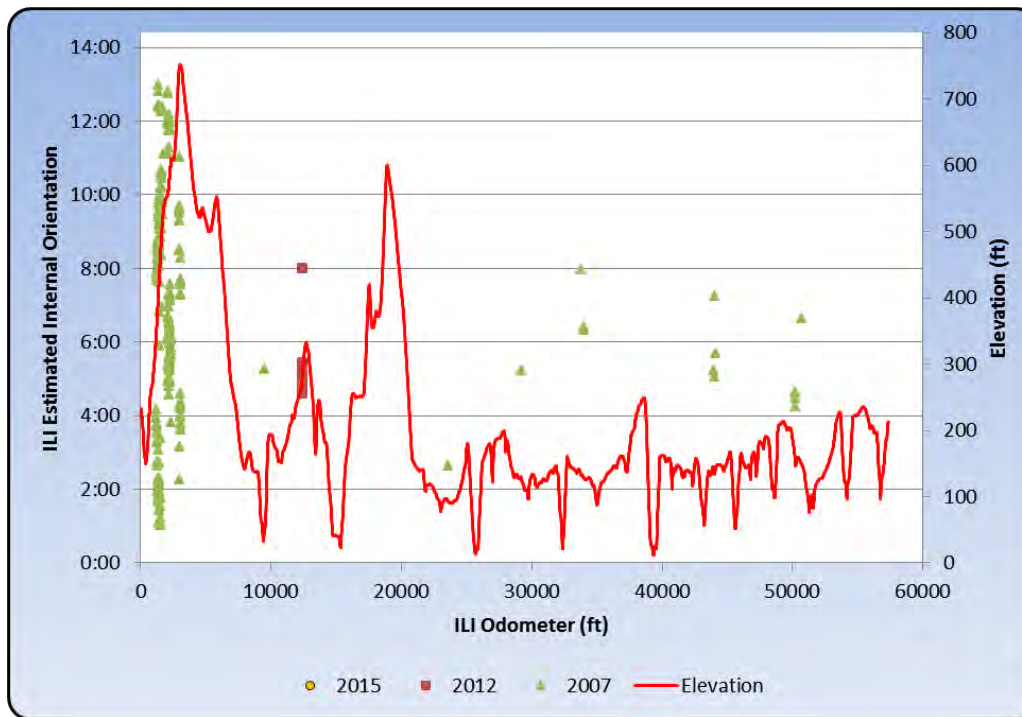


Figure 4. Distribution of internal metal loss anomalies by clock position.

Plains had previously identified the shrink sleeve coating applied over the girth welds as a priority corrosion issue. Figure 5 shows the distance of each metal loss >20% depth in relation to the nearest girth weld as identified in the 2012 inspection.

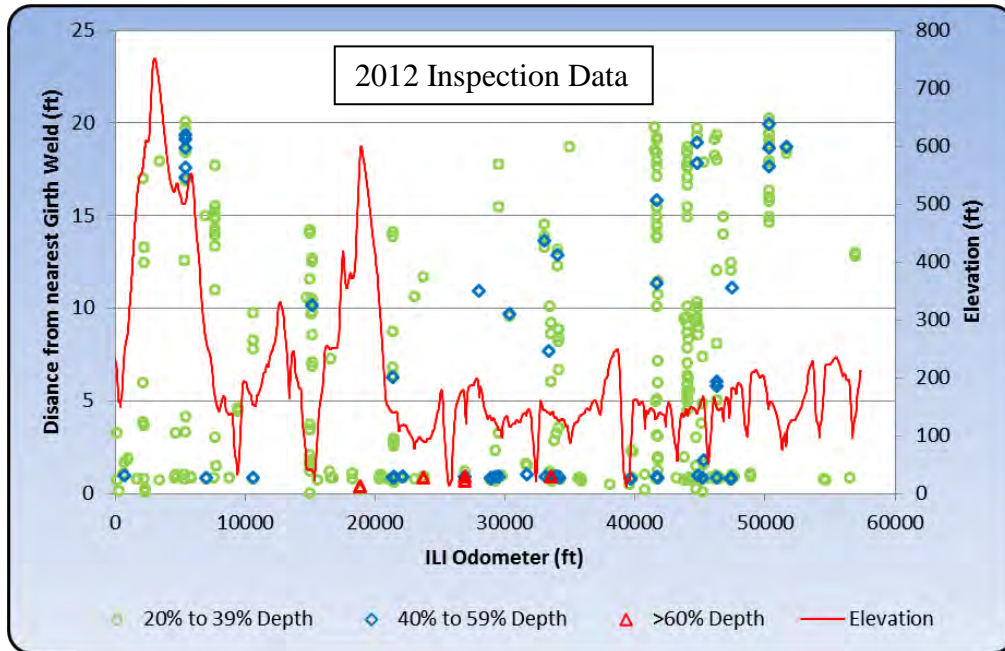


Figure 5. Distance of metal loss to the nearest girth weld in 2012.

The percentage of anomalies by depth within 18” of the nearest girth weld is presented in Table 1. This distance was examined in consideration of the 34” length of shrink sleeve employed (1” greater due to coating interface). The depths were found to have greater criticality nearer the girth welds in the 2012 data than in either of the 2007 or 2015 data. The 2007 and 2015 data approximate an even spread of depth whether under a shrink sleeve or not.

Table 1. Percentage of metal loss by depth under shrink sleeves.

Anomaly Depth	Percentage of Anomalies Within 18" of Girth Weld		
	2007	2012	2015
20% to 39%	53%	36%	35%
40% to 59%	50%	56%	50%
>60%	50%	100%	57%

In-Line Inspection Comparison and Growth Rate Estimation

The in-line inspection results from the 2007, 2012, and 2015 MFL runs were examined. All three inspections were completed by Rosen USA with different tool designations and modifications employed for each run, either in hardware or software. Table 2 details the inspection results. There is a trend indicating an increase in the number of metal loss anomalies greater than 10% depth and therefore active corrosion.

Table 2. In line inspection results.

<i>Inspection</i>	<i># Ext. Metal Loss</i>	<i># Int. Metal Loss</i>	<i># Mill Metal Loss</i>	<i>Total Metal Loss</i>	<i>Metal Loss in First 9450'</i>	<i># Dents</i>	<i># Dents with Metal Loss or on Weld</i>
2007 MFL (≥10%)	386	237	88	711	277	0	0
2012 MFL (≥10%)	1578	6	2	1586	469	22	1
2015 MFL* (≥10%)	1747	0	21	1768	N/A	6	1 (sleeved)

*First 9450' of 2015 data did not record metal loss

An anomaly matching analysis was conducted between the 2007, 2012, and 2015 MFL inspections by aligning each of the runs. Table 3 summarizes the number of metal loss anomalies that have been matched between inspections (considered the same anomaly). The “percent possible” noted represents the percentage aligned of the maximum possible. It is intuitive that the greater the number of matches, the more informed is the determination of growth.

Table 3. Anomaly matches between inspections.

<i>ILI Runs Compared</i>	<i># of Matches for External Metal Loss</i>	<i># of Matches for Internal Metal Loss</i>	<i># of Matches for Mill Metal Loss</i>	<i>Total # Anomaly Matches (% of possible matches)</i>
2007-2012	488	1	2	491 (70%)
2007-2015*	306	0	12	318 (73%)
2012-2015*	802	0	18	820 (73%)

*Consideration given to missing data area

Corrosion growth rates were investigated by analyzing the growth of matched metal loss anomalies between the 2007, 2012, and 2015 MFL inspections. The best statistical fit came from the 2007 to 2015 comparison. A growth rate could only be established for external corrosion as no internal anomalies were delineated in the 2015 inspection and very few in 2012. Figure 6 displays the frequency of growth by percentage from 2007 to 2015. Figure 7 provides a probability plot of the absolute percentage growth. The corrosion rate for the external anomalies was determined to be 0.0166 in/yr by the 99th percentile having a 95% confidence interval. In some instances the growth rate of pitting may be higher than the growth rate of general corrosion. Unfortunately this cannot be delineated as the interaction

rules applied to cluster metal loss in the MFL analysis do not appear appropriate as will be discussed later.

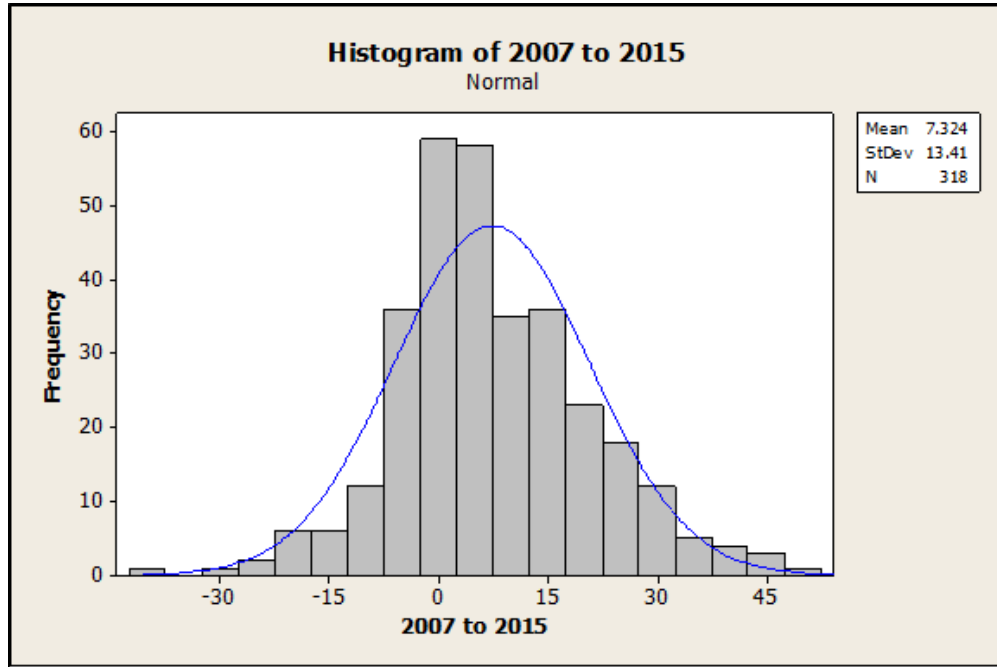


Figure 6. Distribution of growth rates for matching metal loss.

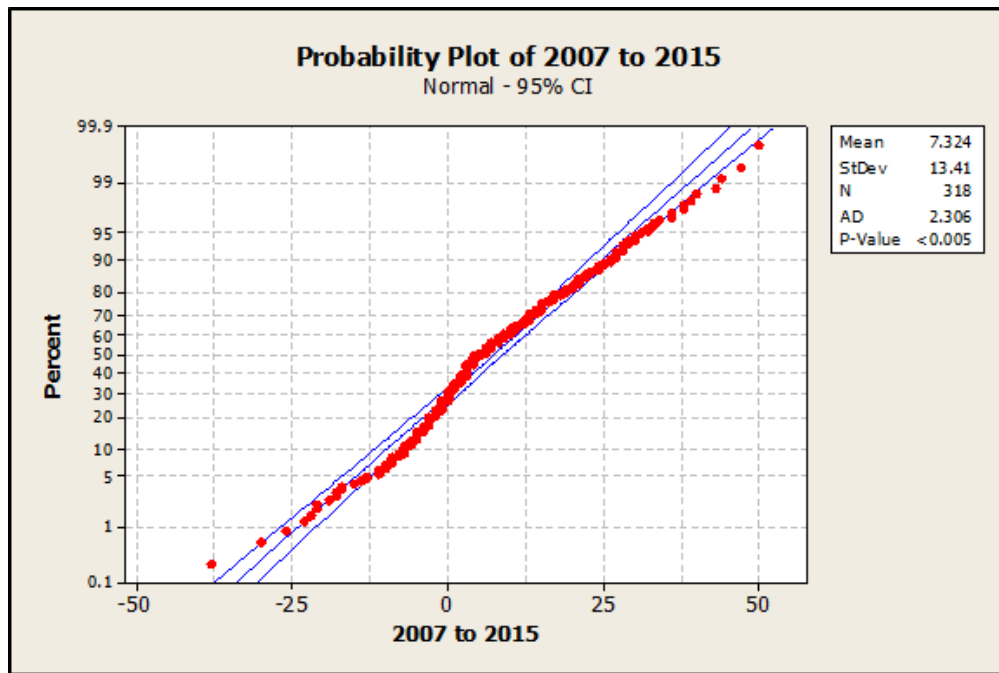


Figure 7. Probability plot of growth rates for a linear rate assumption.

Figure 8 details the 99th percentile growth rate with respect to the absolute variance in the estimated depths from the 2007 and 2015 inspections.

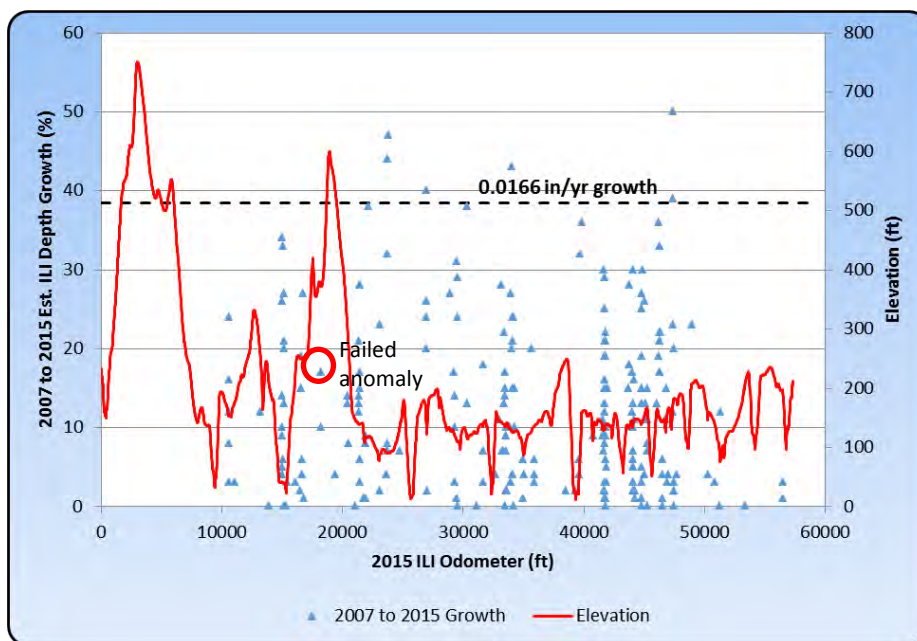


Figure 8. Distribution of external growth by ILI depth variance.

Appendix A examines the ILI growth variance in depth between all inspections similar to Figure 8, except with a finer odometer. It clearly illustrates the greater potential for corrosion and corrosion growth within localized low elevations.

In-Line Inspection Tool Accuracy

The Rosen stated depth sizing accuracy is $\pm 10\%$ with 80 % certainty for pitting and general corrosion. The unity plot in Figure 9 examines the 2015 MFL inspection tool accuracy. The 2015 ILI estimated depths are compared to field measured depths either from the 4 excavations following the failure or the areas recoated after the 2007 and 2012 inspections. The unity plot shows that the 2015 Rosen inspection is within $\pm 10\%$, 57% of the time. It may be seen that the failure location has an uncharacteristically high deviation from the ILI estimate.

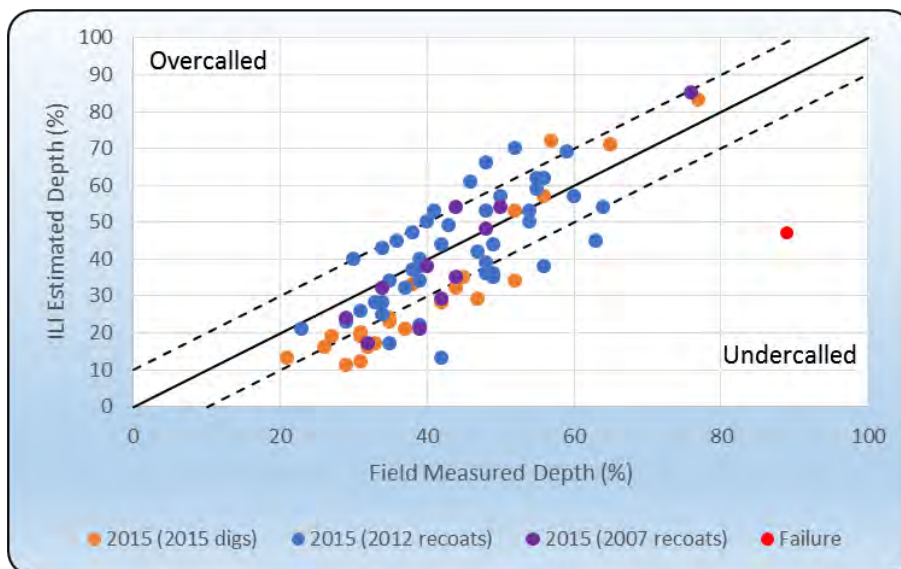


Figure 9. Unity plot for the 2015 MFL inspection.

The unity plot for the 2012 inspection is provided in Figure 10. The 2012 Rosen inspection is within $\pm 10\%$, 58% of the time with respect to the 2012 excavations (blue) and 2007 excavation recoats (violet). When comparing to the 2015 field excavated results based on the 2012 ILI data, growth may have occurred, causing the comparisons between field and ILI to be undercalled (orange). The 2015 digs were not considered in the above stated accuracy.

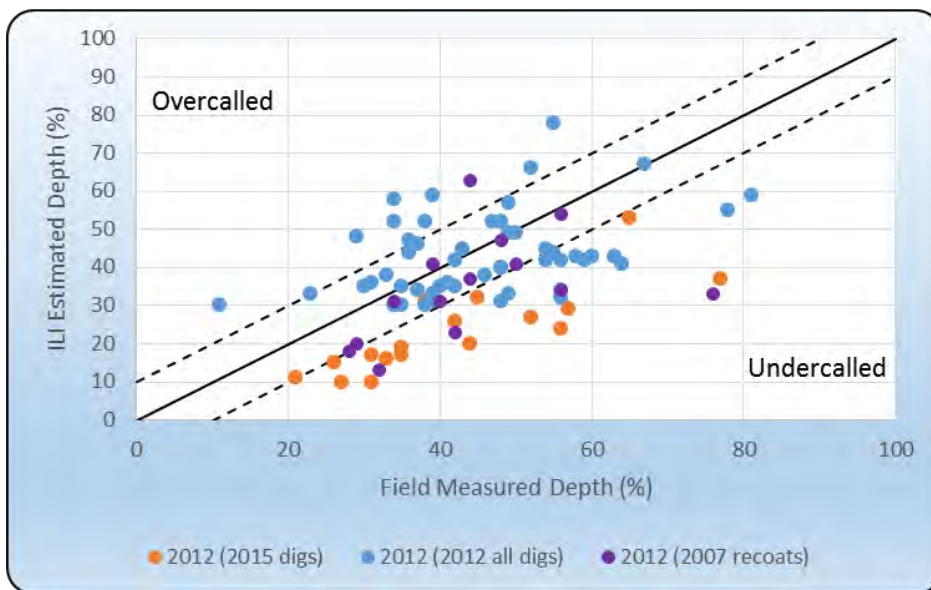


Figure 10. Unity plot for the 2012 MFL inspection.

The unity plot for the 2007 inspection is provided in Figure 11. The 2007 Rosen inspection is within $\pm 10\%$, 33% of the time with respect to the 2007 excavations.

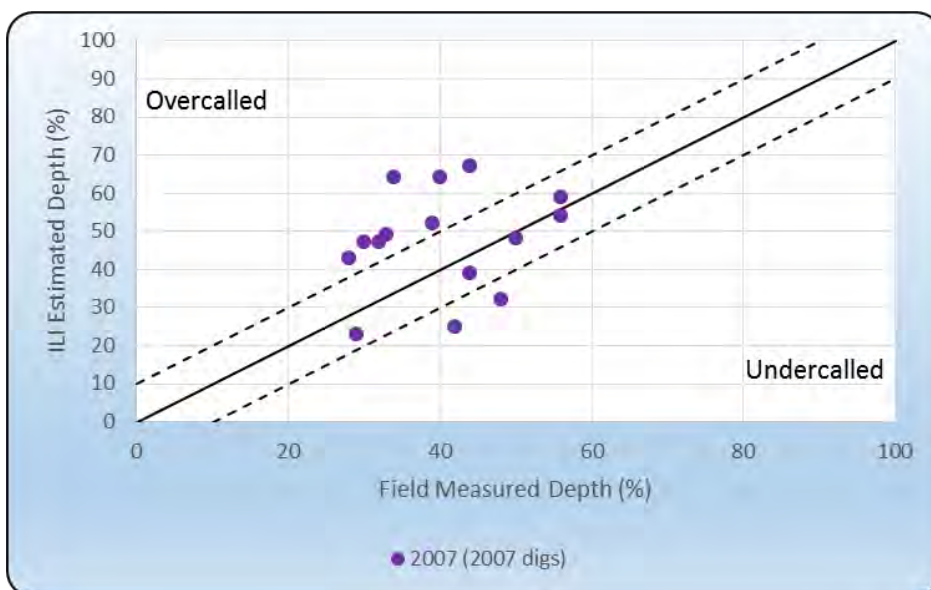


Figure 11. Unity plot for the 2007 MFL inspection.

Likewise, employing API 1163, the tool performance was not within stated specifications. If overcalled anomalies were considered (i.e. $>10\%$ over actual) then in all years the unities would be $\pm 10\%$, $>70\%$ of the time.

The length and width dimensions of metal loss anomalies also play a key part in the sentencing of metal loss with respect to the remaining strength. The depth and axial length of metal loss are primary factors in the remaining strength evaluations, whilst the width estimates can affect the estimated depth of an anomaly during grading by the ILI vendor. Parameters that affect the accuracy of the sizing estimate are the aspect ratio of the corrosion, corrosion geometry, corrosion complexity, defect spacing, tool velocity, and pipe line magnetic permeability amongst others.

All ILI vendors employ software that examine the flux leakage characteristics and amplitude then automatically “box” the metal loss anomalies. The automated boxing determines the depth, length and width for each anomaly based on proprietary algorithms developed by each vendor. These algorithms are created for each model and diameter of inspection tool by pulling (i.e. pull test) the instrument through many known metal loss sizes under controlled conditions. From the signal response the algorithms are created or calibrated. Vendors may create algorithms specifically for particular metal loss characteristics such as general metal loss (large area) or pitting (small and isolated). This is done to more accurately size anomalies as the signal strength and characteristics can and do vary. During the process of characterization the vendor’s proprietary software extracts specific signals from the inspection by an automated algorithm, then classifies the “metal loss”, then quantifies the depth, length and width by the algorithm. The proprietary algorithms must take into account the signal dimensions and typically follow the generic relationship

$$dep_{predict} = \left(\frac{width}{length} \right)^a \frac{amplitude^b}{background^c}$$

(K. Reber, A. Belanger, **Reliability of Flaw Size Calculation based on Magnetic Flux Leakage Inspection of Pipelines**, ECNDT 2006 - Tu.3.1.1, pp 1-11)

This characterization “boxes” individual metal loss anomalies. Once the metal loss is individually “boxed”, interaction routines are applied to “cluster” individual indications into a more realistic representation of the corrosion area. Clusters can also be grouped; however, Plains did not request that Rosen do any grouping. Generally, the interaction criteria are specified by the operator (Plains) as part of the inspection contract. Internal and external corrosion must be considered at the same time. If they are at a coincident location, they should be considered additive. There are five general categories of interaction criteria to “cluster” and/or “group” the “boxed” anomalies

- 1) Length and/or width dependence
- 2) Absolute value
- 3) Wall thickness dependent
- 4) Combinations
- 5) Sector defined

The choice of interaction criteria is important as it may need to be varied depending on the characteristics of the metal loss in the segment being inspected. Plains specifies an interaction criteria to be a combination of absolute value for the length component (1”) and wall thickness dependence for the width component (6t). The 1” x 6t interaction rule is one of the most commonly employed throughout industry and is the example given in ASME B31.4.

To form a metal loss “cluster” from “boxes”, two or more “boxes” must be within 1” of axial separation or within 6 wall thicknesses circumferentially. An example of this process may be seen in Figure 12 which shows the boxes and clusters delineated at the failed anomaly in the 2015 inspection. Solid yellow boxes are metal loss with depths 10%-20%. Solid green boxes are 20-40% depth and solid blue boxes have depths greater than 40%. As requested by Plains, only 15%, and greater metal loss, are to be included for “clustering”. The dashed boxes represent the metal loss “cluster” formed by employing the above interaction rule to the boxes (>15%). The resulting size of a clustered anomaly is the length and width extent with a depth represented by the deepest metal loss box within the cluster.

The clusters formed by Rosen (green and blue dashed) in Figure 12 by the interaction process overlap and do not accurately represent the extent of the actual corrosion area. The two clusters identified overlap due to clustering of metal loss ≥15% depth only, as per Plains. If all “boxes” down to 10% depth were included in the interaction parameter then the cluster would have been represented as per the orange dashed box in Figure 12. Consideration of all metal loss would have defined the actual area much more accurately or alternatively, grouping of clusters could be considered.

The importance of interacting “boxes” appropriately to form “clusters” of an area as closely approximating the actual corrosion area cannot be emphasized enough. The importance of the depth and length measurement will be explored in more detail in the discussion to follow.

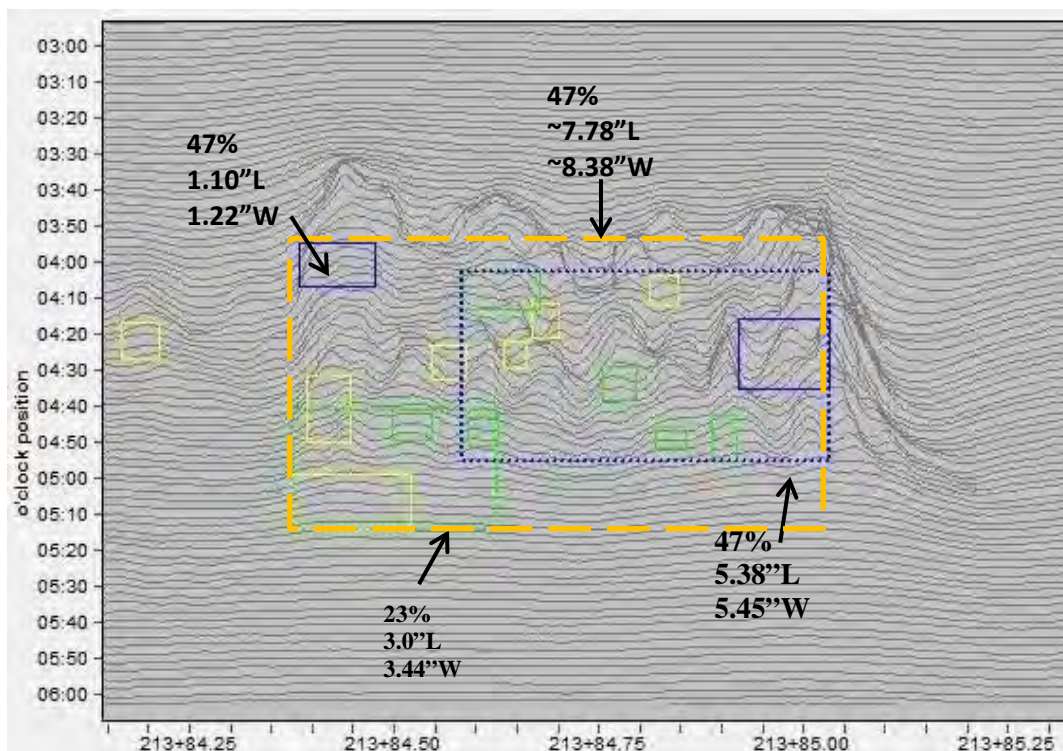


Figure 12. Interacted MFL metal loss in failed anomaly.

During this review process a variance was seen in the length and width sizing of anomalies between inspections as detailed in Tables 4 and 5. The 2007 inspection delineated generally larger metal loss features in length and width dimensions. The 2012 inspection defined the smallest anomalies. The 2012 inspection greatly undercalled the length and width of the

failed defect. All 3 inspections were to have used the 1” x 6t interaction of the boxes although it is unknown if there were changes in the minimum depth requirements. All three inspections were carried out using different MFL tool generations. There have been no details provided as to what changes were made in the proprietary sizing algorithms between tool generations or analysis processes.

Table 4. Distribution of metal loss lengths for boxes and clusters.

Length (in)	2007 Boxes	2012 Boxes	2015 Boxes	Length (in)	2007 Clusters	2012 Clusters	2015 Clusters
0-0.5	16	379	166	0-5	263	83	121
0.5-1	151	683	907	5-10	90	0	1
1-1.5	59	238	304	10-15	20	0	0
1.5-2	21	154	206	15-20	4	0	0
2-2.5	13	49	63	20-25	3	0	0
2.5-3	9	0	0	25-30	3	0	0
3-3.5	20	0	0	30-35	2	0	0
3.5-4	19	0	0	35-40	1	0	0
4-4.5	10	0	0	40-45	1	0	0
4.5-5	1	0	0				
5-5.5	3	0	0				
5.5-6	1	0	0				
6-6.5	1	0	0				

Table 5. Distribution of metal loss widths for boxes and clusters.

Width (in)	2007 Boxes	2012 Boxes	2015 Boxes	Width (in)	2007 Clusters	2012 Clusters	2015 Clusters
0-1	192	632	357	0-5	168	58	90
1-2	84	683	976	5-10	117	21	29
2-3	19	113	198	10-15	68	3	2
3-4	7	40	50	15-20	19	1	1
4-5	5	19	29	20-25	8	0	0
5-6	3	9	18	25-30	3	0	0
6-7	5	5	8	30-35	2	0	0
7-8	3	1	6	35-40	1	0	0
8-9	4	1	2	40-45	1	0	0
9-10	2	0	0				
10-11	0	0	1				
11-12	0	0	1				

Now consider the length and width sizing with respect to that measured in excavations. Figures 13 and 14 compare the tool estimates of length and width to measurements taken during a few field excavations and repair. There are only a few as these were all of the length and width measurements from the field that were provided. In both figures the solid line represents the ideal where the estimated tool sizing is equal to the field measurement and the dashed lines represent $\pm 0.59"$, the tool sizing error for length and width specified by the vendor. Figure 13 shows the data to have a couple length estimates within specification but the remainder of length and width estimates were all under estimated. The excavations shown were done after the 2012 inspection and only the locations that were called by all three tool runs are included. The red markers representing the failure lengths and widths will most assuredly not be the same field measurement in 2007 or 2012, this only represents the dimensions as called by the ILI in that year.

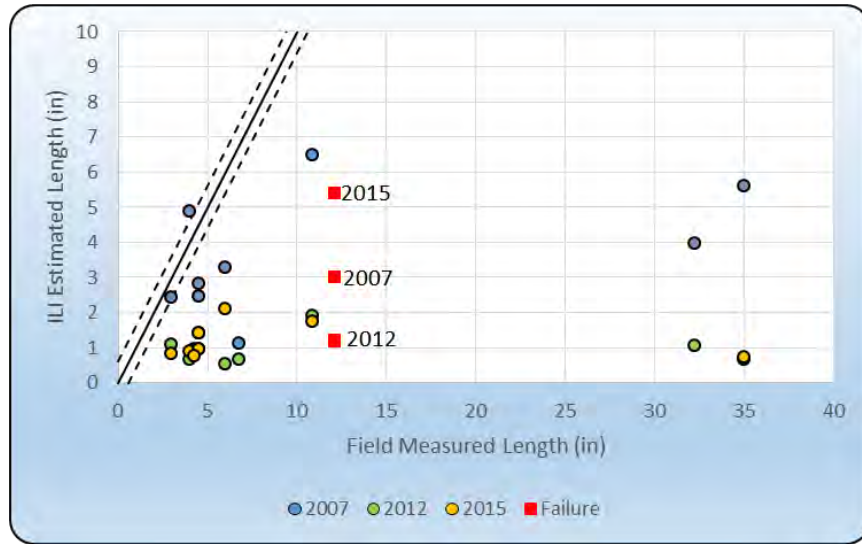


Figure 13. ILI estimated length compared to field measured.

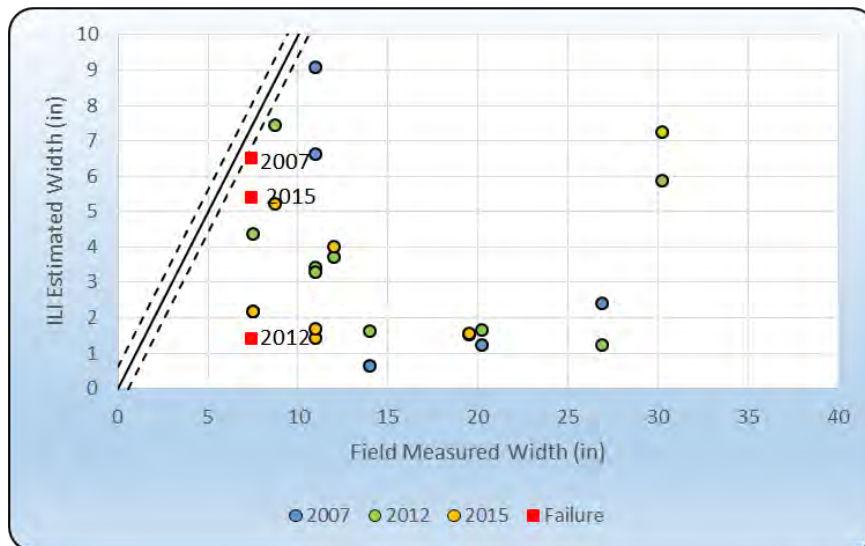


Figure 14. ILI estimated width compared to field measured.

Figure 15 details the depth comparison of the same anomalies. The 2007 depths are primarily undercalled but this could be a result of the 5 years growth from the time of inspection to excavation. The 2012 and 2015 inspections had 56% and 63% of the anomalies overcalled or within specification, respectively. The red markers representing the failure depths will most assuredly not be 89% in 2007 or 2012, this only represents the depth as called by the ILI in that year.

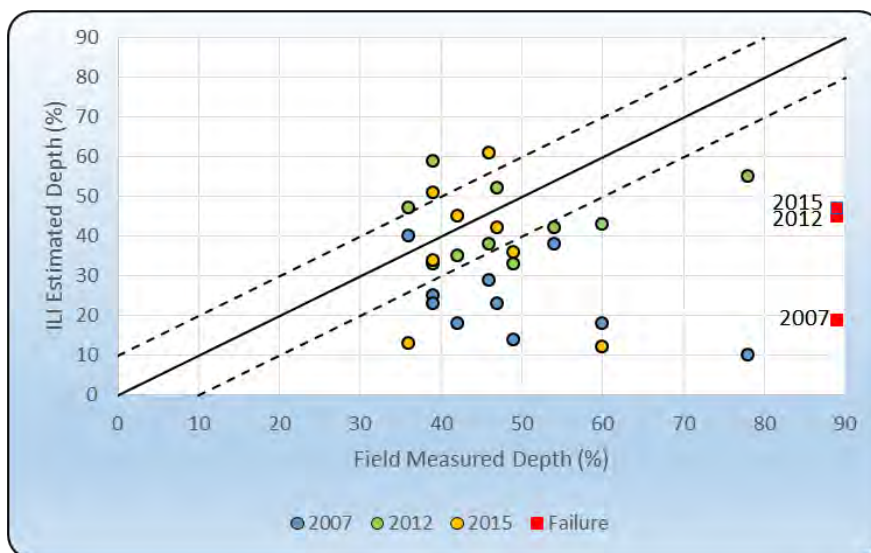


Figure 15. ILI estimated depth compared to field measured.

The issue of underestimating the length and width of a corrosion anomaly will lead to gross underestimations of the corrosion area. Figure 16 delineates all of the Line 901 anomalies with width and length reported from ILI estimates versus excavations made, on a logarithmic scale. As an example, it is showing that 38% of the anomalies had an area stated by the ILI of $\leq 1.5 \text{ in}^2$ when in fact the corrosion areas were between 2.5 in^2 and 7300 in^2 . This being said, there may be a difference in the field measurement technique to consider. It is important that the techniques used in the field be comparable to that required by the ILI analysis to enable a proper assessment of the ILI performance.

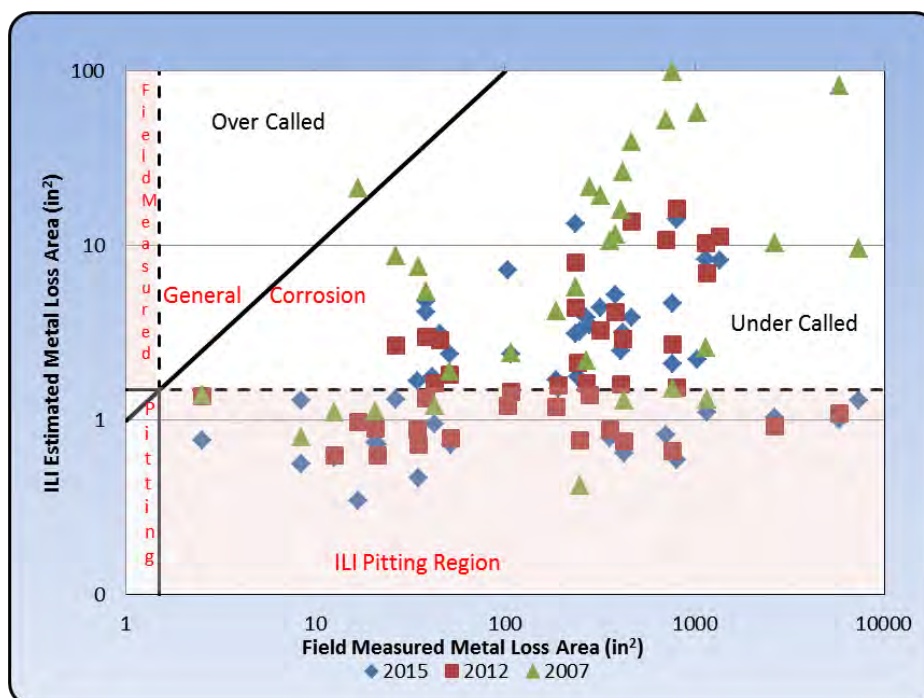


Figure 16. Metal loss area; ILI vs field measurement.

Plains Anomaly Mitigation Strategy

The documented procedure used by Plains entitled “Procedure for the Assessment of In-Line Inspection Results; DOC NO: PAALP-INT-PRC-NJP- 001” was provided as part of the review process. The document outlines the steps Plains personnel are required to take following the receipt of preliminary and final ILI reports. According to this document they comply to the requirements of Code of Federal Regulations 49 Part 195.452 with respect to addressing MFL detectable anomalies.

Part of the Plains document process is a “Close-Out” report that is created following the reception and repair of anomalies related to any ILI Final Report. The most recent “Close-Out” report for the segment in question relates to the 2012 inspection as the 2015 inspection was run only 13 days before the failure. Table 6 is the summary that was provided within the 2012 Las Flores to Gaviota Close-Out report. The table shows that this segment had 382 anomalies addressed. The worst anomalies remaining after repairs, based on the ILI estimated sizing was a 52% deep anomaly and one with an estimated failure pressure of 1608 psi (1.57 factor of safety). It is not clear in the document whether these are one in the same anomaly. It is also unclear as to why an anomaly greater than 50% depth was left as Plains repairs to a minimum of 50% and try to repair to 40% depth (i.e. To attain 50% with the 10% tool tolerance). But the regulations state a $\geq 50\%$ deep area of general corrosion need be repaired, this does not included pitting.

Assuming the remaining $>50\%$ deep anomaly was considered to be pitting then Plains by all accounts met 49 CFR 192.452 requirements as per the 2012 ILI information. Note: the close out report for the 2012 inspection has a later date than the May 19, 2015 release.

Plains has noted in their response to PHMSA on November 23, 2015 with respect to CPF 5-2015-5011H Correction Action Order Amendment 2, page 3, that

“...Furthermore, Plains’ focus on the depth of anomalies, rather than length and width, is supported by the industry standard API 1160, Annex D, *Managing System Integrity for Hazardous Liquid Pipelines*, which states on p. 87: “Growth of an anomaly in depth has a much greater deleterious effect on failure pressure than growth in length, so much so that growth in length can be safely ignored.” “

Although this response is with respect to Line 903, it is misleading and incorrect. The comment quoted above from API 1160 is out of context. Having the most accurate length is very important to the calculation of the remaining strength of every type of anomaly. The length must be defined as accurately as possible. The comment quoted from API 1160 above refers only to the known fact that when corrosion is growing, the depth aspect will be much more influential than the length. This occurs because the percentage depth increases much more rapidly due to the thin wall of the pipe.

Table 6. Close-Out summary for the 2012 inspection of Las Flores to Gaviota.

CLOSE-OUT REPORT										
Line Name:	L901 - Las Flores - Gaviota - 24"			ILI run date:	7/3/2012			Date:	6/22/2015	
Summary of In-Line Inspection Indications										
Metal Loss Anomalies	Ext		Int		Mfg		Total			
	ILI	After	ILI	After	ILI	After	ILI	After		
d/t < 20% WT	1,241	992	6	6	0	0	1,247	998		
20% WT ≤ d/t < 30% WT	182	137	0	0	2	2	184	139		
30% WT ≤ d/t < 40% WT	99	57	0	0	0	0	99	57		
40% WT ≤ d/t < 50% WT	36	9	0	0	0	0	36	9		
50% WT ≤ d/t < 60% WT	15	1	0	0	0	0	15	1		
60% WT ≤ d/t < 70% WT	4	0	0	0	0	0	4	0		
70% WT ≤ d/t < 80% WT	1	0	0	0	0	0	1	0		
d/t ≥ 80% WT	0	0	0	0	0	0	0	0		
Internal ML consistent with internal corrosion	0	0	0	0	0	0	0	0		
Selective Seam Corrosion	0	0	0	0	0	0	0	0		
Total	1,578	1,196	6	6	2	2	1,586	1,204		
Failure Pressures and Deepest Pits										
	ILI	After								
Reported deepest external metal loss (%WT)	78%	52%								
Reported deepest internal metal loss (%WT)	18%	18%								
Calculated lowest Safe_ pressure (based on CGAR)	1,090	1,158								
Calculated lowest P_Burst (based on CGAR)	1,515	1,608								
Seam Weld Anomalies										
	Total	After								
SWA-A	0	0								
SWA-B	0	0								
SWA	0	0								
Deformation Anomalies										
	Total	After								
Dent Depth > 6% OD	0	0								
Dent Depth ≤ 6% OD	22	5								
Dent Depth ≥ 2% OD with metal loss/crack	0	0								
Dent Depth < 2% OD with metal loss/crack	0	0								
Dent Depth ≥ 2% OD affecting weld	0	0								
Dent Depth < 2% OD affecting weld	2	0								
Girth weld anomalies	0	0								
Wrinkle bends	16	0								
Crack Anomalies (Depth)										
Crack Anomalies (Depth)	Crack-Like		Crack Field		Notch-Like		Mid Wall (Lamination/ inclusion)		Total	
	ILI	After	ILI	After	ILI	After	ILI	After	ILI	After
0.040" - 0.079"	0	0	0	0	0	0	0	0	0	0
0.08" - 0.119"	0	0	0	0	0	0	0	0	0	0
0.12" - 0.159"	0	0	0	0	0	0	0	0	0	0
≥ 0.16"	0	0	0	0	0	0	0	0	0	0
No depth	0	0	0	0	0	0	0	0	0	0
Total	0	0	0	0	0	0	0	0	0	0
Results/Comment/Recommendation:										
<p>1. 2012 ILI - 49 anomalies repaired using Type B, 37 anomalies using composite sleeves, 211 anomalies using recoat, and 0 anomaly using pipe replacement.</p> <p>2. The result shows that the ILI tool is within the tool's tolerance specification. No further anomalies need to be investigated.</p> <p>3. The result shows that 73 % of the excavated anomalies were within tool tolerance or overcalled by the ILI tool and no anomalies meet conditions for further evaluations.</p> <p>4. The earliest the remaining ML anomalies to have predicted depth >80%WT or calculated burst pressure < MOP (based on CGAR) is 3/19/2016.</p>										

ILI Details for the Failed Anomaly

All three in-line inspections sized the eventual failure site. Table 7 details the failed anomaly as it was reported by the various inspections.

Table 7. ILI reported dimensions of the failed area.

	Distance (ft)	Length (in)	width (in)	Depth (%)	Clock	Comments
2007	21355.45	3	6.5	19	4:01	Ext Cluster
2012	21384.96	1.2	1.4	45	4:23	Ext metal loss
2015	21384.58	5.38	5.45	47	3:57	External cluster

The anomaly as detailed by the C-Scan (color scan) for each inspection is given in Figure 17.

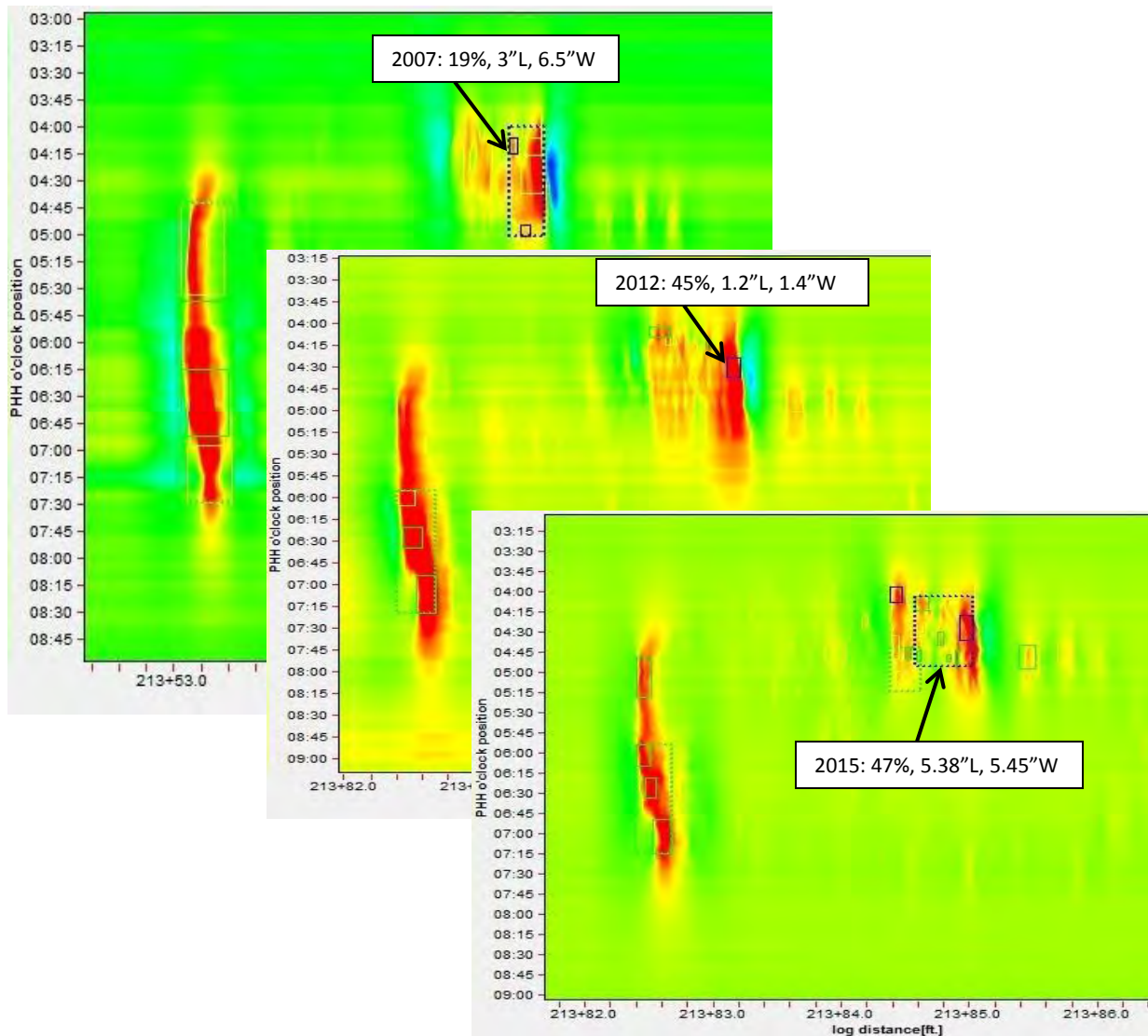


Figure 17. C-Scans with boxes of the failed location as detailed by the 2007, 2012 and 2015 inspections

Figure 18 provides the in-line inspection A-scan in comparison to the in-the-lab laser scan as described in the “Draft Mechanical and Metallurgical Testing Report, Report OAPUS309DNOR (PP136049), DNV, August 6, 2015”.

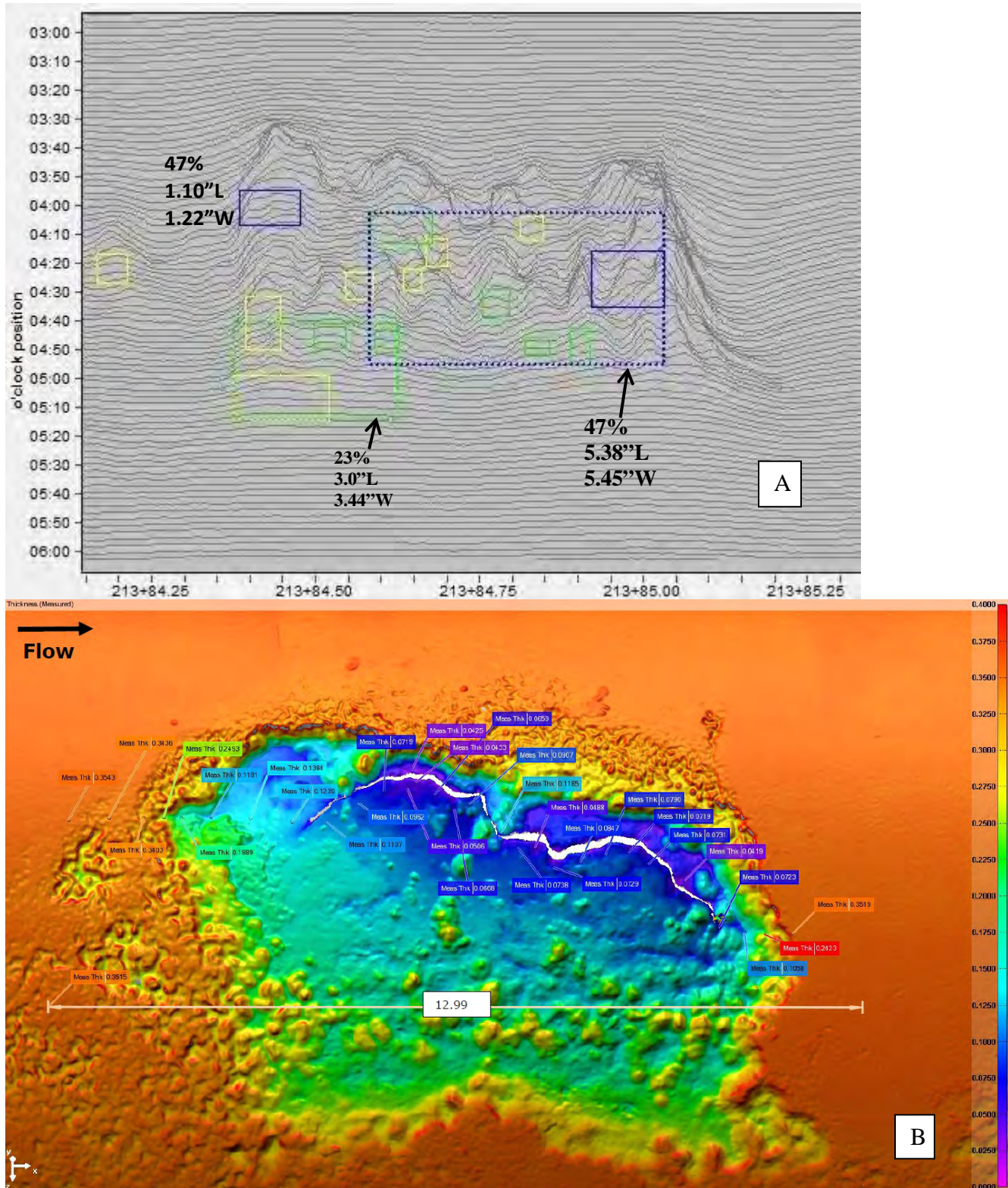


Figure 18. The failed area, A) the Rosen 2015 A-Scan, B) the Laser Scan.

Noted in Table 7 and Figure 17, the last known depth prior to failure was 45% in 2012. The verification of the depth estimate at that time is not available. It is highly likely that there was continued corrosion growth of the anomaly from that time to failure.

The metallurgical report by DNV provided the following information for the depth profile of the failed anomaly in Figure 19. The remaining strength of the anomaly was determined using industry accepted and publicly available software (KAPA, Kiefner and Associates) and is provided in Table 8.

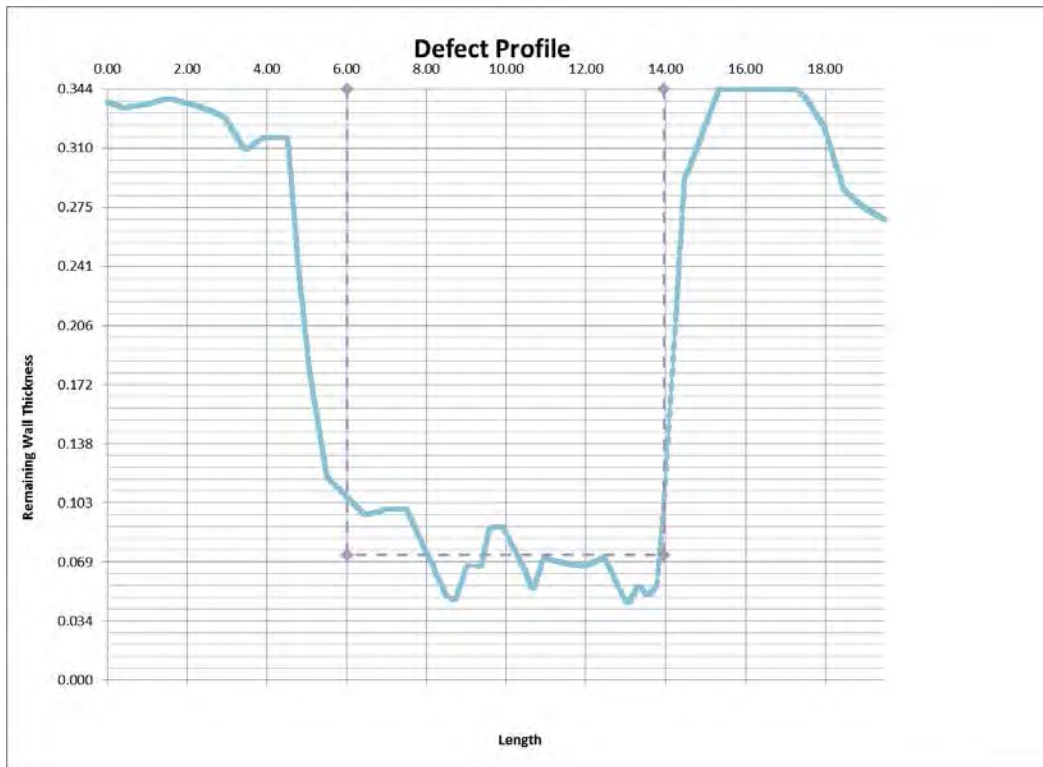


Figure 19. Depth profile of failed anomaly (DNV).

Table 8. Estimated failure pressure from profile in Figure 18.

	Predicted Failure Pressure (Pf, psi)	Factor of Safety (Pf/MOP)	Effective Length (in)
Effective Area Method	684	0.67	7.94
Modified B31G	665	0.65	

The estimated operating pressure at the time and location of failure was 737 psi, the estimated failure pressure as determined by the profile is 685 psi with an effective length of 7.94". This effective length illustrates the difference between the ILI determined cluster length (5.38") and actual. Albeit there was a depth prediction error, an appropriate representation of the corrosion area should be determined through appropriate interaction rules.

Rosen stated in their final report (**RoCombo Inspection Service, Line 901 Las Flores to Gaviota, May 2015, Project # 0-1000-12834**, Rosen Group, June 4, 2015) presented to Plains,

“The data recorded during the RoCombo MFL-A/XT inspection survey, performed on May 6, 2015, was accepted and used for evaluation purposes. During the RoCombo MFL-A/XT inspection survey, there was an area of incomplete data due to odometer slippage. The area starts at ROSEN log distance 111.52 ft and continues to 9412.95 ft totaling 9301.43 ft. The resulting data recorded is 83.79% of the total line length. The survey was correlated to the ROSEN 2012 inspection survey to aid in the evaluation process. During the survey, all sensors were operational in areas outside of the odometer slippage. An additional inspection for this line segment will be performed for coverage in the areas of odometer slippage. The tool velocity during RoCombo MFL-A/XT inspection survey was within the pre-agreed range. Generally, in all areas where the velocity is outside of the optimum range, the ROSEN standard accuracy might not be achieved. Over the complete line length of the RoCombo MFL-A/XT inspection survey, the magnetization level was within the pre-agreed specification of 10 - 30 kA/m. Generally, in all areas where the magnetization level is outside of the optimum range, the ROSEN standard accuracy might not be achieved.”

Further, with respect to the tool velocity,

“The RoCombo MFL-A/XT tool used during this survey was programmed to operate within a velocity range of 0.33 feet per second to 16.41 feet per second.”

The velocity of the 2015 tool in the failed joint was reported to be 0.7 ft/s, which is within the accepted velocity range.

Further, with respect to the magnetization level,

“The magnetization level achieved during the RoCombo MFL-A/XT survey is typically between 10kA/m and 30kA/m in order to meet the Metal Loss Inspection Performance Specifications.”

The magnetization level of the 2015 tool in the failed joint was reported to be approximately 23 kA/m at the failure location, which is within the accepted magnetization range.

The reported maximum depth of the failed anomaly in the 2015 inspection was 47% of the wall thickness $\pm 10\%$. The actual maximum depth was determined by the metallurgical examination to be 89%.

The axial and circumferential (length and width) sizing in the 2015 MFL report, though not fully interacting throughout, provides a respectable representation of the actual anomaly. This feature does have complexity in the feature geometry that should be considered as well.

The depth variance mentioned above raises some question.

Since the inspection tool at the failure location was responding normally and the velocity and magnetization levels were within specification, the tool response is said to be acceptable and within optimal conditions.

When the pipe wall is saturated with magnetic flux there is a specific background signal attained by the MFL sensors. When there is a corrosion area that is free from ferromagnetic material, there will be a flux leakage that is attained and is relative to the length, width and depth of the missing metal. With a tightly adhered magnetic corrosion product such as described in the metallurgical report, the level of flux that “leaks” from the metal loss may have been reduced. This may in turn be partially responsible for the undercalling of the depth based on the observed length and width dimensions. The metallurgical report states that the thickness of the said corrosion product adjacent to the failure area was approximately 0.55” thick.

The corrosion product as detailed in the metallurgical study, Figures 20 and 21, describe a layered strata of Magnetite (Fe_3O_4) and Goethite ($FeO(OH)$). Magnetite (aka. Lodestone) is highly magnetic, whereas Goethite has low magnetic properties but nonetheless is still magnetically susceptible. This magnetic acceptance of the corrosion products provides for the potential retarding of flux leakage. Further study into the actual magnetic properties of the corrosion product has determined that the corrosion product has a slightly increasing magnetic permeability as the magnetic field increases, Figure 22. In the region of the release the magnetization was noted by Rosen to be $\sim 23 \text{ kA/m} = \sim 288 \text{ Oe}$. At this level the amplitude permeability of the corrosion product is approximately 5% that of the steel pipe. Intuitively, the greater the permeability the greater the flux density allowed into a material. That being said, the maximum flux densities derived from testing, given in Table 9, show that the corrosion product will carry, at a maximum, $\sim 5\%$ of the flux density of the steel pipe. Consideration must also be given to the volume of the corrosion product with respect to the flux carrying capacity. A greater volume of corrosion product will carry a greater flux density. Therefore, intrinsically, there will be some “masking” of the flux leakage thereby interfering with an accurate determination of the corrosion depth (less flux leakage=shallower depth). To what degree is beyond the scope of this review. The magnetic study was performed by the Edison Welding Institute, **EWI Project No. 56251CSP** Final Report October 16, 2015.

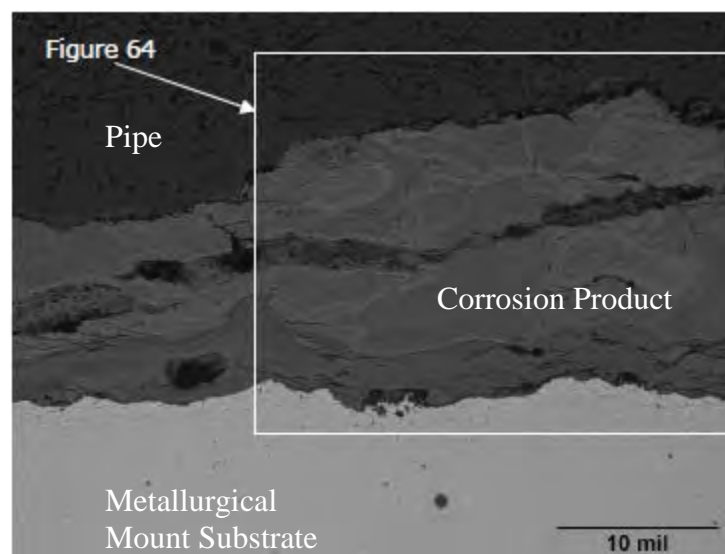


Figure 20. Tightly adhered corrosion product (Fig. 58 from metallurgical report).

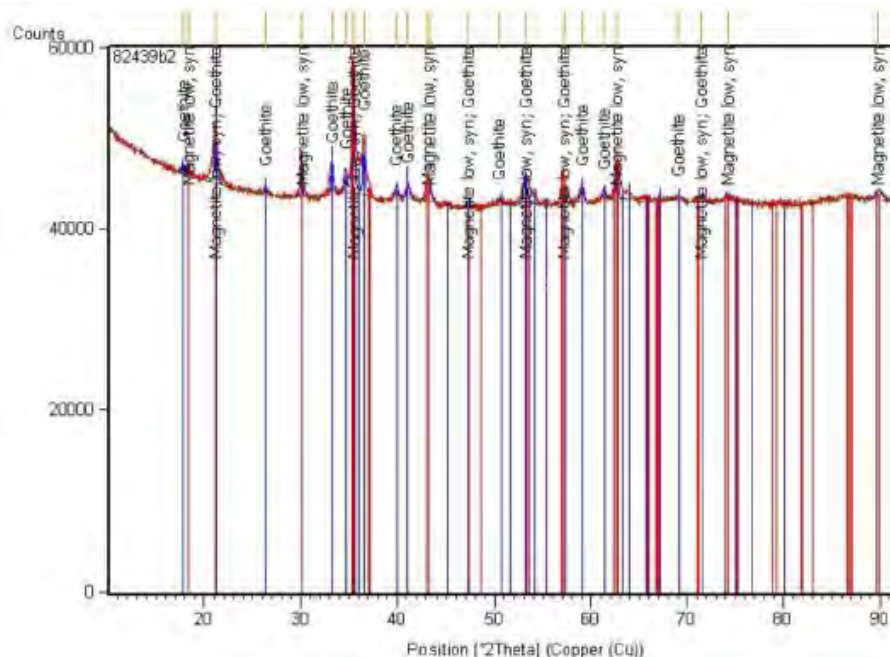


Figure 21. X-Ray Diffraction (XRD) of the corrosion product indicating layering of Magnetite and Goethite (Fig. 62 from metallurgical report).

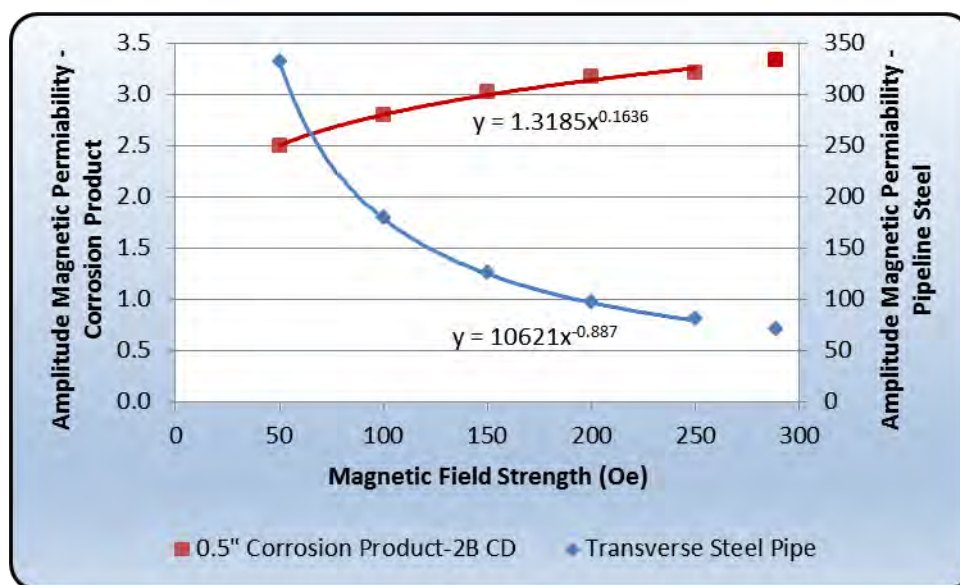


Figure 22. Amplitude magnetic permeability of the pipeline steel and corrosion product (EWI).

Table 9. Magnetic properties of the pipeline steel and corrosion product (EWI).

Specimen	μ_{in}	μ_{max}	H_c	B_r	H_{max}	B_{max}
	-	-	Oe	G	Oe	G
Longitudinal Steel Pipe	149	1467	6.66	12750	1018.2	22193
Transverse Steel Pipe	177.3	1863	6.50	14147	1011.5	22337
0.5" Corrosion Product-2A AB	1.87	2.545	95.16	280	1008.0	1802
0.5" Corrosion Product-2B CD	2.475	3.598	104.40	426	998.3	1987
0.3" Corrosion Product-3A AB	2.229	2.89	86.27	278	1020.6	1680
0.3" Corrosion Product-3B CD	2.511	3.325	92.31	352	1009.9	2050

It should be noted as well that each inspection was carried out by a different model of Rosen MFL inspection tool. The June 2007 inspection employed the Corrosion Detection and Mapping (CDG) tool. The July 2012 inspection utilized the Corrosion Detection and eXtended Geometry tool (CXG). The May 2015 inspection utilized the Axial/eXtended Geometry tool (A/XT). It is unclear by their publicly released specifications the exact differences in the technologies.

It is also unclear what the differences in the sizing algorithms used through the years and on various tools may be. It is conjectured that there was a change in sizing algorithms as the length and width dimensions for the 2012 inspection were typically smaller than that for the 2007 and 2015 inspections. Rosen states that all reports used the 1" by 6t interaction rule, but as stated earlier this may have changed by the minimum depth required for interaction as specified by Plains.

Future Anomaly Mitigation

By using the above determined maximum rate of growth (0.0166 in/yr) and applying this rate to both the length and depth of the corrosion anomalies delineated in the 2012 (first 9450') and 2015 inspection, an anomaly mitigation program can be developed. Two variables were examined with respect to the corrosion growth, the first being the depth and the second being the estimated burst pressure. To examine the effect of growth the rate was applied on a six month interval over a span of ten years.

Depth and remaining strength (estimated burst pressure) limits were set to determine when an anomaly should be excavated. The depth criterion was set at 50% and the burst pressure criterion was set at 139% of the MOP of 1025 psi or 1425 psi. To determine the effects of growth on the estimated burst pressures of each anomaly the 0.85 dL technique, otherwise known as the modified B31G equation, was applied to the growing depth and length estimates.

To be even more aggressive, anomalies were deemed to require excavation six months prior to their estimated burst pressures becoming less than or equal to 139% MOP or having an estimated depth greater than or equal to 50%. *Employing these conservative limits, conservative growth rate and the six month buffer, allows for ILI sizing prediction error.*

The determination of excavation locations and their suggested date were made considering the 2012 inspection data for the first 9450' (no 2015 data collected) and the 2015 data for the remainder. The results were combined and the suggested excavation timeline to the end of 2018 is given in Table 10. Table 11 lists the chainage of the recommended locations for 2015. Some of the locations listed in Table 11 and also in Appendix C may be combined into a single excavation. For a listing of all excavations to 2025 refer to Appendix B and C.

The growth rates, excavations required and re-inspection frequency should be re-examined after every future in line inspection.

Table 10. Suggested excavation timeline.

Dig Date	Anomalies 'Failing' Criteria	Number of Excavations
Jan-15	3	3
May-15	18	17
Nov-15	7	5
Jan-16	3	2
May-16	12	6
Jul-16	2	1
Nov-16	8	5
Jan-17	5	2
May-17	11	5
Jul-17	4	2
Nov-17	7	3
Jan-18	10	6
May-18	20	10
Jul-18	20	8
Nov-18	34	9

Table 11. Suggested excavation locations.

GW	Dig Start	Dig End	Length	Dig Date	GW	Dig Start	Dig End	Length	Dig Date
260	636.44	636.47	0.03	Jan-15	8640/8650	31555.39	31558.11	2.72	May-15
1370	4608.59	4610.89	2.3	Jan-15	9270/9280	33431.52	33460.75	29.23	May-15
1570	5382.03	5382.84	0.81	Jan-15	9280/9290	33469.53	33482.42	12.89	May-15
4150/4160/ 4160.01/4160.02	14945.13	14968.53	23.4	May-15	9420	33999	34026.28	27.28	May-15
					11060	39810.31			Nov-15
4210/4220	15049.79	15076.28	26.49	Nov-15	12410/12420	44708.24	44725.74	17.5	May-15
4220/4230	15086.08	15106.27	20.19	May-15	12420/12430	44745.1	44774.5	29.4	Nov-15
6100/6110	22033.77	22035.46	1.69	May-15	12820/12830	46183.26	46208.59	25.33	May-15
6350/6360	23006.72	23032.43	25.71	May-15	12880	46415.43	46424.28	8.85	May-15
7990	29171.19	29171.21	0.02	May-15	13200/13210	47373.47	47402.54	29.07	May-15
8060	29453.57	29471.01	17.44	May-15	13210	47412.91	47413.4	0.49	May-15
8140	29742.02			Nov-15	13700	48882.16	48882.36	0.2	May-15
8280/8290	30307.15	30333.12	25.97	May-15					

Deformation Discussion

Deformation or dents were examined with consideration to depth, location to welds and their association to corrosion and/or cracking. Table 12 summarizes the details of the three previous deformation inspections. For further delineation of possible dents with metal loss, ILI anomaly alignment was also completed between the 2007, 2012, and 2015 MFL and deformation runs. To which, no locations of a dent with metal loss were found. In order to expedite the May 2015 deformation report after the rupture, Plains asked for the report with

metal loss only. As a result, the report did not provide dent sizing. Consideration should be given to reviewing this further.

Table 12. Dent summary from previous deformation inspections.

Inspection	# Dents	# Geometric Magnetic Anomalies	# Dents with Metal Loss	# Dents on Girth Welds	# Dents on or adjacent to Long Seam
2007 Def ($\geq 2\%$)	0	0	0	0	0
2012 Def ($\geq 1.0\%$)	1	22	0	2 (repaired)	0
2015 Def ($\geq n/a$)	6	0	0	1 (repaired)	0

Discussion to Note

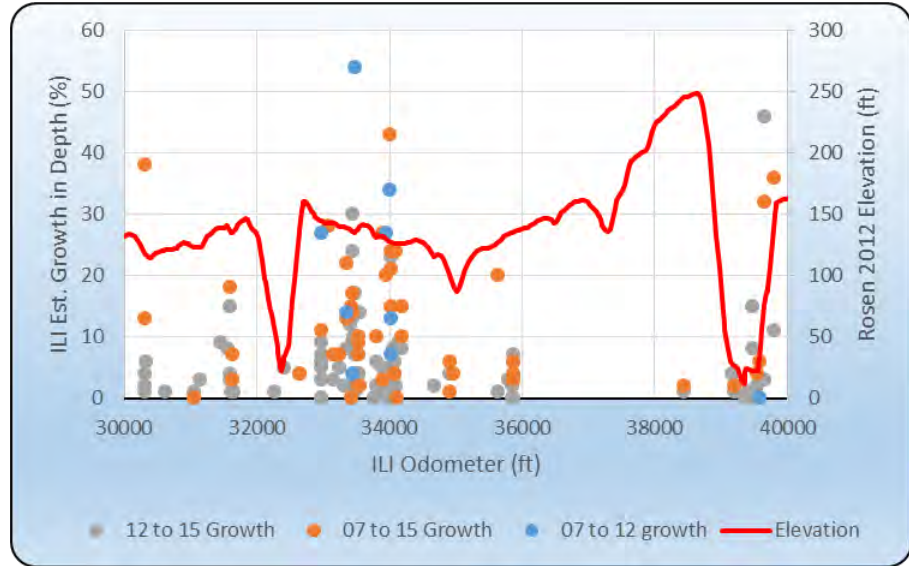
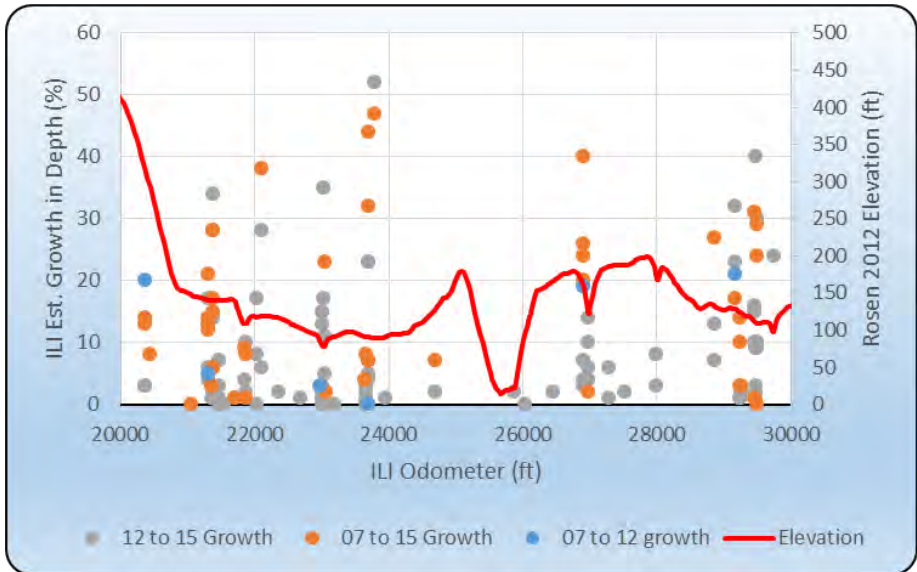
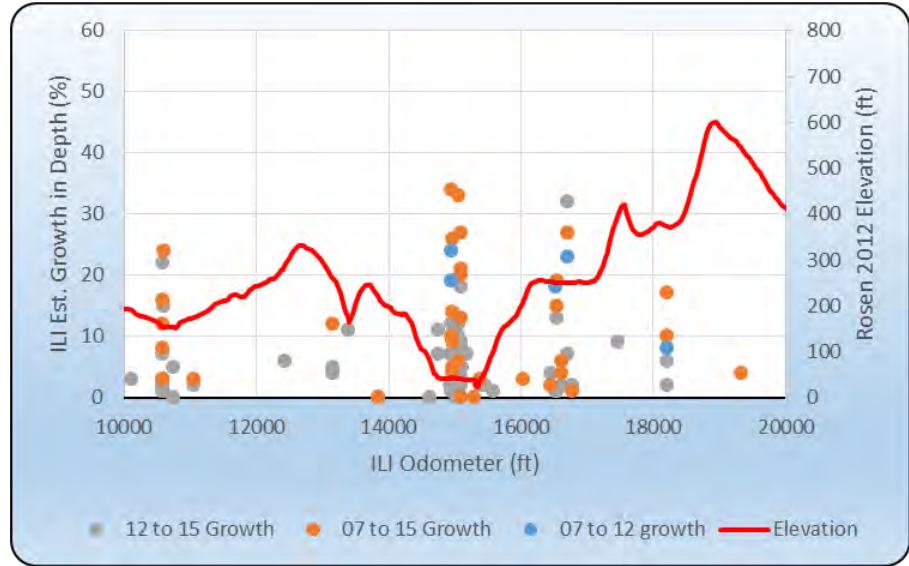
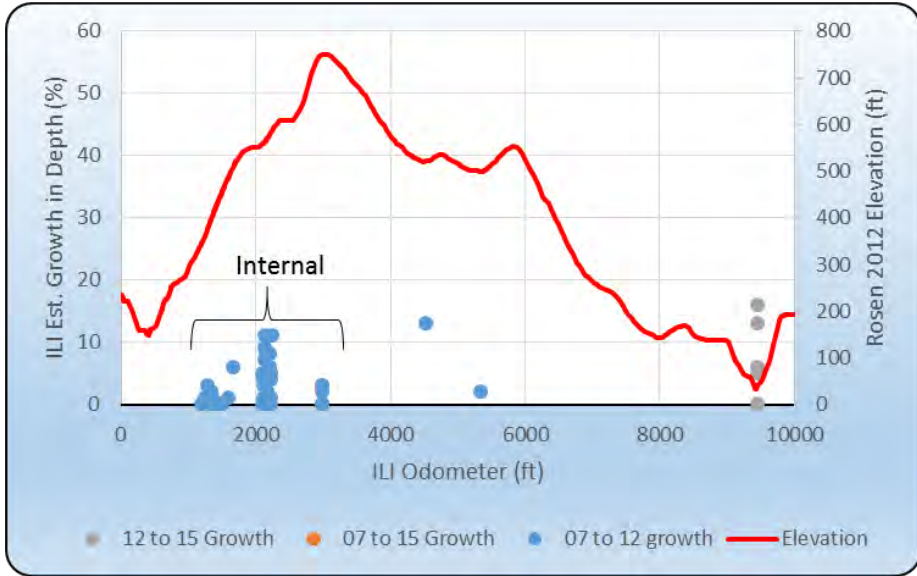
The following points should be considered:

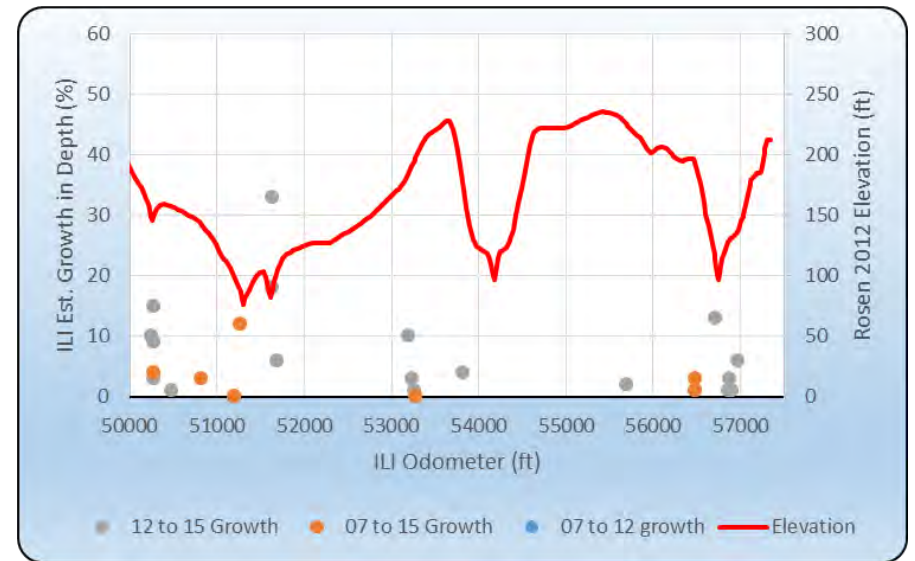
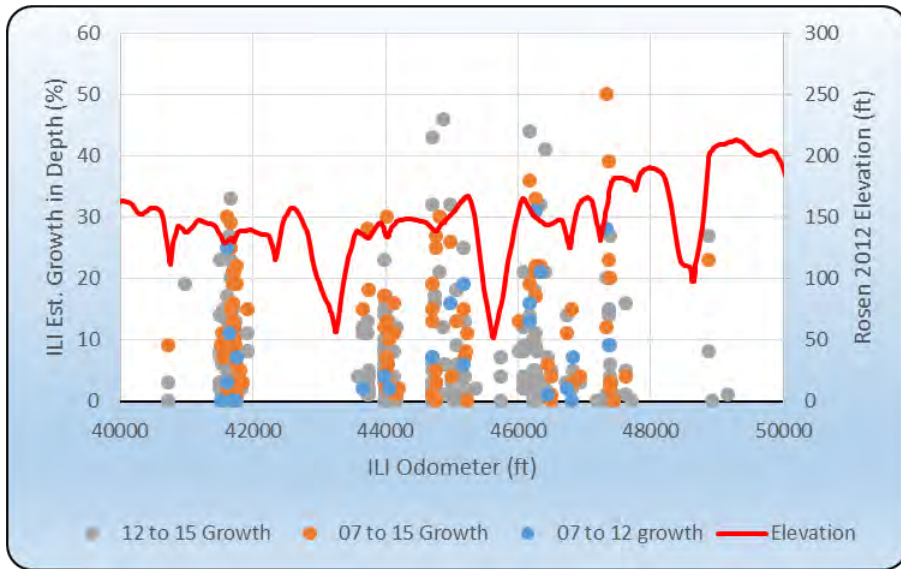
1. This segment should be re-inspected with an ultrasonic wall loss tool. The ultrasonic inspection will provide a measure of the remaining wall thickness without being influenced by the corrosion product. A circumferential MFL may delineate the corrosion lengths more accurately but there is still the issue of depth determination.
2. Interaction rules should be reviewed and changed to provide for adequate sizing of the corrosion anomalies.
3. The field measurements should be comparable to the ILI interaction rules (i.e. the extent of the anomaly is to a depth of 10% with no other metal loss within the specified interaction distance).
4. The dent review found inadequate information from the 2015 inspection.

Other details to consider with respect to this report:

1. Correlations were not made with respect to the agreement in location concerning tees and/or pipe supports or other appurtenances.
2. The defects during the growth stage of this report are not examined for further interaction.
3. This report considers metal loss as delineated by the MFL and deformation tool; no other threats or areas of possible concern were considered.

Appendix A – ILI growth variance in depth between all inspections





Appendix B – Individual Anomaly Excavation Timeline

GW	Distance (ft)	Jan-15	May-15	Nov-15	Jan-16	May-16	Jul-16	Nov-16	Jan-17	May-17	Jul-17	Nov-17	Jan-18	May-18	Jul-18	Nov-18	Jan-19	May-19	Jul-19	Nov-19	Jan-20	May-20	Jul-20	Nov-20	May-21	Nov-21	May-22	Nov-22	May-23	May-24
70.01	125.59										X																			
70.01	125.66																					X								
70.01	125.79																			X										
70.01	128.04																		X											
70.01	128.12																						X							
70.01	128.13												X																	
80	142.7																			X										
80	142.82																						X							
250	597.18																						X							
260	607.51																					X								
260	636.44	X																												
260	636.47																			X										
290	668.45																				X									
290	668.65										X																			
290	668.69																				X									
310	678.73																				X									
310	678.73																				X									
310	678.96																				X									
310	678.96																						X							
420	956.64				X																									
420	956.7								X																					
470	1134.02																						X							
480	1164.9																					X								
480	1186.34																					X								
480	1197.72																						X							
490	1207.96																						X							
490	1224.65																						X							
500	1239.97																						X							
500	1262.12																						X							
500	1277.24																							X						
500	1278.03																					X								
510	1287.34																							X						
510	1296.79																					X								
510	1303.42																						X							
520	1320.27																						X							
520	1325.96																						X							
520	1326.71																						X							
520	1329.16																						X							
520	1329.9																						X							
520	1332.09																						X							
520	1332.19																						X							
520	1334.55																						X							
520	1336.38																						X							
520	1336.89																						X							

GW	Distance (ft)	Jan-15	May-15	Nov-15	Jan-16	May-16	Jul-16	Nov-16	Jan-17	May-17	Jul-17	Nov-17	Jan-18	May-18	Jul-18	Nov-18	Jan-19	May-19	Jul-19	Nov-19	Jan-20	May-20	Jul-20	Nov-20	May-21	Nov-21	May-22	Nov-22	May-23	May-24	
520	1340.58																				X										
520	1342.35																						X								
520	1342.85																						X								
520	1343.33																						X								
520	1346.06																						X								
520	1348.62																					X									
520	1350.34																						X								
520	1352.06																						X								
520	1352.4																						X								
520	1352.78																						X								
530	1360.52																						X								
530	1365.54																						X								
530	1366.72																					X									
530	1367.22																						X								
530	1369.08																						X								
530	1369.47																						X								
530	1371.74																					X									
530	1372.27																					X									
530	1372.95																						X								
530	1373.79																						X								
530	1373.85																						X								
530	1375.95																		X												
530	1380.45																						X								
530	1381.38																						X								
530	1383.55																						X								
530	1385.47																						X								
530	1386.43																						X								
530	1387.57																						X								
530	1388.73																						X								
530	1391.81																						X								
530	1397.07																						X								
530	1398.29																						X								
530	1398.49																						X								
540	1400.11																						X								
540	1402.31																						X								
540	1405.69																						X								
540	1412.65																						X								
540	1413.85																						X								
540	1414.07																						X								
540	1416.93																						X								
540	1417.69																						X								
540	1418.47																						X								
540	1418.65																						X								
540	1419.33																						X								
540	1419.71																						X								
540	1420.81																						X								
540	1424.87																						X								
540	1425.32																						X								
540	1427.32																						X								

GW	Distance (ft)	Jan-15	May-15	Nov-15	Jan-16	May-16	Jul-16	Nov-16	Jan-17	May-17	Jul-17	Nov-17	Jan-18	May-18	Jul-18	Nov-18	Jan-19	May-19	Jul-19	Nov-19	Jan-20	May-20	Jul-20	Nov-20	May-21	Nov-21	May-22	Nov-22	May-23	May-24
540	1436.11																						X							
540	1437.2																						X							
550	1446.49																						X							
550	1448.82																						X							
550	1454.62																						X							
550	1464.27																						X							
550	1465.12																						X							
550	1466.98																						X							
550	1473.06																						X							
560	1477.26																						X							
560	1488.7																						X							
560	1491.34																						X							
560	1491.94																						X							
560	1492.65																						X							
560	1504.82																					X								
560	1509.34																						X							
560	1511.45																						X							
560	1512.66																						X							
560	1512.99																						X							
570	1515.58																						X							
570	1517.55																						X							
570	1525.05																						X							
570	1530.49																						X							
570	1531.75																						X							
570	1535.61																						X							
570	1538.27																						X							
570	1540.72																						X							
580	1555.81																						X							
580	1563.76																						X							
580	1572.03																						X							
580	1572.16																						X							
580	1576.22																						X							
580	1580.67																						X							
580	1581.6																						X							
580	1581.76																						X							
580	1582.47																						X							
580	1585.75																						X							
580	1586.42																						X							
580	1587.4																						X							
580	1588.19																						X							
580	1593.66																						X							
580	1593.8																						X							
590	1595.45																						X							
590	1595.48																						X							
590	1595.49												X																	
590	1597.15																						X							
590	1602.81																						X							
590	1604.13																						X							
600	1673.77																	X												

GW	Distance (ft)	Jan-15	May-15	Nov-15	Jan-16	May-16	Jul-16	Nov-16	Jan-17	May-17	Jul-17	Nov-17	Jan-18	May-18	Jul-18	Nov-18	Jan-19	May-19	Jul-19	Nov-19	Jan-20	May-20	Jul-20	Nov-20	May-21	Nov-21	May-22	Nov-22	May-23	May-24
610	1675.46												X																	
610	1675.53																			X										
610	1690.52																													
610	1696.94																													
610	1700.71																													
610	1708.07																													
620	1752.17																													
620	1753.14																													
640	1817.13																													
650	1823.57																													
650	1823.67																													
650	1824.49																													
650	1824.58																													
650	1825.85																													
650	1826.27																													
650	1826.74																					X								
650	1829.55																													
710	2097.51																X													
720	2104.99																													
720	2107.52																													
720	2107.6																													
720	2108.82																													
720	2112.04																					X								
720	2112.8																													
720	2114.02																		X											
720	2114.85																					X								
720	2116.16																													
720	2118.72																					X								
720	2119.01																													
720	2121.36																													
720	2122.67																													
720	2123.61																													
720	2124.95																					X								
720	2125.85																													
720	2125.86																					X								
720	2126.87																													
720	2127.56																													
720	2127.59																													
720	2130.47																													
720	2133.54																													
720	2134.62																													
720	2136.99																													
720	2138.56																													
720	2139.86																													
730	2146.91																													
730	2148.13																													
730	2148.65																													
730	2150.9																													
730	2153.36																													

GW	Distance (ft)	Jan-15	May-15	Nov-15	Jan-16	May-16	Jul-16	Nov-16	Jan-17	May-17	Jul-17	Nov-17	Jan-18	May-18	Jul-18	Nov-18	Jan-19	May-19	Jul-19	Nov-19	Jan-20	May-20	Jul-20	Nov-20	May-21	Nov-21	May-22	Nov-22	May-23	May-24
730	2153.69																						X							
730	2153.96																						X							
730	2157.94														X															
730	2160.08																		X											
730	2161.52																		X											
730	2162.49																					X								
730	2170.35																						X							
730	2175.05																		X											
730	2175.97																					X								
730	2177.25														X															
730	2179.72																					X								
730	2179.92																						X							
730	2180.45																							X						
740	2182.2																X													
740	2184.73																		X											
740	2193.05																		X											
740	2194.6																							X						
740	2194.96																							X						
740	2200.92																		X											
740	2209.22																							X						
740	2211.03																					X								
740	2219.16																		X											
740	2220.09																		X											
740	2220.66																		X											
740	2220.85																					X								
740	2220.87														X															
750	2221.36																							X						
750	2221.77														X															
750	2221.82																		X											
750	2222.91																							X						
750	2223.28																							X						
750	2227.11																							X						
750	2227.17																							X						
750	2228.41																		X											
750	2229.25																								X					
750	2233.5														X															
750	2233.65																								X					
750	2233.74																		X											
750	2233.89																					X								
750	2234.83																		X											
750	2235.72																								X					
750	2237.39																								X					
750	2238.53																					X								
750	2238.53																						X							
750	2239.45																					X								
750	2240.02																							X						
750	2241.7														X															
750	2244.41																		X											
750	2247.51												X																	

GW	Distance (ft)	Jan-15	May-15	Nov-15	Jan-16	May-16	Jul-16	Nov-16	Jan-17	May-17	Jul-17	Nov-17	Jan-18	May-18	Jul-18	Nov-18	Jan-19	May-19	Jul-19	Nov-19	Jan-20	May-20	Jul-20	Nov-20	May-21	Nov-21	May-22	Nov-22	May-23	May-24	
750	2249.24																		X												
750	2249.78																							X							
750	2250.65																						X								
750	2256.47																		X												
750	2257.86																		X												
750	2258.59																		X												
750	2259.85																							X							
750	2260.65																		X												
750	2260.74																							X							
760	2260.95														X																
760	2261.29																					X									
760	2261.78																					X									
760	2262.28																						X								
760	2262.46																					X									
760	2266.49																					X									
760	2278.68																						X								
760	2286.7																						X								
760	2290.04																						X								
760	2290.15																						X								
760	2290.97																					X									
760	2291.48																						X								
760	2296.34																						X								
760	2299.62																						X								
760	2300.07																					X									
760	2300.63																		X												
760	2300.67									X																					
770	2310.45																							X							
770	2310.99														X																
780	2314.34																					X									
800	2368.43																						X								
800	2368.66																					X									
800	2368.77																		X												
800	2368.81																						X								
970	2990.53																						X								
970	2991.4																					X									
970	2991.74																						X								
970	2992.27																						X								
970	2993.37																							X							
970	2994.13																					X									
970	2994.77																						X								
970	3002.23																						X								
970	3002.4																		X												
970	3020.01																						X								
970	3023.98																						X								
970	3027.15																						X								
970	3027.86																						X								
980	3032.13																						X								
980	3035.79																						X								
980	3035.9																						X								

GW	Distance (ft)	Jan-15	May-15	Nov-15	Jan-16	May-16	Jul-16	Nov-16	Jan-17	May-17	Jul-17	Nov-17	Jan-18	May-18	Jul-18	Nov-18	Jan-19	May-19	Jul-19	Nov-19	Jan-20	May-20	Jul-20	Nov-20	May-21	Nov-21	May-22	Nov-22	May-23	May-24
980	3049.07																						X							
980	3051.26																						X							
980	3052.62																						X							
980	3052.71																						X							
980	3052.82																						X							
980	3052.94																						X							
980	3055.48																						X							
980	3056.12																				X									
980	3058.1																						X							
980	3058.21																					X								
980	3059.16																						X							
980	3059.32																					X								
980	3059.38																						X							
980	3059.51																						X							
980	3059.57																				X									
980	3059.81																				X									
980	3060.04																						X							
980	3060.15																						X							
980	3060.2																						X							
980	3060.42																	X												
980	3060.44																		X											
980	3060.54																		X											
980	3060.64																						X							
980	3060.97																						X							
980	3061.27																						X							
980	3061.34																						X							
980	3061.48																						X							
980	3061.72																				X									
980	3061.74																					X								
980	3061.83																					X								
980	3061.86																						X							
980	3061.9																		X											
980	3062.02																						X							
980	3062.14																						X							
980	3062.27																					X								
980	3062.36																						X							
980	3062.51																						X							
980	3062.52																						X							
980	3062.87																						X							
980	3062.95																					X								
980	3063.14																						X							
980	3063.42																						X							
980	3063.65																						X							
980	3063.74																						X							
980	3064.76																						X							
980	3065.41																						X							
980	3065.82																						X							
980	3066.31																		X											
980	3069.28																			X										

GW	Distance (ft)	Jan-15	May-15	Nov-15	Jan-16	May-16	Jul-16	Nov-16	Jan-17	May-17	Jul-17	Nov-17	Jan-18	May-18	Jul-18	Nov-18	Jan-19	May-19	Jul-19	Nov-19	Jan-20	May-20	Jul-20	Nov-20	May-21	Nov-21	May-22	Nov-22	May-23	May-24
990	3074.62																						X							
1050	3347.6																X													
1050	3347.6																							X						
1050	3347.71														X															
1070	3406.47														X															
1070	3427.76																													
1070	3427.81																X													
1070	3427.82																					X								
1090	3489.91																					X								
1350	4530.98																						X							
1350	4530.99																					X								
1360	4532.7						X																							
1370	4608.59														X															
1370	4608.6																		X											
1370	4608.73																						X							
1370	4610.87	X																												
1370	4610.88																			X										
1370	4610.89																				X									
1480	5026.35																		X											
1520	5186.17																			X		X								
1550	5295.01																			X										
1550	5295.13																				X									
1550	5296.73																			X										
1560	5318.53																					X								
1560	5318.54														X															
1560	5319.35																			X										
1560	5319.85																						X							
1570	5382.03	X																												
1570	5382.15																X													
1570	5382.72																					X								
1570	5382.74																							X						
1570	5382.84														X															
1580	5425.09																							X						
1590	5427.07																					X								
1600	5449.97																					X								
1700	5833.49																			X										
1700	5833.51										X																			
1700	5833.55								X																					
1980	6902.95																					X								
1990	6927.55																													
1990	6928.82														X															
2170	7618.29				X																									
2170	7618.32																					X								
2170	7618.79																						X							
2170	7618.86																					X								
2170	7618.95																					X								
2170	7639.79				X																									
2170	7640.31																			X										
2170	7640.88																			X										

GW	Distance (ft)	Jan-15	May-15	Nov-15	Jan-16	May-16	Jul-16	Nov-16	Jan-17	May-17	Jul-17	Nov-17	Jan-18	May-18	Jul-18	Nov-18	Jan-19	May-19	Jul-19	Nov-19	Jan-20	May-20	Jul-20	Nov-20	May-21	Nov-21	May-22	Nov-22	May-23	May-24
2170	7641.34																				X									
2170	7641.56																		X											
2170	7641.78																					X								
2170	7641.99												X																	
2170	7642.1																					X								
2170	7642.23												X																	
2170	7642.57										X																			
2170	7642.69														X															
2170	7643.22								X																					
2170	7643.34														X															
2170	7643.37																		X											
2170	7643.57								X																					
2170	7643.58														X															
2170	7643.61																					X								
2170	7643.74																		X											
2170	7644.11																					X								
2170	7644.12												X																	
2170	7644.21																					X								
2170	7644.64																					X								
2170	7645.18																					X								
2170	7646.5						X																							
2170	7647.12																		X											
2170	7647.26																							X						
2170	7647.55																					X								
2170	7647.91																					X								
2170	7648.22																						X							
2170	7654.47								X																					
2170	7654.78														X															
2210	7786.93																					X								
2210	7787.14												X																	
2370	8428.95																						X							
2430	8654.45																						X							
2450	8733.29																X													
2450	8733.3																					X								
2450	8733.33												X																	
2450	8733.39																		X											
2500	8898.57																						X							
2640	9452.13																										X			
2640	9452.84																											X		
2640	9453.04																											X		
2640	9458.19																									X				
2640	9458.78																	X												
2640	9459.51																							X						
2640	9459.88												X																	
2640	9460.01								X																					
2830	10119.9 9																									X				
2940	10515.1 5																												X	

GW	Distance (ft)	Jan-15	May-15	Nov-15	Jan-16	May-16	Jul-16	Nov-16	Jan-17	May-17	Jul-17	Nov-17	Jan-18	May-18	Jul-18	Nov-18	Jan-19	May-19	Jul-19	Nov-19	Jan-20	May-20	Jul-20	Nov-20	May-21	Nov-21	May-22	Nov-22	May-23	May-24	
2960	10584.1 2																												X		
2960	10584.2																												X		
2960	10584.2																													X	
2960	10584.7 5																												X		
2960	10586.5 7															X															
2960	10586.9 7																												X		
2960	10587.1 5																												X		
2960	10587.3 4																								X						
2960	10587.5 6																												X		
2960	10587.7 5																												X		
2960	10587.9 2																												X		
2960	10587.9 8																						X								
2960	10588.2																												X		
2960	10588.4 7					X																									
2960	10588.7 5																											X			
2960	10588.9																								X						
2960	10589.0 3																								X						
2960	10589.4 3																												X		
3010	10755.9 2																									X					
3010	10756.3 5																												X		
3090	11060																											X			
3220	11615.8 5																												X		
3370	12195.9 1																												X		
3430	12427.1 6																											X			
3630	13155.9 1																												X		
3630	13155.9 3																						X								
3630	13156.1 8																							X							
3680	13394.4 4																						X								
3680	13394.4 4																												X		
3750	13645.5 6																												X		
3750	13645.7 5																										X				
3810	13852.5																												X		

GW	Distance (ft)	Jan-15	May-15	Nov-15	Jan-16	May-16	Jul-16	Nov-16	Jan-17	May-17	Jul-17	Nov-17	Jan-18	May-18	Jul-18	Nov-18	Jan-19	May-19	Jul-19	Nov-19	Jan-20	May-20	Jul-20	Nov-20	May-21	Nov-21	May-22	Nov-22	May-23	May-24
	4																													
3810	13853.79																										X			
3810	13853.93																									X				
3850	14002.02																											X		
4080	14751.62																	X												
4080	14751.84																	X												
4080	14753.1																								X					
4080	14753.35																									X				
4080	14753.65																							X						
4080	14753.91																											X		
4080	14754.98																											X		
4080	14757.57																												X	
4140	14909.43																												X	
4150	14932.19																		X											
4150	14934.69																									X				
4150	14945.13									X																				
4150	14945.33					X																								
4160	14960.09																													X
4160.01	14960.87																											X		
4160.01	14966.41																													X
4160.01	14967.06		X																											
4160.01	14967.49																													X
4160.01	14967.92																											X		
4160.02	14968.53																													X
4200	15015.82																									X				
4200	15024.47																												X	
4200	15024.48																												X	
4200	15024.49																												X	
4210	15026.16																												X	
4210	15049.79																										X			

GW	Distance (ft)	Jan-15	May-15	Nov-15	Jan-16	May-16	Jul-16	Nov-16	Jan-17	May-17	Jul-17	Nov-17	Jan-18	May-18	Jul-18	Nov-18	Jan-19	May-19	Jul-19	Nov-19	Jan-20	May-20	Jul-20	Nov-20	May-21	Nov-21	May-22	Nov-22	May-23	May-24	
4210	15052.4 2																													X	
4210	15053.3 7																									X					
4210	15053.8 9																											X			
4210	15054.9 1																										X				
4210	15054.9 5																									X					
4210	15055.1 7																	X													
4210	15055.6 7																							X							
4210	15055.7			X																											
4210	15056.0 4																											X			
4210	15056.1 5																								X						
4210	15059.4 9																									X					
4210	15061.4 4																										X				
4220	15069.4 7																							X							
4220	15069.7 4																												X		
4220	15073.6 1																												X		
4220	15073.8 5																								X						
4220	15074.0 2																								X						
4220	15074.1 8																		X												
4220	15076.1 1																												X		
4220	15076.2 8																								X						
4220	15086.0 8																											X			
4220	15086.2 2																							X							
4220	15086.4 7																												X		
4220	15086.6 1																												X		
4220	15092.7 8							X																							
4220	15092.9 7																												X		
4220	15092.9 9															X															
4220	15093.8 9																												X		
4220	15093.9 7																											X			
4220	15094.8 6																								X						

GW	Distance (ft)	Jan-15	May-15	Nov-15	Jan-16	May-16	Jul-16	Nov-16	Jan-17	May-17	Jul-17	Nov-17	Jan-18	May-18	Jul-18	Nov-18	Jan-19	May-19	Jul-19	Nov-19	Jan-20	May-20	Jul-20	Nov-20	May-21	Nov-21	May-22	Nov-22	May-23	May-24
4220	15094.95																			X										
4220	15095.07		X																											
4220	15095.29					X																								
4220	15095.63																	X												
4220	15095.94																										X			
4220	15096.31																												X	
4220	15096.88									X																				
4220	15097.09																	X												
4220	15098.37									X																				
4220	15098.86																											X		
4220	15104.59																									X				
4230	15106.27																										X			
4240	15184.5																													X
4240	15184.5																													X
4240	15184.54																						X							
4250	15186.2																													X
4260	15263.79																										X			
4270	15275.43																											X		
4270	15275.43																													X
4270	15275.44																									X				
4270	15275.45																									X				
4300	15295.63																													X
4340	15366.08																										X			
4340	15366.08																											X		
4360	15377.43																													X
4360	15377.59																								X					
4390	15454.72																									X				
4410	15505.12																											X		
4430	15585.19																								X					
4540	16038.87																											X		
4620	16377.7																													X

GW	Distance (ft)	Jan-15	May-15	Nov-15	Jan-16	May-16	Jul-16	Nov-16	Jan-17	May-17	Jul-17	Nov-17	Jan-18	May-18	Jul-18	Nov-18	Jan-19	May-19	Jul-19	Nov-19	Jan-20	May-20	Jul-20	Nov-20	May-21	Nov-21	May-22	Nov-22	May-23	May-24
	1																													
4640	16458.49																											X		
4650	16460.62									X																				
4660	16532.12																	X												
4660	16532.64																											X		
4660	16538.55																												X	
4660	16538.65																	X												
4660	16538.65																											X		
4660	16538.67													X																
4680	16618.79																											X		
4690	16620.54																									X				
4690	16620.54																										X			
4690	16620.54																												X	
4690	16620.57																									X				
4690	16620.66																												X	
4730	16780.45																												X	
4730	16780.77																											X		
4900	17473.17																												X	
5100	18203.47																		X											
5100	18203.62																											X		
5120	18213.52																												X	
5120	18213.58														X															
5180	18453.36																							X						
5400	19323.51																										X			
5400	19324.23																												X	
5620	20203.62																												X	
5660	20363.63													X																
5660	20363.82																						X							
5680	20442.48																								X					
5840	21048.9																						X							

GW	Distance (ft)	Jan-15	May-15	Nov-15	Jan-16	May-16	Jul-16	Nov-16	Jan-17	May-17	Jul-17	Nov-17	Jan-18	May-18	Jul-18	Nov-18	Jan-19	May-19	Jul-19	Nov-19	Jan-20	May-20	Jul-20	Nov-20	May-21	Nov-21	May-22	Nov-22	May-23	May-24			
5870	21150.0 1																													X			
5930	21367.1 1																														X		
5930	21367.6 7																										X						
5930	21368.4 3																														X		
5930	21368.8 8																														X		
5930	21369.2 6																										X						
5930	21369.3 2																									X							
5930	21369.4 9																											X					
5930	21369.5 6																		X														
5930	21369.5 7																														X		
5930	21369.9 9																										X						
5930	21370.1 3																										X						
5930	21370.3 8																														X		
5930	21370.4 8																									X							
5930	21371.2 1																										X						
5930	21382.4									X																							
5930	21382.4																						X										
5930	21383.8 7																														X		
5930	21384.1 7																														X		
5930	21384.3 8				X																												
5930	21384.3 8																							X									
5930	21384.3 9																														X		
5930	21384.5 4																														X		
5930	21384.5 8				X																												
5930	21384.6 3																															X	
5930	21385.3 9																						X										
5930	21385.6 9																										X						
5980	21552.3 3																															X	
6010	21710.2 8																										X						
6060	21845.4 3																									X							

GW	Distance (ft)	Jan-15	May-15	Nov-15	Jan-16	May-16	Jul-16	Nov-16	Jan-17	May-17	Jul-17	Nov-17	Jan-18	May-18	Jul-18	Nov-18	Jan-19	May-19	Jul-19	Nov-19	Jan-20	May-20	Jul-20	Nov-20	May-21	Nov-21	May-22	Nov-22	May-23	May-24	
6060	21873.53													X																	
6060	21873.53																													X	
6070	21875.21																									X					
6070	21875.23																											X			
6070	21875.26																								X						
6090	21955.27																												X		
6100	22033.77		X																												
6100	22033.79																								X						
6100	22034.04																										X				
6100	22034.05																											X			
6110	22035.41																			X											
6110	22035.46																										X				
6180	22354.2																										X				
6180	22354.2																													X	
6270	22682.66																													X	
6270	22682.99																									X					
6310	22812.91																													X	
6350	23006.72																											X			
6350	23007																										X				
6350	23007.05																								X						
6350	23007.49															X															
6350	23007.71																										X				
6350	23008.54																										X				
6360	23018.59																													X	
6360	23018.95																										X				
6360	23019.23																											X			
6360	23019.6																										X				
6360	23020.83																										X				
6360	23021.31																													X	
6360	23021.79																						X								
6360	23022.85																								X						

GW	Distance (ft)	Jan-15	May-15	Nov-15	Jan-16	May-16	Jul-16	Nov-16	Jan-17	May-17	Jul-17	Nov-17	Jan-18	May-18	Jul-18	Nov-18	Jan-19	May-19	Jul-19	Nov-19	Jan-20	May-20	Jul-20	Nov-20	May-21	Nov-21	May-22	Nov-22	May-23	May-24	
6360	23022.89																											X			
6360	23023																													X	
6360	23023.3																										X				
6360	23023.7																													X	
6360	23023.8																													X	
6360	23024.39																										X				
6360	23024.82																											X			
6360	23024.88		X																												
6360	23028.38																													X	
6360	23028.66																	X													
6360	23028.86																											X			
6360	23029.76																									X					
6360	23030.14																											X			
6360	23030.41																													X	
6360	23031.76																								X						
6360	23032.43																													X	
6360	23040.25																								X						
6360	23040.57																									X					
6370	23053.14											X																			
6370	23060.55																													X	
6370	23063.48																											X			
6370	23074.6																													X	
6400	23198.67																													X	
6520	23639.84																									X					
6520	23667.04																										X				
6520	23667.31															X															
6520	23667.5																											X			
6520	23668.17																													X	
6520	23668.7																													X	
6520	23669																									X					
6520	23669.09																										X				
6580	23867.6																								X						
6590	23945.68																									X					

GW	Distance (ft)	Jan-15	May-15	Nov-15	Jan-16	May-16	Jul-16	Nov-16	Jan-17	May-17	Jul-17	Nov-17	Jan-18	May-18	Jul-18	Nov-18	Jan-19	May-19	Jul-19	Nov-19	Jan-20	May-20	Jul-20	Nov-20	May-21	Nov-21	May-22	Nov-22	May-23	May-24
6600	23947.6 2																										X			
6790	24696.3 2																									X				
6990	25487.1 8																										X			
6990	25525.0 5																												X	
7010	25570.0 1																											X		
7120	25875.1 3																										X			
7120	25912.1 3																												X	
7160	26035.2 1																											X		
7260	26444.2 5																										X			
7260	26454.2 6																											X		
7400	26969.9 4																										X			
7400	26970																												X	
7400	26970.7 3																											X		
7400	26970.7 4																						X							
7400	26970.8 4																											X		
7420	26985.1																							X						
7420	26985.1 1																												X	
7420	26985.1 3																												X	
7420	26985.3 1																	X												
7420	26985.4 3																								X					
7490	27284.6 7																												X	
7490	27285.0 6																										X			
7520	27356.4 8																												X	
7550	27515.0 6																												X	
7550	27515.2 9																								X					
7670	27985.6 1																										X			
7670	27987.8 2																							X						
7670	27992.0 4																						X							
7670	27992.3 3																												X	
7760	28302.3 7																											X		

GW	Distance (ft)	Jan-15	May-15	Nov-15	Jan-16	May-16	Jul-16	Nov-16	Jan-17	May-17	Jul-17	Nov-17	Jan-18	May-18	Jul-18	Nov-18	Jan-19	May-19	Jul-19	Nov-19	Jan-20	May-20	Jul-20	Nov-20	May-21	Nov-21	May-22	Nov-22	May-23	May-24	
8280	30308.63																													X	
8280	30308.91																										X				
8280	30309.22																							X							
8280	30309.45																													X	
8290	30333.12																								X						
8300	30357.49																													X	
8300	30395.95																													X	
8300	30396.32																											X			
8340	30517.65																													X	
8360	30621.83																												X		
8360	30624.35																													X	
8460	30970.79																											X			
8460	30970.88																									X					
8500	31060.9																										X				
8520	31153.53																												X		
8520	31153.86																									X					
8520	31154.3																								X						
8520	31154.98																											X			
8590	31450.88																											X			
8590	31450.96																								X						
8640	31555.39		X																												
8640	31555.44																			X											
8640	31555.71																										X				
8650	31558.06																										X				
8650	31558.06																												X		
8650	31558.11																												X		
8660	31597.75																												X		
8660	31598.12																												X		
8660	31598.14																										X				
8660	31598.17																											X			

GW	Distance (ft)	Jan-15	May-15	Nov-15	Jan-16	May-16	Jul-16	Nov-16	Jan-17	May-17	Jul-17	Nov-17	Jan-18	May-18	Jul-18	Nov-18	Jan-19	May-19	Jul-19	Nov-19	Jan-20	May-20	Jul-20	Nov-20	May-21	Nov-21	May-22	Nov-22	May-23	May-24
8660	31598.18																								X					
8660	31598.21																	X												
8660	31598.28																							X						
8660	31599.89																												X	
8660	31600.23																												X	
8660	31612.77																											X		
8680	31632.19																											X		
8680	31632.34																							X						
8690	31634.25																											X		
8690	31635.4																							X						
8700	31656.41																											X		
8700	31695.07																										X			
8910	32268.11																										X			
8910	32268.22																												X	
8960	32400.7																										X			
8980	32410.99																								X					
9030	32563.95																											X		
9030	32564.03																											X		
9040	32564.8																												X	
9040	32564.85																												X	
9060	32644.89																										X			
9060	32644.93																										X			
9160	32962.22																											X		
9160	32975.48							X																						
9160	32975.75																								X					
9160	32975.76							X																						
9160	32976.05																												X	
9160	32976.06																		X											
9160	32976.06																										X			
9160	32976.06																												X	
9160	32976.0																											X		

GW	Distance (ft)	Jan-15	May-15	Nov-15	Jan-16	May-16	Jul-16	Nov-16	Jan-17	May-17	Jul-17	Nov-17	Jan-18	May-18	Jul-18	Nov-18	Jan-19	May-19	Jul-19	Nov-19	Jan-20	May-20	Jul-20	Nov-20	May-21	Nov-21	May-22	Nov-22	May-23	May-24	
	7																														
9160	32976.19																													X	
9160	32976.23																										X				
9160	32976.69															X															
9160	32977.13																										X				
9160	32977.14																											X			
9160	32978.35																													X	
9200	33161.16																													X	
9210	33162.93																									X					
9220	33240.91																													X	
9220	33241.33																										X				
9220	33241.53																										X				
9220	33241.58																										X				
9230	33242.21																										X				
9250	33322.96																											X			
9250	33354.59							X																							
9250	33355.15															X															
9250	33356.79																											X			
9250	33356.8																											X			
9250	33359.42																							X							
9250	33360.47																													X	
9250	33360.82																										X				
9250	33361																										X				
9260	33371.68																												X		
9260	33371.79																				X										
9260	33371.83																													X	
9260	33372.14																											X			
9260	33400.71																										X				
9270	33402.69															X															
9270	33425.22																								X						
9270	33431.5			X																											

GW	Distance (ft)	Jan-15	May-15	Nov-15	Jan-16	May-16	Jul-16	Nov-16	Jan-17	May-17	Jul-17	Nov-17	Jan-18	May-18	Jul-18	Nov-18	Jan-19	May-19	Jul-19	Nov-19	Jan-20	May-20	Jul-20	Nov-20	May-21	Nov-21	May-22	Nov-22	May-23	May-24
	2																													
9270	33436.25																								X					
9270	33440.39										X																			
9270	33440.62		X																											
9270	33441.11																							X						
9270	33441.24																												X	
9270	33441.59																							X						
9270	33441.66															X														
9270	33441.66													X																
9280	33443.96																									X				
9280	33452.49																										X			
9280	33453.38																									X				
9280	33454.04																										X			
9280	33454.28																										X			
9280	33455.77																											X		
9280	33456																						X							
9280	33456.25																											X		
9280	33457.78																											X		
9280	33458.68																											X		
9280	33458.7																			X										
9280	33459.28																									X				
9280	33460.07																									X				
9280	33460.75																											X		
9280	33469.53																										X			
9280	33469.68																										X			
9280	33469.86																										X			
9280	33470.43																											X		
9280	33470.61																												X	
9280	33472.3																												X	
9280	33472.4																											X		
9280	33473.47																							X						
9280	33473.94																									X				

GW	Distance (ft)	Jan-15	May-15	Nov-15	Jan-16	May-16	Jul-16	Nov-16	Jan-17	May-17	Jul-17	Nov-17	Jan-18	May-18	Jul-18	Nov-18	Jan-19	May-19	Jul-19	Nov-19	Jan-20	May-20	Jul-20	Nov-20	May-21	Nov-21	May-22	Nov-22	May-23	May-24
9280	33474.08																									X				
9280	33474.4																										X			
9280	33474.4																											X		
9280	33474.46																											X		
9280	33474.48															X														
9280	33474.49																										X			
9280	33474.55																												X	
9280	33474.61																							X						
9280	33474.85																							X						
9280	33474.94																												X	
9280	33474.96																									X				
9280	33475.18																										X			
9280	33475.41																								X					
9280	33475.43																												X	
9280	33475.6																			X										
9280	33476.02																											X		
9280	33476.08																								X					
9280	33476.26																							X						
9280	33476.32		X																											
9280	33476.57																									X				
9280	33476.75																			X										
9280	33476.9																										X			
9280	33477.16																											X		
9280	33477.36																												X	
9280	33477.37																											X		
9280	33477.5																										X			
9280	33477.56																											X		
9280	33477.66																									X				
9280	33477.75																									X				
9280	33478.02																											X		
9280	33478.37																											X		

GW	Distance (ft)	Jan-15	May-15	Nov-15	Jan-16	May-16	Jul-16	Nov-16	Jan-17	May-17	Jul-17	Nov-17	Jan-18	May-18	Jul-18	Nov-18	Jan-19	May-19	Jul-19	Nov-19	Jan-20	May-20	Jul-20	Nov-20	May-21	Nov-21	May-22	Nov-22	May-23	May-24	
9280	33479.85																													X	
9290	33482.37																												X		
9290	33482.38																										X				
9290	33482.42																											X			
9300	33527.69																								X						
9300	33527.99																									X					
9300	33528.75																											X			
9300	33528.83																									X					
9300	33529.18																												X		
9300	33529.5																												X		
9300	33529.51																									X					
9300	33529.96																									X					
9300	33530.39													X																	
9300	33530.47																												X		
9300	33530.56																						X								
9300	33530.99																											X			
9300	33531.02																							X							
9300	33531.04																									X					
9300	33531.19																						X								
9310	33562.56													X																	
9310	33562.61																									X					
9310	33562.8																											X			
9360	33764.38																										X				
9360	33764.65																	X													
9360	33764.89																										X				
9360	33765.2																											X			
9360	33766.34																									X					
9360	33766.62																										X				
9360	33766.89																												X		
9360	33788.65																												X		
9360	33789.4																												X		

GW	Distance (ft)	Jan-15	May-15	Nov-15	Jan-16	May-16	Jul-16	Nov-16	Jan-17	May-17	Jul-17	Nov-17	Jan-18	May-18	Jul-18	Nov-18	Jan-19	May-19	Jul-19	Nov-19	Jan-20	May-20	Jul-20	Nov-20	May-21	Nov-21	May-22	Nov-22	May-23	May-24
	7																													
9360	33789.54																												X	
9360	33789.71																									X				
9390	33867.52													X																
9390	33903.09																												X	
9390	33903.37																										X			
9390	33903.6									X																				
9390	33903.9																												X	
9390	33904.08																												X	
9420	33999																									X				
9420	33999.07																									X				
9420	33999.32																							X						
9420	33999.59																									X				
9420	33999.73																												X	
9420	33999.86		X																											
9420	34000.18																							X						
9420	34000.4																								X					
9420	34000.58																												X	
9420	34026.21																											X		
9420	34026.22													X																
9420	34026.24																											X		
9420	34026.28								X																					
9430	34059															X														
9430	34063.61					X																								
9430	34063.76																									X				
9430	34063.93																										X			
9450	34139.92																												X	
9450	34140.74							X																						
9460	34156.58																									X				
9460	34157.5															X														
9460	34158.2																											X		

GW	Distance (ft)	Jan-15	May-15	Nov-15	Jan-16	May-16	Jul-16	Nov-16	Jan-17	May-17	Jul-17	Nov-17	Jan-18	May-18	Jul-18	Nov-18	Jan-19	May-19	Jul-19	Nov-19	Jan-20	May-20	Jul-20	Nov-20	May-21	Nov-21	May-22	Nov-22	May-23	May-24
	4																													
9470	34188.4 1													X																
9470	34188.4 3															X														
9470	34188.4 4																	X												
9470	34188.4 4																									X				
9470	34188.4 5																	X												
9590	34670.2 6																												X	
9650	34912.2 3																									X				
9650	34913.7 5																										X			
9660	34962.4 9																												X	
9670	34971.8 9																										X			
9690	35051.4 6																												X	
9860	35635.8 5													X																
9890	35794.2 9																			X										
9890	35794.3 2																											X		
9910	35853.4 8																										X			
9910	35853.5 6																												X	
9920	35875.9 5																			X										
9920	35875.9 6																										X			
9920	35875.9 8																						X							
9920	35875.9 8																										X			
9920	35876																						X							
9920	35876.0 2																									X				
9920	35876.0 2																												X	
1007	36496.6 8																												X	
1051	37951.3 1																												X	
1054	38046.7 1																										X			
1062	38363.7																												X	
1064	38444.4 1																										X			
1064	38444.4 2																												X	

GW	Distance (ft)	Jan-15	May-15	Nov-15	Jan-16	May-16	Jul-16	Nov-16	Jan-17	May-17	Jul-17	Nov-17	Jan-18	May-18	Jul-18	Nov-18	Jan-19	May-19	Jul-19	Nov-19	Jan-20	May-20	Jul-20	Nov-20	May-21	Nov-21	May-22	Nov-22	May-23	May-24	
10640	38444.43																											X			
10830	39159.96																													X	
10830	39176.57																								X						
10830	39176.57																													X	
10830	39176.66																												X		
10840	39205.66																												X		
10920	39375.25																										X				
10920	39375.31																													X	
10920	39396.11																												X		
10930	39425.07																										X				
10950	39466.96																													X	
10950	39467.04																													X	
10950	39467.06																			X											
10950	39467.08																													X	
10950	39467.09																									X					
10950	39467.23																										X				
10950	39470.93												X																		
10950	39471.56																													X	
10950	39485.51																						X								
10950	39492.71																													X	
10950	39493.03																												X		
10960	39506.92																													X	
10960	39540.92																										X				
10960	39541.34																								X						
10960	39541.57																													X	
10980	39551.41																										X				
10980	39551.98																													X	
10980	39554.39																											X			
10990	39592.17																													X	
10990	39592.4																								X						

GW	Distance (ft)	Jan-15	May-15	Nov-15	Jan-16	May-16	Jul-16	Nov-16	Jan-17	May-17	Jul-17	Nov-17	Jan-18	May-18	Jul-18	Nov-18	Jan-19	May-19	Jul-19	Nov-19	Jan-20	May-20	Jul-20	Nov-20	May-21	Nov-21	May-22	Nov-22	May-23	May-24
0	4																													
1100	39614.6																													
0	8																												X	
1100	39615.1																													
0	7																									X				
1100	39615.2																											X		
0	2																													
1100	39615.3																													
0	6																												X	
1100	39615.3																												X	
0	6																												X	
1100	39615.4																													
0	7																										X			
1103	39703.1																											X		
0	2																													
1103	39703.3																													
0	6																											X		
1103	39703.4																												X	
0	4																													
1105	39768.1																												X	
0	9																													
1106	39810.3			X																										
0	1																													
1131	40732.5																				X									
0	3																													
1131	40732.6																													
0	3																												X	
1131	40732.6																											X		
0	4																													
1133	40751.9																													
0	9																												X	
1133	40752.0																													
0	6																										X			
1133	40752.1																										X			
0	3																												X	
1141	40991.6																												X	
0	6																													
1141	40991.6																											X		
0	7																													
1141	40992.2																										X			
0	5																													
1141	40993.5																												X	
0	5																													
1141	40993.5															X														
0	9																													
1141	40999.3																											X		
0	3																													
1141	40999.5																										X			
0	4																													
1141	40999.6																												X	
0	5																												X	
1141	40999.6																											X		
0	8																											X		
1146	41205.1																									X				
0	8																													
1147	41230.3																											X		
0	2																													

GW	Distance (ft)	Jan-15	May-15	Nov-15	Jan-16	May-16	Jul-16	Nov-16	Jan-17	May-17	Jul-17	Nov-17	Jan-18	May-18	Jul-18	Nov-18	Jan-19	May-19	Jul-19	Nov-19	Jan-20	May-20	Jul-20	Nov-20	May-21	Nov-21	May-22	Nov-22	May-23	May-24
0	7																													
11540	41512.16																										X			
11540	41512.24																			X										
11540	41512.26																											X		
11540	41512.37																												X	
11540	41512.42																											X		
11540	41512.44																			X										
11540	41512.46												X																	
11540	41512.5																							X						
11540	41512.74																	X												
11540	41513.01																			X										
11540	41513.01																												X	
11540	41513.04																						X							
11540	41513.04																												X	
11540	41513.1																											X		
11540	41513.1																												X	
11540	41530.5																									X				
11550	41531.48																												X	
11550	41531.52																											X		
11550	41531.52																												X	
11550	41531.53																							X						
11550	41531.53																												X	
11550	41531.53																												X	
11550	41531.54																											X		
11550	41531.69																												X	
11550	41531.71																									X				
11550	41531.71																										X			
11550	41538.65																								X					
11550	41539.15																												X	
11550	41550.93																									X				

GW	Distance (ft)	Jan-15	May-15	Nov-15	Jan-16	May-16	Jul-16	Nov-16	Jan-17	May-17	Jul-17	Nov-17	Jan-18	May-18	Jul-18	Nov-18	Jan-19	May-19	Jul-19	Nov-19	Jan-20	May-20	Jul-20	Nov-20	May-21	Nov-21	May-22	Nov-22	May-23	May-24	
11550	41551.06																													X	
11550	41551.26																											X			
11550	41551.48																											X			
11550	41551.6																												X		
11550	41551.8																												X		
11550	41551.95																											X			
11550	41551.97																			X										X	
11550	41551.98																												X		
11550	41552.66																													X	
11550	41552.72																												X		
11550	41553.21																													X	
11550	41553.25																										X				
11550	41560.55																													X	
11550	41562.43																													X	
11550	41562.44																													X	
11550	41563.37																													X	
11550	41565.01																													X	
11550	41565.3																													X	
11550	41565.62																										X				
11550	41566.26																													X	
11550	41566.34																										X				
11550	41569.55																													X	
11550	41569.62																													X	
11560	41570.78																											X			
11560	41571.38																													X	
11560	41571.38																													X	
11560	41571.68																	X													
11560	41572.01																													X	
1157	41641.6																											X			

GW	Distance (ft)	Jan-15	May-15	Nov-15	Jan-16	May-16	Jul-16	Nov-16	Jan-17	May-17	Jul-17	Nov-17	Jan-18	May-18	Jul-18	Nov-18	Jan-19	May-19	Jul-19	Nov-19	Jan-20	May-20	Jul-20	Nov-20	May-21	Nov-21	May-22	Nov-22	May-23	May-24
0	8																													
11570	41642.64																												X	
11570	41645.67																					X								
11570	41646.35																												X	
11570	41646.56																												X	
11580	41678.65																												X	
11580	41679.48																									X				
11580	41689.85																										X			
11580	41690.68																										X			
11580	41690.77																											X		
11590	41690.96																											X		
11590	41691.15																									X				
11590	41691.15																										X			
11590	41691.75																										X			
11590	41691.83																											X		
11590	41691.86																							X						
11590	41700.43																									X				
11590	41700.74																										X			
11590	41700.98																											X		
11590	41701																									X				
11590	41701.36																										X			
11590	41701.41																									X				
11590	41701.45																							X						
11590	41701.5																										X			
11590	41701.51																								X					
11590	41701.56																											X		
11590	41701.73																						X							
11590	41701.86									X																				
11590	41701.92																										X			
11590	41702.05																											X		

GW	Distance (ft)	Jan-15	May-15	Nov-15	Jan-16	May-16	Jul-16	Nov-16	Jan-17	May-17	Jul-17	Nov-17	Jan-18	May-18	Jul-18	Nov-18	Jan-19	May-19	Jul-19	Nov-19	Jan-20	May-20	Jul-20	Nov-20	May-21	Nov-21	May-22	Nov-22	May-23	May-24	
11590	41702.12																											X			
11590	41702.13																													X	
11590	41702.37																													X	
11590	41702.39																												X		
11590	41702.45																												X		
11590	41702.66																										X				
11590	41702.7																													X	
11590	41702.72																													X	
11590	41702.74																										X				
11590	41702.75																													X	
11590	41702.76																												X		
11590	41702.85																													X	
11590	41702.89																									X					
11590	41703.06																										X				
11590	41703.06																											X			
11590	41703.07																							X							
11590	41703.33																													X	
11590	41703.8																										X				
11590	41707.27																													X	
11590	41707.71																												X		
11590	41707.72																									X					
11590	41707.97																														
11590	41708.04																														
11590	41709.24																														
11590	41709.96																														
11590	41711.18																														
11590	41711.86																														
11590	41711.94																														
11590	41711.95																														
11590	41712.1																														

GW	Distance (ft)	Jan-15	May-15	Nov-15	Jan-16	May-16	Jul-16	Nov-16	Jan-17	May-17	Jul-17	Nov-17	Jan-18	May-18	Jul-18	Nov-18	Jan-19	May-19	Jul-19	Nov-19	Jan-20	May-20	Jul-20	Nov-20	May-21	Nov-21	May-22	Nov-22	May-23	May-24
0	2																													
11590	41712.2																									X				
11590	41712.2																												X	
11590	41712.5																											X		
11590	41712.7																												X	
11590	41712.8																												X	
11590	41712.9											X																		
11590	41713.0																												X	
11590	41713.3															X														
11590	41713.6																										X			
11590	41713.6																												X	
11590	41713.6															X														
11590	41714.5																												X	
11590	41714.7																									X				
11590	41714.7																											X		
11590	41714.7																												X	
11590	41715.2																												X	
11590	41715.4																												X	
11590	41715.8																										X			
11590	41715.8																												X	
11590	41715.9																												X	
11590	41716.1															X														
11590	41716.4																												X	
11590	41716.4																											X		
11590	41716.7																											X		
11590	41716.9																												X	
11590	41716.9																										X			
11590	41717.0																										X			
11590	41717.4																										X			
11590	41717.6																										X			

GW	Distance (ft)	Jan-15	May-15	Nov-15	Jan-16	May-16	Jul-16	Nov-16	Jan-17	May-17	Jul-17	Nov-17	Jan-18	May-18	Jul-18	Nov-18	Jan-19	May-19	Jul-19	Nov-19	Jan-20	May-20	Jul-20	Nov-20	May-21	Nov-21	May-22	Nov-22	May-23	May-24	
11590	41717.65																													X	
11590	41717.73																											X			
11590	41717.76																													X	
11590	41717.9																								X						
11590	41717.95																												X		
11590	41718.01																												X		
11590	41718.71															X															
11590	41719.26																								X						
11590	41719.46																													X	
11590	41719.89																										X				
11590	41719.97																											X			
11590	41720.06																												X		
11590	41720.35																											X			
11590	41720.52																												X		
11590	41720.63																							X							
11590	41720.72																											X			
11590	41721.18																													X	
11590	41721.35																													X	
11590	41721.54																													X	
11590	41721.64																						X								
11590	41721.68																											X			
11590	41721.7																								X						
11590	41721.91																											X			
11590	41721.96																													X	
11590	41722																													X	
11590	41722.06																													X	
11590	41722.1																													X	
11590	41722.17																													X	
11590	41722.17																													X	
11590	41722.17																													X	
11590	41722.17																													X	
11590	41722.2																													X	

GW	Distance (ft)	Jan-15	May-15	Nov-15	Jan-16	May-16	Jul-16	Nov-16	Jan-17	May-17	Jul-17	Nov-17	Jan-18	May-18	Jul-18	Nov-18	Jan-19	May-19	Jul-19	Nov-19	Jan-20	May-20	Jul-20	Nov-20	May-21	Nov-21	May-22	Nov-22	May-23	May-24
11600	41742.1																											X		
11600	41742.13																					X								
11600	41742.22																							X						
11600	41742.23																								X					
11610	41744.25																												X	
11610	41746.67																									X				
11610	41747.31																					X								
11610	41747.78																											X		
11620	41804.18																								X					
11620	41804.44																												X	
11620	41805.07																												X	
11630	41812.07																												X	
11630	41812.93																									X				
11630	41813.21																												X	
11630	41839.82																											X		
11630	41839.85																										X			
11640	41851.24																										X			
11640	41852.07																										X			
11640	41852.33																												X	
11650	41930.2																		X											
11660	41931.85																			X										
11660	41931.86																							X						
11660	41931.89																												X	
11660	41931.89																												X	
11670	41985.39																										X			
11670	41985.4																											X		
11670	42010.35																							X						
11930	42952.49																										X			
11990	43171.61																						X							
1212	43585.0																										X			

GW	Distance (ft)	Jan-15	May-15	Nov-15	Jan-16	May-16	Jul-16	Nov-16	Jan-17	May-17	Jul-17	Nov-17	Jan-18	May-18	Jul-18	Nov-18	Jan-19	May-19	Jul-19	Nov-19	Jan-20	May-20	Jul-20	Nov-20	May-21	Nov-21	May-22	Nov-22	May-23	May-24		
0	1																															
1213	43608.1																													X		
0	9																															
1213	43608.4																									X						
0	3																															
1215	43666.9																													X		
0	6																															
1215	43666.9																		X													
0	8																															
1215	43667.0																		X													
0	3																															
1216	43716.9									X																						
0	4																															
1216	43734.4																													X		
0	7																															
1216	43735.8																													X		
0	2																															
1216	43736.5																		X													
0	6																															
1216	43736.6																													X		
0	1																															
1216	43736.7																												X			
0	6																															
1216	43736.9																									X						
0																																
1216	43745.0																								X							
0	1																															
1216	43745.0									X																						
0	4																															
1216	43745.1																													X		
0	5																															
1217	43746.6																												X			
0	5																															
1217	43746.7																										X					
0	2																															
1217	43746.7												X																			
0	4																															
1217	43748.0																						X									
0	2																															
1217	43749.8																												X			
0	4																															
1217	43750.3																													X		
0	2																															
1217	43750.6																											X				
0	9																															
1217	43751.2																															
0	1																									X						
1217	43752.0																													X		
0	6																															
1217	43752.4																												X			
0	8																															
1217	43756.8																												X			
0	3																															
1219	43814.1																											X				
0	3																															
1223	44011.9																												X			
0	3																															
1223	44012.3																										X					
0	9																															

GW	Distance (ft)	Jan-15	May-15	Nov-15	Jan-16	May-16	Jul-16	Nov-16	Jan-17	May-17	Jul-17	Nov-17	Jan-18	May-18	Jul-18	Nov-18	Jan-19	May-19	Jul-19	Nov-19	Jan-20	May-20	Jul-20	Nov-20	May-21	Nov-21	May-22	Nov-22	May-23	May-24
12230	44013.5																											X		
12240	44018.59					X																								
12240	44019.64																	X												
12240	44019.83																												X	
12240	44020.12																							X						
12240	44020.91																											X		
12240	44021.03																											X		
12240	44021.34																					X								
12240	44021.8																										X			
12240	44023.6																											X		
12240	44023.61																												X	
12240	44023.67																												X	
12240	44024.02																										X			
12240	44024.62																										X			
12240	44024.63																												X	
12240	44026.71																										X			
12240	44026.77																									X				
12240	44027.28																								X					
12240	44028.1																												X	
12240	44029.89																												X	
12240	44031.61																												X	
12240	44032.53																										X			
12240	44033.17																										X			
12240	44033.39																												X	
12240	44033.82																												X	
12240	44033.97																											X		
12240	44035.69																										X			
12240	44037.15																												X	
12240	44038.19																											X		
12240	44041.0																									X				

GW	Distance (ft)	Jan-15	May-15	Nov-15	Jan-16	May-16	Jul-16	Nov-16	Jan-17	May-17	Jul-17	Nov-17	Jan-18	May-18	Jul-18	Nov-18	Jan-19	May-19	Jul-19	Nov-19	Jan-20	May-20	Jul-20	Nov-20	May-21	Nov-21	May-22	Nov-22	May-23	May-24				
0	6																																	
1224	44046.6																								X									
0	8																																	
1224	44047.5																											X						
0	7																																	
1224	44048.1																						X											
0	44048.1																																	
1224	44048.5																											X						
0	8																																	
1224	44049.1																													X				
0	3																																	
1224	44049.3																													X				
0	8																																	
1224	44051.3																										X							
0	44051.3																																	
1224	44053.3																																	
0	4																																	
1224	44053.3																																	
0	5																			X														
1224	44053.3																				X													
0	6																																	
1224	44053.3																																	
0	8																														X			
1224	44053.3																																	
0	8																														X			
1224	44053.4																																	
0	44053.4																																	
1224	44053.4																																	
0	3																																	
1225	44055.1																																	
0	6																																	
1225	44055.1																																	
0	7																				X													
1225	44055.1																																	
0	7																									X								
1225	44055.1																																	
0	8																															X		
1225	44055.2																																	
0	44055.2																																	
1227	44126.3																																	
0	9																																	
1227	44126.4							X																										
0	1																																	
1228	44170.4																																	
0	44170.4																																	
1228	44171.0																																	
0	7																																	
1228	44171.1																																	
0	8																																	
1228	44171.2																																	
0	9																																	
1228	44173.1																																	
0	8																																	
1228	44204.7																																	
0	44204.7																																	
1228	44204.7																																	
0	5																																	
1231	44286.7																																	
0	2																																	

GW	Distance (ft)	Jan-15	May-15	Nov-15	Jan-16	May-16	Jul-16	Nov-16	Jan-17	May-17	Jul-17	Nov-17	Jan-18	May-18	Jul-18	Nov-18	Jan-19	May-19	Jul-19	Nov-19	Jan-20	May-20	Jul-20	Nov-20	May-21	Nov-21	May-22	Nov-22	May-23	May-24
12410	44708.24		X																											
12410	44708.56															X														
12410	44708.64																													X
12410	44708.99																			X										
12410	44709.36																											X		
12410	44709.39																							X						
12420	44709.76																												X	
12420	44710																	X												
12420	44710.66																			X										
12420	44710.93																										X			
12420	44710.94																									X				
12420	44711.28																									X				
12420	44712.17																										X			
12420	44712.32																												X	
12420	44712.44																										X			
12420	44712.73																												X	
12420	44712.78												X																	
12420	44713.31																									X				
12420	44725.74															X														
12420	44745.1																								X					
12420	44745.65																									X				
12420	44745.84																			X										
12420	44747.51																												X	
12420	44747.53																												X	
12420	44747.59																									X				
12420	44747.74																			X										
12420	44747.78																												X	
12420	44747.8															X														
12420	44747.8																	X												
12420	44747.8															X														

GW	Distance (ft)	Jan-15	May-15	Nov-15	Jan-16	May-16	Jul-16	Nov-16	Jan-17	May-17	Jul-17	Nov-17	Jan-18	May-18	Jul-18	Nov-18	Jan-19	May-19	Jul-19	Nov-19	Jan-20	May-20	Jul-20	Nov-20	May-21	Nov-21	May-22	Nov-22	May-23	May-24
0	2																													
1242	44748.5																													
0	5																													X
1243	44748.7																													X
0	8																													
1243	44748.9																													
0	6																										X			
1243	44749.0																													
0	4																										X			
1243	44749.6																													
0	2																										X			
1243	44749.7																													
0	2																													X
1243	44750.1																													
0	8																									X				
1243	44750.3																													
0	1																										X			
1243	44750.4																													X
0	5																													X
1243	44750.6																													X
0	3																													X
1243	44753.3																													
0	1																										X			
1243	44753.7																													X
0	7																													X
1243	44765.6																													
0	8																										X			
1243	44766.2																													
0	3																										X			
1243	44766.7																													X
0	4																													
1243	44766.8																													
0	2																										X			
1243	44767.0																													X
0	3																													
1243	44767.3																										X			
0	4																													
1243	44768.0													X																
0	4																													
1243	44768.4																													
0	7																				X									
1243	44768.7																													
0	9																									X				
1243	44769.4																													X
0	2																													
1243	44769.9																													
0	2			X																										
1243	44770.9																													
0	5																										X			
1243	44770.9													X																
0	9																													
1243	44771.6																													
0	2																										X			
1243	44774.5																											X		
0	4																										X			
1243	44784.0																													
0	3																													
1243	44784.3																										X			
0	8																													

GW	Distance (ft)	Jan-15	May-15	Nov-15	Jan-16	May-16	Jul-16	Nov-16	Jan-17	May-17	Jul-17	Nov-17	Jan-18	May-18	Jul-18	Nov-18	Jan-19	May-19	Jul-19	Nov-19	Jan-20	May-20	Jul-20	Nov-20	May-21	Nov-21	May-22	Nov-22	May-23	May-24	
12430	44784.68																													X	
12430	44788.3																										X				
12430	44788.44																									X					
12430	44788.67																											X			
12460	44908.13																												X		
12470	44909.82																								X						
12480	44987.97																											X			
12490	44989.6					X																									
12490	44989.6																										X				
12490	44989.68																												X		
12490	45010.92																								X						
12500	45034.21																										X				
12500	45039.78																											X			
12500	45044.49																												X		
12500	45044.54																											X			
12500	45068																											X			
12500	45068.11																												X		
12510	45070																								X						
12510	45070.04																									X					
12510	45072.89					X																									
12510	45073.14																							X							
12510	45074.18																	X													
12510	45074.45																					X									
12510	45075.29																		X												
12510	45076.53																							X							
12510	45077.5																										X				
12510	45083.16																									X					
12510	45083.29																									X					
12510	45083.69																	X													
12510	45084.0																								X						

GW	Distance (ft)	Jan-15	May-15	Nov-15	Jan-16	May-16	Jul-16	Nov-16	Jan-17	May-17	Jul-17	Nov-17	Jan-18	May-18	Jul-18	Nov-18	Jan-19	May-19	Jul-19	Nov-19	Jan-20	May-20	Jul-20	Nov-20	May-21	Nov-21	May-22	Nov-22	May-23	May-24		
0	3																															
12510	45084.2																												X			
12510	45084.49																												X			
12510	45085.76																										X					
12510	45086.74																												X			
12510	45088.2																											X				
12510	45088.77																									X						
12510	45089.11																									X						
12510	45089.79																							X								
12510	45090.11																								X							
12510	45090.29																										X					
12510	45090.43																												X			
12510	45090.54																						X									
12530	45150.07																													X		
12530	45178.24																									X						
12530	45178.47																													X		
12540	45197.18									X																						
12540	45197.62																										X					
12540	45200.05																										X					
12540	45200.57																													X		
12540	45204.09																													X		
12540	45204.4																						X									
12550	45205.01																														X	
12550	45205.06																										X					
12550	45205.47																									X						
12550	45205.82																										X					
12550	45206.21																													X		
12550	45206.69																															
12550	45222.48																							X								
12550	45238.94																													X		

GW	Distance (ft)	Jan-15	May-15	Nov-15	Jan-16	May-16	Jul-16	Nov-16	Jan-17	May-17	Jul-17	Nov-17	Jan-18	May-18	Jul-18	Nov-18	Jan-19	May-19	Jul-19	Nov-19	Jan-20	May-20	Jul-20	Nov-20	May-21	Nov-21	May-22	Nov-22	May-23	May-24		
12590	45370.38																														X	
12590	45370.46																														X	
12590	45370.62																						X									
12590	45371.02																														X	
12710	45748.34																			X												
12710	45748.36																									X						
12710	45748.38																											X				
12710	45748.42																													X		
12710	45748.44																									X						
12720	45812.87																														X	
12730	45814.21																														X	
12780	46022.48																			X												
12790	46024.29																													X		
12790	46044.18																										X					
12800	46082.37																							X								
12800	46082.72																								X							
12800	46082.84																														X	
12800	46083.07													X																		
12800	46083.56																														X	
12800	46083.57																													X		
12800	46083.64																										X					
12800	46083.89																											X				
12800	46084.42																										X					
12800	46084.47																										X					
12800	46084.84																						X									
12800	46085																													X		
12800	46085.42																													X		
12800	46085.63																										X					
12800	46085.72																													X		
12800	46085.9																													X		

GW	Distance (ft)	Jan-15	May-15	Nov-15	Jan-16	May-16	Jul-16	Nov-16	Jan-17	May-17	Jul-17	Nov-17	Jan-18	May-18	Jul-18	Nov-18	Jan-19	May-19	Jul-19	Nov-19	Jan-20	May-20	Jul-20	Nov-20	May-21	Nov-21	May-22	Nov-22	May-23	May-24	
0	8																														
1280	46086.6																				X										
0	2																														
1280	46086.6																													X	
0	4																														
1280	46087.2																														
0	8															X															
1280	46087.3																														
0	2																									X					
1280	46087.6																									X					
0	1																														
1280	46087.7																														
0	3																													X	
1280	46087.9																														
0	7																											X			
1280	46088.3																														
0	3																										X				
1280	46088.5																														
0	2																									X					
1280	46088.5																														
0	5																													X	
1280	46088.9																														
0	1																											X			
1280	46089.1																														
0	7																													X	
1280	46089.4																										X				
0	5																														
1280	46089.5																														
0	1																														
1280	46089.8																														
0	3																													X	
1280	46090.0																														
0	3																														
1280	46090.2																									X					
0	2																														
1280	46091.3																														
0	8																														
1280	46091.9																														
0	3																														
1280	46092.6																														
0	4																													X	
1280	46092.7																														
0	7																													X	
1280	46093.1																														
0	1																														
1280	46093.5																														
0	6																													X	
1280	46093.6																														
0	3																										X				
1280	46093.8																														
0	8																									X					
1280	46094.0																														
0	4																														
1280	46094.4																														
0	6																														
1280	46094.6																														
0	4																													X	
1280	46102.9																														
0	6																								X						

GW	Distance (ft)	Jan-15	May-15	Nov-15	Jan-16	May-16	Jul-16	Nov-16	Jan-17	May-17	Jul-17	Nov-17	Jan-18	May-18	Jul-18	Nov-18	Jan-19	May-19	Jul-19	Nov-19	Jan-20	May-20	Jul-20	Nov-20	May-21	Nov-21	May-22	Nov-22	May-23	May-24
12800	46103.01																										X			
12800	46103.07															X														
12820	46183.26																						X							
12820	46183.33					X																								
12820	46183.34																											X		
12820	46183.35		X																											
12820	46183.39									X																				
12820	46183.42																										X			
12830	46204.85																										X			
12830	46204.95																										X			
12830	46205.43																												X	
12830	46207.43																						X							
12830	46207.43																										X			
12830	46208.09																							X						
12830	46208.5																								X					
12830	46208.59																												X	
12840	46226.61																											X		
12840	46237.96																											X		
12840	46238.56																											X		
12840	46239																									X				
12840	46239.23																							X						
12840	46239.28																										X			
12840	46239.95																											X		
12840	46239.99																									X				
12840	46240.18																											X		
12840	46240.84																										X			
12840	46240.92																										X			
12840	46241.1																											X		
12840	46241.41																										X			
12840	46250.2																										X			

GW	Distance (ft)	Jan-15	May-15	Nov-15	Jan-16	May-16	Jul-16	Nov-16	Jan-17	May-17	Jul-17	Nov-17	Jan-18	May-18	Jul-18	Nov-18	Jan-19	May-19	Jul-19	Nov-19	Jan-20	May-20	Jul-20	Nov-20	May-21	Nov-21	May-22	Nov-22	May-23	May-24
0	3																													
12840	46251.8																												X	
12840	46251.97																									X				
12840	46252.16																									X				
12840	46252.34																										X			
12840	46252.56											X																		
12840	46252.69																					X								
12840	46253.28																								X					
12840	46253.47																										X			
12840	46257.04																											X		
12840	46257.06																										X			
12850	46272.68															X														
12850	46272.75																								X					
12850	46272.81																											X		
12850	46273.2																										X			
12850	46273.76																												X	
12850	46274.2																								X					
12850	46274.79																								X					
12850	46284.58																											X		
12850	46284.67																							X						
12850	46285.4																					X								
12850	46285.7																									X				
12850	46286.12																											X		
12850	46286.21																										X			
12850	46286.75																											X		
12850	46286.84																								X					
12850	46287.18																												X	
12850	46288.49															X														
12850	46293.89																												X	
12850	46294.35																										X			

GW	Distance (ft)	Jan-15	May-15	Nov-15	Jan-16	May-16	Jul-16	Nov-16	Jan-17	May-17	Jul-17	Nov-17	Jan-18	May-18	Jul-18	Nov-18	Jan-19	May-19	Jul-19	Nov-19	Jan-20	May-20	Jul-20	Nov-20	May-21	Nov-21	May-22	Nov-22	May-23	May-24	
12850	46295.87																													X	
12860	46342.56																										X				
12860	46342.71																											X			
12860	46343.01																								X						
12860	46343.57																										X				
12860	46343.91																												X		
12870	46345.58																												X		
12870	46345.6					X																									
12870	46345.6															X															
12870	46345.6																										X				
12880	46415.43																										X				
12880	46415.83																												X		
12880	46423.86																										X				
12880	46423.92																										X				
12880	46423.92																											X			
12880	46423.98								X																						
12880	46423.98																								X						
12880	46424.03																												X		
12880	46424.06		X																												
12880	46424.06																											X			
12880	46424.28																												X		
12890	46449.27																											X			
12890	46449.54																												X		
12890	46449.88																								X						
12890	46451.5																									X					
12900	46504.23																	X													
12910	46505.92																										X				
12910	46511.14																										X				
12970	46721.34																										X				
1298	46735.9																											X			

GW	Distance (ft)	Jan-15	May-15	Nov-15	Jan-16	May-16	Jul-16	Nov-16	Jan-17	May-17	Jul-17	Nov-17	Jan-18	May-18	Jul-18	Nov-18	Jan-19	May-19	Jul-19	Nov-19	Jan-20	May-20	Jul-20	Nov-20	May-21	Nov-21	May-22	Nov-22	May-23	May-24
0	1																													
12980	46738.94															X														
13000	46796.38																													X
13000	46796.43																											X		
13000	46798.69																											X		
13000	46800.26																										X			
13000	46806.47																												X	
13000	46806.74																													
13000	46806.76																	X												
13000	46807.38																		X											
13000	46807.59																											X		
13000	46807.71																										X			
13010	46837.79																										X			
13010	46837.81																											X		
13020	46838.68																											X		
13020	46838.97																						X							
13040	46944.38																											X		
13110	47203.53																											X		
13110	47206.47																											X		
13110	47206.57																											X		
13110	47206.92																											X		
13110	47207.19																											X		
13140	47272.56																													
13170	47319.31																													X
13170	47329.39																										X			
13170	47329.58																								X					
13170	47329.58																										X			
13170	47329.59																												X	
13180	47330.84																												X	
13200	47373.47																										X			

GW	Distance (ft)	Jan-15	May-15	Nov-15	Jan-16	May-16	Jul-16	Nov-16	Jan-17	May-17	Jul-17	Nov-17	Jan-18	May-18	Jul-18	Nov-18	Jan-19	May-19	Jul-19	Nov-19	Jan-20	May-20	Jul-20	Nov-20	May-21	Nov-21	May-22	Nov-22	May-23	May-24	
13200	47373.55													X																	
13200	47373.97					X																									
13200	47374.19		X																												
13200	47400.36							X																							
13200	47400.44																											X			
13200	47400.46																												X		
13200	47400.49																								X						
13200	47400.52																										X				
13200	47400.59																										X				
13200	47400.66																			X											
13200	47400.67																												X		
13200	47400.7																											X			
13200	47400.7																											X			
13200	47400.71																													X	
13200	47400.71																													X	
13210	47402.35																												X		
13210	47402.36																												X		
13210	47402.38																							X							
13210	47402.39																										X				
13210	47402.39																											X			
13210	47402.54																										X				
13210	47412.91		X																												
13210	47413.4																								X						
13220	47448.57																													X	
13220	47480.61																										X				
13230	47482.33																													X	
13260	47623.55																				X										
13260	47623.67																								X						
13260	47623.6																											X			

GW	Distance (ft)	Jan-15	May-15	Nov-15	Jan-16	May-16	Jul-16	Nov-16	Jan-17	May-17	Jul-17	Nov-17	Jan-18	May-18	Jul-18	Nov-18	Jan-19	May-19	Jul-19	Nov-19	Jan-20	May-20	Jul-20	Nov-20	May-21	Nov-21	May-22	Nov-22	May-23	May-24
0	7																													
13260	47623.72																							X						
13260	47623.73																									X				
13320	47780.08																												X	
13570	48607.3																											X		
13570	48607.89																									X				
13570	48607.92																								X					
13700	48882.16		X																											
13700	48882.17																											X		
13700	48882.26					X																								
13700	48882.36																											X		
14020	50168.38																							X						
14020	50168.38																												X	
14040	50246.66																												X	
14040	50246.85																									X				
14040	50246.88																							X						
14040	50246.97																					X								
14060	50259.59																												X	
14060	50264.77																										X			
14060	50266.19																												X	
14060	50267.77																									X				
14060	50269.11																											X		
14060	50269.28																											X		
14060	50269.57																												X	
14060	50269.57																												X	
14060	50269.67																											X		
14060	50269.87																												X	
14060	50270.44																												X	
14060	50270.55																												X	
14060	50270.98																											X		

GW	Distance (ft)	Jan-15	May-15	Nov-15	Jan-16	May-16	Jul-16	Nov-16	Jan-17	May-17	Jul-17	Nov-17	Jan-18	May-18	Jul-18	Nov-18	Jan-19	May-19	Jul-19	Nov-19	Jan-20	May-20	Jul-20	Nov-20	May-21	Nov-21	May-22	Nov-22	May-23	May-24
14060	50271.28																									X				
14060	50271.8																												X	
14060	50271.82																									X				
14060	50272.07																										X			
14060	50272.39																								X					
14060	50272.56																									X				
14060	50272.6																					X								
14060	50273.19																										X			
14060	50273.19																												X	
14060	50273.27																											X		
14060	50273.28																									X				
14110	50475.51																											X		
14200	50820.9																											X		
14200	50821.08																									X				
14300	51203.96																										X			
14310	51271.21																							X						
14310	51271.22																											X		
14310	51271.44																												X	
14310	51271.67																										X			
14310	51271.78																											X		
14310	51271.84																					X								
14310	51271.84																										X			
14310	51271.95																												X	
14470	51642.63																												X	
14500	51691.64																									X				
14590	51974.46																												X	
14650	52251.87																										X			
14650	52251.88																											X		
14890	53192.12																							X						
1490	53193.8																												X	

GW	Distance (ft)	Jan-15	May-15	Nov-15	Jan-16	May-16	Jul-16	Nov-16	Jan-17	May-17	Jul-17	Nov-17	Jan-18	May-18	Jul-18	Nov-18	Jan-19	May-19	Jul-19	Nov-19	Jan-20	May-20	Jul-20	Nov-20	May-21	Nov-21	May-22	Nov-22	May-23	May-24
0	4																													
1490	53193.8																													
0	6																												X	
1491	53234.2																													
0	8																											X		
1492	53274.9																													
0	4																											X		
1492	53275.2																													
0	4																												X	
1492	53313.0																													
0	9																												X	
1505	53823.9																													
0	9																									X				
1553	55653.5																													
0	5																												X	
1554	55696.3																													
0	4																									X				
1577	56478.4																													
0	5																										X			
1577	56478.4																													
0	7																										X			
1578	56480.1																													
0	1																												X	
1578	56480.1																													
0	3																												X	
1585	56711.6																													
0	4																										X			
1585	56712.9																													
0	7																												X	
1585	56713.4																													
0	1																												X	
1585	56713.5																													
0	9																										X			
1585	56713.6																						X							
0	1																													
1585	56713.7																													
0	1																												X	
1585	56714.4																													
0	3																										X			
1585	56714.4																													
0	9																									X				
1585	56716.3																													
0	6																										X			
1585	56717.4																													
0	5																												X	
1588	56809.4																													
0																													X	
1588	56809.4																													
0	1																												X	
1590	56850.4																													
0	5																												X	
1590	56850.9																													
0	4																										X			
1590	56851.1																													
0	8																												X	
1590	56858.6																													
0	8																												X	
1590	56868																													
0																											X			

GW	Distance (ft)	Jan-15	May-15	Nov-15	Jan-16	May-16	Jul-16	Nov-16	Jan-17	May-17	Jul-17	Nov-17	Jan-18	May-18	Jul-18	Nov-18	Jan-19	May-19	Jul-19	Nov-19	Jan-20	May-20	Jul-20	Nov-20	May-21	Nov-21	May-22	Nov-22	May-23	May-24
15900	56878.5																												X	
15900	56882.65																										X			
15910	56895.87																												X	
15910	56895.95																										X			
15910	56902.79																											X		
15910	56902.98																		X											
15910	56903.92																										X			
15910	56914.19																										X			
15910	56916.54																											X		
15910	56922.03																												X	
15910	56922.08																												X	
15950	56972.51																												X	
15950	56974.24																									X				

Appendix C – Full Excavation Timeline (30’ limit)

GW	Dig Start (ft)	Dig End (ft)	Length (ft)	Dig Date
70.01/80	125.59	142.82	17.23	Jul-17
250/260	597.18	607.51	10.33	Jan-20
260	636.44	636.47	0.03	Jan-15
290/310	668.45	678.96	10.51	Jul-17
420	956.64	956.7	0.06	Jan-16
470	1134.02			Jul-20
480	1164.9	1186.34	21.44	Jan-20
480/490	1197.72	1224.65	26.93	Jul-20
500	1239.97	1262.12	22.15	Jul-20
500/510	1277.24	1303.42	26.18	Jul-19
520	1320.27	1348.62	28.35	Jan-20
530	1350.34	1375.95	25.61	Jul-19
530/540	1380.45	1405.69	25.24	Jul-20
540	1412.65	1437.2	24.55	Jul-20
550	1446.49	1473.06	26.57	Jul-20
560	1477.26	1504.82	27.56	Jan-20
560/570	1509.34	1538.27	28.93	Jul-20
570/580	1540.72	1563.76	23.04	Jul-20
580/590	1572.03	1604.13	32.1	Jan-18
600/610	1673.77	1700.71	26.94	Jan-18
610	1708.07			Jul-20
620	1752.17	1753.14	0.97	Jul-20
640/650	1817.13	1829.55	12.42	Jan-20
710/720	2097.51	2126.87	29.36	Jan-19
720/730	2127.56	2153.96	26.4	Jul-18
730/740	2157.94	2184.73	26.79	Jul-18
740/750	2193.05	2222.91	29.86	Jul-18

GW	Dig Start (ft)	Dig End (ft)	Length (ft)	Dig Date
750	2223.28	2250.65	27.37	Jan-18
750/760	2256.47	2278.68	22.21	Jul-18
760/770/780	2286.7	2314.34	27.64	Jan-18
800	2368.43	2368.81	0.38	Jul-19
970	2990.53	3020.01	29.48	Jul-19
970/980	3023.98	3052.94	28.96	Jul-20
980/990	3055.48	3074.62	19.14	Jul-19
1050	3347.6	3347.71	0.11	Jul-18
1070	3406.47	3427.82	21.35	Jul-18
1090	3489.91			Jan-20
1350/1360	4530.98	4532.7	1.72	Jul-16
1370	4608.59	4610.89	2.3	Jan-15
1480	5026.35			Jul-19
1520	5186.17			Jan-20
1550/1560	5295.01	5319.85	24.84	Jul-18
1570	5382.03	5382.84	0.81	Jan-15
1580/1590/1600	5425.09	5449.97	24.88	Jan-20
1700	5833.49	5833.55	0.06	Jan-17
1980/1990	6902.95	6928.82	25.87	Jul-18
2170	7618.29	7648.22	29.93	Jan-16
2170	7654.47	7654.78	0.31	Jan-17
2210	7786.93	7787.14	0.21	Jan-18
2370	8428.95			Jul-20
2430	8654.45			Jul-20
2450	8733.29	8733.39	0.1	Jan-18
2500	8898.57			Jul-20
2640	9452.13	9460.01	7.88	May-17

GW	Dig Start (ft)	Dig End (ft)	Length (ft)	Dig Date
2830	10119.99			May-21
2940	10515.15			May-23
2960	10584.12	10589.43	5.31	May-16
3010	10755.92	10756.35	0.43	May-21
3090	11060			May-22
3220	11615.85			May-23
3370	12195.91			May-23
3430	12427.16			May-22
3630	13155.91	13156.18	0.27	May-20
3680	13394.44			May-20
3750	13645.56	13645.75	0.19	May-22
3810	13852.54	13853.93	1.39	May-22
3850	14002.02			Nov-22
4080	14751.62	14757.57	5.95	May-19
4140/4150	14909.43	14934.69	25.26	Nov-19
4150/4160/4160.01/4160.02	14945.13	14968.53	23.4	May-15
4200/4210	15015.82	15026.16	10.34	May-22
4210/4220	15049.79	15076.28	26.49	Nov-15
4220/4230	15086.08	15106.27	20.19	May-15
4240/4250	15184.5	15186.2	1.7	May-20
4260/4270	15263.79	15275.45	11.66	Nov-21
4300	15295.63			May-23
4340/4360	15366.08	15377.59	11.51	May-21
4390	15454.72			May-21
4410	15505.12			Nov-22
4430	15585.19			May-21
4540	16038.87			Nov-22
4620	16377.71			May-23
4640/4650	16458.49	16460.62	2.13	Nov-17
4660	16532.12	16538.67	6.55	May-18

GW	Dig Start (ft)	Dig End (ft)	Length (ft)	Dig Date
4680/4690	16618.79	16620.66	1.87	May-22
4730	16780.45	16780.77	0.32	Nov-22
4900	17473.17			May-23
5100/5120	18203.47	18213.58	10.11	Nov-18
5180	18453.36			Nov-20
5400	19323.51	19324.23	0.72	May-22
5620	20203.62			May-23
5660	20363.63	20363.82	0.19	May-18
5680	20442.48			May-21
5840	21048.9			May-20
5870	21150.01			May-23
5930	21367.11	21385.69	18.58	Nov-15
5980	21552.33			May-23
6010	21710.28			May-22
6060/6070	21845.43	21875.26	29.83	May-18
6090	21955.27			May-23
6100/6110	22033.77	22035.46	1.69	May-15
6180	22354.2			May-22
6270	22682.66	22682.99	0.33	May-22
6310	22812.91			May-23
6350/6360	23006.72	23032.43	25.71	May-15
6360/6370	23040.25	23063.48	23.23	Nov-17
6370	23074.6			May-23
6400	23198.67			May-23
6520	23639.84	23669.09	29.25	Nov-18
6580	23867.6			Nov-20
6590/6600	23945.68	23947.62	1.94	May-21
6790	24696.32			May-21
6990	25487.18			May-22
6990	25525.05			May-23

GW	Dig Start (ft)	Dig End (ft)	Length (ft)	Dig Date
7010	25570.01			Nov-22
7120	25875.13			May-22
7120	25912.13			May-23
7160	26035.21			Nov-22
7260	26444.25	26454.26	10.01	May-22
7400/7420	26969.94	26985.43	15.49	May-19
7490	27284.67	27285.06	0.39	Nov-21
7520	27356.48			May-23
7550	27515.06	27515.29	0.23	May-21
7670	27985.61	27992.33	6.72	May-20
7760	28302.37			Nov-22
7860	28674.28	28674.43	0.15	Nov-22
7990	29171.19	29171.21	0.02	May-15
8060	29453.57	29471.01	17.44	May-15
8060/8070	29485.33	29496.67	11.34	Nov-20
8140	29742.02			Nov-15
8280/8290	30307.15	30333.12	25.97	May-15
8300	30357.49			May-23
8300	30395.95	30396.32	0.37	Nov-22
8340	30517.65			May-23
8360	30621.83	30624.35	2.52	Nov-22
8460	30970.79	30970.88	0.09	Nov-21
8500	31060.9			May-22
8520	31153.53	31154.98	1.45	May-21
8590	31450.88	31450.96	0.08	May-21
8640/8650	31555.39	31558.11	2.72	May-15
8660	31597.75	31612.77	15.02	May-19
8680/8690/8700	31632.19	31656.41	24.22	Nov-20
8700	31695.07			May-22
8910	32268.11	32268.22	0.11	May-22

GW	Dig Start (ft)	Dig End (ft)	Length (ft)	Dig Date
8960/8980	32400.7	32410.99	10.29	May-21
9030/9040	32563.95	32564.85	0.9	Nov-22
9060	32644.89	32644.93	0.04	May-22
9160	32962.22	32978.35	16.13	Nov-16
9200/9210	33161.16	33162.93	1.77	May-21
9220/9230	33240.91	33242.21	1.3	Nov-21
9250	33322.96			May-22
9250/9260	33354.59	33372.14	17.55	Nov-16
9260/9270	33400.71	33425.22	24.51	Nov-18
9270/9280	33431.52	33460.75	29.23	May-15
9280/9290	33469.53	33482.42	12.89	May-15
9300	33527.69	33531.19	3.5	May-18
9310	33562.56	33562.8	0.24	May-18
9360	33764.38	33789.71	25.33	May-19
9390	33867.52			May-18
9390	33903.09	33904.08	0.99	May-17
9420	33999	34026.28	27.28	May-15
9430	34059	34063.93	4.93	May-16
9450/9460	34139.92	34158.24	18.32	Nov-16
9470	34188.41	34188.45	0.04	May-18
9590	34670.26			Nov-22
9650	34912.23	34913.75	1.52	May-21
9660/9670	34962.49	34971.89	9.4	May-22
9690	35051.46			May-23
9860	35635.85			May-18
9890	35794.29	35794.32	0.03	Nov-19
9910/9920	35853.48	35876.02	22.54	Nov-19
10070	36496.68			May-23
10510	37951.31			May-23
10540	38046.71			Nov-21

GW	Dig Start (ft)	Dig End (ft)	Length (ft)	Dig Date
10620	38363.7			May-23
10640	38444.41	38444.43	0.02	Nov-21
10830	39159.96	39176.66	16.7	May-21
10840	39205.66			Nov-22
10920	39375.25	39396.11	20.86	May-22
10930	39425.07			May-22
10950	39466.96	39493.03	26.07	May-18
10960	39506.92			May-23
10960/10980	39540.92	39554.39	13.47	May-21
10990/11000	39592.17	39615.47	23.3	May-21
11030	39703.12	39703.44	0.32	May-22
11050	39768.19			Nov-22
11060	39810.31			Nov-15
11310/11330	40732.53	40752.13	19.6	Nov-19
11410	40991.66	40999.68	8.02	Nov-18
11460/11470	41205.18	41234.92	29.74	Nov-21
11540/11550	41506.78	41531.71	24.93	Nov-16
11550	41538.65	41566.34	27.69	Nov-19
11550/11560	41569.55	41572.01	2.46	May-19
11570	41641.68	41646.56	4.88	May-20
11580/11590	41678.65	41708.04	29.39	May-17
11590	41709.24	41726.2	16.96	Nov-17
11600/11610	41741.6	41747.78	6.18	Nov-18
11620/11630	41804.18	41813.21	9.03	May-21
11630/11640	41839.82	41852.33	12.51	May-22
11650/11660	41930.2	41931.89	1.69	Nov-19
11670	41985.39	42010.35	24.96	Nov-20
11930	42952.49			May-22
11990	43171.61			May-20
12120/12130	43585.01	43608.43	23.42	Nov-21

GW	Dig Start (ft)	Dig End (ft)	Length (ft)	Dig Date
12150	43666.96	43667.03	0.07	May-19
12160/12170	43716.94	43746.74	29.8	May-17
12170	43748.02	43756.83	8.81	May-20
12190	43814.13			May-22
12230/12240	44011.93	44041.06	29.13	May-16
12240/12250	44046.68	44055.2	8.52	Nov-19
12270	44126.39	44126.41	0.02	Nov-16
12280	44170.48	44173.18	2.7	May-20
12280	44204.7	44204.75	0.05	Nov-19
12310	44286.72			May-23
12410/12420	44708.24	44725.74	17.5	May-15
12420/12430	44745.1	44774.5	29.4	Nov-15
12430	44784.03	44788.67	4.64	May-21
12460/12470	44908.13	44909.82	1.69	May-21
12480/12490	44987.97	45010.92	22.95	May-16
12500	45034.21	45044.54	10.33	May-22
12510	45068	45090.54	22.54	May-16
12530	45150.07	45178.47	28.4	May-21
12540/12550	45197.18	45222.48	25.3	May-17
12550	45238.94			May-23
12590	45370.38	45371.02	0.64	May-20
12710	45748.34	45748.44	0.1	Nov-19
12720/12730	45812.87	45814.21	1.34	Nov-22
12780/12790	46022.48	46044.18	21.7	Nov-19
12800	46082.37	46103.07	20.7	May-18
12820/12830	46183.26	46208.59	25.33	May-15
12840	46226.61	46253.47	26.86	Nov-18
12840/12850	46257.04	46286.84	29.8	Nov-18
12850	46287.18	46295.87	8.69	Nov-18
12860/12870	46342.56	46345.6	3.04	May-16

GW	Dig Start (ft)	Dig End (ft)	Length (ft)	Dig Date
12880	46415.43	46424.28	8.85	May-15
12890	46449.27	46451.5	2.23	May-21
12900/12910	46504.23	46511.14	6.91	May-19
12970/12980	46721.34	46738.94	17.6	Nov-18
13000	46796.38	46807.71	11.33	May-19
13010/13020	46837.79	46838.97	1.18	May-20
13040	46944.38			May-22
13110	47203.53	47207.19	3.66	May-22
13140	47272.56			Nov-21
13170/13180	47319.31	47330.84	11.53	May-21
13200/13210	47373.47	47402.54	29.07	May-15
13210	47412.91	47413.4	0.49	May-15
13220	47448.57			May-23
13220/13230	47480.61	47482.33	1.72	May-22
13260	47623.55	47623.73	0.18	Nov-19
13320	47780.08			May-23
13570	48607.3	48607.92	0.62	Nov-21
13700	48882.16	48882.36	0.2	May-15
14020	50168.38			Nov-20
14040/14060	50246.66	50273.28	26.62	May-20
14110	50475.51			Nov-22

GW	Dig Start (ft)	Dig End (ft)	Length (ft)	Dig Date
14200	50820.9	50821.08	0.18	May-21
14300	51203.96			May-22
14310	51271.21	51271.95	0.74	May-20
14470	51642.63			May-23
14500	51691.64			May-21
14590	51974.46			May-23
14650	52251.87	52251.88	0.01	May-22
14890/14900	53192.12	53193.86	1.74	Nov-20
14910	53234.28			Nov-22
14920	53274.94	53275.24	0.3	Nov-22
14920	53313.09			May-23
15050	53823.99			May-22
15530	55653.55			May-23
15540	55696.34			Nov-21
15770/15780	56478.45	56480.13	1.68	May-22
15850	56711.64	56717.45	5.81	May-20
15880	56809.4	56809.41	0.01	May-23
15900	56850.45	56878.5	28.05	May-22
15900/15910	56882.65	56903.92	21.27	Nov-19
15910	56914.19	56922.08	7.89	May-22
15950	56972.51	56974.24	1.73	Nov-21

Appendix H

PHMSA's Independent Analysis of In-Line Inspection Data

Appendix H: PHMSA's Independent Analysis of ILI Data

Plains' IMP provides written procedures for reviewing an ILI vendor's final report and describes how they are to analyze the data provided to create a dig list. The corrosion growth rate is assumed to be a linear growth that has taken place over 75% of the time since construction. This is considered similarly for both the depth and length growth. Plains' IMP Group then considers two failure modes, leak (80% depth limit) and rupture at maximum operating pressure (MOP). The rupture date is set to the date that is 70% of the estimated time taken to reach failure at the MOP. An anomaly is scheduled for excavation when the nearest date from either mode occurs prior to the next proposed ILI assessment survey date.

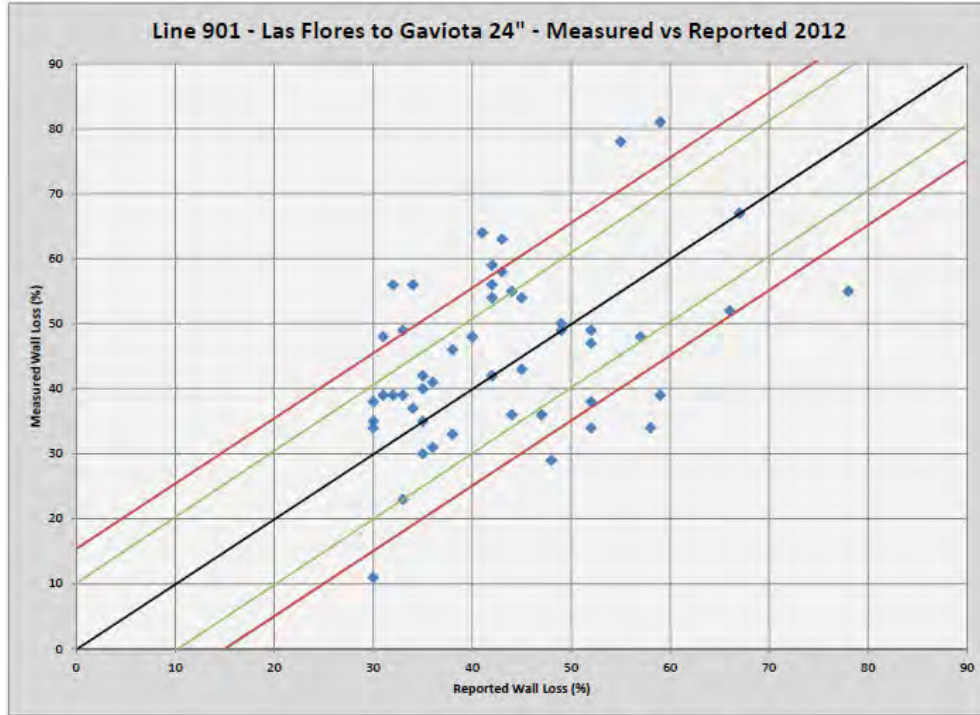
Anomaly dig sheets are then created in Houston and they are sent to the field for execution. The field obtains appropriate permits, conducts the digs and hires a company to come in and perform the NDE on each anomaly. A dig package is then created for each anomaly and includes pictures, data forms, NDE measurements, etc. Once an anomaly dig is completed, the dig package is sent back to the IMP Group in Houston, TX.

Plains' IMP has procedures directing the IMP Group how to analyze the data once the dig information arrives back in Houston from the field. Their procedures are contained in Section 6 and Appendix E1 Magnetic Flux Leakage In-Line Inspection Tool Specification of Plains' IMP.

A short section from page 6-17 and 6-18 of Section 6 of the Plains IMP [Date of Revision: 10 July 2008] are excerpted below.

“Validation of ILI Results To validate the ILI results, Plains will record field found anomaly data on the Anomaly Tracker spreadsheet for the anomalies selected for investigation from the PHMSA Compliance Report. A list of data columns of the Anomaly Tracker spreadsheet is included at the end of this Section. The PHMSA Records Specialists will be responsible for inputting the data into this spreadsheet using data from the Form 501 Pipeline Inspection Reports. Once the data on a pipeline segment is compiled, it will be analyzed by various methods, such as, plotting unity graphs and performing statistical analysis. The field found anomaly data will also be entered into a database, where it can be integrated with other pipeline data for additional analysis.”

PHMSA requested all records and analysis performed after each of the ILI Surveys on line 901. Plains' submitted a Unity Plot for as-found versus as-called depth that was created in 2013 – after the 2012 survey and the ILI digs. The plot is shown here.



The black line is the one to one line where any “as-called equal as-found” anomalies would be plotted. The green lines are +/- 10% lines and the red lines are +/- 15% lines. ~57% of the plotted anomalies are within the +/- 10% lines. Reported tool accuracy is +/- 10% 80% of the time. There is no documentation regarding any further analysis or discussion which may have ensued after the creation of this Unity Plot for wall loss (depth).

Appendix E-1 has more specific written procedures concerning contracting with an MFL Tool vendor. This information is excerpted from the Plains IMP with a Date of Revision: “20 December, 2005 APPENDIX E Integrity Management Plan”.

On page E1-7 and E1-8 it states:

“6.2 Detection and Anomaly Sizing Specification

The MFL tool shall meet the minimum detection and anomaly sizing specifications listed in Table E1-1. The Tool Vendor will submit their MFL tool’s actual specifications with their bid. The Company may modify these specifications.

Table E1-1 Detection and Sizing Accuracy at 80% Confidence Level

	Seam Welded		Seamless	
	Isolated Corrosion < 3t x 3t	Generalized Corrosion > 3t x 3t	Isolated Corrosion < 3t x 3t	Generalized Corrosion > 3t x 3t
Minimum Detectable Depth	0.2 t	0.1 t	0.3 t	0.15 t
Depth Accuracy	± 0.15 t	± 0.15 t	± 0.15 t	± 0.15 t
Length Accuracy	± 1.0"	± 1.0"	± 1.0"	± 1.0"
Width Accuracy	± 1.4"	± 1.4"	± 1.4"	± 1.4"
Axial Location Accuracy	± 1 %	± 1 %	± 1 %	± 1 %
Orientation	± 15 °	± 15 °	± 15 °	± 15 °
Probability of Detection (POD)	90 %	90 %	90 %	90 %

Where t = the nominal wall thickness
 Depth = maximum metal loss anomaly depth
 Length = metal loss in the axial direction
 Width = metal loss in the circumferential direction

6.3 Interaction Criteria

The Tool Vendor shall use the 1”x 6t interaction criteria in data analysis. For the 1”x 6t interaction criteria, two anomalies will interact if the distance between them is less than or equal to 1” in the axial direction and the circumferential distance between them is less than or equal to 6 times the nominal wall thickness.”

The Plains’ IMP also includes a section on verification of tool data as follows:

“8.0 Verification of the Inspection Data

8.1 Selection of Verification Digs

The investigation of selected anomalies that the Company and Tool Vendor agree upon will be used to compare actual vs. predicted dimensions to provide anomaly verification data to the Tool Vendor. The Tool Vendor’s bid must contain a provision for adjusting the anomaly grading based on the verification data at no cost to Company.

8.2 Verification of External Anomalies

External anomalies will be measured by Company field personnel who are qualified to perform API Covered Tasks 8.1 and 8.3. Measurements will be made and recorded for the depth, length and width of the anomaly, as well as the location of the anomaly relative to the reference girth weld. Digital photographs and a sketch or etchings of the anomalies will be made and included in the record. Length of the affected joint and its location relative to the reference marker will be included for comparison to information provided by Tool Vendor. The Company will provide copies of all information obtained from the selected anomalies to the Tool Vendor as soon as possible. The Tool Vendor will review the field data for any corrections to the data analysis for the Final Report.”

Independent Review of Smart Pig Data and Field Found Data

PHMSA contracted with Oak Ridge National Laboratories (ORNL) to provide a Subject Matter Expert (SME) to assist in the investigation by performing an analysis of the MFL smart

pig in-line-inspection (ILI) data and by comparing that data with the digs made and the information gathered by the non-destructive-examination (NDE) of the anomalies in the field. The analysis included a review of the raw ILI data from the 2007, 2012 and 2015 ILI surveys and comparing that data to the as found data when each anomaly was excavated and measured in the field. All of the data used in the ILI-SME report was provided by the Plains' IMP Group.

Unity plots (as-found versus as-called) were made for length, width and depth. Generally, if a point is called a certain value and the field measured value is the same value, the point will fall on a line that runs at a 45 degree angle from zero up and to the right on a Cartesian coordinate graph. Dotted lines are added parallel to the unity line, placed at +/- 10% which is the reported tool tolerance. The smart pigs utilized for each of the surveys in 2007, 2012, and 2015 were from the same vendor and were high resolution magnetic flux leakage (MFL) smart pigs.

Note: The tools differed slightly but utilized the same MFL technology. See the full report for the full discussion.

The first item of note in the ILI-SME Report is that external corrosion was active on line 901. "Table 2. In line inspection results" from that report is copied below. The table shows that from survey to survey (5 years then 3 years), the number of external corrosion anomalies greater than or equal to 10% increased by 1192 and 169 from 2007 to 2012 and 2012 to 2015 respectively.

Table 2. In line inspection results.

<i>Inspection</i>	<i># Ext. Metal Loss</i>	<i># Int. Metal Loss</i>	<i># Mill Metal Loss</i>	<i>Total Metal Loss</i>	<i>Metal Loss in First 9450'</i>	<i># Dents</i>	<i># Dents with Metal Loss or on Weld</i>
2007 MFL (≥10%)	386	237	88	711	277	0	0
2012 MFL (≥10%)	1578	6	2	1586	469	22	1
2015 MFL* (≥10%)	1747	0	21	1768	N/A	6	1 (sleeved)

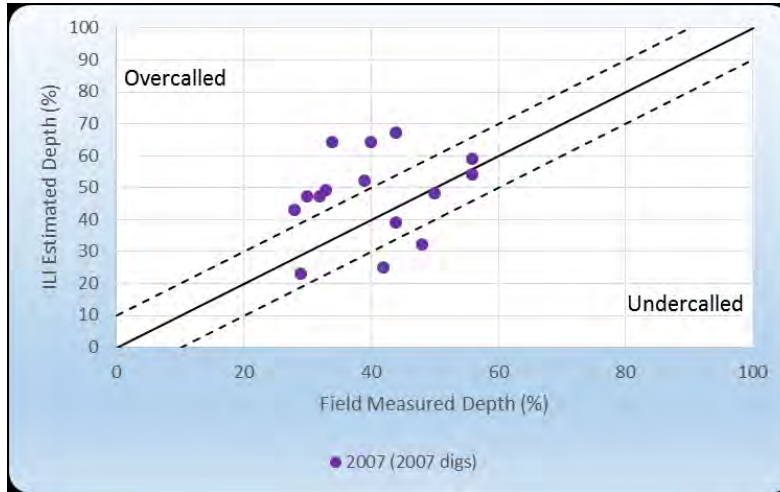
***First 9450' of 2015 data did not record metal loss**

The ILI-SME report goes on to describe the accuracy of the data presented by the ILI tool vendor compared with the actual measurements found when excavated and measured. The stated accuracy of the tool in the vendor-operator contract was not met for any of the ILI surveys. Also, the tool accuracy using the accepted industry standard, API 1163, was not within stated specifications either.

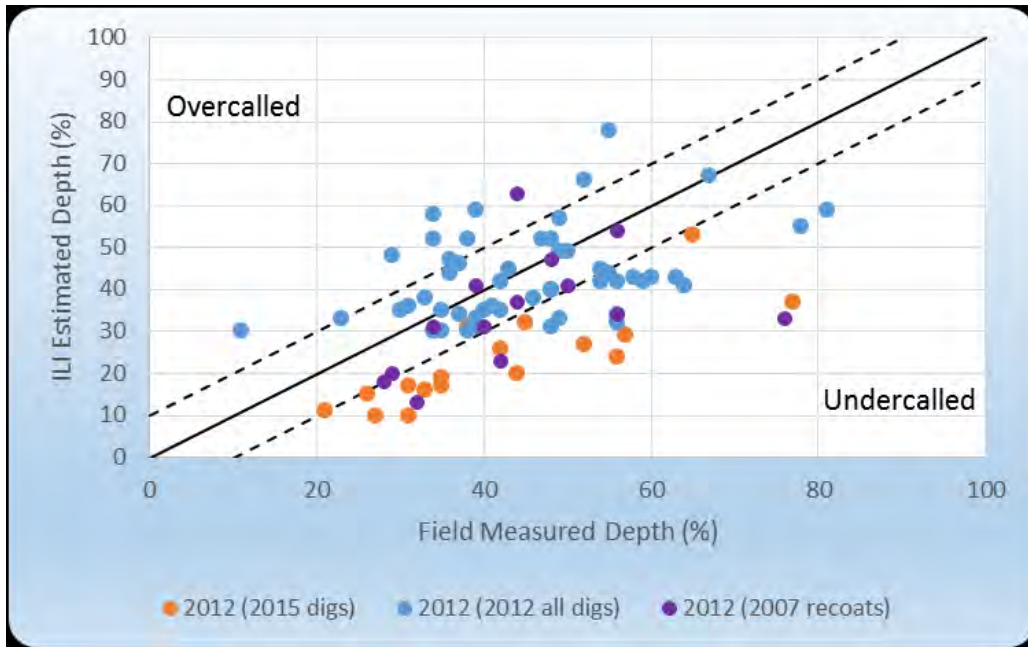
Note: The report does conclude that: “If overcalled anomalies were considered (i.e. >10% over actual) then in all years the unities would be $\pm 10\%$, >70% of the time for depth.”

The report concludes the following with respect to the accuracies reported by the ILI Tool vendor after the field reported measurements for the same anomalies.

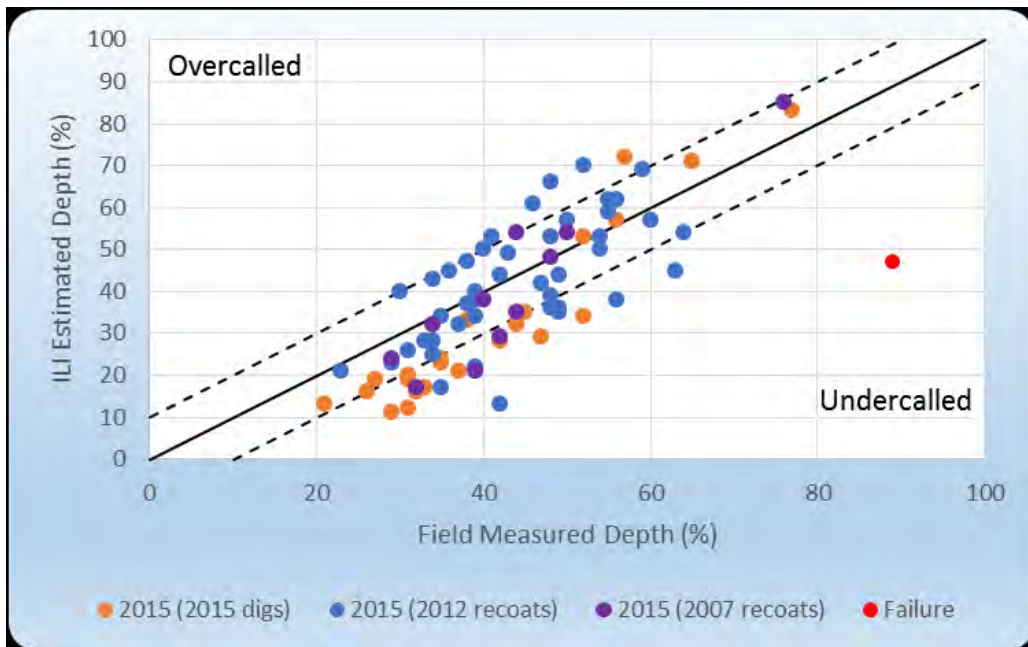
“The unity plot for the 2007 inspection is within $\pm 10\%$, 33% of the time with respect to the 2007 excavations.”



“The unity plot for the 2012 inspection is within $\pm 10\%$, 58% of the time with respect to the 2012 excavations (blue) and 2007 excavation recoats (violet). When comparing to the 2015 field excavated results based on the 2012 ILI data, growth may have occurred, causing the comparisons between field and ILI to be under-called (orange). The 2015 digs were not considered in the above stated accuracy.”



“The 2015 ILI estimated depths are compared to field measured depths either from the 4 excavations following the failure or the areas recoated after the 2007 and 2012 inspections. The unity plot shows that the 2015 Rosen inspection is within $\pm 10\%$, 57% of the time. It may be seen that the failure location has an uncharacteristically high deviation from the ILI estimate.”



The ILI-SME describes the process for calculating the remaining strength of a pipe based on the length, width and depth of an anomaly. He also describes the manner in which ILI vendors’ interact individual pits into boxes and then how the boxes interact to form clusters and how clusters can be grouped. Suffice it to say that there is a defined process for

interacting metal loss anomalies. The only interaction criterion requested by Plains IMP Group was the industry standard one inch by 6 wall thicknesses (1" X 6t) which is normally used for isolated pitting.

From the ILI-SME report: "Plains specifies an interaction criteria to be a combination of absolute value for the length component (1") and wall thickness dependence for the width component (6t). The 1" x 6t interaction rule is one of the most commonly employed throughout industry and is the example given in ASME B31.4."

The ILI-SME report goes on to describe why accurate length and width measurements are important when analyzing external corrosion anomalies.

From the ILI-SME report: "The issue of underestimating the length and width of a corrosion anomaly will lead to gross underestimations of the corrosion area. Figure 16 delineates all of the line 901 anomalies with width and length reported from ILI estimates versus excavations made, on a logarithmic scale. As an example, it is showing that 38% of the anomalies had an area stated by the ILI of $\leq 1.5 \text{ in}^2$ when in fact the corrosion areas were between 2.5 in^2 and 7300 in^2 . This being said, there may be a difference in the field measurement technique to consider. It is important that the techniques used in the field be comparable to that required by the ILI analysis to enable a proper assessment of the ILI performance."

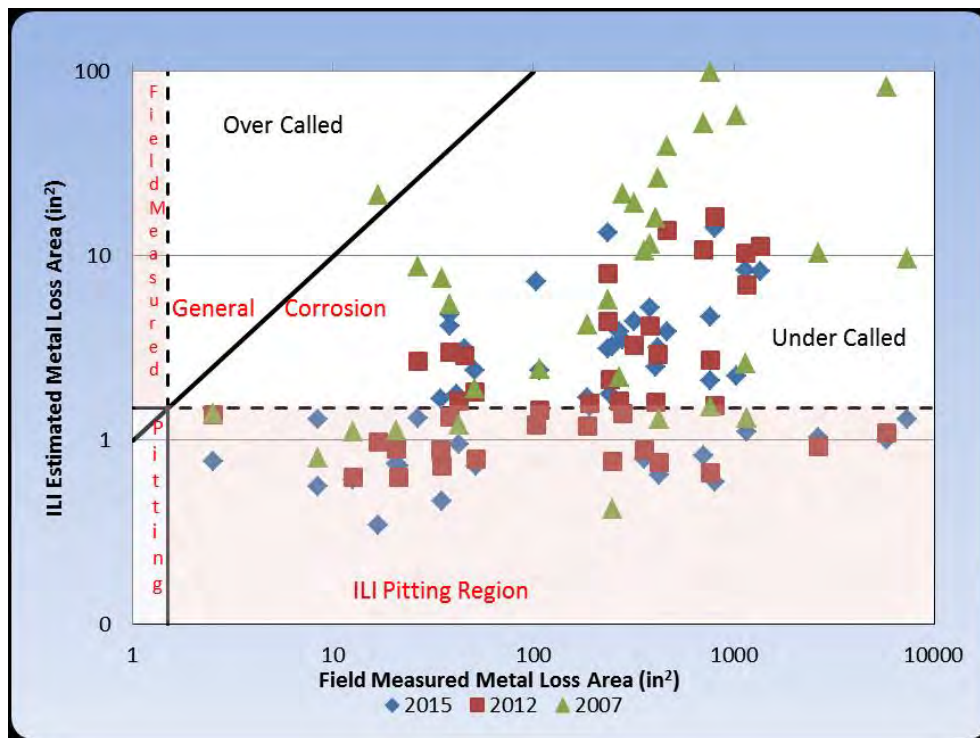


Figure 16. Metal loss area; ILI vs field measurement.

The following are two "Close-Out Reports" provided by the Plains IMP Group. The first one is for the 2007 ILI survey and anomaly digs and the second is for the 2012 ILI survey and

anomaly digs. The 2007 Close-Out Report states in the, “Results/Comments/Recommendations”, at the bottom of the form, “2. The results show that 86% of the excavated anomalies were within tool tolerance or over-called by the ILI tool and no anomalies meet conditions for further evaluations.” This report was completed on 6/21/2015.

The 2012 Close-Out Report states in the “Results/Comments/Recommendations”, at the bottom of the form:

“2. The results show that the ILI tool is within the tool’s tolerance specification.

3. The results show that 73% of the excavated anomalies were within tool tolerance or over-called by the ILI tool and no anomalies meet conditions for further evaluations.”

CLOSE-OUT REPORT

Line Name: ILI tool run date: Date:

Summary of In-Line Inspection Indications

Metal Loss Anomalies	Ext		Int		Mfg		Total	
	ILI	After	ILI	After	ILI	After	ILI	After
d/t < 20% WT	257	248	228	228	71	71	556	545
20% WT ≤ d/t < 30% WT	82	76	5	5	16	16	103	97
30% WT ≤ d/t < 40% WT	33	27	4	4	1	1	38	32
40% WT ≤ d/t < 50% WT	9	3	0	0	0	0	9	3
50% WT ≤ d/t < 60% WT	3	0	0	0	0	0	3	0
60% WT ≤ d/t < 70% WT	2	0	0	0	0	0	2	0
70% WT ≤ d/t < 80% WT	0	0	0	0	0	0	0	0
d/t > 80% WT	0	0	0	0	0	0	0	0
Internal ML consistent with internal corrosion	0	0	0	0	0	0	0	0
Selective Seam Corrosion	0	0	0	0	0	0	0	0
Total	388	352	237	237	88	88	711	677

Failure Pressures and Deepest Pits	ILI	After
Reported deepest external metal loss (%WT)	67%	42%
Reported deepest internal metal loss (%WT)	34%	34%
Calculated lowest Safe_pressure (based on CGAR)	885	1,201
Calculated lowest P_Burst (based on CGAR)	1,230	1,669

Seam Weld Anomalies	Total	After
SWA-A	0	0
SWA-B	0	0
SWA	0	0

Deformation Anomalies	Total	After
	Dent Depth > 6% OD	0
Dent Depth ≤ 6% OD	0	0
Dent Depth > 2% OD with metal	0	0
Dent Depth < 2% OD with metal	0	0
Dent Depth ≥ 2% OD affecting weld	0	0
Dent Depth < 2% OD affecting weld	0	0
Girth weld anomalies	0	0
Wrinkle bends	0	0

Crack Anomalies (Depth)	Crack-Like		Crack Field		Notch-Like		Mid Wall		Total	
	ILI	After	ILI	After	ILI	After	ILI	After	ILI	After
0.040" - 0.079"	0	0	0	0	0	0	0	0	0	0
0.08" - 0.119"	0	0	0	0	0	0	0	0	0	0
0.12" - 0.159"	0	0	0	0	0	0	0	0	0	0
> 0.16"	0	0	0	0	0	0	0	0	0	0
No depth	0	0	0	0	0	0	0	0	0	0
Total	0	0	0	0	0	0	0	0	0	0

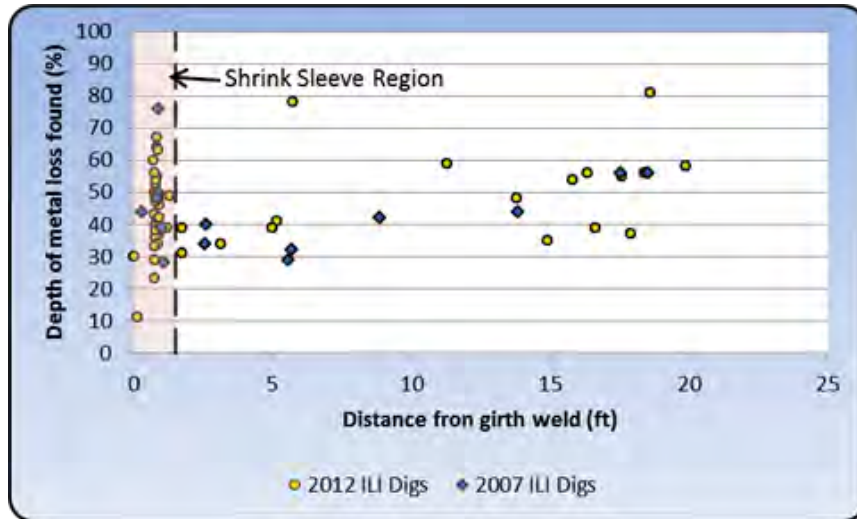
Results/Comment/Recommendation:

- 1 anomaly (cluster) repaired using type B sleeve, 11 anomalies/clusters using composite sleeves, 28 anomalies/clusters using recoat, and 0 anomaly using pipe replacement.
- The results show that 86% of the excavated anomalies were within tool tolerance or overcalled by the ILI tool and no anomalies meet conditions for further evaluations.
- The earliest the remaining ML anomalies to have predicted depth >80%WT or calculated burst pressure < MOP (based on CGAR) is > 2012.

CLOSE-OUT REPORT										
Line Name	L901 - Las Flores - Gaviota - 24"			ILI tool run date:	7/3/2012		Date:	6/22/2015		
Summary of In-Line Inspection Indications										
Metal Loss Anomalies	Ext		Int		Mfg		Total			
	ILI	After	ILI	After	ILI	After	ILI	After		
d/t < 20% WT	1,241	992	6	6	0	0	1,247	998		
20% WT ≤ d/t < 30% WT	182	137	0	0	2	2	184	139		
30% WT ≤ d/t < 40% WT	99	57	0	0	0	0	99	57		
40% WT ≤ d/t < 50% WT	36	9	0	0	0	0	36	9		
50% WT ≤ d/t < 60% WT	15	1	0	0	0	0	15	1		
60% WT ≤ d/t < 70% WT	4	0	0	0	0	0	4	0		
70% WT ≤ d/t < 80% WT	1	0	0	0	0	0	1	0		
d/t ≥ 80% WT	0	0	0	0	0	0	0	0		
Internal ML consistent with internal corrosion	0	0	0	0	0	0	0	0		
Selective Seam Corrosion	0	0	0	0	0	0	0	0		
Total	1,578	1,196	6	6	2	2	1,586	1,204		
Failure Pressures and Deepest Pits	ILI	After	Deformation Anomalies				Total	After		
Reported deepest external metal loss (%WT)	78%	52%	Dent Depth > 6% OD				0	0		
Reported deepest internal metal loss (%WT)	18%	18%	Dent Depth ≤ 6% OD				22	5		
Calculated lowest Safe Pressure (based on	1,090	1,158	Dent Depth ≥ 2% OD with metal				0	0		
Calculated lowest P Burst (based on CGAR)	1,515	1,608	Dent Depth < 2% OD with metal				0	0		
Seam Weld Anomalies			Total	After	Dent Depth ≥ 2% OD affecting weld				0	0
SWA-A	0	0	Dent Depth < 2% OD affecting weld				2	0		
SWA-B	0	0	Girth weld anomalies				0	0		
SWA	0	0	Wrinkle bends				16	0		
Crack Anomalies (Depth)	Crack-Like		Crack Field		Notch-Like		Mid Wall		Total	
	ILI	After	ILI	After	ILI	After	ILI	After	ILI	After
0.040" - 0.079"	0	0	0	0	0	0	0	0	0	0
0.08" - 0.119"	0	0	0	0	0	0	0	0	0	0
0.12" - 0.159"	0	0	0	0	0	0	0	0	0	0
> 0.16"	0	0	0	0	0	0	0	0	0	0
No depth	0	0	0	0	0	0	0	0	0	0
Total	0	0	0	0	0	0	0	0	0	0
Results/Comment/Recommendation:										
1. 2012 ILI - 49 anomalies repaired using Type B, 37 anomalies using composite sleeves, 211 anomalies using recoat, and 0 anomaly using pipe replacement.										
2. The result shows that the ILI tool is within the tool's tolerance specification. No further anomalies need to be investigated.										
3. The result shows that 73 % of the excavated anomalies were within tool tolerance or overcalled by the ILI tool and no anomalies meet conditions for further evaluations.										
4. The earliest the remaining ML anomalies to have predicted depth >80%WT or calculated burst pressure < MOP (based on CGAR) is 3/19/2016.										

Two additional analyses were performed by the ILI-SME which was not included in the final filed report. One data set was the number of anomaly digs that were within one and a half feet of a girth weld. Below is the analysis stated and presented graphically.

“Within the 2007 excavation locations approximately 50% were within 1.5’ of a GW (blue diamonds). Within the 2012 excavation locations approximately 76% were within 1.5’ of a GW (yellow circles). (The shrink sleeve utilized was 34” total, therefore the length from each side of the GW is app 1.5’). The depth of metal loss found within these excavations relative to distance from the girth weld is shown below.”



The second analysis had to do with the estimated cubic yards of dirt excavated during each anomaly dig. Plains’ personnel explained to PHMSA that they were required to keep their excavations below 100 cubic feet. This is important because PHMSA was told by the Plains’ IMP Group that Santa Barbara County has strict requirements for excavators and that obtaining a permit for larger excavations would take from six months or more to obtain a permit. However, Plains’ IMP Group reported that there is an exception for excavations made that are less than 100 cubic yards of dirt. Below is an excerpt from the “Santa Barbara County, Planning and Development, Building and Safety Division Grading Plan Submittal Requirements for Projects (Other than Subdivisions)” delineating exception #4.

(b) Aside from areas designated as open space on the Orcutt Community Plan Open Space Areas Map, these regulations shall not apply to the following exceptions:

- (4) The initial excavation and fill necessary to effect such temporary repair or maintenance of oil and gas and utility lines (located outside of an existing oil producing area) as can be completed within seven days of commencement where such excavation or fill does not exceed a total of one hundred cubic yards of material and where all work is protected, as may be required, by a safety fence or other similar protective device;

The following spreadsheet is a calculated estimate of the amount of dirt excavated during a number of the anomaly digs in 2007 and 2012. On the right of the figure there are some noted assumptions including:

- “* Assuming 10’ width and 8’ depth
- ** Does not include side or end wall terracing
- Lengths taken from individual “Pipeline Inspection and Repair Reports”
- *** Lengths in Repair Reports are inconsistent
- Some refer to the full dig opening and others refer to the repaired/recoat length only.”

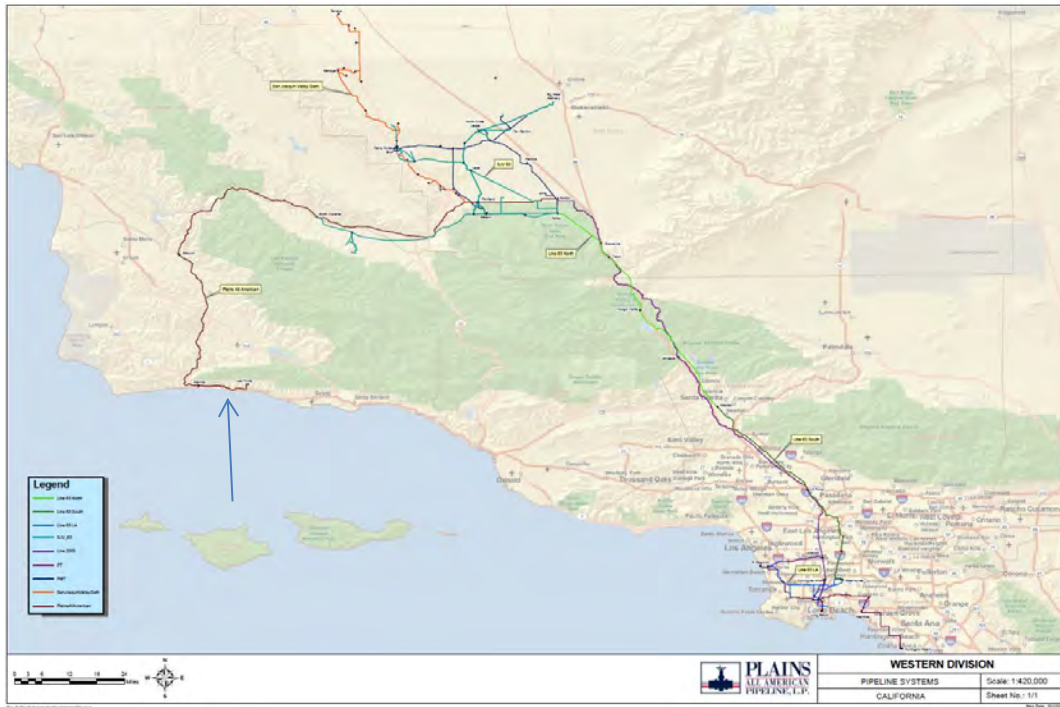
2007 Excavations			2012 Excavations			NOTE
Dig #	Lengt h	App. Volume*	Dig#	Lengt h	App. Volume*	
3	4.8	14.2	1	11.2	33.2	*Assuming 10' width and 8' depth
3A	10.3	30.5	2	9.6	28.4	
4	13.5	40.0	3	14.6	43.3	**does not include side or end wall terracing
5	3.0	8.9	4	16.8	49.8	Lengths taken from individual "Pipeline Inspection and Repair Reports"
6	8.0	23.7	5	13.5	40.0	
7	7.1	21.0	6	9.3	27.6	***Lengths in Repair Reports are inconsistent - Some refer to the full dig opening and others refer to the repaired/recoat length only
8	11.3	33.5	7	12.1	35.9	
9	4.4	13.0	8	7.8	23.1	6' d/s of failure
10	11.1	32.9	9	2.1	6.2	
11	2.5	7.4	10	12.0	35.6	
11B	3.0	8.9	11	11.3	33.5	
12	2.7	8.0	12	6.6	19.6	
13	3.0	8.9	13	8.0	23.7	
			14	6.7	19.9	
			15	8.3	24.6	
			16	6.5	19.3	
			17	7.1	21.0	
			18	6.0	17.8	
			19	9.6	28.4	
			20	7.7	22.8	
			20A	8.7	25.8	
			21	5.8	17.2	
			21A	5.5	16.3	
			22	6.3	18.7	
			23	5.8	17.2	
			24	7.1	21.0	
			25	7.3	21.6	
			26	5.0	14.8	
			27	7.9	23.4	
			28	9.0	26.7	
			29	6.9	20.4	
			30	6.6	19.6	
			31	5.8	17.2	
			32	12.2	36.1	
			33	6.2	18.4	
			33A	6.7	19.9	
			34	5.6	16.6	
			35	8.6	25.5	
			36	16.0	47.4	
			37	4.0	11.9	
			38	12.1	35.9	
			39	6.1	18.1	
			40	8.8	26.1	
			41	4.8	14.2	

This spreadsheet was created to estimate excavated soil volumes for each anomaly dig. Dig numbers are provided as well as volume estimates and assumptions used. Volume was calculated in Cubic Feet and converted to Cubic Yards.

If the volume estimates are doubled, they all still come in under the 100 cubic yard threshold. Dig #13 in 2012, was located only six feet downstream of the failure location.

Appendix I
Maps and Photographs

Appendix I: Maps and Photographs



Map of Plains' Western Division Pipelines. The arrow in the ocean is pointing to the approximate release site on line 901.



Overview from Santa Barbara Spill Web Site



Release Site with Culvert in the foreground. Vacuum Truck sucking up pooled oil in the background.



Culvert Under Highway and RR Tracks to Ocean



This picture shows the release site wrapped in plastic 6 feet upstream from girth weld 5940 where the coating repair is visible. The repair was identified as Dig #13 from the Post 2012 ILI Survey Anomaly Digs.



This is one of the first pictures of the release location after removal from the ditch.

Plains All American Pipeline, L.P.
Line 901 Release (05-19-15): Mechanical and Metallurgical Testing



Figure 2. Photograph showing Pipe Section 1 following removal from the ditch.

This picture was copied from the Final Metallurgical Report. One can see the bare pipe where the insulation and other coatings were removed to allow the pipe to be cut.

Appendix J

National Response Center Report #1



Pipeline & Hazardous Materials Safety Administration (Version 4.0.0 PROD)

HMIS->INCIDENTS->TELEPHONICS

[Rules of Behavior](#)

[Home](#)

[Logout](#)

[Menu](#)

[\[Return to Search\]](#)

NRC Number: 1116950
 Call Date: 05/19/2015 Call Time: 15:43:00

Caller Information

First Name: _____ Last Name: 2457
 Company Name: SANTA BARBARA DISPATCH
 Address: MSD SANTA BARBARA
 City: SANTA BARBARA State: CA
 Country: USA Zip: 93019
 Phone 1: 8056832724 Phone 2: _____
 Organization Type: PRIVATE I Is caller the spiller? Yes No No Response
 Confidential: Yes No No Response

Discharger Information

First Name: _____ Last Name: UNKNOWN
 Company Name: _____
 Address: _____
 City: _____ State: XX
 Country: USA Zip: _____
 Phone 1: _____ Phone 2: _____
 Organization Type: UNKNOWN

Spill Information

State: CA County: SANTA BARBARA
 Nearest City: _____ Zip Code: _____
Location
 HWY 101 AT REFUGIO BEACH

Spill Date: 05/19/2015 (mm/dd/yyyy) Spill Time: 12:39:00 (24h:mm:ss)
 DTG Type: <- Select DTG Type ->
 Incident Type: ALL Reported Incident Type: UNKNOWN SHEEN

Description
 CALLER REPORTED AND UNKNOWN SHEEN COMING FROM AN UNKNOWN SOURCE.

Materials Involved

Material / Chris Name	Chris Code	Total Qty.	Water Qty.
UNKNOWN OIL	OUN	0 UNKNOWN AMOUNT	0 UNKNOWN AMOUNT

Medium Type: <- Select Medium Type ->

Additional Medium Information:

PACIFIC OCEAN

Injuries: _____ Fatalities: _____
 Evacuations: Yes No Unknown No. of Evacuations: _____
 Damages: Yes No Unknown Damage Amount: _____
 Federal Agency Notified: Yes No Unknown State Agency Notified: Yes No Unknown
 Other Agency Notified: Yes No Unknown

Remedial Actions

Additional Info
VERY LIMITED INFORMATION.

<u>Latitude</u>				
Degrees:	<input type="text"/>	Minutes:	<input type="text"/>	Seconds: <input type="text"/> Quadrant: <input type="text"/>
<u>Longitude</u>				
Degrees:	<input type="text"/>	Minutes:	<input type="text"/>	Seconds: <input type="text"/> Quadrant: <input type="text"/>
Distance from City:	<input type="text"/>		Direction:	<input type="text"/>
Section:	<input type="text"/>		Township:	<input type="text"/>
Range:	<input type="text"/>		Milepost:	<input type="text"/>

Rescinded Comments (max 250 characters)

<< Previous

11..11 of 26

Next >>

Appendix K

National Response Center Report #2



[\[Return to Search\]](#)

NRC Number: 1116972
 Call Date: 05/19/2015 Call Time: 17:56:00

Caller Information

First Name: JAMES Last Name: BUCHAIAN
 Company Name: PLAINS ALL AMERICAN PIPELINE
 Address: 3600 BOWMAN CT
 City: BAKERSFIELD State: CA
 Country: USA Zip: 93308
 Phone 1: 6613367906 Phone 2: 6614371459
 Organization Type: PRIVATE I Is caller the spiller? Yes No No Response
 Confidential: Yes No No Response

Discharger Information

First Name: JAMES Last Name: BUCHANAN
 Company Name: PLAINS ALL AMERICAN PIPELINE
 Address: 3600 BOWMAN CT
 City: BAKERSFIELD State: CA
 Country: USA Zip: 93308
 Phone 1: 6613367906 Phone 2: 6614371459
 Organization Type: PRIVATE I

Spill Information

State: CA County: SANTA BARBARA
 Nearest City: GOLETA Zip Code:

Location
 SEE LAT/LONG

Spill Date: 05/19/2015 (mm/dd/yyyy) Spill Time: 13:30:00 (24h:mm:ss)
 DTG Type: <- Select DTG Type ->
 Incident Type: ALL Reported Incident Type: PIPELINE

Description
 CALLER STATED THAT CRUDE OIL WAS DISCOVERED TO BE COMING OUT OF A TRANSMISSION PIPELINE AT A CULVERT UNDER HWY 1 BY THE PACIFIC OCEAN. THE SPILL DID IMPACT AN UNNAMED BEACH AS WELL AS THE OCEAN. CALLER IS ESTIMATING THE AMOUNT SPILLED IS GREATER THAN 500 BARRELS BUT THERE IS LIMITED INFORMATION AT THIS TIME.

Materials Involved

Material / Chris Name	Chris Code	Total Qty.	Water Qty.
OIL: CRUDE	OIL	500 BARREL(S)	0 UNKNOWN AMOUNT

Medium Type: <- Select Medium Type ->

Additional Medium Information:

PACIFIC OCEAN

Injuries: Fatalities:
 Evacuations: Yes No Unknown No. of Evacuations:
 Damages: Yes No Unknown Damage Amount:
 Federal Agency Notified: Yes No Unknown State Agency Notified: Yes No Unknown
 Other Agency Notified: Yes No Unknown

Remedial Actions

LINE HAS BEEN SHUT IN. CONTRACTORS ARE ONSCENE.

Additional Info

Latitude

Degrees: 34 Minutes: 27 Seconds: 43 Quadrant: N

Longitude

Degrees: 120 Minutes: 5 Seconds: 24 Quadrant: W

Distance from City: Direction:

Section: Township:

Range: Milepost:

Rescinded Comments (max 250 characters)

<< Previous

1..1 of 1

<< Save >>

Appendix L

Form PHMSA F 7000.1: Accident Report for Hazardous Liquid Pipeline Systems

NOTICE: This report is required by 49 CFR Part 195. Failure to report can result in a civil penalty not to exceed \$100,000 for each violation for each day that such violation persists except that the maximum civil penalty shall not exceed \$1,000,000 as provided in 49 USC 60122.		OMB NO: 2137-0047 EXPIRATION DATE: 12/31/2016
 U.S. Department of Transportation Pipeline and Hazardous Materials Safety Administration	Original Report Date:	06/17/2015
	No.	20150224 - 21010 ----- (DOT Use Only)

**ACCIDENT REPORT - HAZARDOUS LIQUID
PIPELINE SYSTEMS**

A federal agency may not conduct or sponsor, and a person is not required to respond to, nor shall a person be subject to a penalty for failure to comply with a collection of information subject to the requirements of the Paperwork Reduction Act unless that collection of information displays a current valid OMB Control Number. The OMB Control Number for this information collection is 2137-0047. All responses to the collection of information are mandatory. Send comments regarding this burden or any other aspect of this collection of information, including suggestions for reducing the burden to: Information Collection Clearance Officer, PHMSA, Office of Pipeline Safety (PHP-30) 1200 New Jersey Avenue, SE, Washington, D.C. 20590.

INSTRUCTIONS

Important: Please read the separate instructions for completing this form before you begin. They clarify the information requested and provide specific examples. If you do not have a copy of the instructions, you can obtain one from the PHMSA Pipeline Safety Community Web Page at <http://www.phmsa.dot.gov/pipeline/library/forms>.

PART A - KEY REPORT INFORMATION

Report Type: (select all that apply)	Original:	Supplemental:	Final:
		Yes	
Last Revision Date:	12/23/2015		
1. Operator's OPS-issued Operator Identification Number (OPID):	300		
2. Name of Operator	PLAINS PIPELINE, L.P.		
3. Address of Operator:			
3a. Street Address	333 CLAY STREET, SUITE 1600		
3b. City	HOUSTON		
3c. State	Texas		
3d. Zip Code	77002		
4. Local time (24-hr clock) and date of the Accident:	05/19/2015 10:57		
5. Location of Accident:			
Latitude:	34.462434		
Longitude:	-120.086714		
6. National Response Center Report Number (if applicable):	1116972		
7. Local time (24-hr clock) and date of initial telephonic report to the National Response Center (if applicable):	05/19/2015 14:56		
8. Commodity released: (select only one, based on predominant volume released)	Crude Oil		
- Specify Commodity Subtype:			
- If "Other" Subtype, Describe:			
- If Biofuel/Alternative Fuel and Commodity Subtype is Ethanol Blend, then % Ethanol Blend:			
- If Biofuel/Alternative Fuel and Commodity Subtype is Biodiesel, then Biodiesel Blend e.g. B2, B20, B100			
9. Estimated volume of commodity released unintentionally (Barrels):	2,934.00		
10. Estimated volume of intentional and/or controlled release/blowdown (Barrels):			
11. Estimated volume of commodity recovered (Barrels):	1,100.00		
12. Were there fatalities?	No		
- If Yes, specify the number in each category:			
12a. Operator employees			
12b. Contractor employees working for the Operator			
12c. Non-Operator emergency responders			
12d. Workers working on the right-of-way, but NOT associated with this Operator			
12e. General public			
12f. Total fatalities (sum of above)			
13. Were there injuries requiring inpatient hospitalization?	No		
- If Yes, specify the number in each category:			
13a. Operator employees			
13b. Contractor employees working for the Operator			
13c. Non-Operator emergency responders			
13d. Workers working on the right-of-way, but NOT associated with this Operator			
13e. General public			

13f. Total injuries (sum of above)	
14. Was the pipeline/facility shut down due to the Accident?	Yes
- If No, Explain:	
- If Yes, complete Questions 14a and 14b: (use local time, 24-hr clock)	
14a. Local time and date of shutdown:	05/19/2015 11:30
14b. Local time pipeline/facility restarted:	
- Still shut down? (* Supplemental Report Required)	Yes
15. Did the commodity ignite?	No
16. Did the commodity explode?	No
17. Number of general public evacuated:	1
18. Time sequence (use local time, 24-hour clock):	
18a. Local time Operator identified Accident - effective 7- 2014 changed to "Local time Operator identified failure":	05/19/2015 13:27
18b. Local time Operator resources arrived on site:	05/19/2015 13:27
PART B - ADDITIONAL LOCATION INFORMATION	
1. Was the origin of the Accident onshore?	Yes
	<i>If Yes, Complete Questions (2-12)</i>
	<i>If No, Complete Questions (13-15)</i>
- If Onshore:	
2. State:	California
3. Zip Code:	93117
4. City:	Goleta
5. County or Parish:	Santa Barbara
6. Operator-designated location:	Milepost/Valve Station
	Specify: 4
7. Pipeline/Facility name:	Las Flores to Gaviota 24"
8. Segment name/ID:	Line 901
9. Was Accident on Federal land, other than the Outer Continental Shelf (OCS)?	No
10. Location of Accident:	Pipeline Right-of-way
11. Area of Accident (as found):	Underground
	Specify: Under soil
	- If Other, Describe:
	Depth-of-Cover (in): 56
12. Did Accident occur in a crossing?	No
- If Yes, specify type below:	
- If Bridge crossing –	
	Cased/ Uncased:
- If Railroad crossing –	
	Cased/ Uncased/ Bored/drilled
- If Road crossing –	
	Cased/ Uncased/ Bored/drilled
- If Water crossing –	
	Cased/ Uncased
	- Name of body of water, if commonly known:
	- Approx. water depth (ft) at the point of the Accident:
	- Select:
- If Offshore:	
13. Approximate water depth (ft) at the point of the Accident:	
14. Origin of Accident:	
- In State waters - Specify:	
	- State:
	- Area:
	- Block/Tract #:
	- Nearest County/Parish:
- On the Outer Continental Shelf (OCS) - Specify:	
	- Area:
	- Block #:
15. Area of Accident:	
PART C - ADDITIONAL FACILITY INFORMATION	
1. Is the pipeline or facility:	Interstate
2. Part of system involved in Accident:	Onshore Pipeline, Including Valve Sites
- If Onshore Breakout Tank or Storage Vessel, Including Attached Appurtenances, specify:	
3. Item involved in Accident:	Pipe
- If Pipe, specify:	Pipe Body
3a. Nominal diameter of pipe (in):	24

3b. Wall thickness (in):	.344
3c. SMYS (Specified Minimum Yield Strength) of pipe (psi):	65,000
3d. Pipe specification:	X-65
3e. Pipe Seam , specify:	Longitudinal ERW - High Frequency
- If Other, Describe:	
3f. Pipe manufacturer:	Nippon Steel
3g. Year of manufacture:	1986
3h. Pipeline coating type at point of Accident, specify:	Coal Tar
- If Other, Describe:	
- If Weld, including heat-affected zone, specify. If Pipe Girth Weld, 3a through 3h above are required:	
- If Other, Describe:	
- If Valve, specify:	
- If Mainline, specify:	
- If Other, Describe:	
3i. Manufactured by:	
3j. Year of manufacture:	
- If Tank/Vessel, specify:	
- If Other - Describe:	
- If Other, describe:	
4. Year item involved in Accident was installed:	1990
5. Material involved in Accident:	Carbon Steel
- If Material other than Carbon Steel, specify:	
6. Type of Accident Involved:	Leak
- If Mechanical Puncture – Specify Approx. size:	
in. (axial) by	
in. (circumferential)	
- If Leak - Select Type:	Other
- If Other, Describe:	Narrow slit opening.
- If Rupture - Select Orientation:	
- If Other, Describe:	
Approx. size: in. (widest opening) by	
in. (length circumferentially or axially)	
- If Other – Describe:	
PART D - ADDITIONAL CONSEQUENCE INFORMATION	
1. Wildlife impact:	Yes
1a. If Yes, specify all that apply:	
- Fish/aquatic	Yes
- Birds	Yes
- Terrestrial	Yes
2. Soil contamination:	Yes
3. Long term impact assessment performed or planned:	Yes
4. Anticipated remediation:	Yes
4a. If Yes, specify all that apply:	
- Surface water	Yes
- Groundwater	
- Soil	Yes
- Vegetation	Yes
- Wildlife	Yes
5. Water contamination:	Yes
5a. If Yes, specify all that apply:	
- Ocean/Seawater	Yes
- Surface	Yes
- Groundwater	
- Drinking water: (Select one or both)	
- Private Well	
- Public Water Intake	
5b. Estimated amount released in or reaching water (Barrels):	500.00
5c. Name of body of water, if commonly known:	Pacific Ocean.
6. At the location of this Accident, had the pipeline segment or facility been identified as one that "could affect" a High Consequence Area (HCA) as determined in the Operator's Integrity Management Program?	Yes
7. Did the released commodity reach or occur in one or more High Consequence Area (HCA)?	Yes
7a. If Yes, specify HCA type(s): (Select all that apply)	
- Commercially Navigable Waterway:	Yes
Was this HCA identified in the "could affect" determination for this Accident site in the Operator's	Yes

Integrity Management Program?	
- High Population Area:	
Was this HCA identified in the "could affect" determination for this Accident site in the Operator's Integrity Management Program?	
- Other Populated Area	
Was this HCA identified in the "could affect" determination for this Accident site in the Operator's Integrity Management Program?	
- Unusually Sensitive Area (USA) - Drinking Water	
Was this HCA identified in the "could affect" determination for this Accident site in the Operator's Integrity Management Program?	
- Unusually Sensitive Area (USA) - Ecological	Yes
Was this HCA identified in the "could affect" determination for this Accident site in the Operator's Integrity Management Program?	Yes
8. Estimated cost to Operator – effective 12-2012, changed to "Estimated Property Damage":	
8a. Estimated cost of public and non-Operator private property damage paid/reimbursed by the Operator – effective 12-2012, "paid/reimbursed by the Operator" removed	\$ 0
8b. Estimated cost of commodity lost	\$ 144,000
8c. Estimated cost of Operator's property damage & repairs	\$ 9,868,173
8d. Estimated cost of Operator's emergency response	\$ 90,701,042
8e. Estimated cost of Operator's environmental remediation	\$ 22,421,933
8f. Estimated other costs	\$ 19,796,736
Describe:	Government Agency Costs and Media Relations.
8g. Estimated total costs (sum of above) – effective 12-2012, changed to "Total estimated property damage (sum of above)"	\$ 142,931,884
PART E - ADDITIONAL OPERATING INFORMATION	
1. Estimated pressure at the point and time of the Accident (psig):	750.00
2. Maximum Operating Pressure (MOP) at the point and time of the Accident (psig):	1,056.00
3. Describe the pressure on the system or facility relating to the Accident (psig):	Pressure did not exceed MOP
4. Not including pressure reductions required by PHMSA regulations (such as for repairs and pipe movement), was the system or facility relating to the Accident operating under an established pressure restriction with pressure limits below those normally allowed by the MOP?	No
- If Yes, Complete 4.a and 4.b below:	
4a. Did the pressure exceed this established pressure restriction?	
4b. Was this pressure restriction mandated by PHMSA or the State?	
5. Was "Onshore Pipeline, Including Valve Sites" OR "Offshore Pipeline, Including Riser and Riser Bend" selected in PART C, Question 2?	Yes
- If Yes - (Complete 5a. – 5f below) effective 12-2012, changed to "(Complete 5.a – 5.e below)"	
5a. Type of upstream valve used to initially isolate release source:	Remotely Controlled
5b. Type of downstream valve used to initially isolate release source:	Check Valve
5c. Length of segment isolated between valves (ft):	56,752
5d. Is the pipeline configured to accommodate internal inspection tools?	Yes
- If No, Which physical features limit tool accommodation? (select all that apply)	
- Changes in line pipe diameter	
- Presence of unsuitable mainline valves	
- Tight or mitered pipe bends	
- Other passage restrictions (i.e. unbarred tee's, projecting instrumentation, etc.)	
- Extra thick pipe wall (applicable only for magnetic flux leakage internal inspection tools)	
- Other -	
- If Other, Describe:	
5e. For this pipeline, are there operational factors which significantly complicate the execution of an internal inspection tool run?	No
- If Yes, Which operational factors complicate execution? (select all that apply)	

- Excessive debris or scale, wax, or other wall buildup	
- Low operating pressure(s)	
- Low flow or absence of flow	
- Incompatible commodity	
- Other -	
- If Other, Describe:	
5f. Function of pipeline system:	> 20% SMYS Regulated Trunkline/Transmission
6. Was a Supervisory Control and Data Acquisition (SCADA)-based system in place on the pipeline or facility involved in the Accident?	Yes
If Yes -	
6a. Was it operating at the time of the Accident?	Yes
6b. Was it fully functional at the time of the Accident?	Yes
6c. Did SCADA-based information (such as alarm(s), alert(s), event(s), and/or volume calculations) assist with the detection of the Accident?	Yes
6d. Did SCADA-based information (such as alarm(s), alert(s), event(s), and/or volume calculations) assist with the confirmation of the Accident?	Yes
7. Was a CPM leak detection system in place on the pipeline or facility involved in the Accident?	Yes
- If Yes:	
7a. Was it operating at the time of the Accident?	Yes
7b. Was it fully functional at the time of the Accident?	Yes
7c. Did CPM leak detection system information (such as alarm(s), alert(s), event(s), and/or volume calculations) assist with the detection of the Accident?	No
7d. Did CPM leak detection system information (such as alarm(s), alert(s), event(s), and/or volume calculations) assist with the confirmation of the Accident?	No
8. How was the Accident initially identified for the Operator?	Local Operating Personnel, including contractors
- If Other, Specify:	
8a. If "Controller", "Local Operating Personnel", including contractors", "Air Patrol", or "Ground Patrol by Operator or its contractor" is selected in Question 8, specify:	Operator employee
9. Was an investigation initiated into whether or not the controller(s) or control room issues were the cause of or a contributing factor to the Accident?	Yes, specify investigation result(s): (select all that apply)
- If No, the Operator did not find that an investigation of the controller(s) actions or control room issues was necessary due to: (provide an explanation for why the operator did not investigate)	
- If Yes, specify investigation result(s): (select all that apply)	
- Investigation reviewed work schedule rotations, continuous hours of service (while working for the Operator), and other factors associated with fatigue	Yes
- Investigation did NOT review work schedule rotations, continuous hours of service (while working for the Operator), and other factors associated with fatigue	
Provide an explanation for why not:	
- Investigation identified no control room issues	Yes
- Investigation identified no controller issues	Yes
- Investigation identified incorrect controller action or controller error	
- Investigation identified that fatigue may have affected the controller(s) involved or impacted the involved controller(s) response	
- Investigation identified incorrect procedures	
- Investigation identified incorrect control room equipment operation	
- Investigation identified maintenance activities that affected control room operations, procedures, and/or controller response	Yes
- Investigation identified areas other than those above:	Yes
Describe:	Investigation identified that a minor procedure was not followed. This failure was not a cause of or contributing factor to the Accident. Additional training on this procedure has been provided.
PART F - DRUG & ALCOHOL TESTING INFORMATION	

1. As a result of this Accident, were any Operator employees tested under the post-accident drug and alcohol testing requirements of DOT's Drug & Alcohol Testing regulations?	Yes
- If Yes:	
1a. Specify how many were tested:	1
1b. Specify how many failed:	0
2. As a result of this Accident, were any Operator contractor employees tested under the post-accident drug and alcohol testing requirements of DOT's Drug & Alcohol Testing regulations?	No
- If Yes:	
2a. Specify how many were tested:	
2b. Specify how many failed:	
PART G – APPARENT CAUSE	
Select only one box from PART G in shaded column on left representing the APPARENT Cause of the Accident, and answer the questions on the right. Describe secondary, contributing or root causes of the Accident in the narrative (PART H).	
Apparent Cause:	G1 - Corrosion Failure
G1 - Corrosion Failure - only one sub-cause can be picked from shaded left-hand column	
Corrosion Failure – Sub-Cause:	External Corrosion
- If External Corrosion:	
1. Results of visual examination:	Other
- If Other, Describe:	Corrosion under insulation.
2. Type of corrosion: <i>(select all that apply)</i>	
- Galvanic	
- Atmospheric	
- Stray Current	
- Microbiological	
- Selective Seam	
- Other:	Yes
- If Other, Describe:	Corrosion under insulation.
3. The type(s) of corrosion selected in Question 2 is based on the following: <i>(select all that apply)</i>	
- Field examination	
- Determined by metallurgical analysis	Yes
- Other:	
- If Other, Describe:	
4. Was the failed item buried under the ground?	Yes
- If Yes :	
<input type="checkbox"/> 4a. Was failed item considered to be under cathodic protection at the time of the Accident?	Yes
If Yes - Year protection started:	1990
4b. Was shielding, tenting, or disbonding of coating evident at the point of the Accident?	Yes
4c. Has one or more Cathodic Protection Survey been conducted at the point of the Accident?	Yes
If "Yes, CP Annual Survey" – Most recent year conducted:	2015
If "Yes, Close Interval Survey" – Most recent year conducted:	2015
If "Yes, Other CP Survey" – Most recent year conducted:	
- If No:	
4d. Was the failed item externally coated or painted?	
5. Was there observable damage to the coating or paint in the vicinity of the corrosion?	Yes
- If Internal Corrosion:	
6. Results of visual examination:	
- Other:	
7. Type of corrosion <i>(select all that apply)</i> : -	
- Corrosive Commodity	
- Water drop-out/Acid	
- Microbiological	
- Erosion	
- Other:	
- If Other, Describe:	
8. The cause(s) of corrosion selected in Question 7 is based on the following <i>(select all that apply)</i> : -	
- Field examination	
- Determined by metallurgical analysis	
- Other:	

- If Other, Describe:		
9. Location of corrosion (select all that apply): -		
- Low point in pipe		
- Elbow		
- Other:		
- If Other, Describe:		
10. Was the commodity treated with corrosion inhibitors or biocides?		
11. Was the interior coated or lined with protective coating?		
12. Were cleaning/dewatering pigs (or other operations) routinely utilized?		
13. Were corrosion coupons routinely utilized?		
Complete the following if any Corrosion Failure sub-cause is selected AND the "Item Involved in Accident" (from PART C, Question 3) is Tank/Vessel.		
14. List the year of the most recent inspections:		
14a. API Std 653 Out-of-Service Inspection		
- No Out-of-Service Inspection completed		
14b. API Std 653 In-Service Inspection		
- No In-Service Inspection completed		
Complete the following if any Corrosion Failure sub-cause is selected AND the "Item Involved in Accident" (from PART C, Question 3) is Pipe or Weld.		
15. Has one or more internal inspection tool collected data at the point of the Accident?		Yes
15a. If Yes, for each tool used, select type of internal inspection tool and indicate most recent year run: -		
- Magnetic Flux Leakage Tool		Yes
Most recent year:		2015
- Ultrasonic		
Most recent year:		
- Geometry		
Most recent year:		
- Caliper		Yes
Most recent year:		2015
- Crack		
Most recent year:		
- Hard Spot		
Most recent year:		
- Combination Tool		Yes
Most recent year:		2015
- Transverse Field/Triaxial		
Most recent year:		
- Other		
Most recent year:		
Describe:		
16. Has one or more hydrotest or other pressure test been conducted since original construction at the point of the Accident?		No
If Yes -		
Most recent year tested:		
Test pressure:		
17. Has one or more Direct Assessment been conducted on this segment?		No
- If Yes, and an investigative dig was conducted at the point of the Accident::		
Most recent year conducted:		
- If Yes, but the point of the Accident was not identified as a dig site:		
Most recent year conducted:		
18. Has one or more non-destructive examination been conducted at the point of the Accident since January 1, 2002?		No
18a. If Yes, for each examination conducted since January 1, 2002, select type of non-destructive examination and indicate most recent year the examination was conducted:		
- Radiography		
Most recent year conducted:		
- Guided Wave Ultrasonic		
Most recent year conducted:		
- Handheld Ultrasonic Tool		
Most recent year conducted:		
- Wet Magnetic Particle Test		
Most recent year conducted:		
- Dry Magnetic Particle Test		
Most recent year conducted:		
- Other		
Most recent year conducted:		
Describe:		

G2 - Natural Force Damage - only one sub-cause can be picked from shaded left-handed column	
Natural Force Damage – Sub-Cause:	
- If Earth Movement, NOT due to Heavy Rains/Floods:	
1. Specify:	
	- If Other, Describe:
- If Heavy Rains/Floods:	
2. Specify:	
	- If Other, Describe:
- If Lightning:	
3. Specify:	
- If Temperature:	
4. Specify:	
	- If Other, Describe:
- If Other Natural Force Damage:	
5. Describe:	
Complete the following if any Natural Force Damage sub-cause is selected.	
6. Were the natural forces causing the Accident generated in conjunction with an extreme weather event?	
6a. If Yes, specify: <i>(select all that apply)</i>	
	- Hurricane
	- Tropical Storm
	- Tornado
	- Other
	- If Other, Describe:
G3 - Excavation Damage - only one sub-cause can be picked from shaded left-hand column	
Excavation Damage – Sub-Cause:	
- If Previous Damage due to Excavation Activity: Complete Questions 1-5 ONLY IF the "Item Involved in Accident" (from PART C, Question 3) is Pipe or Weld.	
1. Has one or more internal inspection tool collected data at the point of the Accident?	
1a. If Yes, for each tool used, select type of internal inspection tool and indicate most recent year run: -	
	- Magnetic Flux Leakage
	Most recent year conducted:
	- Ultrasonic
	Most recent year conducted:
	- Geometry
	Most recent year conducted:
	- Caliper
	Most recent year conducted:
	- Crack
	Most recent year conducted:
	- Hard Spot
	Most recent year conducted:
	- Combination Tool
	Most recent year conducted:
	- Transverse Field/Triaxial
	Most recent year conducted:
	- Other
	Most recent year conducted:
	Describe:
2. Do you have reason to believe that the internal inspection was completed BEFORE the damage was sustained?	
3. Has one or more hydrotest or other pressure test been conducted since original construction at the point of the Accident?	
	- If Yes:
	Most recent year tested:
	Test pressure (psig):
4. Has one or more Direct Assessment been conducted on the pipeline segment?	
	- If Yes, and an investigative dig was conducted at the point of the Accident:
	Most recent year conducted:
	- If Yes, but the point of the Accident was not identified as a dig site:
	Most recent year conducted:
5. Has one or more non-destructive examination been conducted at the point of the Accident since January 1, 2002?	

5a. If Yes, for each examination, conducted since January 1, 2002, select type of non-destructive examination and indicate most recent year the examination was conducted:	
- Radiography	Most recent year conducted:
- Guided Wave Ultrasonic	Most recent year conducted:
- Handheld Ultrasonic Tool	Most recent year conducted:
- Wet Magnetic Particle Test	Most recent year conducted:
- Dry Magnetic Particle Test	Most recent year conducted:
- Other	Most recent year conducted:
Describe:	
Complete the following if Excavation Damage by Third Party is selected as the sub-cause.	
6. Did the operator get prior notification of the excavation activity?	
6a. If Yes, Notification received from: <i>(select all that apply)</i> -	
- One-Call System	
- Excavator	
- Contractor	
- Landowner	
Complete the following mandatory CGA-DIRT Program questions if any Excavation Damage sub-cause is selected.	
7. Do you want PHMSA to upload the following information to CGA-DIRT (www.cga-dirt.com)?	
8. Right-of-Way where event occurred: <i>(select all that apply)</i> -	
- Public	- If "Public", Specify:
- Private	- If "Private", Specify:
- Pipeline Property/Easement	
- Power/Transmission Line	
- Railroad	
- Dedicated Public Utility Easement	
- Federal Land	
- Data not collected	
- Unknown/Other	
9. Type of excavator:	
10. Type of excavation equipment:	
11. Type of work performed:	
12. Was the One-Call Center notified?	
12a. If Yes, specify ticket number:	
12b. If this is a State where more than a single One-Call Center exists, list the name of the One-Call Center notified:	
13. Type of Locator:	
14. Were facility locate marks visible in the area of excavation?	
15. Were facilities marked correctly?	
16. Did the damage cause an interruption in service?	
16a. If Yes, specify duration of the interruption (hours)	
17. Description of the CGA-DIRT Root Cause <i>(select only the one predominant first level CGA-DIRT Root Cause and then, where available as a choice, the one predominant second level CGA-DIRT Root Cause as well):</i>	
Root Cause:	
- If One-Call Notification Practices Not Sufficient, specify:	
- If Locating Practices Not Sufficient, specify:	
- If Excavation Practices Not Sufficient, specify:	
- If Other/None of the Above, explain:	
G4 - Other Outside Force Damage - only one sub-cause can be selected from the shaded left-hand column	
Other Outside Force Damage – Sub-Cause:	
- If Damage by Car, Truck, or Other Motorized Vehicle/Equipment NOT Engaged in Excavation:	
1. Vehicle/Equipment operated by:	
- If Damage by Boats, Barges, Drilling Rigs, or Other Maritime Equipment or Vessels Set Adrift or Which Have Otherwise Lost Their Mooring:	
2. Select one or more of the following IF an extreme weather event was a factor:	
- Hurricane	
- Tropical Storm	
- Tornado	

- Heavy Rains/Flood	
- Other	
- If Other, Describe:	
- If Previous Mechanical Damage NOT Related to Excavation: Complete Questions 3-7 ONLY IF the "Item Involved in Accident" (from PART C, Question 3) is Pipe or Weld.	
3. Has one or more internal inspection tool collected data at the point of the Accident?	
3a. If Yes, for each tool used, select type of internal inspection tool and indicate most recent year run:	
- Magnetic Flux Leakage	Most recent year conducted:
- Ultrasonic	Most recent year conducted:
- Geometry	Most recent year conducted:
- Caliper	Most recent year conducted:
- Crack	Most recent year conducted:
- Hard Spot	Most recent year conducted:
- Combination Tool	Most recent year conducted:
- Transverse Field/Triaxial	Most recent year conducted:
- Other	Most recent year conducted:
	Describe:
4. Do you have reason to believe that the internal inspection was completed BEFORE the damage was sustained?	
5. Has one or more hydrotest or other pressure test been conducted since original construction at the point of the Accident?	
- If Yes:	
	Most recent year tested:
	Test pressure (psig):
6. Has one or more Direct Assessment been conducted on the pipeline segment?	
- If Yes, and an investigative dig was conducted at the point of the Accident:	Most recent year conducted:
- If Yes, but the point of the Accident was not identified as a dig site:	Most recent year conducted:
7. Has one or more non-destructive examination been conducted at the point of the Accident since January 1, 2002?	
7a. If Yes, for each examination conducted since January 1, 2002, select type of non-destructive examination and indicate most recent year the examination was conducted:	
- Radiography	Most recent year conducted:
- Guided Wave Ultrasonic	Most recent year conducted:
- Handheld Ultrasonic Tool	Most recent year conducted:
- Wet Magnetic Particle Test	Most recent year conducted:
- Dry Magnetic Particle Test	Most recent year conducted:
- Other	Most recent year conducted:
	Describe:
- If Intentional Damage:	
8. Specify:	
	- If Other, Describe:
- If Other Outside Force Damage:	
9. Describe:	
G5 - Material Failure of Pipe or Weld - only one sub-cause can be selected from the shaded left-hand column	
Use this section to report material failures ONLY IF the "Item Involved in Accident" (from PART C, Question 3) is "Pipe" or "Weld."	
Material Failure of Pipe or Weld – Sub-Cause:	
1. The sub-cause shown above is based on the following: <i>(select all that apply)</i>	

- Field Examination	
- Determined by Metallurgical Analysis	
- Other Analysis	
- If "Other Analysis", Describe:	
- Sub-cause is Tentative or Suspected; Still Under Investigation (Supplemental Report required)	
- If Construction, Installation, or Fabrication-related Or If Original Manufacturing-related:	
2. List contributing factors: <i>(select all that apply)</i>	
- Fatigue or Vibration-related	
Specify:	
- If Other, Describe:	
- Mechanical Stress:	
- Other	
- If Other, Describe:	
- If Environmental Cracking-related:	
3. Specify:	
- If Other - Describe:	
Complete the following if any Material Failure of Pipe or Weld sub-cause is selected.	
4. Additional factors: <i>(select all that apply)</i> :	
- Dent	
- Gouge	
- Pipe Bend	
- Arc Burn	
- Crack	
- Lack of Fusion	
- Lamination	
- Buckle	
- Wrinkle	
- Misalignment	
- Burnt Steel	
- Other:	
- If Other, Describe:	
5. Has one or more internal inspection tool collected data at the point of the Accident?	
5a. If Yes, for each tool used, select type of internal inspection tool and indicate most recent year run:	
- Magnetic Flux Leakage	
Most recent year run:	
- Ultrasonic	
Most recent year run:	
- Geometry	
Most recent year run:	
- Caliper	
Most recent year run:	
- Crack	
Most recent year run:	
- Hard Spot	
Most recent year run:	
- Combination Tool	
Most recent year run:	
- Transverse Field/Triaxial	
Most recent year run:	
- Other	
Most recent year run:	
Describe:	
6. Has one or more hydrotest or other pressure test been conducted since original construction at the point of the Accident?	
- If Yes:	
Most recent year tested:	
Test pressure (psig):	
7. Has one or more Direct Assessment been conducted on the pipeline segment?	
- If Yes, and an investigative dig was conducted at the point of the Accident -	
Most recent year conducted:	
- If Yes, but the point of the Accident was not identified as a dig site -	
Most recent year conducted:	
8. Has one or more non-destructive examination(s) been conducted at the point of the Accident since January 1, 2002?	
8a. If Yes, for each examination conducted since January 1, 2002, select type of non-destructive examination and indicate most recent year the examination was conducted: -	

- Radiography	Most recent year conducted:	
- Guided Wave Ultrasonic	Most recent year conducted:	
- Handheld Ultrasonic Tool	Most recent year conducted:	
- Wet Magnetic Particle Test	Most recent year conducted:	
- Dry Magnetic Particle Test	Most recent year conducted:	
- Other	Most recent year conducted:	
	Describe:	

G6 – Equipment Failure - only one **sub-cause** can be selected from the shaded left-hand column

Equipment Failure – Sub-Cause:

- If Malfunction of Control/Relief Equipment:

1. Specify: *(select all that apply)* -

- Control Valve	
- Instrumentation	
- SCADA	
- Communications	
- Block Valve	
- Check Valve	
- Relief Valve	
- Power Failure	
- Stopple/Control Fitting	
- ESD System Failure	
- Other	
	- If Other – Describe:

- If Pump or Pump-related Equipment:

2. Specify:

	- If Other – Describe:
--	------------------------

- If Threaded Connection/Coupling Failure:

3. Specify:

	- If Other – Describe:
--	------------------------

- If Non-threaded Connection Failure:

4. Specify:

	- If Other – Describe:
--	------------------------

- If Other Equipment Failure:

5. Describe:

--	--

Complete the following if any Equipment Failure sub-cause is selected.

6. Additional factors that contributed to the equipment failure: *(select all that apply)*

- Excessive vibration	
- Overpressurization	
- No support or loss of support	
- Manufacturing defect	
- Loss of electricity	
- Improper installation	
- Mismatched items (different manufacturer for tubing and tubing fittings)	
- Dissimilar metals	
- Breakdown of soft goods due to compatibility issues with transported commodity	
- Valve vault or valve can contributed to the release	
- Alarm/status failure	
- Misalignment	
- Thermal stress	
- Other	
	- If Other, Describe:

G7 - Incorrect Operation - only one **sub-cause** can be selected from the shaded left-hand column

Incorrect Operation – Sub-Cause:

--	--

- If Tank, Vessel, or Sump/Separator Allowed or Caused to Overfill or Overflow	
1. Specify:	
- If Other, Describe:	
- If Other Incorrect Operation	
2. Describe:	
Complete the following if any Incorrect Operation sub-cause is selected.	
3. Was this Accident related to <i>(select all that apply)</i> : -	
- Inadequate procedure	
- No procedure established	
- Failure to follow procedure	
- Other:	
- If Other, Describe:	
4. What category type was the activity that caused the Accident?	
5. Was the task(s) that led to the Accident identified as a covered task in your Operator Qualification Program?	
5a. If Yes, were the individuals performing the task(s) qualified for the task(s)?	
G8 - Other Accident Cause - only one sub-cause can be selected from the shaded left-hand column	
Other Accident Cause – Sub-Cause:	
- If Miscellaneous:	
1. Describe:	
- If Unknown:	
2. Specify:	
PART H - NARRATIVE DESCRIPTION OF THE ACCIDENT	
<p>Crude oil was released from a 24-inch pipeline, located along Highway 101 in Santa Barbara County, California. The released crude reached a culvert which leads to the Pacific Ocean and, as a result, impacted the shoreline and ocean water. The cause of the release is currently under investigation. The pipe has been excavated. The affected portion of pipe was securely packaged to preserve its condition and has been transported to a secure, independent facility for an independent third-party analysis and investigation. A supplemental report will be submitted upon receipt of the third party, metallurgical analysis. In the meantime, Plains personnel are actively engaged in cleanup and environmental remediation efforts.</p> <p>Part A. Question 7. - 14:56 is the time Operator notified the National Response Center (NRC). The NRC was first notified at 12:43 by an unrelated third party.</p> <p>Part A. Question 9. - Answer is a best-estimate as of 6/17/2015.</p> <p>Part A. Question 11.- Response reflects current estimate as of 6/17/2015. The volume of recovered commodity will be revised upward in the supplemental report as more information becomes available.</p> <p>Part A. Question 17. -The number of people evacuated from local State Park campsites is currently undetermined as no estimates are included in the initial first responder reports we have received. We are investigating this further and will revise the Supplemental report as more information becomes available.</p> <p>Part D. Question 8. - Answer reflects estimated costs incurred through 6/16/2015.</p> <p>Supplemental Narratives:</p> <p>Part A, Number 11 and Part D, Number 8 have also been updated to reflect new information as of 7/10/2015.</p> <p>As of 8/4/15 the current estimated release volume remains approx. 2,400 bbls. Preliminary data from the purge activity estimates the release could be potentially 3,400 bbls. While Plains believes the volume estimate listed in Part A, Question 9 best represents the potential discharge volume, we are working with an outside expert to reconcile the differences and will provide additional updates as appropriate.</p> <p>As of 11/24/2015, based on the work performed by our independent third party consultant (i.e. the 'outside expert' mentioned above), our best estimate of the spill volume is 2,934 barrels.</p> <p>The results of the metallurgical analysis of the pipeline segment indicate that the failure occurred at an area of wall thinning from external corrosion that ultimately failed by ductile overload under the imposed operating pressure. The morphology of the external corrosion observed on the pipe section is consistent with corrosion under insulation facilitated by wet-dry cycling.</p> <p>Line 901 remains shut down and subject to Corrective Action Order CPF No. 5-2015-5011H and Amendments. Updated costs for the repair and restart of this line, remains the only outstanding item in order to finalize this 7000-1 form.</p>	
PART I - PREPARER AND AUTHORIZED SIGNATURE	
Preparer's Name	Chrystah Carter
Preparer's Title	Compliance Specialist
Preparer's Telephone Number	713-993-5080
Preparer's E-mail Address	crarter@paalp.com
Preparer's Facsimile Number	713-646-4310
Authorized Signer Name	Troy E Valenzuela

Authorized Signer Title	VP of Environmental Health and Safety
Authorized Signer Telephone Number	713-646-4614
Authorized Signer Email	tevalenzuela@paalp.com
Date	12/23/2015

Appendix M

**Det Norske Veritas (U.S.A.), Inc. (DNV GL): Line 901
Release (5/19/15) Mechanical and Metallurgical Testing**

Final Report

Line 901 Release (5/19/15): Mechanical and Metallurgical Testing

Plains All American Pipeline, L.P.
Houston, Texas

Report No.: OAPUS309DNOR (PP136049)
September 18, 2015

Plains All American Pipeline, L.P.
Line 901 Release (05-19-15): Mechanical and Metallurgical Testing

Project Name:	Line 901 Release (05-19-15): Mechanical and Metallurgical Testing	DET NORSKE VERITAS (U.S.A.), INC. (DNV GL) Materials & Corrosion Technology Center Incident Investigation 5777 Frantz Road Dublin, OH 43017-1886 United States Tel: (614) 761-1214 Fax: (614) 761-1633 www.dnvgl.com
Customer:	Plains All American Pipeline, P.L.	
Contact Person:		
Date of Issue:	September 18, 2015	
Project No.:	PP136049	
Organization Unit:	Incident Investigation	
Report No.:	OAPUS309DNOR	

Task and Objective:

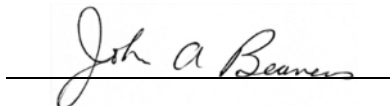
Please see Executive Summary.

Prepared by



David M. Norfleet, Ph.D., P.E.
Principal Engineer

Verified by



John A. Beavers, Ph.D., FNACE
Director – Incident Investigation

Approved by



Neil G. Thompson, Ph.D., FNACE
Senior VP, Pipeline Services

- Unrestricted Distribution (internal and external)
- Unrestricted Distribution within DNV GL
- Limited Distribution within DNV GL after 3 years
- No Distribution (confidential)
- Secret

Keywords

Rev. No.	Date	Reason for Issue:	Prepared by:	Verified by:	Approved by:
0	2015-08-06	First Issue			
1	2015-09-18	Final			

Copyright © DNV GL 2015. All rights reserved. This publication or parts thereof may not be copied, reproduced, or transmitted in any form, or by any means, whether digitally or otherwise without the prior written consent of DNV GL. DNV GL and the Horizon Graphic are trademarks of DNV GL AS. The content of this publication shall be kept confidential by the customer, unless otherwise agreed in writing. Reference to part of this publication, which may lead to misinterpretation, is prohibited.

Executive Summary

Plains All American Pipeline, L.P. (Plains) retained Det Norske Veritas (U.S.A.), Inc. (DNV GL) to perform a metallurgical analysis and mechanical testing on a section of pipe from Line 901 - Las Flores to Gaviota (L901), 24-inch nominal diameter crude oil pipeline that failed while in service. The failure occurred on May 19, 2015 in Goleta (Santa Barbara County), California at milepost (MP) 4, 33.5 feet downstream (D/S) of the nearest upstream (U/S) girth weld and 4.05 miles D/S of the nearest U/S pump station. A failure of a pipe segment can be characterized either as a leak or a rupture; the failure on L901 is characterized as a leak.¹

The section of the pipeline that failed is comprised of 24-inch diameter by 0.344-inch wall thickness, API 5L Grade X65 line pipe steel that contains a high frequency electric resistance welded (ERW) longitudinal seam and was manufactured by Nippon Steel in 1986. The maximum operating pressure (MOP) is 1,341² pounds per square inch gauge (psig) (72% of the specified minimum yield strength [SMYS]). The pressure at the time of failure was reported by Plains to be 737 psig (39.6% of SMYS) at the failure location and time of failure.

The pipeline was installed in 1990 and constructed using pipe that was externally coated with a coal tar urethane coating on the steel substrate, 1.5-inch thick rigid polyurethane foam, and an external polyethylene tape. The pipeline has an impressed current cathodic protection (CP) system with the nearest rectifier located 4.05 miles U/S of the failure location, at the Las Flores Pump Station. A hydrostatic test was performed at the time of commissioning for 8 hours at 1719 psi (Gaviota Station) on November 25th, 1990. In-line inspection (ILI) runs, consisting of deformation and magnetic flux leakage (MFL) tools, were performed in 2007, 2012, and 2015.

The failed pipe joint and 5 feet of the U/S and D/S joints were removed from the failure location and delivered to DNV GL in two pipe sections for analysis. Pipe Section 1 (PS 1) was 19.05 feet in length and contained 5.05 feet of the U/S joint, the U/S girth weld, and

-
- 1 According to the *FRACTURE CONTROL TECHNOLOGY FOR NATURAL GAS PIPELINES CIRCA 2001* (the PRCI report superseding NG-18 Report 208), "The distinction between leak and rupture for the pipeline community is based on the size and configuration of the breach, not how it develops. A "leak" is characterized by a narrow slit-like hole with length less than the diameter, which limits the fluid volume that escapes through the breach. In contrast, a "rupture" involves a longer, open hole that can be bulged over its length, which is on the order of a diameter or longer and can permit escape of a significant fluid volume." Similarly, the research performed as part of the historical NG-18 work identified empirical equations to predict the length at which a feature will propagate versus pop through and arrest; the leak/rupture length. Based on these calculations and visual observations, the length of the feature is consistent with a leak, arresting within the corrosion feature, and did not propagate outside of the feature into nominal wall-thickness pipe.
 - 2 Theoretical maximum operating pressure at the lowest elevation using the lowest pressure of either 80% of the commissioning hydro-test pressure, the 72% of SMYS, or the lowest component rating along the line segment.

15 feet of the failure joint located U/S of the failure. Pipe Section 2 (PS 2) was 31.06 feet in length and contained the failure location, the D/S girth weld, a 2013 composite repair sleeve, and 5 feet of the D/S joint. The objective of the analysis was to determine the metallurgical (or immediate) cause of the failure.

Metallurgical Cause: *The results of the metallurgical analysis indicate that the failure occurred at an area of wall thinning from external corrosion that ultimately failed by ductile overload under the imposed operating pressure. The morphology of the external corrosion observed on the pipe section is consistent with corrosion under insulation facilitated by wet-dry cycling.*

The following steps were performed for this analysis. The pipe sections were visually inspected and photographed. The external polyethylene (PE) tape was removed from PS 1 and PS 2 and visually inspected and photographed. The external pipe surfaces (with insulation) were laser scanned using a FaroArm™ to produce digital maps. The insulation from PS 2 was then removed and the pipe was visually inspected and photographed. The coal tar coating was then removed around the failure location, areas of corrosion, and at the ends of each pipe section.

Wall thicknesses, diameters, and circumferences were measured at various locations on PS 1 and PS 2 where coating was removed and there was no measurable corrosion. Corrosion products were collected from PS 2 for characterization. Analyses performed on these products included: (1) pH testing using litmus paper, (2) spot tests for carbonates and sulfides using 2-normal hydrochloric acid (2N HCl), (3) elemental analyses using energy dispersive spectroscopy (EDS) with a scanning electron microscope (SEM) and (4) compound identification using x-ray diffraction (XRD).

Swab samples were also obtained for bacteria analyses at two locations; an area of external corrosion and an area where the coating was disbonded but there was negligible external corrosion. Separate swab samples were taken for serial dilution and microscopic analysis. Liquid culture media for acid-producing bacteria (APB), sulfate-reducing bacteria (SRB), nitrate-reducing bacteria (NRB), aerobic bacteria (AERO), anaerobic bacteria (ANA), and iron-related bacteria (IRB) was used for the serial dilutions to evaluate growth of various types of bacteria. A five vial serial dilution (1:10,000) was performed using each type of media.

Coupons containing the failure location and areas of corrosion were cut from PS 2 using cold-cutting techniques. Coupon 1 contained the failure location and was a full ring section removed between 30.66 and 35.95 feet from the U/S GW. Coupon 2 contained external corrosion features further U/S from the failure location and was removed between 14.00 and 20.60 feet from the U/S GW; between the 4- and 8-o'clock orientations. The internal

and external surfaces were visually inspected and photographed. Where necessary, the samples were cleaned using a degreaser (LPS Presolve®) and acetone. Ultrasonic testing (UT) was performed on the samples removed from PS 2, using a 1-inch by 1-inch grid spacing, to produce a thickness map. The external and internal pipe surfaces of these coupons were laser scanned to produce a thickness contour dataset. Magnetic particle inspection (MPI) was performed on the external and internal pipe surfaces of the coupon containing the failure location.

The fracture surfaces were cleaned with methanol and acetone, optically examined, and photographed. Samples were then removed from one of the mating fracture surfaces, cleaned with Rhodine inhibited HCl solution and ENPREP® 214 to remove corrosion products, and examined at high magnifications in an SEM to document the fracture morphology. Transverse cross sections were removed from the suspected failure origin, an area of corrosion further U/S, and across the longitudinal seam weld of the failure joint. The transverse cross sections were mounted, polished, and etched. Light photomicrographs were taken to document the fracture and corrosion morphologies and steel microstructure. In addition, corrosion products collected from an area adjacent to the failure location and from areas of corrosion further U/S of the failure were mounted in cross-section and polished. Light photomicrographs were taken to document the corrosion product morphologies. Elemental analysis using EDS was performed to identify the elemental constituents of each.

Soil analyses were conducted on a sample removed (in the field) approximately 8 feet U/S of the U/S girth weld (GW). The soil was tested for resistivity, moisture content, pH, total acidity, total alkalinity, concentration of soluble anions and cations, total dissolved solids, and linear polarization resistance.

Mechanical (duplicate tensile tests and full Charpy V-notch [CVN]) curves) testing was performed on specimens removed from the failed pipe joint and U/S and D/S joints to determine the tensile and fracture toughness properties. Chemical analyses were performed on a steel sample removed from the failed pipe joint and U/S and D/S joints to determine the compositions.

CorLAS™ calculations were performed to estimate the failure pressure based on the pipe geometry, base metal mechanical properties, and the measured flaw profile. This value was compared with the estimated pressure at the failure location.

External corrosion was identified at several locations along the bottom of the failed pipe section, including the corrosion feature that ultimately failed on May 19, 2015. The corrosion features were associated with thick layered deposits and areas of compression and water saturation of the thermal insulation. The characteristics of the failure are consistent

with corrosion under insulation in the presence of wet-dry cycling.

Summary of Observations

- The failure was associated with an external corrosion feature located 33.50 feet from the upstream girth weld, at the 4:24 orientation (center of corrosion feature).
- The dimensions of the corrosion feature were 12.1 inches axially by 7.4 inches circumferentially. The maximum depth, as measured using laser scan data, was 0.318 inches or 89% of the measured wall thickness (0.359 inches).
- The failure opening was 6.6 inches in axial length, with the upstream and downstream ends located 33.35 and 33.9 feet from the upstream girth weld.
- The maximum circumferential dimension of the failure opening was 1.14 inches, approximately 33.45 feet from the upstream girth weld, at the 4:15 orientation.
- The fracture surfaces exhibited ductile overload.
- Cracking and wrinkling were observed within the polyethylene tape.
- Compression was observed within the polyurethane insulation at areas on the bottom of the pipe. These areas were saturated with moisture.
- Disbondment of the coal tar coating was observed on the bottom of the pipe along the length of Pipe Section 2.
- External corrosion features, including the feature associated with the failure, were identified at or adjacent to areas of saturated, compressed insulation.
- The corrosion products were rigid, non-friable, and, at some locations, well adhered to the pipe section. The products consist of alternating layers of goethite and magnetite.
- There is no strong evidence to indicate that microbiological influenced corrosion (MIC) contributed to the observed corrosion.
- No evidence of internal corrosion was observed along the length of the pipe sections inspected.
- The average yield strength (YS) for the failure joint is marginally lower than the minimum YS requirements for API 5L X65 line pipe steel of 65.0 ksi. The average is based on two tests values; one slightly higher (65.2 ksi) and one slightly lower (64.4 ksi) than the requirement. The average ultimate tensile strength (UTS) of the failure joint meets the minimum UTS requirements for API 5L X65 line pipe steel of 80 ksi.
- The Charpy V-notch (CVN) properties of the base metal are typical for the vintage and grade of line pipe steel.

- The chemical composition of the base metal meets requirements for the vintage and grade of line pipe steel.
- The microstructure of the base metal is typical for the vintage and grade of line pipe steel.
- The CorLAS™ predicted failure pressure for the failed joint was calculated to be approximately 760 psig, which is in very good agreement with reported pressure at the failure location and time of failure (737 psig).

Table of Contents

1.0	BACKGROUND	1
2.0	TECHNICAL APPROACH	2
3.0	RESULTS AND DISCUSSION.....	4
3.1	Visual Examination	4
3.1.1	External Polyethylene Tape.....	5
3.1.2	Rigid Polyurethane Insulation.....	6
3.1.3	Coal Tar Urethane Coating.....	7
3.1.4	Carbon Steel Line Pipe	7
3.1.5	Composite “Armor Plate” Sleeve.....	8
3.2	3D Laser Scanning	9
3.3	Ultrasonic Testing.....	10
3.4	Magnetic Particle Inspection.....	10
3.5	Fractographic Examination.....	10
3.5.1	Optical.....	10
3.5.2	Scanning Electron Microscopy	11
3.5.3	Fracture/Corrosion Profile	11
3.6	Metallographic Examination	12
3.7	Solid Sampling of Corrosion Products	13
3.7.1	pH Testing and Qualitative Spot Testing	13
3.7.2	X-ray Diffraction	14
3.7.3	Energy Dispersive Spectroscopy	14
3.8	Microbiological Analyses	15
3.8.1	Serial Dilution – Liquid Culture Media	15
3.8.2	Microscopic Examination for Total Bacteria.....	15
3.9	Soil Testing	15
3.10	Mechanical Testing	16
3.11	Chemical Analysis	17
3.12	Failure Pressure Analysis.....	17
4.0	DISCUSSION AND CONCLUSIONS	18



Plains All American Pipeline, L.P.
Line 901 Release (05-19-15): Mechanical and Metallurgical Testing

Appendices

Appendix A – CorLAS™

List of Tables

Table 1.	Summary of the locations and dimensions of corrosion features identified during the laboratory examination on the external surface of PS 2.	21
Table 2.	Results of diameter measurements performed on PS 1 and PS 2 using Pi tape and a tape measure.	22
Table 3.	Results of wall thickness measurements performed on PS 1 and PS 2.	22
Table 4.	Results of thickness measurements performed adjacent (~0.100 inches circumferentially) to the failure opening using the laser scan dataset. See Figure 32.	23
Table 5.	Results of elemental analyses, using EDS, performed on corrosion products from Feature 1 and Feature 4 compared to ideal chemistry compositions of goethite and magnetite; values presented in mass percent (wt.%).	24
Table 6.	Results of bacteria analyses performed on swabs taken, over an ~1 cm ² area, from the external surface of Pipe Section 2 at Feature 1 on the failure joint and at an area of disbonded coating away from significant corrosion.	25
Table 7.	Results of optical microscopy examination for fixed internal swab samples taken, over a ~1 cm ² area, from the external surface of the pipe section at Feature 1 and at an area away from significant corrosion.	25
Table 8.	Summary of soluble cation and anion concentrations for soil sample 10000151761.	26
Table 9.	Summary of various chemical properties for soil sample 10000151761.	26
Table 10.	Summary of various electrochemical properties for soil sample 10000151761.	26
Table 11.	Results of tensile tests performed on transverse base metal specimens from the failure and the U/S and D/S joints compared with requirements for API 5L Grade X65 line pipe steel.	27
Table 12.	Results of Charpy V-notch impact tests for transverse base metal specimens removed from the joint that failed (Joint 5930).	27
Table 13.	Results of Charpy V-notch impact tests for transverse base metal specimens removed from the U/S joint (Joint 5920).	28
Table 14.	Results of Charpy V-notch impact tests for transverse base metal specimens removed from the D/S joint (Joint 5940).	28

Table 15.	Results of analyses of the Charpy V-notch impact energy and percent shear plots for base metal specimens removed from the three pipe joints.....	29
Table 16.	Results of chemical analyses of samples removed from the joint that failed and the U/S and D/S joints compared with composition requirements (product analysis) for API 5L Grade X65 line pipe steel. ¹	30
Table 17.	Results of failure pressure analyses using CorLAS™. The pressure at the failure site was estimated at 737 psig.	31

List of Figures

Figure 1.	Photograph showing the failure location and the locations of the two pipe sections, during excavation.....	32
Figure 2.	Photograph showing Pipe Section 1 following removal from the ditch.	33
Figure 3.	Photograph showing Pipe Section 2 being removed from the ditch.....	34
Figure 4.	Schematic showing the location of the failure and where samples were removed for various analyses.	35
Figure 5.	Photograph showing the cargo container in the as-received condition.....	36
Figure 6.	Photographs showing the pipe sections in the as-received condition, within the cargo container.	36
Figure 7.	Photographs showing failure location on PS 2 a) before and b) after evidence tape and a clear protective wrapping was removed.	37
Figure 8.	Photographs showing the failure location a) while on site (May 28, 2015) and b) after transit to DNV GL's facility (June 15, 2015).	38
Figure 9.	Photograph showing a stamp on the internal surface of the failure joint, near the D/S GW (GW 5940). "NIPPON" and "24" are legible.	39
Figure 10.	Photographs showing the condition of the external tape on the failure joint. Tape measure indicates distance to upstream girth weld.	40
Figure 11.	Photograph showing the internal surface of the external tape from the failure joint.	41
Figure 12.	Photograph showing the internal surface of the external tape at the failure location. Tape measure indicates distance to upstream girth weld.	42
Figure 13.	Photograph showing the external surface of the external tape at the failure location.	43
Figure 14.	Photographs showing the external surface of the PU insulation at a) the U/S end of PS 2 (14' to 20' from U/S GW) and b) the failure location (31.5' to 36.4' from U/S GW). Tape measure indicates distance to upstream girth weld.	44
Figure 15.	Photograph showing a crack in the PU insulation within a wrinkle. White contrast paint was applied to the surface to facilitate laser scanning and visual inspection. Area shown in Figure 14; scale in mm.	45
Figure 16.	Photograph showing a piece of insulation removed from adjacent to the failure location; near 4:30 orientation.	45

Figure 17. Photograph showing corrosion product that was wedged between the pipe surface and polyurethane insulation. Location indicated in Figure 16; scale in mm.46

Figure 18. Photographs showing the amount of compression in the insulation adjacent to the failure location; near 6:00 orientation. Scale in mm.47

Figure 19. Photograph showing the insulation and coal tar coating separating from the pipe in large sheets on the underside of the pipe; approximately 29' from U/S GW.48

Figure 20. Photograph showing the insulation and coal tar coating separating from the pipe in large sheets on the underside of the pipe; approximately 17' from U/S GW.48

Figure 21. Photograph showing blistered coal tar coating along the 12:00 orientation on PS 2; approximately 28' from U/S GW.....49

Figure 22. Photograph showing external corrosion features on PS 2; Feature 1 and Feature 2. Tape measure indicates distance to upstream girth weld.49

Figure 23. Photograph showing an external corrosion feature on PS 2; Feature 3. Tape measure indicates distance to U/S GW.50

Figure 24. Photograph showing external corrosion features on PS 2; Feature 4 and Feature 6. Tape measure indicates distance to U/S GW (Note: tape slipped 0.1' to the right).....50

Figure 25. Photograph showing an external corrosion feature on PS 2; Feature 5. Tape measure indicates distance to U/S GW.51

Figure 26. Photographs showing the a) external and b) internal surfaces of the pipe section at the failure location (Coupon 1).52

Figure 27. Photographs showing Pipe Section 2 from 37.7 feet to 40.4 feet from GW 5930 a) before and b) after the composite repair sleeve was removed. Tape measure indicates distance to U/S GW (GW 5930).....53

Figure 28. Photograph the primary feature repaired on May 13, 2013. Area shown in Figure 27. Tape measure indicates distance to U/S GW.....54

Figure 29. Renderings of PS 1 and PS 2 (viewed from the OD surface) from laser scanning data showing Feature 1 and Feature 2; Coupon 2. The transparency of the insulation was changed to show a correlation between the features observed on the insulation with corrosion features observed on the pipe. The scale on the right is from 0.000 to 0.400 inches.....55

Figure 30. Renderings of PS 1 and PS 2 (viewed from the OD surface) from laser scanning data showing the failure location (Feature 4) and Feature 3, 5, and 6; Coupon 1. The transparency of the insulation was changed to show a correlation between the features observed

on the insulation with corrosion features observed on the pipe. The scale on the right is from 0.000 to 0.400 inches.56

Figure 31. Rendering of the failure location (viewed from the OD surface) from laser scanning data showing the remaining wall thickness along the fracture surface. The scale on the right is from 0.000 to 0.400 inches. Location indicated in Figure 30.57

Figure 32. Rendering of the failure location showing various thickness measurements made along the corrosion feature and failure opening. The scale on the right is from 0.000 to 0.400 inches. Measurements are tabulated in Table 4.58

Figure 33. Renderings of the area under the composite repair sleeve showing the thickness profile for the feature repaired on May 13, 2013. The scale on the right is from 0.000 to 0.400 inches.59

Figure 34. Photograph showing the internal surface of the pipe section at the failure location with the 1 × 1 inch grid painted on the surface. Tape measure indicates distance to U/S GW.60

Figure 35. Results of the UT measurements performed on 1" × 1" grid near the failure location; Feature 4 (Coupon 1).61

Figure 36. Results of the UT measurements performed on 1" × 1" grid near Feature 1 (Coupon 2).62

Figure 37. Results of the UT measurements performed on 1" × 1" grid near Feature 2 (Coupon 2).63

Figure 38. Photographs showing the a) clockwise and b) counterclockwise fractures surfaces following cleaning with a degreaser and acetone and/or methanol. Tape measure indicates distance to U/S GW.64

Figure 39. Stereo light photomicrographs of representative locations along the clockwise fracture surface following cleaning with a) a degreaser and acetone and/or methanol and d), e) an inhibited HCl acid and ENPREP[®]. Photomicrographs b) and d) are from the same location. Tape measure indicates distance to U/S GW.65

Figure 40. SEM image showing the fracture surface at the location identified in Figure 39e.66

Figure 41. SEM image showing the transition between Region 1 and Region 2. Area indicated in Figure 40.66

Figure 42. SEM image showing the ductile fracture morphology of Region 1. Area indicated in Figure 4167

Figure 43. SEM image showing a nondescript/corroded morphology of Region 2. Area indicated in Figure 4167

Figure 44.	SEM image showing the fracture surface at the location identified in Figure 39c.	68
Figure 45.	SEM image showing a representative ductile fracture morphology for Region 1. Area indicated in Figure 44.	68
Figure 46.	Photograph of the clockwise fracture surface showing thickness measurements of the Region 1 along the fracture surface at 5 mm intervals. Scale in mm.	69
Figure 47.	Fracture/Corrosion profile based on three measurement techniques.	70
Figure 48.	Photograph of the mounted transverse cross-section, Mount 195367-1b removed from the suspected failure origin; Feature 4. Mount location indicated in Figure 39.	71
Figure 49.	Photomicrograph showing the suspected failure origin in cross-section; Feature 4. Area indicated in Figure 48. (Mount 195367-1b; 4% Nital Etch)	71
Figure 50.	Photomicrograph showing the negligible grain elongation and plasticity along the CW fracture surface. Area indicated in Figure 49. (Mount 195367-1b; 4% Nital Etch)	72
Figure 51.	Photomicrograph showing the grain elongation and plasticity along the CCW fracture surface. Area indicated in Figure 49. (Mount 195367-1b; 4% Nital Etch)	72
Figure 52.	Photomicrograph showing corrosion products near the CCW fracture surface. Area indicated in Figure 48. (Mount 195367-1b; 4% Nital Etch)	73
Figure 53.	Photomicrograph showing corrosion products with some undercutting near the CCW fracture surface. Area indicated in Figure 49. (Mount 195367-1b; 4% Nital Etch)	73
Figure 54.	Photomicrograph showing base metal microstructure of Mount 195367-1b; 4% Nital Etch)	74
Figure 55.	Photograph of the mounted cross-section of corrosion products, Mount 195331-1 removed from Feature 4.	74
Figure 56.	Photomicrographs of the mounted cross-section, Mount 195331-1, from corrosion products removed from Feature 4; location identified in Figure 55.	75
Figure 57.	Photograph of the transverse mounted cross-section, Mount 195370-1 removed from Feature 1. Mount location indicated in Figure 22.	76
Figure 58.	Photomicrograph of the mounted cross-section, Mount 195370-1 removed from Feature 1 showing the corrosion morphology at the external surface; mirror image of location indicated in Figure 57.	76

Figure 59.	Photograph of the mounted cross-section of corrosion products, Mount 195322-1, removed from Feature 1.....	77
Figure 60.	Photomicrographs of the mounted cross-section, Mount 195322-1, from the corrosion product removed from Feature 1; location indicated in Figure 59.	77
Figure 61.	Photograph of the mounted cross-section, Mount 195365-1, removed from across the longitudinal seam weld. Location indicated in Figure 4.	78
Figure 62.	XRD spectrum acquired from the corrosion products collected from Feature 1, identifying Goethite and Magnetite as the compounds.	79
Figure 63.	XRD spectrum acquired from the corrosion products collected from Feature 2, identifying Goethite and Magnetite as the compounds.	80
Figure 64.	EDS data collected from Mount 195370-1, mirror image of area indicated in Figure 58.	81
Figure 65.	EDS data collected from Mount 195331-1, area indicated in Figure 56.....	82
Figure 66.	EDS line scan collected from Mount 195331-1, area indicated in Figure 56.....	83
Figure 67.	Photograph showing the soil samples collected from below the pipe, 8 feet U/S of GW 5930.....	84
Figure 68.	Percent shear from Charpy V-notch tests as a function of temperature for transverse base metal specimens removed from the failure joint (Joint 5930).....	85
Figure 69.	Charpy V-notch impact energy as a function of temperature for transverse base metal specimens removed from the failure joint (Joint 5930).	85
Figure 70.	Percent shear from Charpy V-notch tests as a function of temperature for transverse base metal specimens removed from U/S joint (Joint 5920).	86
Figure 71.	Charpy V-notch impact energy as a function of temperature for transverse base metal specimens removed from the U/S joint (Joint 5920).....	86
Figure 72.	Percent shear from Charpy V-notch tests as a function of temperature for transverse base metal specimens removed from D/S joint (Joint 5940).	87
Figure 73.	Charpy V-notch impact energy as a function of temperature for transverse base metal specimens removed from the D/S joint (Joint 5940).....	87

Figure 74. Color profile showing the results of average thickness measurements performed on the laser scan dataset following discretizing the data into 1/2-inch cells. The resulting profile is highlighted in blue and plotted in Figure 47.88

1.0 BACKGROUND

Plains All American Pipeline, L.P. (*Plains*) retained Det Norske Veritas (U.S.A.), Inc. (*DNV GL*) to perform a metallurgical analysis and mechanical testing on a section of pipe from Line 901 - Las Flores to Gaviota (L901), 24-inch nominal diameter crude oil pipeline that failed while in service. The failure occurred on May 19, 2015 in Goleta (Santa Barbara County), California at milepost (MP) 4, 33.5 feet downstream (D/S) of the nearest upstream (U/S) girth weld and 4.05 miles D/S of the nearest U/S pump station. A failure of a pipe segment can be characterized either as a leak or a rupture; the failure on L901 is characterized as a leak.¹

The section of the pipeline that failed is comprised of 24-inch diameter by 0.344-inch wall thickness, API 5L Grade X65 line pipe steel that contains a high frequency electric resistance welded (ERW) longitudinal seam and was manufactured by Nippon Steel in 1986. The maximum operating pressure (MOP) is 1,341² pounds per square inch gauge (psig) (72% of the specified minimum yield strength [SMYS]). The pressure at the time of failure was reported by Plains to be 737 psig (39.6% of SMYS) at the failure location and time of failure.

The pipeline was installed in 1990 and constructed using pipe that was externally coated with a coal tar urethane coating on the steel substrate, 1.5-inch thick rigid polyurethane foam, and an external polyethylene tape. The pipeline has an impressed current cathodic protection (CP) system with the nearest rectifier located 4.05 miles U/S of the failure location, at the Las Flores Pump Station. A hydrostatic test was performed at the time of commissioning for 8 hours at 1719 psi (Gaviota Station) on November 25, 1990. In-line inspection (ILI) runs, consisting of deformation and magnetic flux leakage (MFL) tools, were performed in 2007, 2012, and 2015.

The failed pipe joint and 5 feet of the U/S and D/S joints were removed from the failure location and delivered to DNV GL in two pipe sections for analysis. Figure 1 is a photograph showing the failed pipe section at the failure site, while Figure 2 and Figure 3 are

¹ According to the *FRACTURE CONTROL TECHNOLOGY FOR NATURAL GAS PIPELINES CIRCA 2001* (the PRCI report superseding NG-18 Report 208), "The distinction between leak and rupture for the pipeline community is based on the size and configuration of the breach, not how it develops. A "leak" is characterized by a narrow slit-like hole with length less than the diameter, which limits the fluid volume that escapes through the breach. In contrast, a "rupture" involves a longer, open hole that can be bulged over its length, which is on the order of a diameter or longer and can permit escape of a significant fluid volume." Similarly, the research performed as part of the historical NG-18 work identified empirical equations to predict the length at which a feature will propagate versus pop through and arrest; the leak/rupture length. Based on these calculations and visual observations, the length of the feature is consistent with a leak, arresting within the corrosion feature, and did not propagate outside of the feature into nominal wall-thickness pipe.

² Theoretical maximum operating pressure at the lowest elevation using the lowest pressure of either 80% of the commissioning hydro-test pressure, the 72% of SMYS, or the lowest component rating along the line segment.

photographs showing the pipe sections after removal from the ditch. Pipe Section 1 (PS 1) was 19.05 feet in length and contained 5.05 feet of the U/S joint, the U/S girth weld, and 15 feet of the failure joint located U/S of the failure. Pipe Section 2 (PS 2) was 31.06 feet in length and contained the failure location, the D/S girth weld, a 2013 composite repair sleeve, and 5 feet of the D/S joint. The objective of the analysis was to determine the metallurgical (or immediate) cause of the failure.

2.0 TECHNICAL APPROACH

The procedures used in the analysis were in accordance with industry-accepted standards. Five of the general standards governing terminology, specific metallographic procedures, mechanical testing, and chemical analysis used are as follows:

- ASTM E7, "Standard Terminology Relating to Metallography."
- ASTM E3, "Standard Methods of Preparation of Metallographic Specimens."
- ASTM E8, "Test Methods for Tension Testing of Metallic Materials."
- ASTM E23, "Standard Test Methods for Notched Bar Impact Testing of Metallic Materials."
- ASTM A751, "Standard Test Methods, Practices, and Terminology for Chemical Analysis of Steel Products."

The following steps were performed for this analysis. The protective shipping wrap was removed and the pipe sections were visually inspected and photographed. The external polyethylene (PE) tape was removed from PS 1(PS 1-ID 10000152251³) and PS 2 (PS 2-ID 10000152251) and visually inspected and photographed. The external pipe surfaces (with insulation) were laser scanned using a FaroArm™ to produce digital maps. Laser scanning is a non-destructive technique that uses light, in the form of a laser, to make very accurate three-dimensional (3D) data sets, which capture the x, y, and z coordinates from millions of measurements along the scanned surface. The datasets can then be used to generate 3D renderings of the scanned object(s) that can be rotated, manipulated, and measured.

The insulation from PS 2 was then removed and the pipe was visually inspected and photographed. The coal tar coating was then removed around the failure location, areas of corrosion, and at the ends of each pipe section using brass mallets, putty knives, and methyl ethyl ketone (MEK) and/or acetone.

3 Unique DNV GL barcode assigned to each piece of evidence.

Wall thicknesses, diameters, and circumferences were measured at various locations on PS 1 and PS 2 where coating was removed and there was no measurable corrosion. Corrosion products were collected from PS 2 for characterization. Analyses performed on these products included: (1) pH testing using litmus paper, (2) spot tests for carbonates and sulfides using 2-normal hydrochloric acid (2N HCl), (3) elemental analyses using energy dispersive spectroscopy (EDS) with a scanning electron microscope (SEM) and (4) compound identification using x-ray diffraction (XRD). The pH measurements were obtained by placing a few drops of deionized (DI) water on the pH test paper and then the wetted paper was placed in contact with the surface. The pH test paper was examined for color changes and compared to pH color charts.

Swab samples were also obtained for bacteria analyses, over a standard area of 1 cm², at the two locations; at an area of corrosion and area where the coating was disbonded but there was negligible external corrosion. Separate swab samples were taken for serial dilution and microscopic analysis. Liquid culture media for acid-producing bacteria (APB), sulfate-reducing bacteria (SRB), nitrate-reducing bacteria (NRB), aerobic bacteria (AERO), anaerobic bacteria (ANA), and iron-related bacteria (IRB) was used for the serial dilutions to evaluate growth of various types of bacteria. A five vial serial dilution (1:10,000) was performed using each type of media. The swab obtained for the microscopic analysis was fixed in 1% glutaraldehyde. A five microliter spot was removed from the fixed sample and prepared for examination by drying on a microscope slide and staining with 0.1% fluorescein isothiocyanate (FITC). The sample was examined using a CFI PLAN FLUOR 100X oil immersion objective on a Nikon Eclipse 50i epifluorescent microscope equipped with a FITC filter set to determine bacteria cell counts and morphology.

Coupons containing the failure location and areas of corrosion were cut from PS 2 using cold-cutting techniques. Coupon 1 contained the failure location and was full ring section removed between 30.66 and 35.95 feet from the U/S GW. Coupon 2 contained external corrosion features further U/S from the failure location and was removed between 14.00 and 20.60 feet from the U/S GW; between the 4- and 8-o'clock orientations. The internal and external surfaces were visually inspected and photographed. Where necessary, the samples were cleaned using a degreaser (LPS Presolve[®]) and acetone. Ultrasonic testing (UT) was performed on the samples removed from PS 2, using a 1-inch by 1-inch grid spacing, to produce a thickness map. The external and internal pipe surfaces of these coupons were laser scanned to produce a thickness contour dataset. Magnetic particle inspection (MPI) was performed on the external and internal pipe surfaces of the coupon containing the failure location.

The fracture surfaces were cleaned with methanol and acetone, optically examined, and photographed. Samples were then removed from one of the mating fracture surfaces,

cleaned with Rhodine inhibited HCl solution and ENPREP[®] 214 to remove corrosion products, and examined at high magnifications in an SEM to document the fracture morphology. Transverse cross sections were removed from the suspected failure origin, an area of corrosion further U/S, and across the longitudinal seam weld. The transverse cross sections were mounted, polished, and etched; see Figure 4 for locations. Light photomicrographs were taken to document the fracture and corrosion morphologies and steel microstructure. In addition, corrosion products collected from an area adjacent to the failure location and from areas of corrosion further U/S of the failure were mounted in cross-section and polished. Light photomicrographs were taken to document the corrosion morphologies. Elemental analysis using EDS was performed to identify the elemental constituents of each.

Soil analyses were conducted on a sample removed (in the field) approximately 8 feet U/S of the U/S girth weld (GW). The soil was tested for resistivity, moisture content, pH, total acidity, total alkalinity, concentration of soluble anions and cations, total dissolved solids, and linear polarization resistance.

Mechanical (duplicate tensile tests and full Charpy V-notch [CVN] curves) testing was performed on specimens removed from the failed pipe joint and U/S and D/S joints to determine the tensile and fracture toughness properties. Chemical analyses were performed on a steel sample removed from the failed pipe joint and U/S and D/S joints to determine the compositions.

CorLAS[™] calculations were performed to estimate the failure pressure based on the pipe geometry, base metal mechanical properties, and the measured flaw profile. This value was compared with the estimated pressure at the failure location.

3.0 RESULTS AND DISCUSSION

3.1 Visual Examination

The pipe sections were transported to DNV GL's facility near Columbus, Ohio in a sealed cargo container on a flatbed semi-truck. The cargo container was locked and secured with three keyed padlocks, a serialized cargo lock, and evidence tape prior to transport. The corresponding keys for the locks were distributed amongst the interested parties, such that no one person had access to all of the keys. The container was then driven non-stop to a DNV GL storage facility. Upon receipt, the locks and evidence tape were inspected. Figure 5 is a photograph showing the container being loaded into a DNV GL storage facility; the four locks are identified in the figure with yellow circles.

Figure 6 contains photographs showing the two pipe sections in the as-received condition. The pipe sections were wrapped in opaque plastic wrap and boxed. Evidence tape was

applied in the field on top of the plastic wrap approximately 1 foot U/S and D/S of the failure on PS 2. Figure 7 contains photographs showing the failure location before and after removal of the evidence tape and protective plastic wrap at DNV GL's facility. The fracture surfaces were protected with foam insulation that was placed around the clockwise (CW) fracture surface; shown in Figure 7b. Figure 8 contains photographs showing the failure location while on site (Figure 8a - May 28, 2015) and at DNV GL's facility (Figure 8b - June 15, 2015). Some red corrosion products were observed near the failure location, as shown in Figure 8b. The failure opening was 6.6 inches in length and located at the 4:15 orientation, consisting of an irregular fracture path that opened in the clockwise (CW) direction looking D/S. The U/S and D/S ends of the fracture path were located at 33.35 and 33.9 feet, respectively, from the U/S GW. The maximum opening measured 1.14 inches, approximately 33.45 feet from the U/S GW. The failure is associated with a corrosion feature that measured approximately 12.1 inches axially in length by 7.4 inches circumferentially in width. Additional data are presented in Section 3.1.4.

PS 1 was 19.05 feet in length and contained 5.05 feet of the U/S joint, the U/S girth weld (GW) and 14 feet of the failure joint U/S of the failure. Pipe Section 2 was 31.06 feet in length and contained 26.06 feet of the failure joint, including the failure location, the D/S GW, a 2013 composite repair sleeve, and 5 feet of the D/S joint. PS 2 was 31.06 feet in length and contained the failure location, the D/S GW, a composite repair sleeve, and 5 feet of the D/S joint. Reference markings were identified on each pipe section noting the top-dead-center (TDC) and the location of each girth weld. A stamp was identified on the internal surface of the failure joint towards the D/S end, adjacent to GW 5940. Figure 9 is a photograph showing the stamp; "NIPPON", "24", and other indiscernible characters were observed.

3.1.1 External Polyethylene Tape

An external polyethylene tape (external surface of the rigid polyurethane insulation) was present on PS 1 and PS 2, Figure 2 and Figure 10 respectively. The tape is installed in a white condition; however, exposure to the soil and released product discolored the tape to varying shades of brown. Areas of decohesion from the insulation substrate were observed in varying degrees along the length of the two pipe sections. The most pronounced areas were located near the failure location, as shown in the photographs presented at the bottom of Figure 10. Cracks were also observed in the PE tape, primarily at the 12- and 6-o'clock orientations; some of the cracks are identified in Figure 10. Wrinkles in the tape were observed along the entire length of both pipe sections on the bottom half of the pipe (2:00 to 10:00 orientation).

The PE tape was removed from each pipe section, aligned as it was on the pipe, and visually inspected and photographed. Figure 11 is a photograph of the internal surface of the tape looking D/S. The original white coloration of the PE tape is apparent in the figure along with bands of product at the 4:00 and 7:00 orientations, which appear to correlate with the wrinkle bands in the tape along the pipe section. In general, the areas exhibiting wrinkles were disbanded or partially disbanded from the insulation and were much easier to remove from the pipe section. Figure 12 and Figure 13 are photographs showing the internal and external surfaces of the PE tape at the failure location, respectively. Similar to other areas along the pipeline, cracking and wrinkles in the PE tape were observed near the failure location. The cracks in the tape were located at the 6:00 orientation, while the wrinkles were located at the 4:00 and 7:00 orientations.

3.1.2 Rigid Polyurethane Insulation

The polyurethane (PU) insulation was visually inspected after the PE tape was removed. Figure 14 contains photographs from two locations along PS 2; the U/S end and the failure location. The insulation exhibited impressions corresponding to the wrinkles observed in the PE tape and, at one location a small crack in the insulation was identified within a wrinkle impression, refer to Figure 15. The white contrast paint evident in the figure was applied to the insulation to facilitate laser scanning and visual inspection. Compression of the insulation was also observed at locations along the 6:00 orientation; two locations are identified Figure 14. Additional detail is provided in Section 3.2.

The insulation adjacent to the failure location was removed at the 6:00 orientation, refer to Figure 16. Wedged between the insulation and the pipe surface was a piece of corrosion product, which was collected and bagged. Figure 17 is a photograph showing the corrosion product. The corrosion product is dark, saturated with oil, and rigid. The insulation was partially saturated with a clear liquid. Figure 18 contains photographs showing the insulation in cross-section. The liquid line is evident in the lower-left photograph. At this location, the insulation is saturated near the external surface, while the middle photograph shows saturation that is through the full thickness of the insulation. In addition, significant compression of the insulation was observed at this location (center photo). The compressed thickness measured 0.276 inches as compared to the nominal thickness of 1.5 inches, which corresponds to over 80% compression. In general, the compressed insulation was located on the bottom of the pipe and areas of saturation were within the compressed areas. A pH measurement was also made at a saturated location along the insulation using pH paper; location identified in Figure 17. The pH was between 6 and 7.

3.1.3 Coal Tar Urethane Coating

The thickness of the coal tar coating was measured using micrometers on a piece that disbonded near the failure location; area shown in Figure 16. The average of four measurements was 0.043 inches, which corresponds closely with measurements performed further U/S (~20 feet U/S from failure location) that averaged 0.040 inches. Figure 19 is a photograph showing the removal of the PU insulation and coal tar coating. Along the underside of the pipe, the insulation and coal tar coating came off together, such that the coal tar coating had disbonded from the pipe surface. At this location, released product can be seen along the mating surfaces of the pipe and coating.

Disbondment of the coal tar coating was also observed further U/S on PS 2 at areas where released product did not reach, refer to Figure 20. Disbondment was associated with large corrosion cells, evident in the figure, and in areas where no deep corrosion was observed, but exhibited a layer of fine corrosion products on the pipe surface. Approximately 28 feet from the U/S GW on PS 2 an area of blistered coal tar coating was observed; refer to Figure 21. The insulation against this area was moist, but there was no significant corrosion associated with this location. A syringe was used to extract fluid contained within one of the blisters from which a pH measurement was made using pH paper. The pH was between 6 and 7, consistent with the pH measurement performed on a piece of saturated insulation adjacent to the failure location described above.

3.1.4 Carbon Steel Line Pipe

Following removal of the PE tape, PU insulation, and areas of coal tar coating that had disbonded from PS 2, the pipe section was visually inspected. Areas of corrosion were observed on the external surface surrounding the failure location and approximately 14 to 20 feet U/S of the failure location on the bottom of the pipe. The larger features are identified in Figure 22 through Figure 25; a summary of the feature dimensions and locations is presented in Table 1. The corrosion features were located on the bottom of the pipe section in or adjacent to areas that exhibited disbondment of the coal tar coating and compression in the adjacent PU insulation. The corrosion products were dry, rigid, and magnetic. At some locations, a putty knife was required to separate the corrosion products from the pipe body. For the most part, the products associated with each corroded area came off in one piece that was non-friable in nature. The products were dark brown to black or charcoal in appearance and could be handled while remaining intact. The products also appeared to be layered. A Dremel® rotary tool was ultimately used to cut through some of the products for the metallography presented in Section 3.6. The corrosion products from each of the features identified in Table 1 were collected for subsequent analyses.

A 5.3-foot ring coupon (Coupon 1) containing the failure location and Features 3 through 6 was cut from PS 2. The cuts were made at 30.66 and 35.95 feet from the U/S GW. Similarly, a 6.6-foot coupon (Coupon 2) was cut from U/S end of PS 2 capturing Feature 1 and Feature 2. The longitudinal cuts were made at approximately the 4:00 and 8:00 o'clock orientations.

Circumferences/diameters and wall thicknesses were measured on the U/S end of PS 1 (U/S Joint), D/S end of PS 2 (D/S Joint), and on the U/S and D/S ends of the ring section containing the failure location. The measurements were made in areas with no coating or measurable corrosion. The diameters were measured using a Pi tape and are shown in Table 2. The diameter meets API 5L tolerances for 24-inch nominal diameter pipe. The diameters were measured with a tape measure from the 3 to 9 o'clock and 12 to 6 o'clock orientations. The diameters varied from 24.0 to 24.1 inches, indicating no significant ovality, as shown in Table 2. The wall thickness was measured at the 12, 3, 6, and 9 o'clock orientations at the same locations described above; see Table 3 for details. The wall thickness values ranged from 0.356 to 0.362 inches. These wall thickness values meet API 5L tolerances for a nominal wall thickness of 0.344 inches.⁴

The 5.3-foot long ring coupon was cut longitudinally at the 3:00 and 9:00 o'clock orientations to facilitate examination of the internal surface. Figure 26 contains photographs showing the external and internal surfaces of the bottom-half of the ring coupon. There was no observable corrosion on the internal surface. A small, superficial, mill anomaly was identified approximately 6 inches D/S from the failure opening.

3.1.5 Composite "Armor Plate" Sleeve

The composite repair sleeve installed on May 13, 2013, was comprised of composite Armor Fiber[®] and cured resin, overlaid with a green two-part epoxy. There were no indications of water ingress or disbondment of the two-part epoxy. The repair was removed by cutting, chiseling, and ultimately sand blasting. Figure 27 contains photographs showing the pipe before and after removal of the repair sleeve. Throughout the removal process, the pipe section was visually inspected for indications of discoloration and corrosion to determine if additional corrosion had occurred following installation of the sleeve in 2013. Figure 28 is a photograph showing the primary feature that was repaired in 2013 after the composite sleeve was removed. There was no evidence of discoloration or additional corrosion associated with the feature; additional discussion and depth measurements are presented in Section 3.2.

4 API 5LX, 35th Edition, May 1986.

The two-part epoxy and resin were well-adhered, precluding electrolyte from reaching the pipe surface and thus, eliminating additional corrosion of the feature. Similarly, there is no evidence that the repair influenced corrosion of the feature that ultimately failed, i.e. galvanic couple. Without an ionic pathway through the electrolyte there is no means by which to setup such a cell.

3.2 3D Laser Scanning

The external surfaces of PS 1 and PS 2 were laser scanned, using a FaroArm™, following removal of the external polyethylene tape. Similarly, the failure opening and corrosion features along the external surfaces of the pipe section (and the corresponding internal surfaces) were also laser scanned once the polyurethane insulation was removed. The datasets were aligned using reference magnets placed along the pipe sections prior to scanning. With the exception of Feature 1, the features were cleaned with a soft-bristled brush, brass-bristles brush, and methanol and/or acetone. The corrosion products within Feature 1 were left intact for metallographic examination (Section 3.6). As a result of scanning the internal and external surfaces of the pipe at and around the corrosion features, a remaining wall thickness profile was generated to show the extent of corrosion for each feature.

Figure 29 contains renderings of the aligned dataset, highlighting the areas of corrosion on the U/S end of PS 2 (Feature 1 and Feature 2). The pipe was rotated such that the viewing direction is normal to the 6:00 orientation. From this perspective, areas of corrosion are clearly visible along the 6:00 orientation. The transparency of the polyurethane dataset on PS 2 was set to 30% providing an opportunity to identify any correlation between features on the insulation and areas of corrosion. It is clear from these data that the corrosion features are located at or adjacent to areas of compressed insulation.

Similarly, Figure 30 contains renderings highlighting the areas of corrosion at or near the failure location (Features 3-6). Consistent with the observations above, the corrosion features are located at or adjacent to areas of compressed insulation. Figure 31 is a rendering showing Feature 4; the failure location. The maximum depth of each feature was determined, based on a measured nominal wall thickness of 0.359 inches, from the laser scan data and are presented in Table 1. Various thickness measurements were made slightly offset (~0.100 inches circumferentially) from the fracture path to provide data that would not contain necking, providing a better representation of the wall thickness just prior to the failure. A rendering showing the measurement locations is provided in Figure 32, while the data is given in Table 4. Based on this, the maximum depth of Feature 4 was 0.318 inches or 89% of the measured wall thickness. The failure opening measured 6.55

inches in length with a maximum opening of 1.10 inches, which are consistent with the measurements made during the visual examination.

The corrosion areas associated with the 2013 repair were also laser scanned. Figure 33 is a rendering showing the thickness profile of the deepest feature. The maximum corrosion depth was 0.220 inches, which corresponds closely to the maximum depth (0.228 inches) and location within the feature identified in 2013 prior to sleeving the pipe section. It's possible that the discrepancy is due to remnant resin still present within the feature prior to laser scanning.

3.3 Ultrasonic Testing

Ultrasonic testing was performed on the coupons identified in Figure 29 and Figure 30. Thickness measurements were made at 1-inch intervals along a 1 × 1-inch grid that was applied to the internal surfaces of each coupon. Figure 34 is a photograph of the grid applied to the coupon containing the failure location. The corresponding measurements are provided in Figure 35; however, the data or the photograph in Figure 34 would need to be mirrored to match one another, as the data is provided as observed from the external surface. Similar measurements were made on the coupon containing Feature 1 and Feature 2. These data are presented in Figure 35 and Figure 36, respectively. The data are provided with a color overlay; dark red being the thinnest remaining wall thickness. Similar measurements were made on the coupon containing Feature 1 and Feature 2. The results from Feature 2 are provided in Figure 37. The UT data agreed very well with the laser scan data, and given the increased lateral resolution of the laser scan data, subsequent discussions and depth data presented in this report are based on the laser scan datasets.

3.4 Magnetic Particle Inspection

Magnetic particle inspection was performed on the internal and external surfaces surrounding the failure location. There were no features or anomalies identified.

3.5 Fractographic Examination

3.5.1 Optical

Figure 38 contains photographs of the clockwise (CW) and counterclockwise (CCW) fracture surfaces, Figure 38a and Figure 38b, respectively following cleaning with a degreaser and methanol and/or acetone. The fracture surfaces are brown in color and slanted with respect to the radial direction.

Figure 39 contains stereo light photomicrographs of representative locations along the CW fracture surface following cleaning with a degreaser and methanol and/or acetone [(a), (b), (c)] and one location following cleaning with Rhodine inhibited HCl acid and ENPREP® 214 [(d), (e)]. As shown in Figure 39a and Figure 39c, the fracture surface is tapered or slanted through the thickness. This is a typical characteristic of ductile overload. Similarly, the fracture surface along its length is wavy and has characteristics of ductile tearing and overload. Figure 39d and Figure 39e are micrographs of the regions shown in Figure 39b following cleaning with Rhodine inhibited hydrochloric (HCl) acid and ENPREP® 214. At this location, two unique morphologies are present; Region 1, which has a dull/matte finish and is associated with the areas along the slanted fracture surface, and Region 2, which is more reflective and at a shallower angle with respect to the outer or inner surfaces. These areas are identified in Figure 39e. Region 2 extended the deepest at this location, approximately 33.76 feet from the U/S GW, along the fracture surface.

3.5.2 Scanning Electron Microscopy

Figure 40 is an SEM image of the area identified in Figure 39e along the CW fracture surface (Sample 195367-1; 33.76' from the U/S GW). The white dashed line indicates the interface between Region 1 and Region 2. Figure 41 is a higher magnification SEM image showing the transition between Region 1 and Region 2. Region 2 is relatively smooth with spherical-shaped impressions, while Region 1 appears rough with smaller topographical features. Figure 42 contains a high magnification SEM image in Region 1, near the ID. The fracture surface at this location exhibits dimples, which are characteristic of ductile overload. Figure 43 contains a high magnification SEM image in Region 2, near the ID surface. The fracture surface is nondescript having a corroded appearance and is inconsistent with a typical fracture morphology, indicating that this region was present prior to the failure. This observation coupled with the oblique angle of the surface and visual appearance indicates that Region 2 is associated with external corrosion.

Figure 44 is an SEM image from a representative location along the fracture surface exhibiting a shear or slanted fracture surface (Sample 195367-2, 33.55' from the U/S GW). At higher magnification (Figure 45), a rough-dimpled appearance, consistent with ductile overload, was observed. The dimples are elongated in the vertical direction as shown in the figure, which is consistent with the orientation of the sheared fracture plane.

3.5.3 Fracture/Corrosion Profile

Using the observations of the optical and SEM fractographic examinations, a fracture profile was generated showing the boundary of Region 1. Measurements were made along the

fracture surface at 5 mm intervals, refer to Figure 46. The resulting data are plotted in Figure 47 as measured (remaining) wall thickness versus distance to U/S GW. Given that plasticity/ductility was observed along the fracture surface, the measured thickness of Region 1 is not necessarily representative of the remaining wall thickness prior to failure. This is due to necking of the material, a process governed by the Poisson effect, whereby tensile strain on one direction (i.e. circumferential) results in compressive strain in the other two perpendicular directions (i.e. radial and longitudinal) for isotropic materials; such as steel. Therefore, the thickness of Region 1 was larger than the measured values prior to failure. For this reason, two additional profiles are presented in the figure using the laser scan data; one based on a ½-inch by ½-inch grid, which will be discussed in Section 3.12 and one based on the measurements made adjacent to the fracture surface (Figure 32), approximately 0.100 inches circumferentially, presumably at locations not heavily influenced by necking.

3.6 Metallographic Examination

Figure 48 is a photograph of the transverse metallographic cross-section (Mount 195367-1b) removed from across the fracture surface at approximately 33.76 feet D/S of the U/S GW; same location identified in Figure 41. The corrosion profile near the failure opening is relatively uniform; however, transitions sharply with a steep side wall approximately 15 mm CCW from the opening. Figure 49 is a photomicrograph showing the two mating fracture surface in the etched condition. Figure 50 is a photomicrograph showing the mating CW fracture surface. With the exception of a small ligament at the internal surface, there were no obvious indications of plasticity corresponding to Region 1. This suggests that the preexisting corrosion feature was almost through-wall at this location just prior to failure. In comparison, the mating CCW fracture surface, presented in Figure 51, exhibited grain elongation and deformation, consistent with plasticity and the results obtained from the SEM examination showing dimpled failure in Region 1. The discrepancy between microstructural characteristics of the CW and CCW surfaces at this location is due to a small misalignment between the two mating fracture surfaces when the transverse cuts were made to produce the metallographic cross-section.

Figure 52 and Figure 53 are representative photomicrographs showing the corrosion morphology along the external surfaces of Mount 195367-1b. The corrosion is scalloped in most cases (Figure 52), and the remaining corrosion products exhibit a layered texture with alternating light and dark bands. However, at the base of some of these scallops, some undercutting was also observed, as shown in Figure 53. Figure 54 is a photomicrograph showing the typical microstructure of the base metal. The microstructure consists of ferrite

(white areas) and fine pearlite (gray areas). This microstructure is consistent with the vintage and grade of the steel.

Figure 55 is a photograph of the transverse metallographic cross-section (Mount 195331-1) removed from the corrosion products associated with Feature 4; collected adjacent to the failure location. At this location, the thickness of the product is approximately 0.55 inches. Droplets of oil can be seen on the surface of the mount, as the photograph was taken following the SEM examination in which the mount was pumped down to low pressures to facilitate observation in the SEM. Figure 56 contains photomicrographs through the thickness of the corrosion product. The morphology of the corrosion products are similar throughout, consisting of alternating light and dark layers.

Figure 57 is a photograph of the transverse metallographic cross-section (Mount 195370-1) removed through Feature 1, at approximately 16.65 feet D/S of the U/S GW; feature identified in Figure 22. The corrosion depth is much less severe at this location and the profile is relatively uniform. At higher magnification (Figure 58), the corrosion products exhibit a similar layered morphology as those observed near the failure location; Figure 52. Figure 59 is a photograph showing the transverse metallographic cross-section (Mount 195322-1) removed from the corrosion products associated with Feature 1. At this location, the thickness of the product is approximately 0.40 inches. Consistent with the other corrosion products, the morphology contains alternating dark and light layers; refer to Figure 60.

Figure 61 is a photograph showing the transverse metallographic cross-section remove from the longitudinal seam weld of the failure joint. At higher magnification, an hourglass shape (associated with a heat affected zone) can be observed, characteristic of a high-frequency electric resistance weld (ERW).

3.7 Solid Sampling of Corrosion Products

3.7.1 pH Testing and Qualitative Spot Testing

The pH of the external corrosion products collected from Feature 5 was determined using deionized (DI) water and pH test paper. The pH of the deposits was 5 to 6 and the pH of the DI water used in the analysis was also 5 to 6.

Qualitative spot testing, using 2N HCl, was performed on three external corrosion products collected from Feature 1, Feature 2, and Feature 5. Portions of the samples were placed in vials with lead acetate tape and a few drops of the HCl were placed on the products. Vigorous bubbling is a positive indication for the presence of carbonates. A rotten egg odor

and/or discoloration of lead acetate tape are positive indications for the presence of sulfides. All samples tested negative for both carbonates and sulfides.

3.7.2 X-ray Diffraction

X-ray diffraction was performed on corrosion products collected from Feature 1 and Feature 2. The resulting spectrum for each is presented in Figure 62 and Figure 63, respectively. The compounds identified for each were goethite (FeOOH) and magnetite (Fe_3O_4). Goethite is one of the most thermodynamically stable iron oxides under aerobic (high oxygen) conditions. Conversely, magnetite is metastable phase formed under low oxygen conditions.

3.7.3 Energy Dispersive Spectroscopy

Energy dispersive spectroscopy was performed on the corrosion products captured in the metallographic cross-sections. Figure 64 contains the results of EDS scans performed on the corrosion products in Mount 195370-1, associated with Feature 1. EDS scans were performed within the layered regions identified in the metallographic examination. The results are summarized in Table 5. The two primary constituents are iron (Fe) and oxygen (O), which are characteristic of iron oxides. Small quantities of chlorine (Cl) were identified, likely associated with chlorides, while most of the other constituents are elements common to line pipe steels. A relatively high concentration of copper (Cu) was identified in Scan 1 (8 wt.%), which is atypical of line pipe steel and may be associated with deposits from groundwater. The other three scans identified typical concentrations of Cu. The light area, Scan 3, has an O content of 29.24 wt.%, while the darker bands, Scan 2 and Scan 4, have an average oxygen content of 36.88 wt.%. Given that the XRD analyses identified goethite and magnetite as the two compounds associated with the corrosion products, these values were compared to the calculated oxygen content for goethite (36 wt.%) and magnetite (28 wt.%). These values correlate very closely, indicating that the light areas are likely magnetite and the darker areas are likely goethite.

Figure 65 contains the results of EDS scans performed on the corrosion products on Mount 195331-1, associated with Feature 4. Similar results were obtained for the layers identified in the cross-section. The results are summarized in Table 5, which again shows that the compositions of the light layers correspond to magnetite and the compositions of the darker layers correspond to goethite. The variation in oxygen content is apparent in the line scan presented in Figure 66, which illustrated the decreased oxygen content of the lighter layer.

3.8 Microbiological Analyses

The external surface of the pipe section was swabbed (at DNV GL) over a standard area of approximately 1 cm² for bacterial analysis. The swabs were taken from the bottom of Feature 1, 16.65 feet D/S from the U/S GW and from an area beneath disbonded coal tar coating with no significant corrosion; approximately 5 inches CCW from Feature 1. Separate swab samples were taken from each location for the serial dilution and microscopic examination analyses. The results of the microbiological analyses are discussed below.

3.8.1 Serial Dilution – Liquid Culture Media

Table 6 shows the results of the bacteria serial dilution testing for the swab samples collected from the pipe section. The results reveal a positive indication for five types of bacteria (APB, AERO, ANA, IRB, and NRB) at the corrosion feature, while there were no positive indications for bacteria at the area away with no significant corrosion. As seen in the table, the highest concentration of bacteria detected was 100 bacteria per cm², which is a relatively low value.

3.8.2 Microscopic Examination for Total Bacteria

The swabs collected from Feature 4 and from the area away were fixed in 1% glutaraldehyde and examined using epifluorescent microscopy. The practical minimum detection limit for this method is approximately 10³ cells/ml of fixed sample. The results of the analysis are provided in Table 7. As seen in the table, rod-shaped cells were detected for the swab samples removed at Feature 1 and an area of no apparent corrosion. The calculated concentration of cells for the swab samples were 1.70 × 10⁴ cells/mL and 2.8 × 10⁴ cells/mL. This type of microscopic examination does not differentiate between living and non-living organisms.

3.9 Soil Testing

DNV GL collected six (6) soil samples from the dig site at the failure location. Two samples were collected from under the pipe at each of the three locations: 8 feet U/S of GW 5930 (IDs 10000151761 & 10000151762), 2 feet D/S of failure location (IDs 10000151753 & 1000151759), and 12.5 feet D/S of GW 5940 (IDs 10000151754 & 10000151755). The only samples not contaminated with product were the samples collected 8 feet U/S of GW 5930. Figure 67 is a photograph showing the soil samples collected 8 feet US of GW 5930. The samples were placed in a cooler with ice packs and shipped to DNV GL's laboratory for testing. One of the uncontaminated samples (Sample 10000151761) was sieved in order to conduct the testing.

Testing was conducted to determine the physical and chemical properties of the sample, including: (1) resistivity, (2) moisture content, (3) pH, (4) soluble anions [Cl^- , SO_4^{2-} , S_2^- , NO_2^- , NO_3^- , CO_3^{2-} , HCO_3^-], (5) soluble cations [K^+ , Ca^{2+} , Mg^{2+} , Na^+], (6) total alkalinity, (7) total acidity, (8) linear polarization resistance, and (9) total dissolved solids (TDS). The results of the analyses are provided in Table 8 through Table 10.

The sample exhibited relatively low levels of nitrate (NO_3^-), chloride (Cl^-) and carbonate (HCO_3^-) and high levels of sulfate (SO_4^{2-}) anions; 115, 117, 204, and 3600 mg/L, respectively. The soil resistivity decreased from 3,800 ohm-cm in the as-received condition to 400 ohm-cm when saturated. Based on these data, the soil is considered corrosive.⁵ Corrosion rates were determined for the soil sample in the as-received and saturated condition using linear polarization resistance (LPR). The resulting corrosion rates were 2.5 and 2.7 mils per year (mpy), respectively.

3.10 Mechanical Testing

The results of tensile testing of duplicate, transverse base metal specimens removed from the pipe joint that failed and the U/S and D/S joints are shown in Table 11. The average yield strength (YS) and ultimate tensile strength (UTS) of Joint 5930 were 64.8 ksi and 84.0 ksi, respectively. The average YS of the base-metal samples is marginally lower than the minimum YS requirements for API 5L X65 line pipe steel of 65.0 ksi. The average is based on two tests values of 65.2 and 64.4 ksi. The average UTS of the base-metal samples meets the minimum UTS requirements for API 5L X65 line pipe steel of 80 ksi. The tensile properties of the U/S and D/S joints meet the requirements for API 5L X65 line pipe steel, as shown in Table 11.

Table 12 - Table 14 summarize the results of the Charpy testing for the transverse base metal samples while Figure 68 through Figure 73 show the corresponding Charpy percent shear and impact energy curves. An analysis of the data for the base metal specimens from the failure joint, Joint 5930, indicates that the 85% fracture appearance transition temperature (FATT) is -58.5°F and the upper shelf Charpy energy is 164.8-ft-lbs, full size. These are very good values and typical for modern line pipe steels. The CVN test results can be adjusted to determine the 85% FATT that would be expected for full-scale pipe by applying temperature shifts to the data. This method (full-scale) adjusts the 85% FATT obtained from the Charpy tests to a predicted FATT from the Battelle Drop-Weight Tear Test (BDWTT). The predicted 85% FATT from the BDWTT test most closely represents the

5 *Peabody's Control of Pipeline Corrosion*, 2nd Edition, Table 5.5 and Table 5.7.

expected FATT for full-scale pipe wall material.⁶ The full-scale brittle to ductile transition temperature for the failure joint, based on a pipe wall thickness of 0.359 inches, is shown in Table 15. The pipe joint is expected to exhibit ductile fracture behavior above -78.4°F.⁷ The values for the U/S and D/S joints are also provided in Table 15. The toughness properties of these joints also are very good but not quite as good as the failure joint.

3.11 Chemical Analysis

The results of the chemical analyses performed on samples removed from the failure joint and the U/S and D/S pipe joints are shown in Table 16. The results show that the pipe joints meet the composition specifications for API 5L X65 line pipe steel at the time of manufacture.

3.12 Failure Pressure Analysis

CorLAS™ (Version 3.02) was used to perform Remaining Strength (RSTRENG) calculations to estimate the failure pressure incorporating the effective-area methodology. The calculations were based on the measured mechanical properties and dimensions of the failure joint, and the measured flaw profile. Three flaw profiles were considered for the analysis:

- Case 1: Measurements made along the fracture surface combined with laser scan data on either end of the failure opening, within Feature 4; the black profile presented in Figure 47.
- Case 2: The laser scan data and measurements made adjacent to the fracture surfaces, presumably in areas where necking/plasticity was minimized; the blue profile presented in Figure 47.
- Case 3: The laser scan data and discretizing corrosion Feature 4 into ½-inch cells; columns running axial and rows running circumferential. The average depth for each cell was determined and the lowest values identified within each column were then used to generate the flaw profile; refer to Figure 74 and Figure 47 (green profile).⁸

The measured flaw profiles, presented in Figure 47, were fed into CorLAS™ whereby an algorithm converted each profile into an equivalent semi-elliptical flaw. These effective (or

6 W. A. Maxey, J. F. Kiefner, R. J. Eiber, *Brittle Fracture Arrest in Gas Pipelines*, NG-18 Report No. 135, A.G.A. Catalog No. L51436, April 1983, Battelle Columbus Laboratories.

7 Rosenfeld, M.J., "A Simple Procedure for Synthesizing Charpy Impact Energy Transition Curves from Limited Test Data," International Pipeline Conference, Volume 1, ASME, 1996, Equation 1.

8 The average thickness for each cell was used (instead of minimum values) due to meshing effects along the fracture surface that provided unrealistic minimum wall thickness values as a result of the slanted fracture surfaces.

equivalent) flaws were used to estimate the failure pressure. The results of the analysis are presented in Table 17. The calculated failure pressure for Case 1, Case 2, and Case 3 are 474 psig, 759 psig, and 763 psig, respectively.

The estimated pressure at the failure location at the time of the failure was reportedly 737 psig, which is in very good agreement with the estimated failure pressures for Case 2 and Case 3. As discussed previously, the estimated failure pressure for Case 1 is underestimated due to the presence of necking that resulted from the overload event. Additional results of the analysis, and a description of CorLAS™, are summarized in Appendix A.

4.0 DISCUSSION AND CONCLUSIONS

External corrosion was identified at several locations along the failed pipe section, including the corrosion feature that ultimately failed on May 19, 2015. The corrosion features are located in areas where the external polyethylene tape, thermal polyurethane insulation, and coal tar enamel were compromised, allowing the ingress of moisture to facilitate aqueous corrosion. Cracking in the polyethylene tape, as well as wrinkles, provided pathways for water to collect against the bottom of the pipe section. This in turn may have initiated and/or accelerated the breakdown of the thermal insulation that resulted in compression of the insulation and breakdown of the cellular structure, causing water absorption and retention. The presence of goethite and magnetite in a layered morphology is consistent with aqueous corrosion under wet-dry cycling.⁹ When oxygen transport is high, such as during the drying stages when the electrolyte is relatively thin, goethite is the stable oxide. However, during saturated conditions or when oxygen is limited (i.e. thick products), magnetite is predominant. The alternating nature of the layers suggests that external variables, such as rain, drainage, and operating temperature contributed to the corrosion process.

The term corrosion under insulation (CUI) may be defined as external corrosion of carbon steel piping, pressure vessels, and structural components resulting from water trapped under insulation.¹⁰ Although typically associated with above-ground piping, CUI is the appropriate corrosion mechanism for this particular failure given the contributing role of the thermal insulation to the corrosion process. Thus, the results of the analyses indicate that CUI was the primary corrosion mechanism, facilitated by wet-dry cycling. Although bacteria were identified at a corrosion feature sampled U/S of the failure location, the quantities were low and the layered morphology within the corrosion products is not necessarily

9 Nasrazadani, S. and Raman, A., *Formation and Transformation of Magnetite (Fe₃O₄) on steel surfaces under Continuous and Cyclic Water Fog Testing*, Corrosion, 1993.

10 API Recommended Practice 583, Corrosion Under Insulation and Fireproofing, May 2014.

consistent with MIC, particularly given that the corrosion products are extremely rigid. Therefore, there is no strong evidence to indicate that MIC contributed to the observed corrosion. A summary of our observations are provided below.

Summary of Observations

- The failure was associated with an external corrosion feature located 33.50 feet from the upstream girth weld, at the 4:24 orientation (center of corrosion feature).
- The dimensions of the corrosion feature were 12.1 inches axially by 7.4 inches circumferentially. The maximum depth, as measured using laser scan data, was 0.318 inches or 89% of the measured wall thickness (0.359 inches).
- The failure opening was 6.6 inches in axial length, with the upstream and downstream ends located 33.35 and 33.9 feet from the upstream girth weld.
- The maximum circumferential dimension of the failure opening was 1.14 inches, approximately 33.45 feet from the upstream girth weld, at the 4:15 orientation.
- The fracture surfaces exhibited ductile overload.
- Cracking and wrinkling were observed within the polyethylene tape.
- Compression was observed within the polyurethane insulation at areas on the bottom of the pipe. These areas were saturated with moisture.
- Disbondment of the coal tar coating was observed on the bottom of the pipe along the length of Pipe Section 2.
- External corrosion features, including the feature associated with the failure, were identified at or adjacent to areas of saturated, compressed insulation.
- The corrosion products were rigid, non-friable, and, at some locations, well adhered to the pipe section. The products consist of alternating layers of goethite and magnetite.
- No evidence of internal corrosion was observed along the length of the pipe sections inspected.
- The average yield strength (YS) for the failure joint is marginally lower than the minimum YS requirements for API 5L X65 line pipe steel of 65.0 ksi. The average is based on two tests values; one slightly higher (65.2 ksi) and one slightly lower (64.4 ksi) than the requirement. The average ultimate tensile strength (UTS) of the failure joint meets the minimum UTS requirements for API 5L X65 line pipe steel of 80 ksi.
- The Charpy V-notch (CVN) properties of the base metal are typical for the vintage and grade of line pipe steel.

- The chemical composition of the base metal meets requirements for the vintage and grade of line pipe steel.
- The microstructure of the base metal is typical for the vintage and grade of line pipe steel.
- The CorLAS™ predicted failure pressure for the failed joint was calculated to be approximately 760 psig, which is in very good agreement with reported pressure at the failure location and time of failure (737 psig).

Table 1. Summary of the locations and dimensions of corrosion features identified during the laboratory examination on the external surface of PS 2.

Corrosion Feature (2015 ILI "Log Dist.")	Distance from U/S GW to Center of Feature (feet)	Axial Length (inches)	Distance from TDC to Center of Feature, Clockwise (inches)	Circumferential Length (inches)	O'clock Orientation (TDC to Center of Feature)	Maximum Depth from Laser Scan Data¹¹ (inches)
Feature 1 (21367.67)	16.55	8.3	43.00	7.7	6:50	0.112 (31%)
Feature 2 (21368.88) (21369.26) (21369.49) (21369.56) (21369.57) (21369.99) (21370.13) (21370.48)	18.61	21.9	40.30	9.8	6:24	0.199 (55%)
Feature 3 (21382.40)	31.52	7.7	35.60	17.2	5:40	0.208 (58%)
Feature 4 (21384.17) (21384.38) (21484.39) (21484.54) (21484.58) (21384.63)	33.50	12.1	27.75	7.4	4:24	0.318 (89%)
Feature 5	33.83	1.8	44.80	2.2	7:00	0.025 (7%)
Feature 6 (21385.39)	34.32	2.8	30.10	2.8	4:48	0.122 (34%)

¹¹ Based on measured nominal wall thickness of 0.359 inches.

Table 2. Results of diameter measurements performed on PS 1 and PS 2 using Pi tape and a tape measure.

Location	Diameter Using Pi Tape (inches)	Diameter 3 to 9 o'clock (inches)	Diameter 6 to 12 o'clock (inches)
PS 1 - U/S end; Joint 5920	24.059	24.0	24.0
PS 2 - 30.7' from U/S GW; Joint 5930	24.059	24.0	24.0
PS 2 - 36' from U/S GW; Joint 5930	24.055	24.1	24.0
PS 2 - D/S end; Joint 5940	24.048	24.1	24.0

Table 3. Results of wall thickness measurements performed on PS 1 and PS 2.

O'clock Orientations	Wall Thickness, PS 1 U/S End Joint 5920 (inches)	Wall Thickness, PS 2 30.7' from U/S GW Joint 5930 (inches)	Wall Thickness, PS 2 36' from U/S GW Joint 5930 (inches)	Wall Thickness, PS 2 D/S End Joint 5940 (inches)
12:00	0.356	0.359	0.359	0.358
3:00	0.360	0.362	0.362	0.359
6:00	0.356	0.359	0.358	0.359
9:00	0.357	0.359	0.357	0.358
Average	0.357	0.360	0.359	0.359

Table 4. Results of thickness measurements performed adjacent (~0.100 inches circumferentially) to the failure opening using the laser scan dataset. See Figure 32.

Distance to U/S GW (feet)	Measured Wall Thickness (inches)
33.02	0.354
33.07	0.344
33.12	0.340
33.15	0.249
33.17	0.189
33.21	0.118
33.26	0.138
33.32	0.124
33.36	0.111
33.41	0.096
33.44	0.072
33.47	0.051
33.48	0.043
33.48	0.043
33.51	0.066
33.53	0.067
33.55	0.091
33.60	0.119
33.62	0.074
33.64	0.049
33.67	0.073
33.70	0.085
33.73	0.079
33.76	0.072
33.79	0.073
33.84	0.042
33.89	0.072
33.92	0.106
33.95	0.242
33.98	0.352

Table 5. Results of elemental analyses, using EDS, performed on corrosion products from Feature 1 and Feature 4 compared to ideal chemistry compositions of goethite and magnetite; values presented in mass percent (wt.%).

Element	Mount 195370-1 (Feature 1 Products)				Mount 195331-1 (Feature 4 Products)			Goethite (FeOOH)	Magnetite (Fe ₃ O ₄)
	Scan 1 (Mixed Layers)	Scan 2 (Dark Layer)	Scan 3 (Light Layer)	Scan 4 (Light Layer)	Scan 1 (Light Layer)	Scan 2 (Light Layer)	Scan 3 (Dark Layer)		
Oxygen (O)	33.52	35.78	29.24	37.97	27.85	29.45	37.83	36.01	27.64
Silicon (Si)	0.19	0.40	0.41	0.26	0.21	0.20	0.22	–	–
Chlorine (Cl)	0.19	0.06	0.07	0.15	–	–	–	–	–
Sulfur (S)	–	–	–	–	–	–	0.18	–	–
Manganese (Mn)	0.79	0.80	0.68	0.73	0.59	0.93	0.98	–	–
Magnesium (Mg)	–	–	–	–	–	–	0.48	–	–
Iron (Fe)	56.87	62.46	69.60	60.71	71.35	69.41	60.30	62.85	72.36
Copper (Cu)	8.44	0.49	–	0.18	–	–	–	–	–

Table 6. Results of bacteria analyses performed on swabs taken, over an ~1 cm² area, from the external surface of Pipe Section 2 at Feature 1 on the failure joint and at an area of disbanded coating away from significant corrosion.

Bacteria Type	Feature 1 (16.65 ft D/S from U/S GW)		Area of No Significant Corrosion (Outside of Feature 1; ~ 5 inches CCW)	
	Test Result	Number of Positive Vials	Test Result	Number of Positive Vials
Aerobic (AERO)	Positive	2	Not detected	–
Anaerobic (ANA)	Positive	2	Not detected	–
Acid-Producing (APB)	Positive	2	Not detected	–
Sulfate-Reducing (SRB)	Not detected	–	Not detected	–
Iron-Related (IRB)	Positive	2	Not detected	–
Nitrate-Reducing (NRB)	Positive	2	Not detected	–

Bacteria Concentration Key:

- 1 10 bacteria per cm²
- 2 100 bacteria per cm²,
- 3 1,000 bacteria per cm²,
- 4 10,000 bacteria per cm²,
- 5 100,000 bacteria per cm²

Table 7. Results of optical microscopy examination for fixed internal swab samples taken, over a ~1 cm² area, from the external surface of the pipe section at Feature 1 and at an area away from significant corrosion.

Sample Identification	Aliquot Volume, uL	Total Cells Observed	Calculated № cells/mL	Morphology
Feature 1 (16.65 ft D/S from U/S GW)	5	12	1.70 × 10 ⁴	Rod
Area of No Apparent Corrosion (Outside of Feature 1; ~ 5 inches CCW)	5	>20	2.80 × 10 ⁴	Rod

Table 8. Summary of soluble cation and anion concentrations for soil sample 10000151761.

Sample ID	Soluble cations mg/L				Soluble anions mg/L						
	Na ⁺	K ⁺	Ca ²⁺	Mg ²⁺	NO ₂ ⁻	NO ₃ ⁻	Cl ⁻	SO ₄ ⁻	S ₂ ⁻	CO ₃ ²⁻	HCO ₃ ⁻
10000151761 (8' U/S of GW 5930; below pipe)	898	320.	495	9.64	< 2.1	115	117	3600	< 0.67	< 13.3	204

Table 9. Summary of various chemical properties for soil sample 10000151761.

Sample ID	pH soil	Total Acidity mg CaCO ₃ /kg	Total Alkalinity mg CaCO ₃ /kg	As-Received Moisture Content %	Total Dissolved Solids (mg/L)
10000151761 (8' U/S of GW 5930; below pipe)	7.95	< 66.5	204	(a) 27.59% (b) 21.62%	6350

a – Percent moisture per AASHTO T265 & ASTM D2216

b – Percent moisture per EPA Method 1684, Eq. 2.

Table 10. Summary of various electrochemical properties for soil sample 10000151761.

Sample ID	Resistivity Ohm-cm (as-received)	Resistivity Ohm-cm (saturated)	LPR mpy (as-received)	LPR mpy (saturated)
10000151761 (8' U/S of GW 5930; below pipe)	3,800	400	2.5	2.7

Table 11. Results of tensile tests performed on transverse base metal specimens from the failure and the U/S and D/S joints compared with requirements for API 5L Grade X65 line pipe steel.

	Failure Joint (10000151970)	U/S Joint (10000151968)	D/S Joint (10000151969)	API 5L Grade X52 (Minimum Values) ³
Yield Strength, ksi ¹	64.8 ²	65.9	68.4	65
Tensile Strength, ksi ¹	84.0	84.6	87.7	80
Elongation in 2 inches, % ¹	35.0	33.6	32.8	21.25
Reduction of Area, % ¹	60.1	62.8	57.6	–

1 – Average of duplicate tests.

2 – Average of 65.2 ksi (extensometer on OD) and 64.4 ksi (extensometer on ID)

3 – API 5LX, 35th Edition, May 1986.

Table 12. Results of Charpy V-notch impact tests for transverse base metal specimens removed from the joint that failed (Joint 5930).

Sample ID	Temperature, °F	Sub-size Impact Energy, ft-lbs	Full Size Impact Energy, ft-lbs	Shear, %	Lateral Expansion, mils
15446-1-6	-238	2	2	0	0.006
15446-1-10	-189	4	5	1	0.006
15446-1-4	-148	24	28	8	0.017
15446-1-2	-103	33	38	29	0.022
15446-1-8	-65	103	120	83	0.076
15446-1-7	-29	124	144	91	0.084
15446-1-1	-4	119	138	99	0.081
15446-1-3	32	130	151	100	0.082
15446-1-5	68	158	184	100	0.083
15446-1-9	100	142	165	100	0.080

Table 13. Results of Charpy V-notch impact tests for transverse base metal specimens removed from the U/S joint (Joint 5920).

Sample ID	Temperature, °F	Sub-size Impact Energy, ft-lbs	Full Size Impact Energy, ft-lbs	Shear, %	Lateral Expansion, mils
15446-2-9	-312	1	1	0	0.001
15446-2-3	-238	2	2	0	0.001
15446-2-2	-193	4	5	3	0.001
15446-2-5	-148	5	6	15	0.002
15446-2-1	-103	18	22	20	0.012
15446-2-10	-51	48	58	41	0.045
15446-2-4	-4	101	122	92	0.075
15446-2-6	32	104	126	100	0.073
15446-2-7	75	111	135	100	0.078
15446-2-8	100	117	142	100	0.079

Table 14. Results of Charpy V-notch impact tests for transverse base metal specimens removed from the D/S joint (Joint 5940).

Sample ID	Temperature, °F	Sub-size Impact Energy, ft-lbs	Full Size Impact Energy, ft-lbs	Shear, %	Lateral Expansion, mils
15446-3-9	-312	1	1	0	0.000
15446-3-3	-238	2	2	1	0.002
15446-3-2	-193	3	4	3	0.002
15446-3-5	-148	5	6	15	0.003
15446-3-1	-103	12	15	15	0.007
15446-3-10	-51	40	48	36	0.040
15446-3-4	-4	83	101	83	0.068
15446-3-6	32	92	112	100	0.077
15446-3-7	75	96	116	100	0.079
15446-3-8	100	103	125	100	0.080

Table 15. Results of analyses of the Charpy V-notch impact energy and percent shear plots for base metal specimens removed from the three pipe joints.

	Failure Joint; Joint 5930 (10000151970)	U/S Joint; Joint 5920 (10000151968)	D/S Joint; Joint 5940 (10000151969)
Upper Shelf Impact Energy (Full Size), Ft-lbs	164.8	138.9	121.3
85% FATT, °F	-58.5	-1.6	4.8
85% FATT, °F (Full Scale Pipe) ¹	-78.4	-19.4	-12.7

1 – Full Scale Pipe FATT = 85% FATT + $((66 * (t_w^{0.55} / t_c^{0.7}) - 100))$ where t_w = pipe wall thickness and t_c = width of the CVN specimen.

Table 16. Results of chemical analyses of samples removed from the joint that failed and the U/S and D/S joints compared with composition requirements (product analysis) for API 5L Grade X65 line pipe steel.¹

Element	Failure Joint; 5930 (10000151970) (Wt. %)	U/S Joint; 5920 (10000151968) (Wt. %)	D/S Joint; 5940 (10000151969) (Wt. %)	API 5L Grade X65 Spec (Wt. %) ¹
C (Carbon)	0.082	0.083	0.078	0.30 (max)
Mn (Manganese)	1.110	1.160	1.120	1.50 (max)
P (Phosphorus)	0.011	0.010	0.010	0.050 (max)
S (Sulfur)	0.007	0.007	0.007	0.060 (max)
Si (Silicon)	0.170	0.190	0.160	–
Cu (Copper)	0.268	0.270	0.274	–
Sn (Tin)	0.000	0.000	0.000	–
Ni (Nickel)	0.008	0.008	0.006	–
Cr (Chromium)	0.035	0.027	0.028	–
Mo (Molybdenum)	0.000	0.000	0.000	–
Al (Aluminum)	0.010	0.016	0.012	–
V (Vanadium)	0.022	0.024	0.028	0.010 (min)
Nb (Niobium)	0.063	0.065	0.062	0.005 (min)
Zr (Zirconium)	0.000	0.000	0.000	–
Ti (Titanium)	0.011	0.016	0.015	–
B (Boron)	0.0006	0.0005	0.0005	–
W (Tungsten)	0.000	0.000	0.000	–
Co (Cobalt)	0.000	0.000	0.000	–
Fe (Iron)	98.200	98.100	98.200	Balance

1 – API 5L, 35th Edition, May 1986.

Table 17. Results of failure pressure analyses using CorLAS™. The pressure at the failure site was estimated at 737 psig.

Case №	Equivalent Flaw Profile	Properties	Estimated Failure Pressure (psig)
1	As-measured along fracture surface (includes necking)	Measured	474
2	Laser scan data adjacent to fracture surface	Measured	759
3	Laser scan data ½ x ½ inch grid (average)	Measured	763

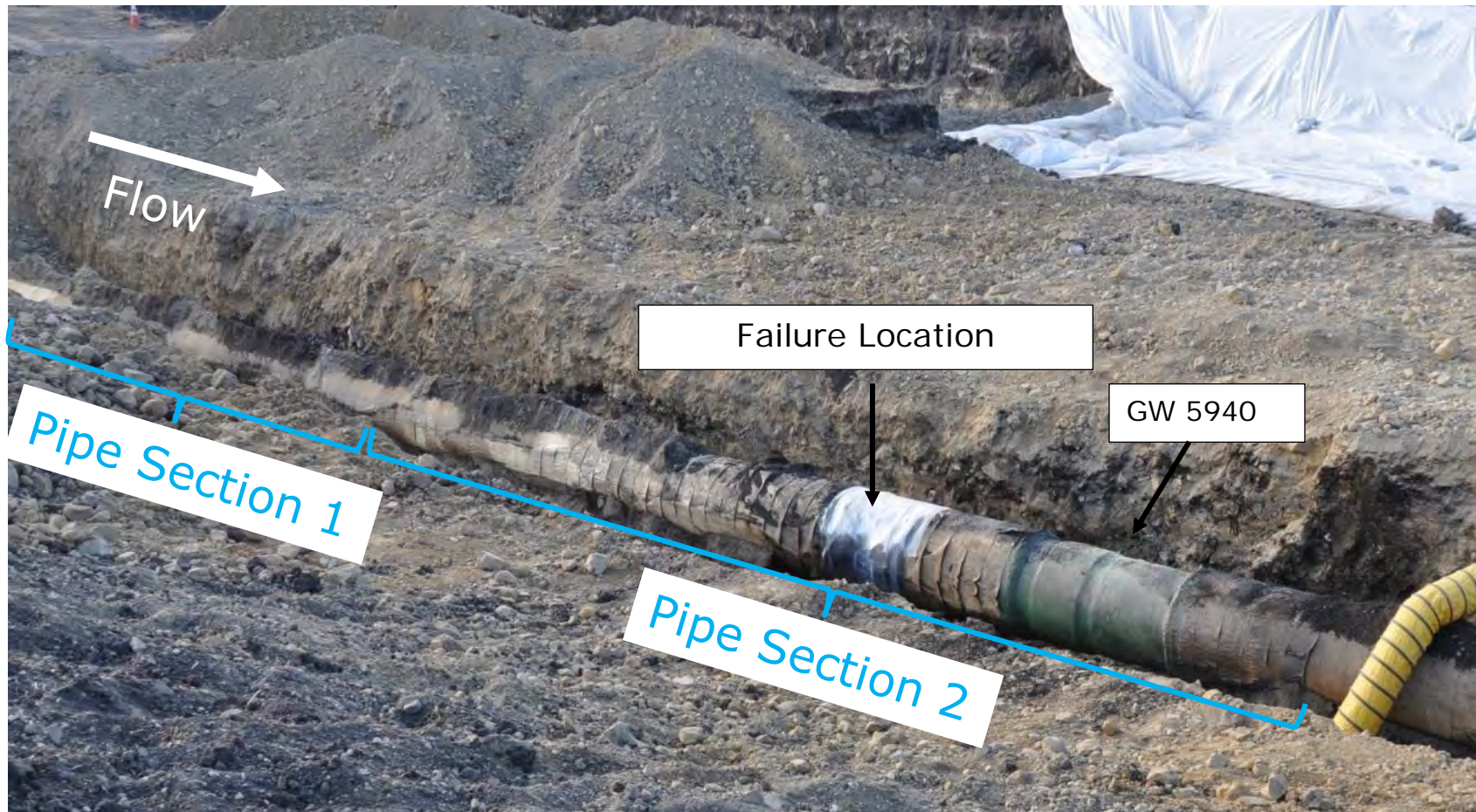


Figure 1. Photograph showing the failure location and the locations of the two pipe sections, during excavation.

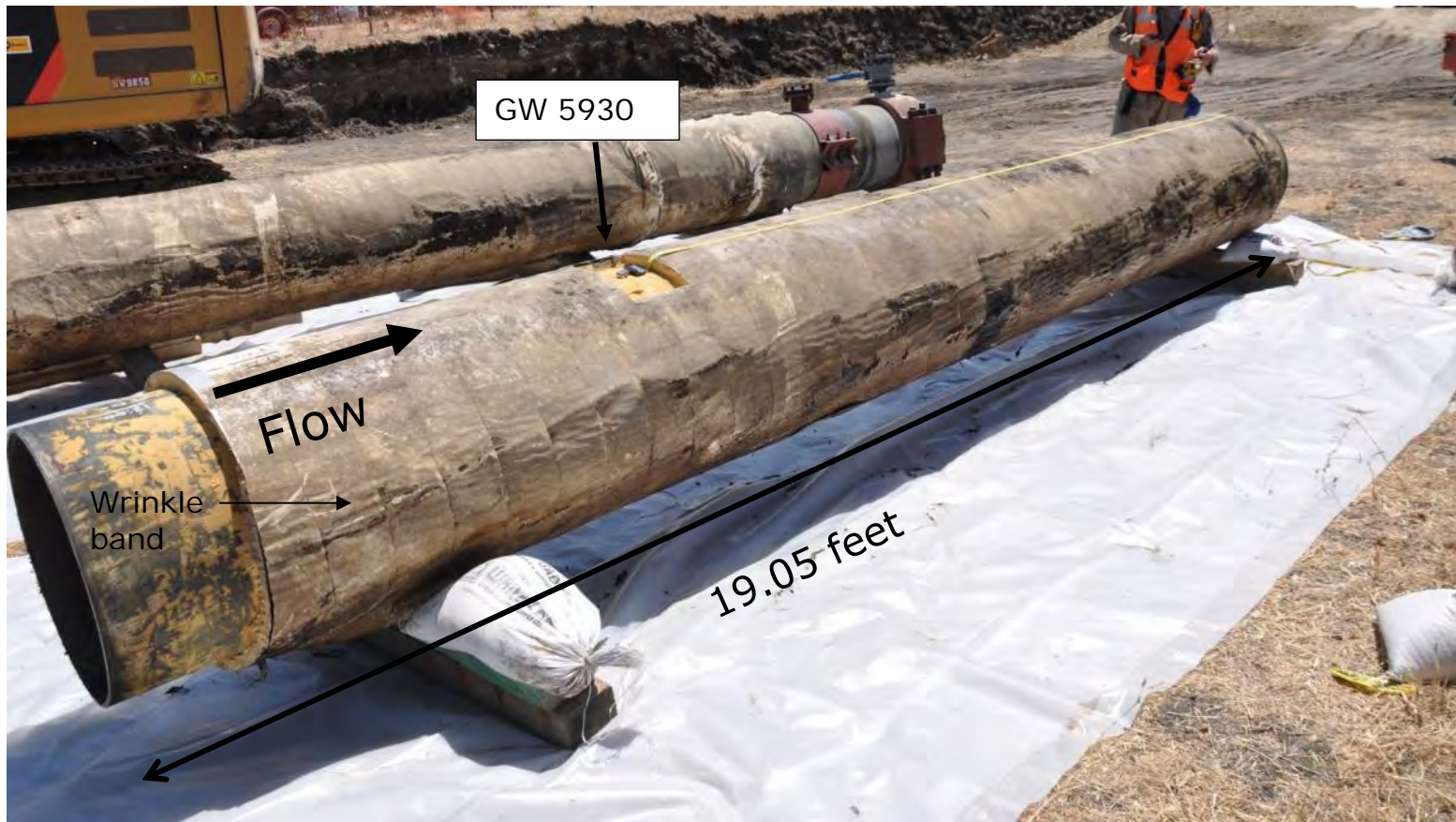


Figure 2. Photograph showing Pipe Section 1 following removal from the ditch.



Figure 3. Photograph showing Pipe Section 2 being removed from the ditch.

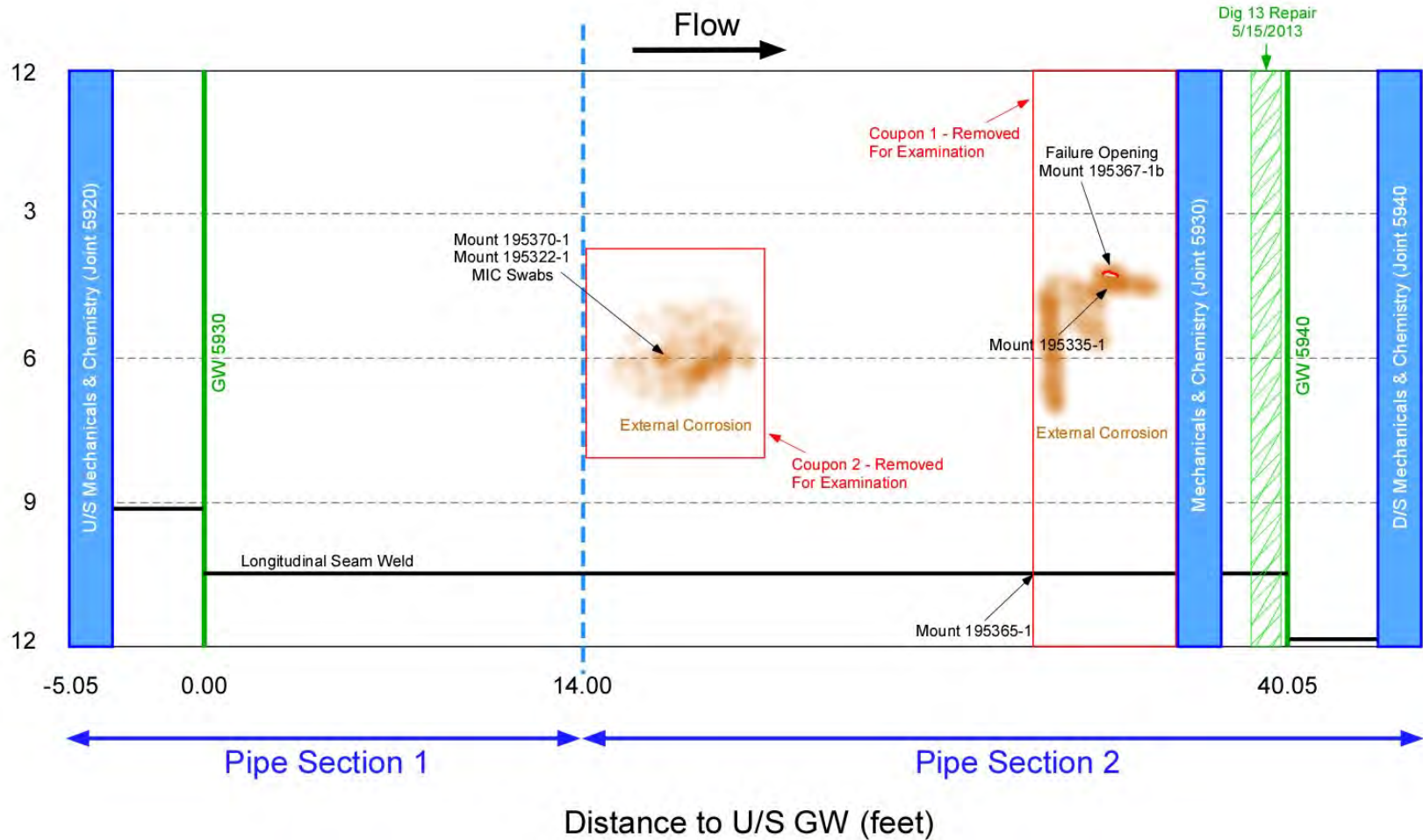


Figure 4. Schematic showing the location of the failure and where samples were removed for various analyses.



Figure 5. Photograph showing the cargo container in the as-received condition.

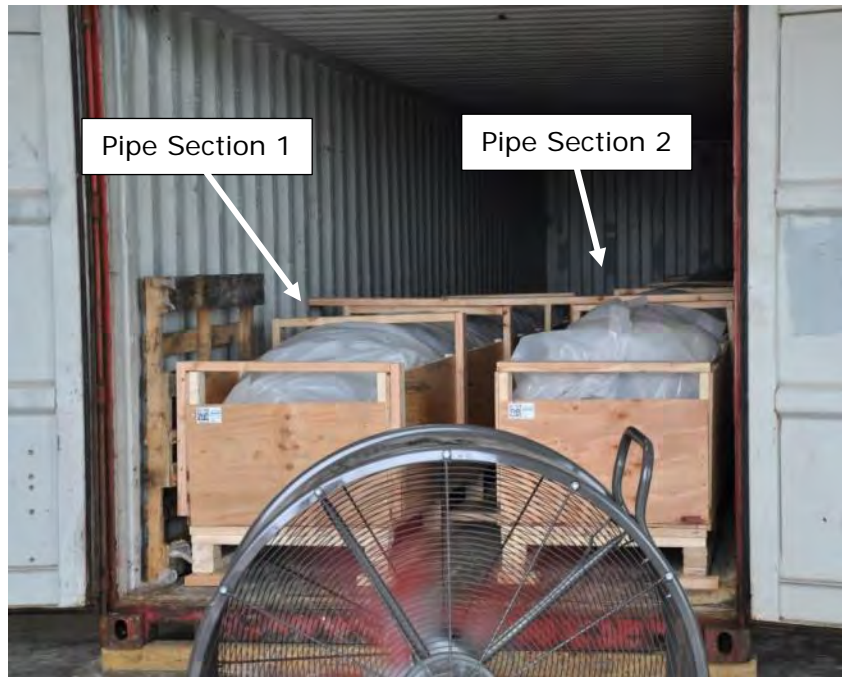
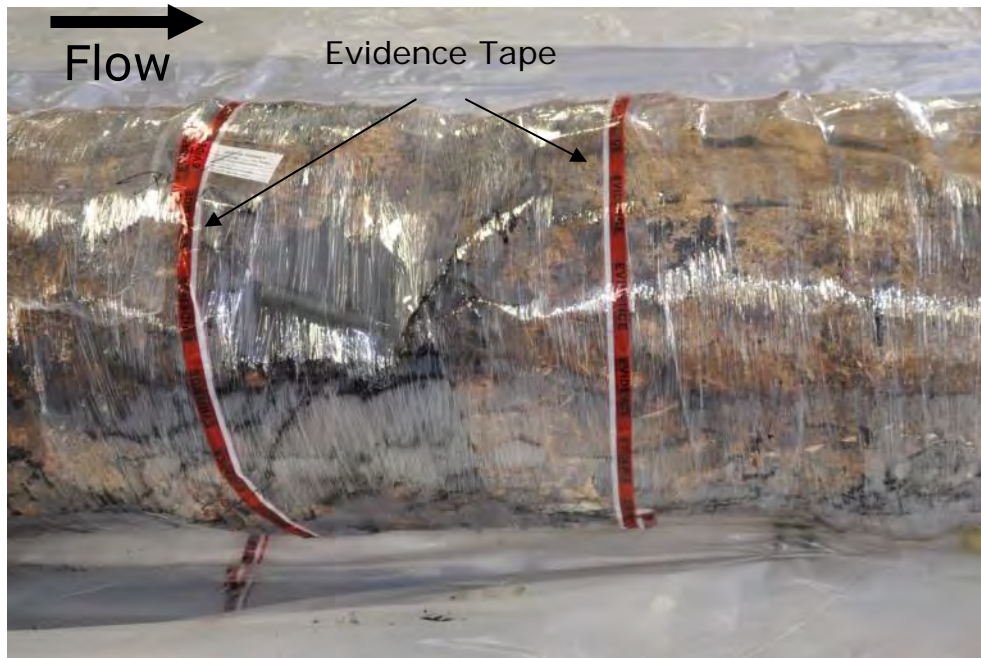


Figure 6. Photographs showing the pipe sections in the as-received condition, within the cargo container.



(a)



(b)

Figure 7. Photographs showing failure location on PS 2 a) before and b) after evidence tape and a clear protective wrapping was removed.



(a)



(b)

Figure 8. Photographs showing the failure location a) while on site (May 28, 2015) and b) after transit to DNV GL's facility (June 15, 2015).



Figure 9. Photograph showing a stamp on the internal surface of the failure joint, near the D/S GW (GW 5940). "NIPPON" and "24" are legible.

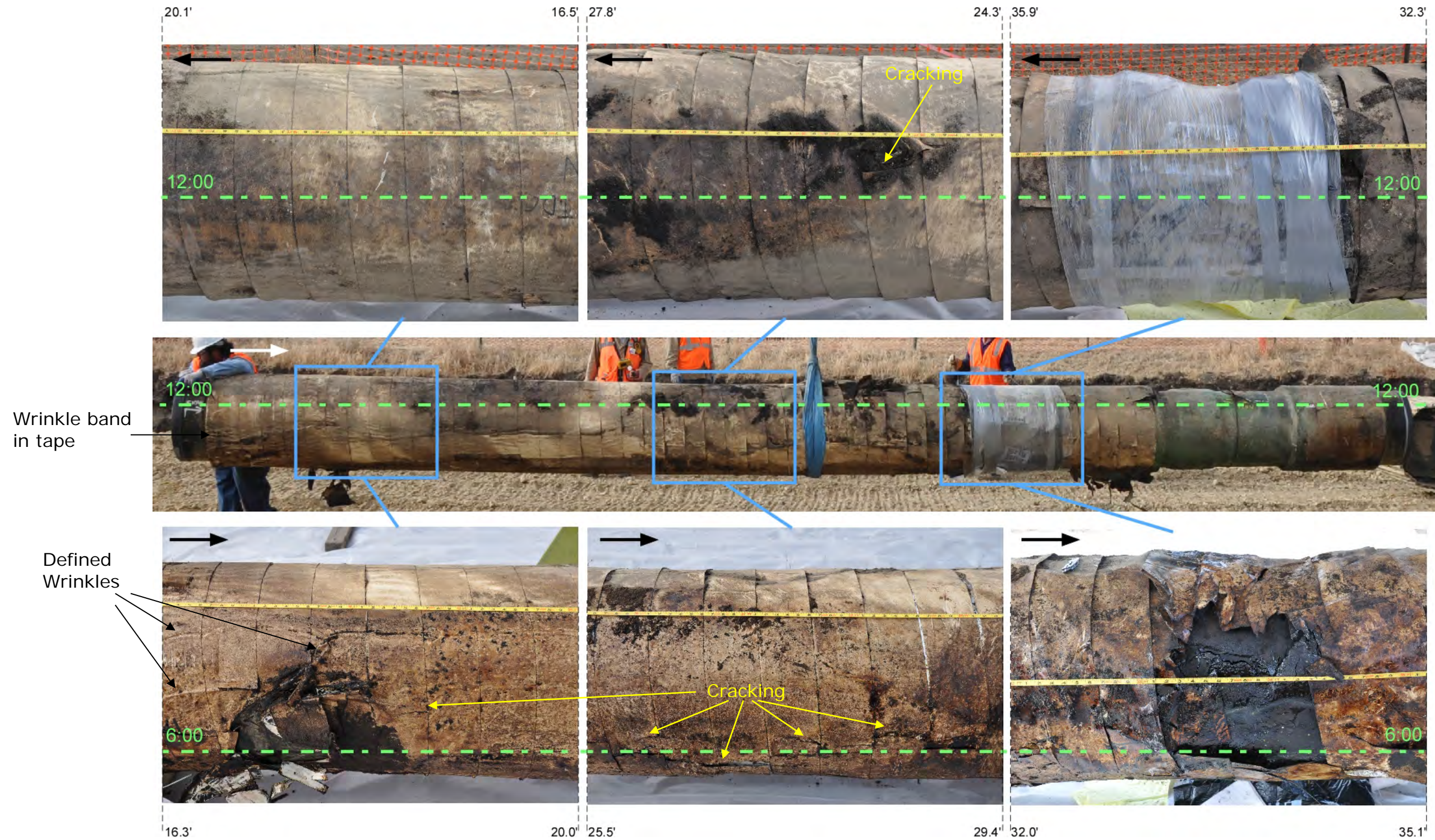


Figure 10. Photographs showing the condition of the external tape on the failure joint. Tape measure indicates distance to upstream girth weld.

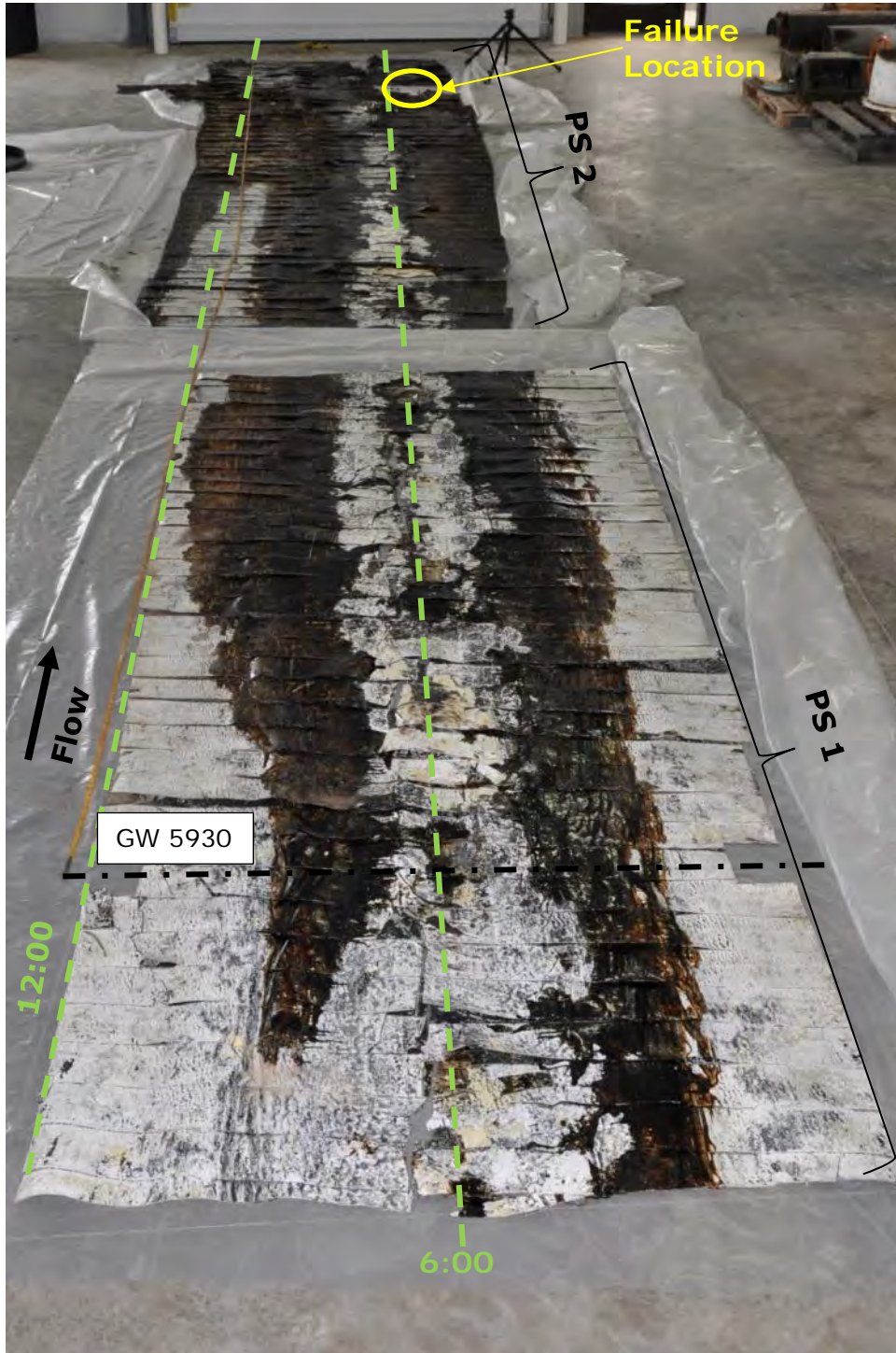


Figure 11. Photograph showing the internal surface of the external tape from the failure joint.



Figure 12. Photograph showing the internal surface of the external tape at the failure location. Tape measure indicates distance to upstream girth weld.

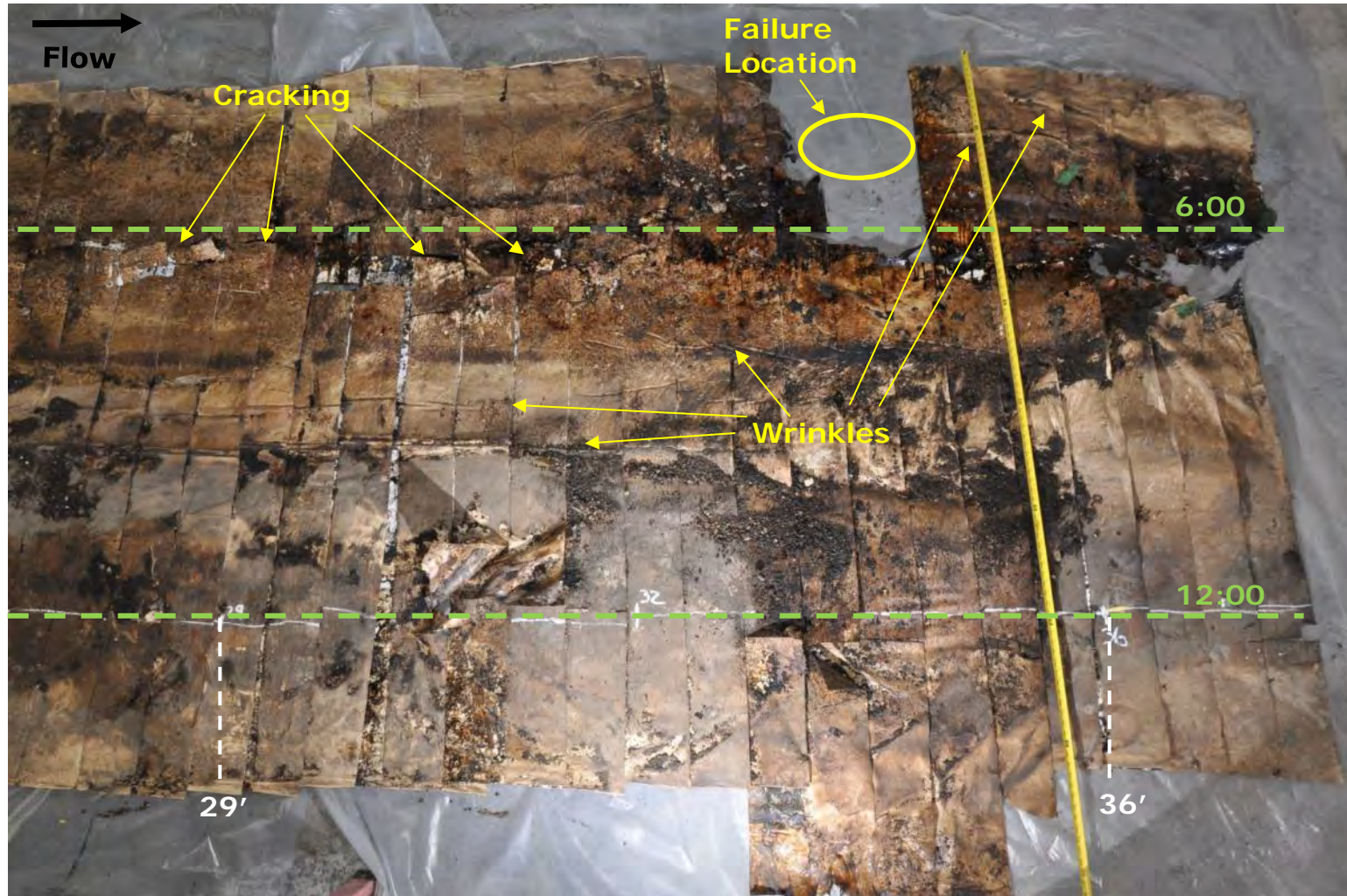


Figure 13. Photograph showing the external surface of the external tape at the failure location.

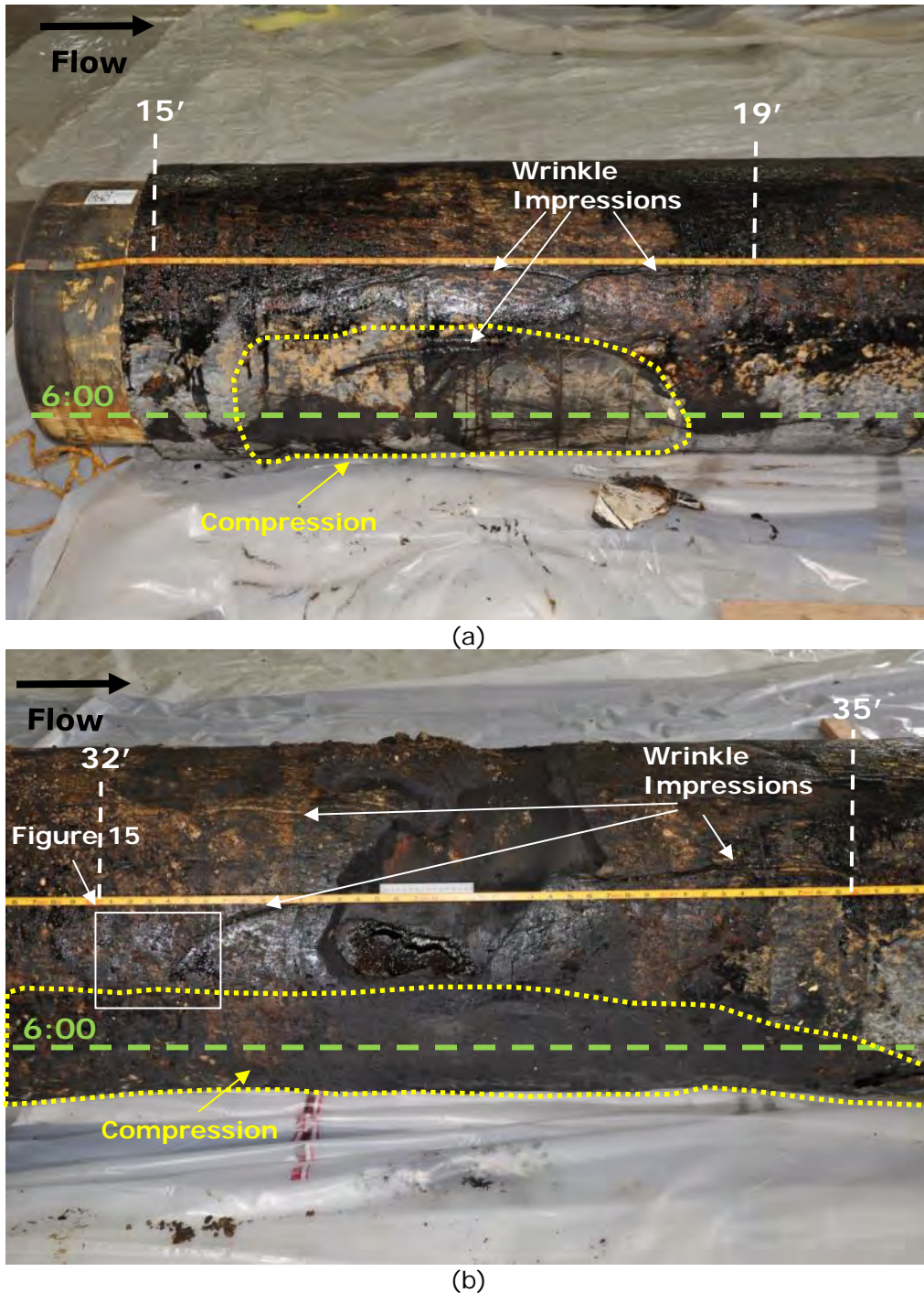


Figure 14. Photographs showing the external surface of the PU insulation at a) the U/S end of PS 2 (14' to 20' from U/S GW) and b) the failure location (31.5' to 36.4' from U/S GW). Tape measure indicates distance to upstream girth weld.

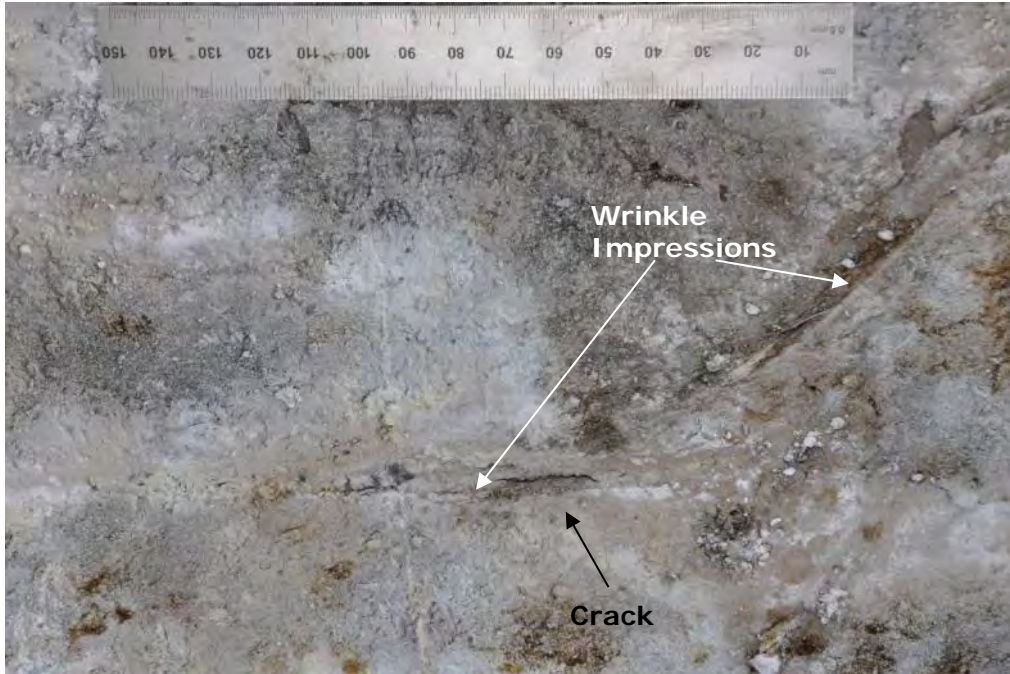


Figure 15. Photograph showing a crack in the PU insulation within a wrinkle. White contrast paint was applied to the surface to facilitate laser scanning and visual inspection. Area shown in Figure 14; scale in mm.

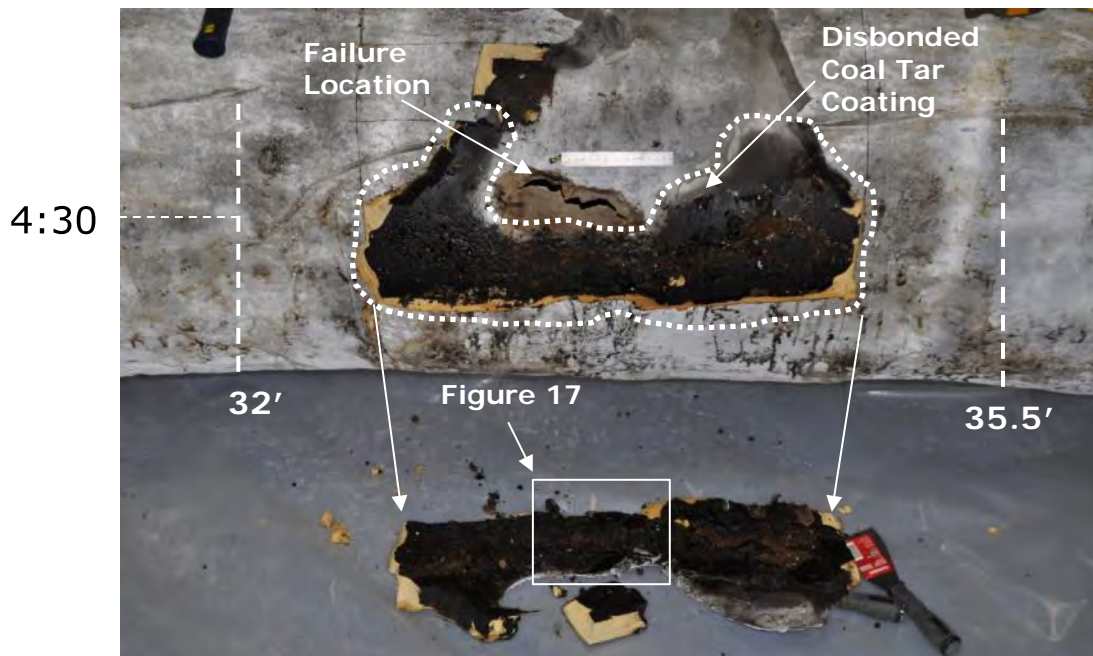


Figure 16. Photograph showing a piece of insulation removed from adjacent to the failure location; near 4:30 orientation.

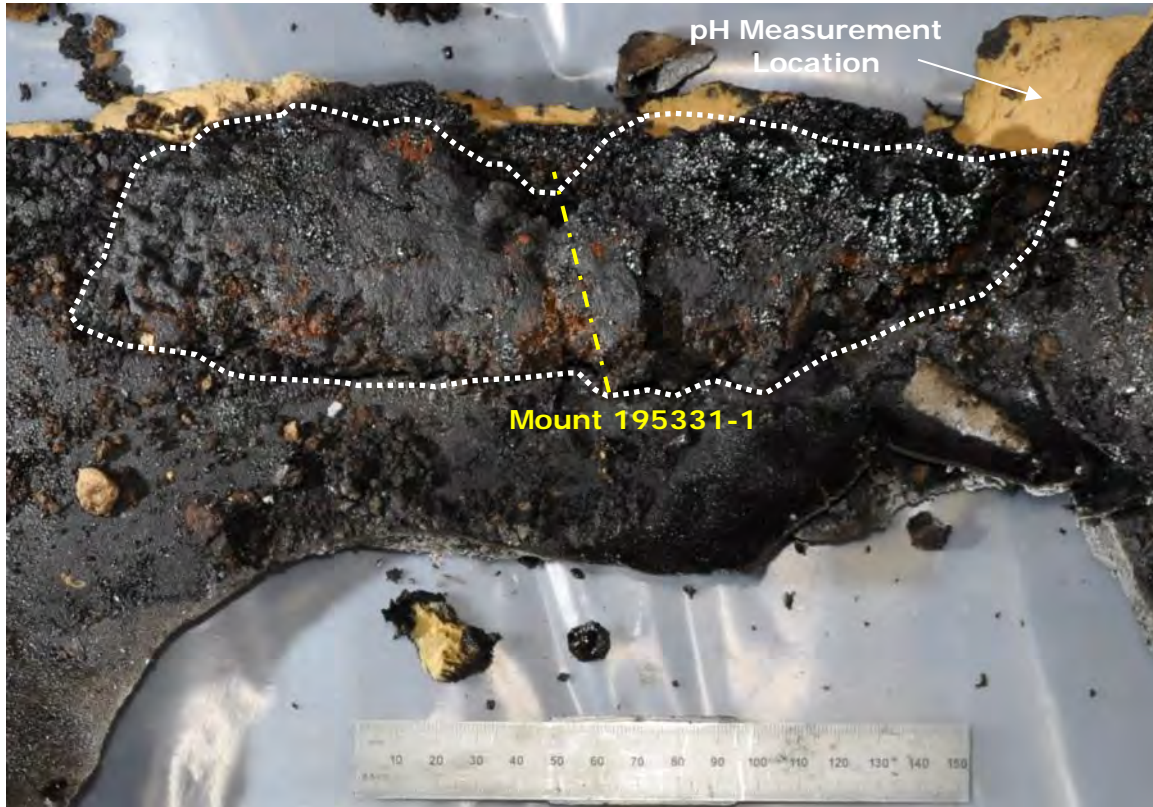


Figure 17. Photograph showing corrosion product that was wedged between the pipe surface and polyurethane insulation. Location indicated in Figure 16; scale in mm.

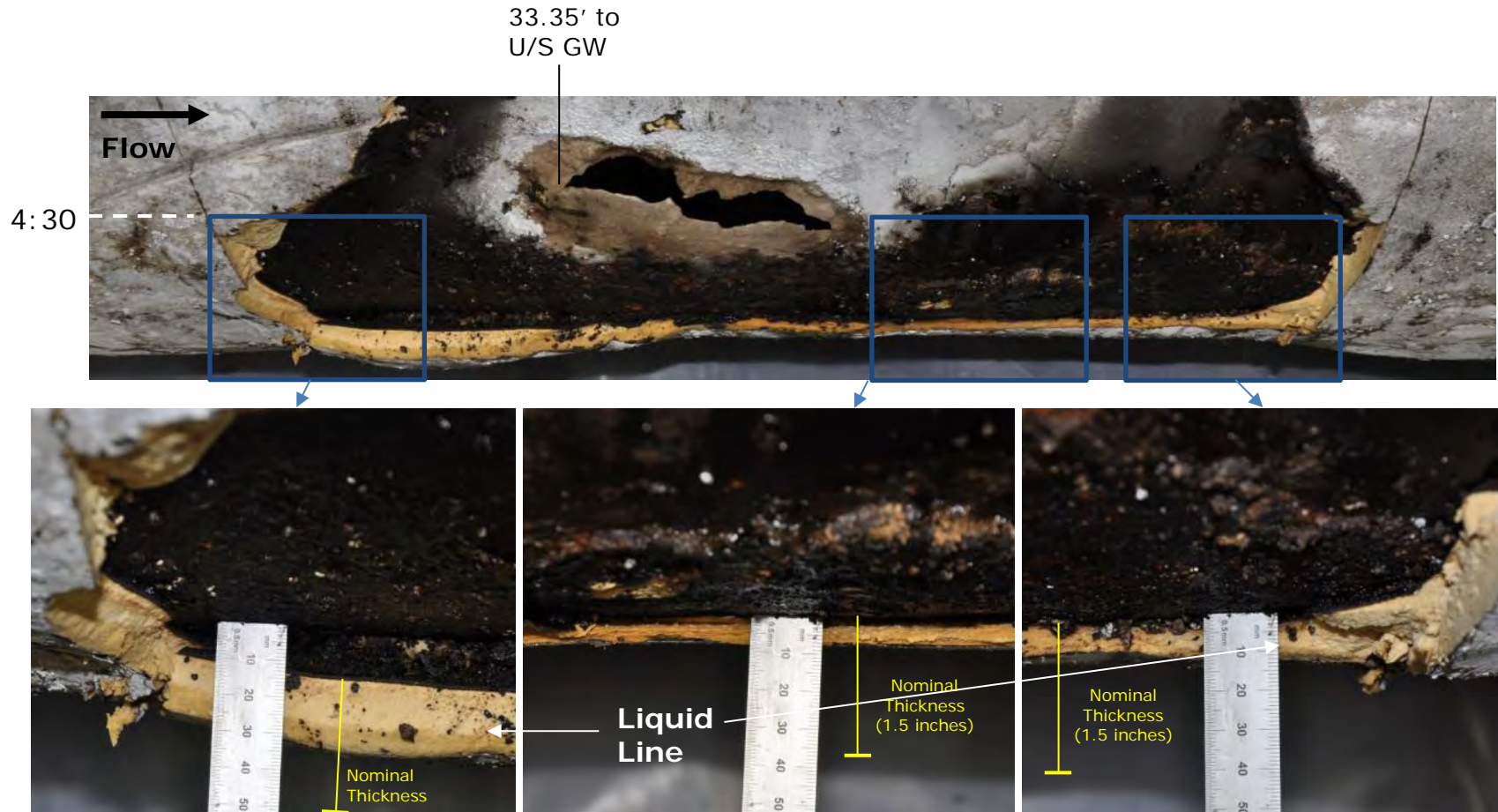


Figure 18. Photographs showing the amount of compression in the insulation adjacent to the failure location; near 6:00 orientation. Scale in mm.

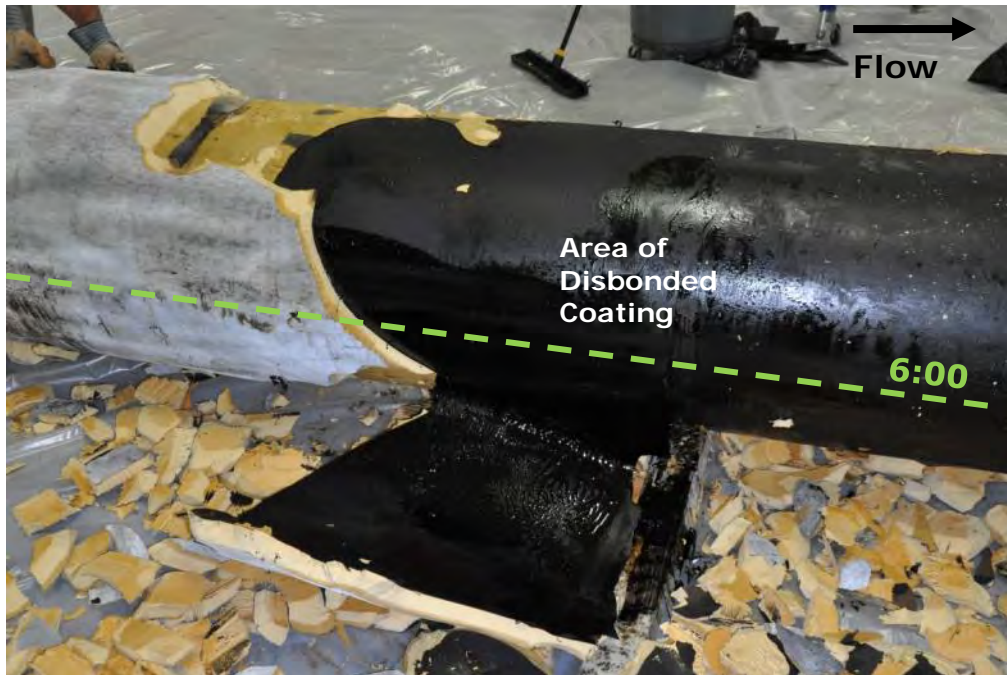


Figure 19. Photograph showing the insulation and coal tar coating separating from the pipe in large sheets on the underside of the pipe; approximately 29' from U/S GW.



Figure 20. Photograph showing the insulation and coal tar coating separating from the pipe in large sheets on the underside of the pipe; approximately 17' from U/S GW.

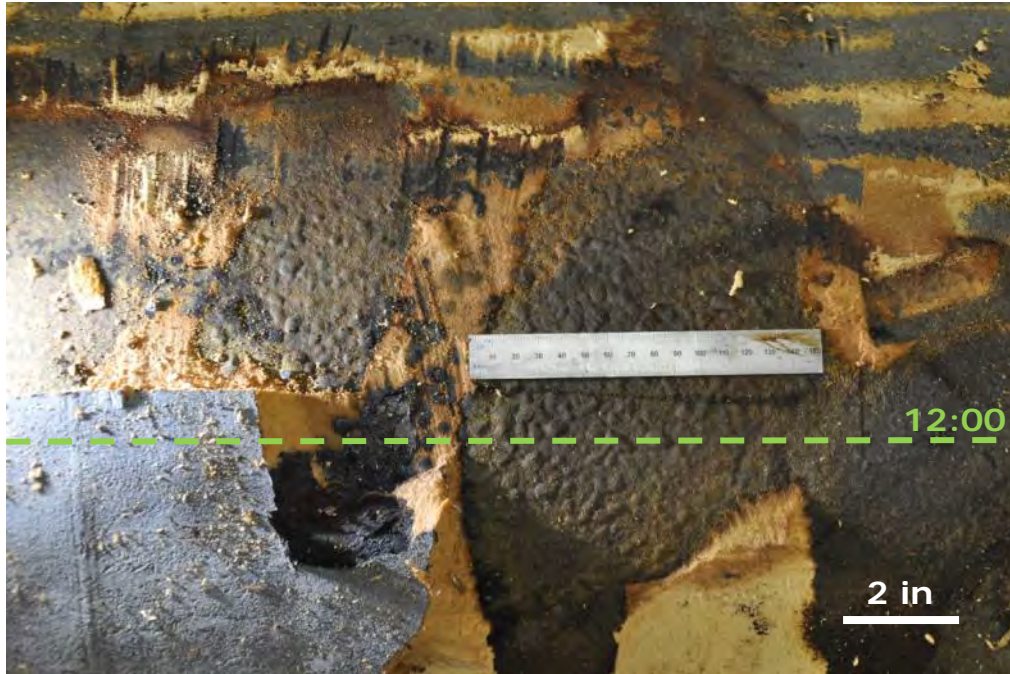


Figure 21. Photograph showing blistered coal tar coating along the 12:00 orientation on PS 2; approximately 28' from U/S GW.

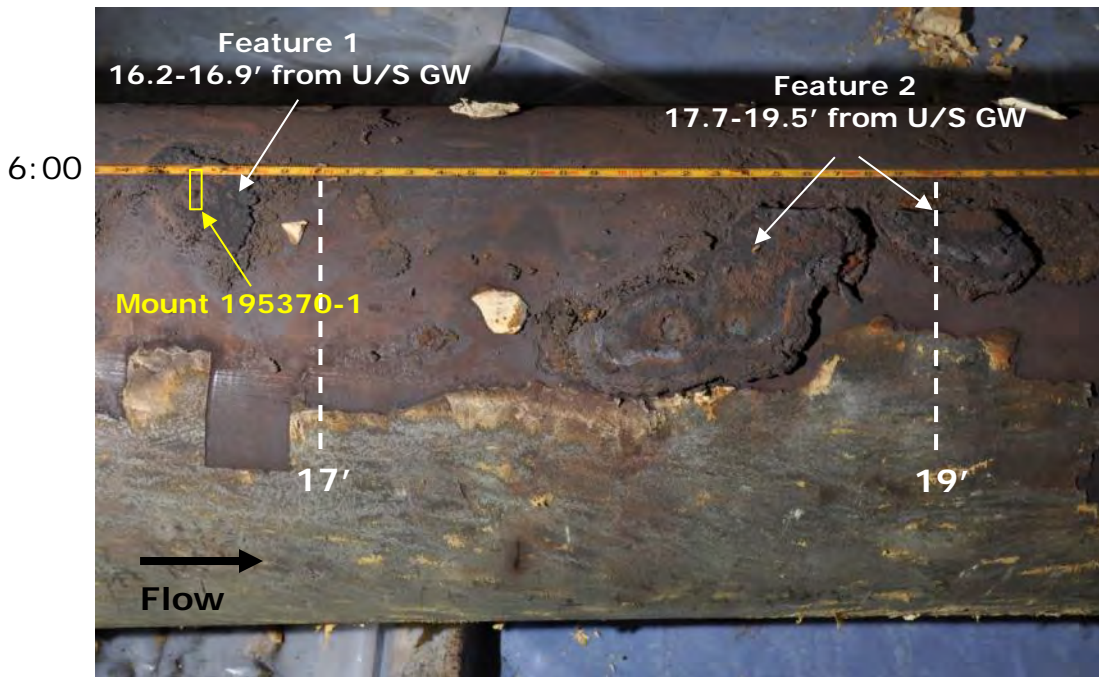


Figure 22. Photograph showing external corrosion features on PS 2; Feature 1 and Feature 2. Tape measure indicates distance to upstream girthing weld.

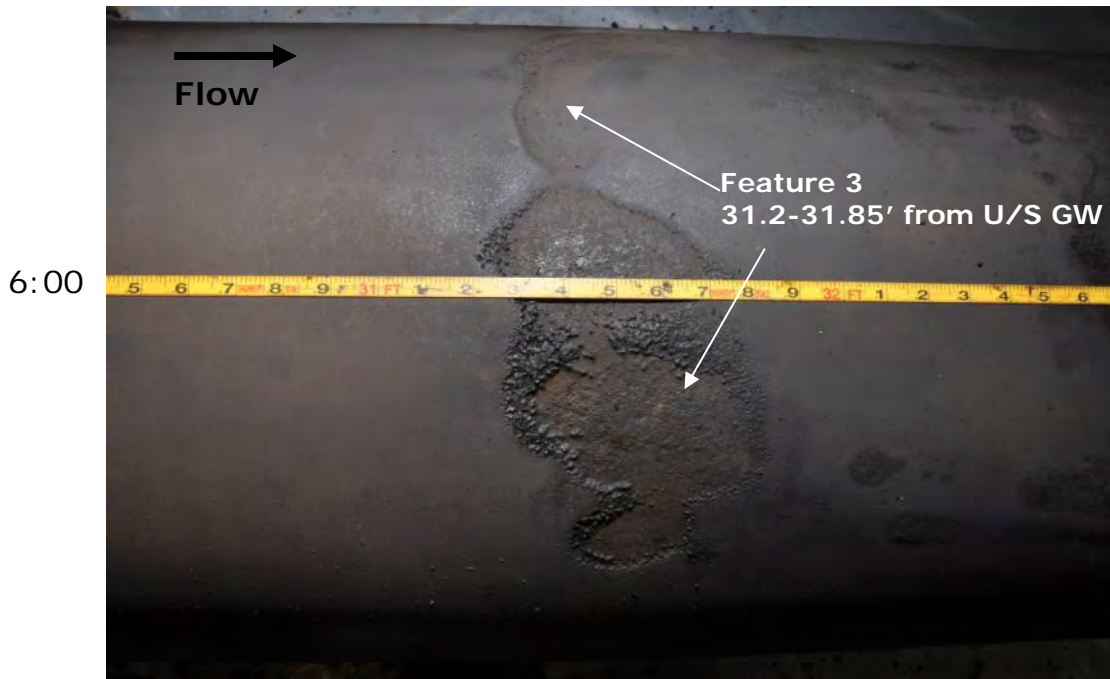


Figure 23. Photograph showing an external corrosion feature on PS 2; Feature 3. Tape measure indicates distance to U/S GW.

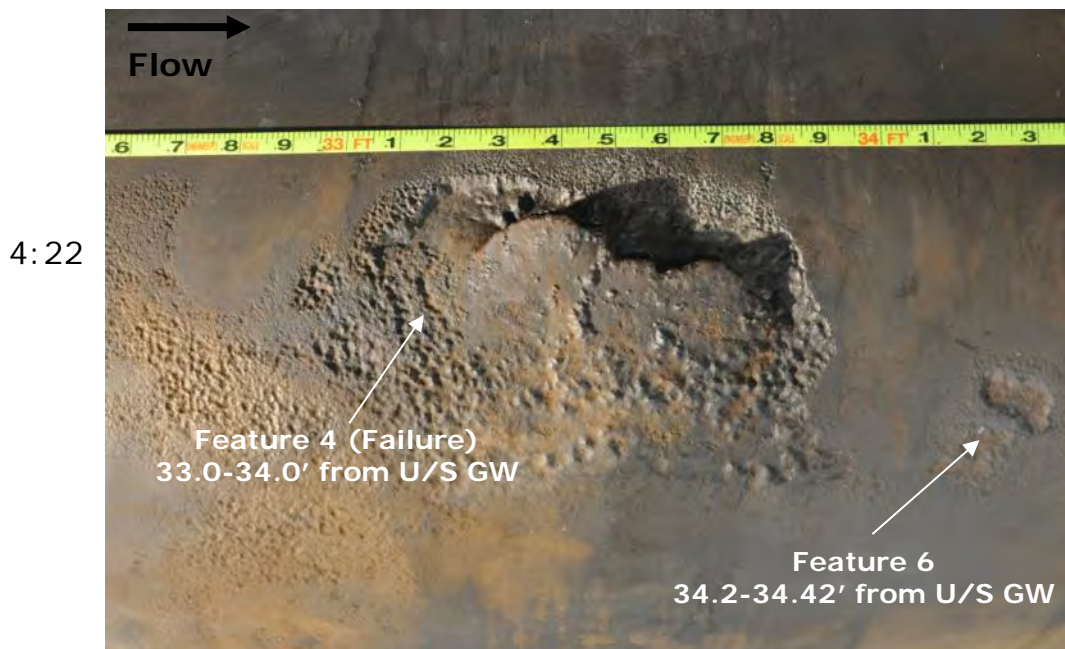


Figure 24. Photograph showing external corrosion features on PS 2; Feature 4 and Feature 6. Tape measure indicates distance to U/S GW (Note: tape slipped 0.1' to the right).

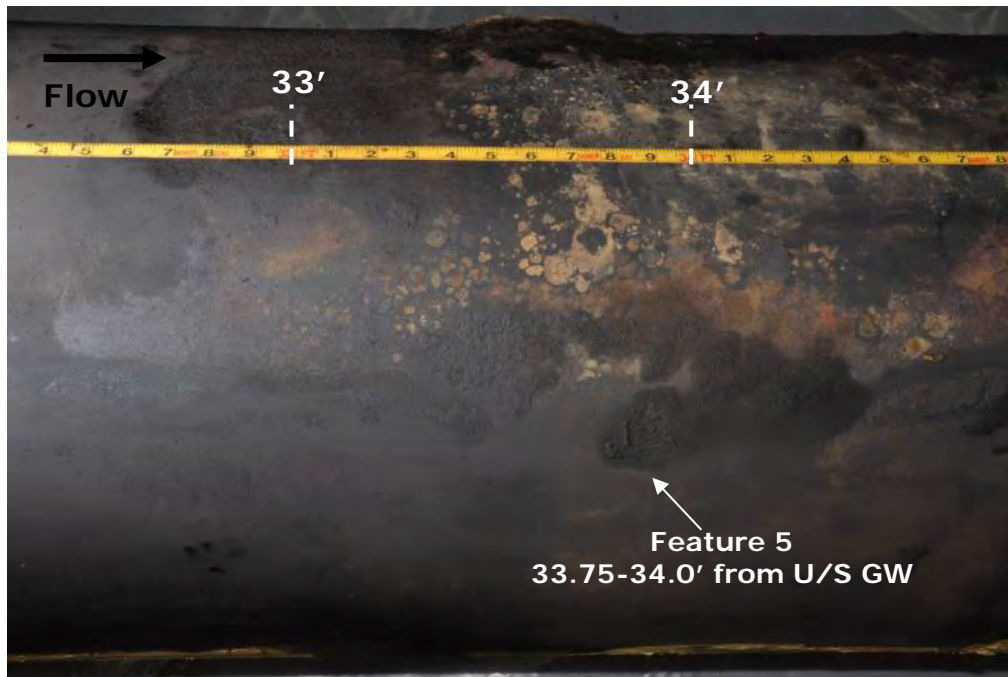
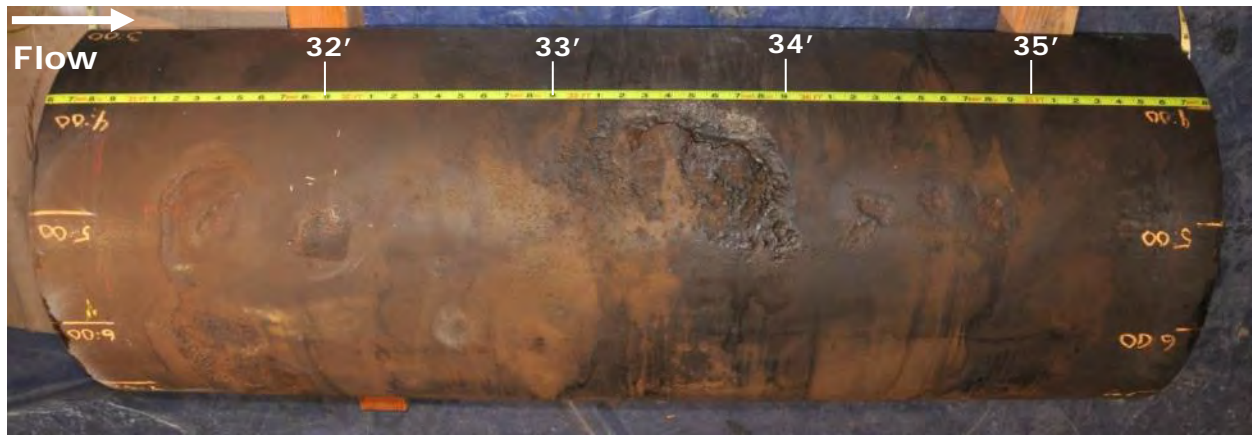
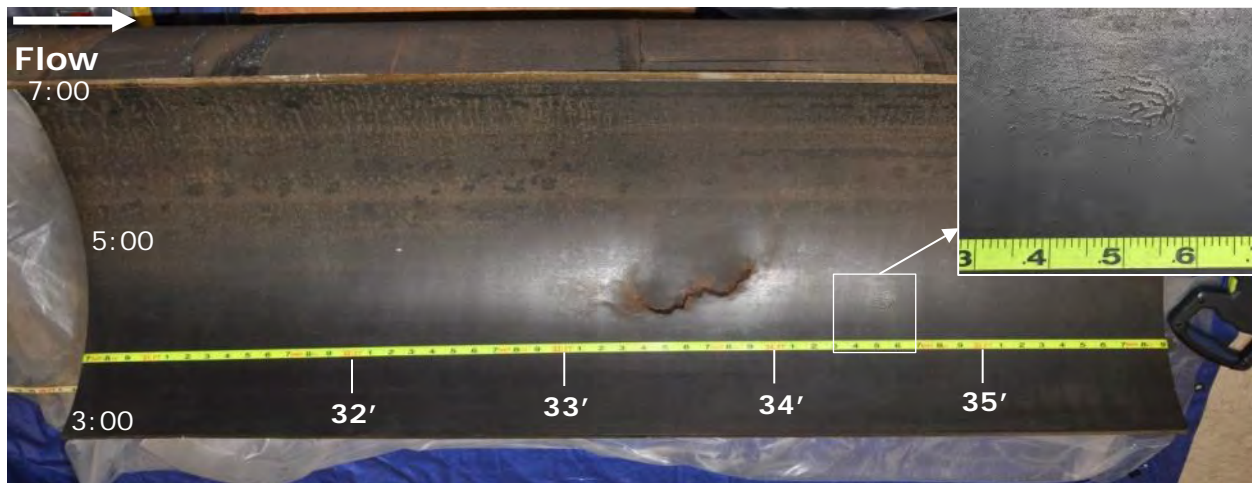


Figure 25. Photograph showing an external corrosion feature on PS 2; Feature 5. Tape measure indicates distance to U/S GW.



(a)

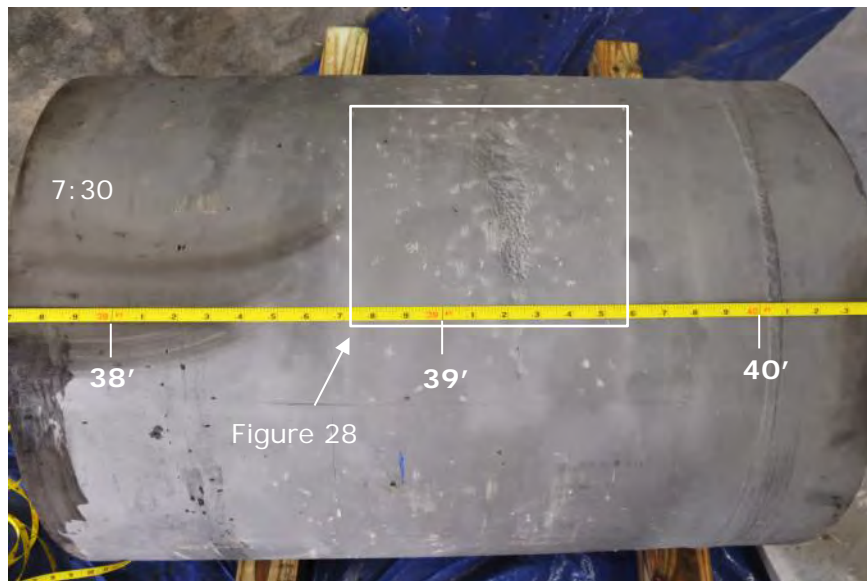


(b)

Figure 26. Photographs showing the a) external and b) internal surfaces of the pipe section at the failure location (Coupon 1).



(a)



(b)

Figure 27. Photographs showing Pipe Section 2 from 37.7 feet to 40.4 feet from GW 5930 a) before and b) after the composite repair sleeve was removed. Tape measure indicates distance to U/S GW (GW 5930).



Figure 28. Photograph the primary feature repaired on May 13, 2013. Area shown in Figure 27. Tape measure indicates distance to U/S GW.

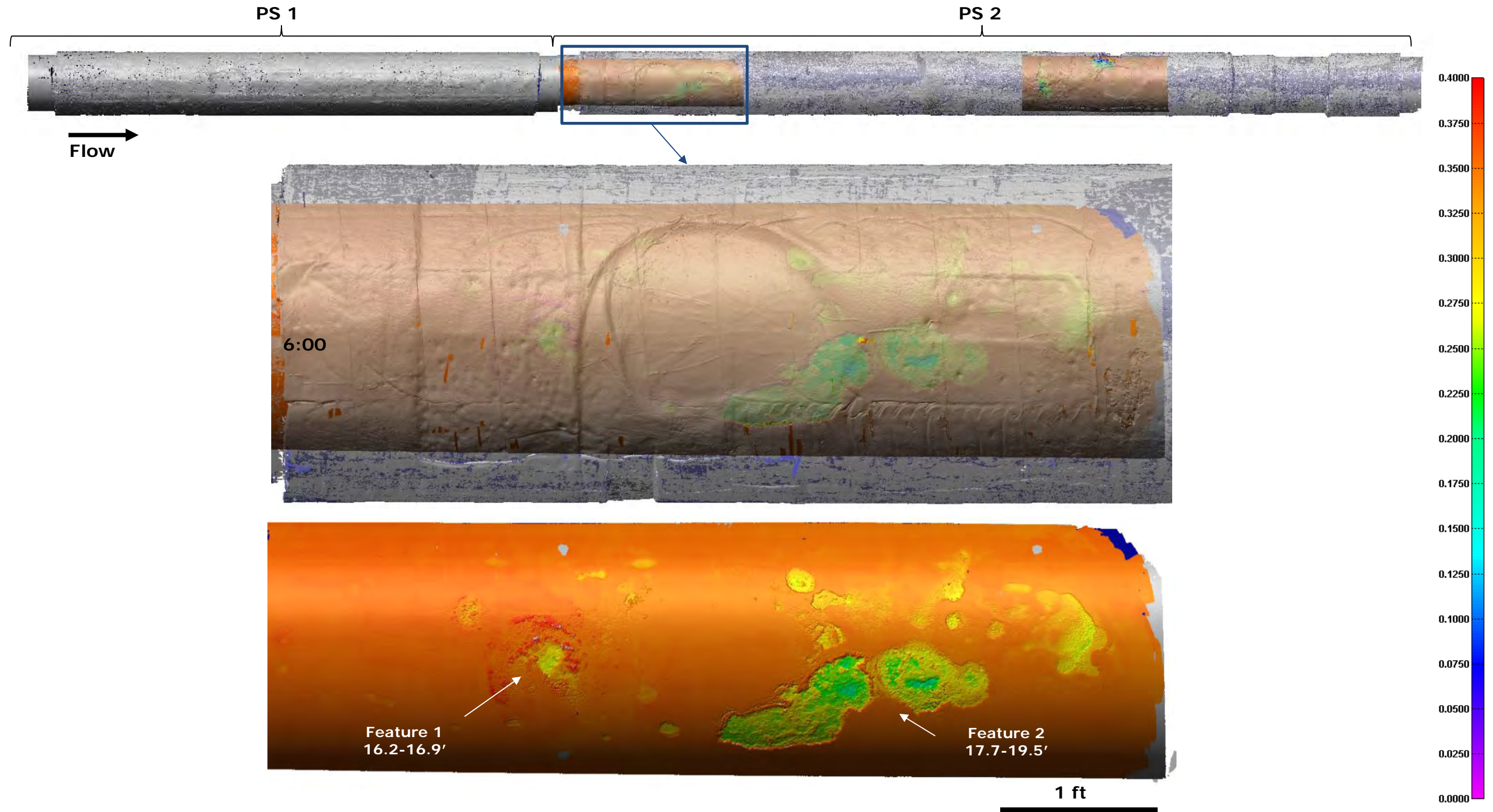


Figure 29. Renderings of PS 1 and PS 2 (viewed from the OD surface) from laser scanning data showing Feature 1 and Feature 2; Coupon 2. The transparency of the insulation was changed to show a correlation between the features observed on the insulation with corrosion features observed on the pipe. The scale on the right is from 0.000 to 0.400 inches.

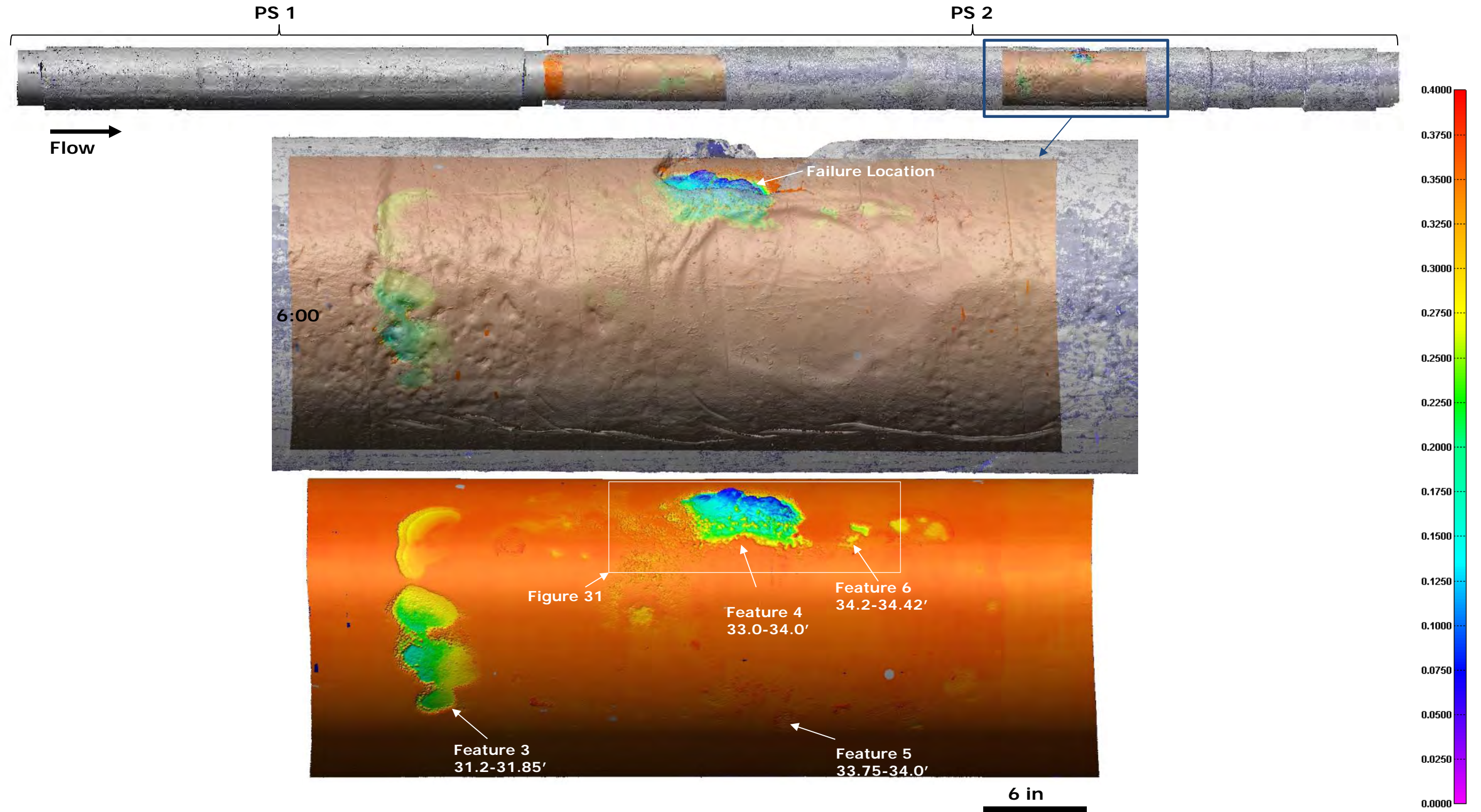


Figure 30. Renderings of PS 1 and PS 2 (viewed from the OD surface) from laser scanning data showing the failure location (Feature 4) and Feature 3, 5, and 6; Coupon 1. The transparency of the insulation was changed to show a correlation between the features observed on the insulation with corrosion features observed on the pipe. The scale on the right is from 0.000 to 0.400 inches.

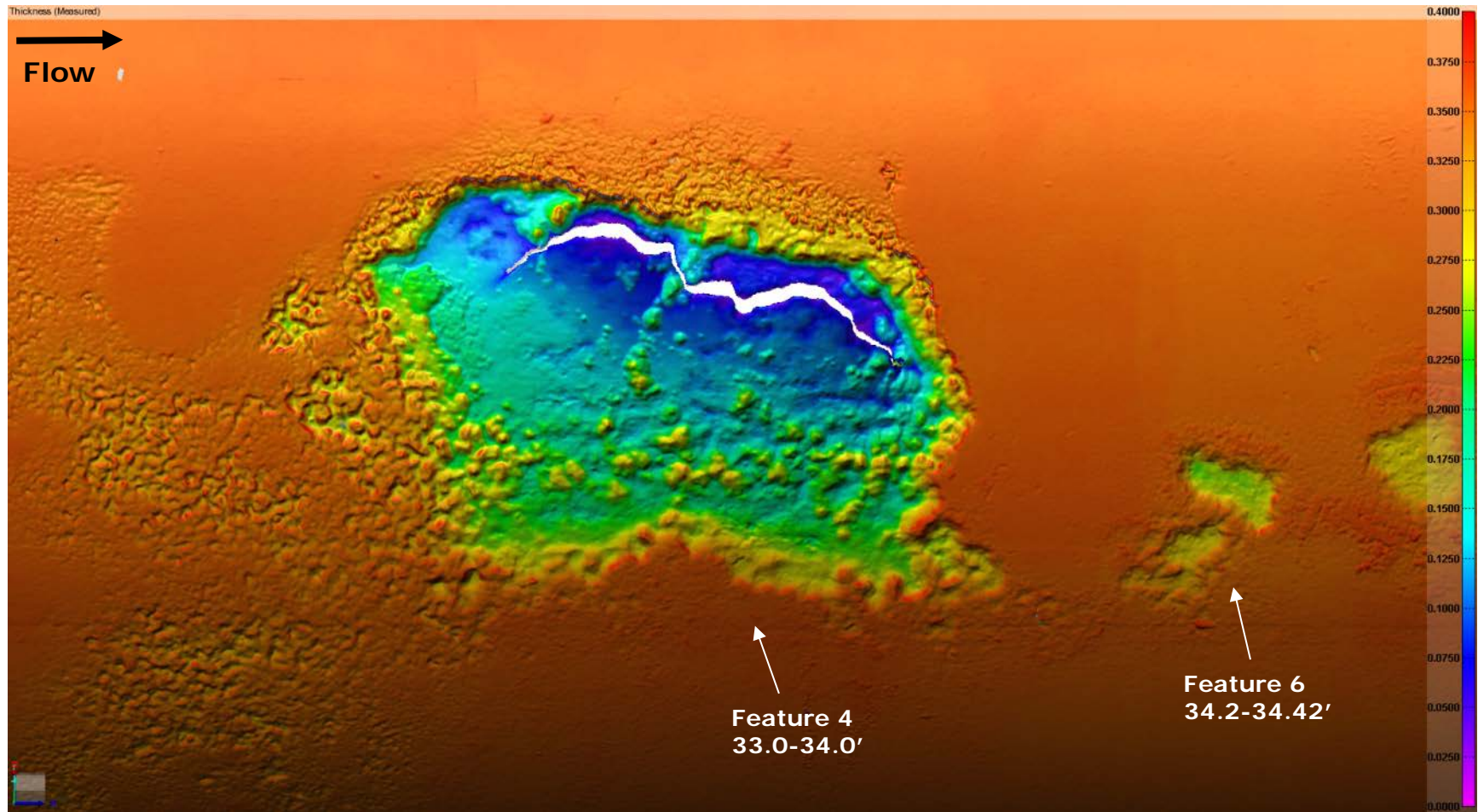


Figure 31. Rendering of the failure location (viewed from the OD surface) from laser scanning data showing the remaining wall thickness along the fracture surface. The scale on the right is from 0.000 to 0.400 inches. Location indicated in Figure 30.

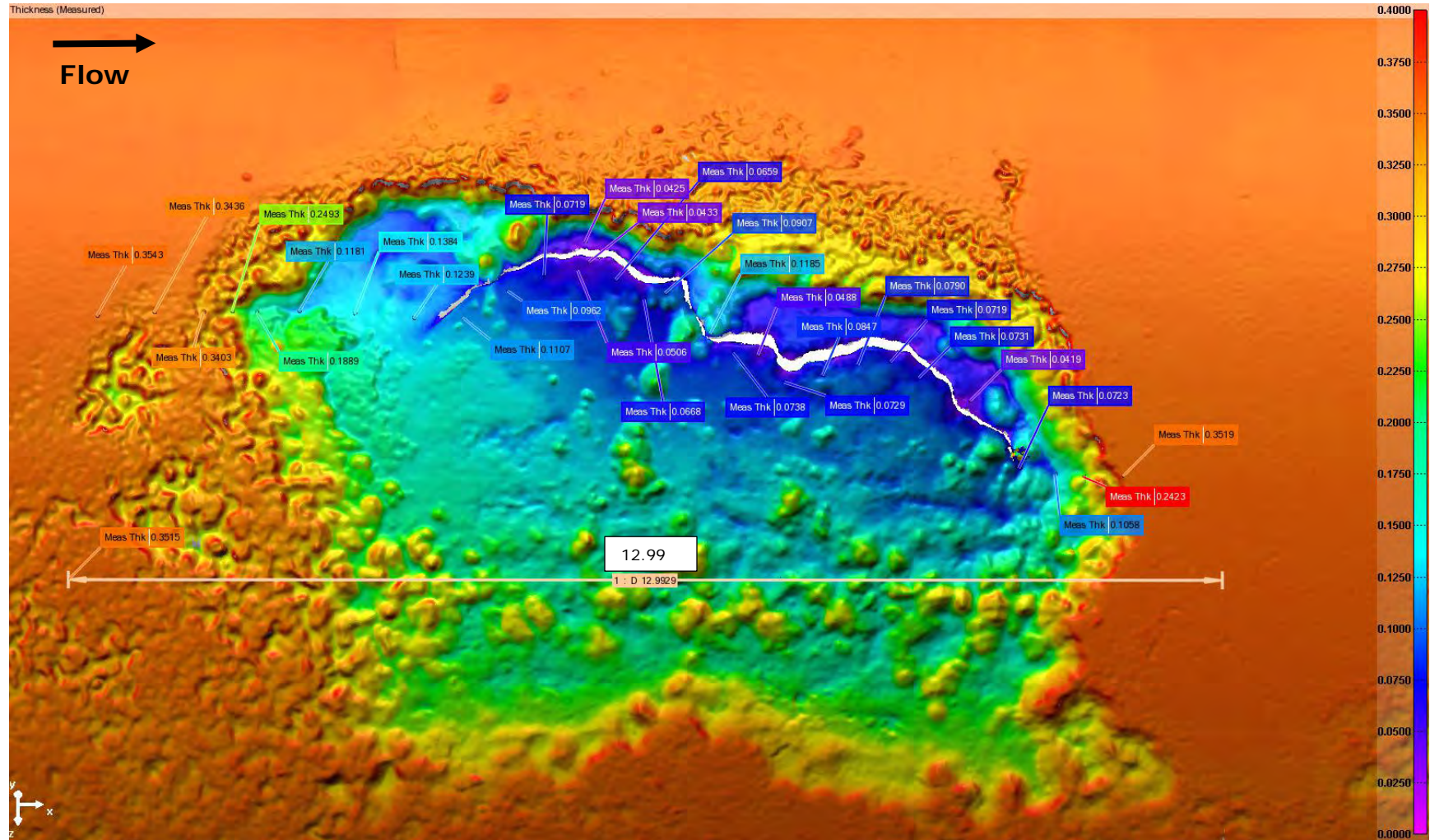


Figure 32. Rendering of the failure location showing various thickness measurements made along the corrosion feature and failure opening. The scale on the right is from 0.000 to 0.400 inches. Measurements are tabulated in Table 4.

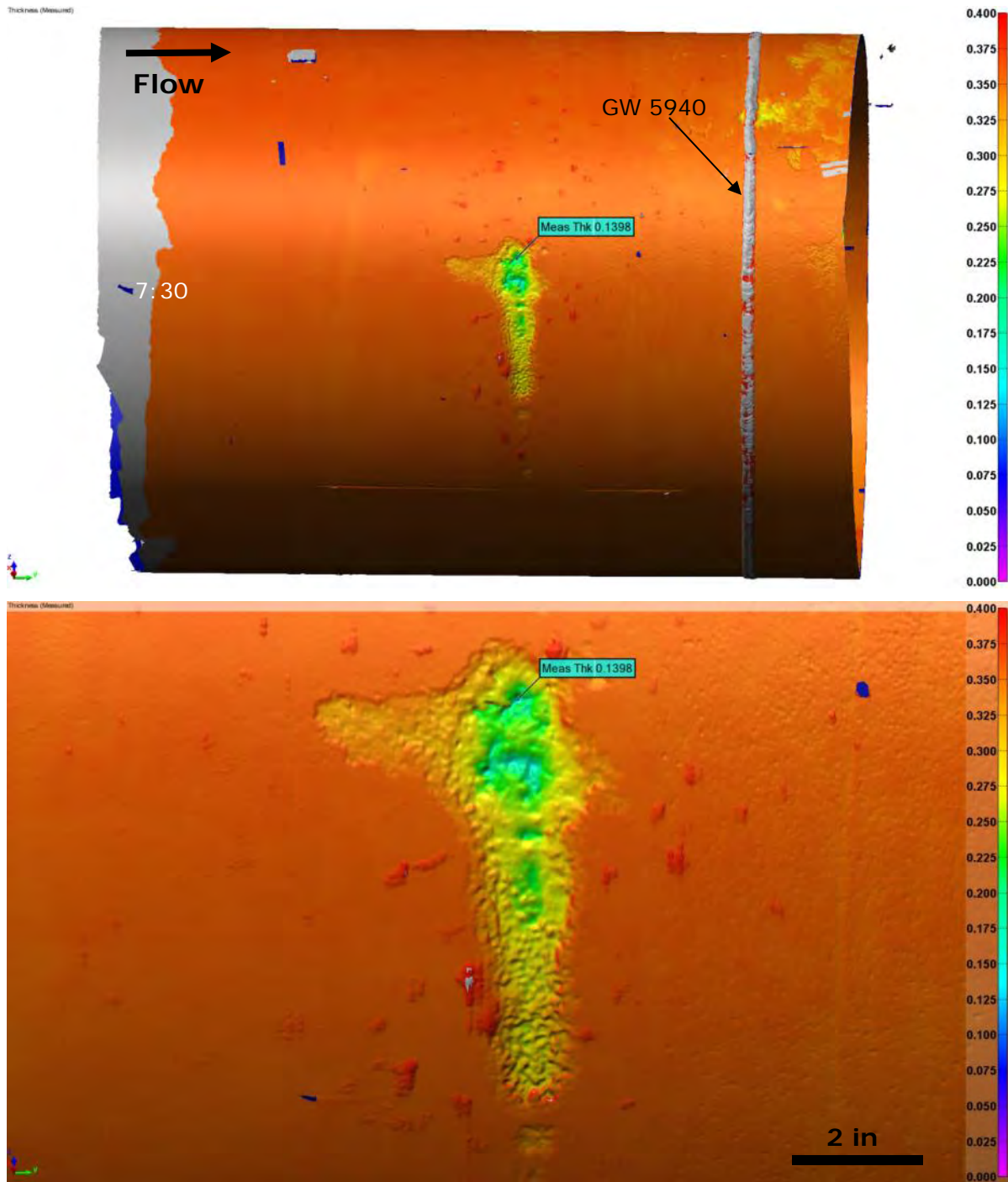


Figure 33. Renderings of the area under the composite repair sleeve showing the thickness profile for the feature repaired on May 13, 2013. The scale on the right is from 0.000 to 0.400 inches.

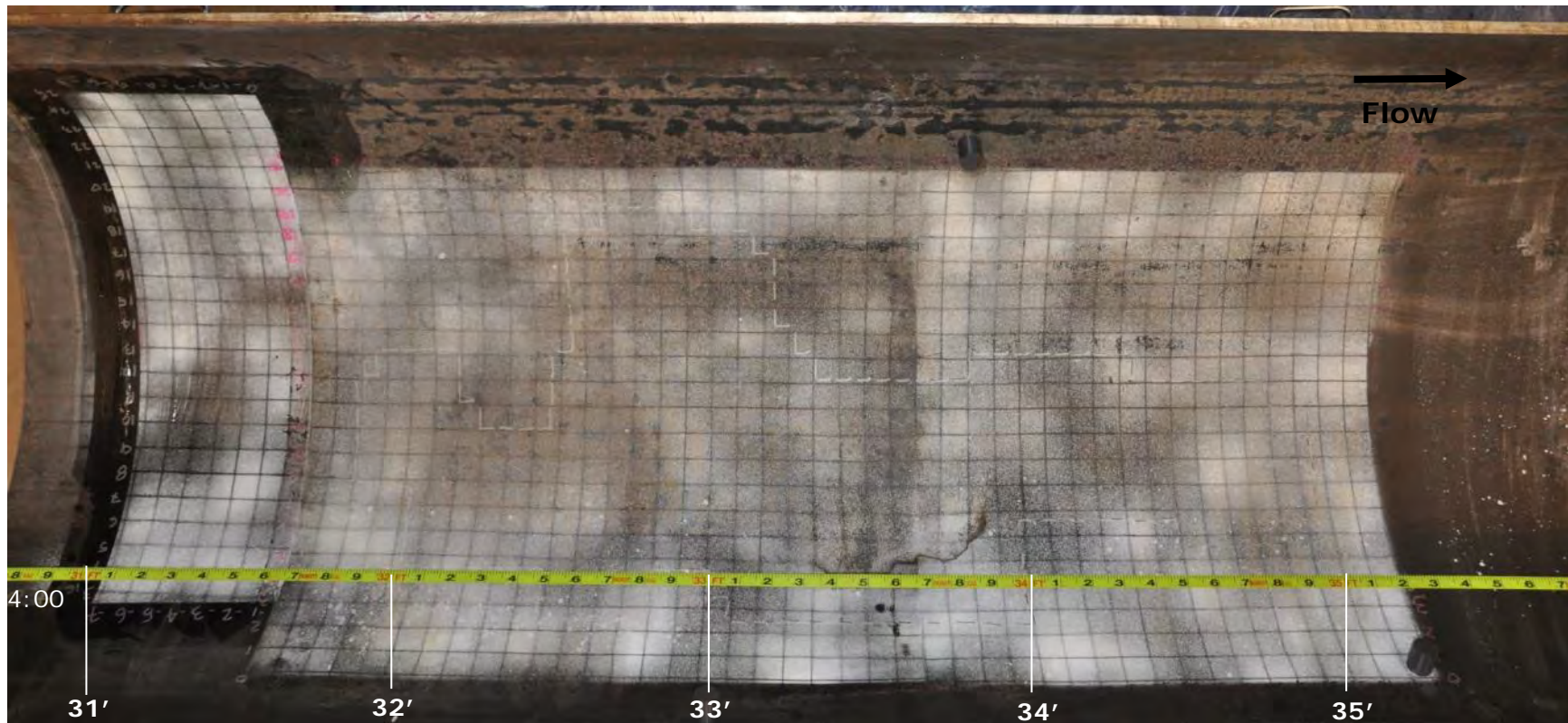


Figure 34. Photograph showing the internal surface of the pipe section at the failure location with the 1 × 1 inch grid painted on the surface. Tape measure indicates distance to U/S GW.

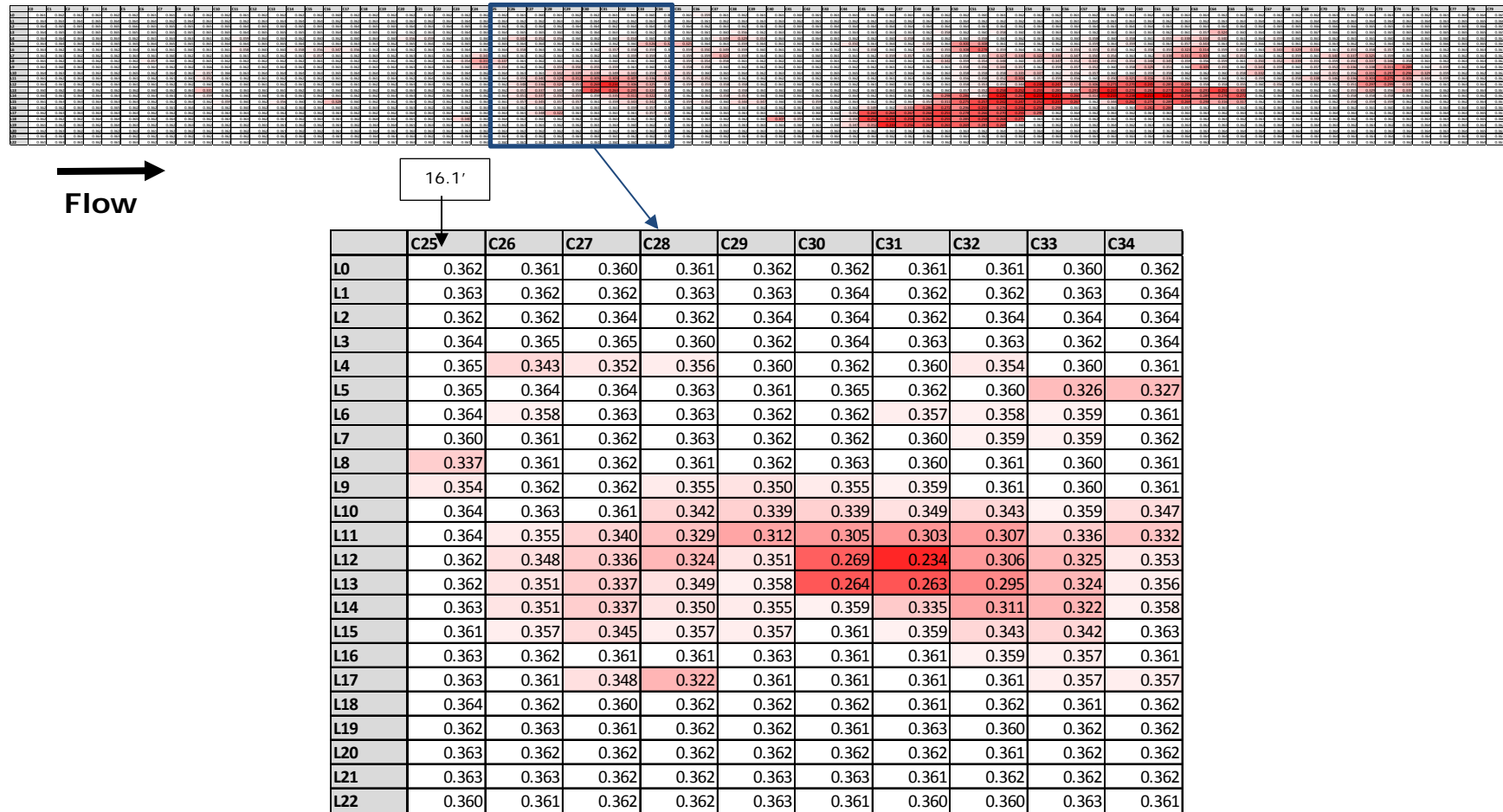


Figure 36. Results of the UT measurements performed on 1" x 1" grid near Feature 1 (Coupon 2).

Plains All American Pipeline, L.P.
 Line 901 Release (05-19-15): Mechanical and Metallurgical Testing

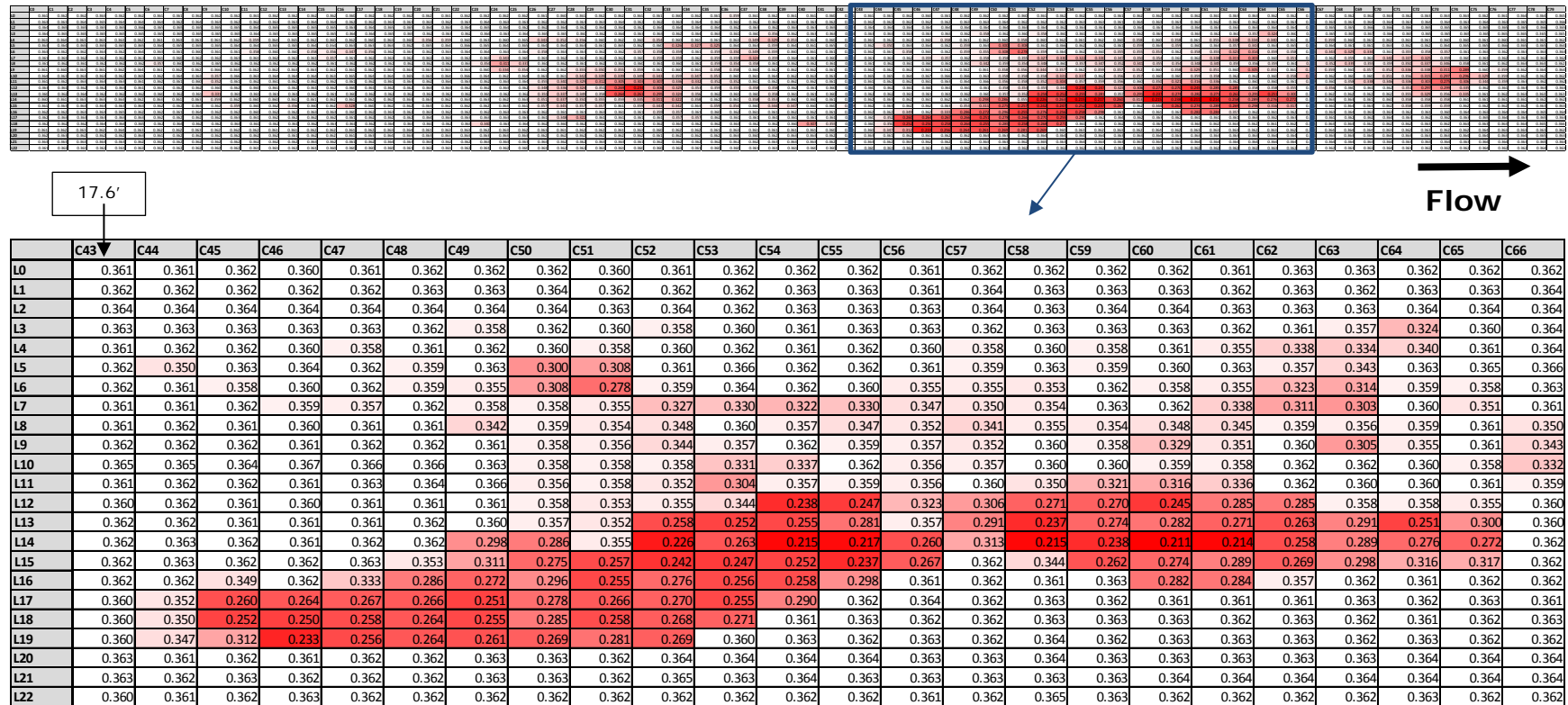


Figure 37. Results of the UT measurements performed on 1" x 1" grid near Feature 2 (Coupon 2).



(a)



(b)

Figure 38. Photographs showing the a) clockwise and b) counterclockwise fractures surfaces following cleaning with a degreaser and acetone and/or methanol. Tape measure indicates distance to U/S GW.

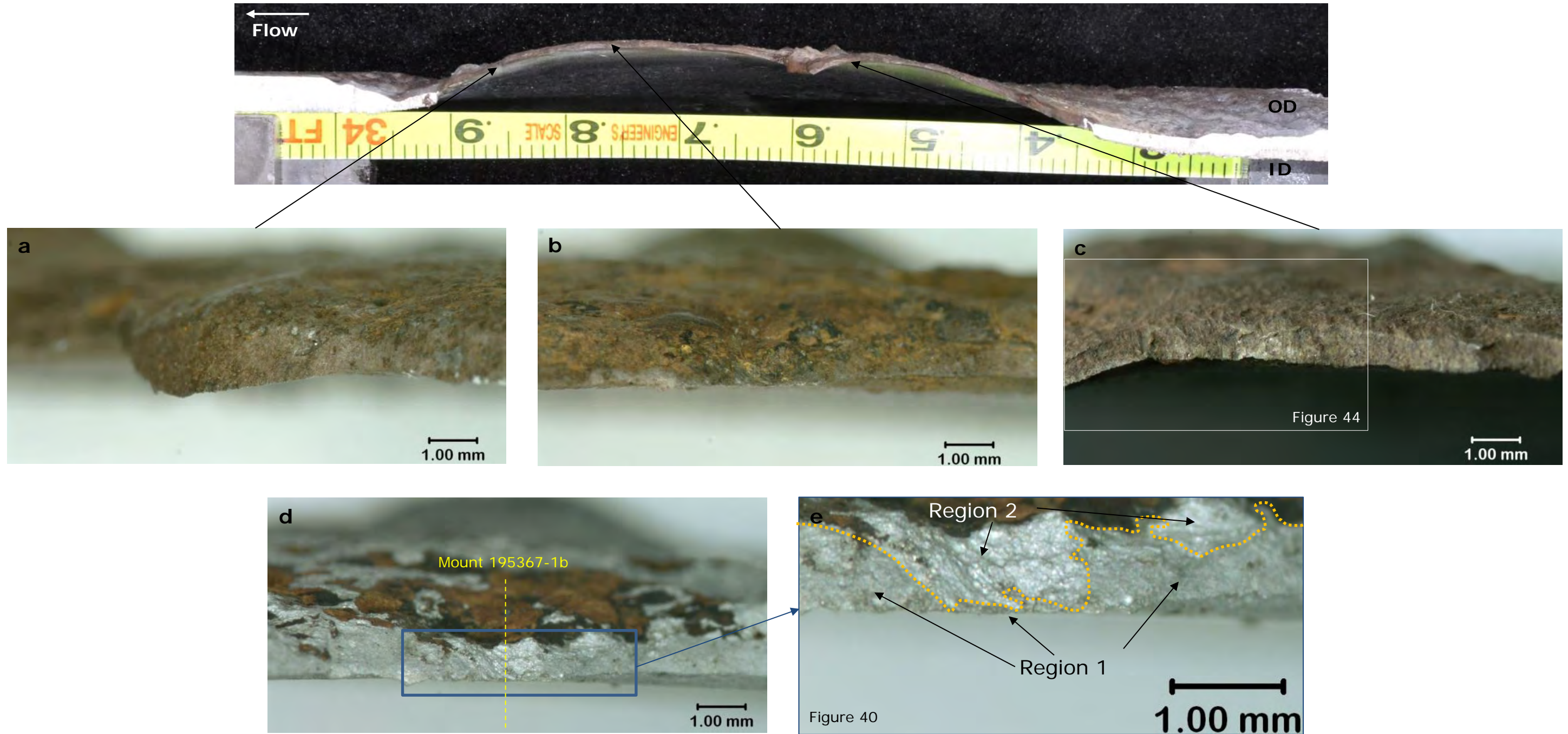


Figure 39. Stereo light photomicrographs of representative locations along the clockwise fracture surface following cleaning with a), b), c) a degreaser and acetone and/or methanol and d), e) an inhibited HCl acid and ENPREP®. Photomicrographs b) and d) are from the same location. Tape measure indicates distance to U/S GW.

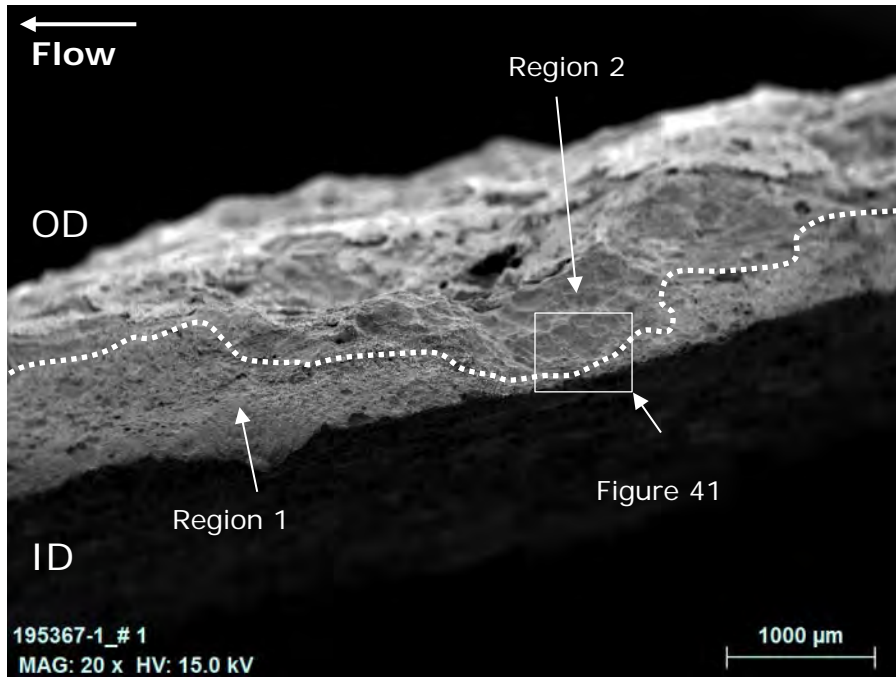


Figure 40. SEM image showing the fracture surface at the location identified in Figure 39e.

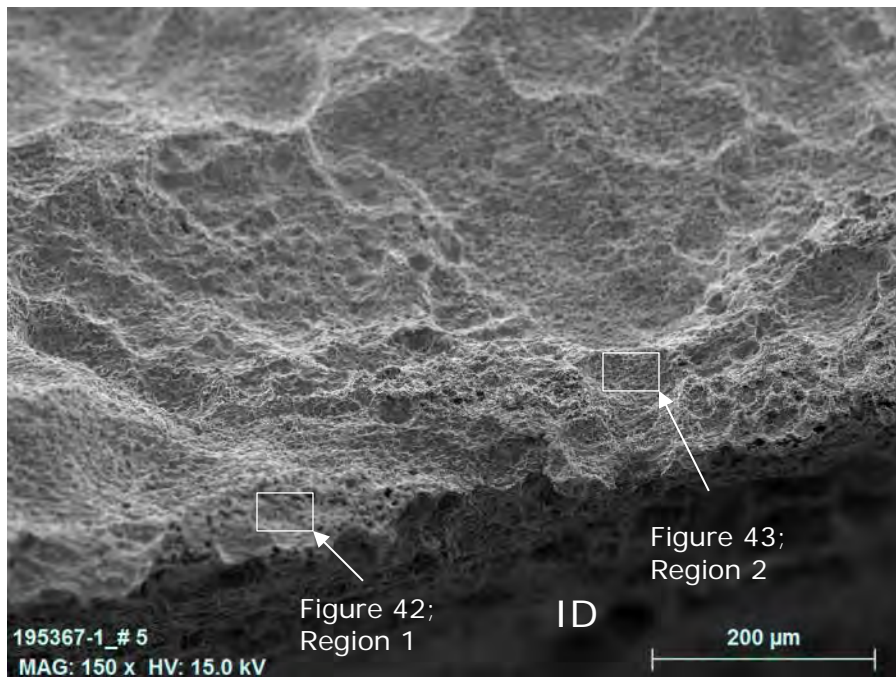


Figure 41. SEM image showing the transition between Region 1 and Region 2. Area indicated in Figure 40.

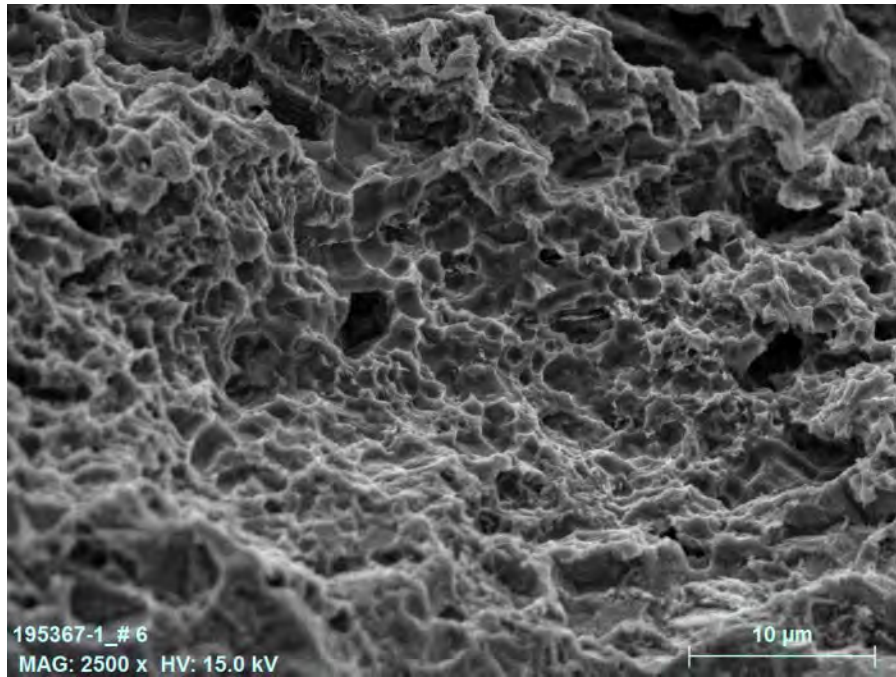


Figure 42. SEM image showing the ductile fracture morphology of Region 1. Area indicated in Figure 41

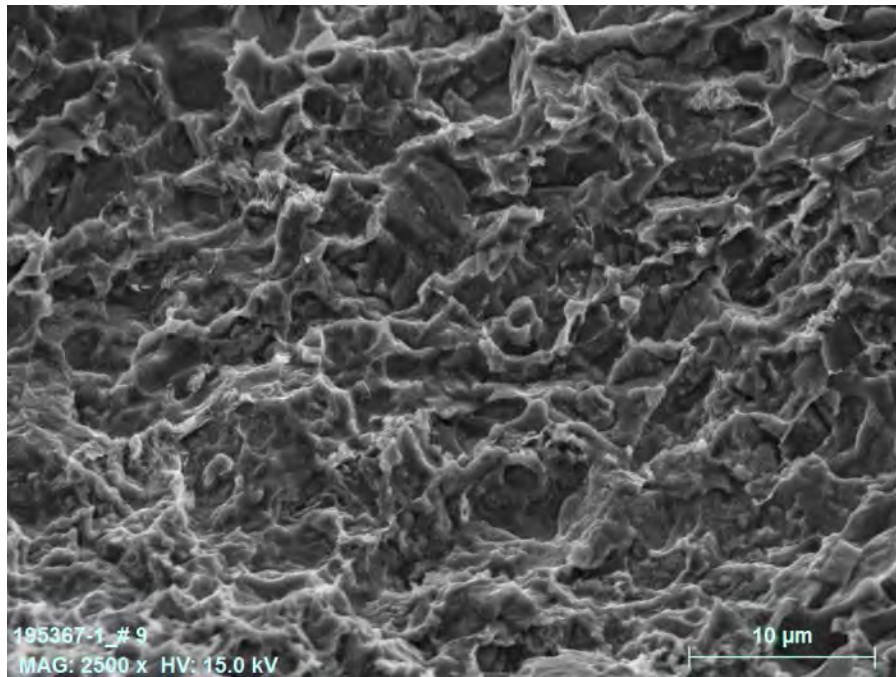


Figure 43. SEM image showing a nondescript/corroded morphology of Region 2. Area indicated in Figure 41

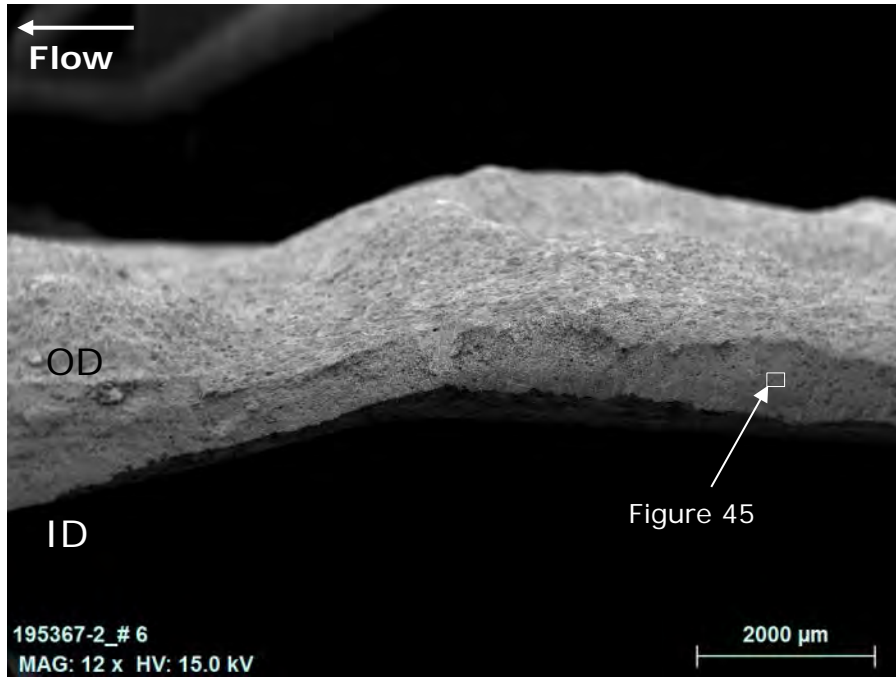


Figure 44. SEM image showing the fracture surface at the location identified in Figure 39c.

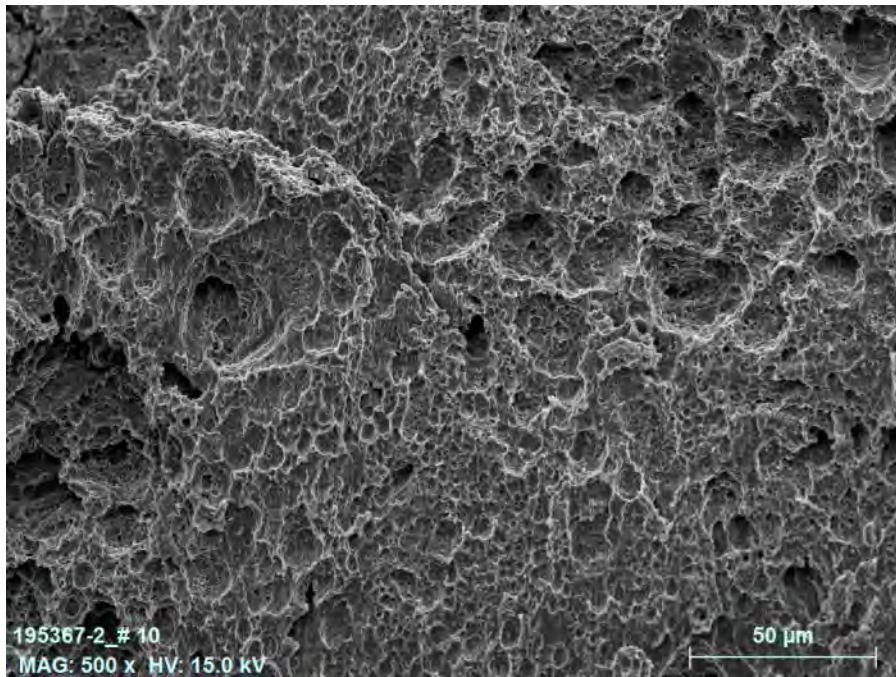


Figure 45. SEM image showing a representative ductile fracture morphology for Region 1. Area indicated in Figure 44.

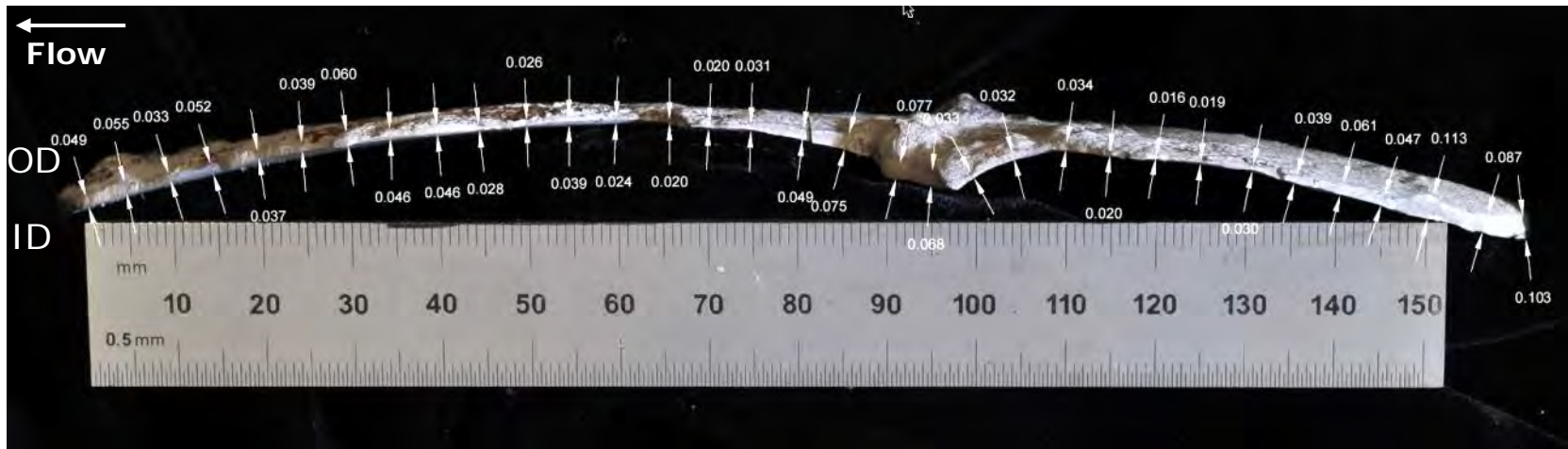


Figure 46. Photograph of the clockwise fracture surface showing thickness measurements of the Region 1 along the fracture surface at 5 mm intervals. Scale in mm.

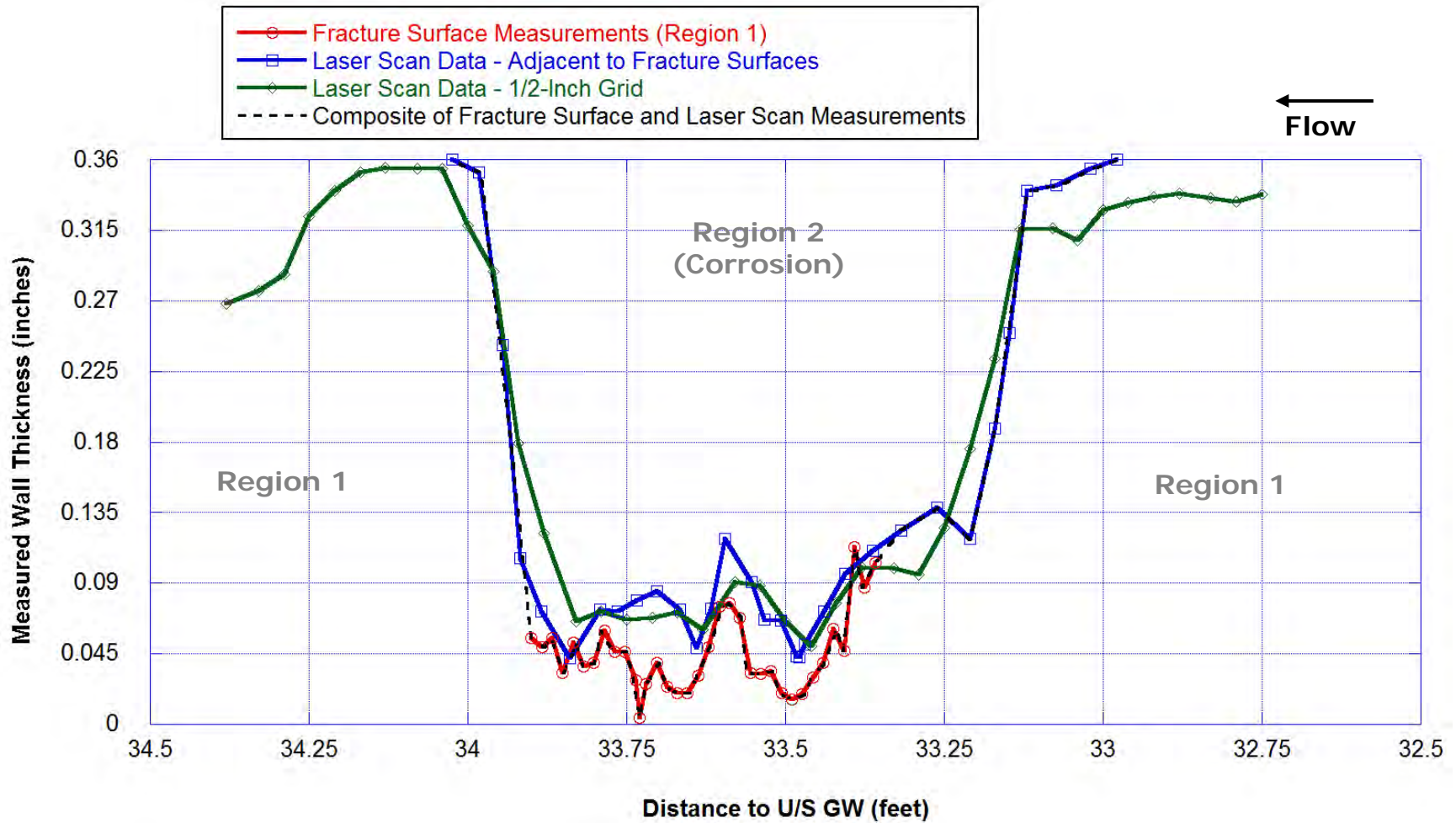


Figure 47. Fracture/Corrosion profile based on three measurement techniques.

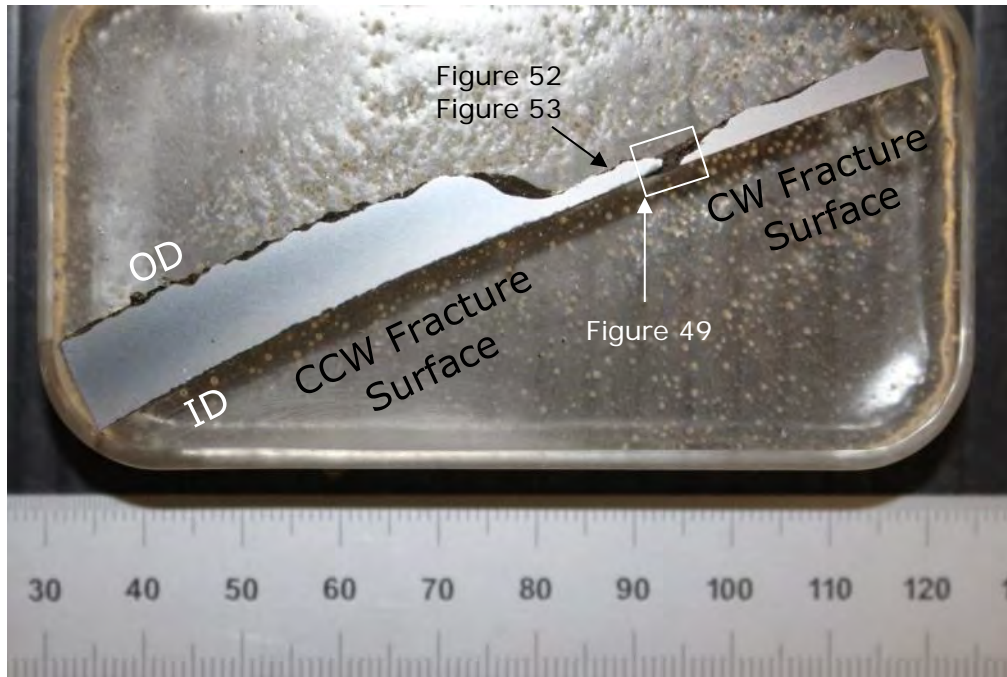


Figure 48. Photograph of the mounted transverse cross-section, Mount 195367-1b removed from the suspected failure origin; Feature 4. Mount location indicated in Figure 39.

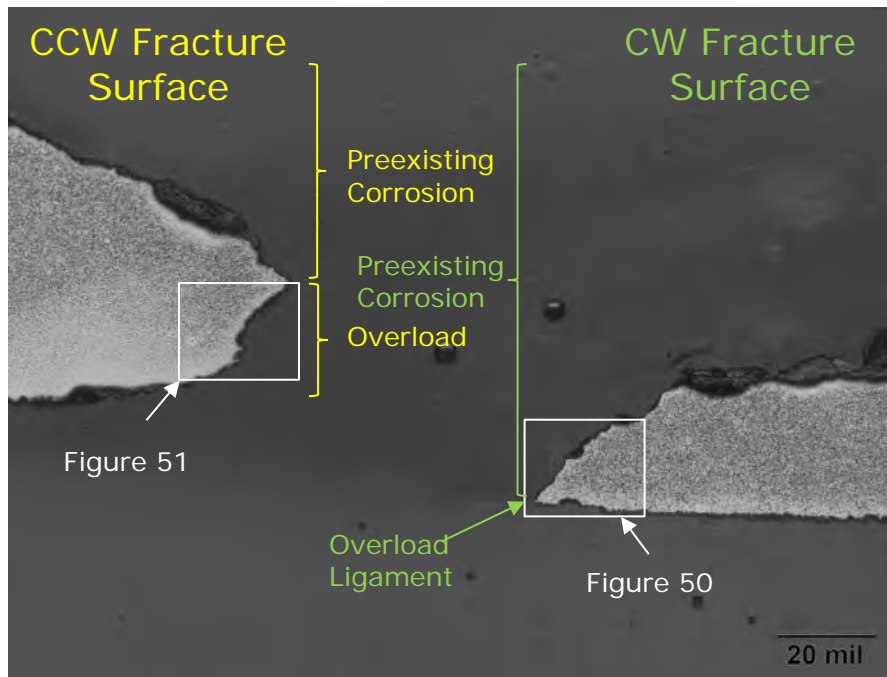


Figure 49. Photomicrograph showing the suspected failure origin in cross-section; Feature 4. Area indicated in Figure 48. (Mount 195367-1b; 4% Nital Etch)

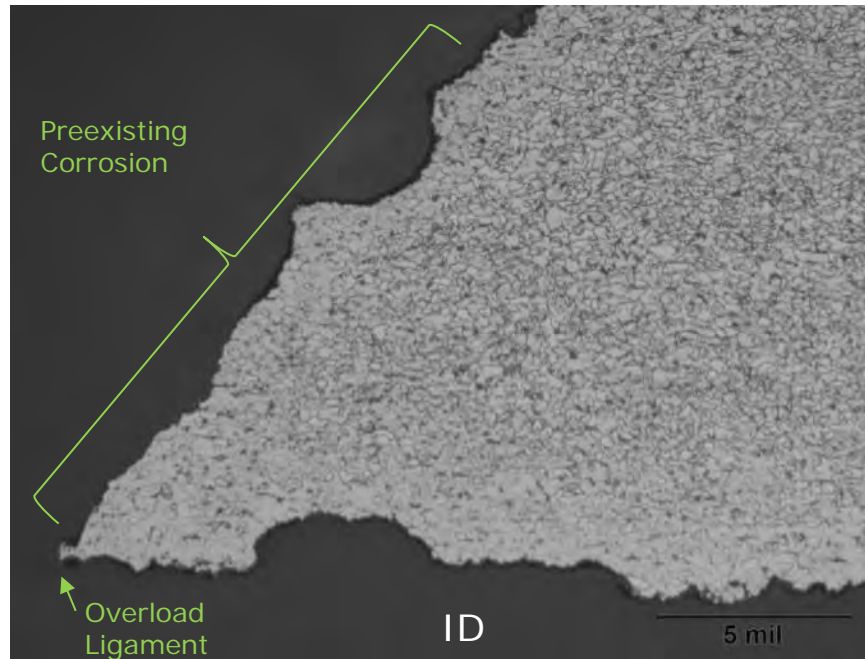


Figure 50. Photomicrograph showing the negligible grain elongation and plasticity along the CW fracture surface. Area indicated in Figure 49. (Mount 195367-1b; 4% Nital Etch)

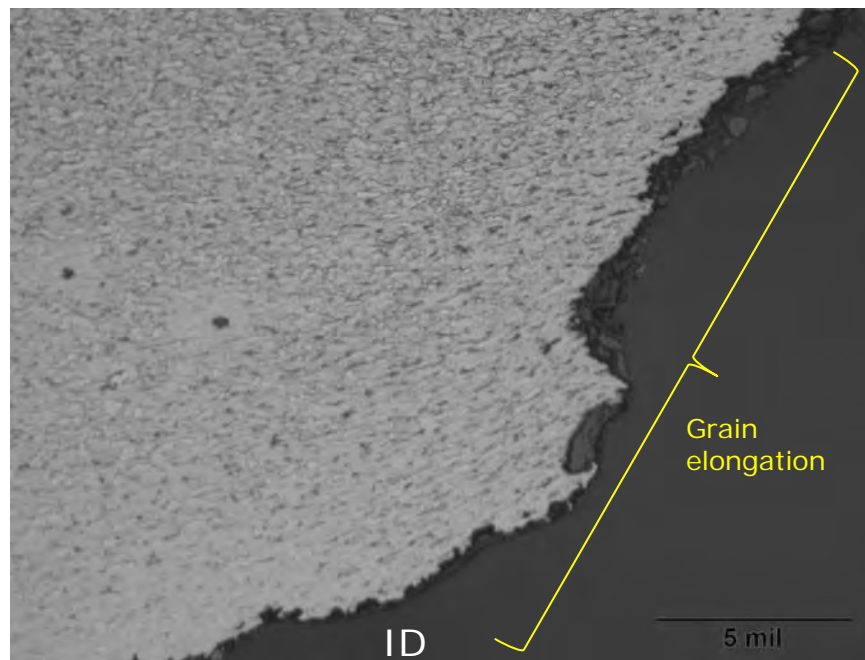


Figure 51. Photomicrograph showing the grain elongation and plasticity along the CCW fracture surface. Area indicated in Figure 49. (Mount 195367-1b; 4% Nital Etch)

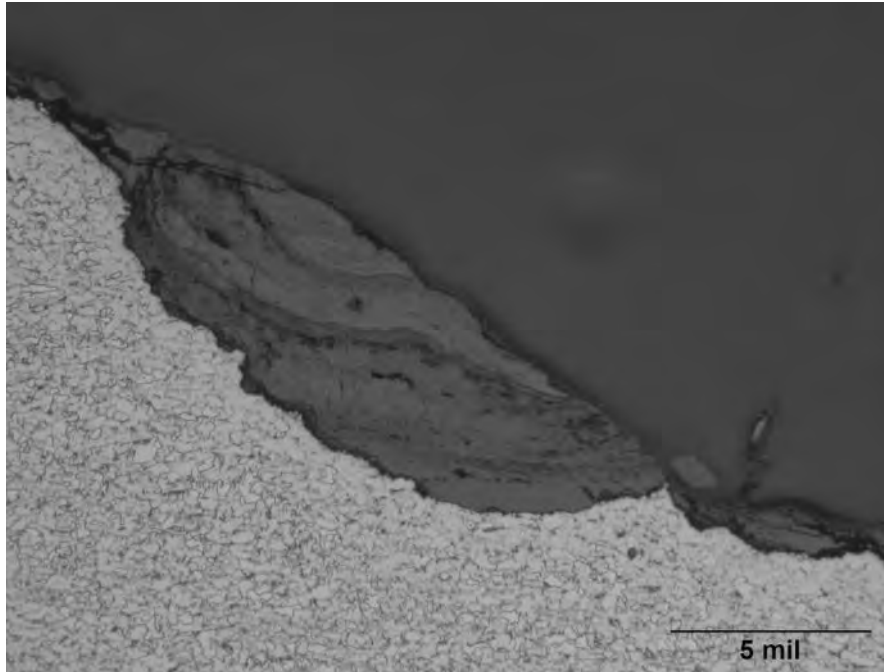


Figure 52. Photomicrograph showing corrosion products near the CCW fracture surface. Area indicated in Figure 48. (Mount 195367-1b; 4% Nital Etch)

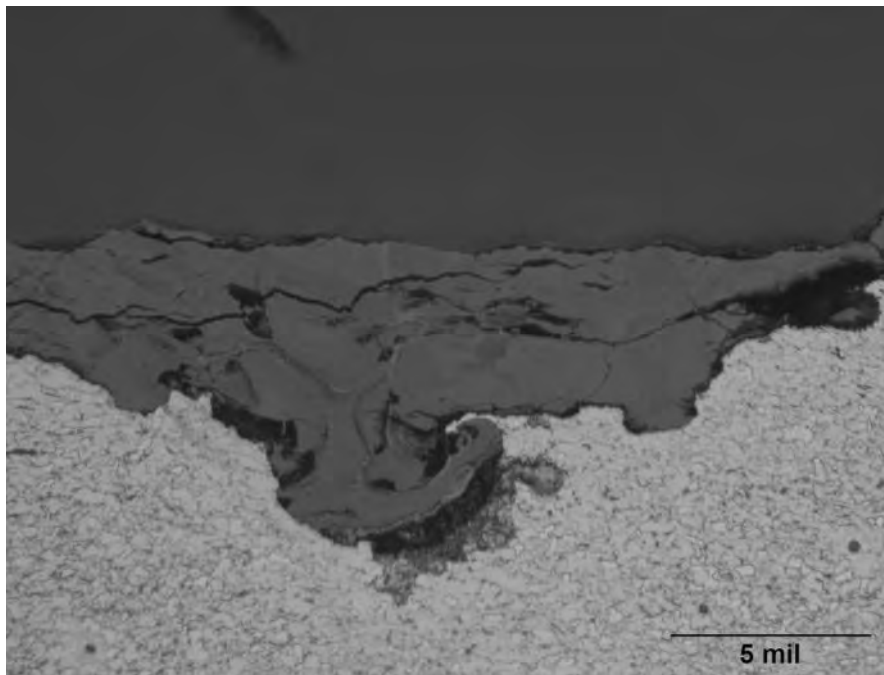


Figure 53. Photomicrograph showing corrosion products with some undercutting near the CCW fracture surface. Area indicated in Figure 49. (Mount 195367-1b; 4% Nital Etch)

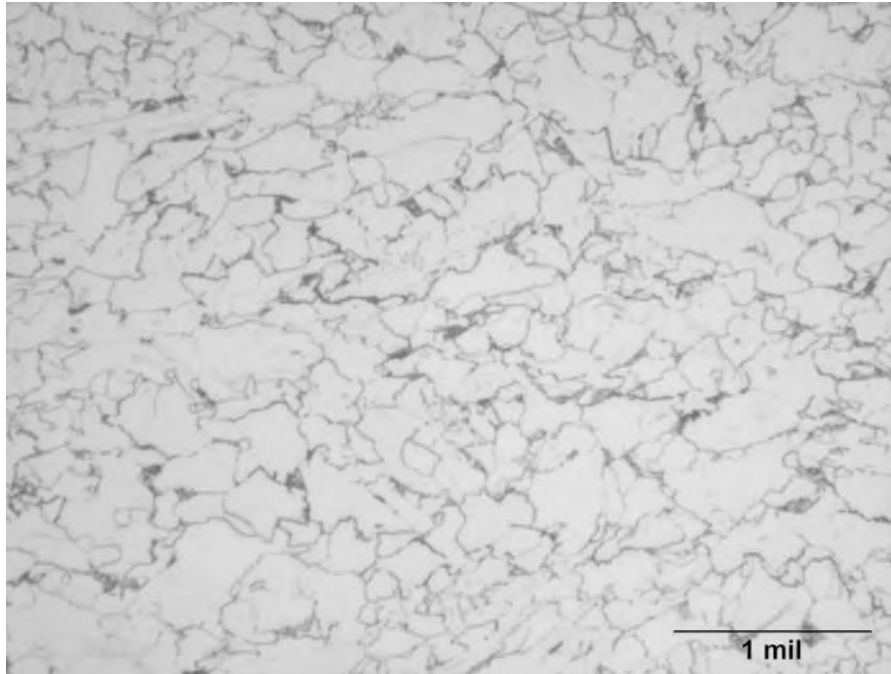


Figure 54. Photomicrograph showing base metal microstructure of Mount 195367-1b; 4% Nital Etch)

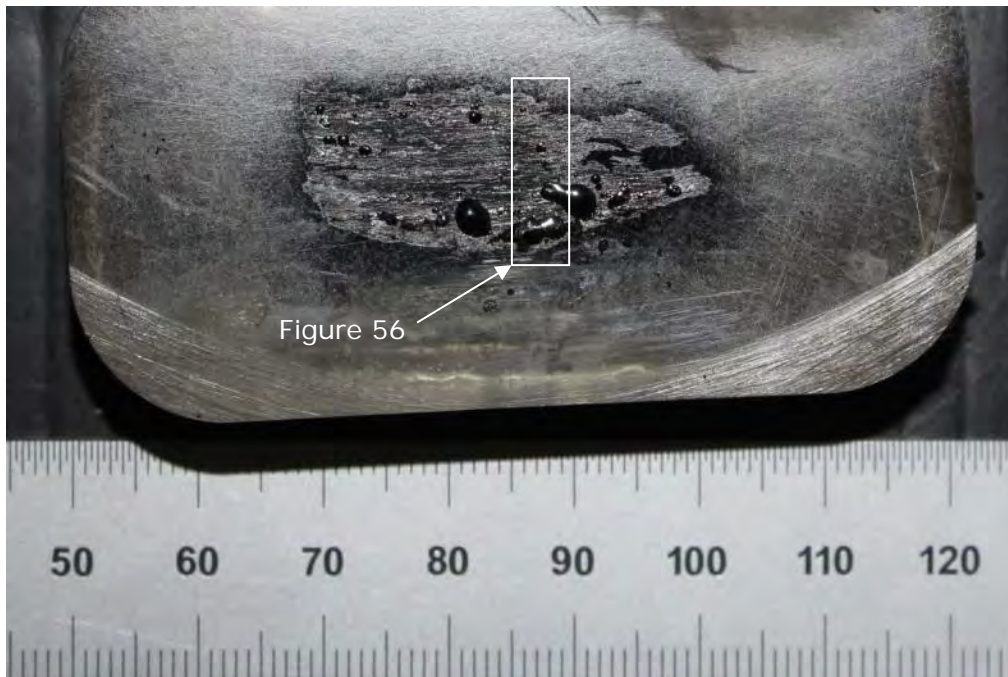


Figure 55. Photograph of the mounted cross-section of corrosion products, Mount 195331-1 removed from Feature 4.

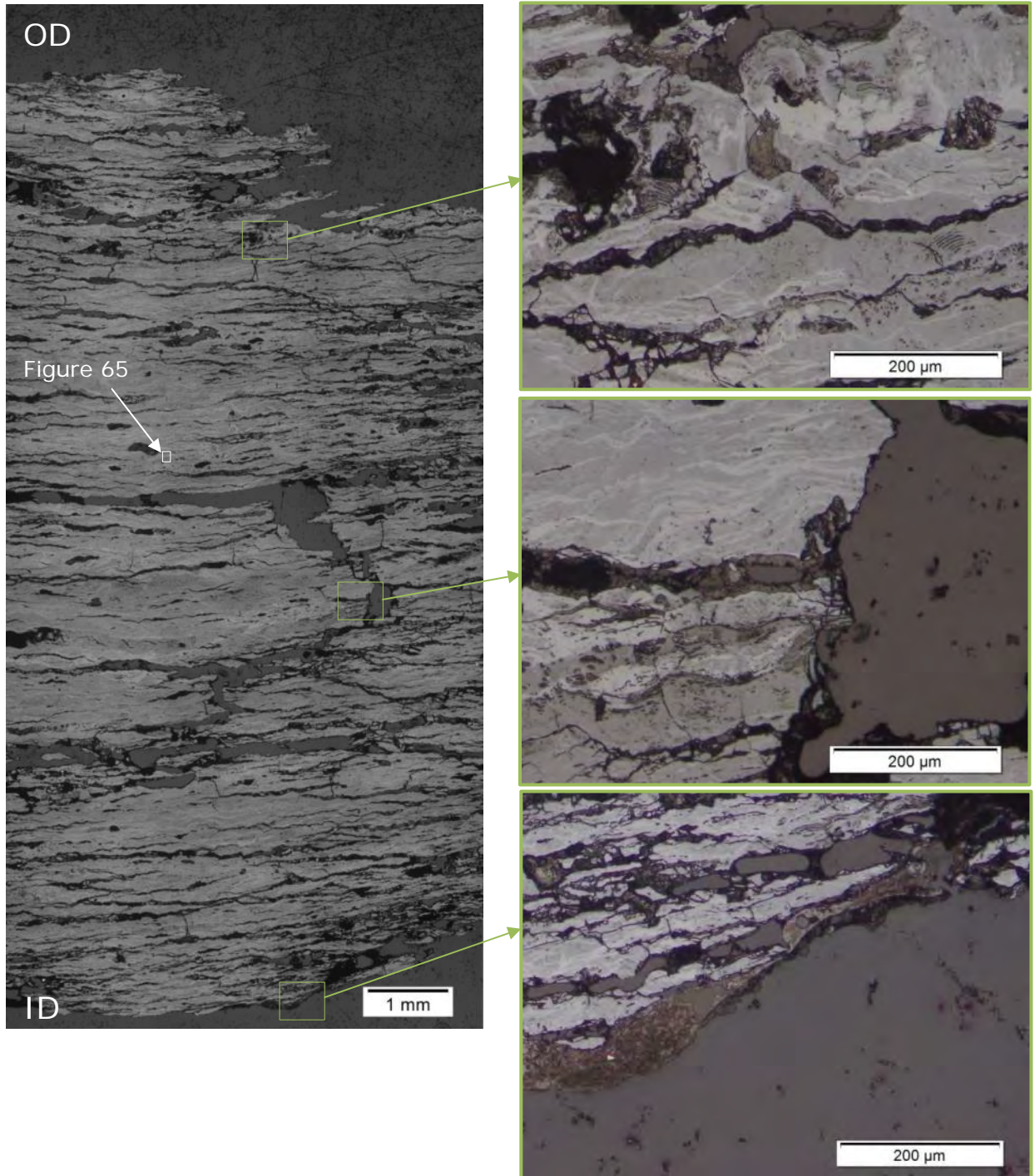


Figure 56. Photomicrographs of the mounted cross-section, Mount 195331-1, from corrosion products removed from Feature 4; location identified in Figure 55.

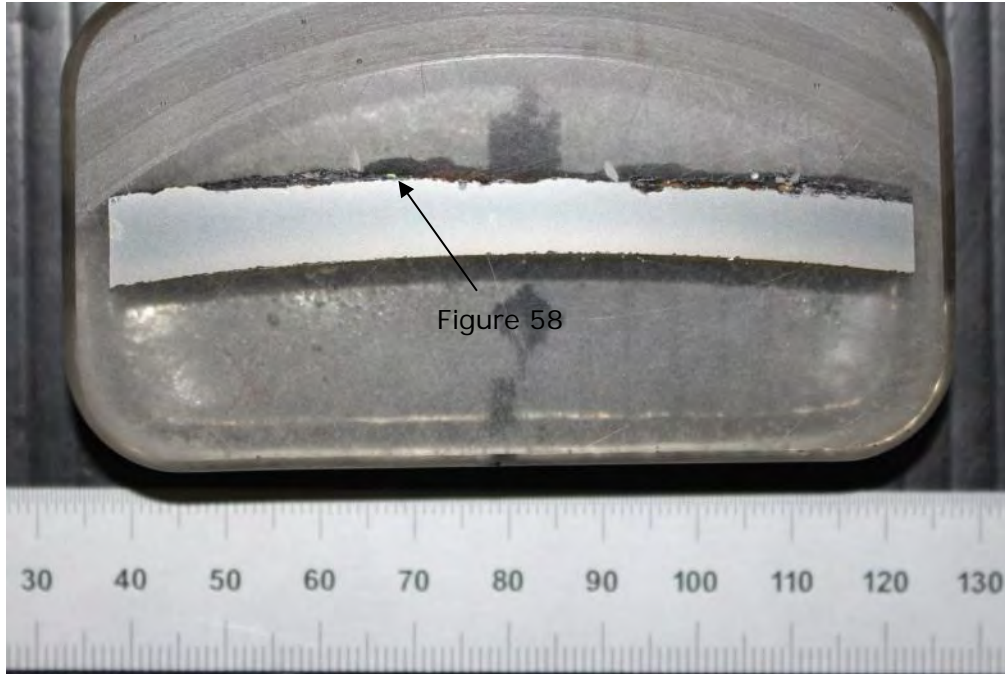


Figure 57. Photograph of the transverse mounted cross-section, Mount 195370-1 removed from Feature 1. Mount location indicated in Figure 22.

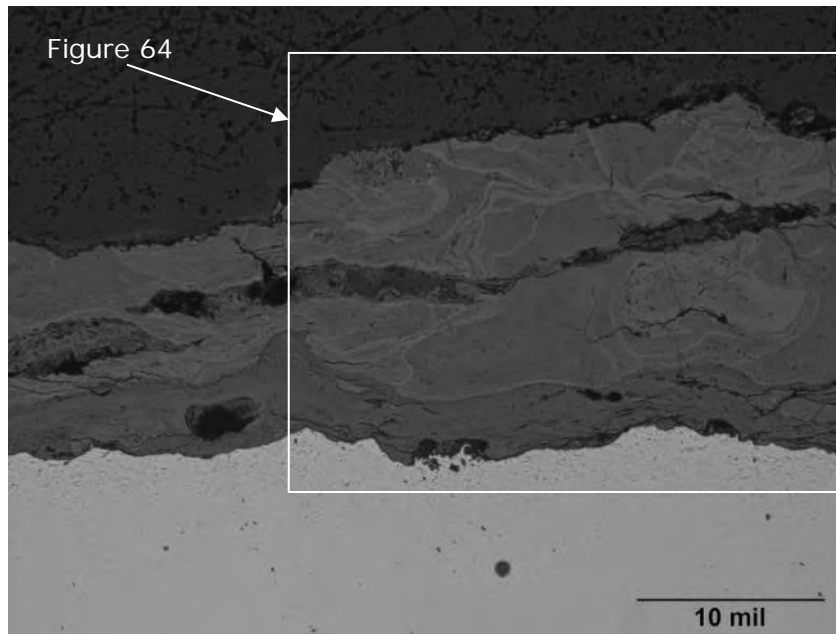


Figure 58. Photomicrograph of the mounted cross-section, Mount 195370-1 removed from Feature 1 showing the corrosion morphology at the external surface; mirror image of location indicated in Figure 57.

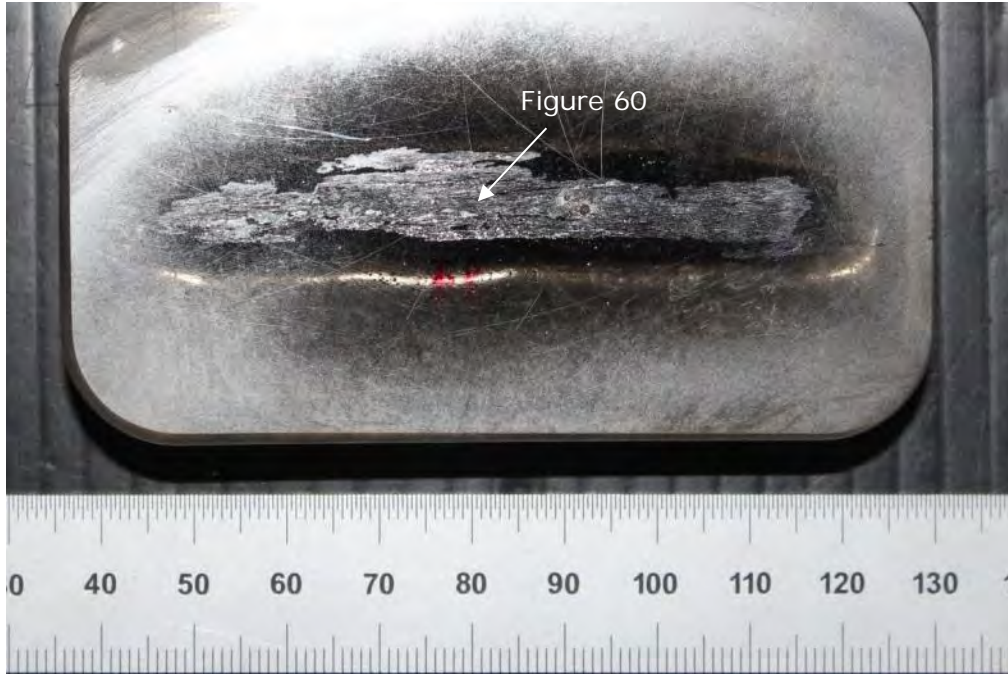


Figure 59. Photograph of the mounted cross-section of corrosion products, Mount 195322-1, removed from Feature 1.

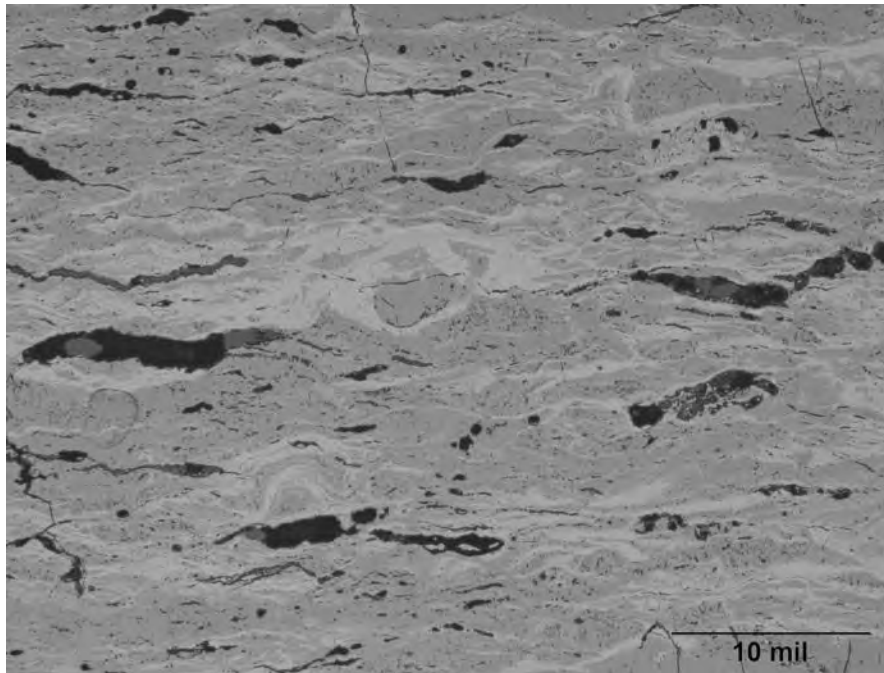


Figure 60. Photomicrographs of the mounted cross-section, Mount 195322-1, from the corrosion product removed from Feature 1; location indicated in Figure 59.

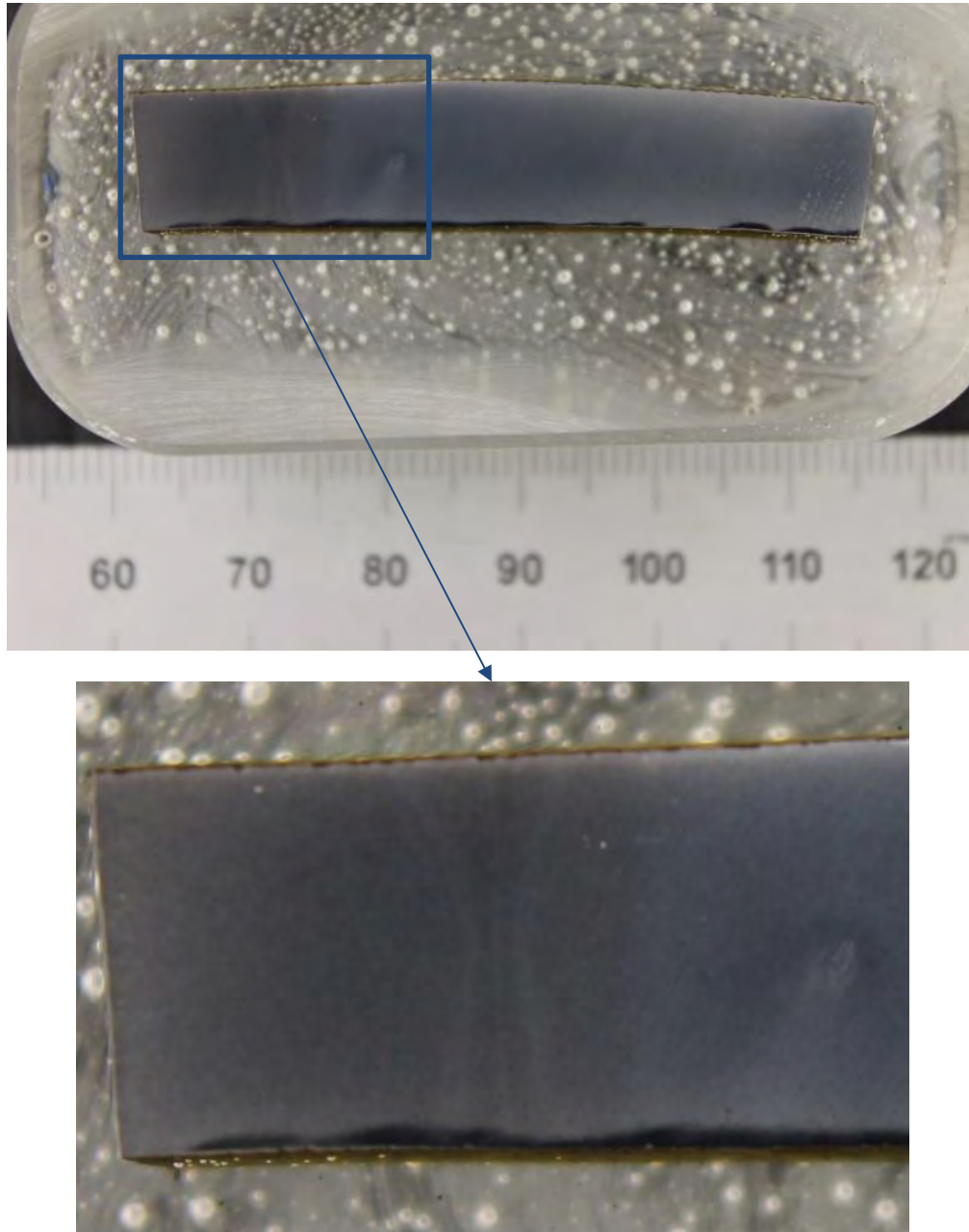


Figure 61. Photograph of the mounted cross-section, Mount 195365-1, removed from across the longitudinal seam weld. Location indicated in Figure 4.

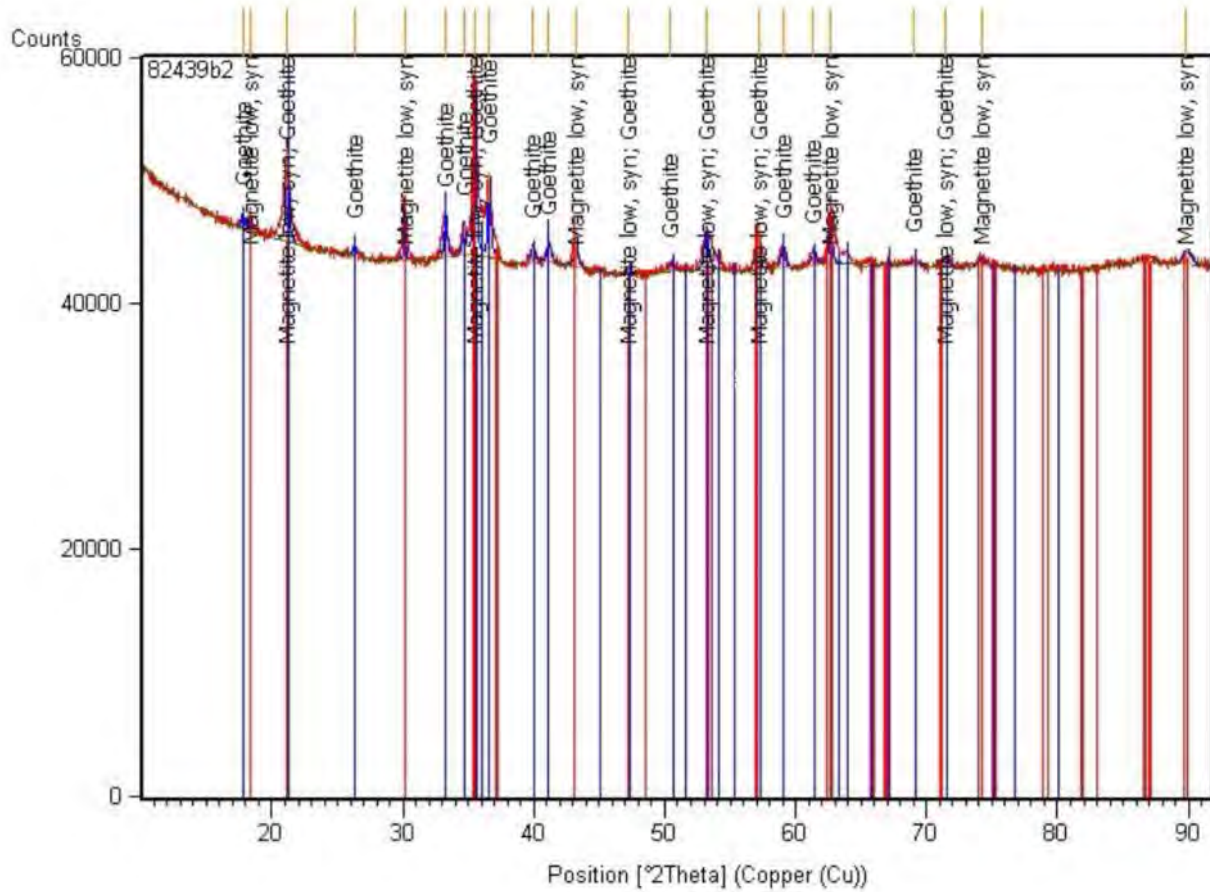


Figure 62. XRD spectrum acquired from the corrosion products collected from Feature 1, identifying Goethite and Magnetite as the compounds.

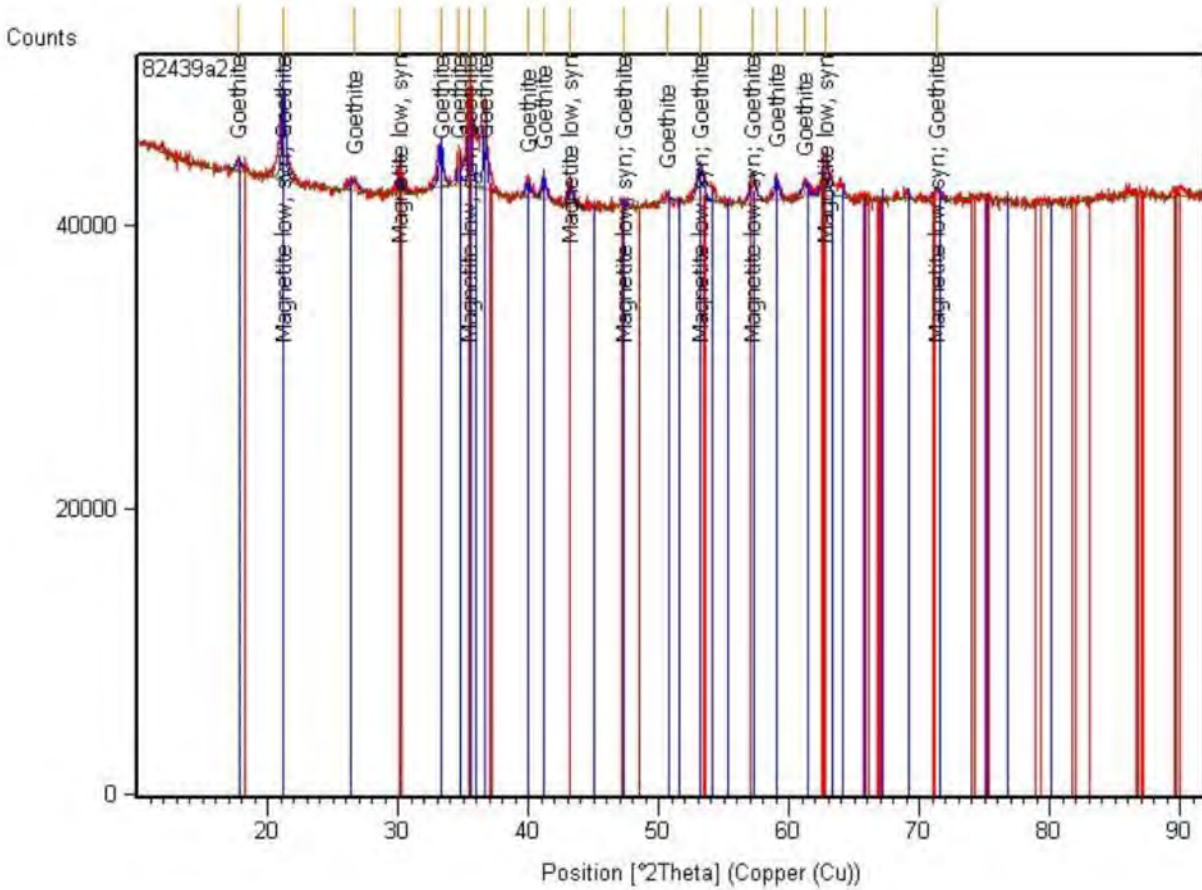
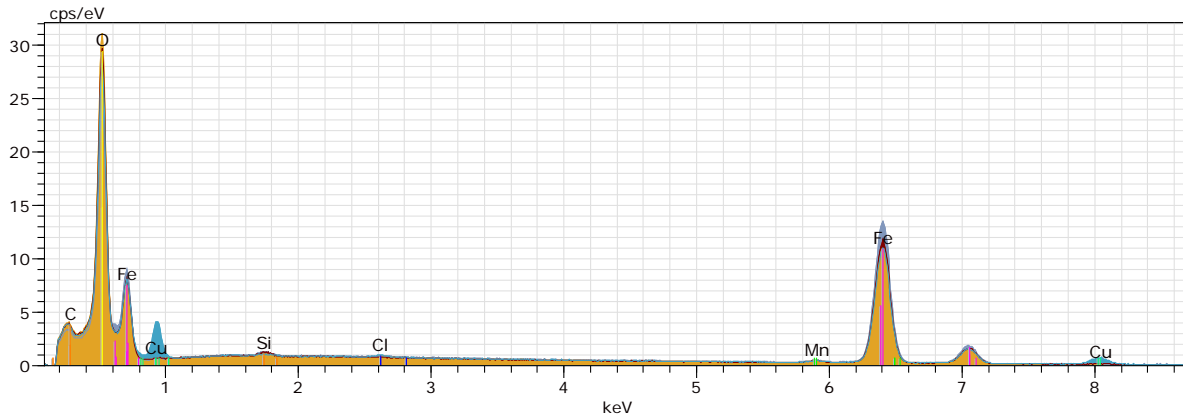
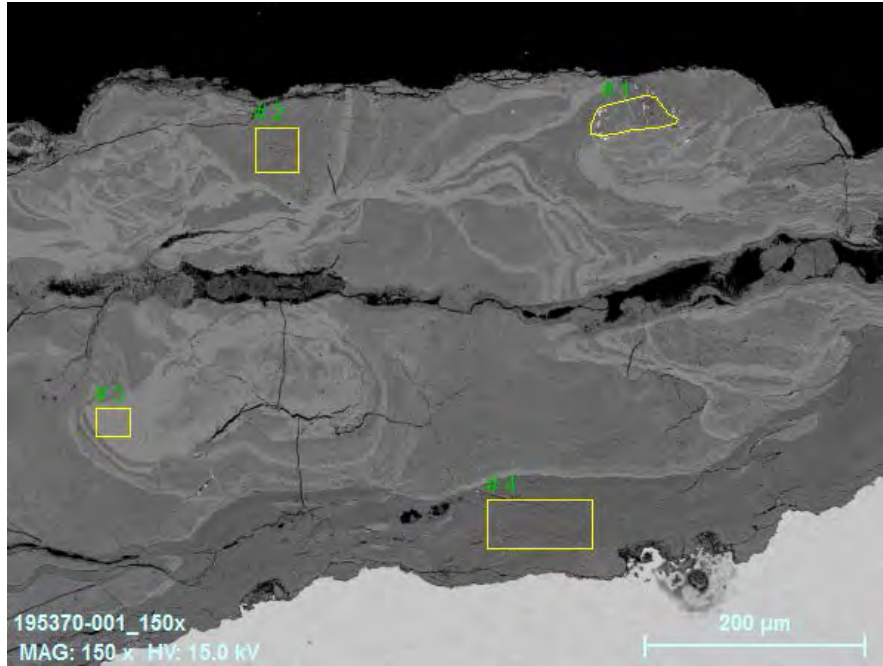


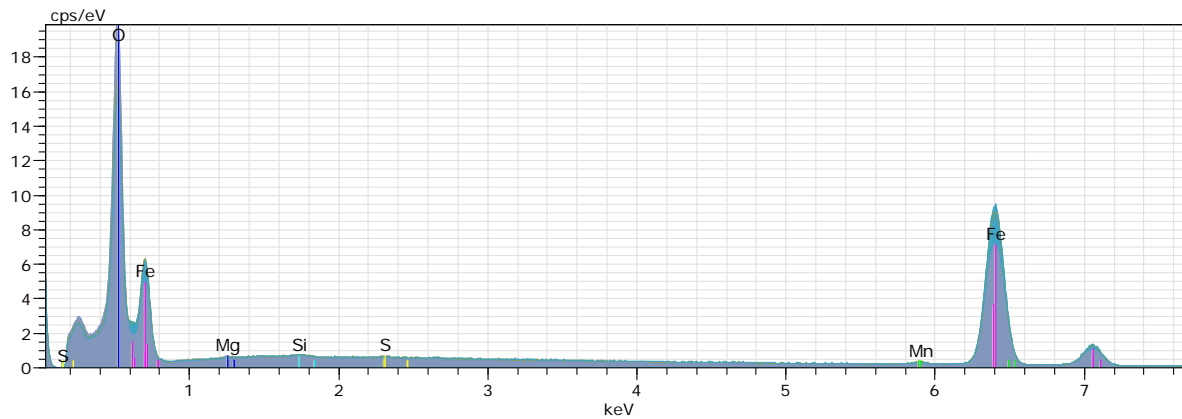
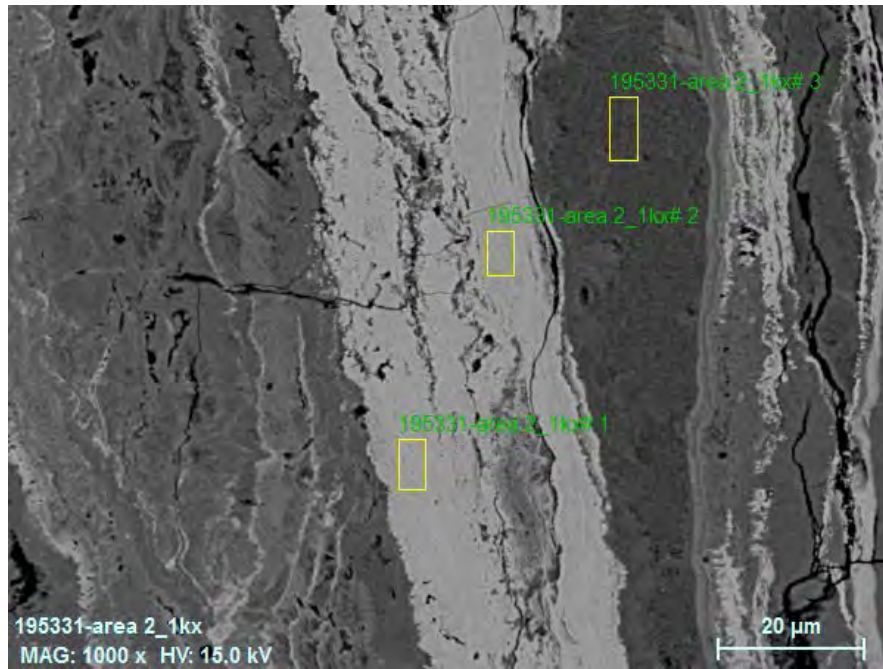
Figure 63. XRD spectrum acquired from the corrosion products collected from Feature 2, identifying Goethite and Magnetite as the compounds.



Norm. mass percent (%)

Spectrum	C	O	Si	Cl	Mn	Fe	Cu
# 1	0.00	33.52	0.19	0.19	0.79	56.87	8.44
# 2	0.00	35.78	0.40	0.06	0.80	62.46	0.49
# 3	0.00	29.24	0.41	0.07	0.68	69.60	-
# 4	0.00	37.97	0.26	0.15	0.73	60.71	0.18
Mean value:	0.00	34.13	0.32	0.12	0.75	62.41	3.04
Sigma:	0.00	3.73	0.11	0.06	0.06	5.33	4.68
Sigma mean:	0.00	1.87	0.05	0.03	0.03	2.67	2.34

Figure 64. EDS data collected from Mount 195370-1, mirror image of area indicated in Figure 58.



Norm. mass percent (%)

Spectrum	O	Mg	Si	S	Mn	Fe
195331-area 2_1kx# 1	27.85	-	0.21	-	0.59	71.35
195331-area 2_1kx# 2	29.45	-	0.20	-	0.93	69.41
195331-area 2_1kx# 3	37.83	0.48	0.22	0.18	0.98	60.30
Mean value:	31.71	0.48	0.21	0.18	0.83	67.02
Sigma:	5.36	0.00	0.01	0.00	0.21	5.90
Sigma mean:	3.09	0.00	0.01	0.00	0.12	3.41

Figure 65. EDS data collected from Mount 195331-1, area indicated in Figure 56.

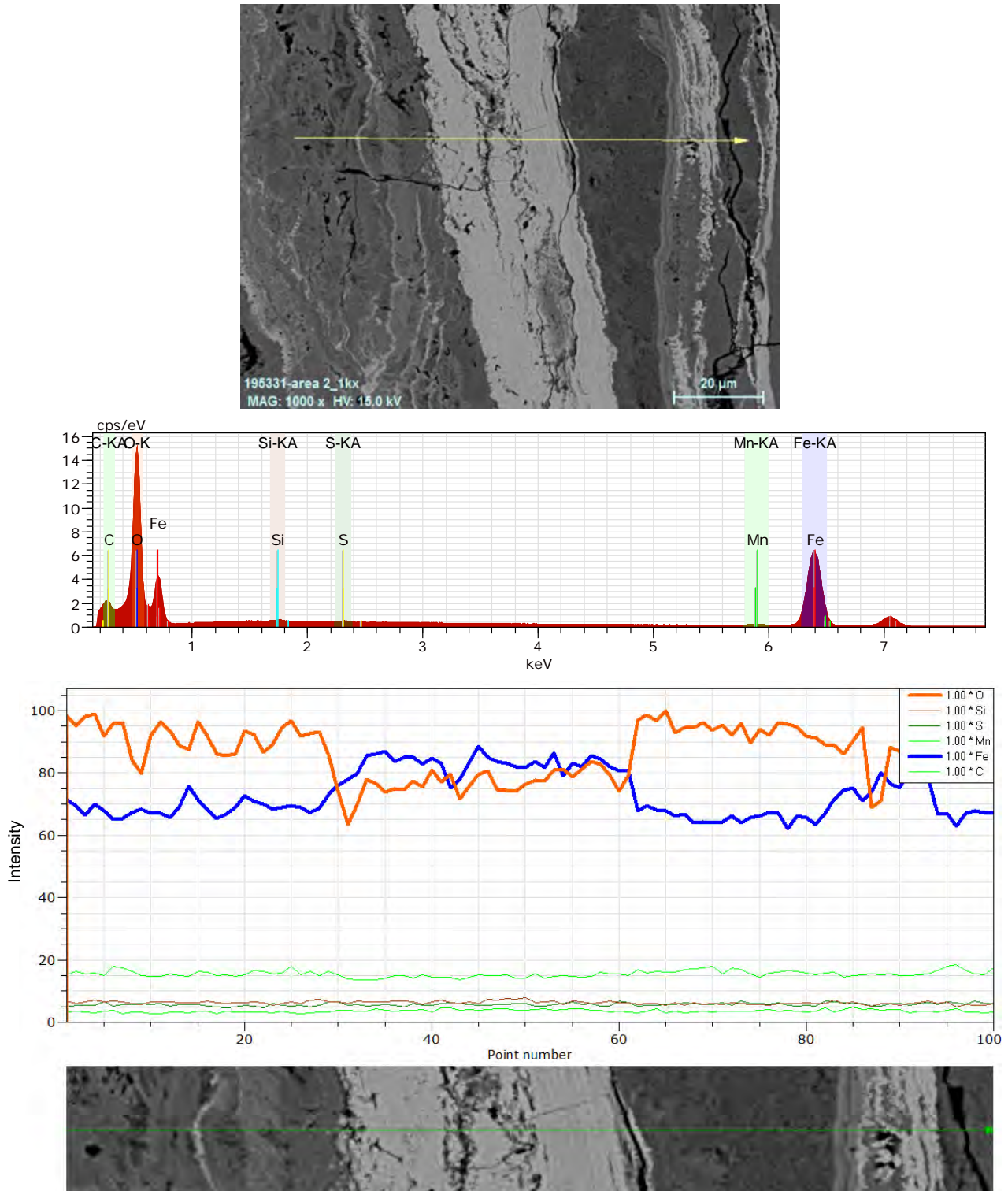


Figure 66. EDS line scan collected from Mount 195331-1, area indicated in Figure 56.



Figure 67. Photograph showing the soil samples collected from below the pipe, 8 feet U/S of GW 5930.



Figure 68. Percent shear from Charpy V-notch tests as a function of temperature for transverse base metal specimens removed from the failure joint (Joint 5930).

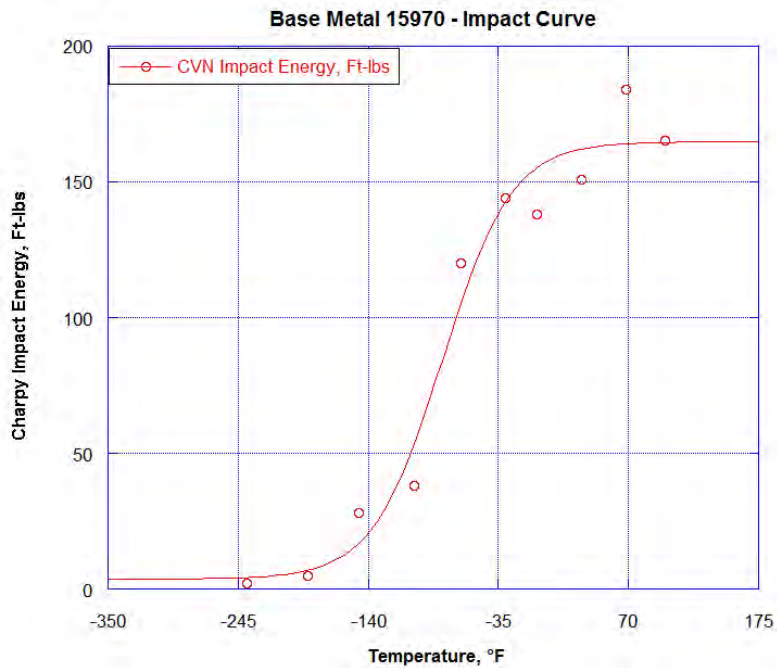


Figure 69. Charpy V-notch impact energy as a function of temperature for transverse base metal specimens removed from the failure joint (Joint 5930).



Figure 70. Percent shear from Charpy V-notch tests as a function of temperature for transverse base metal specimens removed from U/S joint (Joint 5920).

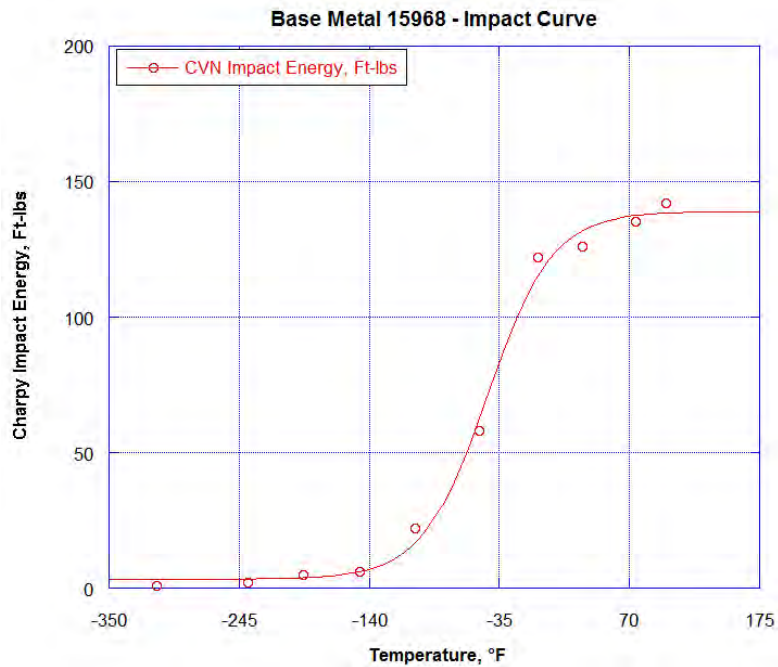


Figure 71. Charpy V-notch impact energy as a function of temperature for transverse base metal specimens removed from the U/S joint (Joint 5920).

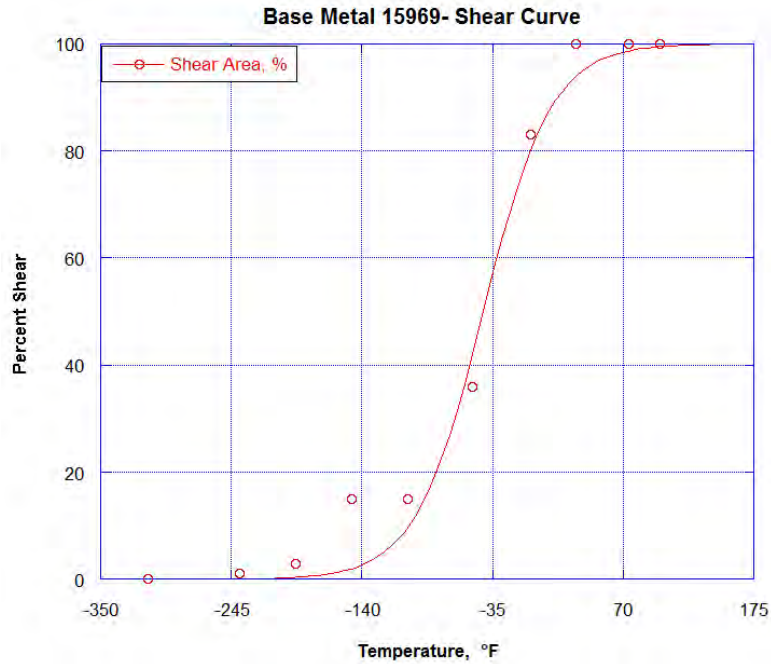


Figure 72. Percent shear from Charpy V-notch tests as a function of temperature for transverse base metal specimens removed from D/S joint (Joint 5940).

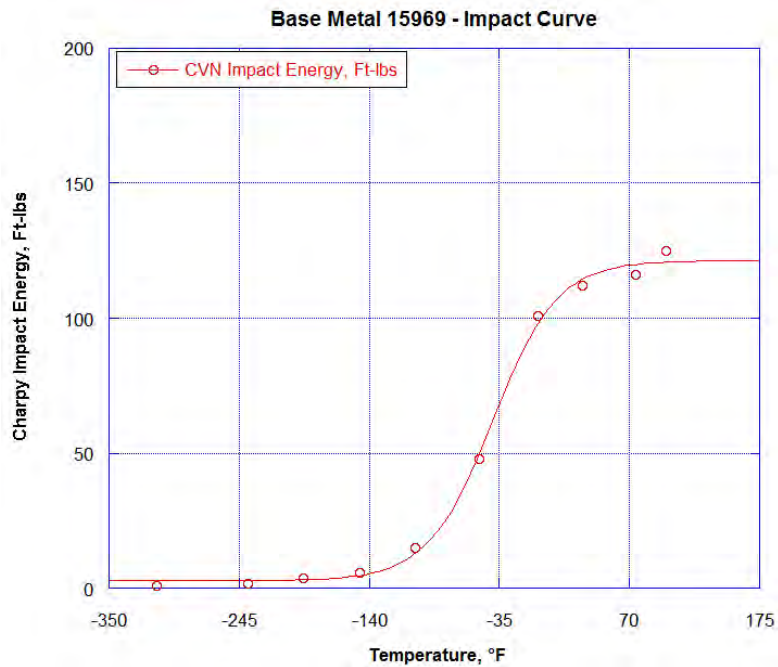


Figure 73. Charpy V-notch impact energy as a function of temperature for transverse base metal specimens removed from the D/S joint (Joint 5940).

Plains All American Pipeline, L.P.
 Line 901 Release (05-19-15): Mechanical and Metallurgical Testing

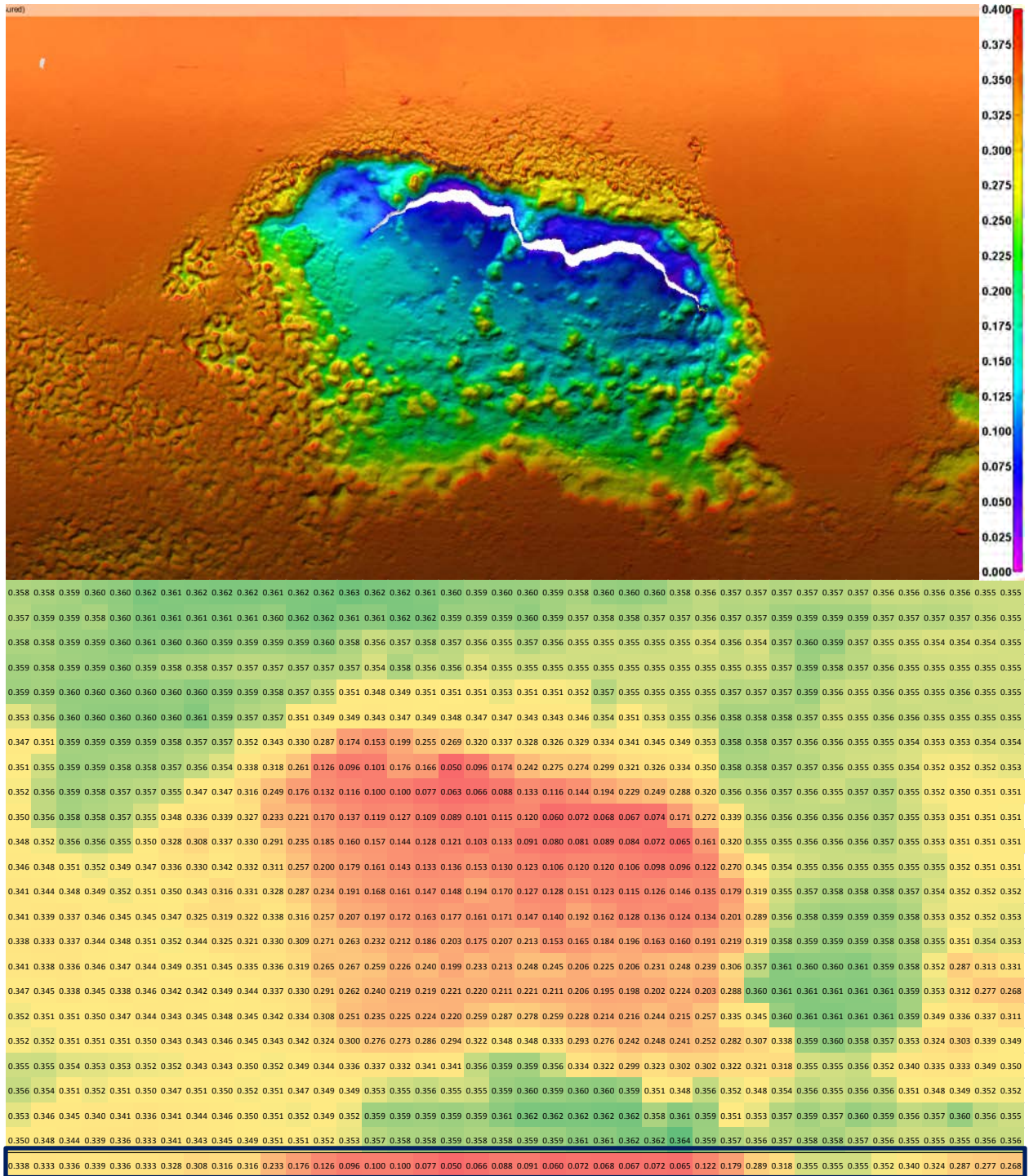


Figure 74. Color profile showing the results of average thickness measurements performed on the laser scan dataset following discretizing the data into 1/2-inch cells. The resulting profile is highlighted in blue and plotted in Figure 47.

APPENDIX A

CorLAS™

Appendix A

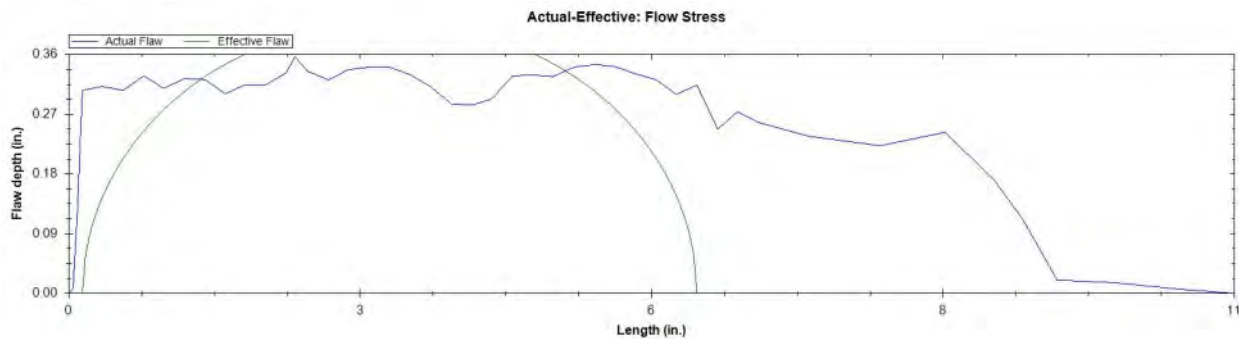
Description of CorLAS™

The CorLAS™ computer program was developed by Det Norske Veritas (U.S.A.), Inc. (formerly CC Technologies) to evaluate crack-like flaws in pipelines based on inelastic fracture mechanics. Using the effective area of the actual, measured crack length-depth profile, an equivalent semi-elliptical surface flaw is modeled and used to compute the effective stress and the applied value of J for internal pressure loading. The effective stress and applied J are then compared with the flow strength (σ_{fs}) and fracture toughness (J_C), respectively, to predict the failure pressure.

The program also contains a similar inelastic fracture mechanics analysis for through-wall flaws. The fracture toughness of the steel can be estimated from Charpy data or measured by means of a J_{IC} test. In the most recent version of CorLAS™, the fracture toughness analysis automatically checks for plastic instability and only the fracture toughness curve needs to be considered for crack-like flaws. The actual tensile and Charpy properties of the pipe joint, measured from the samples removed, can be used for the critical leak/rupture length calculation.

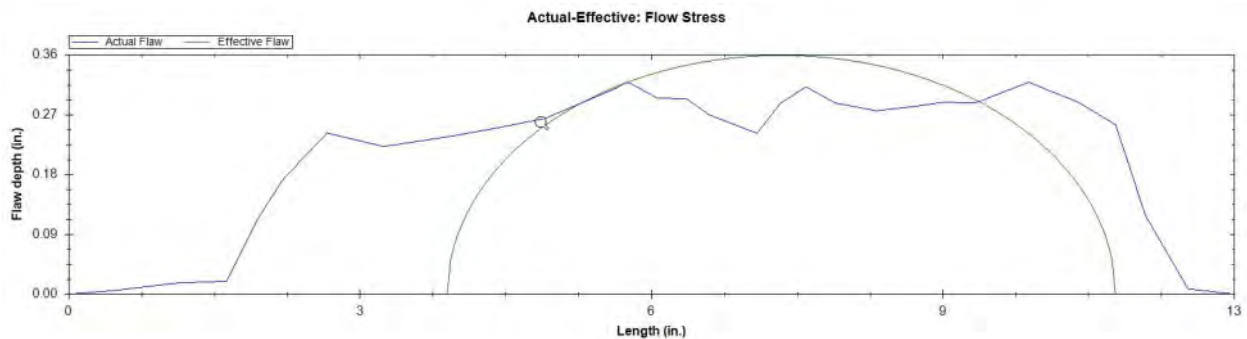
Case 1: Fracture Surface Measurements & Laser Scan Data

Plains Line 901	Semi-Elliptical Flaw Profile	
	API X65 - Joint 5930	
	Maximum Operating Pressure (psig)	1341
	UTS (psi)	84000
	YS (psi)	64800
	FS (psi)	74800
	E (ksi)	29500
	nexp	0.098
	Jc (lb/in)	12097
	Thin-wall (OD) formula for hoop stress	
	Tmat	208.9
	OD (in.)	24
	Wall Thickness (in.)	0.359
Summary of Results for Effective Area Method		
	Flaw: Start (in.)	0.13
	Length (in.)	5.9
	Area (in. ^2)	1.889
	Depth (in.) Maximum	0.356
	Equivalent Flaw	0.408
	For Design Factor	0.72
	Design Pressure (psig)	1395.79
	Failure Stress (psi)	15523
	Failure Pressure (psig)	464.41
	For Design Factor	0.72
	Maximum Safe Pressure (psig)	334.38
Summary of Results for 0.85dL Eff. Area Method		
	Failure Stress (psi)	16205
	Failure Pressure (psig)	484.79
	For Design Factor	0.72
	Maximum Safe Pressure (psig)	349.05



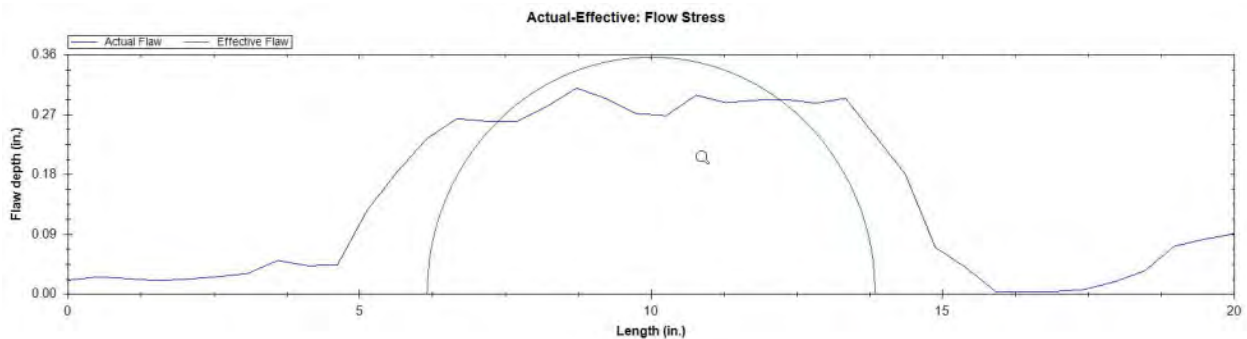
Case 2: Laser Scan Data - Offset from Fracture Surface

Plains Line 901	Semi-Elliptical Flaw Profile	
	API X65 - Joint 5930	
	Maximum Operating Pressure (psig)	1341
	UTS (psi)	84000
	YS (psi)	64800
	FS (psi)	74800
	E (ksi)	29500
	nexp	0.098
	Jc (lb/in)	12097
	Thin-wall (OD) formula for hoop stress	
	Tmat	208.9
	OD (in.)	24
	Wall Thickness (in.)	0.359
Summary of Results for Effective Area Method		
	Flaw: Start (in.)	4.076
	Length (in.)	7.2
	Area (in. ^2)	2.026
	Depth (in.) Maximum	0.318
	Equivalent Flaw	0.358
	For Design Factor	0.72
	Design Pressure (psig)	1395.79
	Failure Stress (psi)	25388
	Failure Pressure (psig)	759.53
	For Design Factor	0.72
	Maximum Safe Pressure (psig)	546.86
Summary of Results for 0.85dL Eff. Area Method		
	Failure Stress (psi)	23779
	Failure Pressure (psig)	711.39
	For Design Factor	0.72
	Maximum Safe Pressure (psig)	512.2



Case 3: Laser Scan Data - 1/2-Inch Grid (Average)

Plains Line 901	Semi-Elliptical Flaw Profile	
	API X65 - Joint 5930	
	Maximum Operating Pressure (psig)	1341
	UTS (psi)	84000
	YS (psi)	64800
	FS (psi)	74800
	E (ksi)	29500
	nexp	0.098
	Jc (lb/in)	12097
	Thin-wall (OD) formula for hoop stress	
	Tmat	208.9
	OD (in.)	24
	Wall Thickness (in.)	0.359
Summary of Results for Effective Area Method		
	Flaw: Start (in.)	6
	Length (in.)	7.5
	Area (in.^2)	2.095
	Depth (in.) Maximum	0.309
	Equivalent Flaw	0.356
	For Design Factor	0.72
	Design Pressure (psig)	1395.79
	Failure Stress (psi)	25516
	Failure Pressure (psig)	763.35
	For Design Factor	0.72
	Maximum Safe Pressure (psig)	549.61
Summary of Results for 0.85dL Eff. Area Method		
	Failure Stress (psi)	23715
	Failure Pressure (psig)	709.46
	For Design Factor	0.72
	Maximum Safe Pressure (psig)	510.81





ABOUT DNV GL

Driven by our purpose of safeguarding life, property, and the environment, DNV GL enables organizations to advance the safety and sustainability of their business. We provide classification and technical assurance along with software and independent expert advisory services to the maritime, oil and gas, and energy industries. We also provide certification services to customers across a wide range of industries. Operating in more than 100 countries, our 16,000 professionals are dedicated to helping our customers make the world safer, smarter, and greener.

Appendix N

**Det Norske Veritas (U.S.A.), Inc. (DNV GL): Line 901
Release (5/19/15) Technical Root Cause Analysis**

Final Report

Line 901 Release (5/19/15) Technical Root Cause Analysis

**Plains All American Pipeline, L.P.
Houston, Texas**

Report No.: OAPUS307KKRA (PP136049)
December 4, 2015

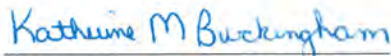
Plains All American Pipeline, L.P.
 Line 901 Release (5/19/15) Technical Root Cause Analysis

Project Name:	Line 901 Release (5/19/15) Technical Root Cause Analysis	DET NORSKE VERITAS (U.S.A.), INC. (DNV GL) Materials & Corrosion Technology Center Incident Investigation
Customer:	Plains All American Pipeline, L.P.	5777 Frantz Road
Contact Person:		Dublin, OH 43017-1886
Date of Issue:	December 4, 2015	United States
Project No.:	PP136049	Tel: (614) 761-1214
Organization Unit:	Incident Investigation	Fax: (614) 761-1633
Report No.:	OAPUS307KKRA	www.dnvgl.com

Task and Objective:

Please see Executive Summary.

Prepared by



Katherine M. Buckingham, Ph.D.
Principal Engineer



Barbara N. Padgett, Ph.D.
Senior Engineer



Steven J. Polasik, M.S., P.E.
Senior Engineer



Angel Kowalski
Head of Section - Fitness for Service

Verified by



John A. Beavers, Ph.D., FNACE
Director - Incident Investigation

Approved by



Neil G. Thompson, Ph.D., FNACE
Vice President, Pipeline Services

- Unrestricted Distribution (internal and external)
- Unrestricted Distribution within DNV GL
- Limited Distribution within DNV GL after 3 years
- No Distribution (confidential)
- Secret

Keywords

Copyright © DNV GL 2015. All rights reserved. This publication or parts thereof may not be copied, reproduced, or transmitted in any form, or by any means, whether digitally or otherwise without the prior written consent of DNV GL. DNV GL and the Horizon Graphic are trademarks of DNV GL AS. The content of this publication shall be kept confidential by the customer, unless otherwise agreed in writing. Reference to part of this publication, which may lead to misinterpretation, is prohibited.

Rev. No.	Date	Reason for Issue:	Prepared by:	Verified by:	Approved by:
0	2015-09-21	First Issue			
1	2015-12-04	Final Issue			

Executive Summary

Plains All American Pipeline, L.P. (Plains) retained Det Norske Veritas (U.S.A.), Inc. (DNV GL) to perform a root cause analysis (RCA) of a failure that occurred on Line Segment 901, which transports heated crude oil from the outer continental shelf (OCS) of California. The failure occurred on May 19, 2015 in Goleta, California (Santa Barbara County) and was located near milepost (MP) 4. The location was approximately 4.05 miles downstream (D/S) from Las Flores Pump Station and approximately 6.2 feet upstream (U/S) from the nearest girth weld, identified as Girth Weld (GW) 5940. Approximately 2,934¹ barrels of crude oil were released.

The portion of the pipeline that contained the failure is comprised of 24-inch diameter by 0.344 inch wall thickness, API 5L Grade X65 line pipe steel that was manufactured by Nippon Steel and contains a high frequency (HF) electric resistance welded (ERW) longitudinal seam. The pipeline (Line 901) was installed in 1990 and is approximately 10.87 miles in length, spanning between Las Flores Station on the U/S end and Gaviota Station on the D/S end. The pipeline is externally covered with the following: (1) a protective coating of coal tar urethane (CTU) that is in intimate contact with the steel pipe, (2) a layer of rigid thermal polyurethane (PU) foam insulation, and (3) an outer layer of polyethylene (PE) tape. The pipeline has an impressed cathodic protection (CP) system that was energized at the time of installation.

The normal operating pressure and maximum discharge pressure (MDP) for the line are 616 psig and 1,025 psig, respectively. These pressures correspond to 33% and 55% of the specified minimum yield strength (SMYS), respectively. The pressure at the time and location of the failure was reported by Plains to be 737 psig [Ref 2], which corresponds to 39.6% of the SMYS and 71.9% of the MDP.

The leak occurred in a mostly rural area that runs along the coastline of the Pacific Ocean. The topography in the area is hilly, with the pipeline oriented uphill from the ocean. The failure was located near a local low point along the pipeline. Several road crossings, such as Highway 1, are present in the area with drainage toward the coast via culverts. It is via these culverts that the released oil reached the Pacific Ocean at Refugio State Beach.

The objective of the RCA was to identify factors contributing to the failure and document the decisions made preceding the failure. The portion of the pipeline that contained the failure location was removed and sent to DNV GL to determine the metallurgical cause of the failure and to identify any contributing factors. The conclusions and recommendations for this RCA are based on the findings from the final metallurgical report as well as information

¹ [Ref 6] The final volume estimate for the released oil at the time of this report.

provided and publically reported by Plains. Based on the findings of the analysis, recommendations for improvements also are identified.

The methodology used by DNV GL for the RCA of the Line 901 release was based on the DNV GL Loss Causation Model (LCM). This model is built on the concept that incidents can be attributed to immediate causes, basic causes, and failures of management systems to control hazards. The analysis uses a systematic method of processing evidence gathered during an investigation in order to identify the factors that led to the incident. This methodology assists in the development of corrective and/or remedial measures.

The LCM approach used by DNV GL is called a Barrier-based Systematic Causal Analysis Technique (BSCAT). BSCAT™ is a technique that applies a Systematic Causal Analysis Technique (SCAT) model to each barrier, as opposed to the incident as a whole. This method results in a thorough review of the effectiveness of individual barriers identified in the risk assessment. BSCAT provides a methodology that allows for the analysis of complex incidents that involve multiple barriers.

The results of the metallurgical analysis indicated that the immediate metallurgical cause for the Line 901 failure was wall thinning from external corrosion that ultimately failed by ductile overload under the imposed operating pressure [Ref ¶1]. The flaw that failed was not through wall prior to ductile overload and, therefore, the failure event was sudden in nature. The morphology of the external corrosion was determined to be consistent with corrosion under insulation (CUI), facilitated by wet-dry cycling.

The results of the root cause analysis presented below are based on the provided documentation referenced in Appendix B. DNV GL reserves the right to modify or supplement these conclusions should new information become available. DNV GL identified four c basic root causes of the failure:

1. The external coating system failed to prevent moisture from reaching the pipe steel, allowing the external corrosion process to occur.

Basis:

Based on the metallurgical analysis, the protective coal tar urethane coating, thermal polyurethane foam insulation, and polyethylene tape were compromised at the failure location. The damage included wrinkles, cracks, staining, and decohesion of the polyethylene tape; staining, water saturation and retention, and compression of the polyurethane foam; and disbondment of the coal tar urethane.

2. The cathodic protection system was ineffective due to shielding by the thermal polyurethane insulation and external polyethylene wrap.

Basis:

Based on the provided documentation, Plains met the regulatory requirements for monitoring the cathodic protection (CP) system on Line 901, and the measured pipe to soil potential values met the required levels for protection. However, the presence of the polyurethane insulation and the polyethylene wrap shielded the cathodic protection current and prevented voltage monitoring of the shielded portions of the pipe. As a result, the CP current did not reach the pipe surface and the measured potentials did not represent the potentials at the areas of corrosion under the insulation.

3. The contracted in-line inspection significantly undersized the external corrosion feature that failed on Line 901.

Basis:

Based on the provided documentation, the 2015 MFL tool significantly undersized the external corrosion feature that ultimately leaked (i.e. a tool determined depth of 47% of the nominal wall thickness vs. a laboratory measured depth of 89% of the nominal wall thickness). The MFL tool likely also undersized the same feature in the 2012 ILI run based on a review and comparison of the 2007, 2012, and 2015 raw signal data for the feature that failed.

4. The mitigative actions taken by Plains on Line 901 did not adequately address the elevated integrity threat of corrosion under insulation.

Basis:

The results of the metallurgical analysis indicated that the immediate metallurgical cause of the failure was CUI. Corrosion under insulation is a unique corrosion mechanism that necessitates its own integrity risk assessment. Plains did not apply sufficient mitigative strategies specific to CUI to prevent this anomaly from failing. The measures could include enhancement of existing barriers and additional preventative barriers.

Additional observations for improvement in the Integrity Management Program

The following provides perspective on Plains' integrity management plan (IMP) as related to the failure on Line 901. Coating systems, as a barrier to external corrosion related integrity threats, (i) are never perfect and (ii) age over time, thereby decreasing the effectiveness of the barrier. The cathodic protection (CP) system is another barrier to external corrosion integrity threats. Cathodic protection can be effective for many external corrosion related integrity threats; e.g., corrosion at holidays (holes in the coating) and microbiological influenced corrosion (MIC).

There are limits to the effectiveness of CP for corrosion related integrity threats and mitigation barriers can be strengthened and/or other mitigation barriers can be employed in conjunction with CP; e.g., stray current enhanced corrosion, AC induced corrosion, stress corrosion cracking, and corrosion beneath disbanded coatings that shield CP current. For these, multiple barriers may be used depending on the individual integrity threat, but the ILI program in conjunction with a dig program becomes a more important barrier since it is known that the other barriers of coating and CP are not always effective.

In the case of Line 901, Plains targeted 70 metal loss features in 2012, which included 31 features beyond those required by code and used for validation of the ILI program. These additional digs constitute a strengthened barrier in the prevention of a pipe failure due to a corrosion related integrity threat. Several of the digs were based on the strengthening of the ILI/dig barrier for the purpose of identifying and repairing corrosion under shrink sleeves used at girth welds; a known corrosion related integrity threat involving coatings that shield CP. In addition, the ILI re-inspection interval was decreased from a minimum of 5 years to 3 years (performed at 2.8 years). This also is a strengthening of a barrier in the prevention of a pipe failure due to a corrosion related integrity threat.

Plains IMP aggressively addressed several of the corrosion related integrity threats; but, as mentioned under contributing causes, Plains did not apply sufficient mitigative strategies to prevent the CUI anomaly from failing. In addition, an IMP is only as good as the data that are utilized to monitor and measure its performance. As addressed as a contributing cause, the ILI significantly undersized (47% versus an actual value of 89% through wall) the feature that eventually failed.

The RCA identified improvements that could be made within the integrity management program, which were not direct causes of the failure. These observations are given below.

1. Based on the information provided, Plains could adopt additional practices to identify and address any inaccuracies in future ILI runs.

Basis:

DNV GL performed an analysis of the 2012 ILI and dig data using API 1163, which is not a regulatory requirement or part of the IMP, and determined that the tool performance was not within the stated specifications. There was no produced documentation to indicate that Plains communicated with the ILI vendor, such as requesting a re-grade, following production of the unity plot[s] to account for the scatter observed within the data. However, using the recalculated tool tolerance would still result in a similar re-inspection interval as that used by Plains for the 2015 ILI run.

2. Based on the provided information, Plains could better incorporate the results from multiple ILI runs into their corrosion growth rate calculations.

Basis:

Plains IMP Section 9.2.2 states, "External and internal corrosion growth rates are estimated from multiple ILI runs, field observations, and observed historical growth rates." The procedure specifies calculation of a corrosion growth rate in mils per year using the increase in corrosion depth during the time between consecutive ILI runs. There is no documentation provided to indicate that Plains performed such calculations using the historical ILI data.

DNV GL calculated a corrosion growth rate for the feature that failed based on data from the 2007 and 2012 ILI runs. Although a higher corrosion rate was calculated than that determined using the CGAR process, this rate results in a similar re-inspection interval to that performed by Plains.

Additional analyses that go beyond the IMP, codes, and standards, include:

- Statistically active corrosion (SAC) analysis performed on Line 901 resulted in a similar re-inspection interval as that used by Plains (2.8 years) for the 2015 ILI run. The analysis identified a remaining life for the feature that failed that is greater than the re-inspection interval used by Plains.

3. Based on the provided information, Plains should improve their documentation and/or record-keeping of their decision-making processes related to actions taken.

Basis:

Over the course of the investigation, DNV GL identified areas within the integrity management process that were not sufficiently documented. For example, no justification (i.e. assumptions, analyses, etc.) was provided for determining the reassessment interval of 3 years based on the 2012 ILI data.

Although a form explicitly identifying the justification for the reduction of their re-inspection interval from 5 years to 3 years was not provided, DNV GL's assessments and calculations resulted in a similar re-inspection interval as that used by Plains.

Table of Contents

1.0	INTRODUCTION	1
2.0	TECHNICAL APPROACH	2
2.1	Methodology.....	2
2.2	Approach	2
3.0	TIMELINE OF EVENTS	3
3.1	Key Events on Line 901 from 1990 to May 19, 2015	3
3.2	Key Events on Line 901 on May 19, 2015	5
3.3	Probable Time of Failure.....	5
3.3.1	Pressure Data	5
3.3.2	Leak Detection.....	6
4.0	IMMEDIATE / METALLURGICAL CAUSE	8
4.1.1	Summary of Metallurgical Findings	8
4.1.2	Immediate Cause Conclusion	9
5.0	SUPPLEMENTAL ANALYSES	10
6.0	BASIC ROOT CAUSES	12
6.1	External Corrosion Control System	13
6.1.1	External Protective Coating System	13
6.1.2	Cathodic Protection System	16
6.1.2.1	External Corrosion Data Review and Analysis.....	18
6.2	Integrity Program.....	21
6.2.1	Summary of Processes / Procedures Pertaining to Risk Assessments.....	21
6.2.2	Summary of Processes / Procedures Pertaining to ILI Assessments	22
6.2.2.1	Conducting Assessments and Processing Results	22
6.2.2.2	Pipeline Repair Requirements.....	23
6.2.2.3	Continual Assessment and Evaluation of Pipeline Integrity	23
6.2.2.4	Identification of Preventive and Mitigative Measures	24
6.2.3	Available In-Line Inspection Data	25
6.2.4	Summary of Events Following the 2012 and 2015 In-Line Inspection Final Reports	25
6.2.5	Description and Review of the 2012 ILI CGAR Analysis as Applied to Joint 5930.....	26

Table of Contents (Cont'd)

6.2.6	Description and Review of 2012 DOT Compliance Report (2012 Final Repair List)	29
6.2.7	Description and Review of the Validation of ILI Results	30
6.2.8	Description and Review of Re-Assessment Interval Determination	32
6.2.9	Continual Evaluation and Assessment of Pipeline Integrity.....	35
7.0	SUMMARY AND CONCLUSIONS	35

Appendices

Appendix A – BSCAT™ Methodology

Appendix B – Documents Reviewed

Appendix C – Supplemental Analyses for 2015 Digs

Appendix D – Corrosion Product Supplemental Analyses - Density Testing

Appendix E – Corrosion Product Supplemental Analyses - Magnetic Permeability

Appendix F – Statistically Active Corrosion Assessment

List of Tables

Table 1.	Summary of inspection data from aerial patrols of Line Segment 901 between January 7, 2015 and May 11, 2015.....	40
Table 2.	Assessments on potential external corrosion mechanisms for the failure.....	41
Table 3.	Historical moisture conditions, based on 2007 and 2012 ILI dig information, for pipe joints near the 2015 failure location.....	42
Table 4.	Timeline of external corrosion control monitoring and inspection data.....	43
Table 5.	Comparison of Rate Estimation Methods between 2007 and 2012 ILI.....	44
Table 6.	Comparison of estimated time to reach 80% WT for features on Joint 5930.....	45
Table 7.	Summary of features selected for excavation following the 2012 ILI.....	46
Table 8.	Comparison of re-assessment intervals for the feature associated with the 2015 Failure.....	47

List of Figures

Figure 1.	Photographs showing the topography in the vicinity of the failure location.....	48
Figure 2.	Topographical map and plot showing the elevation profile for Line 901. The white triangles on the map correspond to mile post markers. The green star on the map and the green line on the plot identify the location of the May 19, 2015 failure.....	49
Figure 3.	Photographs showing two of the culverts through which released product flowed.....	50
Figure 4.	Schematic showing the Loss Causation Model.....	51
Figure 5.	Timeline showing key events for Line 901 from the time of construction to the day of the incident (May 19, 2015).....	52
Figure 6.	Timeline showing key events for Line 901 on the day of the incident (May 19, 2015).....	53
Figure 7.	Plot of pressure versus time showing the discharge pressure for Las Flores (red), the incoming pressure for Gaviota (blue), and the calculated pressure for Joint 5930 (green) on May 19, 2015 [Ref 227].....	54
Figure 8.	Plot of pressure versus time showing the discharge pressure for Las Flores (red), the incoming pressure for Gaviota (blue), and the calculated pressure for Joint 5930 (green) on May 19, 2015 between 10:00 am and 12:00 pm [Ref 227].....	55
Figure 9.	Schematic showing Line 901 from Las Flores to Gaviota showing the approximate location of the pipeline and the elevation profile of the pipeline. The red arrows indicate the locations of flow meters [Ref 248].....	56
Figure 10.	Schematic showing Line 903 from Gaviota to Sisquoc the approximate location of the pipeline and the elevation profile of the pipeline. The red arrows indicate the locations of flow meters [Ref 249].....	57
Figure 11.	Schematic showing Line 903 from Sisquoc to Station Number 1595 + 16 the approximate location of the pipeline and the elevation profile of the pipeline. The red arrows indicate the locations of flow meters [Ref 250].....	58

List of Figures (Cont'd)

Figure 12.	Schematic showing Line 903 from Station Number 1595 + 16 to Pentland the approximate location of the pipeline and the elevation profile of the pipeline. The red arrows indicate locations of flow meters [Ref 251].	59
Figure 13.	Plot showing volume versus time data for the Las Flores to Pentland line segment between May 18, 2015 at 5:00am and May 20, 2015 at 12:00am.	60
Figure 14.	Plot showing volume versus time data for the Las Flores to Pentland line segment between May 19, 2015 at 1:00am and May 20, 2015 at 12:00am.	60
Figure 15.	Photograph showing the failure location before (Top) and after (Bottom) cleaning. Tape measure indicates distance to U/S GW (Note: tape slipped 0.1' to the right).	61
Figure 16.	BowTie diagram, generated using the BSCA T™ methodology, summarizing the preventative barriers in place for the Line 901 Release. The barriers shown as two rectangles on either side of the horizontal line correspond to failed barriers, while the thin rectangles that span the horizontal line correspond to ineffective barriers.	62
Figure 17.	Schematic and photograph showing the protective external coating and the PU foam and PE tape layers present on the Line 901 pipeline.	63
Figure 18.	Photographs showing compromised protective coating and PU foam/PE tape layers at the failure location.	64
Figure 19.	Photograph of wrinkles in the PE tape, located away from the failure location.	65
Figure 20.	Photographs showing compromised coating and PU foam away from the failure location.	66
Figure 21.	Plot showing the distribution of external metal loss features vs. o'clock orientation identified for Line 901 during the 2007, 2012, and 2015 ILI runs.	67
Figure 22.	Photographs showing recoated pipe on Line 901 after: (a) 2007 ILI Dig #5 and (b) 2012 ILI Dig #13 [Ref 147 & 169].	68
Figure 23.	Plot of temperature data, provided by Plains, for Las Flores Station between May 2014 and May 2015 [Ref 226].	69

List of Figures (Cont'd)

Figure 24.	Plains All American Line 901 "IRF" pipe-to-soil potential annual test point survey data years 2008, 2014, and 2015. Note: IRF: free of IR error.....	70
Figure 25.	Plains All American Line 901 In-Line Inspection 2007 maximum external metal loss depth reported aligned with 2008 Close Interval Survey (- Pipe Nominal Wall Thickness).....	71
Figure 26.	Plains All American Line 901 In-Line Inspection 2012 maximum external metal loss depth reported aligned with 2015 Close Interval Survey (- Pipe Nominal Wall Thickness).....	72
Figure 27.	Plains All American Pipeline Las Flores I Rectifier: Direct current (DC) output recorded between 2005 - 2015.....	73
Figure 28.	Plains All American Pipeline Las Flores II Rectifier: Direct current (DC) output recorded between 2005 - 2015.....	74
Figure 29.	Plains All American Pipeline Gaviota I Rectifier: Direct current (DC) output recorded between 2005 - 2015.....	75
Figure 30.	Plains All American Pipeline Gaviota II Rectifier: Direct current (DC) output recorded between 2005 - 2015.....	76
Figure 31.	Plains All American Pipeline L 901 Cathodic Protection Rectifiers: Average direct current (DC) output recorded between 2005 - 2015.....	77
Figure 32.	Plains All American Line 901 2015 close interval potential survey and annual test point survey data recorded between 2009 and 2014.....	78
Figure 33.	Timeline of events associated with Line 901, following the 2012 ILI.....	79
Figure 34.	Excerpt from IMP Fig 9-2 illustrating process to estimate corrosion growth rates [Ref 22].....	80
Figure 35.	Representation of reported metal loss features on Joint 5930.....	80
Figure 36.	Depths of ILI-reported metal loss features on Joint 5930.....	81
Figure 37.	Metal loss depth unity plot using Plains data.....	82
Figure 38.	Metal loss depth unity plot using Plains data. Light blue diamonds correspond to features located greater than 2 feet from a girth weld. Purple diamonds correspond to features within 2 feet of a girth weld.....	83
Figure 39.	DNV GL-produced metal loss depth unity plot for the 2015 ILI of the Las Flores to Gaviota line segment.....	84

List of Figures (Cont'd)

Figure 40. Excerpt from API 1163 used to establish consistency with performance specification (Table 8 in Appendix E, [Ref 309]).	85
Figure 41. Snapshot showing portion of Figure 6-1 from Section 6.2 of Plains' IMP, regarding regrading [Ref 20].	85

Acronyms

BSCAT™	Barrier-based Systematic Cause Analysis Technique
CGAR	Corrosion Growth Analysis Report
COF	Consequence of failure
CP	Cathodic Protection
CPM	Computation Pipeline Monitoring
CTU	Coal tar urethane
D/S	Downstream
ERW	Electric resistance weld
GIS	Geographic information system
GW	Girth weld
HF	High frequency
ICCP	Impressed Current Cathodic Protection
ILI	In-line Inspection
IMP	Integrity Management Plan
LCM	Lost Causation Model
LOF	Likelihood of failure
LDS	Leak Detection System
MDP	Maximum Discharge Pressure
ML	Metal loss
MFL	Magnetic Flux Leakage
MOP	Maximum Operating Pressure
MP	Mile Post
MPI	Magnetic Particle Inspection
NWT	Nominal wall thickness
OCS	Outer Continental Shelf
OEM	Office of Emergency Management
P&M	Preventative & Mitigative
PE	Polyethylene
PHMSA	Pipeline and Hazardous Materials Safety Administration
PLM	Pipeline Monitor
PU	Polyurethane
RCA	Root Cause Analysis
RGW	Reference Girth Weld
ROF	Risk of failure
SBC	Santa Barbara County
SBCFD	Santa Barbara County Fire Department
SCADA	Supervisory Control and Data Acquisition
SCAT	Systematic Causal Analysis Technique
SMYS	Specified Minimum Yield Strength
U/S	Upstream
WT	Wall Thickness

1.0 INTRODUCTION

Plains All American Pipeline, L.P. (Plains) retained Det Norske Veritas (U.S.A.), Inc. (DNV GL) to perform a root cause analysis (RCA) of a failure that occurred on Line Segment 901, which transports heated crude oil from the outer continental shelf (OCS). The failure occurred on May 19, 2015 in Goleta, California (Santa Barbara County) and was located near milepost (MP) 4. The location was approximately 4.05 miles downstream (D/S) from Las Flores Pump Station and approximately 6.2 feet upstream (U/S) from the nearest girth weld, identified as Girth Weld (GW) 5940. As a result of the failure, approximately 2,934² barrels of crude oil were estimated to have been released.

The leak occurred in a mostly rural area that runs along the coastline of the Pacific Ocean. The topography in the area is hilly, with the pipeline oriented uphill from the ocean. Figure 1 contains photographs showing the topography in the vicinity of the failure. Figure 2 contains a topographical map and elevation plot of Line 901. As shown in the figure, the failure was located near a local low point along the pipeline. Several road crossings, such as Highway 1, are present in the area with drainage toward the coast via culverts. It is via these culverts that the released oil reached the Pacific Ocean at Refugio State Beach. Figure 3 contains photographs showing the first two culvert through which the released product flowed. The photograph to the left in the figure corresponds to the culvert closest to the release site. A makeshift berm was created at this culvert to prevent any additional product from flowing through the culvert. The photograph to the right in the figure corresponds to the second culvert through which product flowed. This culvert ran beneath Highway 101.

The portion of the pipeline that contained the failure is comprised of 24-inch diameter by 0.344 inch wall thickness, API 5L Grade X65 line pipe steel that was manufactured by Nippon Steel and contains a high frequency (HF) electric resistance welded (ERW) longitudinal seam. The pipeline (Line 901) was installed in 1990 and is approximately 10.87 miles in length, spanning between Las Flores Station on the U/S end and Gaviota Station on the D/S end. The pipeline is externally covered with the following: (1) a protective coating of coal tar urethane (CTU) that is in intimate contact with the steel pipe, (2) a layer of rigid thermal polyurethane (PU) foam insulation, and (3) an outer layer of polyethylene (PE) tape. The pipeline has an impressed cathodic protection (CP) system that was energized at the time of installation.

The normal operating pressure and maximum discharge pressure (MDP) for the line are 616 psig and 1,025 psig, respectively. These pressures correspond to 33% and 55% of the

² [Ref 6] The final volume estimate for the released oil at the time of this report.

specified minimum yield strength (SMYS), respectively. The pressure at the time and location of the failure was reported by Plains to be 737 psig [Ref 2], which corresponds to 39.6% of the SMYS and 71.9% of the MDP.

The portion of the pipeline that contained the failure location was removed and sent to DNV GL to determine the metallurgical cause of the failure and to identify any contributing factors. The conclusions and recommendations for this RCA are based on the findings from the final metallurgical report as well as information provided and publically reported by Plains. The objective of the RCA was to identify factors contributing to the failure and document the decision-making process. Based on the findings of the analysis, recommendations for improvements also are identified.

2.0 TECHNICAL APPROACH

2.1 Methodology

The methodology used by DNV GL for the RCA of the Line 901 release was based on DNV GL's Loss Causation Model (LCM). The DNV GL LCM used in the analysis is shown in Figure 4. This model is built on the concept that incidents can be attributed to immediate causes, basic causes, and failures of management systems to control hazards. The analysis uses a systematic method of processing evidence gathered during an investigation in order to identify the factors that led to the incident. This methodology assists in the development of corrective and/or remedial measures.

The LCM approach used by DNV GL is called a Barrier-based Systematic Causal Analysis Technique (BSCAT™). BSCAT™ is a technique that applies a Systematic Causal Analysis Technique (SCAT) model to each barrier, as opposed to the incident as a whole. This method results in a thorough review of the effectiveness of individual barriers identified in the risk assessment. BSCAT™ provides a methodology that allows for the analysis of complex incidents that involve multiple barriers. Detailed information about the BSCAT™ methodology and its application is provided in Appendix A.

2.2 Approach

DNV GL reviewed various materials provided and publically reported by Plains (i.e. technical documents, manuals, maps, and data) and produced by DNV GL. The materials are grouped into the following categories: (1) incident related documents - References 1 – 7, (2) integrity-related documents (i.e. integrity management plan, cathodic protection surveys, in-line inspections, and excavation reports and digs) - References 8 – 200, (3) leak detection documents - References 201 – 223, (4) operations documents - References 224 – 242, (5) historical documents - References 243 – 246, (6) drawings, maps, and diagrams -

References ¶247 - ¶293, (7) public reports issued by Plains - Reference ¶294 - ¶298 and (8) standards, papers, etc. - References ¶299 - ¶316. A complete list of the materials reviewed for the RCA is provided in Appendix B.

The documents listed above were used for the following tasks:

1. Timeline creation of events leading up to the incident.
2. Immediate (Metallurgical) cause determination for the incident.
3. Basic cause(s) determination for the incident.
4. Technical root cause(s) determination for the incident.

It is important to note that the analyses described within this report were only performed for the segment of the pipeline affected by the incident (i.e. Line 901). The findings and discussion presented in this report are not representative or indicative of the entire pipeline system and programs covered by Plains and Plains subsidiaries. The results and analysis incorporated herein are based on the provided documentation listed in Appendix B. DNV GL reserves the right to modify or supplement the report should new information become available.

3.0 TIMELINE OF EVENTS

Two timelines were developed to help visualize the events that occurred leading up to the incident. Documents provided by and public reports issued by Plains were used to populate the timelines with relevant information. The first timeline incorporates key events that occurred on Line 901 between the time of construction to the day of the incident (May 19, 2015). The second timeline incorporates key events that occurred on the day of the incident up until the identification of the failure. These timelines were used to identify the barriers in place to prevent the incident and to identify the probable time of failure.

3.1 Key Events on Line 901 from 1990 to May 19, 2015

Figure 5 is a timeline showing key events for Line 901 from the time of construction to the day of the incident. The timeline includes dates for (1) construction (olive green circles), (2) system ownership change (green circle), (3) in-line inspections (ILIs) (purple triangles), (4) ILI excavation digs (red lines), (5) close-interval surveys (blue lines), and (6) the May 19, 2015 failure (teal square).

Five key events were identified relating to the construction and ownership of Line 901. The line pipe was manufactured in 1985 [Ref ¶246], but it was not installed until 1990 by All American Pipeline [Ref ¶2]. It was coated with mill-applied coal tar urethane and insulated

with 1.5 inches of mill-applied polyurethane foam in a double-joint configuration [Ref 244]. Girth welds performed during construction were coated using Raychem WPC M100-27000 x 34/A/Uni shrink sleeves combined with Raychem #S-1142 primer kits [Ref 244]. Cathodic protection in the form of impressed current was installed in 1990, the same year as the pipeline installation [Ref 2]. A hydrostatic test of the line was performed at Gaviota Station on Nov. 25, 1990. The test pressure of 1719 psig was held for 8 hours [Ref 2]. In 1994, the Las Flores Canyon Pump Station was constructed [Ref 296]. Four years later, All American Pipeline was acquired by Plains and Line 901 became part of Plains assets [Ref 297].

Four ILIs were performed on Line 901 between 1996 and May 19, 2015 [Ref 294]. Details about the vendor, tool(s) used, and the results for the 1996 ILI (ILI 1) were not available for review. The ILI vendor in the 2007 (ILI 2), 2012 (ILI 3), and 2015 (ILI 4) inspections was ROSEN, located in Houston, TX [Refs. 50, 91, 138]. For ILI 2, two tools were run– a geometry tool and a metal loss tool (magnetic flux leakage [MFL]). The tool type used for ILI 3 and ILI 4 was a combination MFL and deformation tool. Based on the results of the ILIs, digs were initiated in prioritized areas identified by Plains' integrity management plan (IMP) within one year of the ILI tool runs. Thirteen digs³ were conducted between February 21, 2008 and March 3, 2009. Between October 15, 2012 and October 3, 2013, 44 digs were performed⁴. After the 2015 ILI and the failure, 4 digs were performed in prioritized areas.⁵

Cathodic Protection Close-Interval Criteria Survey (CIS) assessments were conducted in December of 2008 (CIS1) and April of 2015 (CIS2) [Ref 31 – 44]. The CIS vendor was Hanson Survey & Design, from Houston, TX.

As part of the monitoring program utilized by Plains for leak detection, aerial patrols were conducted routinely on Line 901 (on a weekly basis, approximately). The patrols were conducted by Kern Charter Inc. (*Kern*) of Line 901 from Las Flores to Gaviota and Line 902 from Gaviota Station to the Gaviota Booster [Refs. 216 – 220]. Table 1 summarizes the inspection data from aerial patrols of Line Segment 901 between January 7, 2015 and May 11, 2015. Between these dates, 18 reports were completed. Three to twelve days separated the inspection dates. On three occasions (January 16, April 1, and April 17, 2015), weather prevented the inspection of Line 901. No leaks were identified by these aerial patrols. Surface patrols of the right of way (ROW) were not performed as part of

³ 2007: Digs 3 (WC5365.72), Dig 3 (WC 5342.18), Digs 4 – Dig 11, Dig 11B, Dig 12, & Dig 13. [Refs. 144 - 156]

⁴ 2012: Digs 1 – 19, Dig 20, Dig 20A, Dig 21, Dig 21A, Digs 22 – 33, Dig 33A, Digs 34 – Dig 41. [Refs. 157 -199]

⁵ 2015: Digs 1 through 4. [Ref 200]

Plains IMP of Line 901. The last aerial patrol prior to the failure was performed on May 11, 2015 by Kern.

3.2 Key Events on Line 901 on May 19, 2015

Figure 6 is a timeline showing key events for Line 901 on the day of the incident (May 19, 2015). The timeline includes times for (1) operational events (blue triangles), (2) calls to the National Response Center [NRC] (purple "X"s), (3) responses by local personnel to NRC calls (green triangles), and (4) and failure confirmation by Plains (teal square).

At approximately 10:55 am [Ref 294], an unplanned pump shutdown at the Sisquoc station occurred. The pump was successfully restarted. At 11:15 am, the pump at Sisquoc station was shut down [Ref 294]. Fifteen minutes later, the pump at Las Flores Station was shut down by Midland Control to prevent packing of the line [Ref 298].⁶ Line 901 was isolated at this time. Three calls were placed to emergency response entities, one call was placed to the Santa Barbara County (SBC) Fire Department and two calls were placed to the National Response Center (NRC). The SBC Fire Department was first notified of an odor near Refugio Beach at 11:42 am by an unidentified member of the public. State Parks staff were alerted to the 911 call and attempted to locate the source of the odor around 12:00 pm. SBC Emergency Management was then notified of the presence of oil on Refugio State Beach at 12:30 pm by SBC Fire Department. A call was placed, by an unidentified caller, to the NRC at 12:43 pm (1116950) reporting an oil sheen on Refugio State Beach. Around 1:30 pm, Plains confirmed a failure on Line 901 near Refugio State Beach. A call was placed by Plains to the NRC at 2:56 pm (1116972).

3.3 Probable Time of Failure

3.3.1 Pressure Data

Figure 7 is a plot of pressure versus time data for the discharge pressure for Las Flores (red, Ref 227), the incoming pressure for Gaviota (blue, [Ref 227]), and the calculated pressure for Joint 5930 (green) on May 19, 2015.⁷ The maximum recorded discharge pressure for Las Flores and incoming pressure for Gaviota on May 19 was 721 psig and 707 psig, respectively. These pressures were recorded at 12:55 pm and 12:54 pm, respectively. The maximum pressure data from Las Flores and Gaviota correspond to a pressure of 814 psig⁸

⁶ The remaining times referenced in this paragraph are from [Ref 298].

⁷ Calculated pressures determined by DNV GL.

⁸ Calculated value based on OPS TTO5 – Low Frequency ERW and Lap Welded Longitudinal Seam Evaluation (p. 23), April 2004. Discrepancy with the value reported by Plains may be associated with the equation used to

calculate value. This equation used by DNV GL:

$$P_x = \left(P_{us} + \left(\frac{SG}{2.31} h_{us} \right) - P_{ds} - \left(\frac{SG}{2.31} h_{ds} \right) \right) \left(\frac{L-x}{L} \right) - \left(\frac{SG}{2.31} (h_x - h_{ds}) \right) + P_{ds}$$

at the location of the failure. The time at which the maximum pressure was recorded occurred between the first call to the NRC and before Plains confirmed the failure on Line 901.

Figure 8 plot of pressure versus time data for the discharge pressure for Las Flores (red), the incoming pressure for Gaviota (blue), and the calculated pressure for Joint 5930 (green) on May 19, 2015 between 10:00 am and 12:00 pm. The corresponding times for key events associated with operational events (blue triangles shown in Figure 6) are indicated. Based on the pressure data, the unplanned and planned shutdowns at Sisquoc did not cause an increase in pressure, which would be expected due to line packing. There is a slight increase in pressure after the Las Flores Pump was shut down. Twelve minutes after the Las Flores pump was shutdown, a 911 call was placed to the SBC Fire Department notifying of the odor near Refugio State Beach.

3.3.2 Leak Detection

Leak detection is performed on the Plains pipeline system using computation pipeline monitoring (CPM). Plains uses two systems for CPM: (1) Pipeline Monitor (PLM) and (2) SimSuite Leak Detection System (LDS) [Ref 201]. For the affected line segment, the PLM approach was utilized. PLM compares the metered in to the metered out using SCADA at all inlet and outlet connections. Figure 9 through Figure 12 contain alignment sheets for Line 901 from Las Flores to Gaviota, Line 903 from Gaviota to Sisquoc, Line 903 from Sisquoc to Station Number 1596+16, and Line 903 from Station Number 1596+16 to Pentland, respectively. Calculations performed using the PLM were done using all of the inlet and outlet metered data between Las Flores and Pentland. In total, there are eleven locations that are part of the calculation, five inlets and six outlets (locations shown as red arrows in the figures).

There are six rolling time periods that are examined as part of PLM: (1) LT1 – 1 hour, (2) LT2 – 5 hour, and (3) LT3 – 24 hour, (4) ST1, (5) ST2, and (6) ST3.⁹ For Line 901 between Las Flores and Pentland, LT2 and LT3 were utilized in calculating the metered amount in that portion of the line segment in barrels. Plains calculated the overshoot in two ways (1) historical and (2) estimated. The historical data are based on real-time data from SCADA and the estimated data are based on an approximation of total metered amount if the real-time data were not available. The calculated overshoot data are monitored in the by a Leak Detection Engineer in the Plains' Control Center located in Midland, Texas.

⁹ Acronyms LT and ST are not defined in provided documentation.

Threshold alarm set points are selected by the Leak Detection Engineer based on the historical operating data for the pipeline and the events taking place on the pipeline. For instance, when product is flowing, an overshort value of 150 bbls is typical; however, when there is a pump shutdown (like the one preceding the detection of product outside the pipeline on May 19) a threshold value of 600 bbls is used. When the upper or lower threshold limits are violated, a PLM alarm indicating the over or the short is recorded in the SCADA. These instances are recorded as “critical” and have an audible sound associated with the event. An investigation into these types of events is immediately launched by the Leak Detection Controller.

Figure 13 and Figure 14 are plots showing volume versus time data for the Las Flores to Pentland line segment for the for LT2 and LT3 rolling time calculations [Ref 226]. These span the time frames of May 18, 2015 at 5:00 am and May 20, 2015 at 12:00 am and between May 19, 2015 at 1:00 am and May 20, 2015 at 12:00am, respectively. As shown in the figures, there is a downward trend in the total metered amount around 12:30 pm on May 19. The estimated and historical lines then diverge at ~1:23 pm around a short of 600 bbls.

In the SCADA between May 5, 2015 and May 19, 2015, twelve PLM alarms associated with Las Flores to Pentland segment of the pipeline were logged [Ref 206]. Ten of the PLM alarms were associated with events on May 6, 2015. These were associated with the ILI of the line pipe by ROSEN on that date. The two remaining PLMs took place on May 19, 2015 at 1:22:58 pm – the first was an alarm event and the second was the corresponding control description. The alarm event was associated with a violation of the “short” threshold (600 bbls) of the PML. The PLM was inhibited¹⁰ as a control by the leak detection engineer. By inhibiting the line, real-time recording of the inlet and outlet meters stopped. Hence, historical data were used to estimate the overshort values starting at 1:23 pm on May 19 (see Figure 13 and Figure 14). The pipeline was not shut-in at this time; however, an investigation into the alarm was initiated per Plains’ requirements outlined in Chapter 100-8 [Ref 201].

Based on a review of Plains Leak Detection methodologies, the overshort plots from the day of the event, and the SCADA from the two weeks prior, there is no evidence to suggest a slow leak was present within the system, which is consistent with the findings of the metallurgical report that indicated a sudden failure event.

¹⁰ The term “inhibited” means that the alarm was acknowledged by the leak detection engineer, and then silenced in order to begin an investigation in the alarm.

4.0 IMMEDIATE / METALLURGICAL CAUSE

4.1.1 Summary of Metallurgical Findings

DNV GL performed a metallurgical analysis on the portion of the pipeline that failed and concluded that *"the failure occurred at an area of wall thinning from external corrosion that ultimately failed by ductile overload under the imposed operating pressure. The morphology of the external corrosion observed on the pipe section is consistent with corrosion under insulation facilitated by wet-dry cycling."*[Ref 1] Figure 15 contains photographs of the failure location, provided in the metallurgical report, before and after cleaning. The failure opening was determined to be 6.6 inches in length axially with a maximum opening of 1.14 inches. The failure was located at the 4:15 o'clock orientation within an area of external corrosion that extended 12.1 inches in the longitudinal direction and 7.4 inches in the circumferential direction. The maximum depth of the external corrosion was 89% of the measured wall thickness at the failure location. No portion of the flaw was through wall prior to the ductile overload failure and, therefore, the failure event was sudden in nature.

During the investigation, several external corrosion features were identified along the bottom of the joint that failed. These features were in addition to the corrosion feature associated with the failure and were covered by thick, layered deposits that were magnetic. Chemical analyses performed on the deposits revealed that they were primarily comprised of layers of goethite and magnetite¹¹, two forms of iron oxide. No evidence of calcareous deposits was detected within the deposits, indicating that CP likely did not reach these areas. The areas where the external corrosion features were located corresponded to areas of compromised coating. The coating at these locations consisted of a combination of disbanded coal tar urethane, compressed and water saturated insulation, and wrinkled polyethylene tape. The nature of the coating damage allowed for the ingress of water to the pipe surface, which facilitated the corrosion.

Examination of the fracture surfaces from the failure location revealed the presence of two regions. The region near the external surface was nondescript and consistent with corrosion, while the region near the internal surface was dimpled and consistent with ductile overload. No evidence of in-service growth was identified on the fracture surface, indicating that the failure corresponded to a single sudden event.

Chemical and mechanical testing was performed on the pipe joint that failed. The results of those tests revealed that the steel was consistent with the vintage and grade of steel. No

¹¹ The chemical formula for goethite and magnetite are FeO(OH) and Fe₃O₄, respectively.

evidence of any metallurgical defects that may have played a role in the failure was identified within the steel.

4.1.2 Immediate Cause Conclusion

The potential for various mechanisms that may have caused the external corrosion at the failure location were considered during the metallurgical investigation. The mechanisms considered included the following: (1) AC stray current corrosion, (2) DC stray current corrosion, (3) galvanic corrosion, (4) microbiologically influenced corrosion (MIC), and (5) corrosion under insulation (CUI). Table 2 summarizes assessments for the potential external corrosion mechanisms at the failure location. The table is broken into three columns. The first column lists potential mechanisms (i.e. AC stray current corrosion, galvanic corrosion, etc.) that may have caused the corrosion. The second column contains the relevance of each mechanism to the corrosion observed at the failure location. The third column lists supporting evidence for the assessment given in column two.

AC and DC stray current corrosion were both eliminated as potential mechanisms for several reasons. These phenomena do not occur beneath shielding coatings. The morphology of the corrosion and the associated corrosion products are not consistent with AC or DC stray current corrosion. Furthermore, field measurements indicated there was negligible AC voltages on the pipeline at the failure location and there was no high voltage AC (HVAC) lines or sources of DC stray current in the right of way (ROW).

Galvanic corrosion was also eliminated as the primary cause of the corrosion. This is based on the fact that there was no evidence of dissimilar metals near the corrosion features observed on the failed pipe joint.

MIC was eliminated as the primary cause of the corrosion, but may have played a contributing role. Bacteria were identified at a corrosion feature sampled U/S from the failure location. The levels of bacteria detected, however, were low. This finding coupled with the dense layered morphology of the corrosion products is not consistent with MIC.

Based upon the results of the analysis, the most probable cause of the external corrosion is the mechanism of CUI. This conclusion is based upon (1) the morphology of the corrosion [i.e. mix of general corrosion and pits], (2) the thick layered morphology of the corrosion products, (3) the location of the corrosion [beneath saturated insulation], and (4) the association of the corrosion with compromised coating. The presence of wrinkling and cracks in the outer polyethylene tape coating likely allowed for the ingress of water to reach the pipe surface and facilitate corrosion.

Thus, the immediate cause of the failure on Line 901 was determined to be external corrosion due to a CUI mechanism. Based on this finding, DNV GL reviewed historical documents regarding the service history of the line to identify contributing factors to the failure.

5.0 SUPPLEMENTAL ANALYSES

Four priority digs, identified as Digs 1 - 4, were performed between May 29, 2015 and June 3, 2015, based on the preliminary findings of the 2015 ILI run. These locations were selected based on the maximum depths, identified by the tool, for external metal loss features on Line 901. DNV GL personnel were present during all four digs and collected various samples. The collected samples included the following: (1) corrosion products associated with the features, (2) swab samples for bacteria testing, (3) soil samples, and (4) coating insulation removed at the feature locations. The results of these analyses are summarized below and details are provided in Appendix C.

- The corrosion products
 - ◆ Are primarily dark brown in appearance with some areas that were rust-colored.
 - ◆ Are dry, rigid, and magnetic.
 - ◆ Consist of a layered morphology comprised primarily of goethite and magnetite.
- There is no strong evidence to indicate that MIC played a primary role in the observed external corrosion observed for Digs 1 - 4.
- The results of analyses performed on soil samples, removed near the failure and dig locations, revealed that the soil removed near the failure location exhibited higher corrosive properties.
- Analyses of liquids extracted from insulation samples removed near the corrosion features from Digs 1 - 4 revealed higher concentrations of corrosive species (i.e. chlorides) than their respective soil samples.

The corrosion products removed near the failure location were found to be tightly adhered to the surface of the pipe, such that mechanical means (i.e. hammer and chisel) were necessary to remove the products. The products were fairly rigid, coming off in sheets. Compound analyses performed on the products revealed that they are comprised of multiple alternating layers of magnetite and goethite. The products are also attracted to a magnet, indicating that the products may have affected the response seen by the tool. Based on these findings, analyses were performed on corrosion product samples removed from the

pipe joint that failed to assess the potential impact, if any, they had on the sizing capabilities of the MFL tool.

The influence of corrosion products on MFL depth sizing has previously been noted in the literature. Bowerman et al. observed inaccuracies in pit depths, as reported by an MFL tool, when ferromagnetic debris was present within corrosion features [Ref 307]. Specific compounds identified within the debris included magnetite, iron sulfide, siderite, and hematite. These researchers tested deeper corrosion features that contained the products than had been reported by the tool. They speculated that the deposits decreased the induced magnetic flux and reduced the quality of the acquired data. Similar findings were observed by Kasai et al. [Ref 308]. These researchers observed that ferro- and semi-magnetic products within corrosion features caused distortion of the flux field pattern that impacted the ILI detection and sizing performance. In their cases, the features appeared smaller than their actual size.

Based on the nature of the deposits, density and magnetic permeability measurements were performed on corrosion product samples removed near the 2015 failure location on Line 901. The results of the density testing are presented in Appendix D and revealed that a representative corrosion product, identified as Corrosion Product Sample 10000195318, had an approximate density of 3.53 g/cm³, which is approximately 45% of the density of low carbon steel. The product tested was removed from Feature 2 on the pipe joint that contained the 2015 failure (i.e. Pipe Joint 5930).

The results of the magnetic permeability testing are presented in Appendix E and revealed the following:

- The corrosion product specimens were less magnetic than the steel specimens.
- No significant differences were determined for the magnetic properties of the specimens removed from the two corrosion product samples.
- There were differences between the magnetic properties of the steel specimen in the axial (longitudinal) direction and the magnetic properties of the steel specimen in the transverse (circumferential direction).
- At the field strengths typically associated with MFL tools, the magnetic permeability values of the corrosion product specimens were significantly lower than the magnetic permeability values of the steel specimens. The values for the corrosion product specimens were less than 5% of the values determined for the steel specimens.

These results indicate that the magnetic nature of the deposits alone likely did not significantly impact the sizing capabilities of the MFL tool.

6.0 BASIC ROOT CAUSES

Basic root causes are contributing factors that are usually determined during the review of engineering controls and operational procedures. They may also be referred to as “indirect” causes. As shown in the schematic of the Loss Causation Model (See Figure 4), basic causes lead to the immediate cause(s).

There are a number of integrity assessment and integrity assurance methodologies that can be used on a pipeline. These methodologies are engineering controls that are typically used to prevent and/or assess for threats to pipeline integrity. The controls are considered “barriers” from the perspective of a root cause analysis. For this incident, the barriers fall into two main categories: (1) external corrosion control system and (2) integrity management program. Within each category, several areas that may have affected/contributed to the failure were considered. These areas are outlined below:

1. External Corrosion Control System

External protective coating system – a method used to prevent moisture ingress to prevent corrosion.

Cathodic protection (CP) system – an applied current used to counteract the natural electrochemistry of corrosion.

2. Integrity Program

Contracted In-line inspection - a technology used to identify sections of metal loss in the pipeline.

Mitigative actions – measures to address a specific threat that can include enhancement of existing barriers and/or the use of additional preventative barriers

An analysis of these areas was performed using the BSCAT™ methodology. Ineffective, failed, and missing barriers related to the failure were identified. Effective, ineffective, failed, and/or missing barriers related to the failure were identified. The term “Effective” is used to describe a barrier that is performing in the manner as originally intended. “Ineffective” is a term used to describe a barrier that is in place and operating, but its performance is deficient. The term “Failed” is used to describe a barrier that was originally in place, but has degraded and no longer functions as originally intended. “Missing” is used to describe a barrier that was never in place. These barriers are graphically represented in Figure 16 and discussed below by area.

6.1 External Corrosion Control System

The results of the metallurgical analysis [Ref ¶1] indicate that the leak occurred at an area of external metal loss due to corrosion that ultimately failed by ductile overload under the imposed operating pressure. Buried carbon steel pipelines are normally protected against external corrosion by a combination of an external coating and cathodic protection (CP). Plains' Operations and Maintenance Manual O&M - 412 (OM412) [Ref ¶31] provides procedures to ensure the implementation of a sound corrosion control program to meet or exceed the minimum federal safety standards as defined by Title 49, Part 195 of the Code of Federal Regulations for Hazardous Liquids [Ref ¶316], developed by the U.S. Department of Transportation (DOT) Pipeline and Hazardous Materials Safety Administration (PHMSA). Both an external coating and CP system were in place on Line 901 to minimize the threat of external corrosion. Since the immediate cause of the failure is external corrosion, factors associated with one or both of these barriers failed and/or was ineffective. Details on both the external protective coating and CP system are described below.

6.1.1 External Protective Coating System

The use of an external protective coating is one of the primary barriers used to prevent degradation of the external surface of a pipeline. The coating serves to prevent exposure of the external pipe surface to the surrounding soil environment and potentially corrosive conditions. When coating failure does occur, the remaining intact coating reduces the surface area of exposed metal, thereby decreasing the CP current requirements for protection.

Line 901 is externally coated with a protective CTU. In addition to the protective coating, the external surface of the pipeline is also covered with a rigid PU foam and a white Polyken (PE) tape [Ref ¶244]. The use of the PU foam and PE tape was selected at the time of construction, by All American Pipeline, to maintain the temperature of the heated oil within the pipeline and minimize heat losses during transit. The PU foam was well bonded to the CTU coating and the PE tape was wrapped around the PU foam to reduce the ingress of water. Figure 17 contains a schematic and a photograph showing the location of the CTU coating, the PU foam, and the PE tape with respect to the bare pipe steel. The CTU was identified as LAC-450 [Ref ¶131] and is in intimate contact with the steel. The average thickness of the coating ranged from 0.040 to 0.043 inches, as reported in the metallurgical report [Ref ¶1]. The outer PU foam was approximately 1.5 inches thick at the time of installation [Ref ¶244]. .

The protective CTU coating, PU foam layer, and PE tape were compromised at the failure location, based on the evidence provided in the metallurgical report. The damage included

wrinkles, cracks, staining, and decohesion of the PE tape; staining, water saturation, and compression of the PU foam; and disbondment of the CTU [Ref ¶1]. The compression and saturation of the PU foam were found to be concentrated only along the bottom of the pipeline. The PU foam was found to exhibit minor to no evidence of compression and saturation along the top of the pipe. Figure 18 contains representative photographs of the damage observed on the protective coating and the outer layers at the failure location. In addition to the damage, thick layers of corrosion products were found wedged between the protective CTU coating and the pipe steel. The presence of the corrosion products beneath the protective coating indicates that the coating had to have failed at this location such that water reached the pipe steel and established a corrosion cell. The morphology and location of the corrosion products are consistent with a CUI mechanism.

The compromised coating on Line 901 was not isolated to just the failure location. Evidence of wrinkles and cracks were observed within the PE tape along the length of the excavated pipeline during the incident investigation. The wrinkles were concentrated at the bottom of the pipe along the 4:00 and 7:00 o'clock orientations [Ref ¶1], while the cracks were primarily along the 12:00 and 6:00 o'clock orientations. Figure 19 is a photograph showing evidence of wrinkles within the PE tape layer, away from the failure location. Similarly, evidence of saturation/compression of the PU foam and thick deposits beneath the disbonded CTU coating were concentrated along the bottom of the pipe at Priority Dig 1 in 2015; see Figure 20. These findings indicate that the environment along the bottom of the pipe is likely more corrosive than the environment along the top of the pipe. This conclusion is supported by the results of the 2007, 2012, and 2015 ILI runs, which show a higher distribution of external corrosion anomalies between the 3:00 and 9:00 o'clock orientations of the pipe; see Figure 21. Thus, the protective external coating did not provide an effective barrier against the initiation and subsequent propagation of external corrosion.

Repairs and excavations performed on Line 901 since 2007 have utilized a two part epoxy to recoat the pipeline. The recoat did not include the application of the PU foam insulation. Figure 22 contains photographs showing two examples of recoats performed after representative 2007 and 2012 ILI digs [Ref ¶147 & ¶169]. The use of an epoxy protective coating with no PU foam helps to minimize the possibility of CP shielding in these areas. These steps increase the chance that CP can assist with mitigating external corrosion in areas where the two part epoxy coating is compromised.

Probable contributing factors to the failure of the CTU protective coating are considered to be:

- Temperature of operation
- Shearing stresses on the protective coating (insulation compression / land movement)
- Design (outer coverings)
- Wet / dry cycling

The temperature of the product during operation of Line 901 averaged approximately 135 °F, based on data provided for a year prior to the failure [Ref 226]. Under typical operating conditions, this temperature was generally maintained between May 2014 and May 2015. During this time period, the temperature had a range between approximately 50 °F – 145 °F; see Figure 23. The lower temperature excursions appear to be isolated events. Only two low temperature excursions were noted over the time period for which data were provided. One of the excursions corresponded to the time of the 2015 ILI run. In contrast, the high temperature excursions were a bit more frequent but shorter in duration. Hickey et al. [Ref 306] showed that, at these higher temperatures (i.e. ~ 150 °F), and when exposed to a chloride environment, CTU coatings exhibited poor cathodic disbondment properties. Thus, the operating temperature may have influenced the adhesion of the CTU coating to the pipeline steel. In addition to the effect that the operating temperature may have played on the CTU coating, the temperature may have also promoted CUI. Corrosion under insulation is a phenomenon that is well established in above ground piping facilities, like oil refineries and chemical process plants [Refs 301 and 310] and is known for underground pipelines [Ref 311]. CUI is identified as a concern in above-ground piping systems operating in a temperature range of 32 °F to 212 °F. The operating temperature of Line 901 falls within this range. Given the geometry of the CTU coating, PU insulation, and PE tape layer; the primary cause of failure from the metallurgical analysis; and the operating temperature of the line; the environment is consistent with circumstances conducive to CUI in above ground facilities. Thus, temperature may have been a contributing factor to the CUI.

In combination with the temperatures discussed above, shearing stresses acting on the protective CTU coating likely contributed to the failure. In order for the corrosion to occur, the protective CTU coating had to disbond from the steel surface. Once the coating disbonded, the steel pipe was exposed to an electrolyte and corrosion could occur. Evidence of shearing due to soil stresses was observed along the pipeline, as evidenced by the presence of wrinkles and folds within the PE tape and compression of the PU foam. Based on the strong bond between the CTU coating and the PU foam, any soil stresses acting on the PE tape and PU foam were likely transferred to the CTU coating.

The design of the insulating layers on Line 901 also contributed to the failure of the CTU coating. PE tape may have been selected to prevent water ingress to the PU foam and / or protection of the PU foam; however, tape is known to exhibit integrity issues in buried systems (i.e. wrinkling and poor corrosion control capabilities). Thus, when the PE tape was compromised, water was able to reach and saturate the PU foam. This water reached the CTU coating, which was absorbed by the PU foam.

Wet / dry cycling is another probable contributor to the failure. Historical moisture data for the pipe joints at and adjacent to the May 19, 2015 failure location were reviewed due to: (1) the findings of the soil analyses in the metallurgical report and supplemental analyses (i.e. higher corrosive properties for saturated soils), (2) the presence of saturated PU foam adjacent to the failure location, and (3) the findings from the metallurgical report that indicate that the CUI was facilitated by wet/dry cycling. The data reviewed include the soil conditions reported in 2007 ILI Dig #5 and 6 [Ref ¶147 & ¶148] and reported in 2012 ILI Digs #12 and 13 [¶168 & ¶169]. The pipe joints excavated during these digs included Pipe Joints 5910 - 5950.¹² These data were compared to historical average monthly precipitation reports for Santa Barbara, California and are presented in ¶Table 3. Both moist and dry soil conditions were encountered during the digs. The soils were found to be moist in February and March and dry in May. These findings correlate to the historic monthly rainfall patterns for Santa Barbara County, CA. The only pipe joint that was excavated during both a historically wet and dry month was Pipe Joint 5920. This pipe joint is directly adjacent to Pipe Joint 5930, which contained the failure location, on the U/S side. The fact that the soil adjacent to the pipe joint that failed exhibited wet-dry cycling indicates that wet-dry cycling likely occurred within the soil at the failure location and thus contributed to the failure. In addition, the location of Pipe Joint 5930 along Line 901 has the potential for extended periods of exposure to moisture as it falls within a low point along the line; see Figure 2.

Based on the metallurgical analysis, the protective coal tar urethane (CTU) coating, thermal polyurethane (PU) foam insulation, and polyethylene (PE) tape were compromised at the failure location. The damage included wrinkles, cracks, staining, and decohesion of the PE tape; staining, water saturation, and compression of the PU foam; and disbondment of the CTU. The damage to the external protective coating system allowed for water ingress, retention of water, and subsequent CUI.

6.1.2 Cathodic Protection System

CP is intended to mitigate external corrosion at exposed coating holidays. OM412 indicates that all buried or submerged interstate hazardous liquid pipelines that are constructed,

¹² The May 19, 2015 leak was associated with Pipe Joint 5930

relocated, replaced, or otherwise changed subsequent to March 1, 1970 must have CP installed [Ref §231]. OM412 also indicates that the CP system must be installed within one year after the pipeline is constructed, relocated, replaced, or otherwise changed. Both of these requirements were met for Line 901.

OM412 indicates that all pipelines shall be electrically surveyed at least once each calendar year, but with intervals not exceeding 15 months, to determine whether the level of CP is adequate. The criteria for protection shall be a negative 0.850 volt with cathodic protection current applied. The pipe-to-soil potential shall be measured with reference to a copper-copper sulfate reference electrode (CSE) placed on the ground above the pipeline. Voltage (IR) drops other than those across the structure-to-electrolyte boundary shall be considered when evaluating the measured pipe-to-soil potentials.

OM412 provides a second criterion for adequate CP, defined by a minimum of 100 millivolts of negative polarization voltage shift. The polarization voltage shift must be determined by interrupting the protective current (turning off all cathodic protection current sources, including those from any foreign system that may affect the pipeline pipe-to-soil potential) and measuring the polarization decay. The voltage reading after the immediate voltage shift occurs (when current is initially interrupted) shall be used as the base reading from which to measure the polarization decay.

Section 6: Criteria and Other Considerations for Cathodic Protection of NACE International Standard Practice SP0169-2013 "Control of External Corrosion on Underground or Submerged Metallic Piping" [Ref §301], lists criteria for CP that indicate whether adequate CP of a metallic piping system has been achieved. The two criteria included in OM412 are included in SP0169, however, paragraph 6.2.1.4.2 indicates that at elevated temperatures (> 40 °C [104 °F]), the criteria listed in OM412 may not be sufficient, and also indicates that at temperatures greater than 60 °C (140 °F), the polarized potential of -0.950 volt CSE or more negative might be required. Experimental work performed by Jung-Gu and Yong-Wook [Ref §302] concluded that, for buried pipe under thermal insulation, adequate CP could not be obtained at -0.85 volt of polarization at temperatures greater than 25 °C [77 °F].

Paragraph 6.3.7 of SP0169-2013, indicates reliable measurement of potentials and therefore interpretation of CP criteria can be significantly affected by the presence of electrical shielding. Electrical shielding can be caused by disbanded coatings, thermal insulation, loose wrappers, high-resistivity rock or soils, metal structures or pipelines that are close to the structure being protected, and other man-made materials partially or completely surrounding the pipeline. The external coating system of L901 consists of a coal tar urethane coating on the steel substrate, 1.5-inch thick rigid polyurethane foam, and an external polyethylene tape. This type of coating systems has been reported to limit the

effectiveness of the cathodic protection in mitigating corrosion on areas where the electrolyte has reached the external surface of the steel pipe [Refs §302, §304, §305].

Pipe-to-soil potential data recorded at CP test stations located along L901 were provided between years 2005 and 2015 [Ref ¶46], for review and analysis.

OM412 indicates all CP rectifiers shall be inspected at intervals not to exceed 2½ months, but at least 6 times each calendar year. The inspection shall include recording direct current (DC) output volts and amps, coarse and fine tap settings, and a visual inspection of rectifier components. Measurement of DC output volts and amps, and pipe-to-soil instant off potentials shall be completed as necessary to assure the rectifier is calibrated and adjusted properly.

DC output volts and amperes, and taps settings of rectifiers Las Flores I, Las Flores II, Gaviota Station I, and Gaviota Station II, were provided for review and analysis between years 2005 and 2015 [Ref ¶47 and ¶49]. The analysis is discussed below.

OM412 indicates a detailed potential survey, typically refer to as a close-interval potential survey (CIS) should be conducted where practicable and determined necessary by sound engineering practice, to accomplish the following objectives, established in paragraph 10.1.1.3 of NACE Standard SPO169-2007 [Ref §300]:

- Assess the effectiveness of the CP system;
- Provide base-line operating data;
- Locate areas of inadequate protection levels;
- Identify locations likely to be adversely affected by construction, stray currents, or other unusual environmental conditions; or
- Select areas to be monitored periodically.

CIS data recorded on L901 in years 2008 and 2015 were provided for review and analysis [Ref §33], [Ref §34].

External metal loss data from MFL ILI runs conducted in the years 2007, 2012 and 2015 were provided for analysis and review, [Ref §85], [Ref ¶126], and [Ref ¶139].

6.1.2.1 External Corrosion Data Review and Analysis

The purpose of the data review and analysis was to identify possible direct cause or causes that may have contributed to the failure that occurred on May 19th, 2015 in Goleta (Santa Barbara County), California at mile post (MP) 4, of pipeline L901.

The first step when evaluating the performance of the external corrosion control system is to review the timeline of the data available. Based on the available data, some assumptions may be needed to establish operating conditions on the years where no data are available. The timeline of the data available to external corrosion is presented in Table 4.

As can be seen in Table 4, the line started operation in 1990. Assuming that the external metal loss occurred at a constant rate since installation, a maximum wall loss of 0.318-inch reported at the leak [Ref 1], and 25 years of exposure (2015-1990), an average corrosion rate of 12.7 mils (1 mil = one thousandths of an inch) per year (mpy) is calculated. This corrosion rate value is consistent with the value provided in Appendix C3 of NACE International Standard SP0520-2010 [Ref 299] 12.2 mpy, which corresponds to the corrosion rate of a pipeline segment that had at least 40 mV of polarization (considering IR drop) for a significant fraction of the time since installation. This corrosion rate would not be expected on a pipeline segment with polarized annual pipe to soil potential values (IRF potentials stand for pipe-to-soil potentials free of IR error, also referred to as interrupted potentials) presented in Figure 24. The IRF potentials recorded in the vicinity of the 2015 leak site meet both the criterion for adequate CP indicated in OM412 and the criterion suggested in NACE SP0502 for pipelines operating at temperatures higher than 60 °C (140 °F). However, data from only three years (recorded on one day of the specific year), of a pipeline that has been in operation for 25 years, may not be a good representation of the operational history of the external corrosion control system. Therefore additional data were aligned and analyzed.

2008 CIS data were aligned to 2007 ILI data, and 2015 CIS data were aligned to 2012 ILI, to check whether or not there was any correlation between external metal loss reported by the ILI runs and the pipe-to-soil potential profile along the pipeline route. The results are presented in Figure 25 and Figure 26, respectively. The interrupted pipe-to-soil potentials reported in 2008 and 2015 are more negative than -0.85 V CSE, and the 2015 interrupted potentials pipe-to-soil potentials are more negative than -0.95 V CSE along the entire length of L901. The locations where the 2008 CIS pipe-to-soil potential values were less negative than -0.95 V CSE (boxed in red rectangles in Figure 25), don't coincide with the locations where the deepest external metal loss were reported by the ILI tool.

However, when ILI data are aligned and compared with CIS data, the validity (in time) of the CIS data needs to be checked. ILI data reports the cumulative metal loss that has occurred until the date of the inspection. CIS data report the pipe-to-soil potential values at the time of the survey and under the operating conditions of the CP system at the time of the survey. The CIS potential profile will only be valid on the days of the life of the pipeline in which the CP system was operating under the same conditions present at the time of the

survey (these conditions include the condition of the electrical insulators, foreign CP systems that affect the pipeline segment, rain fall, etc.).

The operating conditions of the CP rectifiers Las Flores I, Las Flores II, Gaviota Station I, and Gaviota Station II, that provide CP current to L901 were plotted and analyzed between years 2005 and 2015. The results are presented in Figure 27 – Figure 30, respectively. To facilitate the analysis of the operating condition of the CP system, the yearly average of the DC current output was calculated for each year and for each rectifier. The total DC current outputs were plotted between years 2005 and 2015 and the ILI run and CIS inspections years were included in the plot presented in Figure 31. As can be seen, the 2015 CIS data do not represent the operating conditions at which the CP system operated between 2008 and 2015. If it did, it could account for the external metal loss that occurred between 2007 and 2015 and could show consistency when compared to 2007 and 2015 ILI results. The limited validity of the CIS and ILI alignment is also evident in Figure 32. The annual pipe-to-soil potential data recorded prior to the 2015 CIS show less polarization than the one recorded during the CIS.

Despite the limitation of the CIS data, neither the annual test point data, nor the operating conditions of the rectifiers are consistent with the external metal loss reported by the ILI inspections. This inconsistency between the CP level and the external metal loss is likely a result of the electrical shielding produced by the coating system. The cathodic protection current cannot reach (or marginally reaches) the steel surface exposed to trapped electrolyte and the sensitivity of the electrical surveys used to monitor the condition of the buried pipe is significantly limited and not reliable.

Probable contributing factors to the ineffectiveness of the CP system were considered and include:

- Design of pipeline (insulation layers)
- High resistive nature of the soil

With the existing coating system, external corrosion will occur on the pipe surface at locations where the external polyethylene jacket allows the ingress of moisture, probably at field joints or areas where the topography of the right-of-way made it difficult to install the pipe. Areas where this moisture is trapped, together with seasonal changes that promote dry / humid cycles, may accelerate the degradation mechanism. This premise is validated by the preference of external metal loss on the bottom of the pipe where moisture will tend to accumulate due to gravity. Figure 21 shows the distribution of the external metal loss anomalies around the circumference of the pipe. In 2015, more than 71% of the external

metal loss anomalies reported by the ILI were between the 3 and 9 o'clock position, i.e. the bottom of the pipe.

Resistivity measurements were taken on soil samples removed near the failure location and at the four priority dig sites; see Appendix C. The resistivities of the unsaturated (i.e. as-received) samples ranged from 2,500 – 78,000 Ohm-cm. Three of the five samples tested exhibited unsaturated resistivities that were greater than 14,000 Ohm-cm, which is highly resistive. High resistivity soils can be detrimental to the effectiveness of the CP system.

In summary, Plains met the regulatory requirements for monitoring cathodic protection system on Line 901, and based on the data provided, met the required levels for protection. However, the presence of polyurethane insulation and a polyethylene wrap shielded cathodic protection and the measured potentials are not representative of the electrochemical potentials at the areas of CUI.

6.2 Integrity Program

Within its Integrity Management Plan (IMP), Plains implements a process of assessment and evaluation to maintain pipeline integrity. This investigation focused on the provided procedures to conduct a risk analysis and assess the integrity of the pipeline, including those used following the acceptance of the final ILI report related to assessments of internal and external corrosion.

6.2.1 Summary of Processes / Procedures Pertaining to Risk Assessments

Plains utilize a relative risk indexing system (algorithm), which is described in "Risk Assessment Procedures" (Section 3 of the IMP). Nine likelihood of failure (LOF) types are identified and are consistent with general industry practices: external corrosion, internal corrosion, third party, equipment, construction, manufacturing, incorrect operations, weather and outside forces, and stress corrosion cracking.

The description of the algorithm, including the weighting of each LOF type and the scoring mechanism for each variable category, is in Appendix D1 of IMP Section. For this investigation, external corrosion is the LOF type of interest. Plains identified this failure type in the relative risk model and it makes up 27% of the total likelihood score. This failure type has the highest weighting of all nine failure types identified. Plains provided DNV GL with their scoring mechanism for the failure type of external corrosion, which considered factors such as soil type, soil condition, asset age, coating type, the presence of insulation, and CP type [Ref ¶13]. For Line 901, the external corrosion risk "contribution" to the LOF algorithm remained relatively consistent from 2009-2014 (i.e. ranging between 0.94 and 1.16 according to Ref ¶14).

Recommended Practice (RP) API 1160 provides guidance on managing system integrity to pipeline operators that transport hazardous liquids. Within the RP, a list of threats for underground pipelines is provided. All nine of the failure types (i.e. threats) identified by Plains are included in the practice. The specific threat of CUI is not addressed for underground pipelines in API 1160 or in Title 49, Part 195 of the Code of Federal Regulations for Hazardous Liquids [Ref ¶16]. Plains did identify external corrosion issues associated with field coatings (shrink sleeves) based on experience [Ref ¶90 and ¶131] and actions were taken to address this specific threat through the use of more stringent dig criteria and a shorter reassessment interval. Other than the accelerated re-inspection interval implemented on the line, Plains the mitigative actions taken by Plains on Line 901 did not adequately address the elevated integrity threat of CUI

6.2.2 Summary of Processes / Procedures Pertaining to ILI Assessments

Portions of Sections 6, 8, and 9 of the IMP specify the procedures and guidance for “Conducting Assessments and Processing Results,” “Pipeline Repair Requirements,” and “Continual Assessment and Evaluation of Pipeline Integrity,” respectively [Ref ¶20, ¶21, and ¶22]. Section 11 of the IMP contains the procedure used for the “Identification of Preventive and Mitigative Measures” [Ref ¶23]. The relevant portions of each section are summarized below.

6.2.2.1 Conducting Assessments and Processing Results

Section 6.3 “Review of New ILI Results – Repair Determinations and Schedules” includes the process used to evaluate ILI results and identify detected anomalies that require further evaluation and/or remediation. Two of the eight sub-sections are applicable to this review:

- **Tool Tolerance and Anomaly Classification:** Specifies that the reported depths of “all significant corrosion anomalies” from the final ILI report are increased by a tool tolerance of 10% wall thickness. Anomalies are classified by comparing the Modified B31G burst pressure and Safe Operating Pressure to the MOP of the pipeline. The Corrosion Growth Analysis Report (CGAR)¹³ is used to calculate the estimated corrosion growth as part of the repair list generation.
- **Classification of Corrosion and Deformation Anomalies – Generate Initial Repair Lists:** Specifies how corrosion and deformation anomalies are separated into Immediate, 60-Day, 180-Day, and other condition anomalies and the timeframes these conditions must be evaluated.

¹³ The CGAR process will be described in more detail later.

Section 6.4 “Data Integration of Pipeline ILI Results and Risk-Factor Data – Finalize Repair Scope and Schedule” describes the “procedures [to] be used to integrate other pipeline system information to finalize and supplement [§195.452(h)(4)-based] repair lists and set the repair schedule priorities.” Four of the five subsections are applicable to this review:

- **Manual Process for Data Integration:** Integration of geographic information systems (GIS), current and previous ILI, previous repairs, cathodic protection data and estimated remaining lives are used to determine the final repair locations and schedule.
- **ILI Results Evaluation based on Data Integration:** The compiled and integrated data are reviewed to identify subsequent actions. Results are documented on the “PHMSA Compliance Report”.¹⁴
- **Repair Decisions based on Data Integration:** Identification of additional repairs or evaluations, which may add additional repairs or exploratory digs to the repair schedule. When digs are performed in Santa Barbara County as part of the IMP, a grading plan for the dig has to be submitted to the County of Santa Barbara Planning and Development – Building and Safety Division. Specific requirements for grading on the dig are provided within the Santa Barbara County, California – Code of Ordinances in Chapter 14 [Ref 298].
- **Validation of ILI Results:** Comparison of ILI-reported anomaly data and field-measured data, which is subject to analysis such as, plotting unity graphs and performing statistical analysis.

6.2.2.2 Pipeline Repair Requirements

Section 8.3 “Repair Categorization” provides the definitions of repair categories (e.g., Immediate Condition) from §195.452(h)(4). These category definitions are also contained in the process schematic in Section 6.3 “Review of New ILI Results – Repair Determinations and Schedules”.

6.2.2.3 Continual Assessment and Evaluation of Pipeline Integrity

The evaluation to determine a re-assessment interval for internal and external corrosion is presented in Section 9.2.2 “Procedures for Evaluating External and Internal Corrosion”. The external and internal corrosion procedures are intended to determine “the hypothetical time to failure (including safety factors) from internal and external corrosion growth and

¹⁴ The PHMSA Compliance report is also referred to as the “DOT Compliance Report” in the documentation provided to DNV GL

calculates an appropriate Re-Assessment interval to detect corrosion anomalies prior to the point at which the anomaly could potentially cause an operations failure.”

Plains developed an Excel®-based program that performs the calculations described in Section 9.2.2 called “Corrosion Growth Analysis Report.” The CGAR program is also used during the procedures in Sections 6.3 and 6.4 to generate the final repair and evaluation schedule.

As stated in Section 9.2.2, the procedure to determine a re-assessment interval for internal and external corrosion involves estimating the:

- *“Initial Corrosion Anomaly Size. The largest potential corrosion anomalies that could remain after the last assessment repairs were made are determined from ILI or hydrotest data.”*
- *“Corrosion Growth Rates. External and internal corrosion growth rates are estimated from multiple ILI runs, field observations, and observed historical growth rates.”*
- *“Time to Grow Corrosion Anomaly to Repair Condition. The time required to grow the initial corrosion anomaly size to failure is determined. The Reassessment interval based on corrosion growth is set at 70% of the predicted time to failure at the normal operating hoop stress of the system.”*

The recommended re-assessment interval is recorded on Form F11-2, Part A per Section 9.2.5 “Determination of the Re-Assessment Interval.” Changes to the re-assessment schedule are documented on the revision log for the assessment schedule per Section 9.3 “Revisions to Re-Assessment Schedule”.

Periodic evaluations to assess overall pipeline integrity are required by §195.452(j)(2) and the procedural requirements for these evaluations are specified in Section 9.5 “Continual Evaluation and Assessment of Pipeline Integrity.” Evaluations occur at the midpoint between the last Preventative & Mitigative (P&M) evaluation and next scheduled assessment, after multiple leaks or failures by the same cause, following a “significant increase in risk analysis score” of a pipeline section and a “significant change in operations” of the pipeline section. The evaluations are documented on Form F9-1.

6.2.2.4 Identification of Preventive and Mitigative Measures

Preventive and Mitigative Evaluation Meetings are defined in Section 11 of the IMP “Identification of Preventive and Mitigative Measures.” Section 11.3 specifies that “Division P&M Evaluation Teams meet yearly” and “P&M evaluations of assessments will occur within

15 months of the receipt of the final reports [to allow] time for reviewing the assessment results and investigating the worst anomalies to develop confidence in the validity of the assessment and to understand the pipeline segment's condition."

6.2.3 Available In-Line Inspection Data

Plains provided results and documentation related to ILI assessments performed in 2007, 2012, and 2015. All three assessments were performed by Rosen using high resolution axial magnetic flux leakage (MFL) ILI tools.

The 2015 MFL run was completed on May 6, 2015, approximately 13 days prior to the failure; however, the ILI data were still being analyzed by Rosen at the time of the failure. Plains received the preliminary ILI report on May 22, 2015 and the final ILI report on May 31, 2015. Although documentation was available for all three assessments, this review focused primarily on the information and analysis performed using the 2012 ILI as it pertains to processing the ILI results for excavations and determining an appropriate reassessment interval. The 2007 ILI is included in that process. The analysis is also supplemented with information from the 2015 ILI as appropriate.

6.2.4 Summary of Events Following the 2012 and 2015 In-Line Inspection Final Reports

The timeline of events related to and following the receipt of the 2012 ILI final report on September 24, 2012 (including the 2015 ILI) is shown in Figure 33. The CGAR analysis process began around September 26, 2012.¹⁵ Excavations were completed between October 18, 2012 and October 3, 2013. The DOT Compliance Report [Ref ¶124] was completed July 10, 2013. The Assessment Schedule [Ref ¶127] dated December 31, 2012 specified a three year reassessment interval for Line 901. As required in Section 9.3, the Assessment Plan revision log was updated. Form F11-2 [Ref ¶131], required as part of Section 9.2.5, for the 2012 ILI was completed on May 21, 2015. PHMSA conducted an inspection of procedures and records pertaining to Line 901 between August 19 and October 4, 2013 and provided Plains with the results of their inspection on September 11, 2015 [Ref ¶7]. On March 26, 2014, the highest pressure recorded at the Las Flores station between the 2012 ILI and May 18, 2015 (the day before the failure) was 888 psig. In April, a CIS and an aerial patrol were completed on the 9th and 28th, respectively. Between May 29, 2015 and June 3, 2015 four excavations were performed by Plains based on the 2015 ILI data. [Ref ¶200]

¹⁵ Plains provided an intermediate CGAR analysis file [Ref ¶128] dated September 26, 2012 indicating that the CGAR process began around this timeframe.

6.2.5 Description and Review of the 2012 ILI CGAR Analysis as Applied to Joint 5930

The CGAR analysis is used within multiple steps during the analysis of ILI data and the reassessment interval determination. The initial and final repair lists are based on the results of this analysis and the calculations form the basis for the reassessment interval.

In the 2012 CGAR analysis [Ref ¶128], the initial flaw size for all reported ILI features were increased by the ILI tool tolerances (equal to 10% of the nominal wall thickness (WT) for depth and 0.472-in (12 mm) for length). This is consistent with IMP Section 6.3 for depth; the addition of the length tolerance exceeds the requirements in Section 6.3. The MOP used was 1140 psig.

(b) (4)

[REDACTED]

[REDACTED]

[REDACTED]

[REDACTED]

[REDACTED]

[REDACTED] This is consistent with the equation presented in Figure 9-2 of Section 9.2.2 for depth; the estimate of corrosion growth for length exceeds the requirements in Section 9.2.2.

The CGAR analysis file [Ref ¶128] calculated the estimated dates features reach a depth of 80% WT, a modified B31G burst pressure less than MOP and the estimated reassessment date [Ref ¶312]. The estimated time to reach 80% of the WT is used as part of the requirements in Sections 6.3 and 6.4. The estimated reassessment date calculated by the CGAR analysis file [Ref ¶128] is consistent with Section 9.2.2 and is 70% of the estimated time for the features to reach a modified B31G burst pressure less than MOP.

Section 9.2.2 states, "External and internal corrosion growth rates are estimated from multiple ILI runs, field observations, and observed historical growth rates." An excerpt of IMP Figure 9-2 is presented in Figure 34, which describes the requirements for estimating corrosion growth rates. For the case when multiple ILI runs that "allow depth comparisons of the same corrosion anomalies" are available, the procedure (see Figure 34) specifies a corrosion growth rate in mils per year using the increase in corrosion depth during the time between ILI runs. It is DNV GL's interpretation that, as presented in Figure 34, the corrosion growth rate calculated using multiple ILI runs is then compared with the rate calculated using the CGAR analysis. The larger of the two values is intended to be used in the remainder of the CGAR analysis.

The 2012 CGAR analysis file [Ref ¶128] provides a column to enter the reported metal loss depths from previous assessments; this column is not referenced by existing equations or embedded macros. On Aug 20, 2015, Plains confirmed¹⁶ that the previous analysis results are not incorporated into the CGAR program calculations; instead the difference in depth is reviewed by the Integrity Specialist while finalizing the repair list. Therefore, the process followed by Plains to incorporate previous ILI results compared differences in reported depths, but did not directly calculate rates in mpy to compare them to the automated CGAR calculations. Evidence was not provided to indicate that the process was in strict adherence with the requirements of IMP Section 9.2.2.

DNV GL performed a comparison of metal loss features reported in the 2007, 2012, and 2015 ILI runs on Joint 5930¹⁷. The distance to the upstream girth weld, orientation, length, and width were compared. A graphical representation of this alignment is shown in Figure 35. Blue and green boxes represent the locations of the metal loss features reported in the 2007 ILI and 2012 ILI, respectively. Black boxes represent the location of metal loss features in the 2015 ILI. The odometer location is presented in terms of the 2015 ILI to provide consistency with the Metallurgical Report [Ref ¶1]. Features identified within the Metallurgical Report [Ref ¶1] in the vicinity are shown as red boxes and the laser-scan measured depths are provided. The ILI-estimated depths of the reported metal loss features that are greater than 20% WT, and were not identified to be under a repair, are also included in the figure. In general, the locations of the ILI-reported metal loss and features found through physical examination correlate well. The 2015 ILI depths are less than the laser-scan measured depths as can be seen in Figure 35 and Figure 36. Figure 36 contains a graphical representation of the reported metal loss depths from the 2007 (blue diamonds), 2012 (green squares) and 2015 (orange triangles) ILI runs in the region near the failure location. The failure location and the area recoated as part of the 2012, "Dig 13," are also shown. The maximum depth of ILI-reported features undersize the depth at the failure location (measured to be 89% WT) for the 2015 ILI data.

Defect characterization (i.e., depth sizing) is affected by the geometry of the anomaly. For the defect that led to the release, the edges were particularly 'sharp' meaning the depth profile changed rapidly from shallow to deep. To evaluate the potential impact of sharpness, DNV GL reviewed "Magnetic Flux Leakage (MFL) Technology for Natural Gas Pipeline Inspection", prepared by J. B. Nestleroth and T. A. Bubenik, Battelle, for The Gas Research Institute, February 1999. This report along with data taken during the same time period show that a sharp defect can produce less flux leakage than a gradual defect.

¹⁶ Teleconference with AZA and Plains on August 20, 2015.

¹⁷ The 2015 failure location.

However, the effect is modest (for the defects studied in the report, the leakage field strength is reduced by up to about 20%). Thus, sharpness could explain some, but not all, of the discrepancy between the defect depth reported by the ILI tool and the actual depth.

Depth sizing by the ILI vendor is influenced by the defect depth and width relative to the pipe wall thickness (deep and/or narrow defects are difficult to size), length-to-width ratio (large length-to-width ratios are difficult to size), proximity to adjacent anomalies (overlapping inspection signals can complicate the analyses), and other parameters (e.g. magnetic nature of corrosion products, magnetization, and tool velocity). In this case, the most significant factor is probably the depth of the flaw relative to the pipe wall thickness, as it is especially difficult to size defects over 70% to 80% of the wall thickness. From an MFL inspection perspective, the defect is not particularly narrow and its length-to-width ratio is modest. In addition, the defect is away from other defects whose signals could have complicated the analysis. Nonetheless, each of these factors could have contributed to the undersizing.

Given the fact that the 2012 ILI reported depth is within 2% WT of the 2015 ILI reported depth (compare 45% to 47%, respectively) and expected corrosion growth rates would not result in growth from ~47% WT to 89% WT in 13 days (the difference from the survey to the failure), it is conceivable that the actual depth in 2012 was much closer to 89% WT. The maximum pressure recorded at Las Flores station is 888 psig on March 26, 2014. The failure opening was measured at 6.6 in. If a feature of this length is assumed to exist on that date, then the depth needed to reach a modified B31G failure pressure equal to 888 psig is above 80% WT, suggesting that the depth of this feature in 2014 could have been up to 80% WT. If a flaw with a length of 12 inches is assumed, then the depth corresponding to a modified B31G failure pressure of 888 psig is 79% WT¹⁸, also suggesting that the depth of this feature could have been close to 80% WT.

Table 5 contains a listing of the metal loss features reported in the 2012 ILI data on Joint 5930, the CGAR estimated growth rate per Equation (1), and the rate estimated by the single anomaly comparison method (see excerpt of IMP Figure 9-2 in Figure 34). For five out of the ten 2012 ILI features, the single anomaly-based rate between the 2007 and 2012 ILI is less than the 2012 CGAR estimated rate. The feature that corresponds to the release location is highlighted in bold in Table 5. The estimated single anomaly-based rate for the feature associated with the 2015 failure is over two times faster (in mils per year) than is estimated by the CGAR process.

¹⁸ 24-in OD, 0.344-in WT, API Grade X65

Table 6 compares the time to reach 80% WT¹⁹ for each feature in Joint 5930 reported by the 2012 ILI. The initial depths in Table 6 from the 2012 ILI were increased by the specified tool tolerance to be consistent with IMP Section 6.3 and the 2012 CGAR analysis file. The minimum time to reach 80% WT for the feature corresponding to the failure and is greater than the three-year re-assessment interval specified for this line as documented in the 2012 Assessment Plan [Ref ¶127]. Based solely on this criterion¹⁹, the feature corresponding to the failure would not have been selected for excavation. Discussions of the other failure criterion, other rate calculations, and initial flaw sizes are given below.

The process followed by Plains to incorporate previous ILI results compared differences in reported depths, but did not directly calculate rates in mpy and compare them to the automated CGAR calculations. There was no evidence provided that their process was in strict adherence with the requirements of IMP Section 9.2.2. The feature corresponding to the release location was estimated to reach 80% WT after the specified reassessment interval using the process followed by Plains. The same conclusion would have been reached had Plains used the single anomaly comparison rate.

6.2.6 Description and Review of 2012 DOT Compliance Report (2012 Final Repair List)

The final repair list is documented in the DOT Compliance Report [Ref ¶124] per the requirements of IMP Section 9.4. The 88 features (70 are metal loss) across 41 dig sites selected for excavation and repair are summarized in Table 7. Table 7 contains the documented selection criteria for the inclusion of the features in the repair list. The documented selection criterion for 21 (30% of 70 targeted metal loss) were based on their depth (greater than or equal to 40% WT) and close proximity (less than or equal to 2.0 feet) to a girth weld. The total number of targeted metal loss features that were within 2.0 feet of a girth weld is 50 (71% of 70 targeted metal loss).

Only one feature in the 2012 ILI met the requirements for Immediate, 60-Day or 180-Day conditions in §195.452(h)(4)(i)-(iii). This feature, a top side dent, was included in the repair list and documented in the DOT Compliance report. The remaining selection criteria are Plains-specific criteria.

¹⁹ The estimated time to reach 80% of the WT is used as part of the requirements in Sections 6.3 and 6.4 to establish the final repair scope and schedule; features that are estimated to grow to 80% WT prior to the “due date” are selected for excavation and repair.

6.2.7 Description and Review of the Validation of ILI Results

Section 6.4 of the IMP, subsection "Validation of ILI Results" requires validation of the ILI results "by various methods, such as, plotting unity graphs and performing statistical analysis."

Fifteen field depth measurements were matched by Plains to 15 of the 2007 ILI-reported depths in a file [Ref #87]. DNV GL performed least squares linear regression on the field-ILI data for the 15 data points, as shown in Figure 37. Figure 37 presents the ILI-reported depth on the x-axis and the field-measured depth on the y-axis. The unity line and 10% WT tolerances are indicated. The upper region of the plot is where the ILI undersized the depths. The slope of the least squares regression equation is 0.1508 ± 0.4044 (95% confidence) and the R^2 value is 0.0475. The 95% confidence interval on the slope includes 0, indicating that there is not enough statistical evidence at 95% confidence to support a relationship between the 2007 ILI-reported depth and the actual field-measured depth.

Plains provided 52 field depth measurements matched to 52 of the 2012 ILI-reported depths in a file [Ref #129].²¹ DNV GL performed least squares linear regression on the field-ILI data for the 52 data points, as shown in Figure 38. The slope of the least squares regression equation is 0.4988 ± 0.3113 (95% confidence) and the R^2 value is 0.1716. The 95% confidence interval on the slope does not include 0, indicating that there is a relationship between the ILI-reported depth and the actual field-measured depth. Figure 38 shows that the distribution of metal loss features more than 2.0 feet from a girth weld and those near a girth weld may be different. Those features near a girth weld exhibit depths both under and over the ILI-reported depths; whereas, those greater than 2.0 feet from a girth weld tend to be undersized by the 2012 ILI (none are over reported). The largest difference between the ILI-reported depth and the field-measured depth, when the ILI under-reports the field depth, is 24% WT. This difference is for a feature that was not within 2.0 feet of a girth weld. Figure 38 suggests that some metal loss features away from the girth weld, like the feature associated with the 2015 failure, were under-reported by the 2012 ILI.

Six field depth measurements were matched by Plains to six of the 2015 ILI-reported depths [Ref #200]. An additional five measurements, obtained using laser scanning, were matched to five 2015 ILI-reported depths in the Metallurgical Failure Report [Table 1 of

²⁰ The R^2 value ranges from 0.0 to 1.0 and measures how close the data are to the fitted regression line. The higher the R^2 value, the better the linear model fits the data.

²¹ [Ref #129] is from 2015; the data are consistent with a unity plot generated by Plains in 2013 [Ref #130].

Ref [1]. Twenty-two field measurements taken in 2013 and under recoat or composite sleeves, in response to the 2012 ILI, were matched to 22 of the 2015 ILI-reported depths by DNV GL by comparing the 2012 and 2015 ILI feature listings. The unity plot of the 33 total field to 2015 ILI correlations is shown in Figure 39.

DNV GL performed least squares linear regression on the field-ILI data for the 33 data points, as shown in Figure 39. The green squares denote the field measurements correlated by comparing the 2012 and 2015 ILI, the purple diamonds are the laser scan measurements and the blue triangles are the measurements reported in the 45 Day CAO report. Features within two feet of a GW are indicated by purple circles. The slope of the least squares regression equation is 0.4815 ± 0.1999 (95% confidence) and the R^2 value is 0.4402. The 95% confidence interval on the slope does not include 0, indicating that there is a relationship between the 2015 ILI-reported depth and the actual field-measured depth. Features matched by comparing the 2012 and 2015 ILI are both over and undersized. The tendency to over or undersize features does appear to be influenced by the measurement technique; features measured in the field are all over called and features measured in a laboratory using laser scanning are undersized.

Comparing the 2012 and 2015 field-ILI unity plots demonstrates that the slope of the least squares regression equation is similar (close to, but below 0.5) for both with the 2015 ILI exhibiting less variability around the regression line (the R^2 value is larger and the 95% interval on the slope has a smaller range). The intercepts are also similar (close to 25). The similarities in the least square regression equations for the 2012 and 2015 unity plots suggest that the mean (expected) field depth for a given ILI-reported depth in either 2012 or 2015 would be similar, but that the 2015 would have a smaller standard deviation around the mean.

Although not a regulatory requirement, API Standard 1163 (API 1163) [Ref [309]] provides guidelines for the qualification of in-line inspection systems used in gas and hazardous liquid in-line inspection system pipelines. In Appendix E of API 1163 the overall number of verification measurements, N , versus the number of verification measurements *within tolerance*, N_{in} , is used to establish consistency with performance specifications. Figure 40 is an excerpt of API 1163 Appendix E containing a table that can be used to establish consistency with performance specifications. Figure 40 was calculated assuming a tool performance specification of depths sized within a given tolerance with 80% certainty and a 95% confidence level.

According to API 1163 (see Figure 40, Ref [309]) there must be at least 37 features within the specified tolerance with a sample size of 52 total features to establish consistency with

the stated performance specification. In Figure 38, 29 measurements are within the tool tolerance used throughout the CGAR analysis (e.g., $\pm 10\%$ WT). Based on API 1163, there is not enough evidence to support that the 2012 ILI met the stated performance specification.

Section 6.4 of the IMP requires validation of the ILI results “by various methods, such as, plotting unity graphs and performing statistical analysis,” but does not directly specify the requirements when the ILI does not meet the performance specifications. The only direct reference in the documents provided to DNV GL relating to discrepancies between the ILI and field measurements is in the process flowchart in Section 6.2 of the IMP (excerpt in Figure 41). The text in this flow chart states that if there are “Large discrepancies between pig calls and actual size of dents, metal loss or crack like anomalies,” then the “Integrity Specialist initiates ILI tool vendor re-grading of raw tool data.” There is no guidance as to what constitutes a large discrepancy. There is no information or documentation indicating that Plains initiated a regrade of either the 2007 or 2012 inspection data.

In order to evaluate the potential for other means to respond when the ILI tool does not meet the performance specifications, DNV GL redefined the assumed tool tolerance using API 1163. The intent was to determine a revised tolerance that would provide a similar confidence as the vendor-stated tolerance that is included in the requirements of IMP Section 6.3. For the 2012 ILI, a redefined tolerance of $\pm 16\%$ WT is needed to be consistent with API 1163 (i.e., 37 of 52 within tolerance per Figure 40). The redefined tolerance is greater than the tolerance used by Plains in the CGAR analysis performed subsequent to the 2012 ILI.

In Section 6.4 of the IMP, the data integration process is used to identify results requiring subsequent actions that “may include regrading the ILI anomaly tally; exploratory digs and repairs beyond those required for §195.452(h)(4)(i, ii & iii); special bellhole inspections (e.g. mag particle testing); and, similar efforts to resolve questions raised by the data integration analysis.” It is DNV GL’s opinion that the excavation results conducted as part of the ILI validation should be included in the data integration process.

6.2.8 Description and Review of Re-Assessment Interval Determination

Plains based the re-assessment interval on the estimated time for the predicted burst pressure of any given feature to be less than MOP, specifically 70% of that time (refer to Section 9.2.2 of the IMP).

In the Assessment Plan from 2012 [Ref #127] dated December 31, 2012, the reassessment interval is specified as three years; the “Change Inspection Interval” section states “Reduce

L901 Las Flores to Gaviota 24", L903 Gaviota to Sisquoc 30", L903 Sisquoc to Pentland 30" and L903 Pentland to Emidio 30" from 5 years to 3 years." The date the decision was made to change the inspection interval and the reason for the change were not included in documents provided to DNV GL.

DNV GL performed calculations, using the CGAR process, to evaluate whether the three year inspection interval was justified for the feature associated with the 2015 failure. Table 8 compares the reassessment interval based on the tolerance and rate scenarios discussed previously. Specifically, the initial flaw size is based on a 10% and a 16% tolerance and the rates are based on either the CGAR methodology or the single anomaly comparison. The time to reach the 80% WT and modified B31G burst pressure (P_{Fail}) is calculated. For all cases, the feature associated with the 2015 failure is predicted to reach 80% WT before $P_{Fail} \leq MOP$. Section 9.2.2 of the IMP defines the reassessment interval as "70% of the predicted time to failure at the normal operating hoop stress of the system." It is unclear from the procedures provided by Plains how to handle these cases as modified B31G is not applicable for depths greater than 80% WT [Ref 315]. For the calculations in Table 8, DNV GL has assumed that the reassessment interval is taken as 70% of the time to reach either 80% WT or $P_{Fail} \leq MOP$. Based on the CGAR process, the estimated reassessment interval using a $\pm 10\%$ and $\pm 16\%$ tool tolerance are 7.3 and 5.5 years, respectively. Based on feature to feature matching, the estimated reassessment interval using a $\pm 10\%$ and $\pm 16\%$ tool tolerance are 3.4 and 2.5 years, respectively. While the most conservative reassessment interval of 2.5 years is less than the three year reassessment interval specified by Plains; the actual reassessment interval was 2.8 years²² and is similar when accounting for operational and logistical requirements for ILI.

DNV GL applied the 2012 CGAR process using a 16% tool tolerance to all remaining unrepaired features from the 2012 ILI. The minimum predicted failure pressure for unrepaired features using the 2012 CGAR process after five years is 1452 psig, which is greater than the MOP used by Plains. If the 70% time frame per Section 9.2.2 is applied, then all features should have a predicted failure pressure above the MOP for at least 4.2 years to justify a three year assessment interval²³. In addition, the minimum time to reach 80% WT for unrepaired features is 6.01 years (70% is 4.3 years). Therefore, the CGAR process as applied by Plains to the 2012 ILI supports a three year assessment interval.

If a 16% "tolerance" is incorporated²⁴ instead of the 10% used in 2012, then the minimum predicted failure pressure for unrepaired features using the procedure in the 2012 CGAR

²² Using a survey date of July 3, 2012 and May 6, 2015

²³ Three years is approximately 70% of 4.2 years (i.e., $3.0 / 0.7 = 4.2$)

²⁴ This is the "redefined tolerance" needed to meet the requirements in API 1163, see Section 6.2.7

analysis file after five years is 1352 psig, which is also greater than the MOP used by Plains. The minimum time to reach 80% WT for unrepaired features is 3.9 years for a reported feature from the 2012 ILI²⁵ (this corresponds to a 2.7 year inspection interval). The CGAR process using the larger tolerance resulted in a re-inspection that is of the same order that Plains used to initiate the 2015 ILI run. Thus, reevaluating the 2012 ILI data in this manner may not have prevented the failure.

Multiple methods exist to compare ILI data and estimate corrosion growth rates. DNV GL performed an additional analysis comparing the 2007 and 2012 ILI data that is neither required in Plains' IMP nor in the CFR. The analysis is termed statistically active corrosion (SAC). DNV GL developed the SAC methodology with the objective to identify pipeline locations for which ILI data indicates a likelihood of corrosion growth and predict corrosion rates. For selected joints with the potential for significant growth, a manual review of the ILI signal data was performed to determine whether the likely growth is evident in the ILI signal or a result of ILI sensitivity differences. Based on the results of the corrosion growth screening and probabilistic assessment, DNV GL manually reviewed 169 pipe joints and identified evidence of growth in 82 (49% of the total reviewed). As a result of the statistical analysis and manual review, DNV GL determined that the joint that failed in 2015 (Joint 5930) showed evidence of significant change in the signal data and is predicted to have a SAC growth rate (15 mpy), which is between the rate used in the CGAR process (8 mpy) and the rate obtained via pit-to-pit matching (18 mpy). With the SAC rate, the feature that led to the 2015 failure is estimated to reach 80% WT in 5.8 years (70% of that time is 4.0 years). Appendix F contains a description of the SAC methodology as well as the compiled summaries of the manual signal review and estimated rates.

One of the minimum P&M measures that must be considered within the Preventive and Mitigative Evaluation Meeting is the potential for establishing shorter inspection intervals (see IMP Section 11.4 [Ref ¶23]). While the assessment interval was shortened from five to three years [Ref ¶127] prior to December 31, 2012, there is no documentation (e.g., Form F11-2) provided to DNV GL specifying the assumptions or calculations that were used to justify the three-year assessment interval.

No information was provided documenting a Preventive and Mitigative Evaluation Meeting within the 15 month window of the receipt of the final report required in Section 11.3 "Forming Division Preventive and Mitigative Evaluation Teams." On May 21, 2015 (after the 2015 failure) Form F11-2 [Ref ¶131] was completed. This form references the 2012 ILI data (not the 2015 ILI) and:

²⁵ A 53% WT, 0.75-in metal loss feature on Joint 14470 (odometer 51640.14).

- States that the current inspection interval is three years (Part A-1: Review of Design, Operation and Risk Data)
- References the release on 5/19/2015 (Part A-3: Leaks from Segment or Facility)
- Recommends a reduction in the reassessment interval from three to two years to “ensure the control of growth of external corrosion under shrink sleeves” (Part B).

6.2.9 Continual Evaluation and Assessment of Pipeline Integrity

Documents pertaining to the periodic evaluation process required in Section 9.5, specifically Form F9-1, were requested but were not provided to DNV GL. On September 11, 2015 Plains stated²⁶ that Form F11-2 is similar to Form F9-1 and is therefore used in the place of Form F9-1.

There is no documentation provided to DNV GL that a periodic evaluation process meeting took place prior to the 2015 release, as it pertains to the 2012 ILI data. Plains has not demonstrated that the requirements in Section 9.5 have been met.

7.0 SUMMARY AND CONCLUSIONS

The results of the metallurgical analysis indicated that the immediate metallurgical cause for the Line 901 failure was wall thinning from external corrosion that ultimately failed by ductile overload under the imposed operating pressure [Ref ¶1]. The flaw that failed was not through wall prior to ductile overload and, therefore, the failure event was sudden in nature. The morphology of the external corrosion was determined to be consistent with corrosion under insulation (CUI), facilitated by wet-dry cycling.

The results of the root cause analysis presented below are based on the provided documentation referenced in Appendix B. DNV GL reserves the right to modify or supplement these conclusions should new information become available. DNV GL identified four c basic root causes of the failure:

1. The external coating system failed to prevent moisture from reaching the pipe steel, allowing the external corrosion process to occur.

Basis:

Based on the metallurgical analysis, the protective coal tar urethane coating, thermal polyurethane foam insulation, and polyethylene tape were compromised at the failure location. The damage included wrinkles, cracks, staining, and decohesion of

the polyethylene tape; staining, water saturation and retention, and compression of the polyurethane foam; and disbondment of the coal tar urethane.

2. The cathodic protection system was ineffective due to shielding by the thermal polyurethane insulation and external polyethylene wrap.

Basis:

Based on the provided documentation, Plains met the regulatory requirements for monitoring the cathodic protection (CP) system on Line 901, and the measured pipe to soil potential values met the required levels for protection. However, the presence of the polyurethane insulation and the polyethylene wrap shielded the cathodic protection current and prevented voltage monitoring of the shielded portions of the pipe. As a result, the CP current did not reach the pipe surface and the measured potentials did not represent the potentials at the areas of corrosion under the insulation.

3. The contracted in-line inspection significantly undersized the external corrosion feature that failed on Line 901.

Basis:

Based on the provided documentation, the 2015 MFL tool significantly undersized the external corrosion feature that ultimately leaked (i.e. a tool determined depth of 47% of the nominal wall thickness vs. a laboratory measured depth of 89% of the nominal wall thickness). The MFL tool likely also undersized the same feature in the 2012 ILI run based on a review and comparison of the 2007, 2012, and 2015 raw signal data for the feature that failed.

4. The mitigative actions taken by Plains on Line 901 did not adequately address the elevated integrity threat of corrosion under insulation.

Basis:

The results of the metallurgical analysis indicated that the immediate metallurgical cause of the failure was CUI. Corrosion under insulation is a unique corrosion mechanism that necessitates its own integrity risk assessment. Plains did not apply sufficient mitigative strategies specific to CUI to prevent this anomaly from failing. The measures could include enhancement of existing barriers and additional preventative barriers.

Additional observations for improvement in the Integrity Management Program

The following provides perspective on Plains' integrity management plan (IMP) as related to the failure on Line 901. Coating systems, as a barrier to external corrosion related integrity threats, (i) are never perfect and (ii) age over time, thereby decreasing the effectiveness of the barrier. The cathodic protection (CP) system is another barrier to external corrosion integrity threats. Cathodic protection can be effective for many external corrosion related integrity threats; e.g., corrosion at holidays (holes in the coating) and microbiological influenced corrosion (MIC).

There are limits to the effectiveness of CP for corrosion related integrity threats and mitigation barriers can be strengthened and/or other mitigation barriers can be employed in conjunction with CP; e.g., stray current enhanced corrosion, AC induced corrosion, stress corrosion cracking, and corrosion beneath disbanded coatings that shield CP current. For these, multiple barriers may be used depending on the individual integrity threat, but the ILI program in conjunction with a dig program becomes a more important barrier since it is known that the other barriers of coating and CP are not always effective.

In the case of Line 901, Plains targeted 70 metal loss features in 2012, which included 31 features beyond those required by code and used for validation of the ILI program. These additional digs constitute a strengthened barrier in the prevention of a pipe failure due to a corrosion related integrity threat. Several of the digs were based on the strengthening of the ILI/dig barrier for the purpose of identifying and repairing corrosion under shrink sleeves used at girth welds; a known corrosion related integrity threat involving coatings that shield CP. In addition, the ILI re-inspection interval was decreased from a minimum of 5 years to 3 years (performed at 2.8 years). This also is a strengthening of a barrier in the prevention of a pipe failure due to a corrosion related integrity threat.

Plains IMP aggressively addressed several of the corrosion related integrity threats; but, as mentioned under contributing causes, Plains did not apply sufficient mitigative strategies to prevent the CUI anomaly from failing. In addition, an IMP is only as good as the data that are utilized to monitor and measure its performance. As addressed as a contributing cause, the ILI significantly undersized (47% versus an actual value of 89% through wall) the feature that eventually failed.

The RCA identified improvements that could be made within the integrity management program, which were not direct causes of the failure. These observations are given below.

1. Based on the information provided, Plains could adopt additional practices to identify and address any inaccuracies in future ILI runs.

Basis:

DNV GL performed an analysis of the 2012 ILI and dig data using API 1163, which is not a regulatory requirement or part of the IMP, and determined that the tool performance was not within the stated specifications. There was no produced documentation to indicate that Plains communicated with the ILI vendor, such as requesting a re-grade, following production of the unity plot[s] to account for the scatter observed within the data. However, using the recalculated tool tolerance would still result in a similar re-inspection interval as that used by Plains for the 2015 ILI run.

2. Based on the provided information, Plains could better incorporate the results from multiple ILI runs into their corrosion growth rate calculations.

Basis:

Plains IMP Section 9.2.2 states, "External and internal corrosion growth rates are estimated from multiple ILI runs, field observations, and observed historical growth rates." The procedure specifies calculation of a corrosion growth rate in mils per year using the increase in corrosion depth during the time between consecutive ILI runs. There is no documentation provided to indicate that Plains performed such calculations using the historical ILI data.

DNV GL calculated a corrosion growth rate for the feature that failed based on data from the 2007 and 2012 ILI runs. Although a higher corrosion rate was calculated than that determined using the CGAR process, this rate results in a similar re-inspection interval to that performed by Plains.

Additional analyses that go beyond the IMP, codes, and standards, include:

- Statistically active corrosion (SAC) analysis performed on Line 901 resulted in a similar re-inspection interval as that used by Plains (2.8 years) for the 2015 ILI run. The analysis identified a remaining life for the feature that failed that is greater than the re-inspection interval used by Plains.

3. Based on the provided information, Plains should improve their documentation and/or record-keeping of their decision-making processes related to actions taken.

Basis:

Over the course of the investigation, DNV GL identified areas within the integrity management process that were not sufficiently documented. For example, no justification (i.e. assumptions, analyses, etc.) was provided for determining the reassessment interval of 3 years based on the 2012 ILI data.

Although a form explicitly identifying the justification for the reduction of their re-inspection interval from 5 years to 3 years was not provided, DNV GL's assessments and calculations resulted in a similar re-inspection interval as that used by Plains.

Table 1. Summary of inspection data from aerial patrols of Line Segment 901 between January 7, 2015 and May 11, 2015.

Patrol Date	Inspection Data
7-Jan-15	Segment OK
16-Jan-15	UF due to Weather ¹
21-Jan-15	Segment OK
28-Jan-15	Segment OK
4-Feb-15	Segment OK
9-Feb-15	Segment OK
19-Feb-15	Segment OK
25-Feb-15	Segment OK
3-Mar-15	Segment OK
13-Mar-15	Segment OK
25-Mar-15	Segment OK
1-Apr-15	UF due to Weather ¹
6-Apr-15	Segment OK
17-Apr-15	UF due to Weather ¹
20-Apr-15	Segment OK
29-Apr-15	Segment OK
4-May-15	Segment OK
11-May-15	Segment OK

1 – UF: Unable to fly.

Table 2. Assessments on potential external corrosion mechanisms for the failure.

Corrosion Mechanism	Relevant to Line 901 Failure	Assessment
AC Stray Current Corrosion	No	AC field measurements were negligible and there was no HVAC lines in the ROW.
DC Stray Current Corrosion	No	The corrosion was not characterized by sharp edged pitting and the absence of corrosion products around the pitted area (i.e. which is typical of DC stray current corrosion.) Also there were no foreign line crossings or parallel lines located in the ROW.
Galvanic Corrosion	No	The corrosion was not associated with the coupling of two dissimilar materials. The corrosion features were found across the length of the line and were not isolated/concentrated to areas of previous armor plate repairs.
Microbiologically Influenced Corrosion	May have contributed to corrosion, but not cause	Bacteria were identified at a corrosion feature sampled U/S of the failure location; however they were not preferentially flourishing within the corroded areas. Furthermore, the levels of bacteria were low and the layered morphology within the corrosion products is not consistent with MIC.
Corrosion Under Insulation	Yes	Based on the morphology (general corrosion mixed with pits) and location (beneath damaged coating combined with wet, thermal insulation) of the corrosion associated with the failure, the corrosion is due to CUI.

Table 3. Historical moisture conditions, based on 2007 and 2012 ILI dig information, for pipe joints near the 2015 failure location.

Pipe Joint	Dig Data					Average Monthly Precipitation (inches) ²
	ILI Year	Dig Number ¹	Dig Date	Soil Condition ¹	Soil Description ¹	
5910	2012	Dig 12	5/9/13	Dry	Clay, Sand, Rock	0.31
5920	2007	Dig 5	3/3/09	Moist	Loam	2.91
	2012	Dig 12	5/9/13	Dry	Clay, Sand, Rock	0.31
5930 ³	2012	Dig 13	5/10/13	Dry	Clay, Sand, Rock	0.31
5940	2012	Dig 1	5/10/13	Dry	Clay, Sand, Rock	0.31
5950	2007	Dig 6	2/21/08	Moist	Loam	4.57

1 – [Ref 50 & Ref 91]

2 – [Ref 314]

3 - Pipe Joint 5930 contained the May 19, 2015 failure location.

Table 4. Timeline of external corrosion control monitoring and inspection data.

#	Event	Year	Month	Date		Comments
				Start	End	
1	Year Pipe in Service	1990				
2	Year CP was commissioned					Information not received
3	Earliest Annual Test Point Data provided	2005	January			
4	1st ILI Metal Loss Run	2007	June	1	–	Report date: August 15, 2007
5	1st CIS	2008	December	5	8	
6	2nd ILI Metal Loss Run	2012	July	3	–	Report date: September 26, 2012
7	2nd CIS	2015	April	8	9	
8	3rd ILI Metal Loss	2015	May	6	–	Report date: June 4, 2012
9	Failure	2015	May	19	–	

Table 5. Comparison of Rate Estimation Methods between 2007 and 2012 ILI.

2007 ILI		2012 ILI		Rate	
Odometer (ft)	Maximum Depth (% WT)	Odometer (ft)	Maximum Depth (% WT)	CGAR † (mpy)	Single Anomaly Comparison ‡ (mpy)
		21367.68	12	2.20	1.38
		21370.50	14	2.57	2.75
21341.79	11	21371.23	13	2.39	1.38
21353.03	23	21382.40	24	4.40	0.69
		21384.36	38	6.97	19.26
		21384.48	11	2.02	0.69
		21384.80	21	3.85	7.57
21355.45	19	21384.96	45	8.26	17.89
		21385.38	13	2.39	2.06
21360.90	26	21390.33	41	7.52	10.32

† Assumes a construction year of 1987, run year of 2012, 0.344-in WT

‡ Assumes five years between inspections, no tolerance added to either 2007 or 2012 reported depths, 0.344-inch WT and a 2007 feature depth of 10% WT for 2012 features without a match in 2007.

Table 6. Comparison of estimated time to reach 80% WT for features on Joint 5930.

2012 ILI		Initial Flaw †	Rate ‡ (mpy)		Time to Reach 80% WT (yrs)	
Odometer (ft)	Maximum Depth (% WT)		CGAR	Single Anomaly Comparison	CGAR	Single Anomaly Comparison
21367.68	12	22	2.20	1.38	90.63	145.00
21370.5	14	24	2.57	2.75	75.00	70.00
21371.23	13	23	2.39	1.38	82.21	142.50
21382.4	24	34	4.40	0.69	35.94	230.00
21384.36	38	48	6.97	19.26	15.79	5.71
21384.48	11	21	2.02	0.69	100.57	295.00
21384.8	21	31	3.85	7.57	43.75	22.27
21384.96	45	55	8.26	17.89	10.42	4.81
21385.38	13	23	2.39	2.06	82.21	95.00
21390.33	41	51	7.52	10.32	13.26	9.67

† The reported ILI depths are increased by a tool tolerance per Section 6.3 of the IMP

‡ Refer to Table 5 for rate estimates

Table 7. Summary of features selected for excavation following the 2012 ILI.

DOT Compliance Report Selection Criteria	Targeted Features		
	> 2 feet from a girth weld	≤ 2 feet from a girth weld	Total
180 Day : Dent >2% on TOP ¹	1	-	1
Calc Growth ≥ 80% : High Priority	-	2	2
Calc Growth ≥ 80%	1	7	8
Additional : ≤ 2 ft from GW & ≥ 40% ML	-	21	21
Additional : GMA near GW ¹	-	2	2
Additional : ML Validation – Freq. in Joint	18	-	18
Additional : ML Validation	1	14	15
Additional : ML Validation : Not Previously Reported	-	6	6
Additional: Noted as Possible Wrinkle ¹	15	-	15
Total Metal Loss	20	50	70
Total	36	52	88

1 – Geometric features.

Table 8. Comparison of re-assessment intervals for the feature associated with the 2015 Failure.

Case ID	Initial Flaw Size ¹	Method for Rate Calculation ²	Time to Criteria ³		Assessment Interval ⁴
			≥ 80% WT	P _{Fail} ≤ MOP	P _{Fail} ≤ MOP
Case 1	2012 ILI + 10%	CGAR	10.4	10.4	7.28
Case 2	2012 ILI + 10%	Single Anomaly Match	4.8	4.8	3.36
Case 3	2012 ILI + 16%	CGAR	7.9	7.9	5.53
Case 4	2012 ILI + 16%	Single Anomaly Match	3.6	3.6	2.52

1 10% is tool tolerance used by Plains during the 2012 CGAR process; 16% is the "redefined tolerance" based on API 1163.

2 CGAR uses Equation (1); Single Anomaly Match rate is based on pit-to-pit matching.

3 The estimated time to reach indicated criteria. The feature is predicted to reach 80% WT in depth before P_{Fail} drops below MOP.

4 IMP Section 9.2.2 defines the reassessment interval as "70% of the predicted time to failure at the normal operating hoop stress of the system." Given that the feature is predicted to reach 80% WT before P_{Fail} ≤ MOP, the reassessment interval is taken as 70% time to reach 80% WT.



(a) View parallel to pipeline showing slope of hill near failure location



a) View perpendicular to pipeline showing slope of hill near failure location

Figure 1. Photographs showing the topography in the vicinity of the failure location.

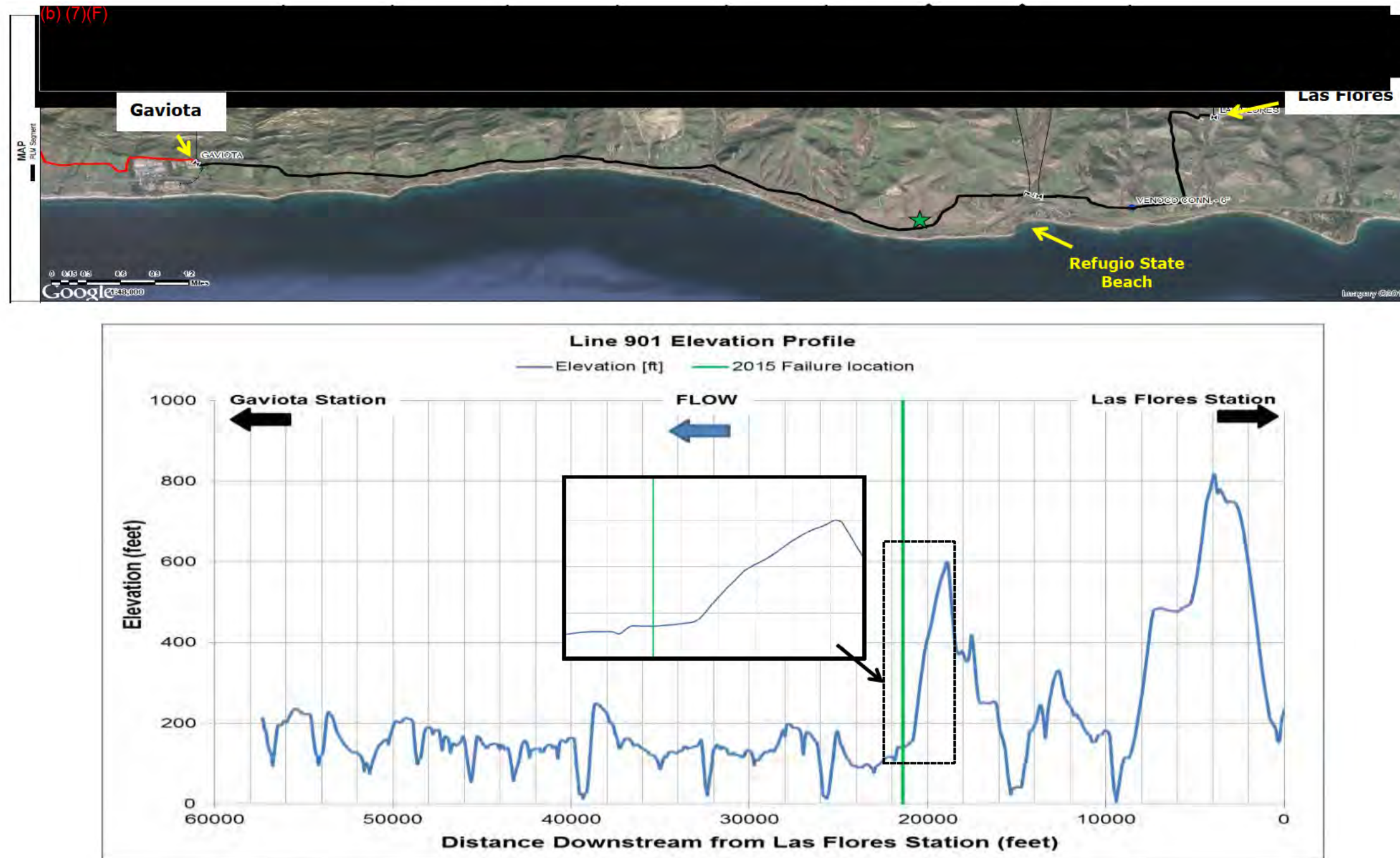


Figure 2. Topographical map and plot showing the elevation profile for Line 901. The white triangles on the map correspond to mile post markers. The green star on the map and the green line on the plot identify the location of the May 19, 2015 failure.



(a) First culvert through which product flowed.

(b) Second culvert through which product flowed.

Figure 3. Photographs showing two of the culverts through which released product flowed.

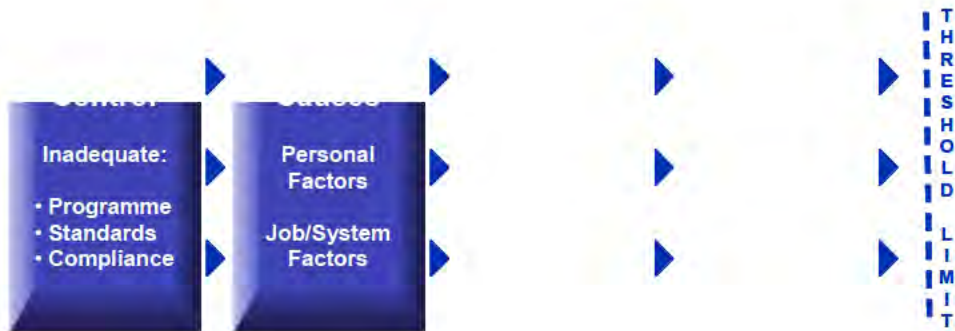


Figure 4 Schematic showing the Loss Causation Model.

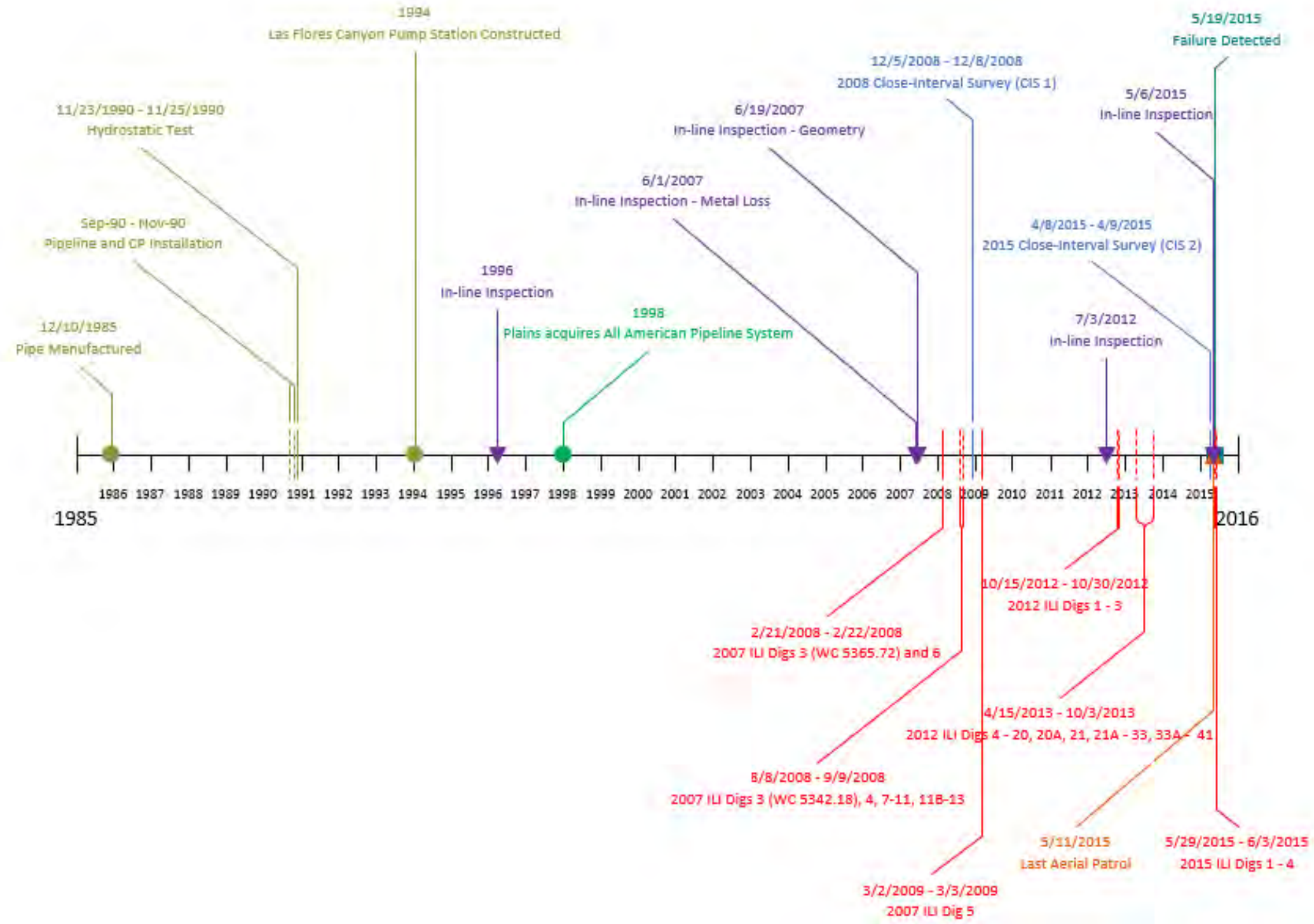


Figure 5. Timeline showing key events for Line 901 from the time of construction to the day of the incident (May 19, 2015).

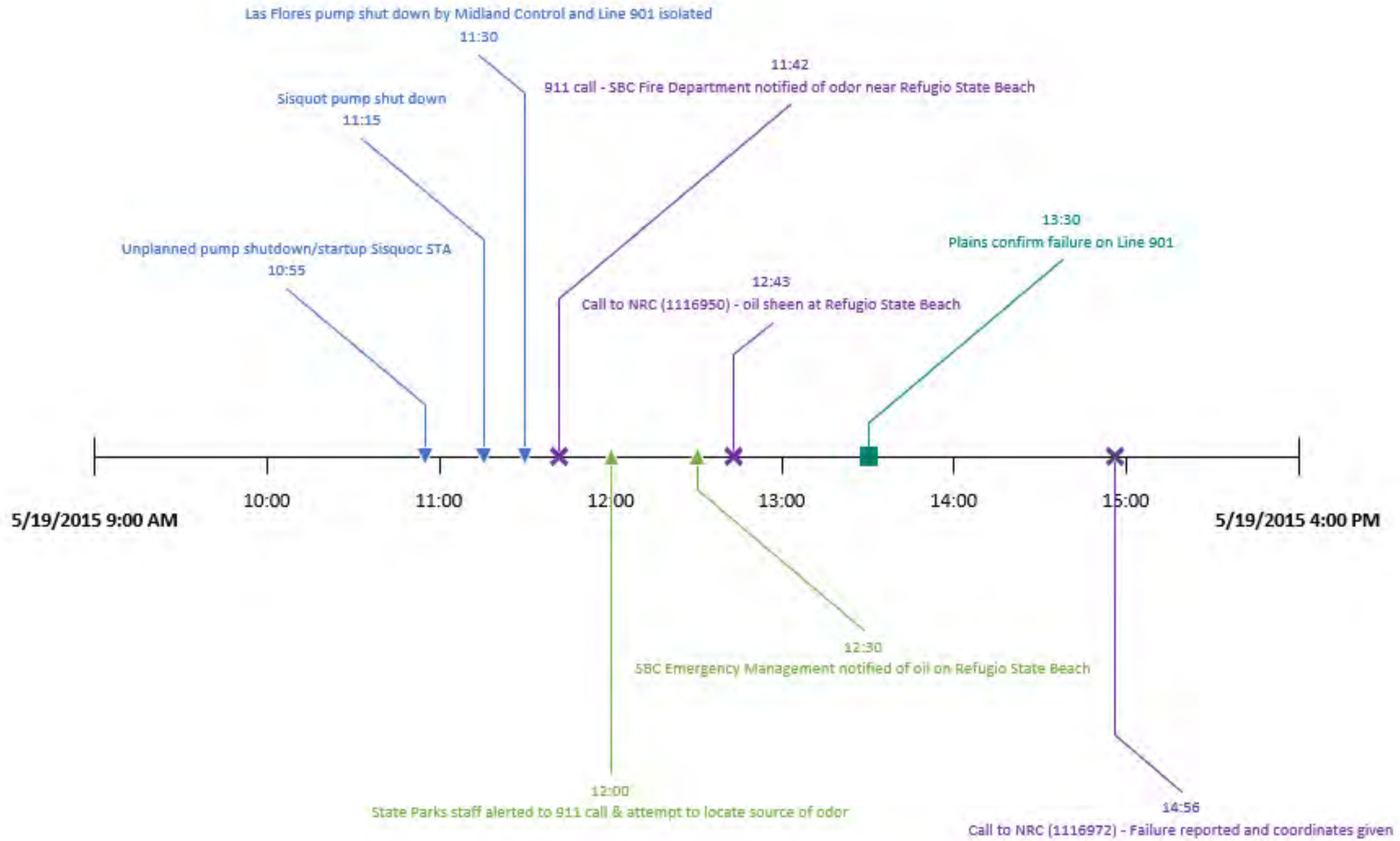


Figure 6. Timeline showing key events for Line 901 on the day of the incident (May 19, 2015).

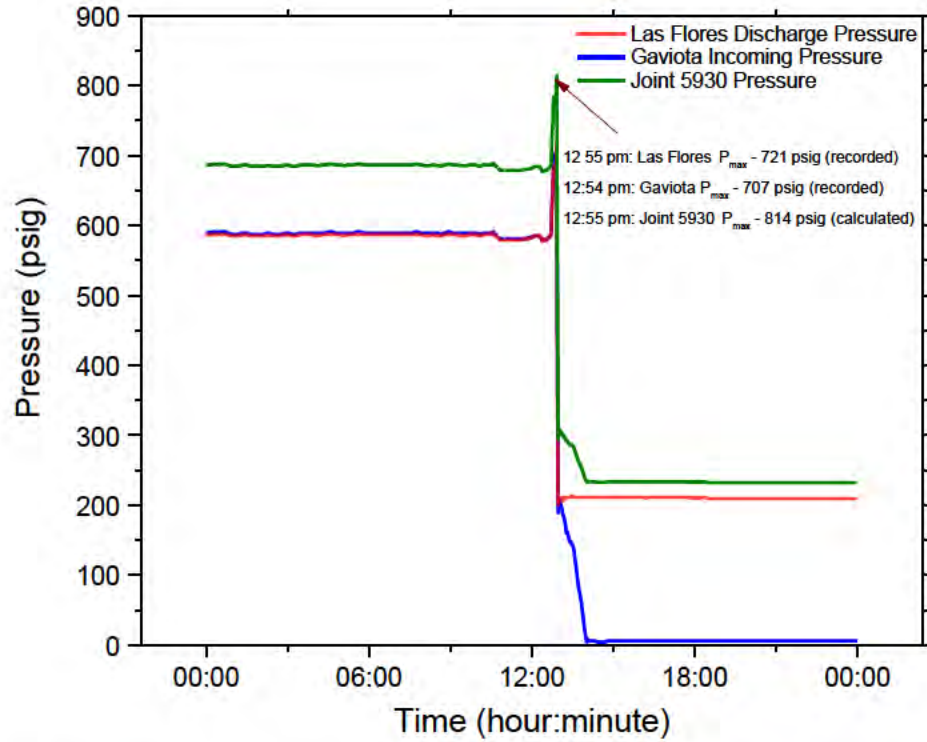


Figure 7. Plot of pressure versus time showing the discharge pressure for Las Flores (red), the incoming pressure for Gaviota (blue), and the calculated pressure for Joint 5930 (green) on May 19, 2015 [Ref 227].

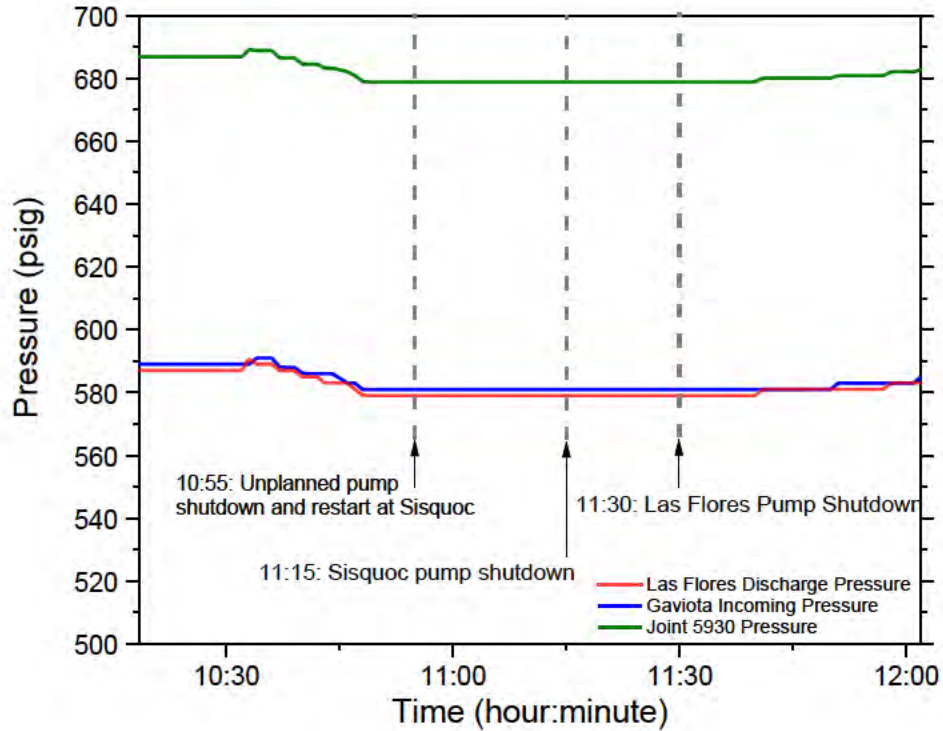


Figure 8. Plot of pressure versus time showing the discharge pressure for Las Flores (red), the incoming pressure for Gaviota (blue), and the calculated pressure for Joint 5930 (green) on May 19, 2015 between 10:00 am and 12:00 pm [Ref 227].



Figure 9. Schematic showing Line 901 from Las Flores to Gaviota showing the approximate location of the pipeline and the elevation profile of the pipeline. The red arrows indicate the locations of flow meters [Ref 248].



Figure 10. Schematic showing Line 903 from Gaviota to Sisquoc the approximate location of the pipeline and the elevation profile of the pipeline. The red arrows indicate the locations of flow meters [Ref 249].



Figure 11. Schematic showing Line 903 from Sisquoc to Station Number 1595 + 16 the approximate location of the pipeline and the elevation profile of the pipeline. The red arrows indicate the locations of flow meters [Ref 250].

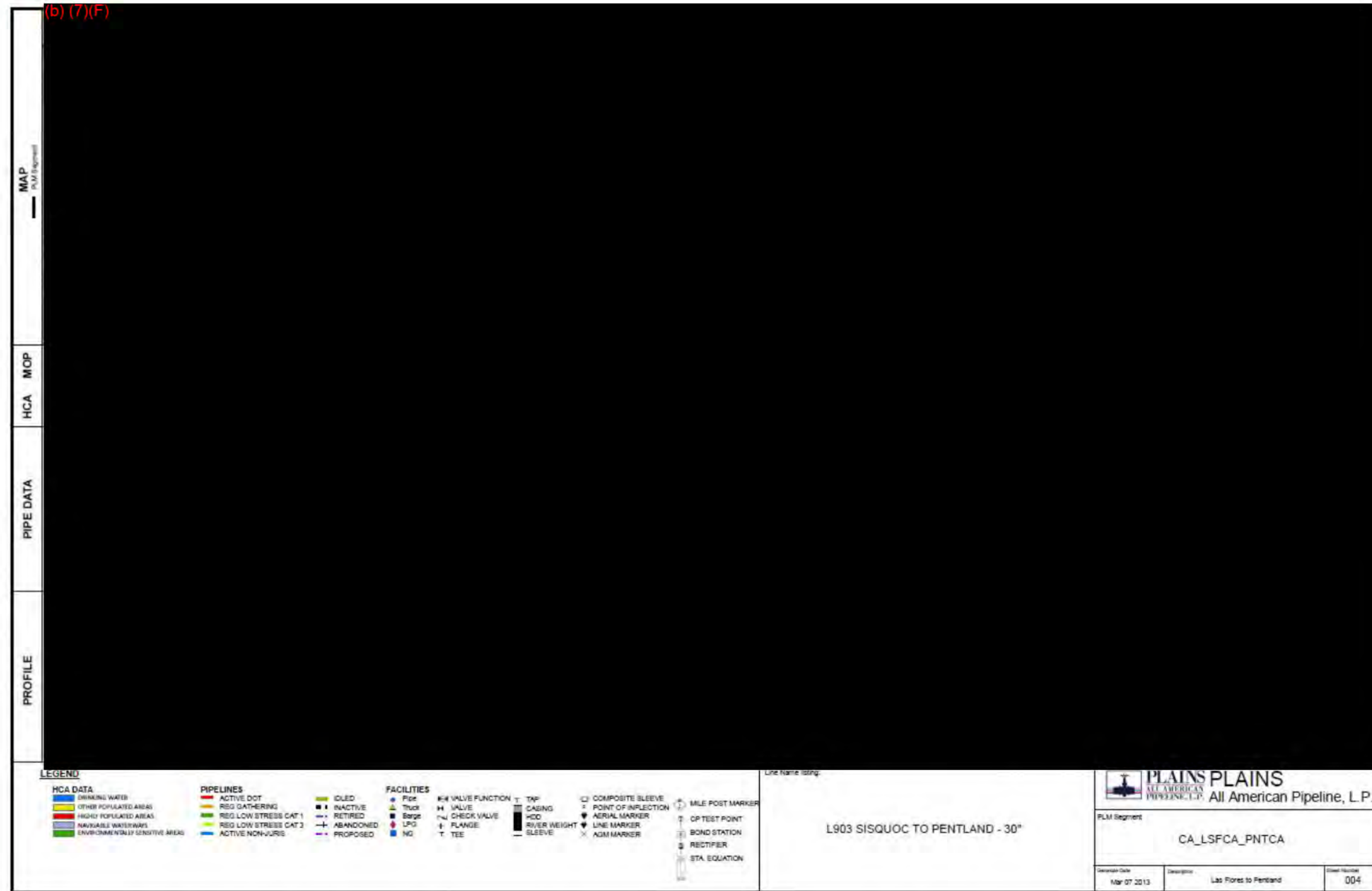


Figure 12. Schematic showing Line 903 from Station Number 1595 + 16 to Pentland the approximate location of the pipeline and the elevation profile of the pipeline. The red arrows indicate locations of flow meters [Ref 251].



Figure 13. Plot showing volume versus time data for the Las Flores to Pentland line segment between May 18, 2015 at 5:00am and May 20, 2015 at 12:00am.

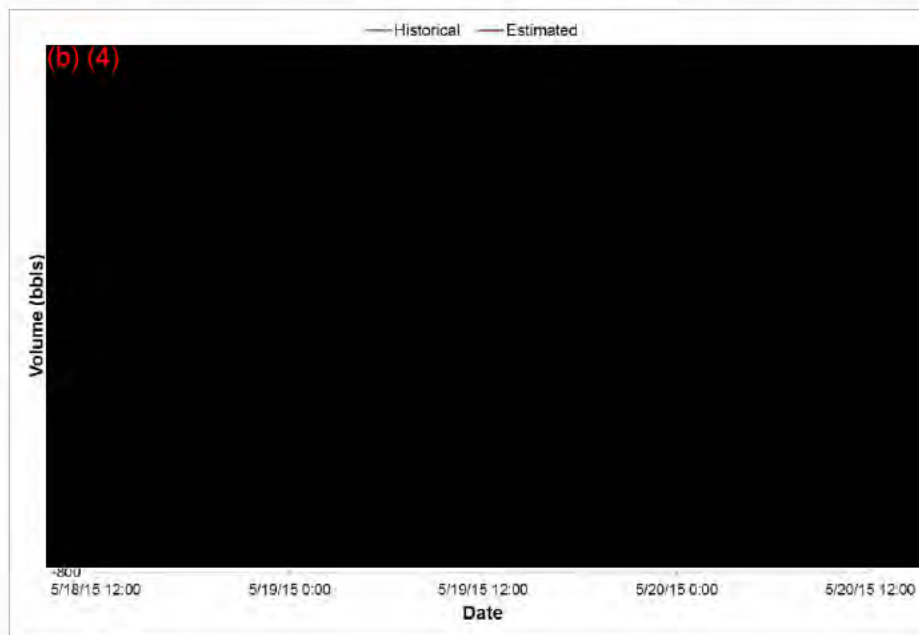


Figure 14. Plot showing volume versus time data for the Las Flores to Pentland line segment between May 19, 2015 at 1:00am and May 20, 2015 at 12:00am.

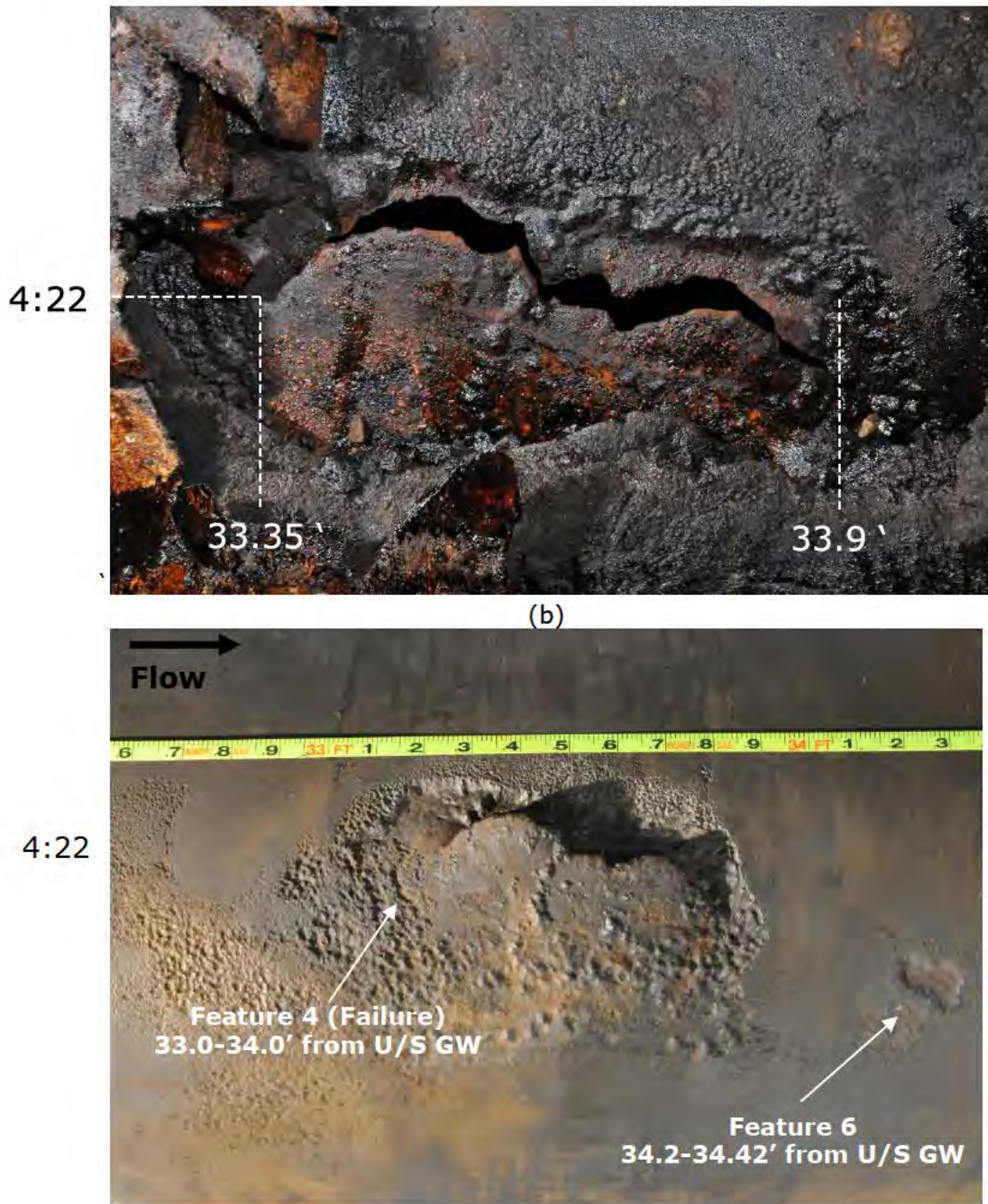


Figure 15. Photograph showing the failure location before (Top) and after (Bottom) cleaning. Tape measure indicates distance to U/S GW (Note: tape slipped 0.1' to the right).

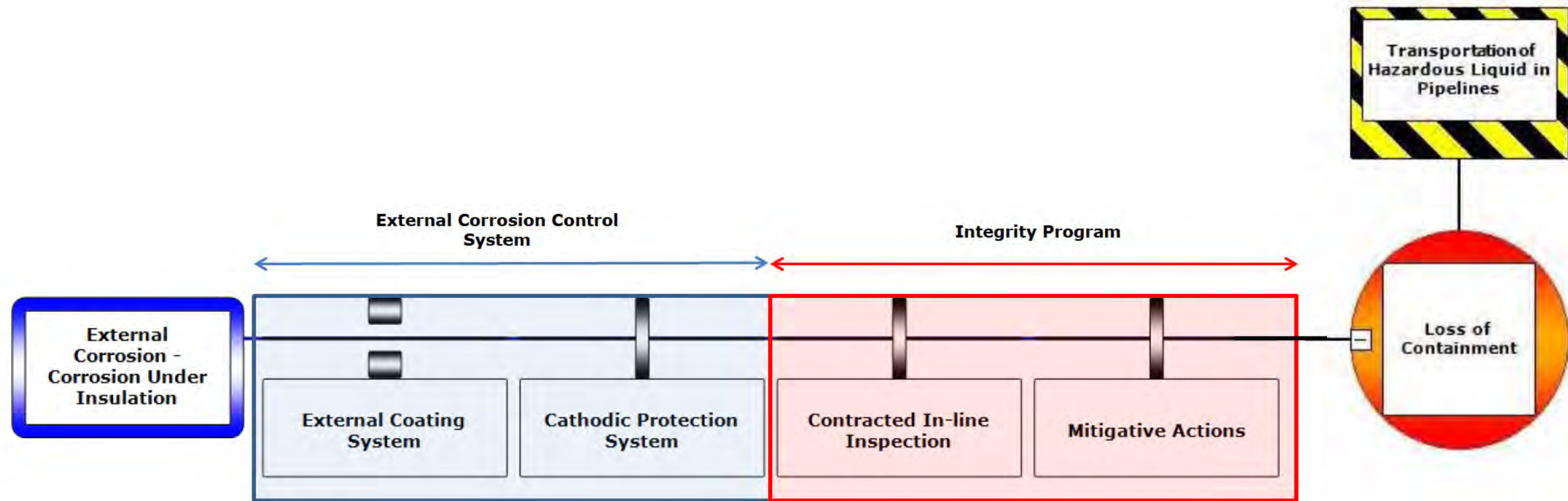


Figure 16. BowTie diagram, generated using the BSCA T™ methodology, summarizing the preventative barriers in place for the Line 901 Release. The barriers shown as two rectangles on either side of the horizontal line correspond to failed barriers, while the thin rectangles that span the horizontal line correspond to ineffective barriers.



Figure 17. Schematic and photograph showing the protective external coating and the PU foam and PE tape layers present on the Line 901 pipeline.

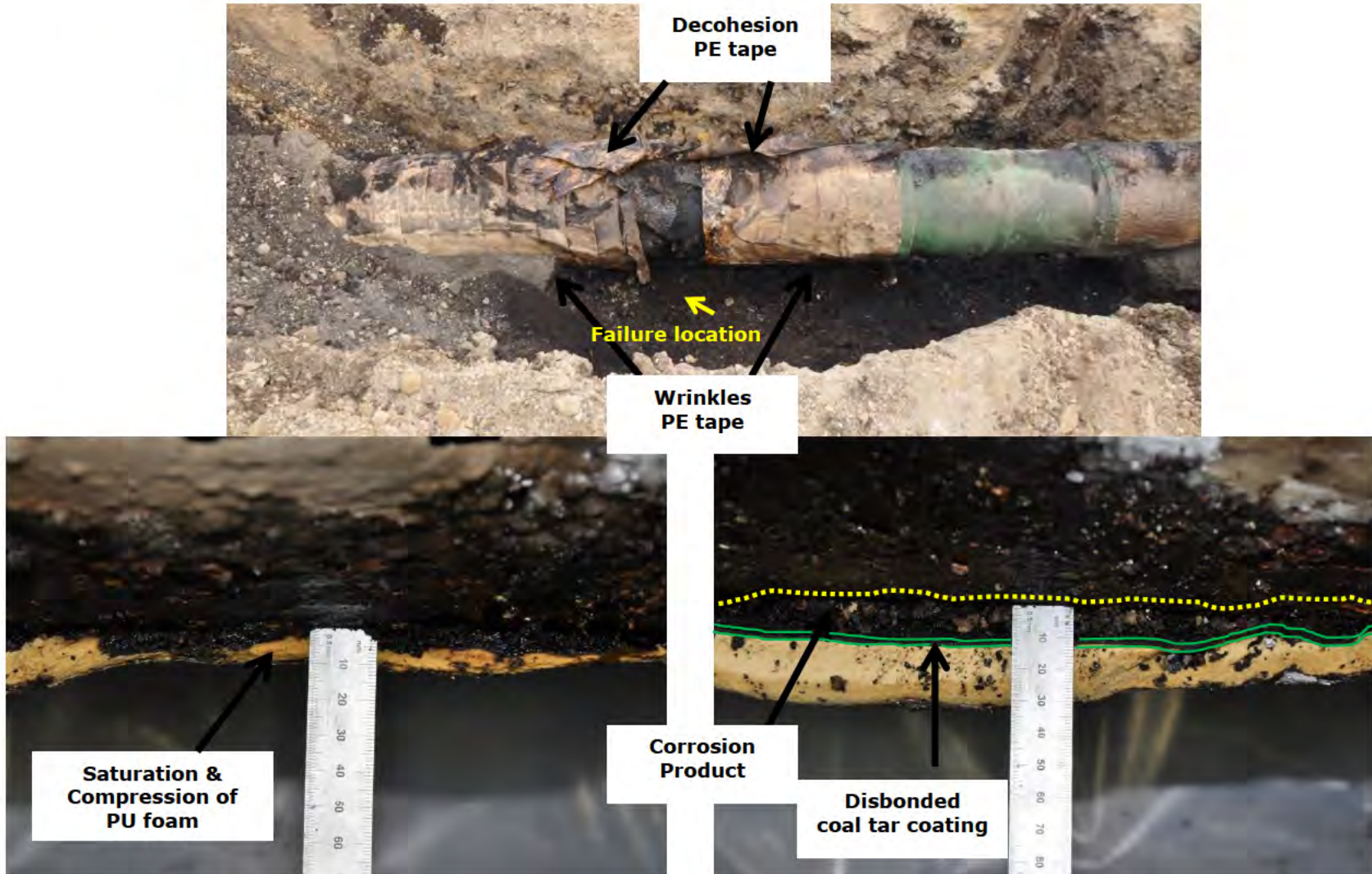


Figure 18. Photographs showing compromised protective coating and PU foam/PE tape layers at the failure location.



Figure 19. Photograph of wrinkles in the PE tape, located away from the failure location.

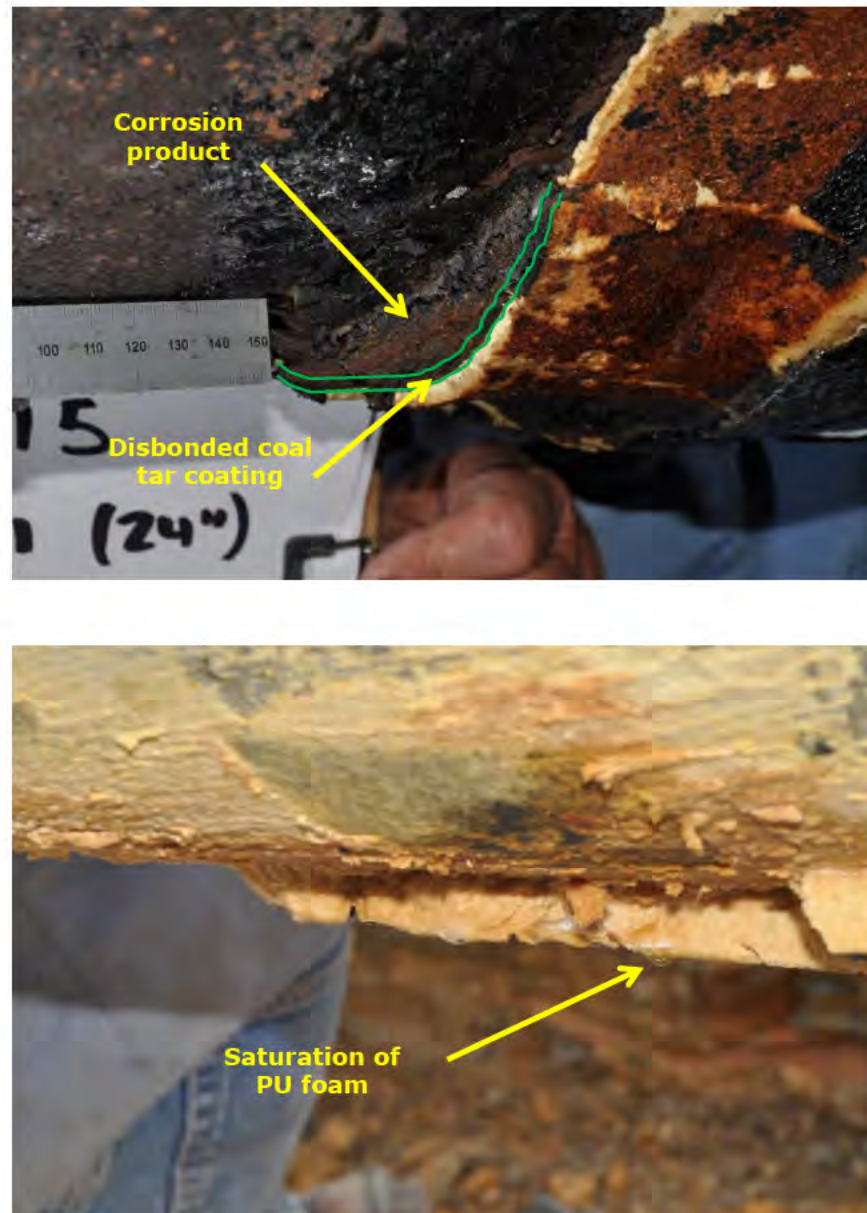


Figure 20. Photographs showing compromised coating and PU foam away from the failure location.

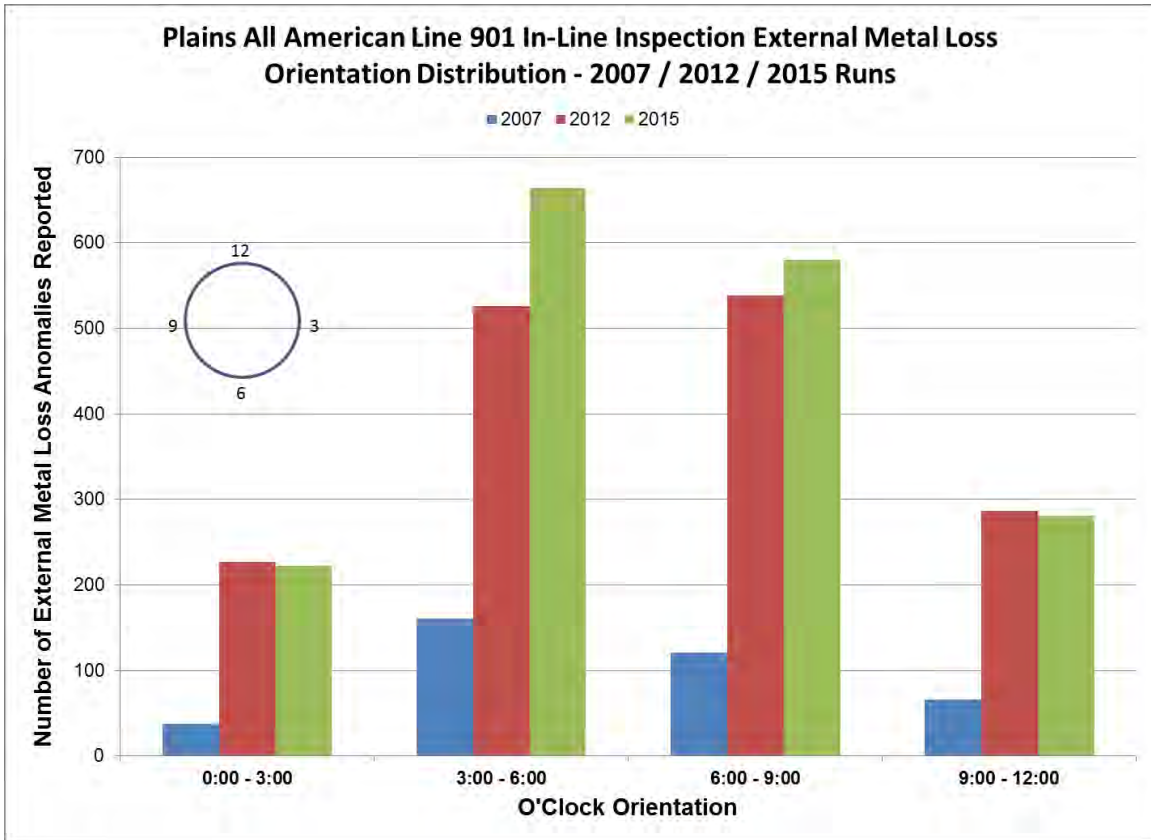
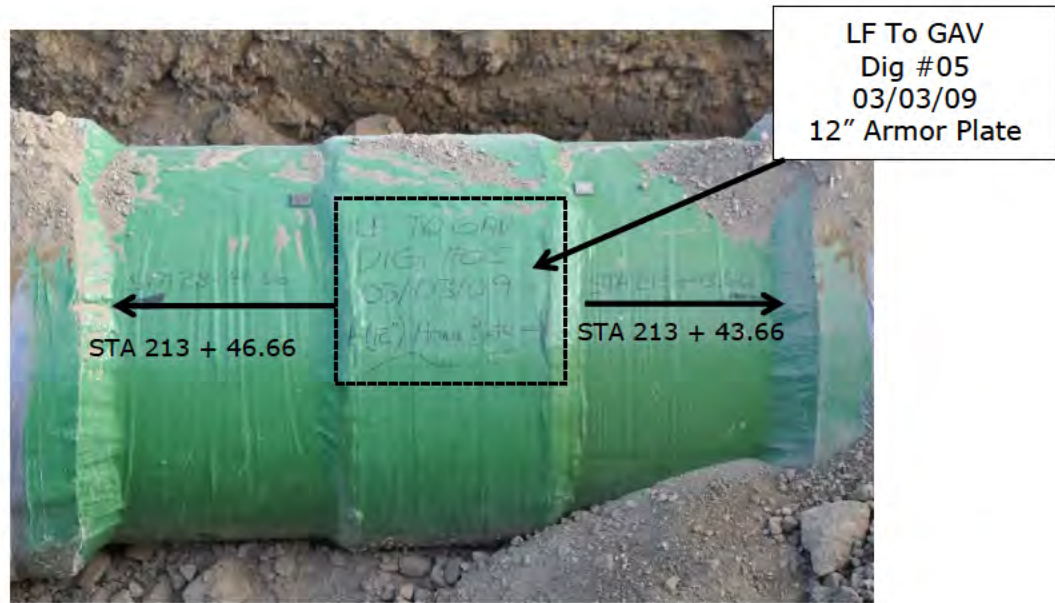
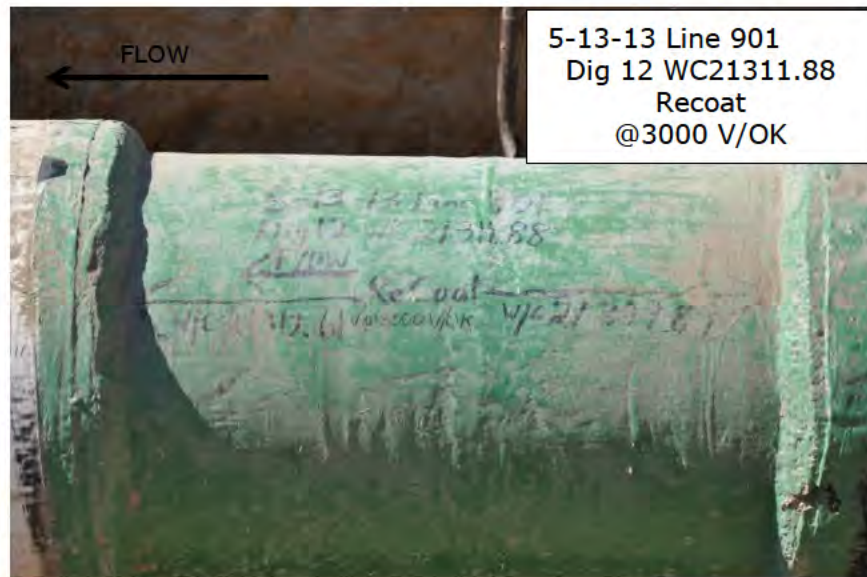


Figure 21. Plot showing the distribution of external metal loss features vs. o'clock orientation identified for Line 901 during the 2007, 2012, and 2015 ILI runs.



(a) 2007 ILI Dig #5



(b) 2012 ILI Dig #13

Figure 22. Photographs showing recoated pipe on Line 901 after: (a) 2007 ILI Dig #5 and (b) 2012 ILI Dig #13 [Ref 147 & 169]

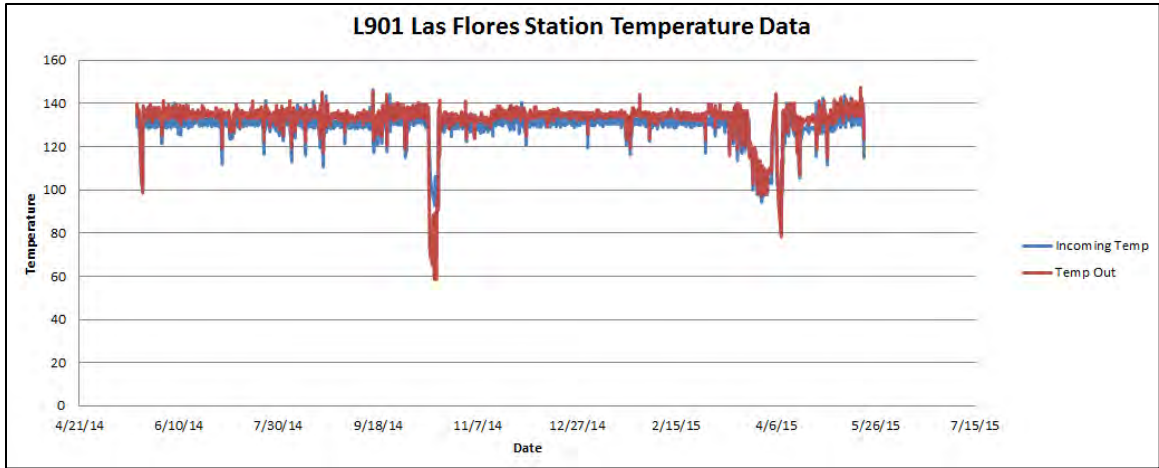


Figure 23. Plot of temperature data, provided by Plains, for Las Flores Station between May 2014 and May 2015 [Ref 226].

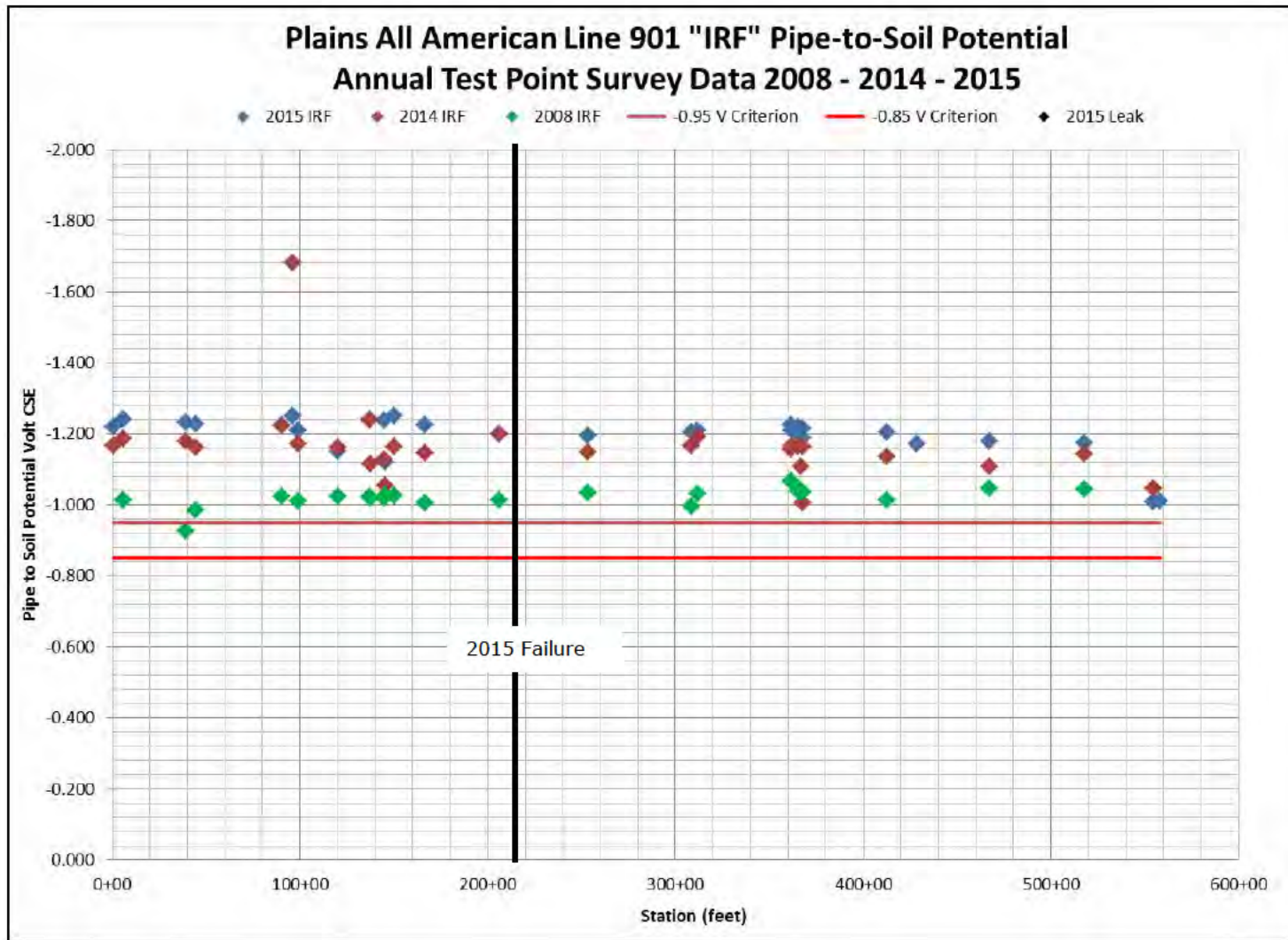


Figure 24. Plains All American Line 901 "IRF" pipe-to-soil potential annual test point survey data years 2008, 2014, and 2015. Note: IRF: free of IR error.

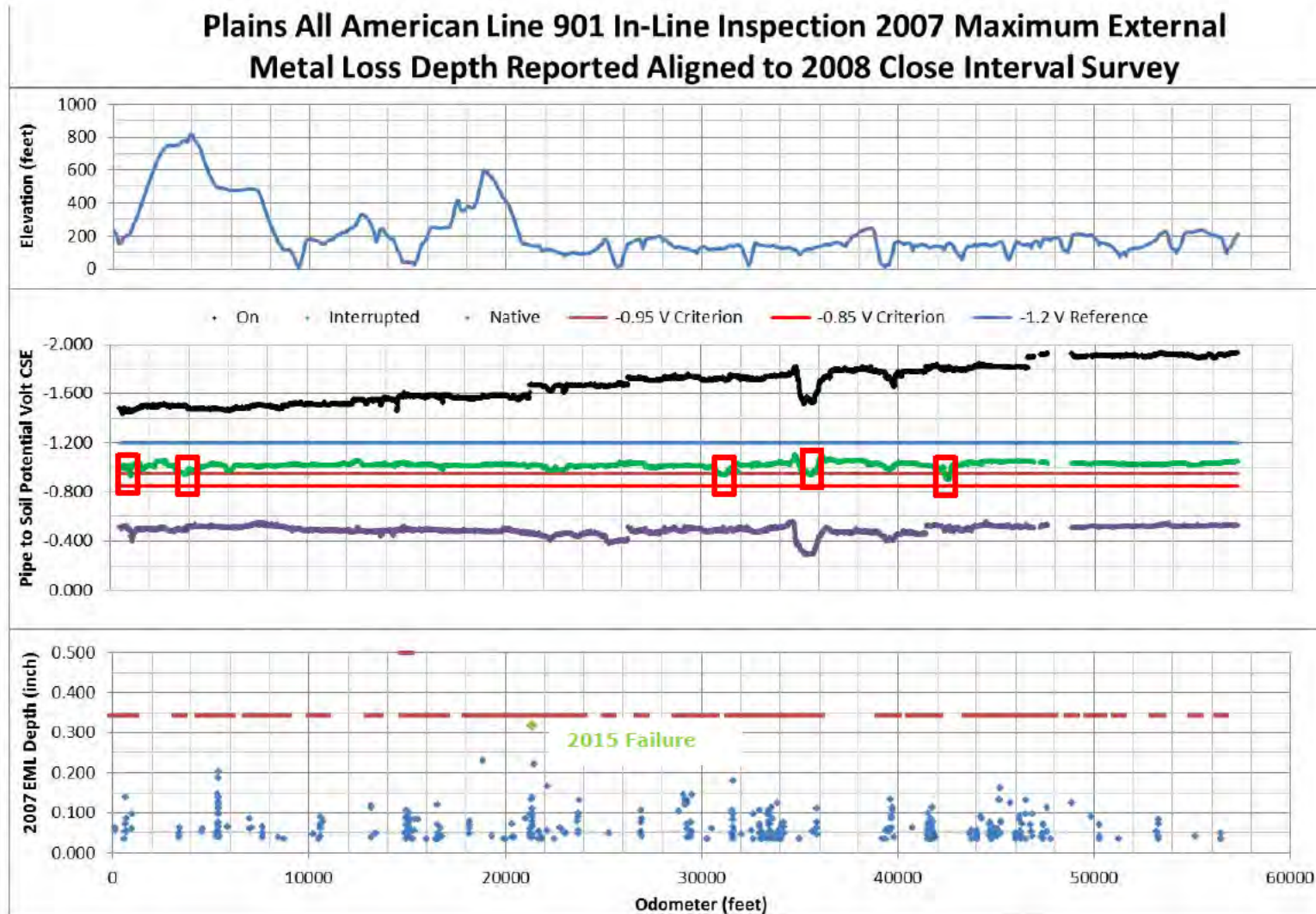


Figure 25. Plains All American Line 901 In-Line Inspection 2007 maximum external metal loss depth reported aligned with 2008 Close Interval Survey (- Pipe Nominal Wall Thickness).

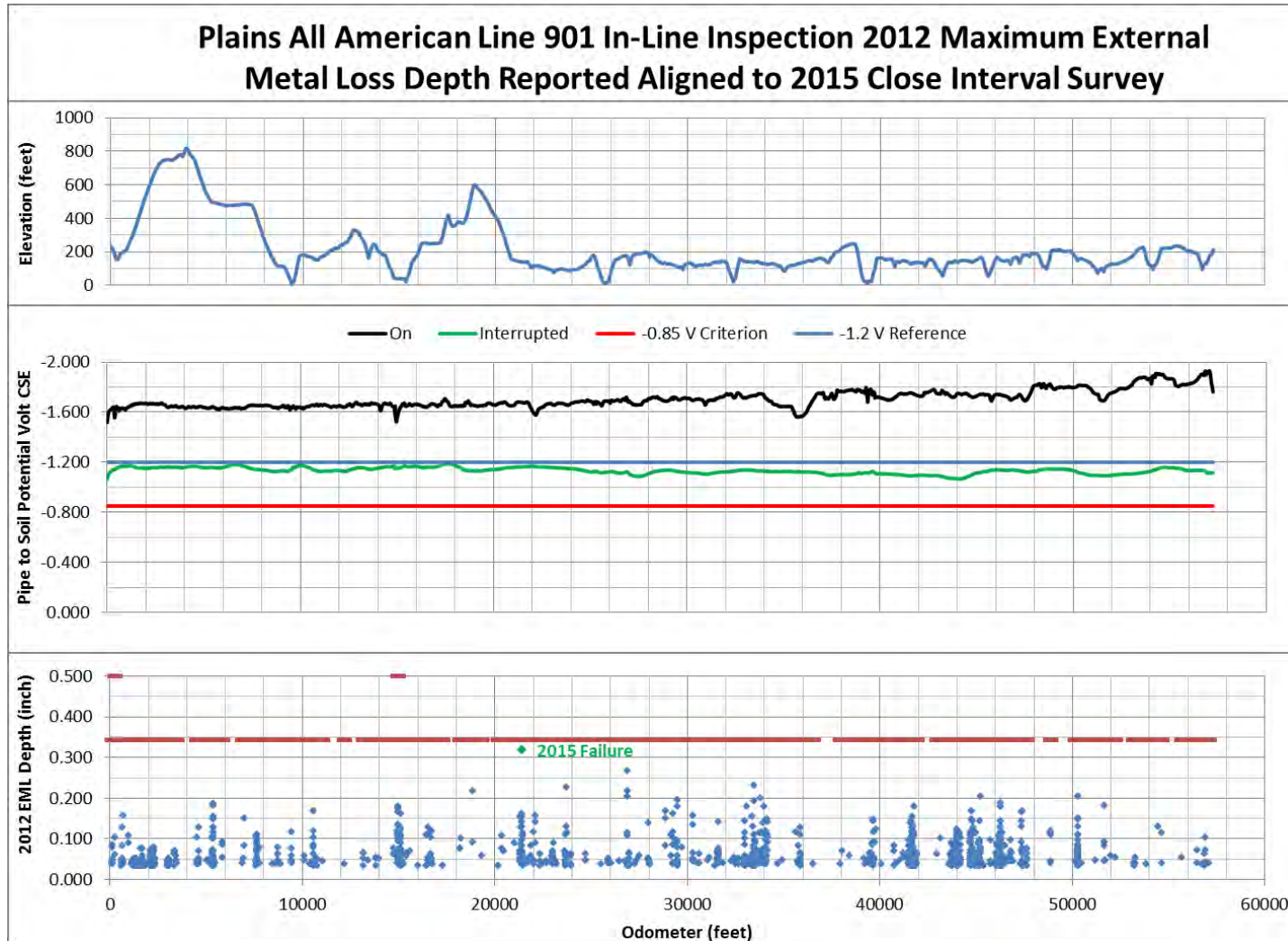


Figure 26. Plains All American Line 901 In-Line Inspection 2012 maximum external metal loss depth reported aligned with 2015 Close Interval Survey (- Pipe Nominal Wall Thickness).

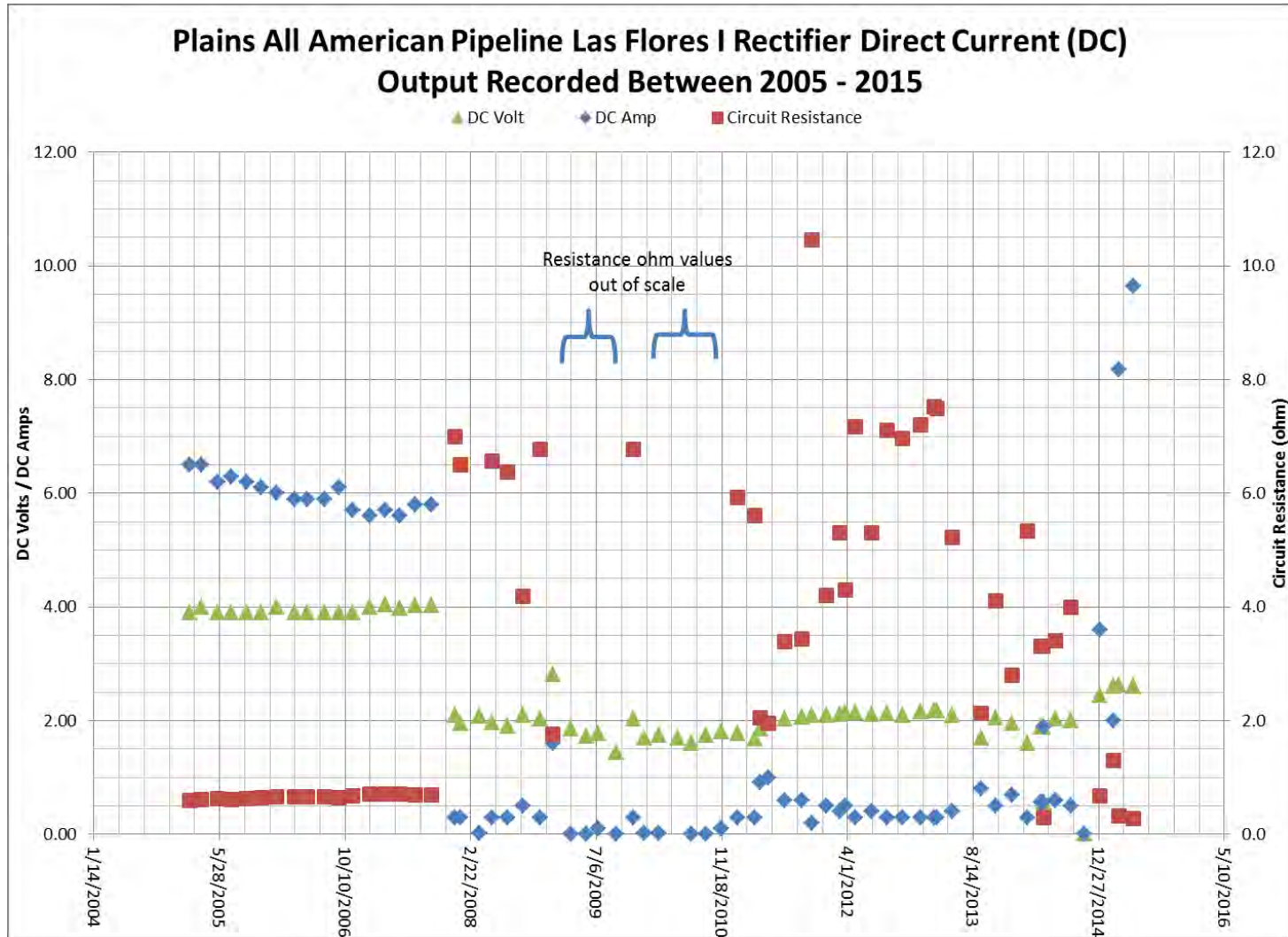


Figure 27. Plains All American Pipeline Las Flores I Rectifier: Direct current (DC) output recorded between 2005 - 2015.

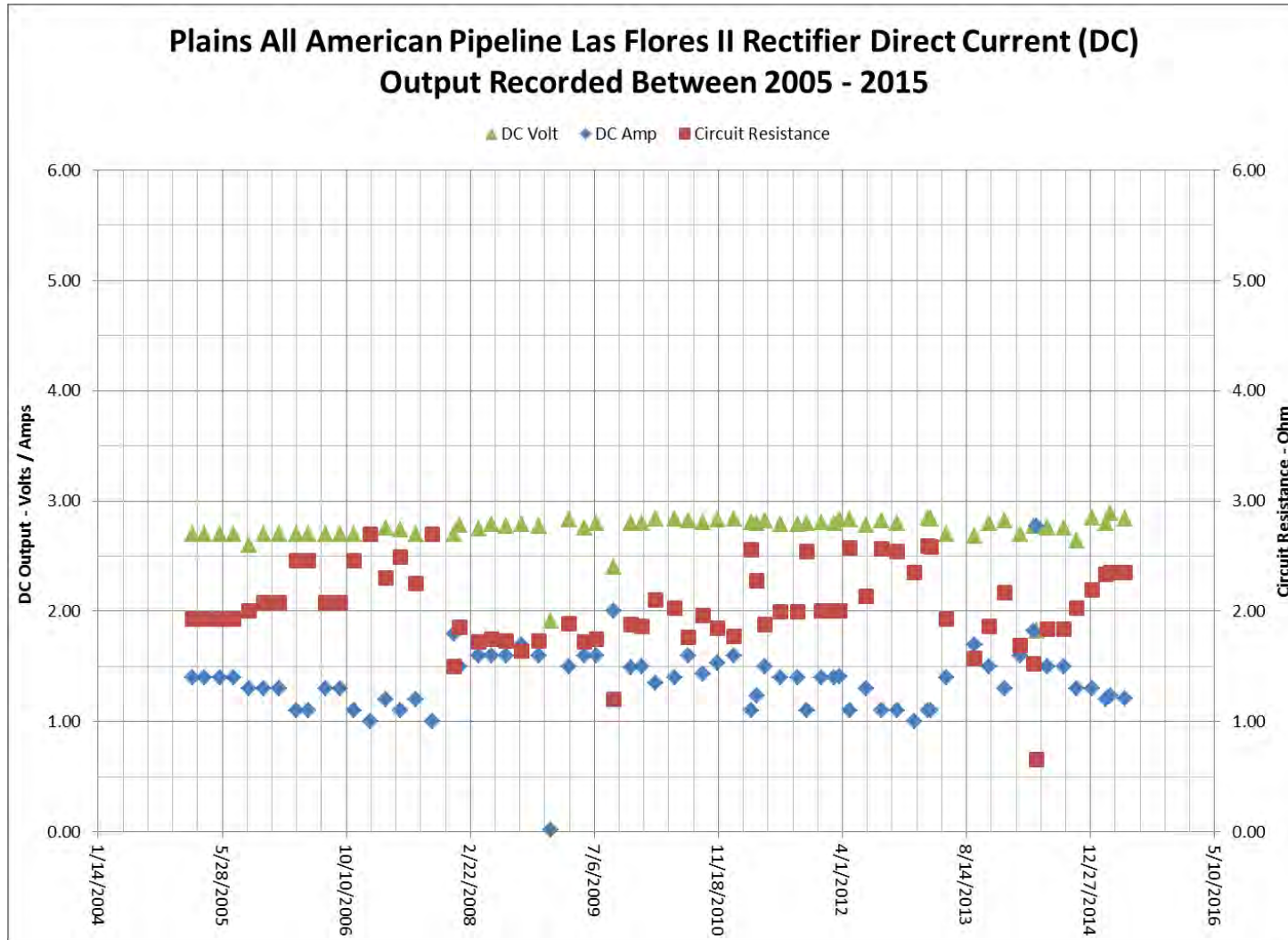


Figure 28. Plains All American Pipeline Las Flores II Rectifier: Direct current (DC) output recorded between 2005 - 2015.

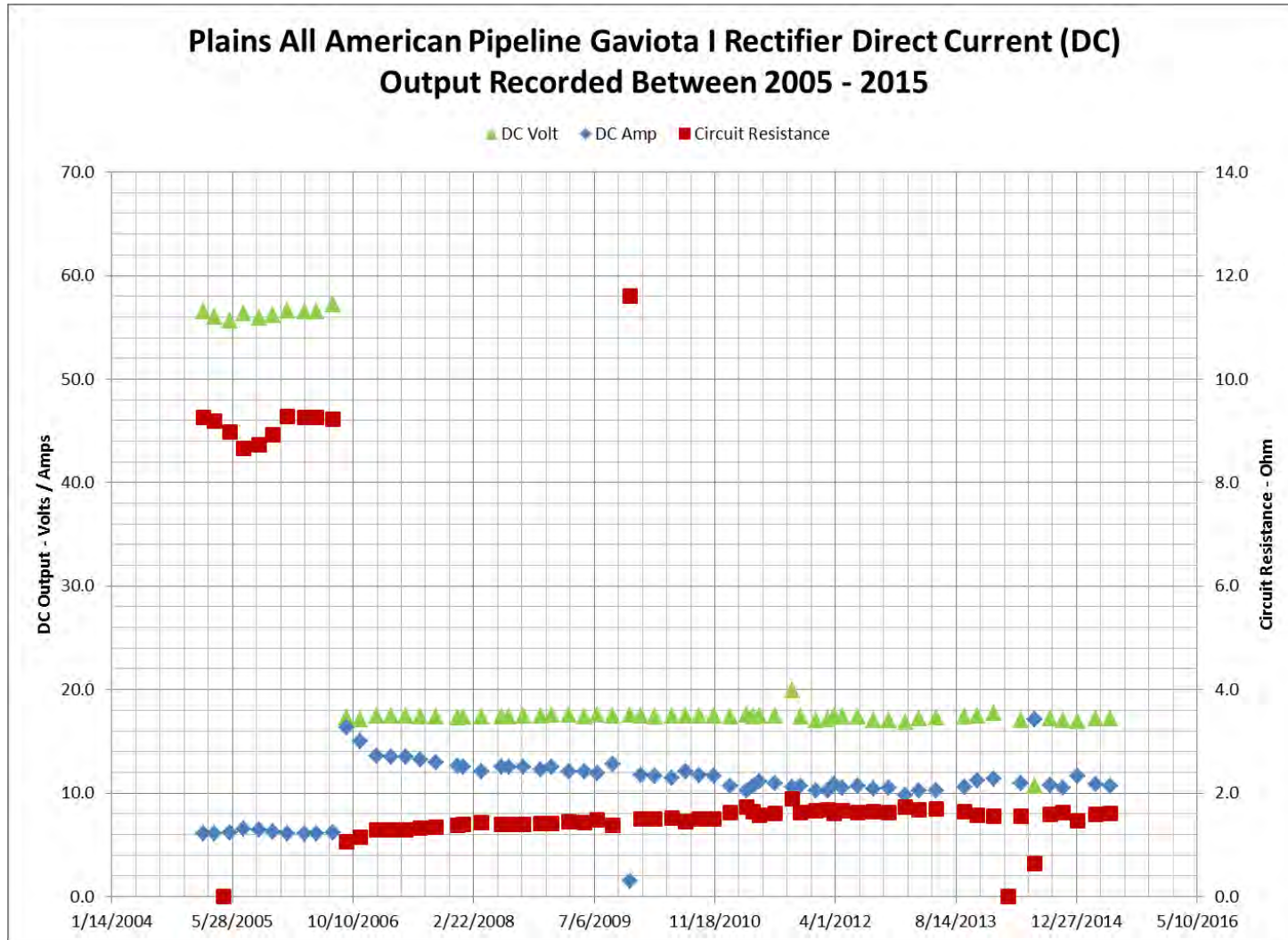


Figure 29. Plains All American Pipeline Gaviota I Rectifier: Direct current (DC) output recorded between 2005 - 2015.

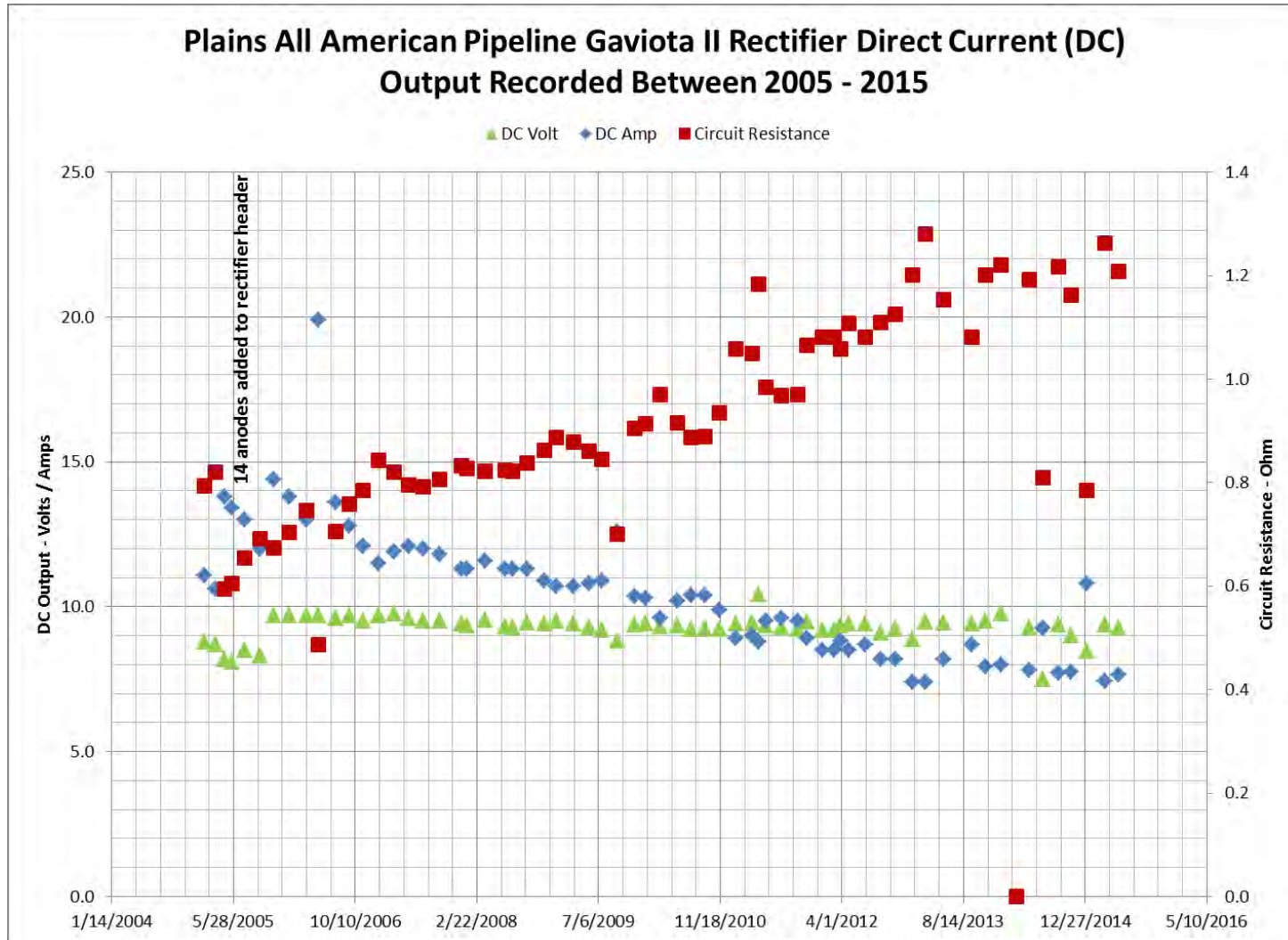


Figure 30. Plains All American Pipeline Gaviota II Rectifier: Direct current (DC) output recorded between 2005 - 2015.

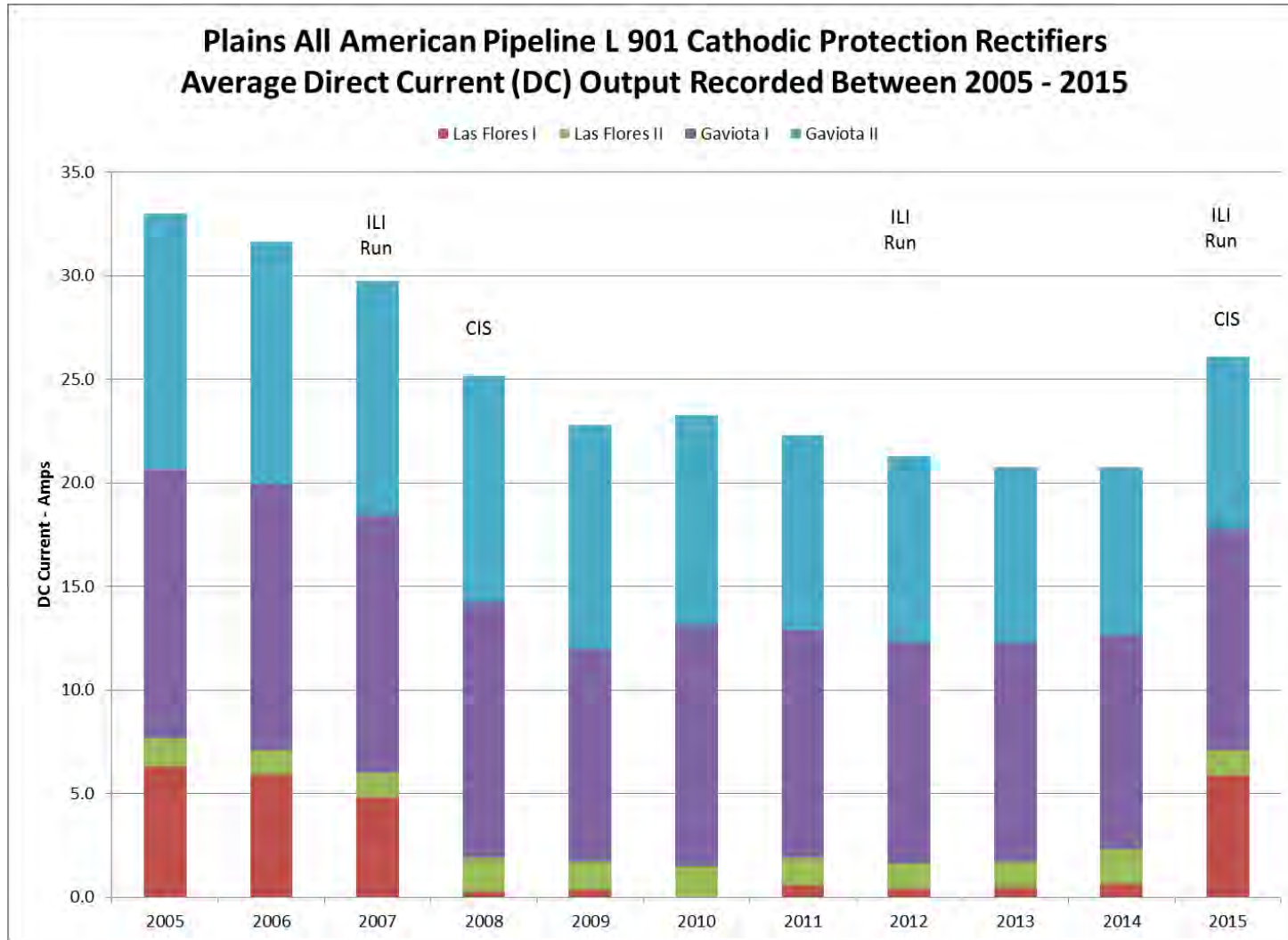


Figure 31. Plains All American Pipeline L 901 Cathodic Protection Rectifiers: Average direct current (DC) output recorded between 2005 - 2015.

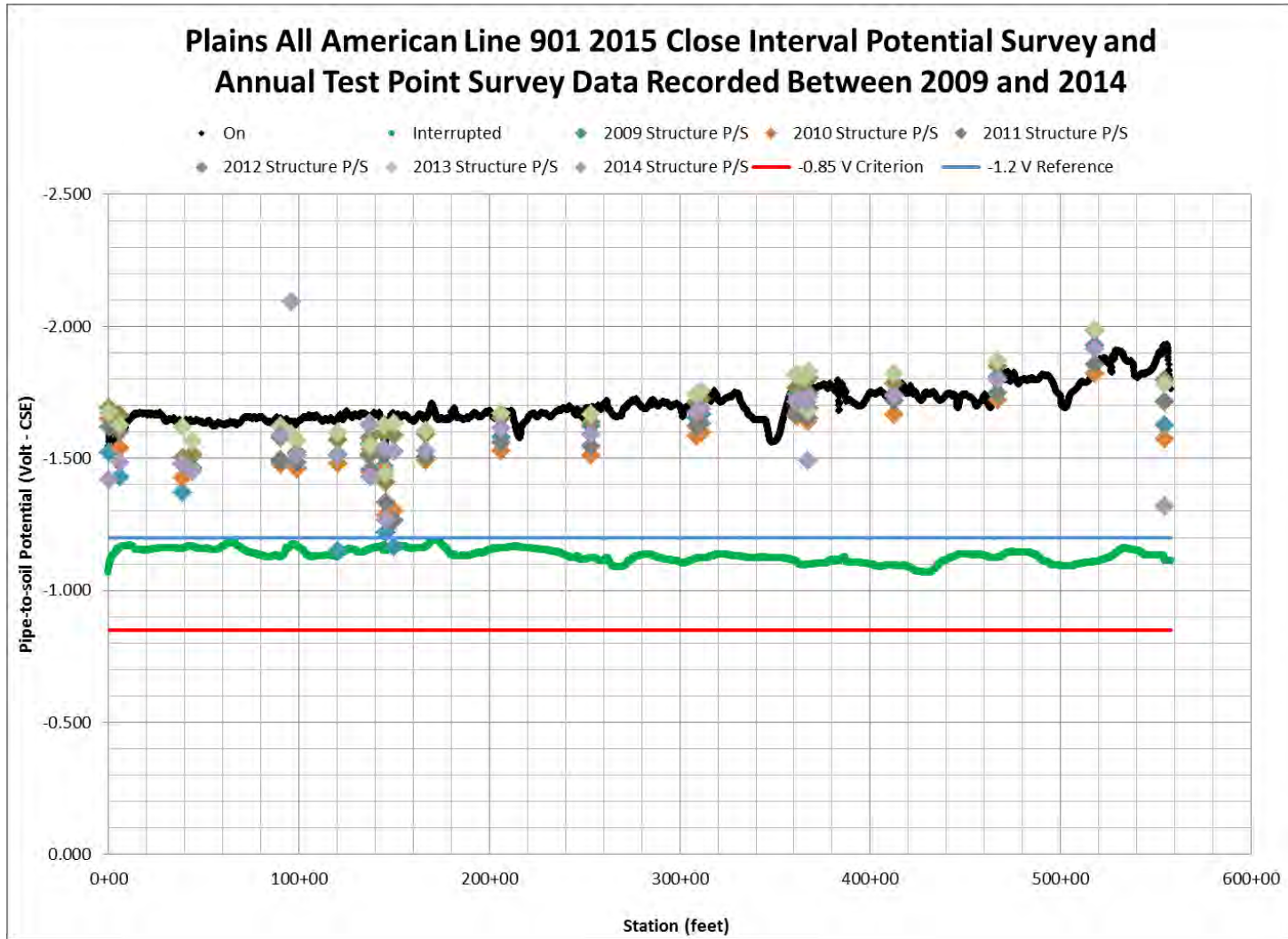


Figure 32. Plains All American Line 901 2015 close interval potential survey and annual test point survey data recorded between 2009 and 2014.

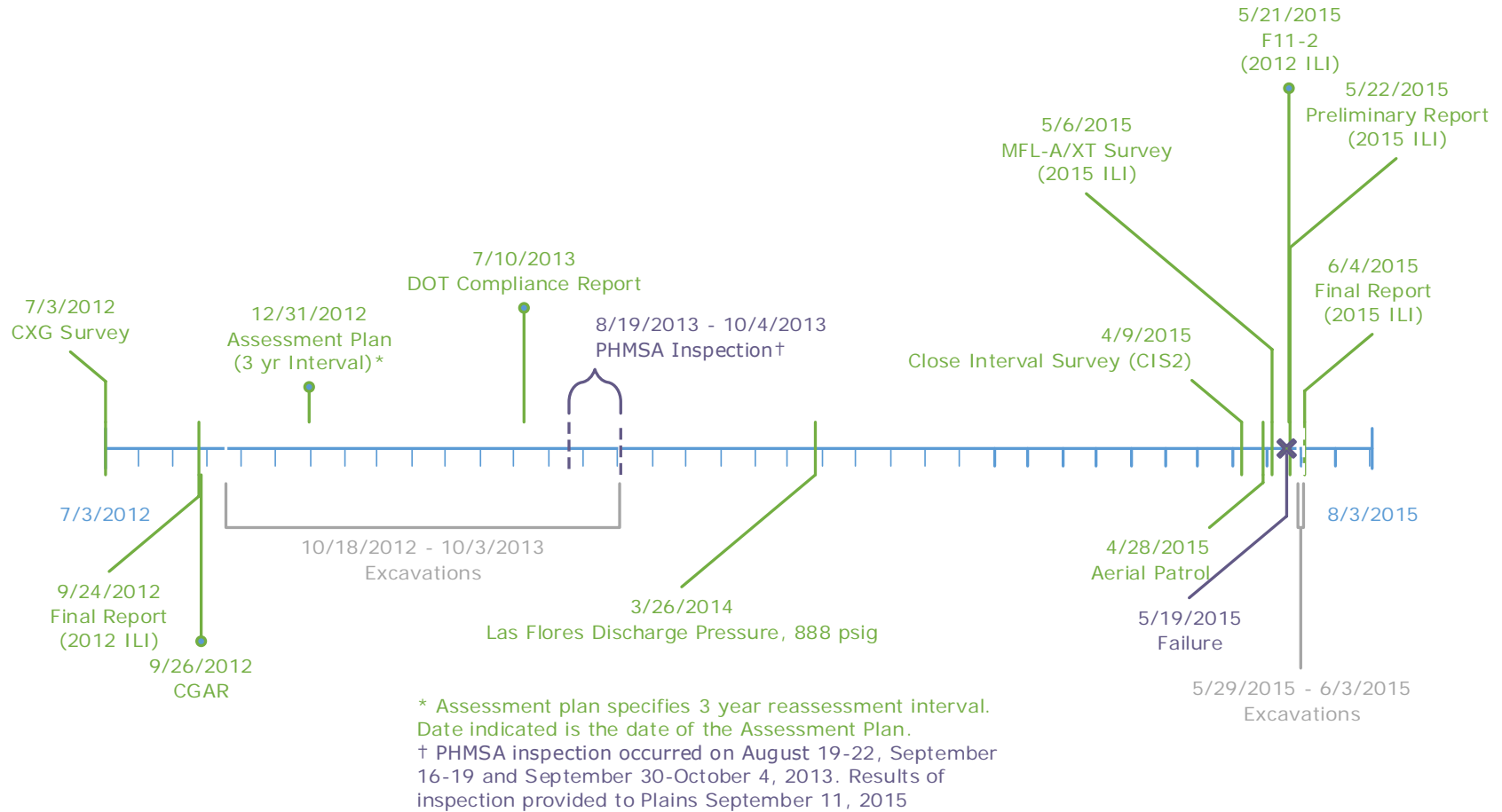


Figure 33. Timeline of events associated with Line 901, following the 2012 ILI.

(b) (4)



Figure 34. Excerpt from IMP Fig 9-2 illustrating process to estimate corrosion growth rates [Ref 22].

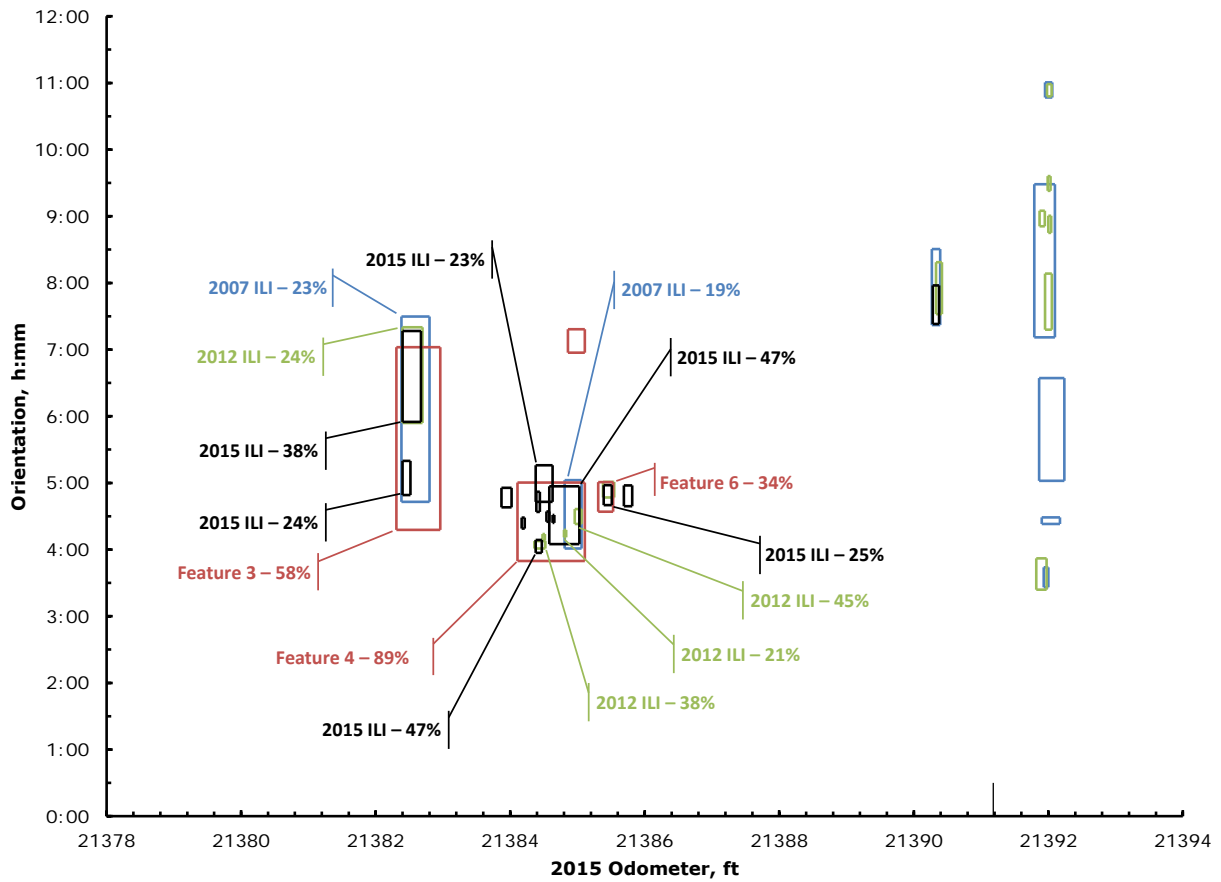


Figure 35. Representation of reported metal loss features on Joint 5930

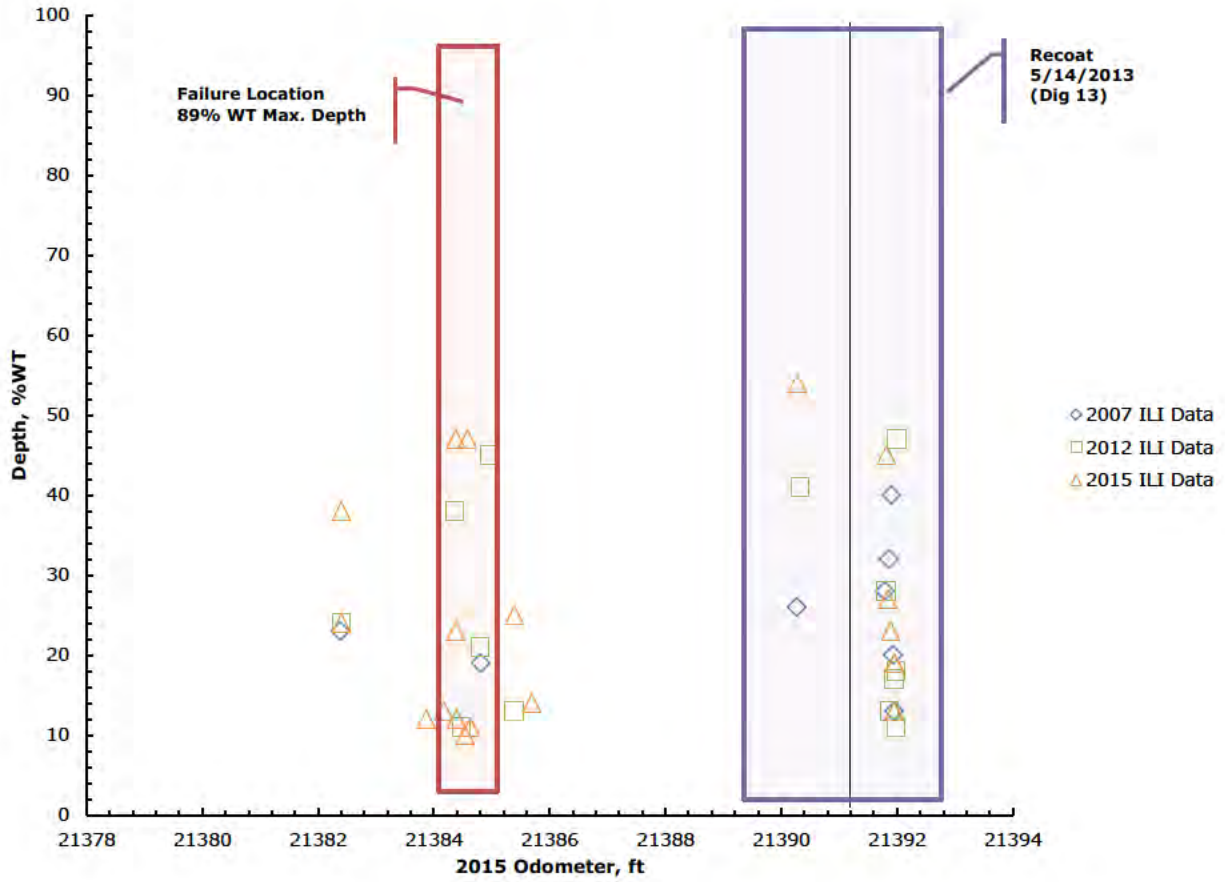


Figure 36. Depths of ILI-reported metal loss features on Joint 5930

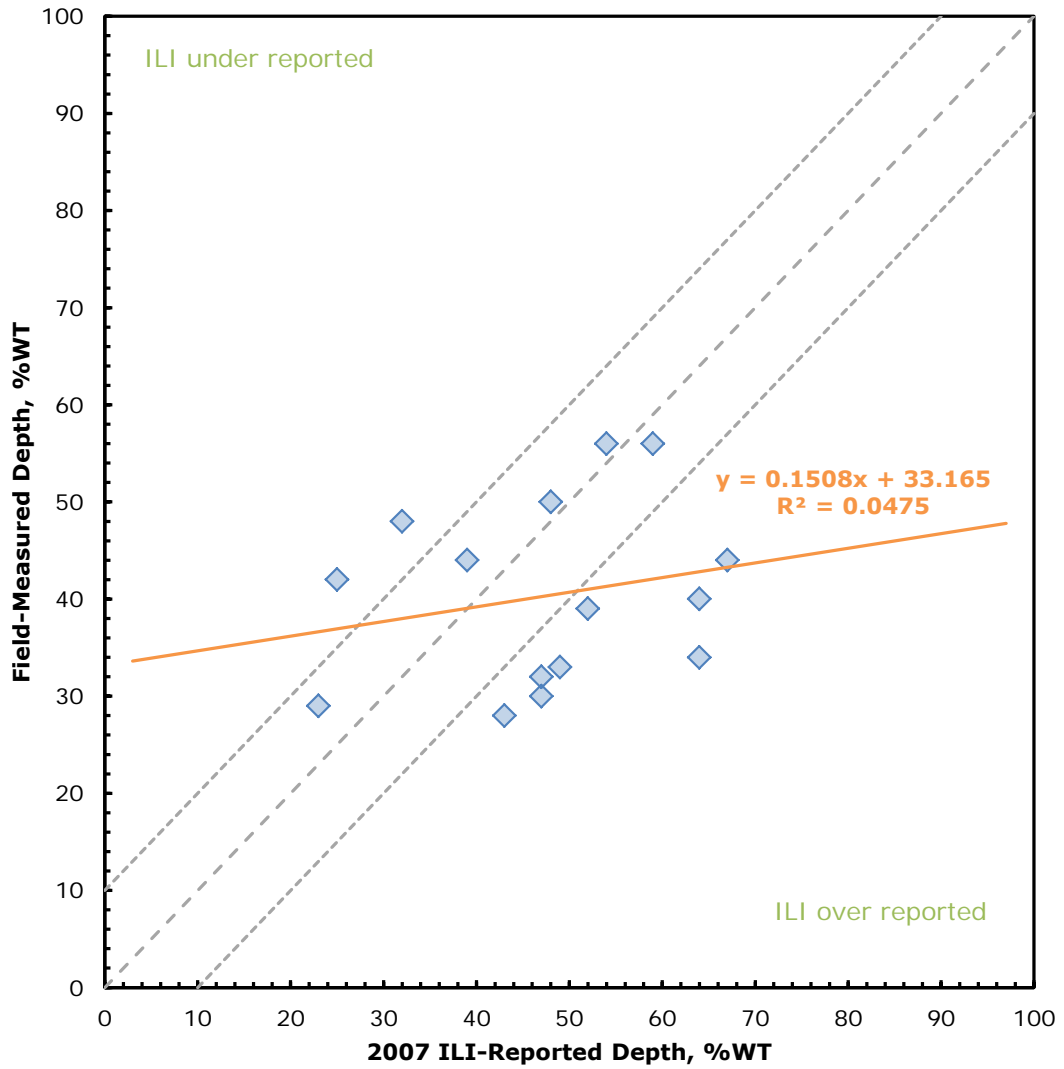


Figure 37. Metal loss depth unity plot using Plains data.

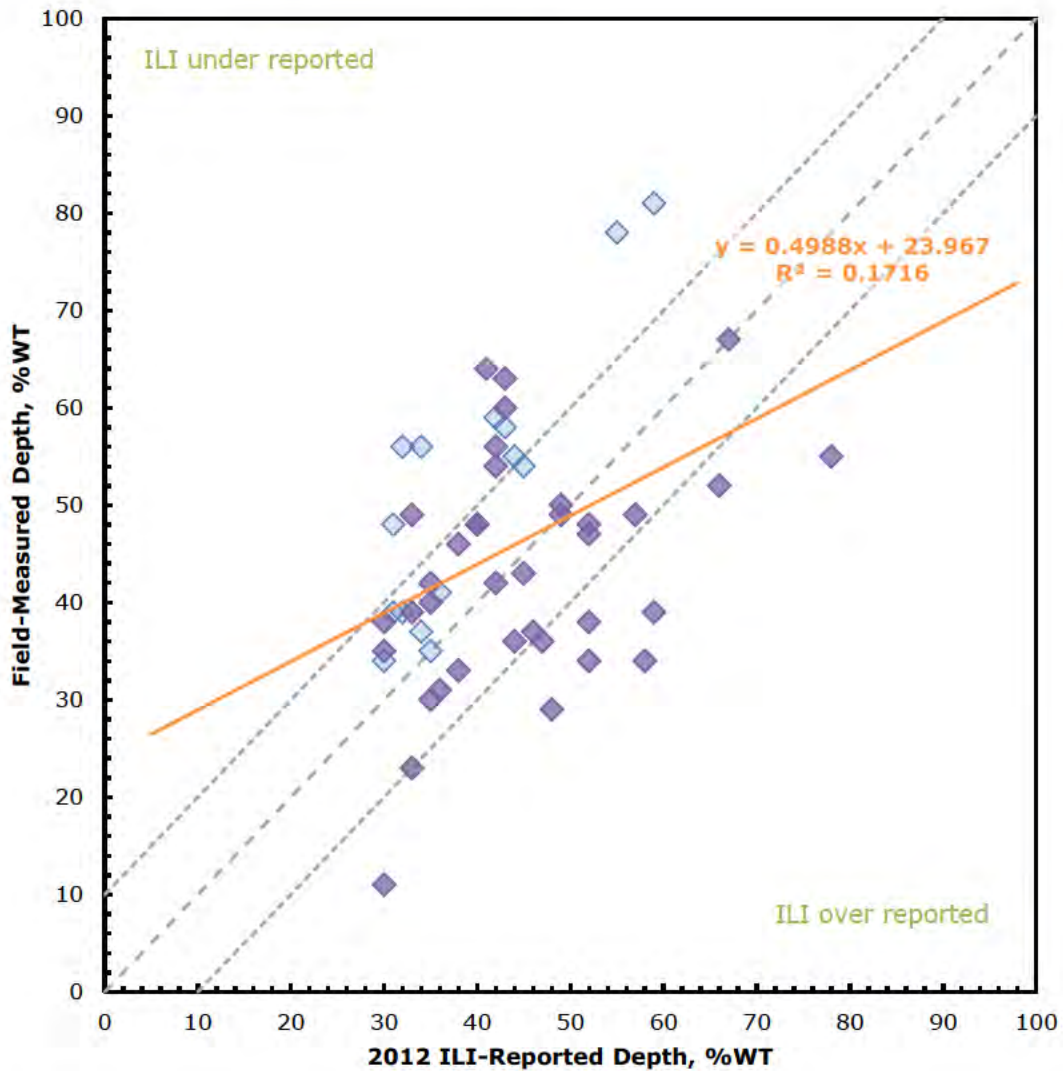


Figure 38. Metal loss depth unity plot using Plains data. Light blue diamonds correspond to features located greater than 2 feet from a girth weld. Purple diamonds correspond to features within 2 feet of a girth weld.

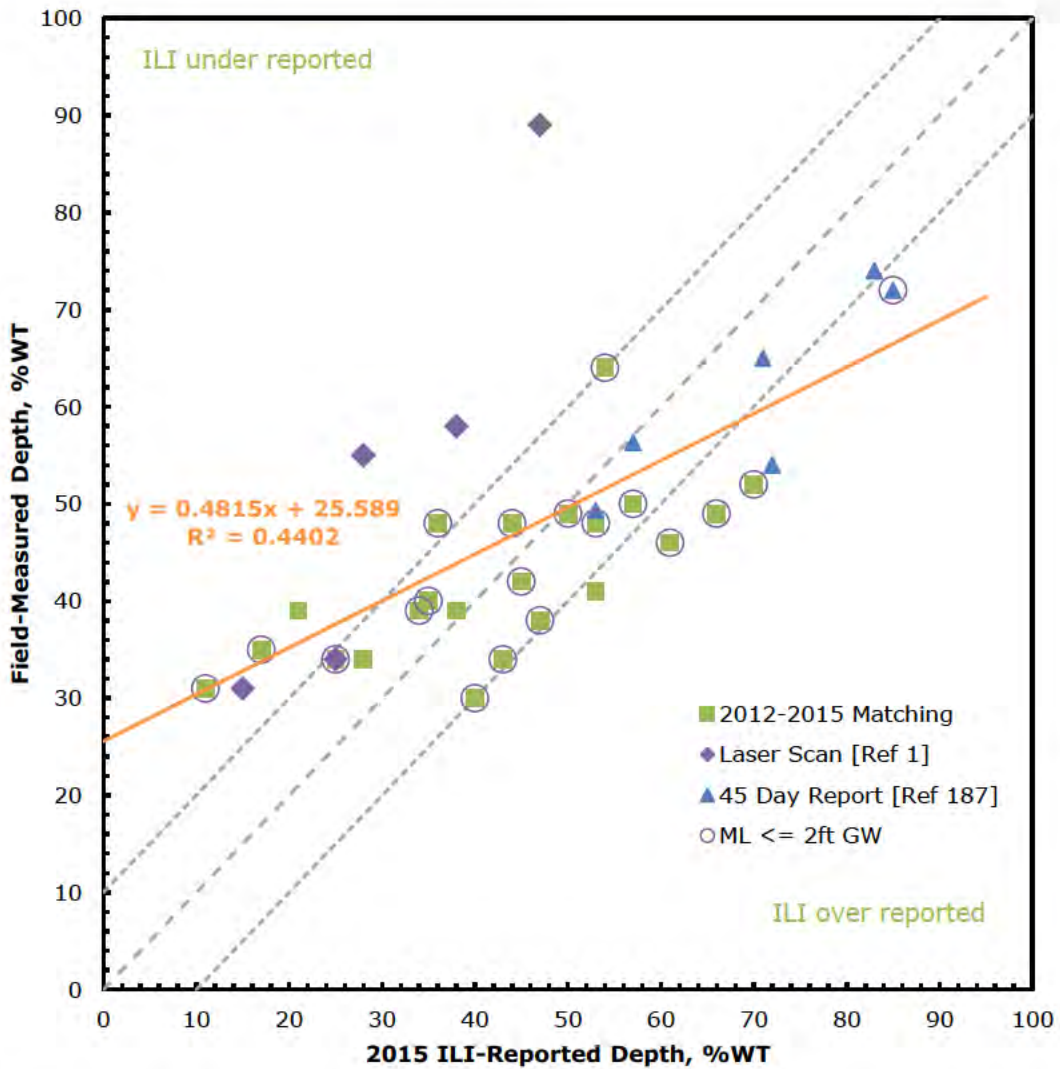


Figure 39. DNV GL-produced metal loss depth unity plot for the 2015 ILI of the Las Flores to Gaviota line segment.

Table 8—Table to Establish Consistency with Performance Specifications (Certainty = 0.80 and Confidence Level = 95%)

N	N _{in}	N	N _{in}	N	N _{in}
5	2	21	14	37	25
6	3	22	14	38	26
7	4	23	15	39	27
8	4	24	16	40	28
9	5	25	17	41	28
10	6	26	17	42	29
11	6	27	18	43	30
12	7	28	19	44	31
13	8	29	20	45	31
14	9	30	20	46	32
15	9	31	21	47	33
16	10	32	22	48	34
17	11	33	22	49	34
18	11	34	23	50	35
19	12	35	24	51	36
20	13	36	25	52	37

Figure 40. Excerpt from API 1163 used to establish consistency with performance specification (Table 8 in Appendix E, [Ref 309]).

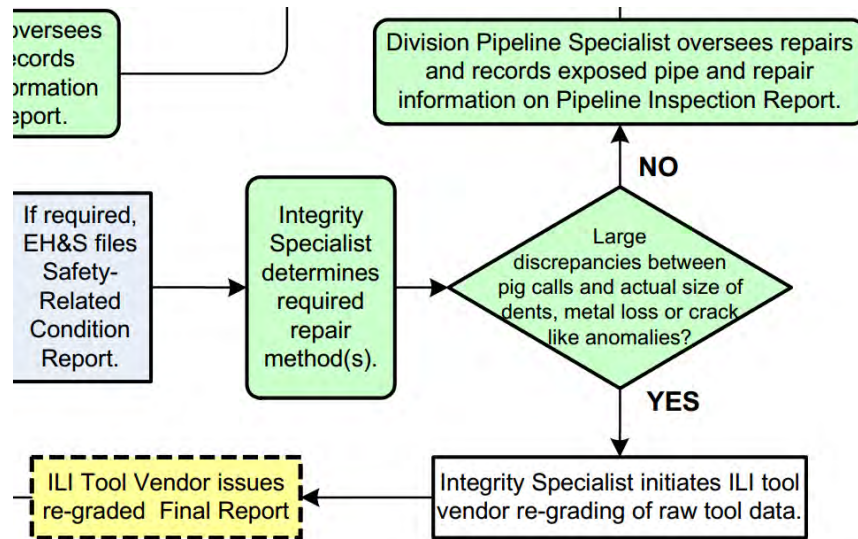


Figure 41. Snapshot showing portion of Figure 6-1 from Section 6.2 of Plains' IMP, regarding regrading [Ref 20].

APPENDIX A

BSCAT™ Methodology

BSCAT Methodology

Causal analysis is the core of an incident investigation. The analysis uses a systematic method of processing evidence gathered during an investigation in order to identify the factors that led to the incident. This approach assists in the development of corrective and/or remedial measures.

For the Line 901 Failure, DNV GL applied its standard Loss Causation Model to the incident. The DNV GL Loss Causation Model used in the analysis is shown in Figure A-1. As seen in the figure, the model involves a progression of factors that lead to an incident. In order to explain why and how the incident occurred, the progression would start at the box on the left-hand side, which is labeled "Lack of Control" and is often used interchangeably with "Root Cause." Typically, the root cause of an incident is related to weaknesses or gaps in the management system. The weaknesses or gaps may be related to programs, processes, standards, or compliance. Weaknesses in the management system then lead to a "Basic Cause." Typically, basic causes are related to engineering decisions, technical events, personal factors, or job/system factors. The basic cause in turn leads to the "Immediate Cause" of the incident. The immediate cause typically involves substandard conditions or acts/practices and is addressed in a metallurgical or materials analysis. Finally, the immediate cause progresses to the incident. Consequences of the incident are shown in the box to the far right. The consequences include a loss to people, property, equipment, a process, and/or the environment. When carrying out the analysis, the figure is applied in the reverse order (i.e. starting with the loss and working backwards toward the "root cause").

By identifying the root cause(s) of each incident, it is possible to derive process-related actions for improvement that can be implemented and managed throughout the site operations. Key lessons learned in this respect can also be shared with other sites exposed to similar conditions and programs.



Figure A-1. Schematic showing loss causation model.

Two approaches typically used by DNV GL include the Systematic Causal Analysis Technique (SCAT™) and the Barrier-based Systematic Causal Analysis Technique (BSCAT). SCAT™ is an RCA approach that uses standardized causation descriptions to convey the immediate and basic causes of an incident. This technique helps incident investigators identify weak areas in the integrity management system. The standard causation descriptions help to categorize commonalities that can be tracked in order to prioritize the weak areas of the management system. BSCAT™ is a technique that applies the SCAT model to each barrier, as opposed to the incident as a whole. This method results in a thorough review of the effectiveness of the individual barriers identified in the risk assessment. BSCAT provides a methodology that allows for the analysis of complex incidents that involve multiple barriers. A summary of the steps involved in the BSCAT process are outlined in Table A-1.

BowTie diagrams are used in BSCAT™ to identify the barriers that are in place to prevent threats from escalating into an incident and the barriers that are in place to mitigate consequences following an incident. A BowTie analysis can be performed before an accident/incident to help assess the barriers that are in place and their current state. BowTies can also be created following an accident/incident to analyze the system's barriers at the time of the accident/incident.

Table A-1. Summary of BSCAT process.

The BSCAT process involves the following steps:

1. **Evidence Capture** – This includes collecting information pertaining to the incident through interviews of the people involved and reviews of documents related to the incident.
2. **Timeline Development** – The evidenced captured is used to create a timeline of the events leading up to the incident.
3. **Barrier Identification** – If a BowTie diagram of the incident has not been created, one is created using the threat that escalated to the main event. The barriers that are in place or could be in place are identified at this time.
4. **Barrier State** – The state of each barrier is determined. The barrier status descriptions include Effective, Ineffective, Failed, and Missing. The term “Effective” is used to describe a barrier that is performing in the manner as originally intended. “Ineffective” is a term used to describe a barrier that is in place and operating, but its performance is deficient. The term “Failed” is used to describe a barrier that was originally in place, but has degraded and no longer functions as originally intended. “Missing” is used to describe a barrier that was never in place.
5. **Causal Analysis** – The SCAT process is then applied to the barriers that are identified as Ineffective, Unreliable, or Missing. This process will show the immediate and basic causes of the barrier’s ineffective state, as well as where the gaps in the Management System Elements, as shown in Table A-1, exist.

APPENDIX B

References

The following is a list of references that were used for the RCA. The reference numbers listed below are used throughout this report to identify the source of information.

Reference Number	Document Name	Issued by	Dated	No of Pages
1. Incident Related Documents				
1.	Plains All American Pipeline- Line 901 - Final Metallurgical Report (PP13 6049) September 18	DNV GL	9/18/15	111
2.	Background Sheet-L901-6-3-15	Plains All American Pipeline, L.P.	6/3/15	3
3.	Corrective_Action_Order_Plains_Pipeline_LP	PHMSA	5/21/15	9
4.	520155011H_Amendment_to_the_Corrective_Action_Order_06032015.pd	PHMSA	6/3/15	7
5.	National Response Center 2015 Current Data 7-16-15 509pm	NRC	7/16/15	
6.	L901 Supplemental (Rev 11.24.15) - PHMSA F 7000.1	Plains All American Pipeline, L.P.	11/24/15	14
7.	520155019_NOPV_PCO_09112015	PHMSA	9/11/15	6
2. Integrity Related Documents				
8.	ILI Review Process Procedure	Plains All American Pipeline, L.P.		41
9.	CGAR Checklist (2010)	Plains All American Pipeline, L.P.		1
10.	Repair Plan Checklist_2012	Plains All American Pipeline, L.P.		1
11.	Repair Plan Checklist_6-16-15	Plains All American Pipeline, L.P.		1
12.	Line 901 Las Flores to Gaviota	AKRI Hydrotesting	1/10/91	34
13.	ExternalCorrosionIndexFactors	Plains All American Pipeline, L.P.		3
14.	RiskResults_2009-2014_23Jun2015	Plains All American Pipeline, L.P.		1
15.	ROSOFT Data Management Version 6.70. Disc 1 of 1. 0646578	Rosen		
16.	Summary Rpt_Las Flores to Gaviota_Final	Plains All American Pipeline, L.P.	9/5/13	92

Reference Number	Document Name	Issued by	Dated	No of Pages
Integrity Management Plan				
17.	Integrity Management Plan Table of Contents	Plains All American Pipeline, L.P.	12/18/03	3
18.	Section 3 - Risk Assessment Procedures	Plains All American Pipeline, L.P.	2/7/07	28
19.	Section 4 Pipeline Assessment Method Selection Proc	Plains All American Pipeline, L.P.	9/11/14	16
20.	IMP Section 6 Procedures for Conducting Assessments & Processing Results	Plains All American Pipeline, L.P.	7/10/08	30
21.	IMP Section 8 Pipeline Repair Requirements	Plains All American Pipeline, L.P.	6/2/06	2
22.	Section 9 Procedure for Continual Assessment_Eval	Plains All American Pipeline, L.P.	2/10/07	18
23.	Section 11 - Plains IMP 2014	Plains All American Pipeline, L.P.	2/8/2007	30
24.	Spec. No. 201-Pipeline Maintenance Welding & Repair Procedure	Plains All American Pipeline, L.P.	6/22/07	26
Cathodic Protection Surveys				
25.	Foreign Line Crossing	Plains All American Pipeline, L.P.		1
26.	Las Flores Annual CP Survey 2012-15	Baker Hughes	5/21/15	3
27.	Revised Rect inspection 5yr	Plains All American Pipeline, L.P.	8/6/15	6
28.	REvisedTest Point Inspections 5 yr	Plains All American Pipeline, L.P.	8/6/15	4
29.	Las Flores 24 In_2008_CRI	Hanson Survey & Design	12/5/08 - 12/8/08	53
30.	Las Flores 24In_2015_Book	Hanson Survey & Design	4/8/15 - 4/9/15	65
Close Interval Surveys				
31.	Gaviota to Emidio 30 In_2009_CRI	Hanson Survey & Design, LLC	9/29/09	544
32.	Gaviota to Emidio 30 In_2009_RAW	Hanson Survey & Design, LLC	7/13/15	5

Plains All American Pipeline, L.P.
 Line 901 Release (5/19/15) Technical Root Cause Analysis

Reference Number	Document Name	Issued by	Dated	No of Pages
33.	Las Flores 24 In_2008_CRI	Hanson Survey & Design, LLC	12/5/08	53
34.	Las Flores 24In_2015_Book	Hanson Survey & Design, LLC		65
35.	Line 903 Hwy 101_2012_Book	Hanson Survey & Design, LLC		86
36.	Line 903 Hwy 101_2012_Depth	Hanson Survey & Design, LLC		1
37.	Line 903 Hwy 101_2012_Raw	Hanson Survey & Design, LLC		496
38.	Line 903 Hwy 101_2012_Rect	Hanson Survey & Design, LLC	July 2012	1
39.	Line 903 MP 54_2012_Book	Hanson Survey & Design, LLC		21
40.	Line 903 MP 54_2012_Raw	Hanson Survey & Design, LLC		1
41.	Line 903 MP 54_2012_Rect	Hanson Survey & Design, LLC		1
42.	Line 903 MP 60_2012_Book	Hanson Survey & Design, LLC		49
43.	Line 903 MP 60_2012_Raw	Hanson Survey & Design, LLC		493
44.	Line 903 MP 60_2012_Rect	Hanson Survey & Design, LLC		1
Rectifier Reports				
45.	2005-2015 Annual TP Survey 903	Baker Hughes	6/4/15	35
46.	2005-2015 Annual TP Survey 901	Baker Hughes	6/11/15	8
47.	L901 Rectifier Inspections 2005-2015	Baker Hughes	6/11/15	5
48.	L-901-CCH224_COUPON	Baker Hughes	5/28/15	1
49.	L903 Rectifier Inspections 2005-2015	Baker Hughes	6/11/15	10
In Line Inspection				
2007 In Line Inspection				

Plains All American Pipeline, L.P.
 Line 901 Release (5/19/15) Technical Root Cause Analysis

Reference Number	Document Name	Issued by	Dated	No of Pages
50.	2007 Rosen Report	Rosen	8/15/07	28
51.	anomaly counts_rtf_converted.docx	Rosen		1
52.	Anomaly Relative to Closest Weld Distance	Rosen	8/15/07	1
53.	Anomaly Type Distribution Chart_Pie Chart	Rosen	8/15/07	1
54.	CDG Magnetization Level	Rosen	8/15/07	1
55.	CDG Tool Rotation	Rosen	8/15/07	1
56.	CDG Tool Temperature	Rosen	8/15/07	1
57.	CDG Tool Velocity	Rosen	8/15/07	1
58.	Conclusions_rtf_converted.docx	Rosen	8/15/07	1
59.	data quality summary_rtf_converted.docx	Rosen		1
60.	Depth Distribution of All Metal Loss Anomalies	Rosen	8/15/07	1
61.	Depth Distribution of Internal Metal Loss Anomalies	Rosen	8/15/07	1
62.	Depth Distribution of Non-Internal Metal Loss Anomalies_2	Rosen	8/15/07	1
63.	Dig Sheets Las Flores to Gaviota	Rosen	8/15/07	45
64.	EGP Tool Rotation	Rosen	8/15/07	1
65.	EGP Tool Temperature	Rosen	8/15/07	1
66.	EGP Tool Velocity	Rosen	8/15/07	1
67.	ERF Distribution Graph	Rosen	8/15/07	1
68.	Given MAOP, Pdesign and Theoretical Safe Pressure Graph	Rosen	8/15/07	1

Plains All American Pipeline, L.P.
Line 901 Release (5/19/15) Technical Root Cause Analysis

Reference Number	Document Name	Issued by	Dated	No of Pages
69.	ISFR_5362_02_	Rosen	8/15/07	3
70.	ISFR_5365_72_	Rosen	8/15/07	3
71.	ISFR_18814_52_	Rosen	8/15/07	3
72.	ISFR_21438_78_	Rosen	8/15/07	3
73.	ISFR_31574_91_	Rosen	8/15/07	3
74.	List of Installations	Rosen	8/15/07	4
75.	List of Marker Positions	Rosen	8/15/07	1
76.	List of Most Severe Anomalies	Rosen	8/15/07	2
77.	List of Significances_2	Rosen	8/15/07	46
78.	O'clock Position of All Metal Loss Anomalies_2	Rosen	8/15/07	1
79.	O'clock Position of Internal Anomalies	Rosen	8/15/07	1
80.	O'clock Position of Non-Internal Anomalies	Rosen	8/15/07	1
81.	Pipe Tally 2007 Las Flores to Gaviota.xls	Rosen	8/15/07	41
82.	pipetally.xls	Rosen	8/16/07	30
83.	report	Rosen	8/15/07	28
84.	Signed 2007 ILI Summary Report	Plains All American	8/23/07	6
85.	2007 Pipetally	Rosen	8/15/07	
86.	CGAR _LasFlores to Gaviota_08_17_07	Plains All American Pipeline, L.P.	8/17/07	6
87.	Close Out Report _LasFlores_Gav_2007	Plains All American Pipeline, L.P.		3

Reference Number	Document Name	Issued by	Dated	No of Pages
88.	#_LCG-C129-A64. Rosen 2007. Disk 1 of 1	LCG >> Discovery Experts.		
89.	#_LCG-C129-A65. Rosen 2007. Disk 2 of 2	LCG >> Discovery Experts.		
90.	L901 Form F11-2_2007	Plains All American Pipeline, L.P.	10/8/09	5
2012 In Line Inspection				
91.	2012 Rosen Report	Rosen	9/24/12	28
92.	AGM sheets	Rosen	9/24/12	24
93.	Anomaly Relative to Closest Weld Distance_2	Rosen	9/24/12	1
94.	Anomaly Type Distribution Chart	Rosen	9/24/12	1
95.	CXG Magnetization Level	Rosen	9/24/12	1
96.	CXG Tool Rotation	Rosen	9/24/12	1
97.	CXG Tool Temperature	Rosen	9/24/12	1
98.	CXG Tool Velocity	Rosen	9/24/12	1
99.	Deformation Distribution	Rosen	9/24/12	1
100.	Deformation Orientation	Rosen	9/24/12	1
101.	Depth Distribution of All Metal Loss Anomalies_2	Rosen	9/24/12	1
102.	Depth Distribution of Internal Metal Loss Anomalies_2	Rosen	9/24/12	1
103.	Depth Distribution of Non-Internal Metal Loss Anomalies	Rosen	9/24/12	1
104.	Dig Sheets_P1	Rosen	9/24/12	3
105.	Dig Sheets_P2	Rosen	9/24/12	38

Plains All American Pipeline, L.P.
Line 901 Release (5/19/15) Technical Root Cause Analysis

Reference Number	Document Name	Issued by	Dated	No of Pages
106.	ERF Distribution	Rosen	9/24/12	1
107.	Gauge Pig Spec Sheet	Rosen	5/7/12	1
108.	Given MAOP, Pdesign and Theoretical Safe Pressure	Rosen	9/24/12	1
109.	ISFR_23707_53_	Rosen	9/24/12	3
110.	ISFR_26907_13_	Rosen	9/24/12	3
111.	ISFR_26907_36_	Rosen	9/24/12	3
112.	ISFR_33480_86_	Rosen	9/24/12	3
113.	ISFR_42570_35_	Rosen	9/24/12	3
114.	List of Installations_2	Rosen	9/24/12	4
115.	List of Markers	Rosen	9/24/12	1
116.	List of Significances	Rosen	9/24/12	102
117.	Metal Loss Distribution	Rosen	9/24/12	1
118.	Metal Loss Orientation	Rosen	9/24/12	1
119.	MFL tool Spec and calibration sheet	Rosen	1/13/12	2
120.	O'clock Position of All Metal Loss Anomalies	Rosen	9/24/12	1
121.	O'clock Position of Internal Metal Loss Anomalies	Rosen	9/24/12	1
122.	O'clock Position of Non-Internal Metal Loss Anomalies	Rosen	9/24/12	1
123.	Pipetally.xls	Rosen	9/24/12	29
124.	Signed 2012 ILI Summary Report	Plains All American Pipeline, L.P.	9/5/13	8

Plains All American Pipeline, L.P.
Line 901 Release (5/19/15) Technical Root Cause Analysis

Reference Number	Document Name	Issued by	Dated	No of Pages
125.	Site Survey Report	Rosen	7/5/12	4
126.	2012 Pipetally	Rosen	9/24/12	
127.	AssessmentPlan_31Dec2012	Plains All American Pipeline, L.P.	12/31/12	1
128.	CGAR 2012_Las Flores to Gaviota_9-26-12	Plains All American Pipeline, L.P.		6
129.	Close Out Report_LasFlores_Gav_2012_rev1	Plains All American Pipeline, L.P.	6/22/15	5
130.	FW Unity Plots for Sisquoc to Pentland 2012 and Las Flores to Gaviota 2008 and 2012.msg	Plains All American Pipeline, L.P.	9/18/15	
131.	L901 Las Flores to Gaviota Form F11-2 2015 rev Approved 6-9-2015	Plains All American Pipeline, L.P.	5/21/15	10
132.	#_LCG-C129-A62. Rosen 2012-A. Disk 1 of 1	LCG >> Discovery Experts		
133.	#_LCG-C129-A63. Rosen 2012-B. Disk 1 of 2	LCG >> Discovery Experts		
134.	#_LCG-C129-A71. Rosen 2012. Disk 2 of 2	LCG >> Discovery Experts		
135.	CGAR_Line 901-Las Flores-Gaviota-2012 DAS	Plains All American Pipeline, L.P.	6/21/13	8
2015 In Line Inspection				
136.	anomaly counts	Rosen		1
137.	conclusions	Rosen		1
138.	Final Rosen Report May 2015 ILI	Rosen	6/4/15	227
139.	2015 Pipetally	Rosen	6/4/15	33
140.	Pipetally.xls	Rosen	6/4/15	
141.	#PA84/A456. Rosen 2015. Disk 1 of 2	LCG >> Discovery Experts		
142.	#PA84/A457. Rosen 2015. Disk 2 of 2	LCG >> Discovery		

Reference Number	Document Name	Issued by	Dated	No of Pages
		Experts		
143.	Preliminary Report 24in Line 901 Las Flores to Gaviota	Rosen	5/22/15	13
Excavation and Repair Reports				
2007 Digs				
144.	Las-Gav-WC 5342.18_Dig 3	Plains All American Pipeline, L.P.		55
145.	Las-Gav-WC 5365.72_Dig 3.PDF	Plains All American Pipeline, L.P.		65
146.	Las-Gav-WC 18814.52 Dig 4	Plains All American Pipeline, L.P.		55
147.	Las-Gav-WC 21307.63 Dig 5	Plains All American Pipeline, L.P.		44
148.	Las-Gav-WC 21438.79_Dig 6	Plains All American Pipeline, L.P.		32
149.	Las-Gav-WC 22083.48 Dig 7	Plains All American Pipeline, L.P.		45
150.	Las-Gav-WC 29052.98_Dig 8	Plains All American Pipeline, L.P.		62
151.	Las-Gav-WC 29206.61_Dig 9.PDF	Plains All American Pipeline, L.P.		57
152.	Las-Gav-WC 31574.91_Dig 10.PDF	Plains All American Pipeline, L.P.		54
153.	Las-Gav-WC 34025.04_Dig 11.PDF	Plains All American Pipeline, L.P.		65
154.	Las-Gav-WC 34137.11_Dig 11B.PDF	Plains All American Pipeline, L.P.		36
155.	Las-Gav-WC 44100.91_Dig 12.PDF	Plains All American Pipeline, L.P.		63
156.	Las-Gav-WC 45139.21_Dig 13	Plains All American Pipeline, L.P.		51
2012 Digs				
157.	Las-Gav_Dig 1 WC 26907.14	Plains All American Pipeline, L.P.		56

Plains All American Pipeline, L.P.
 Line 901 Release (5/19/15) Technical Root Cause Analysis

Reference Number	Document Name	Issued by	Dated	No of Pages
158.	Las-Gav_Dig 2 WC 33480.86	Plains All American Pipeline, L.P.		93
159.	Las-Gav_Dig 3 WC 42570.35	Plains All American Pipeline, L.P.		99
160.	Las-Gav_Dig 4 WC 269.14	Plains All American Pipeline, L.P.		43
161.	Las-Gav_Dig 5 WC 678.93	Plains All American Pipeline, L.P.		31
162.	Las-Gav_Dig 6 WC 4324.14	Plains All American Pipeline, L.P.		75
163.	Las-Gav_Dig 7 WC 6982.96	Plains All American Pipeline, L.P.		37
164.	Las-Gav_Dig 8 WC 10595.52	Plains All American Pipeline, L.P.		43
165.	Las-Gav_Dig 9 WC 14970.32	Plains All American Pipeline, L.P.		40
166.	Las-Gav_Dig 10 WC 16669.12	Plains All American Pipeline, L.P.		39
167.	Las-Gav_Dig 11 WC 17474.02	Plains All American Pipeline, L.P.		35
168.	Las-Gav_Dig 12 WC 21311.88	Plains All American Pipeline, L.P.		40
169.	Las-Gav_Dig 13 WC 21390.33	Plains All American Pipeline, L.P.		45
170.	Las-Gav_Dig 14 WC 23707.53	Plains All American Pipeline, L.P.		39
171.	Las-Gav_Dig 15 WC 28857.22	Plains All American Pipeline, L.P.		37
172.	Las-Gav_Dig 16 WC 29490.43	Plains All American Pipeline, L.P.		36
173.	Las-Gav_Dig 17 WC 32732.65	Plains All American Pipeline, L.P.		66
174.	Las-Gav_Dig 18 WC 32954.85	Plains All American Pipeline, L.P.		79
175.	Las-Gav_Dig 19 WC 33081.18	Plains All American Pipeline, L.P.		35

Plains All American Pipeline, L.P.
Line 901 Release (5/19/15) Technical Root Cause Analysis

Reference Number	Document Name	Issued by	Dated	No of Pages
176.	Las-Gav_Dig 20 WC 33800.97	Plains All American Pipeline, L.P.		37
177.	Las-Gav_Dig 20A WC 33820.56	Plains All American Pipeline, L.P.		59
178.	Las-Gav_Dig 21 WC 33946.08	Plains All American Pipeline, L.P.		38
179.	Las-Gav_Dig 21A WC 33993.62	Plains All American Pipeline, L.P.		65
180.	Las-Gav_Dig 22 WC 34106.54	Plains All American Pipeline, L.P.		33
181.	Las-Gav_Dig 23 WC 34188.43	Plains All American Pipeline, L.P.		32
182.	Las-Gav_Dig 24 WC 35975.10	Plains All American Pipeline, L.P.		77
183.	Las-Gav_Dig 25 WC 39655.36	Plains All American Pipeline, L.P.		46
184.	Las-Gav_Dig 26 WC 41609.94	Plains All American Pipeline, L.P.		93
185.	Las-Gav_Dig 27 WC 41769.64	Plains All American Pipeline, L.P.		41
186.	Las-Gav_Dig 28 WC 43990.86	Plains All American Pipeline, L.P.		50
187.	Las-Gav_Dig 29 WC 44827.97	Plains All American Pipeline, L.P.		32
188.	Las-Gav_Dig 30 WC 45183.16	Plains All American Pipeline, L.P.		42
189.	Las-Gav_Dig 31 WC 45246.50	Plains All American Pipeline, L.P.		32
190.	Las-Gav_Dig 32 WC 46263.62	Plains All American Pipeline, L.P.		54
191.	Las-Gav_Dig 33_33A WC 47191.95	Plains All American Pipeline, L.P.		101
192.	Las-Gav_Dig 34 WC 47341.16	Plains All American Pipeline, L.P.		32
193.	Las-Gav_Dig 35 WC 47726.17	Plains All American Pipeline, L.P.		35

Reference Number	Document Name	Issued by	Dated	No of Pages
194.	Las-Gav_Dig 36 WC 50280.62	Plains All American Pipeline, L.P.		91
195.	Las-Gav_Dig 37 WC 50941.59	Plains All American Pipeline, L.P.		63
196.	Las-Gav_Dig 38 WC 54239.07	Plains All American Pipeline, L.P.		98
197.	Las-Gav_Dig 39 WC 54358.73	Plains All American Pipeline, L.P.		66
198.	Las-Gav_Dig 40 WC 54472.60	Plains All American Pipeline, L.P.		34
199.	Las-Gav_Dig 41 WC 54627.39	Plains All American Pipeline, L.P.		26
2015 Digs				
200.	45 Day Report CAO 7-6-15 FINAL	Plains All American Pipeline, L.P.	7/6/15	7
3. Leak Detection Documents				
201.	100-8 Pipeline Leak Detection	Plains All American Pipeline, L.P.		6
202.	OS_Data	Plains All American Pipeline, L.P.		1
203.	PAA_0000003 - PAA_0000028	Plains All American Pipeline, L.P.		26
204.	PAA_0000090 - PAA_0000095	Plains All American Pipeline, L.P.		6
205.	PAA_0000104_CONFIDENTIAL	Plains All American Pipeline, L.P.		464
206.	PAA_0000105_CONFIDENTIAL	Plains All American Pipeline, L.P.		82
207.	PAA_0000106	Plains All American Pipeline, L.P.		6
208.	PAA_0000112	Plains All American Pipeline, L.P.		1
209.	PAA_0000114	Plains All American Pipeline, L.P.		3

Plains All American Pipeline, L.P.
Line 901 Release (5/19/15) Technical Root Cause Analysis

Reference Number	Document Name	Issued by	Dated	No of Pages
210.	PAA_0000119_CONFIDENTIAL	Plains All American Pipeline, L.P.		51
211.	PAA_0000129_CONFIDENTIAL	Plains All American Pipeline, L.P.		499
212.	PAA00011284	Plains All American Pipeline, L.P.		1
213.	Line 901 5-1-2014 to 5-19-2015	Plains All American Pipeline, L.P.		499
214.	Line 903 5-1-2014 to 5-19-2015	Plains All American Pipeline, L.P.		499
215.	SCADA Tags	Plains All American Pipeline, L.P.		1
Patrol Data				
216.	01 - Jan 07, 2015 - Jan 28, 2015	Plains All American Pipeline, L.P.	1/21/15 - 2/2/15	4
217.	02 - Feb 04, 2015 - Feb 25, 2015	Plains All American Pipeline, L.P.	2/11/15 - 3/4/15	4
218.	03 - Mar 04, 2015 - Mar 25, 2015	Plains All American Pipeline, L.P.	3/12/15 - ?	3
219.	04 - Apr 01, 2015 - April 29, 2015	Plains All American Pipeline, L.P.	4/13/15 - 5/14/15	5
220.	05 - May 04, 2015 - May 11, 2015	Plains All American Pipeline, L.P.	5/14/15 - 5/19/15	2
Written Responses to PHMSA				
221.	PAA_0000102 - PAA_0000103	Plains All American Pipeline, L.P.	5/28/15	2
222.	Responses to PHMSA Investigation Questions 7.2.15	Plains All American Pipeline, L.P.	7/2/15	2
223.	Responses to PHMSA Request for Documents and Information 6.2.15	Plains All American Pipeline, L.P.	6/2/15	2
4. Operations Documents				
224.	BKPlainsPipe	Plains All American Pipeline, L.P.	2/15	29
225.	901_LasFlores_Gaviota_24in_7_2_15	Plains All American Pipeline, L.P.	7/2/15	1

Reference Number	Document Name	Issued by	Dated	No of Pages
226.	901_pressuredata_summary	Plains All American Pipeline, L.P.	4/26/11-5/20/15	7
227.	Pressure Data 5-19-2015	Plains All American Pipeline, L.P.	5/19/15	1
228.	O&M Manual Table of Contents	Plains All American Pipeline, L.P.	9/10	11
229.	O&M Table of Contents	Plains All American Pipeline, L.P.	3/13	4
230.	O & M - 405 System Start-up and Shutdown	Plains All American Pipeline, L.P.	9/10	4
231.	O & M - 412 Corrosion Control	Plains All American Pipeline, L.P.	9/14	16
232.	O & M - 415 Pipeline Repairs	Plains All American Pipeline, L.P.	10/11	8
233.	O & M - 425 Instruction for Recognizing Safety Related Conditions	Plains All American Pipeline, L.P.	9/10	4
234.	O & M - 501 Introduction	Plains All American Pipeline, L.P.	10/13	4
235.	O & M - 502 Unintended Valve Closure	Plains All American Pipeline, L.P.	9/10	2
236.	O & M - 503 Unintended Shutdown	Plains All American Pipeline, L.P.	9/10	2
237.	O & M - 504 Abnormal Pressure or Flow Rates	Plains All American Pipeline, L.P.	9/10	6
238.	O & M - 505 Complete Loss of Communications	Plains All American Pipeline, L.P.	9/10	2
239.	O & M - 506 Operation of a Safety Device or Failure of a Safety Device to Operate	Plains All American Pipeline, L.P.	9/10	2
240.	O & M - 507 Returning to Normal Operation	Plains All American Pipeline, L.P.	9/10	2
241.	O & M - 508 Review of Response to Abnormal Operations	Plains All American Pipeline, L.P.	9/10	2
242.	O & M - 509 Tank Overfill Alarm	Plains All American Pipeline, L.P.	9/10	2
5. Historical Documents				

Plains All American Pipeline, L.P.
Line 901 Release (5/19/15) Technical Root Cause Analysis

Reference Number	Document Name	Issued by	Dated	No of Pages
243.	_Binder 7 of 8_P.O., MTR's, O&M Manuals	All American Pipeline Company		90
244.	Insulations specifications	All American Pipeline Company		49
245.	MTRs 24inch 312wt and 500wt	Nippon Steel Corporation	12/10/85	3
246.	MTRs 24inch 344wt	Nippon Steel Corporation	12/10/85	7
6. Drawings, Maps, and Diagrams				
247.	24in As Built Field Book	Harold D. Hardin Land Surveyor	2/5/91	238
248.	CA_LSFCA_PNTCA - 001	Plains All American Pipeline, L.P.	3/7/13	1
249.	CA_LSFCA_PNTCA - 002	Plains All American Pipeline, L.P.	3/7/13	1
250.	CA_LSFCA_PNTCA - 003	Plains All American Pipeline, L.P.	3/7/13	1
251.	CA_LSFCA_PNTCA - 004	Plains All American Pipeline, L.P.	3/7/13	1
252.	CA_LSFCA_PNTCA-RMS-001	Plains All American Pipeline, L.P.	6/10/15	1
253.	PAA_0000096	Plains All American Pipeline, L.P.	9/27/13	1
254.	PAA_0000097	Plains All American Pipeline, L.P.	-	1
255.	SouthCuyamaGathering	Plains All American Pipeline, L.P.	8/26/15	1
Alignments Line 901				
256.	01 CE-COV	All American Pipeline Company		1
257.	02 CE-IND-1	All American Pipeline Company		1
258.	03 CE-IND-2	All American Pipeline Company		1
259.	04 CE-001A	All American Pipeline Company	9/11/90	1

Plains All American Pipeline, L.P.
Line 901 Release (5/19/15) Technical Root Cause Analysis

Reference Number	Document Name	Issued by	Dated	No of Pages
260.	05 CE-001B	All American Pipeline Company	4/11/90	1
261.	06 CE-001C	All American Pipeline Company	9/11/90	1
262.	07 CE-001D	All American Pipeline Company	9/11/90	1
263.	08 CE-001E	All American Pipeline Company	9/11/90	1
264.	901-D-PP-ALL_REV3	Plains All American Pipeline, L.P.	6/9/15 - 6/16/15	13
Alignments Line 903				
265.	09 CE-002	Celeron Pipeline Company of California	7/13/87	1
266.	10 CE-003	Celeron Pipeline Company of California	7/13/87	1
267.	11 CE-004	Celeron Pipeline Company of California	7/13/87	1
268.	12 CE-005	Celeron Pipeline Company of California	7/13/87	1
269.	13 CE-006	Celeron Pipeline Company of California	7/13/87	1
270.	14 CE-007	Celeron Pipeline Company of California	7/13/87	1
271.	15 CE-008	Celeron Pipeline Company of California	7/13/87	1
272.	16 CE-009	Celeron Pipeline Company of California	7/13/87	1
273.	17 CE-010	Celeron Pipeline Company of California	7/13/87	1
274.	18 CE-011	Celeron Pipeline Company of California	7/13/87	1
275.	19 CE-012	Celeron Pipeline Company of California	7/13/87	1
276.	20 CE-013	Celeron Pipeline Company of California	7/13/87	1

Plains All American Pipeline, L.P.
 Line 901 Release (5/19/15) Technical Root Cause Analysis

Reference Number	Document Name	Issued by	Dated	No of Pages
277.	21 CE-014	Celeron Pipeline Company of California	7/13/87	1
278.	22 CE-015	Celeron Pipeline Company of California	7/13/87	1
279.	23 CE-016	Celeron Pipeline Company of California	7/13/87	1
280.	24 CE-017	Celeron Pipeline Company of California	7/13/87	1
281.	25 CE-018	Celeron Pipeline Company of California	7/13/87	1
282.	26 CE-019	Celeron Pipeline Company of California	7/13/87	1
283.	27 CE-020	Celeron Pipeline Company of California	7/13/87	1
284.	28 CE-021	Celeron Pipeline Company of California	7/13/87	1
285.	29 CE-022	Celeron Pipeline Company of California	7/13/87	1
286.	30 CE-023	Celeron Pipeline Company of California	7/13/87	1
287.	31 CE-024	Celeron Pipeline Company of California	7/13/87	1
288.	32 CE-025	Celeron Pipeline Company of California	7/13/87	1
289.	33 CE-026	Celeron Pipeline Company of California	7/13/87	1
Line 903 Elevation Profile Drawings				
290.	CA_PNTCA_EMDCA-RMS-001	Plains All American Pipeline, L.P	6/10/15	1
291.	CA_LSFCA_PNTCA-RMS-002	Plains All American Pipeline, L.P	6/10/15	1
292.	CA_LSFCA_PNTCA-RMS-003	Plains All American Pipeline, L.P	6/10/15	1
293.	CA_LSFCA_PNTCA-RMS-004	Plains All American Pipeline, L.P	6/10/15	1

Reference Number	Document Name	Issued by	Dated	No of Pages
7. Public Documents				
294.	Plains Pipeline Response to 6-5-15 Congressional Letter	Plains All American Pipeline, L.P	6/19/15	14
295.	Excerpt from PAA's Anticipated 10Q Disclosure Regarding Line 901	Plains All American Pipeline, L.P.	8/7/15	1
296.	http://www.sbcountyplanning.org/energy/projects/PlainsPipeline.asp	County of Santa Barbara, Planning and Development - Energy Division		
297.	https://www.plainsallamerican.com/about-us/company-history	Plains All American Pipeline, L.P.		
298.	Prepared Oral Testimony of Patrick Hodgins - June 26, 2015 http://www.plainsline901response.com/go/doc/7266/2552586/	Plains All American Pipeline, L.P.	6/26/15	
8. Standards, Papers, etc.				
299.	NACE International Standard Practice SP0502-2010, "Pipeline External Corrosion Direct Assessment Methodology"	NACE International	2010	60
300.	NACE International Standard Practice SP0169-2007 "Control of External Corrosion on Underground or Submerged Metallic Piping Systems".	NACE International	2007	36
301.	NACE International Standard Practice SP0169-2013 "Control of External Corrosion on Underground or Submerged Metallic Piping".	NACE International	2013	60
302.	Cathodic protection criteria of thermally insulated pipeline buried in soil	Corrosion Science	43, 2001	
303.	NACE RP0198: Control of Corrosion Under Thermal Insulation and Fireproofing Materials – A Systems Approach	NACE	1998	
304.	Petrobras Transporte S.A. - Transpetro Solution for the Minimization of External Corrosion of Thermal Insulation Pipelines for Underground Heated Oil Transportation in Brazil.	Proceedings of IPC 2004	2004	
305.	On the cathodic protection of thermally insulated pipelines	Engineering Failure Analysis	16 (2009)	2047–2053
306.	Physical and Performance Properties of Coal Tar Urethanes - Pipe	NACE International	April 2 - 6, 1984	8
307.	Under Deposit Corrosion Mitigation and ILI Accuracy Improvement In a Sour Crude Gathering and Transportation System Accomplished Using Novel Chemistry	NACE International	2012	16
308.	Influence of Corrosion Products on Magnetic Flux Leakage Signals in Inspection of Farside Metal-loss Defects in Oil Storage Tank Bottom	Journal of the Japan Petroleum Institute	January 2004	9

Reference Number	Document Name	Issued by	Dated	No of Pages
309.	Recommended Practice 1163 - In-Line Inspection Systems Qualification Standard	American Petroleum Institute	August 2005	50
310.	Recommended Practice 583 - Corrosion Under Insulation and Fireproofing	American Petroleum Institute	May 2014	88
311.	NACE International Publication 10A392 (2006 Edition) Effectiveness of Cathodic Protection on Thermally Insulated Underground Metallic Structures	NACE International	2006	8
312.	ASME B31G Manual for Determining the Remaining Strength of Corroded Pipes	American Society of Mechanical Engineers	2012	60
313.	Santa Barbara County, California - Code of Ordinances - Supplement 32 Update 2 (Ordinance No. 4926) – Chapter 14	Santa Barbara County Code	6/23/15	43
314.	US Climate Data for Santa Barbara County: http://www.usclimatedata.com/climate/santa-barbara/california/united-states/usca1017/2000/1	US Climate Data	8/18/15	-
315.	Citation: A modified criterion for determining the remaining strength of corroded pipe	PRCI Contract PR-3-805	12/22/89	18
316.	49 CFR 195 - Transportation of Hazardous Liquids by Pipeline	U.S. Department of Transportation (DOT) Pipeline and Hazardous Materials Safety Administration (PHMSA)		70

APPENDIX C

Supplemental Analyses from 2015 Digs

SUPPLEMENTAL 2015 DIG ANALYSES

1.0 BACKGROUND

Four priority digs, identified as Digs 1 – 4, were performed on Line 901 between May 29, 2015 and June 3, 2015, based on the preliminary findings of the 2015 ILI run. Figure C-1 contains a topographical map and elevation plot of Line 901 showing the locations of Digs 1 - 4 relative to the failure location. All four digs were located D/S from the failure in relative low areas along the line; see Figure C-2 and Figure C-3. The locations of these digs were selected based on the maximum depths of external metal loss features on Line 901, as identified by the tool. Table C-1 identifies the features associated with the four digs and summarizes the dimensional findings [Ref 181] for each feature. The maximum corrosion depths of the measured features were all lower than the depths identified by the tool (i.e. the features were over-called by the ILI tool).

Figure C-4 – Figure C-7 contain field photographs from the four digs showing representative corrosion products associated with the external corrosion features. For all four digs, the corrosion was located at areas of disbonded coal tar urethane (CTU) coating, beneath an intact PU foam layer. The corrosion products were primarily dark brown in appearance with some areas that were rust-colored. In general, the products were dry, fairly rigid, and magnetic. Although portions of the corrosion products were removed as relatively thick, intact samples, the products were a bit more friable (i.e. crumbled) than the deposits removed near the failure location. All four samples exhibited evidence of a layered morphology; see Figure C-8.

DNV GL personnel were present during all four digs and collected various samples at each dig site for laboratory analysis. The collected samples included the following: (1) corrosion products associated with the external metal loss features, (2) swab samples for bacteria testing removed at and away from the features, (3) soil samples removed from the dig sites, and (4) insulation samples removed at the feature locations. The objectives of the analyses were to characterize the samples and to compare the results for the samples with the results obtained for samples removed near the failure location.

2.0 TECHNICAL APPROACH

The procedures used in the analyses were in accordance with industry-accepted standards. Three of the general standards governing terminology and bacteria testing used are as follows:

- NACE/ASTM G193 – 10a “Standard Terminology and Acronyms Relating to Corrosion.”

- NACE TM0106, "Detection, Testing, and Evaluation of Microbiologically Influenced Corrosion (MIC) on External Surfaces of Buried Pipelines."
- NACE TM0194, "Standard Test Method for Field Monitoring of Bacterial Growth in Oil and Gas Systems."

Corrosion products were collected during each dig for characterization. Analyses performed on these products included: (1) elemental analyses using energy dispersive spectroscopy (EDS) with a scanning electron microscope (SEM) and (2) compound identification using x-ray diffraction (XRD).

Swab samples were also obtained for bacteria analyses, over a standard area of 1 cm², at two locations per dig site (i.e. at an area of corrosion and an area where the coating was disbonded but there was negligible external corrosion). Separate swab samples were taken for serial dilution and microscopic analysis. Liquid culture media for acid-producing bacteria (APB), sulfate-reducing bacteria (SRB), nitrate-reducing bacteria (NRB), aerobic bacteria (AERO), anaerobic bacteria (ANA), and iron-related bacteria (IRB) was used for the serial dilutions to evaluate growth of various types of bacteria. A five vial serial dilution (1:10,000) was performed using each type of media.

The swab obtained for the microscopic analysis was fixed in 1% glutaraldehyde. A five microliter specimen was removed from the fixed sample and prepared for examination by drying on a microscope slide and staining with 0.1% fluorescein isothiocyanate (FITC). The sample was examined using a CFI PLAN FLUOR 100X oil immersion objective on a Nikon Eclipse 50i epifluorescent microscope equipped with a FITC filter set to determine bacteria cell counts and morphology.

Analyses were conducted on soil samples removed (in the field) from each dig site. The soils were tested for resistivity, moisture content, pH, total acidity, total alkalinity, concentration of soluble anions and cations, total dissolved solids, and linear polarization resistance; see Table C-2 for a summary of the soil related procedures. Analyses were also performed on liquids extracted from insulation samples that were removed from the feature locations at each dig site. Due to the limited sample volumes, only two of the extracts were analyzed. The extracts were analyzed for only the following: soluble anions [Cl⁻, SO₄²⁻, NO₂⁻, NO₃⁻, CO₃²⁻, HCO₃⁻], total alkalinity, and total dissolved solids.

3.0 RESULTS

3.1 Corrosion Product Analyses

3.1.1 X-ray Diffraction

Table C-3 shows the results of XRD analyses performed on the corrosion products from Digs 1 – 4. Compounds identified in all four samples were goethite ($\text{FeO}(\text{OH})$) and magnetite (Fe_3O_4). Goethite is one of the most thermodynamically stable iron oxides under aerobic (high oxygen) conditions. Conversely, magnetite is a metastable phase formed under low oxygen conditions. In Dig 4, a third compound, akaganeite ($\text{Fe}^{3+}\text{O}(\text{OH},\text{Cl})$) was also identified. Akaganeite is indicative of the presence of oxygen.

3.1.2 Energy Dispersive Spectroscopy

The results of the EDS analyses performed on the corrosion products from Digs 1 through 4 are summarized in Table C-4. The two primary constituents are iron (Fe) and oxygen (O), which are characteristic of iron oxides. Small quantities of chlorine (Cl) were identified, likely associated with chlorides. Small quantities of manganese (Mn) were identified, which is a common constituent of line pipe steels. A relatively high concentration of carbon (C) was identified in all scans, which may be from organics within the insulation, soil, and/or bicarbonate compounds found in ground water.

3.2 Microbiological Analyses

The external surfaces of Joints 6550, 12420, 12460, and 14470 from Digs 1 – 4, respectively, were swabbed over a standard area of approximately 1 cm^2 for bacterial analysis. For each pipe joint, the swabs were taken from a representative external corrosion pit and from an area away from the corrosion pit. Separate swab samples were taken from each location for the serial dilution and microscopic examination analyses. The results of the microbiological analyses are discussed below.

3.2.1 Serial Dilution – Liquid Culture Media

Table C-5 shows the results of the bacteria serial dilution testing for the swab samples collected from the pipe joints. The results reveal that the majority of the swab samples exhibited a positive indication for five types of bacteria (APB, AERO, ANA, IRB, and NRB). Only the swab samples taken at an area away from the corrosion feature for Digs 2 and 4 were positive for all six bacteria types (i.e. AERO, ANA, APB, SRB, IRB, and NRB). As seen in the table, the highest concentration of bacteria detected was 100,000 bacteria per cm^2 , which is a relatively high value. There was no evidence to indicate that bacteria were preferentially flourishing at the corrosion pits. In many cases, higher concentrations of bacteria were found in the swabs taken from areas away from the corrosion features.

3.2.2 Microscopic Examination for Total Bacteria

The swabs collected from the four dig locations were fixed in 1% glutaraldehyde and examined using epifluorescent microscopy. The practical minimum detection limit for this method is approximately 10^3 cells/ml of fixed sample. The results of the analysis are provided in Table C-6. As seen in the table, rod-shaped cells were detected for all the swab samples. The calculated concentration of cells for the swab samples ranged between 2.10×10^4 cells/mL and 2.8×10^4 cells/mL, which are high values. This type of microscopic examination does not differentiate between living and non-living organisms.

3.3 Soil Analyses

Table C-7 is a summary of the soil samples collected by DNV GL during the four priority digs performed in 2015. Information on the soil samples collected near the failure location are also provided in the table for comparison. The first column in the table identifies the location where the sample was obtained. Columns 2, 3, and 4 provide DNV GL's designation for the soil, the associated Arcsset number ID, and a brief field description of the soil, respectively. Columns 5 and 6 provide the joint number where the soil was taken and whether the soil was analyzed.

Six (6) soil samples were removed from the dig site near the failure location; see Table C-7. Two samples were collected from under the pipe at each of three locations: 8 feet U/S of GW 5930 (IDs 10000151761 & 10000151762), 2 feet D/S of the failure location (IDs 10000151753 & 10000151759), and 12.5 feet D/S of GW 5940 (IDs 10000151754 & 10000151755). The only samples not contaminated with product, and thus representative of the soil prior to the failure, were the samples collected 8 feet U/S of GW 5930. One of these samples, ID 10000151761, was analyzed. Figure C-9 is a photograph of Soil 10000151761 in the shipped bag. The soil consisted of clumps in a variety of sizes that were cream to tan colored in appearance.

Five (5) additional soil samples were removed during the four priority digs performed following the release; see Table C-7. The soil from Dig 1 (ID 10000151758) was removed below the pipe at a GW on Joint 6550, which was located west or D/S of the failure location. The soils from Dig 2 (ID 100151751) and Dig 3 (ID 1000195234) were removed at the pipe on Reference Joint 12420 and under the pipe at Reference Joint 12460, respectively. Both digs were located D/S of the failure location. The soil samples removed from Dig 4 (IDs 10000195233 and 10000195232) were collected from the top of the pipe from Reference Joint 14470, near a corrosion feature. Dig 4 was located D/S of the failure location. Only one of the samples from Dig 4 (ID 10000195233) was analyzed. Figure C-10 contains photographs of the four soils that were analyzed from Digs 1 – 4. All four soils consisted of

clumps. The soils from Digs 1 and 3 consisted of equally sized larger rocks, while the soils from Digs 2 and 4 consisted of rocks of varying sizes. The soil from Dig 1 was black to charcoal in appearance, while the soils from Digs 2 – 4 were cream to tan in appearance.

The following steps were performed for the soil analyses. The soil samples were collected, shipped, and handled in accordance with DNV GL's standard operating procedure for soils. Analysis began with each soil sample pulverized into small pieces. The soils were then sifted through a #10 sieve (2.0 mm particle size) to remove gravel, leaving soil particles classified as sand, silt, and clay. The selected soils were tested for pH, moisture content, and resistivity. Testing was also performed to estimate the corrosion rate of carbon steel within the soil using linear polarization resistance (LPR), which is an electrochemical technique. Next, water soluble anions and cations were extracted from the soils, using a 5:1 water to soil ratio, to determine their relative concentrations. The extracts were also tested to determine the total acidity, total alkalinity, and total dissolved solids present in each extract. The procedures used in the analysis were in accordance with industry-accepted standards, which are summarized in ¶Table C-2. The results of the analyses are provided in ¶Table C-8 – ¶Table C-10.

In general, the results of the analyses revealed that the soil removed near the failure location exhibited more corrosive properties, as received, than those soils removed from the priority dig locations. This conclusion is based on the following results for the as-received soil removed near the failure location: (1) the higher moisture content, (2) the lower resistivity, (3) the higher determined corrosion rate, and (4) the higher levels of sulfate (SO_4^{2-}) anions. All five soil samples exhibited more corrosive properties in the saturated condition. In general, the soil removed near the failure location exhibited the most corrosive properties. This soil exhibited the lowest resistivity and the second highest corrosion rate in the saturated condition. Based on the findings, the corrosive properties of the soil are impacted by moisture content, which is expected.

3.4 Insulation Extract Analyses

During Digs 1 – 4, DNV GL collected samples of the insulation that had been in contact with the pipe at each feature location. The samples were bagged and shipped to DNV GL's laboratory in Columbus, OH, where the liquids within the samples were extracted. ¶Figure C-11 is a photograph showing the liquids extracted from the insulation samples from each dig. ¶Table C-11 provides a summary and description of the four extracted samples. The volume of extracted liquids varied from approximately 20 to 120 mL. The extracts from the insulation samples from Digs 1 and 4 were relatively clear in appearance, while the extracts from the insulation samples from Digs 2 and 3 were rust-colored in appearance. Based on

the limited extract volumes, two representative samples were selected for chemical analysis. One sample (i.e. Dig 2 sample) was selected to represent a rust-colored extract and the second sample (i.e. Dig 4 sample) was selected to represent a clear extract.

Table C-12 is a summary of the chemical analyses performed on the Dig 2 and Dig 4 insulation extracts. Due to the limited sample volumes, these samples were analyzed for only the following: soluble anions [Cl^- , SO_4^{2-} , NO_2^- , NO_3^- , CO_3^{2-} , HCO_3^-], total alkalinity, and total dissolved solids. The concentrations of soluble anions were consistently higher for the Dig 2 Extracts compared to the Dig 4 Extracts. Both extract samples exhibited higher levels of chlorides (Cl^-), nitrates (NO_3^-), sulfates (SO_4^{2-}), and bicarbonates (HCO_3^-) than the soil samples that were removed from these locations. These findings indicate that a higher concentration of corrosive species may have been in contact with the pipe at these locations. Furthermore, the insulation may facilitate the concentration process as the insulation experiences wet-dry cycling.

4.0 SUMMARY OF FINDINGS

- The corrosion products
 - ◆ Are primarily dark brown in appearance with some areas that were rust-colored.
 - ◆ Are dry, rigid, and magnetic.
 - ◆ Consist of a layered morphology comprised primarily of goethite and magnetite.
- There is no strong evidence to indicate that MIC played a primary role in the observed external corrosion observed for Digs 1 – 4.
- The results of analyses performed on soil samples, removed near the failure and dig locations, revealed that the soil removed near the failure location exhibited more corrosive properties.
- Analyses of liquids extracted from insulation samples removed near the corrosion features from Digs 1 – 4 revealed higher concentrations of corrosive species (i.e. chlorides) than their respective soil samples.

Table C-1. Summary of features identified during Priority Digs 1 – 4 performed in 2015.

Priority Dig Number	Reference Joint	Log Distance of Feature (ft)	Tool Call	Tool Calls		Max Depth Field (%)
				Max Length (in)	Max Depth (%)	
Dig 1	6550	23785.8	External metal loss	0.75	85	72
Dig 2	12420	44719.8	External metal loss	0.87	72	54
Dig 3	12460	44874.43	External metal loss	1.98	53	49.3
		44877.52	External metal loss	0.98	83	74
Dig 4	14470	51640.00	External metal loss	0.88	71	65
		51640.27	External metal loss	0.83	57	56.3

Table C-2. Summary of Soil Related Procedures.

Test Parameter	Methodology	Standard
Soil Handling	Soil Permit Guidelines	N/A
Soil Extraction	Water extraction of soluble anions and cations	SW846-1311, 1312 (modified)
pH	1:1 slurry	ASTM D4972
Resistivity, As Received or Saturated	4pt Wenner method	ASTM G57, AASHTO T288-91
Moisture Content	weight loss technique	ASTM D2216, AASHTO T265
Corrosion Rate of Soil by LPR	Linear Polarization Resistance	ASTM G5, G15, G59, G102, Linear Polarization Resistance Measurement
Soluble Anions		
Nitrite, NO ₂ ⁻	Colorimetric, auto	Analytical method: EPA 353.2
Nitrate		
Chloride, Cl ⁻	Ion chromatography	Analytical method: EPA 300.0
Sulfate, SO ₄ ²⁻		
Sulfide, S ²⁻	Colorimetric	Analytical method: SM 4500-S2-D
Carbonate, CO ₃ ²⁻	Titrimetric	Analytical method: SM2320B
Bicarbonate, HCO ₃ ⁻		
Total Alkalinity		
Total Acidity	Titrimetric	Analytical method: SM2310B
Soluble Cations		
Calcium, Ca ²⁺	ICP	Analytical method: EPA 6010; Preparation Method: EPA 3010
Magnesium, Mg ²⁺		
Potassium, K ⁺		
Sodium, Na ⁺		
Total Dissolved Solids (TDS)	Gravimetric residue	Analytical method: SM2540C

Table C-3. Results of compound analyses, using X-ray diffraction, performed on corrosion products from Digs 1 – 4.

Compound	Dig 1	Dig 2	Dig 3	Dig 4
Goethite – FeO(OH)	Present	Present	Present	Present
Magnetite – Fe ₃ O ₄	Present	Present	Present	Present
Akaganeite – FeO(OH)	–	–	–	Present

Table C-4. Results of elemental analyses, using EDS, performed on corrosion products from Digs 1 – 4 compared to ideal chemistry compositions of goethite and magnetite; values presented in mass percent (wt.%).

Elements	Dig 1	Dig 2	Dig 3	Dig 4	Goethite (FeOOH)	Magnetite (Fe₃O₄)
Carbon (C)	9.9	7.9	4.6	4.8	–	–
Oxygen (O)	34.2	33.2	34.7	34.4	36.01	27.64
Sodium (Na)	–	0.6	–	–	–	–
Silicon (Si)	–	0.2	–	–	–	–
Chlorine (Cl)	0.3	0.4	0.3	0.3	–	–
Manganese (Mn)	0.5	0.5	0.9	0.7	–	–
Iron (Fe)	55.1	57.2	59.5	59.8	62.85	72.36

Table C-5. Results of bacteria analyses performed on swabs taken, over an ~1 cm² area, from the external surfaces of Joints 6550, 12420, 12460, and 14470 during Digs 1 – 4, respectively, at and away from corrosion features.

Bacteria Type	Dig 1 (Joint 6550)				Dig 2 (Joint 12420)			
	Pit		Area Away		Pit		Area Away	
	Test Result	Number of Positive Vials	Test Result	Number of Positive Vials	Test Result	Number of Positive Vials	Test Result	Number of Positive Vials
Aerobic (AERO)	Positive	3	Positive	5	Positive	3	Positive	4
Anaerobic (ANA)	Positive	2	Positive	5	Positive	3	Positive	2
Acid-Producing (APB)	Positive	3	Positive	5	Positive	2	Positive	4
Sulfate-Reducing (SRB)	Not detected	–	Not detected	–	Not detected	–	Positive	2
Iron-Related (IRB)	Positive	1	Positive	5	Not detected	–	Positive	3
Nitrate-Reducing (NRB)	Positive	3	Positive	5	Positive	5	Positive	4

Bacteria Type	Dig 3 (Joint 12460)				Dig 4 (Joint 14470)			
	Pit		Area Away		Pit		Area Away	
	Test Result	Number of Positive Vials	Test Result	Number of Positive Vials	Test Result	Number of Positive Vials	Test Result	Number of Positive Vials
Aerobic (AERO)	Positive	5	Positive	5	Positive	5	Positive	5
Anaerobic (ANA)	Positive	5	Positive	5	Positive	5	Positive	5
Acid-Producing (APB)	Positive	4	Positive	4	Positive	3	Positive	5
Sulfate-Reducing (SRB)	Not Detected	–	Not Detected	–	Not Detected	–	Positive	1
Iron-Related (IRB)	Positive	5	Positive	4	Positive	2	Positive	4
Nitrate-Reducing (NRB)	Positive	5	Positive	5	Positive	4	Positive	4

Bacteria Concentration Key:

- 1 10 bacteria per cm²
- 2 100 bacteria per cm²,
- 3 1,000 bacteria per cm²,
- 4 10,000 bacteria per cm²,
- 5 100,000 bacteria per cm²

Table C-6. Results of optical microscopy examination for fixed swab samples taken, over an ~1 cm² area, from the external surfaces of Joints 6550, 12420, 12460, and 14470 during Digs 1 - 4, respectively, at and away from corrosion features.

Dig Number	Sample Identification	Aliquot Volume, uL	Total Cells Observed	Calculated No cells/mL	Morphology
1	Pit	5	>20	2.80×10^4	Rod
	Area Away	5	>20	2.80×10^4	Rod
2	Pit	5	>20	2.80×10^4	Rod
	Area Away	5	15	2.10×10^4	Rod
3	Pit	5	16	2.20×10^4	Rod
	Area Away	5	>20	2.80×10^4	Rod
4	Pit	5	>20	2.80×10^4	Rod
	Area Away	5	18	2.50×10^4	Rod

Table C-7. Summary of soil samples collected by DNV GL.

	DNV GL Designation	Sample ID (ArcSSETT #)	Field Description	Reference Joint	Analyses Performed
Soils Near Failure Location	Near Failure	10000151761	@ 8 ft U/S of U/S GW 5930 below pipe	5920	Yes
	–	10000151762	@ 8 ft U/S of U/S GW 5930 below pipe	5920	No ¹
	–	10000151753	2 ft D/S of leak location	5930	No ²
	–	10000151759	2 ft D/S of leak location	5930	No ²
	–	10000151754	12.5 ft D/S of GW 5940	5940	No ²
	–	10000151755	12.5 ft D/S of GW 5940	5940	No ²
Priority Dig Soils	Dig 1	10000151758	Soil from dig West of leak location below pipe @ GW	6550	Yes
	Dig 2	10000151751	Dig 2 @ pipe	12420	Yes
	Dig 3	10000195234	Dig 3 Soil under pipe	12460	Yes
	–	10000195232	Dig 4 soil @ top of pipe near corrosion S/N 1 of 2 6/03/15	14470	No ¹
	Dig 4	10000195233	Dig 4 soil @ top of pipe near corrosion S/N 2 of 2 6/03/15	14470	Yes

- 1 - Duplicate sample
- 2 - Sample contaminated with crude oil

Table C-8. Summary of various chemical and electrochemical properties for soil samples.

DNV GL Designation	pH Soil	Moisture Content (%) ¹	Resistivity (Ohm-cm)		Corrosion Rate (mpy)	
			As Received	Saturated	As Received	Saturated
Near Failure	7.95	27.59	3,800	400	2.517	2.718
Dig 1	8.53	18.31	2,500	810	0.359	1.933
Dig 2	8.21	11.57	29,000	580	0.160	2.244
Dig 4	8.52	12.77	78,000	12,000	0.094	2.328
Dig 3	7.56	6.80	14,000	690	0.410	4.405

1 – Percent moisture per AASHTO T265 & ASTM D2216

Table C-9. Summary of soluble cation and anion concentrations for soil samples removed near the failure location and from Digs 1 – 4.

DNV GL Designation	Soluble Cations mg/L				Soluble Anions, mg/L						
	Ca ²⁺	Mg ²⁺	Na+	K+	NO ₂ ⁻	NO ₃ ⁻	Cl ⁻	SO ₄ ²⁻	S ²⁻	CO ₃ ²⁻	HCO ₃ ⁻
Near Failure	898	320.	495	9.64	<2.1	114.84	117	3600	<0.67	<13.3	204
Dig 1	18.0	<6.10	218	<6.10	<2.0	12.68	29	49	<0.61	<12.2	744
Dig 2	53.0	38.7	413	8.88	10.472	40.33	78.6	338.8	<0.57	<11.4	529.5
Dig 3	9.57	<5.77	493	5.88	<1.9	21.18	108	200	<0.58	<11.5	524
Dig 4	60.0	24.8	95.2	<5.41	<1.8	9.09	26	206	<0.54	<10.8	146

Table C-10. Summary of various chemical properties determined for soil samples removed near the failure location and from Digs 1 – 4.

DNV GL Designation	Total Alkalinity (mg CaCO₃/L)	Total Acidity (mg CaCO₃/L)	Total Dissolved Solids (TDS) (mg/L)
Near Failure	204	< 66.5	6350
Dig 1	744	< 61.0	640
Dig 2	530	< 56.9	1550
Dig 3	524	< 57.7	1390
Dig 4	146	< 54.1	622

Table C-11. Summary of liquids extracted from insulation samples collected by DNV GL during Priority Digs 1 – 4 performed in 2015.

Extract Identification	Reference Joint	Sample ID (ArcSSETT #)	pH at Pipe/Insulation Interface (Field measurement)	Estimated Extracted Volume (mL)	Extract Appearance	Chemical Analysis Performed
Dig 1 Extract	6550	10000151104	6 – 7	20	Clear	No
Dig 2 Extract	12420	10000151105	7 – 8	120	Rust-colored	Yes
Dig 3 Extract	12460	10000151106	7	60	Rust-colored	No
Dig 4 Extract	14470	10000151107	6	40	Clear	Yes

Table C-12. Summary of results of chemical analyses performed on liquids extracted from the insulation removed during Priority Digs 2 and 4 performed in 2015.

Sample ID	Soluble Anions (mg/L)						Total Alkalinity As CaCO₃ (mg/L)	Total Dissolved Solids (mg/L)
	NO₂⁻	NO₃⁻	Cl⁻	SO₄⁻	CO₃²⁻	HCO₃⁻		
Dig 2 Extract	48.0	739.28	1080	2000	< 2.0	397	397	7470
Dig 4 Extract	< 1.6	30.10	329	993	< 2.0	102	102	2020

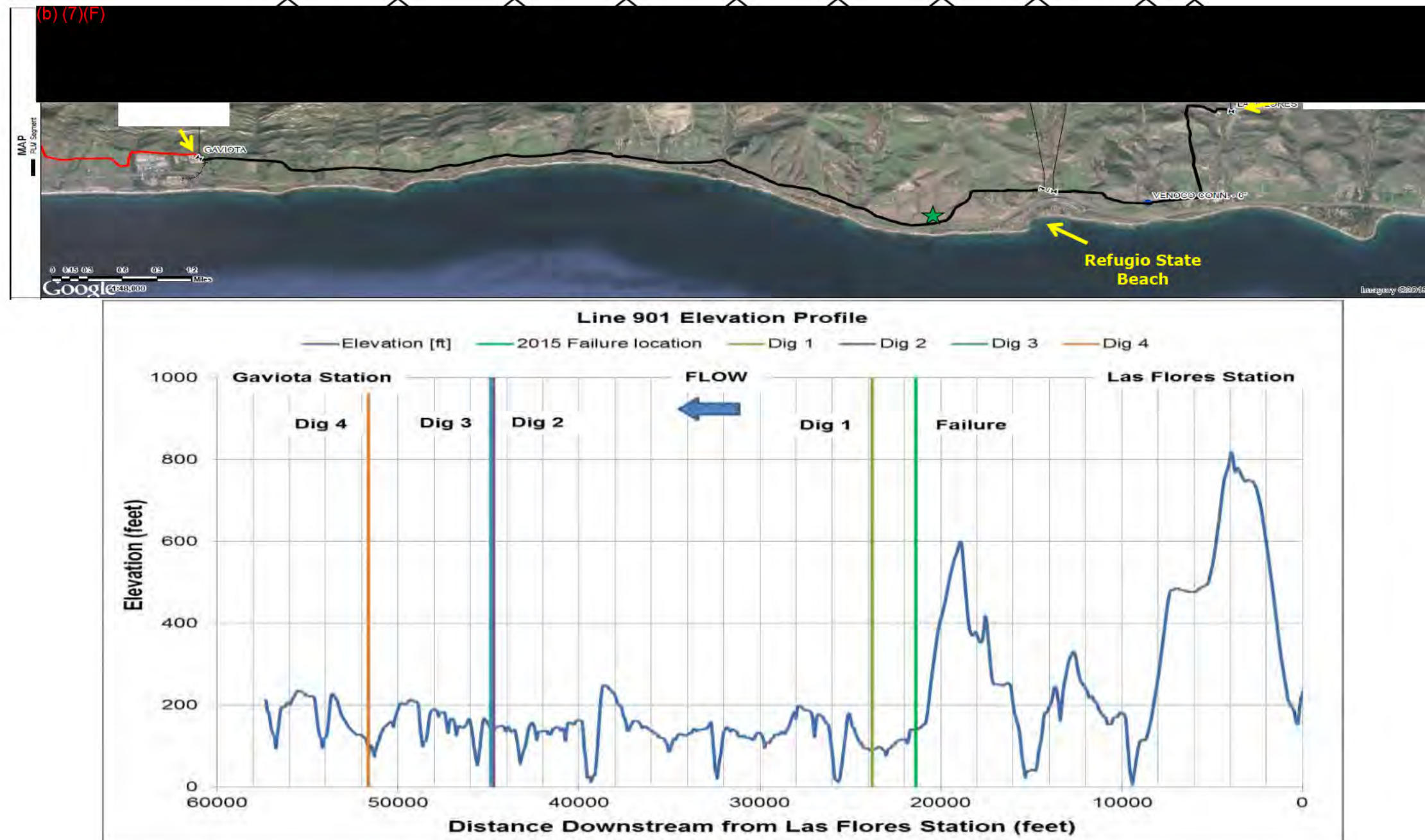
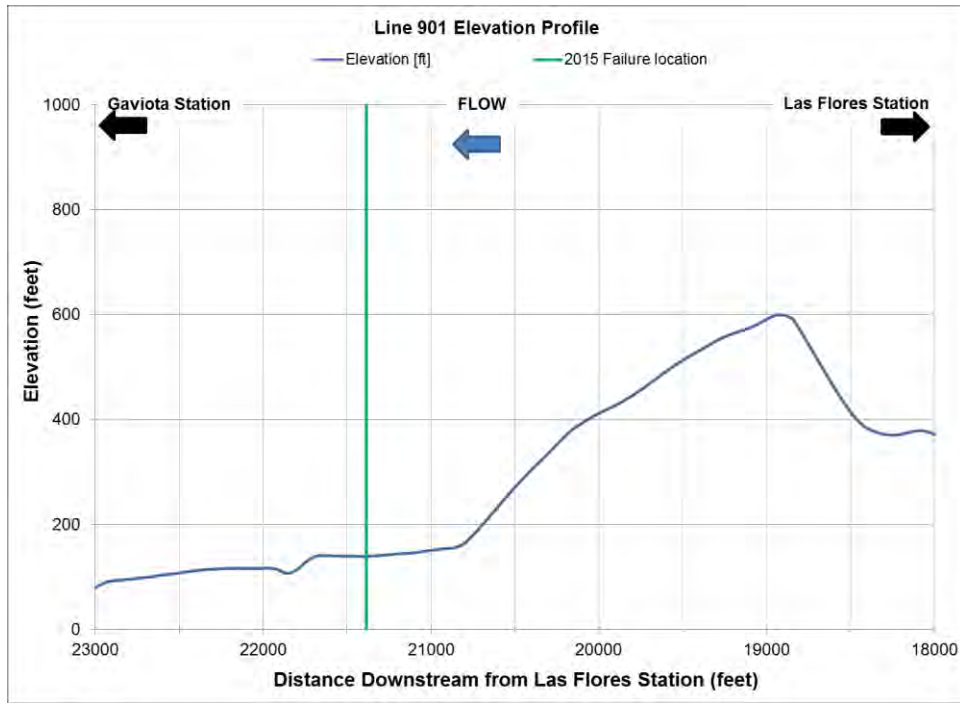
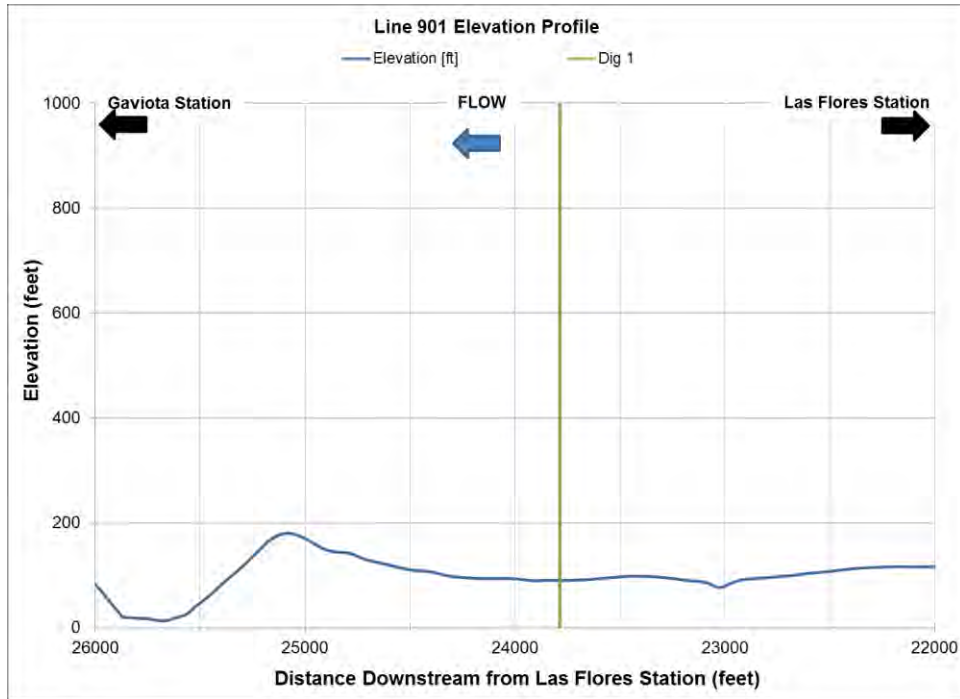


Figure C-1. Topographical map and elevation plot showing the locations of Priority Digs 1 – 4 relative to the failure location. The white triangles on the map correspond to mile post markers. The green star on the map and the green line on the plot identify the location of the May 19, 2015 failure.

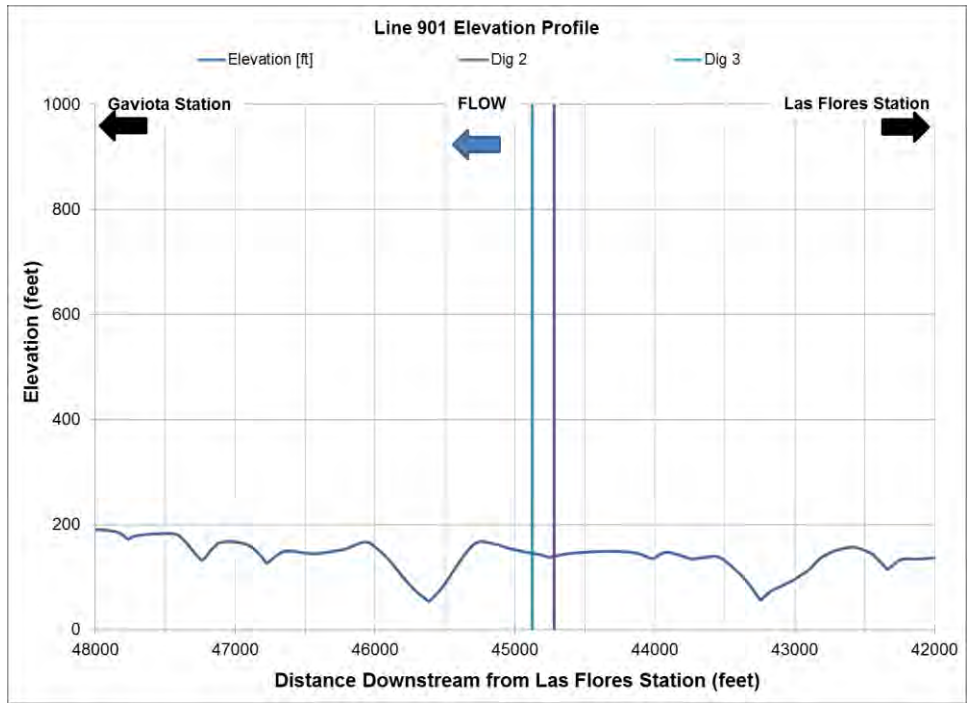


(a) Failure Location

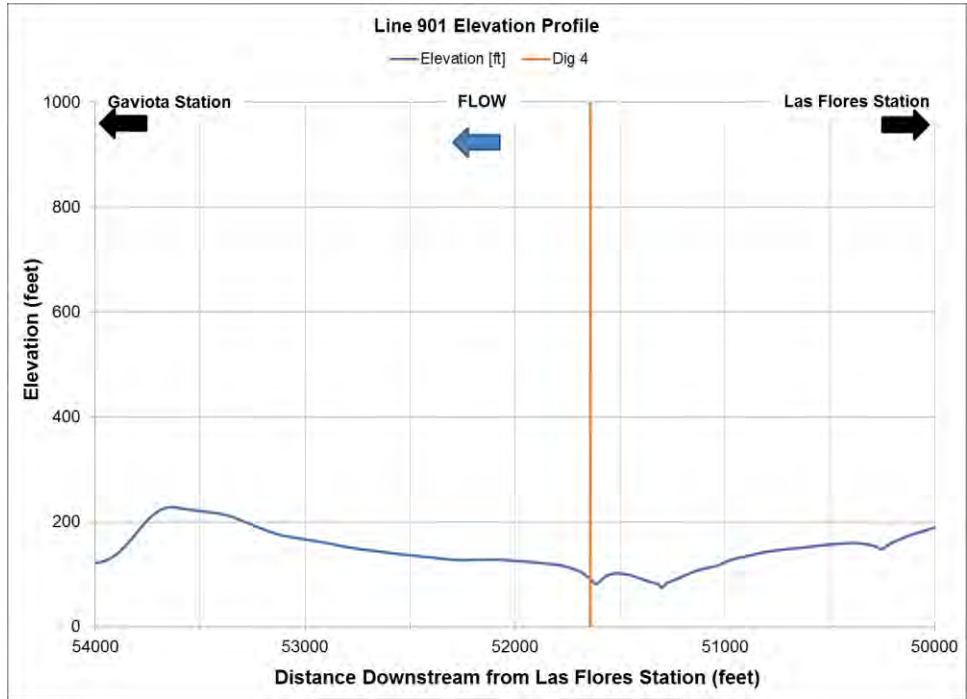


(b) Dig 1 Location

Figure C-2. Plots showing close-ups of the elevation profile of Line 901 at: (a) the failure location and (b) the location of Dig 1.



(a) Dig 2 and 3 Locations



(b) Dig 4 Location

Figure C-3. Plots showing close-ups of the elevation profile of Line 901 at: (a) the locations of Digs 2 and 3 and (b) the location of Dig 4.

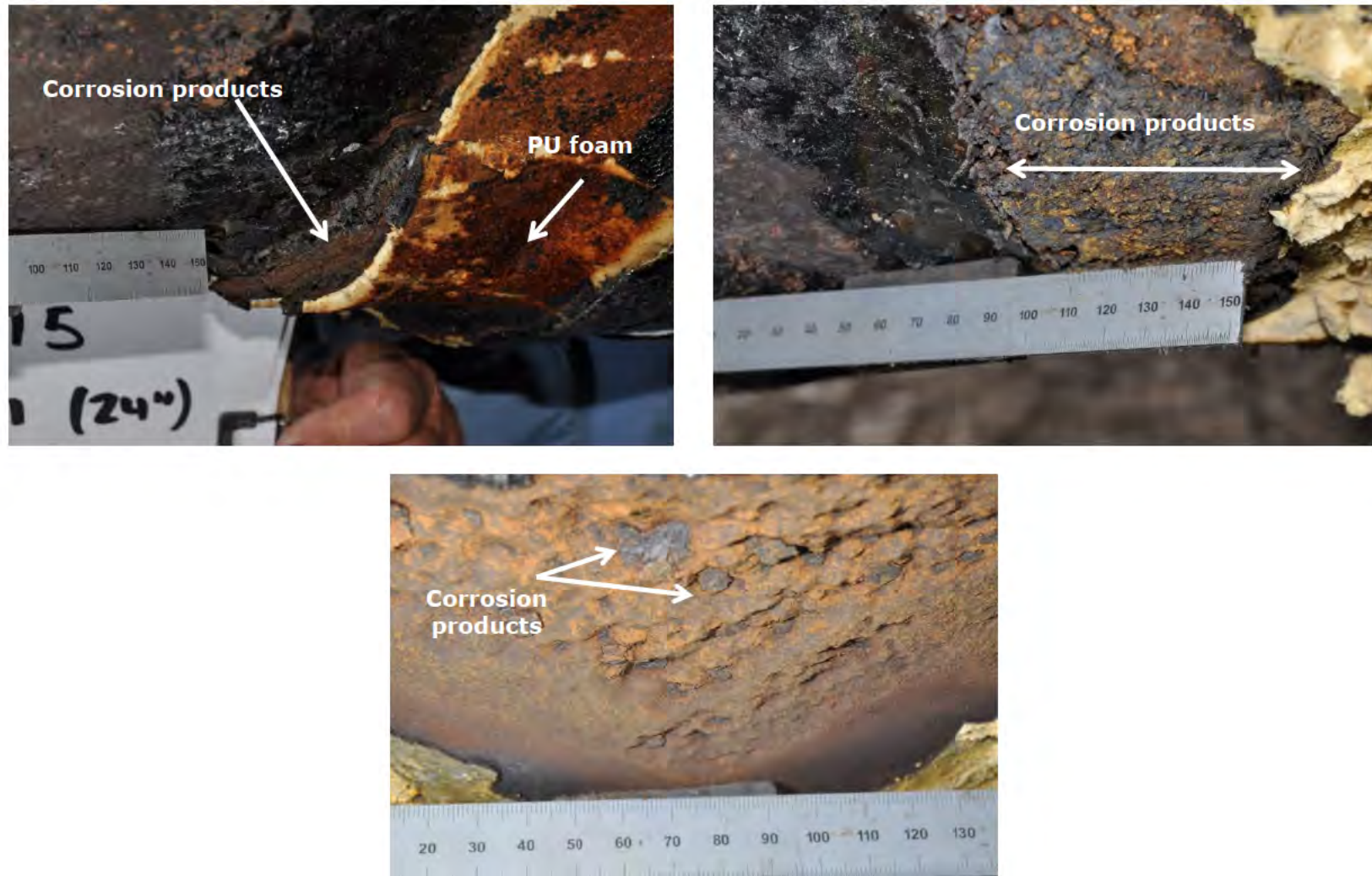


Figure C-4. Field photographs showing the corrosion products associated with the external metal loss feature from Dig 1.

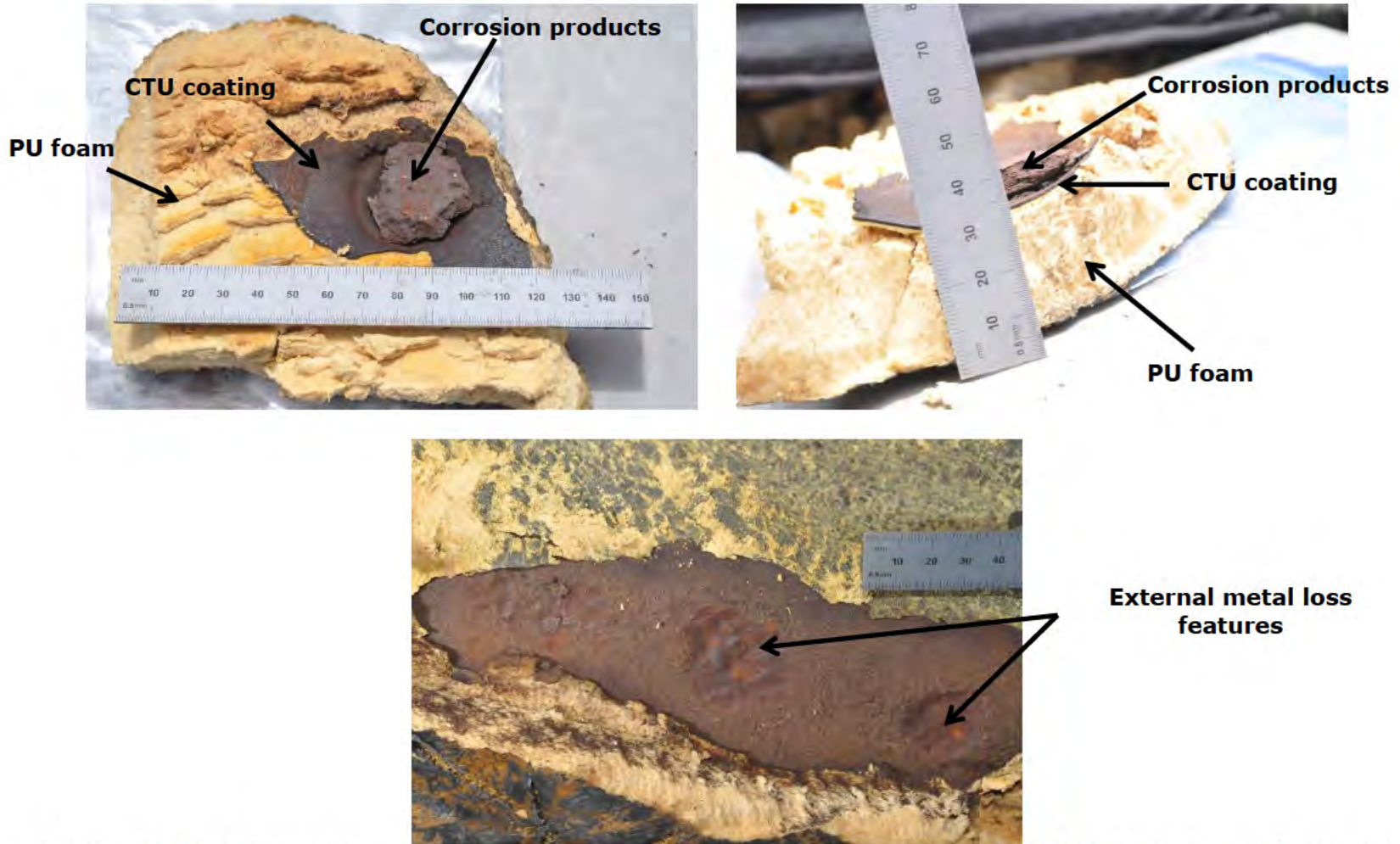


Figure C-5. Field photographs showing representative corrosion products associated with the external metal loss features from Dig 2.

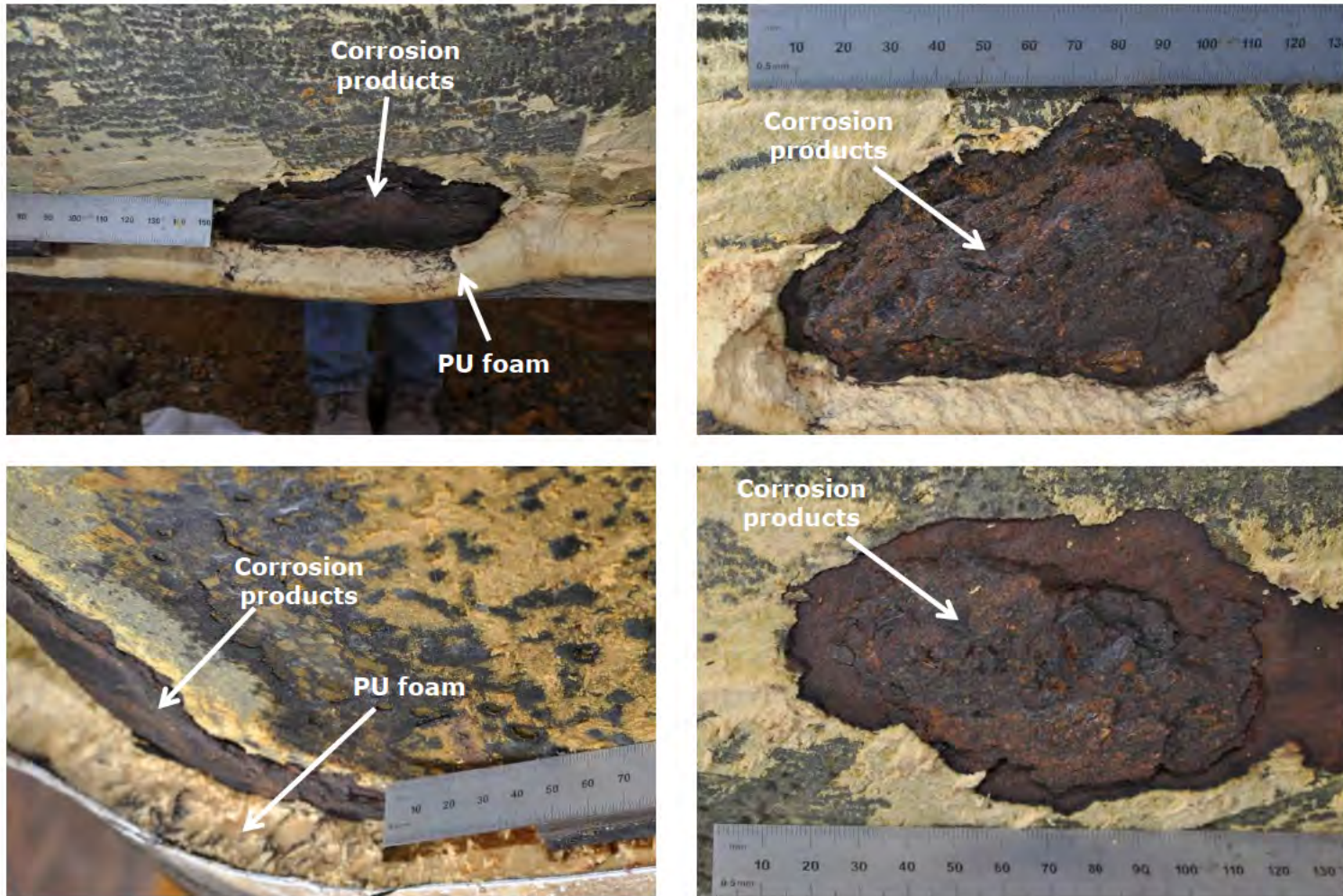


Figure C-6. Field photographs showing representative corrosion products associated with the external metal loss features from Dig 3.



Figure C-7. Field photographs showing representative corrosion products associated with the external metal loss features from Dig 4.



Figure C-8. Photographs showing the layered morphology of representative corrosion products associated with the external metal loss features from Digs 1 – 4.



Figure C-9. Photograph of Soil 10000151761, as-received, that was removed near the failure location. The scale pictured is in mm.



Figure C-10. Photograph of as-received soil for Priority Digs 1 - 4. The scales pictured are in mm.

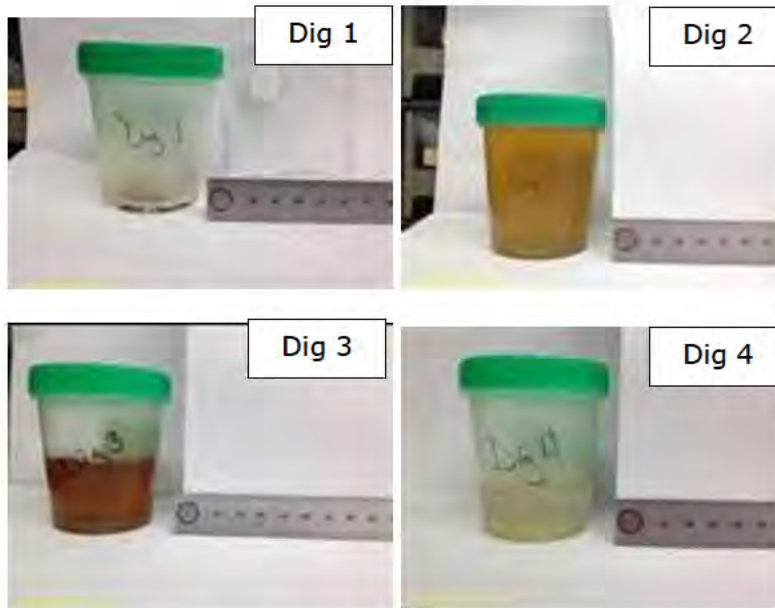


Figure C-11. Photographs of liquids extracted from insulation collected by DNV GL during 2015 Priority Digs 1 - 4.

APPENDIX D

Corrosion Products Supplemental Analyses

Density Testing

CORROSION PRODUCT SUPPLEMENTAL ANALYSES DENSITY TESTING

1.0 BACKGROUND

DNV GL was requested by PHMSA to perform density and magnetic permeability testing on corrosion product samples removed near the 2015 failure location on Line 901. These tests were not part of the original scope of the metallurgical analysis performed by DNV GL and so were added to the root cause analysis (RCA). The results from the density testing are summarized in this appendix, while the results of the magnetic permeability testing are summarized in Appendix E.

Density testing was performed on a representative corrosion product sample, identified as Corrosion Product Sample 10000195318, removed near the 2015 failure. The sample was collected along the 6:00 o'clock orientation, 17.8 – 19.5 feet from the upstream girth weld. The objectives of the analysis were to determine the approximate density of the sample and compare the results with the density of steel.

2.0 TECHNICAL APPROACH

The density testing was performed using a Model XS 205 balance manufactured by Mettler Toledo and equipped with a density determination kit. This equipment was used to calculate the density of the corrosion product sample based upon Archimedes' principle, which states that *"any body immersed in a fluid becomes lighter by an amount equal to the weight of the fluid that has been displaced."*

The testing involved weighing the corrosion product in air and then in an auxiliary fluid; deionized (DI) water. The density of the corrosion product was then calculated using the following two equations:

$$\rho = \frac{A}{A-B}(\rho_o - \rho_L) + \rho_L \quad \text{With compensation for air density}$$

$$\rho = \frac{A \cdot \rho_o}{A-B} \quad \text{Without compensation for air density}$$

Where:

ρ = density of the sample

ρ_o = density of the auxiliary liquid

ρ_L = density of air (0.0012 g/cm³)

A = weight of the sample in air

B = weight of the sample in the auxiliary liquid

3.0 RESULTS

Figure D-1 is a photograph showing the sample that was removed from Corrosion Product Sample 10000195318 for the density testing.¹ The sample was irregular in shape with a maximum length, width, and thickness of approximately 2.33 inches, 1.28 inches, and 0.534 inches, respectively. Note that one edge of the sample was cut with a Dremel tool equipped with a cutting blade. The sample was rigid, non-friable, and easily handled. Figure D-2 and Figure D-3 contain photographs showing the test setup for measuring the weight of the sample in air and in water, respectively. Due to the presence of air within the sample, the weight of the sample in water was taken only after all large air bubbles escaped from the surface of the sample. This process took approximately 30 minutes.

Table D-1 provides a summary of the weights obtained for the sample in both air and water. The weights are provided in both milligrams, which was the value reported by the balance, and in grams. As expected, the weight of the sample in air was greater than the weight of the sample in water. Table D-2 summarizes the density values calculated for the sample, with and without compensation for the density of air, based on the measurements in Table D-1. The values are very similar, ranging from 3.533 to 3.537 g/cm³ with and without compensating for the density of air. These values were compared to the density for mild steel (i.e. 7.87 g/cm³). The densities obtained for the corrosion product samples were approximately 45% of the density of low carbon steel.

¹ Note: Only a portion of Corrosion Product Sample 10000195318 was needed for the density testing (i.e. the entire sample was not consumed for this testing).

Table D-1. Summary of weights measured for Corrosion Product Sample 10000195318 during the density testing.

Testing Environment	Density of Testing Environment (g/cm ³)	Weight (mg)	Weight (g)
Air	0.0012 (P _L)	39794.36	39.79436 (A)
DI water	0.99819 ¹ (P _o)	28563.52	28.56352 (B)

1 – Density of water at 20.2 °C (i.e. temperature measured at time of testing) per Table 7.7 in the operating instructions manual for Excellence Balances, XS Models.

Where: P_o = density of the auxiliary liquid A = weight of the sample in air
 P_L = density of air (0.0012 g/cm³) B = weight of the sample in the auxiliary liquid

Table D-2. Summary of density values calculated for Corrosion Product Sample 10000195318 based on the data in Table D-1.

Density of Corrosion Product (g/cm ³)	Compensation for Air Density	Density of Mild Steel (g/cm ³)
3.533	Yes ¹	7.87 ³
3.537	No ²	

1- $\rho = \frac{A}{A-B}(\rho_o - \rho_L) + \rho_L$; see Table D-1 for A, B, ρ_o , and ρ_L

2- $\rho = \frac{A \cdot \rho_o}{A-B}$; see Table D-1 for A, B, ρ_o , and ρ_L

3 – Density for 0.06% C steel. Metals Handbook Desk Edition, Second Edition 1998 p. 64.



Figure D-1. Photograph showing the portion of Corrosion Product 10000195318 that was used for the density testing. Scale is in inches

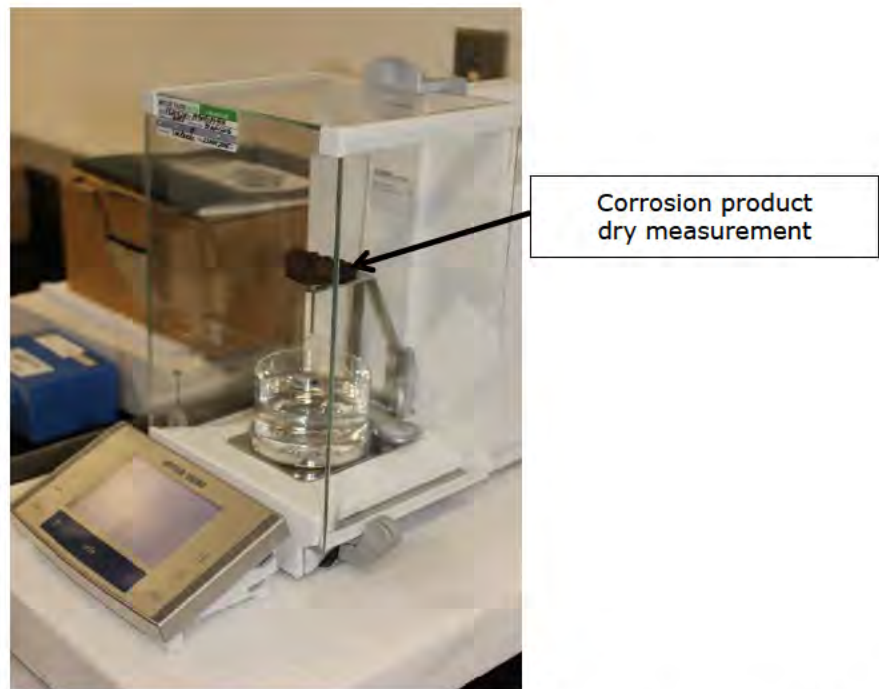


Figure D-2. Photograph showing the test setup used to measure the dry weight of the corrosion product.

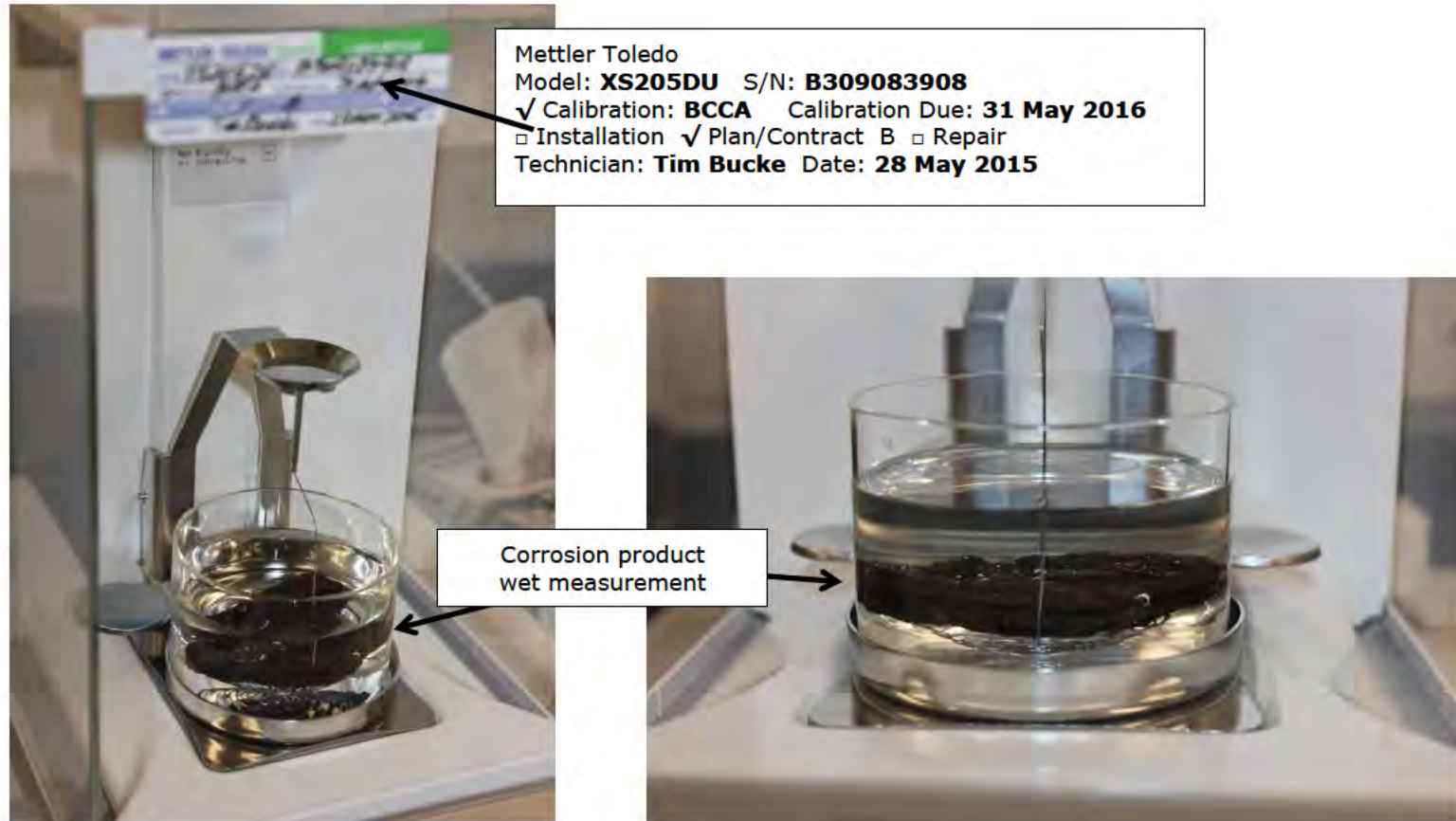


Figure D-3. Photographs showing the test setup (Left) and close-up of the sample (Right) during the submerged testing.

APPENDIX E

Corrosion Products Supplemental Analyses Magnetic Permeability Testing

CORROSION PRODUCT SUPPLEMENTAL ANALYSES MAGNETIC PERMEABILITY TESTING

1.0 BACKGROUND

DNV GL was requested by PHMSA to perform density and magnetic permeability testing on corrosion product samples removed near the 2015 failure location on Line 901. These tests were not part of the original scope of the metallurgical analysis performed by DNV GL and so were added to the root cause analysis (RCA). The results from the magnetic permeability testing are summarized in this appendix, while the results of the density testing are summarized in Appendix D.

Two representative corrosion product samples and a steel plate sample, all removed from the pipe joint that contained the failure, were selected for the magnetic permeability testing. Identifications and descriptions of the selected samples are provided in Table E-1 and photographs of the samples are provided in Figure E-1 and Figure E-2, respectively. The corrosion product samples are identified as Sample 10000195331 (i.e. sample exposed to crude oil) and Sample 10000195318 (i.e. dry sample). The steel sample selected for the testing is identified as Sample 10000195363. Only portions of the corrosion products and the steel sample were used for the testing. Specifically, two specimens were removed from each sample type described above. The testing did not consume all of the product/material available for the three samples.

The objectives of the testing were to measure and compare the magnetic properties of the corrosion product samples with those measured for the plate steel.

2.0 EXPERIMENTAL DETAILS

2.1 Test Technique

The test method used for the magnetic property testing was in accordance with industry-accepted standard ASTM A773 / A773M, "*Standard Test Method for Direct Current Magnetic Properties of Low Coercivity Magnetic Materials Using Hysteresigraphs.*" This test method provides instructions on how to produce plots of magnetic induction (B, magnetic flux density) vs. magnetic field strength (H), from which basic magnetic properties for soft and semi-hard materials are determined.

The curves were evaluated to determine the following parameters (see Figure E-3):

- Coercive force (H_c) in Oersteds (Oe)
- Residual magnetization (B_r) in Gauss (G)

- Maximum magnetic field strength (H_{max}) in Oe
- Maximum induction (B_{max}) in G

Based on the above determine values, the following magnetic permeability values, which are dimensionless, were calculated using the equations provided below.

- Initial magnetic permeability (μ_{in})
- Maximum magnetic permeability ($\mu_{r\ max}$)
- Magnetic permeability amplitude ($\mu_r\ amp$)

$$B = B_i + H \quad \text{Relative magnetic permeability of material}$$

$$\mu_{r\ amp} = \frac{B}{H} \quad \text{Amplitude magnetic permeability}$$

$$\mu_{r\ diff} = \frac{dB}{dH} \quad \text{Differential magnetic permeability}$$

where: H = magnetic field strength [Oe]
 B = normal induction in test specimen [G]
 B_i = intrinsic induction in test specimen [G]

2.2 Specimen Preparation

Based on the test technique identified for this analysis, bar specimens were prepared from the corrosion products and steel samples selected. Two specimens per sample were prepared (i.e. six total specimens).

The initial proposed dimensions for the test specimens were 3-inches in length by 0.5-inches in width by 0.25-inches in height. The width and height selected for the specimens were based on minimum allowances identified for the testing. During the course of the specimen preparation, the actual heights achieved for the corrosion product specimens were greater than the minimum 0.25 inches previously selected. So as not to significantly alter the nature of the deposits from their field condition, it was decided to maximize the heights used for the corrosion product samples. Figure E-4 contains schematics showing the test specimen geometries and Table E-2 summarizes the dimensions of each test specimen.

Details regarding the specific preparation steps for the corrosion product specimens and steel specimens are discussed below by sample type.

2.2.1 Corrosion Product Specimens

The following steps were performed to prepare the corrosion product specimens. First, the deposits samples were laser scanned from both surfaces, using a FaroArm™, to produce 2D and 3D renderings of the samples. The renderings were used to map the thickness of the samples and to determine the optimal locations from which to take specimens. The approximate locations of two test specimens were marked on the flattest surface of each corrosion product sample; see Figure E-5. These markings were made to provide guidance for the initial cuts once the samples were embedded. The markings were made by first preparing a template of the desired specimen geometry (i.e. length vs. width) on a sheet of transparency paper. The transparency paper was cut along the lines of the template, except at the corners. The template was then placed on top of the corrosion product samples and a yellow paint marker was used to trace the cut edges transferring the specimen geometry onto the corrosion products. Consideration to the thickness of the band saw blade (i.e. 0.02-inches) was given when using the template to mark the samples.

Alphabetical reference points (i.e. A, B, C, etc.) were marked on the corrosion product samples to identify the approximate end points of each cut line; see Figure E-5. For ease of discussion, these alphabetical markings will be referenced when identifying sectioning locations on the embedded samples.

Next, the corrosion product samples were embedded in epoxy. Rectangular plastic containers, approximately 7-inches in length by 5-inches in width and 3-inches in height, were used as molds to embed the corrosion product samples in a clear, two-part epoxy. Prior to placing the samples in their molds, a mold release agent was sprayed on the internal surfaces of the containers to facilitate the release of the embedded samples once the epoxy had cured.

The flattest surface of each corrosion product sample was placed on top of plastic spacers positioned within the container. The plastic spacers were positioned so that the surface of each sample was parallel to the bottom of their respective molds. Figure E-6 contains photographs showing the spacers used beneath the samples and the samples once they were placed in their respective molds.

Next, the two-part epoxy was mixed and poured slowly into the molds; see Figure E-7a. The sample molds (i.e. mounts) were then placed in a vacuum chamber in order to remove any trapped air within the uncured epoxy of the mounts; see Figure E-7b. The mounts were allowed to cure overnight in a fume hood. A small fan was positioned to blow on the mounts during the curing process to remove the exothermal heat from the chemical

reaction of the epoxy during curing. Once cured, the mounts were removed from their respective plastic containers; see Figure E-7c and Figure E-7d.

The embedded samples were then cut using a diamond band saw that was lubricated with ethylene glycol; see Figure E-8a. All cuts were made slightly outside of the final desired dimension to ensure that a sufficient amount of material remained for any grinding needed to achieve the final specimen dimension. The embedded samples were first cut along the outer end markings (i.e. along Lines G-H and I-J shown in Figure E-7c and d) in order to facilitate handling of the samples during grinding. The corrosion product surfaces exposed by these cuts were then re-embedded in epoxy. Next, a cut was made along Line C-D on both samples (see Figure E-8b and c). These cuts were the only cuts that were made directly along the line marked on the embedded samples. The corrosion product surfaces exposed by these cuts were then re-embedded in epoxy.

The two remaining pieces of the original embedment were then cut along Lines A-B and E-F followed by re-embedment of the exposed corrosion product surfaces in epoxy (see Figure E-8b and c). Each side of the embedded samples was individually ground by hand in order to achieve the desired over-all dimensions; see Figure E-9a. Grinding was carried out using 600 grit silicon carbide paper strips attached to a flat granite block and ethylene glycol as a lubricant. Based on the integrity of the samples, a protective epoxy layer was not necessary for the final test specimens. Figure E-9b and c are photographs showing the final test specimens for Corrosion Product Samples 10000195318 and 10000195331.

2.2.2 Steel Plate Specimens

The following steps were performed to prepare the steel specimens. The approximate locations of the final test specimens were marked on the steel plate. Two specimens: one in the axial direction and one in the transverse direction were sectioned from the plate; see Figure E-10. Consideration was given to account for the thickness of the saw blade (i.e. 0.02-inches) when marking up the steel plate samples.

The samples were cut using a band saw. All cuts were made slightly outside of the final desired dimension to ensure that a sufficient amount of material was left to allow for any milling needed to achieve the final specimen dimensions. Care was taken to achieve straight cuts. The samples were then milled at slow speeds to the desired dimensions. Figure E-10b and c are photographs showing the final longitudinal and transverse steel specimens.

2.3 Test Procedure

A soft magnetic hysteresigraph tester, Model SMT-700, that was computer automated and manufactured by KJS Associates, Inc., was used to measure the magnetic properties of the test specimens. Figure E-11 contains photographs showing the magnetic tester and a representative test setup for the magnetic property testing. Prior to testing, the prepared specimens were wrapped with insulating tape that was approximately 0.009 inches thick. A 30 gauge magnetic wire was then wound around each specimen. This wire served as a secondary induction winding.

During testing, each specimen was positioned using a pole piece adapter in a KJS Associates Model YOKE-100 electro-magnet and clamped into a closed magnetic test circuit. A calibrated Hall probe was placed at the surface of the coil in order to measure the applied magnetic field (H). The secondary winding was then connected to the system fluxmeter to determine the flux density in the sample. Prior to the start of each test, the test specimen was demagnetized. Once the specimen was demagnetized, the specimen was then magnetized to a maximum applied field of 1000 Oe in the yoke fixture. The full four-quadrant B vs. H curve was then measured at room temperature.

Each test specimen was also measured at lower applied fields to account for the typical field strengths of the magnetic flux leakage (MFL) tool. The higher permeability specimens were tested at an induction level of 12 kG, while the lower permeability specimens were tested to an induction level of 1000 G.

3.0 RESULTS

Several magnetic parameters were measured and/or calculated for this analysis. The parameters include H_{max} , H_c , B_{max} , B_r , μ_{in} , and μ_{max} . Some values are relevant to MFL tools and some are not. The parameters of interest, as related to the Line 901 failure, include the magnetic permeability (μ) and the magnetic field strength (H).

Figure E-12 contains composite plots showing the magnetic induction (B, magnetic flux density) vs. magnetic field strength (H) for the six specimens when tested at strong magnetic fields (up to 1000 Oe). The curves for the steel specimens are shown in red, while the curves for the corrosion product specimens are shown in green (195318) and blue (195331). The plot to the left in Figure E-12 shows the data up to a maximum magnetic induction of 25,000 G, while the plot to the right in Figure E-12 shows the data up to a maximum magnetic induction of 2,500 G. A clear difference is apparent between the steel and corrosion product specimens in both plots. As shown, the saturation magnetization of the corrosion product specimens (i.e. B_{max}) is approximately 10% of the saturation magnetization measured for the steel specimens. These differences indicate that the steel

specimens are more magnetic than the corrosion product specimens. No significant differences were observed between the corrosion product specimens.

The magnetic properties of the specimens were measured when exposed to both a strong magnetic field and a lower magnetic field. Figure E-13 through Figure E-18 contain the individual plots of magnetic induction vs. magnetic field strength for each of the six tested specimens when exposed to the two magnetic fields. The magnetic properties determined from these curves and the data extracted from these curves are summarized in Table E-3. The first column identifies the specimen and the second column shows the sample type. Columns 3 - 6 contain values that were extrapolated from the curves shown in Figure E-13 through Figure E-18 and Columns 7 and 8 provide the initial and maximum differential magnetic permeability values. The values shown in Columns 7 and 8 are the parameters of interest for this analysis. As seen, the permeability values determined for the corrosion product specimens are similar and are much lower than the values determined for the steel specimens (i.e. less than 2% of the values determined for the steel specimens). Differences were observed between the longitudinal and transverse steel specimens, with the transverse specimen exhibiting higher magnetic permeability values. The magnetic permeability values shown in Table E-3 were obtained for a field strength that exceeds the strongest MFL tools. Thus, values were also determined within the typical field strengths of high-field MFL tools.

The typical field strength of high-field MFL tools range from 140 Oe to 180 Oe, reaching a maximum of around 200 Oe.¹ Based on this information, smoothing approximation curves were used in the range from 50 to 300 Oe to calculate the amplitude magnetic permeability. The curves were based on the measured B-H curves for the six test specimens, but were corrected for residual magnetization and non-zero initial field data. The results of these analyses are summarized in Table E-4. The first column identifies the specimen and the second column identified the sample type. Columns three through seven list the amplitude magnetic permeability at the following magnetic field strengths: 50, 100, 150, 200, and 250 Oe. As shown, the amplitude magnetic permeability values for the corrosion product specimens generally increase with increasing magnetic field strength. In contrast, the amplitude magnetic permeability values for the steel specimens decrease with increasing magnetic field strength. Overall, the magnetic permeability values for the corrosion product specimens are much lower than the values measured for the steel samples (i.e. less than 3% of the values determined for the steel specimens).

¹ Development of Dual Field Magnetic Flux Leakage (MFL) Inspection Technology to Detect Mechanical Damage, PRCI Report, 2013.

4.0 SUMMARY OF FINDINGS

A summary of the findings are provided below.

- The corrosion product specimens were less magnetic than the steel specimens.
- No significant differences were determined for the magnetic properties of the specimens removed from the two corrosion product samples.
- There were differences between the magnetic properties of the steel specimen in the axial (longitudinal) direction and the magnetic properties of the steel specimen in the transverse (circumferential direction).
- At the field strengths typically associated with MFL tools, the magnetic permeability values of the corrosion product specimens were significantly lower than the magnetic permeability values of the steel specimens. The values for the corrosion product specimens were less than 5% of the values determined for the steel specimens.

Table E-1. Summary of samples selected for the magnetic permeability testing.

Sample ID (Arcsset #)	Sample Type	Description	Pipe Joint	Distance D/S from GW 5930 (ft)	o'clock orientation
10000195318	Corrosion Product	Corrosion product from Feature 2	5930	17.8 – 19.5	~ 6:24
10000195331		Corrosion product adjacent to leak location (Feature 4)	5930	33.50	~4:24
10000195363	Plate Steel	Counter clockwise fracture surface; small plate	5930		

Table E-2. Summary of the dimensions, as reported by Magnetic Instruments, for the magnetic permeability specimens.

Specimen Identifications	Sample Type	Average Length (in)	Average Width (in)	Average Height (in)
195318 – 3A	Corrosion Product	2.251	0.514	0.327
195318 – 3B		2.251	0.514	0.295
195331 – 2A		2.251	0.518	0.483
195331 – 2B		2.251	0.510	0.463
195363 – 2 Longitudinal	Plate Steel	2.251	0.505	0.250
195363 – 3 Transverse		2.251	0.504	0.249

Table E-3. Summary of magnetic properties for tested specimens.

Specimen Identifications	Sample Type	Values determined from plots				Calculated values	
		Maximum Applied Magnetic Field Strength, H_{max}^1 (Oe)	Coercive force, H_c (Oe)	B_{max}^1 (G)	Residual Magnetization, B_r (G)	Initial Differential Magnetic Permeability μ_{in}	Maximum Differential Magnetic Permeability μ_{max}
195318 – 3A	Corrosion Product	1020.6	86.27	1680	278	2.229	2.890
195318 – 3B		1009.9	92.31	2050	352	2.511	3.325
195331 – 2A		1008.0	95.16	1802	280	1.870	2.545
195331 – 2B		998.3	104.4	1987	426	2.475	3.598
195363 – 2 Longitudinal	Plate Steel	1018.2	6.66	22193	12750	149.0	1467
195363 – 3 Transverse		1011.5	6.5	22337	14147	177.3	1863

¹ Values calculated from corrected curves.

Table E-4. Summary of magnetic permeability amplitudes¹ for the tested specimens at typical magnetic field strengths of MFL tools.

Specimen Identification	Sample Type	Magnetic Field Strength (Oe)				
		50	100	150	200	250
195318 – 3A	Corrosion Product	2.29 ²	2.508	2.632	2.678	2.675
195318 – 3B		2.615	2.812	2.954	3.045	3.086
195331 – 2A		1.872	2.018	2.154	2.249	2.298
195331 – 2B		2.491	2.795	3.027	3.165	3.206
195363 – 2 Longitudinal	Plate Steel	332.3	179.5	125.2	96.99	79.55
195363 – 3 Transverse		330.5	178.7	124.7	96.64	79.28

¹ Smoothing approximation curves used in range from 50 to 300 Oe to calculate amplitude magnetic permeability. Curves were corrected for residual magnetization and non-zero initial field.

² Values shaded in light gray are amplitude magnetic permeability values.



Figure E-1. Photographs of Corrosion Product Sample 10000195318 (Top) and Corrosion Product Sample 10000195331 (Bottom), which were used for the magnetic permeability testing: Surface that was in contact with the pipe surface (Left) and Surface that was in contact with the coating (Right). Top images are flipped about the horizontal axis and bottom images are flipped about the vertical axis.



Figure E-2. Photograph of Steel Plate Sample 10000195363, which was used for the magnetic permeability testing

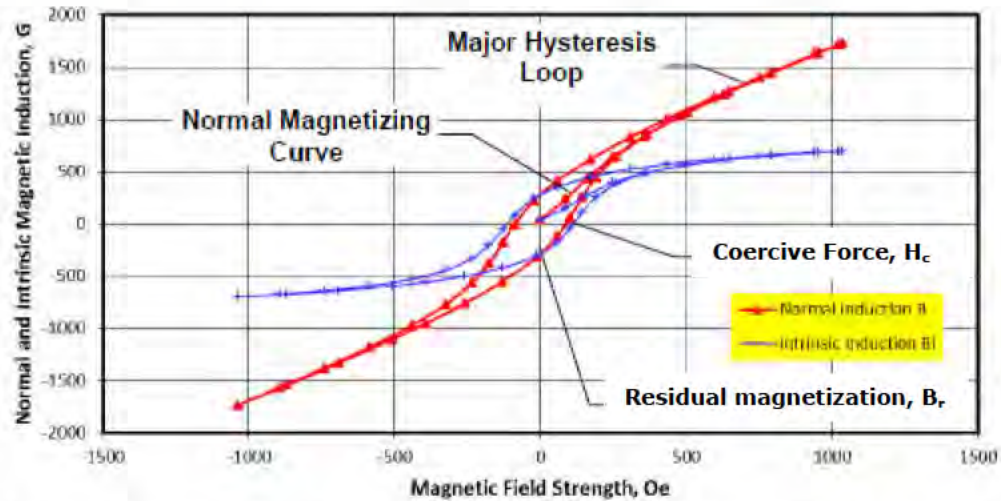


Figure E-3. Plot of normal and intrinsic magnetic induction vs. magnetic field strength for a representative sample, showing how coercive force (H_c) and residual magnetization (B_r) are determined.

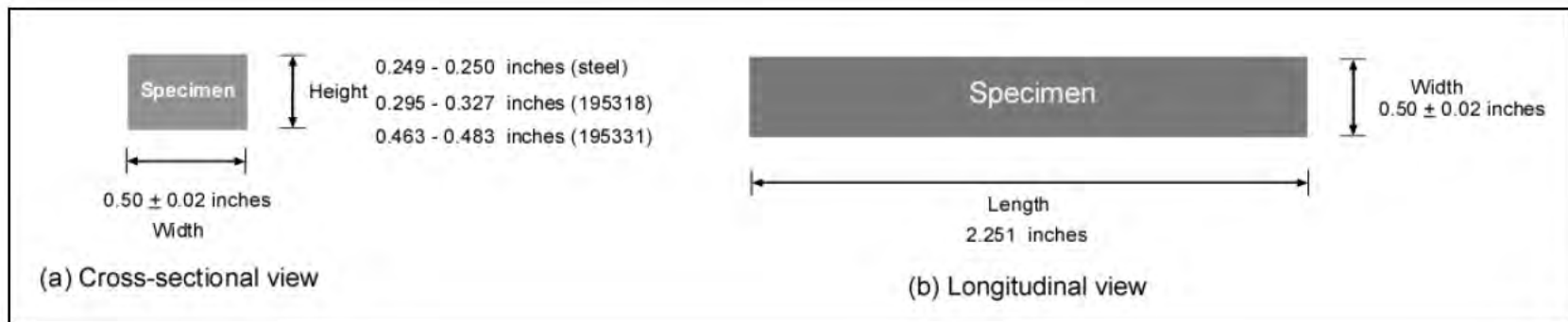


Figure E-4. Schematics showing the dimensions for the magnetic permeability specimens: (a) cross-sectional view and (b) longitudinal view.

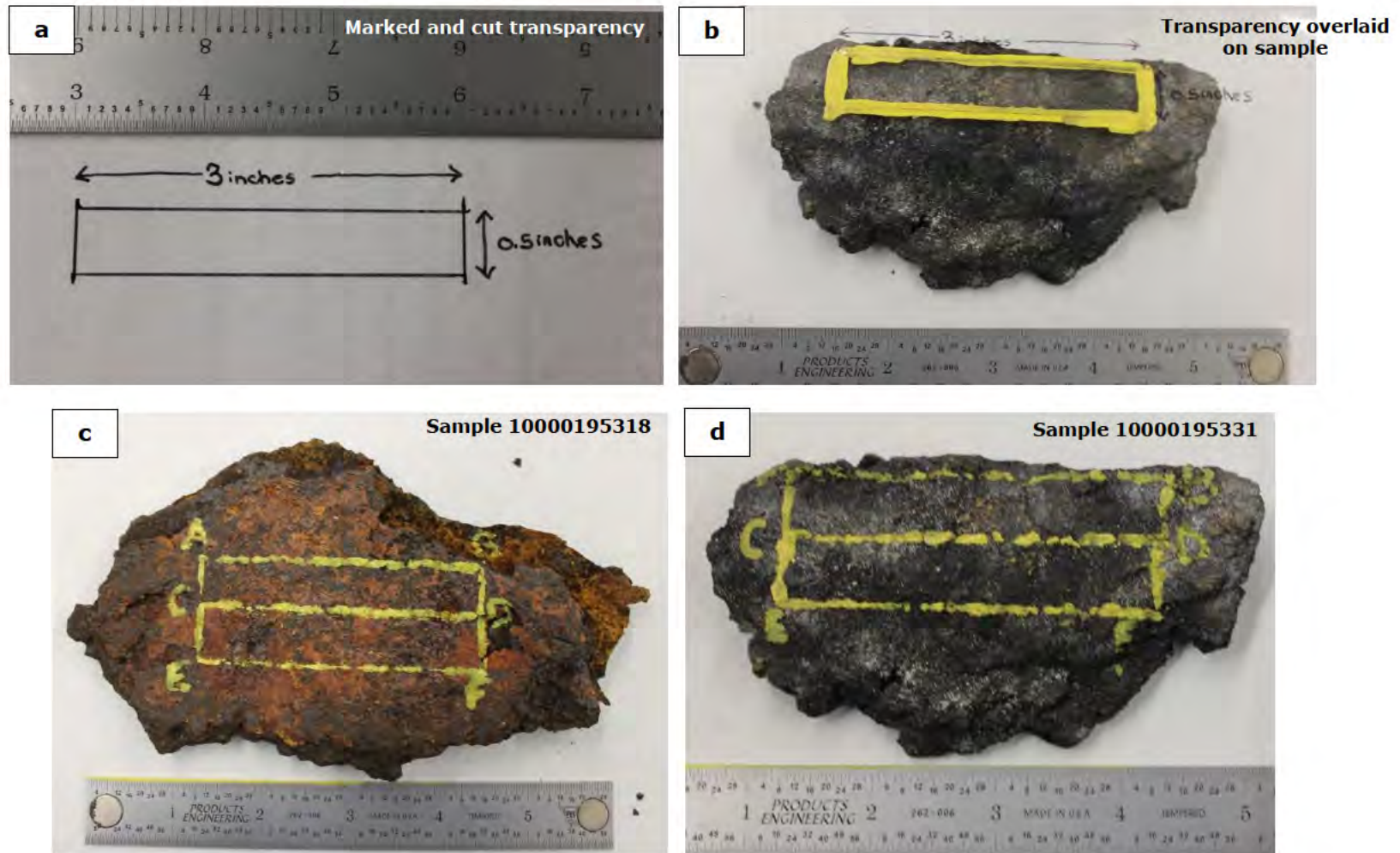


Figure E-5. Photographs showing the labeling process for the corrosion product samples: (a) transparency template, (b) transparency overlaid on Sample 10000195331 for marking, (c) labeled Sample 10000195318, and (d) labeled Sample 10000195331.

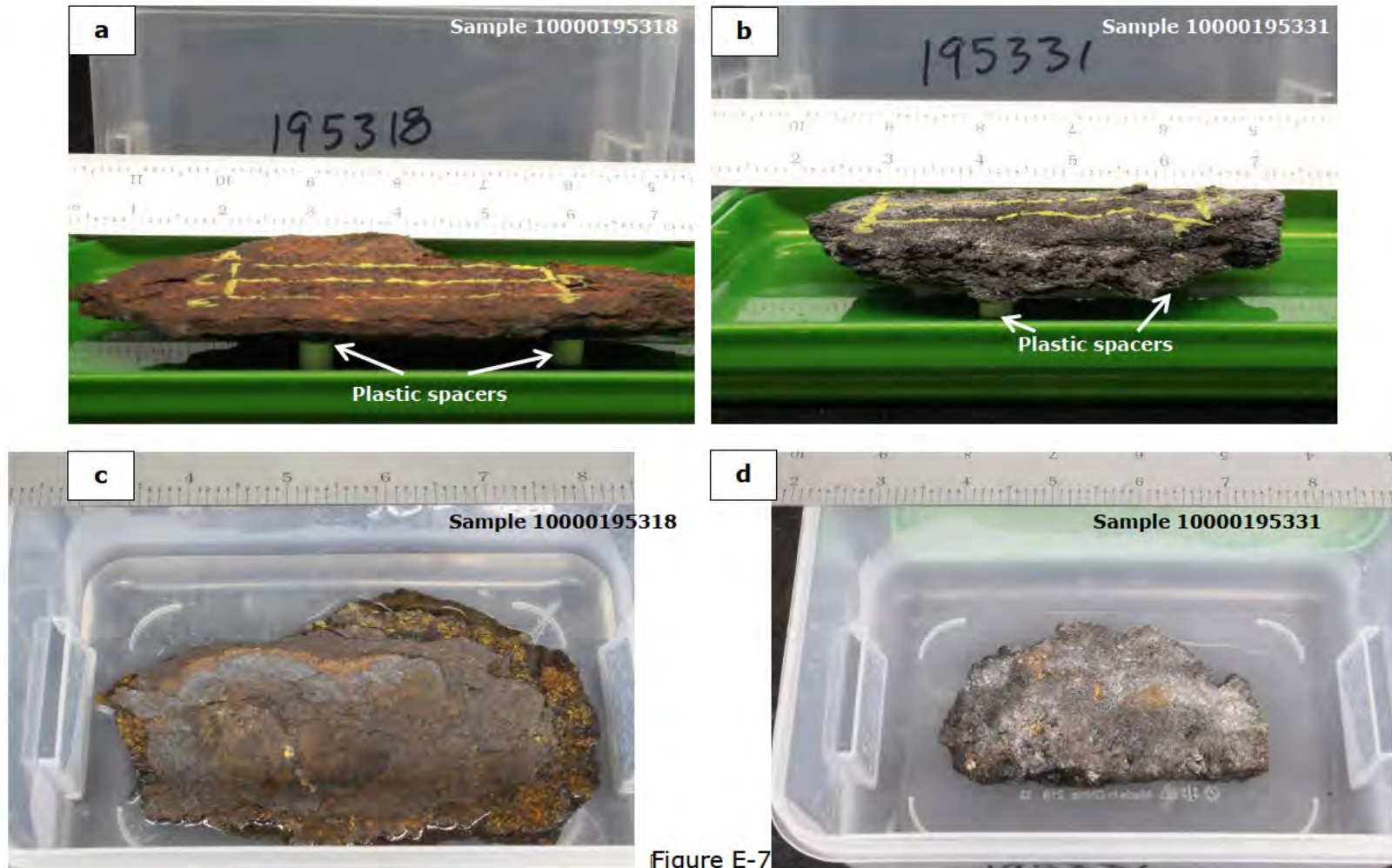


Figure E-7

Figure E-6. Photographs showing preparation of the corrosion product samples for embedment: (a) plastic rod used to elevate Sample 10000195318, (b) plastic rod used to elevate Sample 10000195331, (c) Sample 10000195318 in the mold, and (d) Sample 10000195331 in the mold.

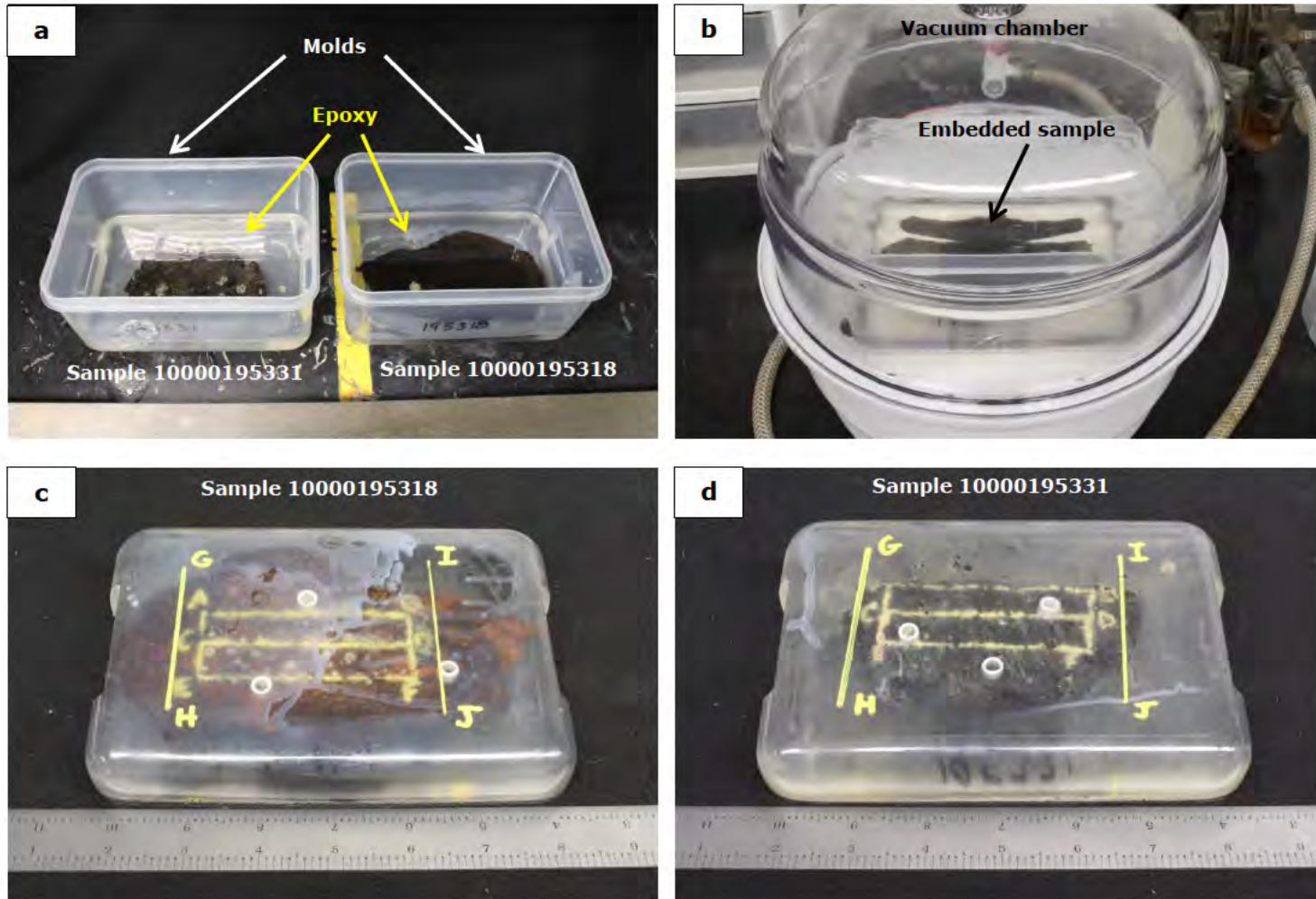


Figure E-7. Photographs showing the embedment process for the corrosion product samples: (a) embedment molds after samples were covered with epoxy, (b) mold samples in vacuum chamber to remove bubbles, (c) embedded Sample 10000195318, and (d) embedded Sample 10000195331.

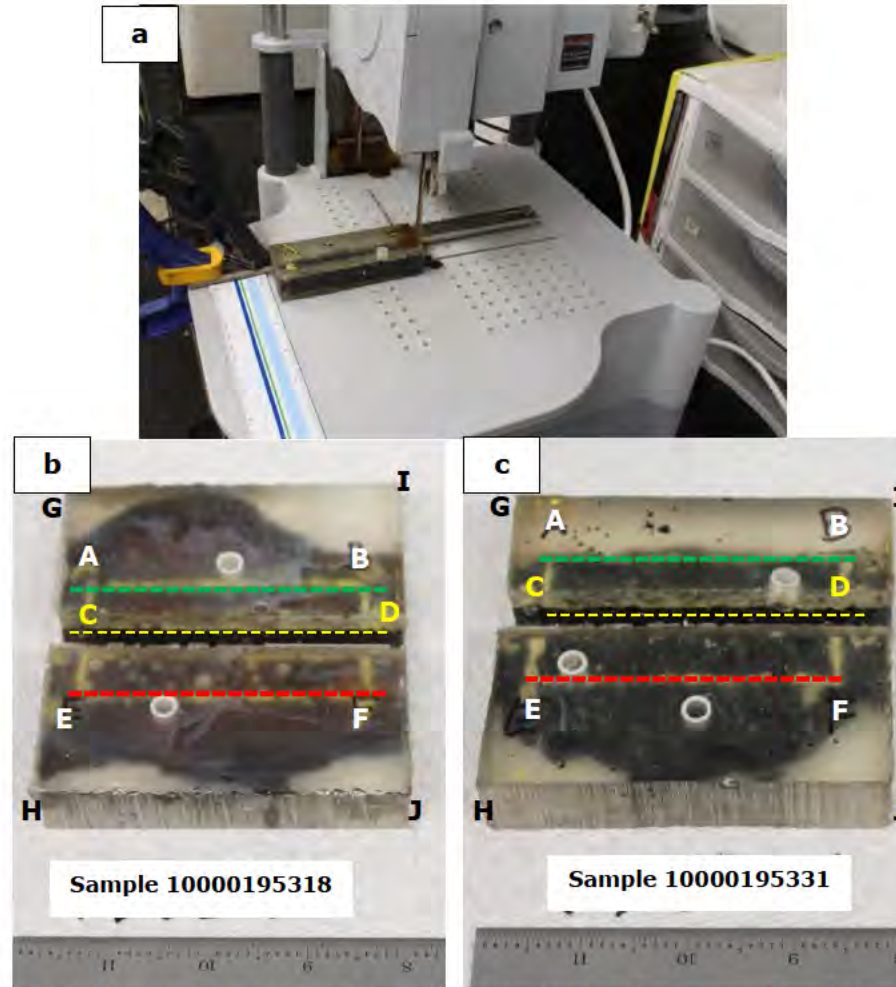


Figure E-8. Photographs showing the cutting process for the corrosion product samples: (a) sample cutting on diamond saw, (b) Sample 10000195318 after cuts were made along Lines G-H, I-J, and C-D and (d) Sample 10000195331 after cuts were made along Lines G-H, I-J, C-D (yellow dashed line), A-B (green dashed line), and E-F (red dashed line). Refer to Figure E-7 for the line identifications.

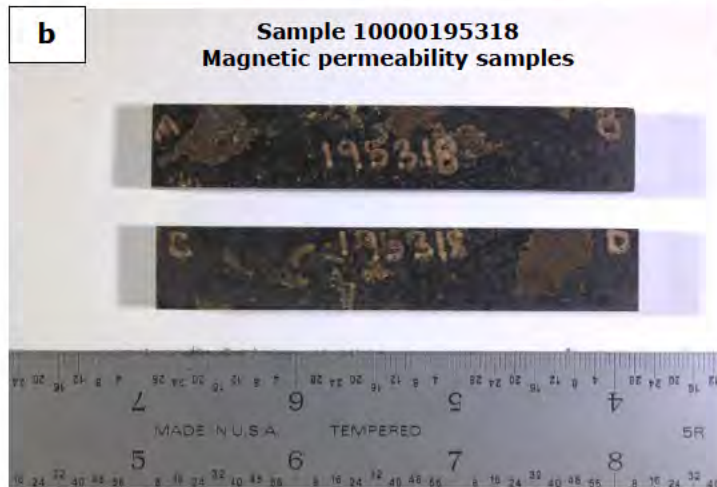
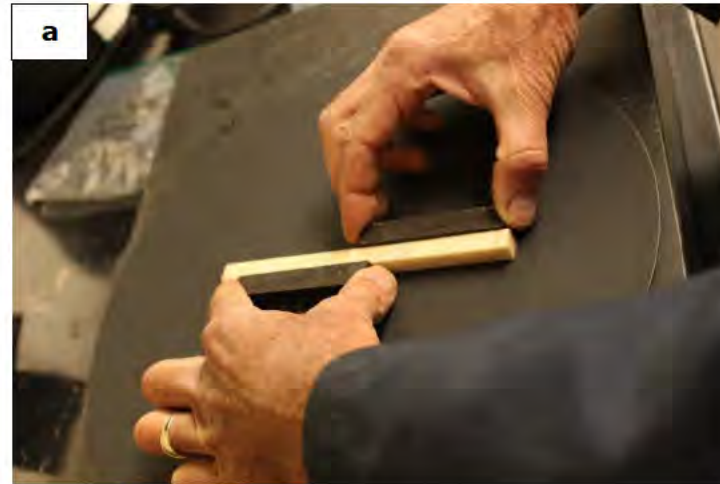


Figure E-9. Photographs showing the finishing process for the corrosion product samples: (a) sample finishing with SiC paper, (b) Sample 10000195318 magnetic permeability samples, and (c) Sample 10000195331 magnetic permeability samples.

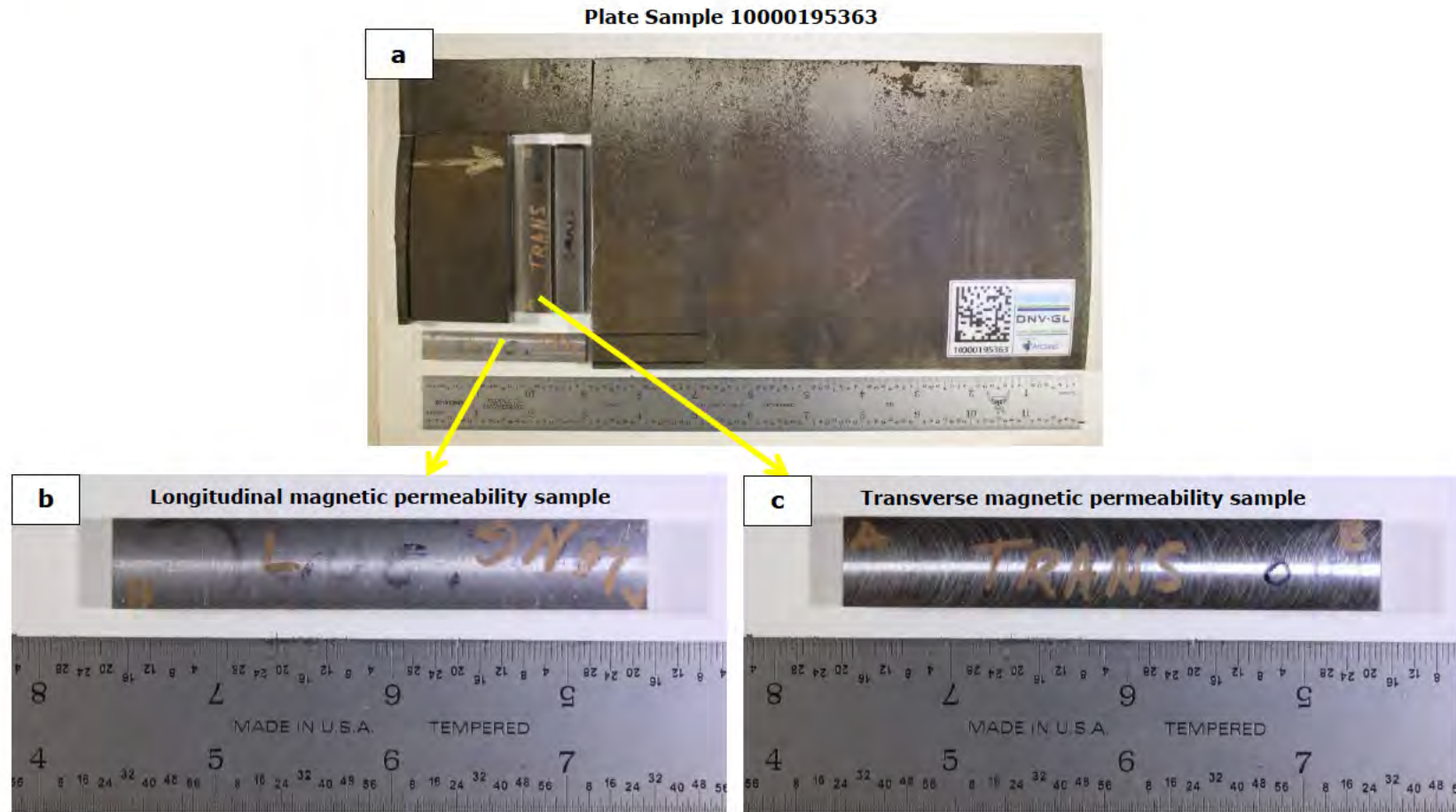


Figure E-10. Photographs showing the plate samples used for the magnetic permeability testing: (a) Plate Sample 1000095363 showing location where samples were removed, (b) Longitudinal magnetic permeability sample, and (c) Transverse magnetic permeability sample.

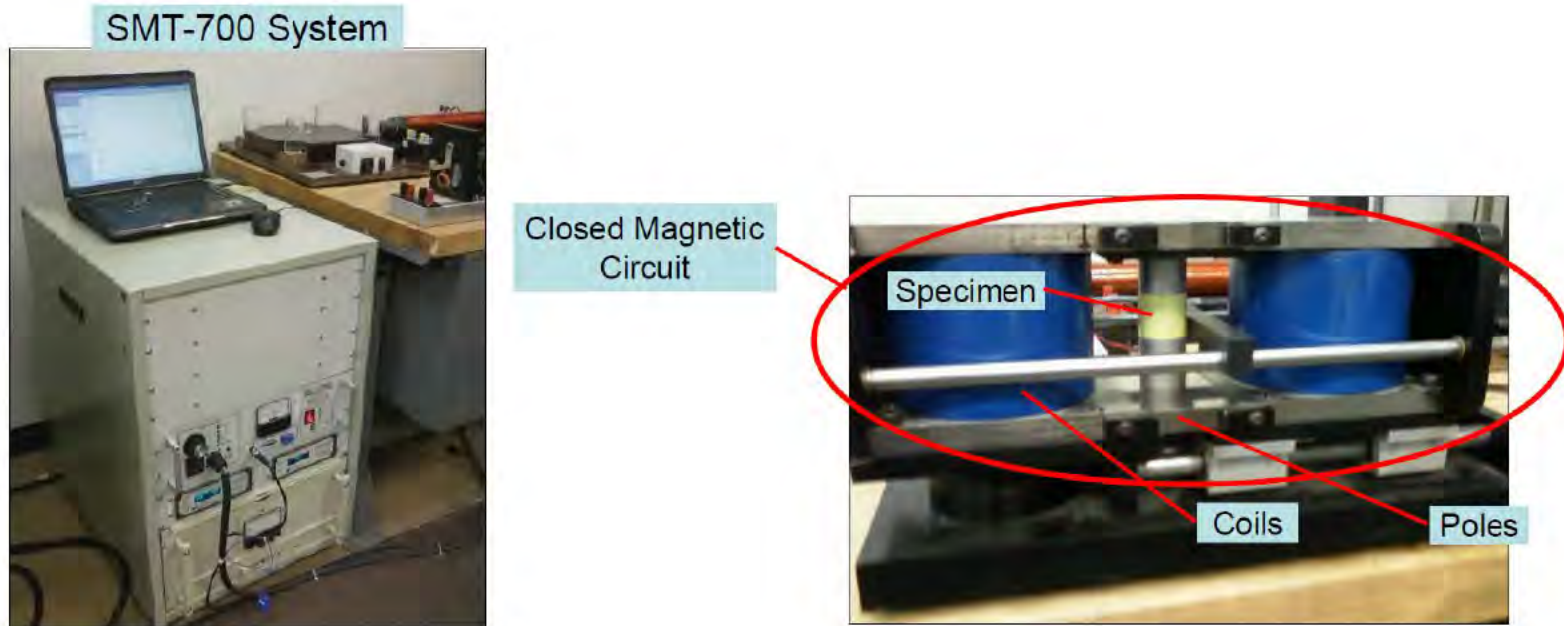


Figure E-11. Photographs showing the tester and a representative test setup for the magnetic property testing.

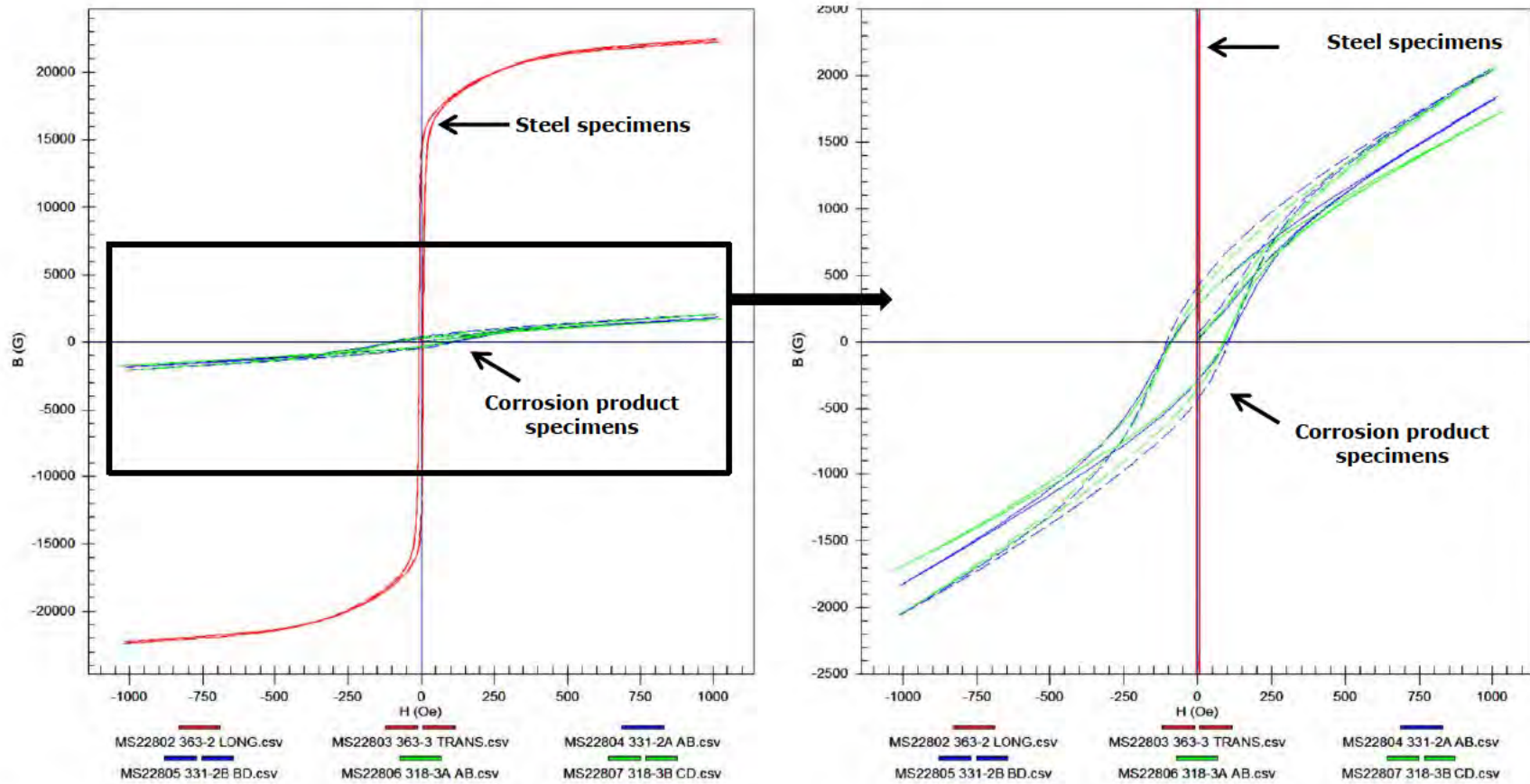


Figure E-12. Composite plots of magnetic induction (B, magnetic flux density) vs. magnetic field strength (H) for the six specimens when tested at strong magnetic fields (up to 1000 Oe): Overall plot (Left) and close-up of overall plot with magnetic induction range of $\pm 2,500$ G.

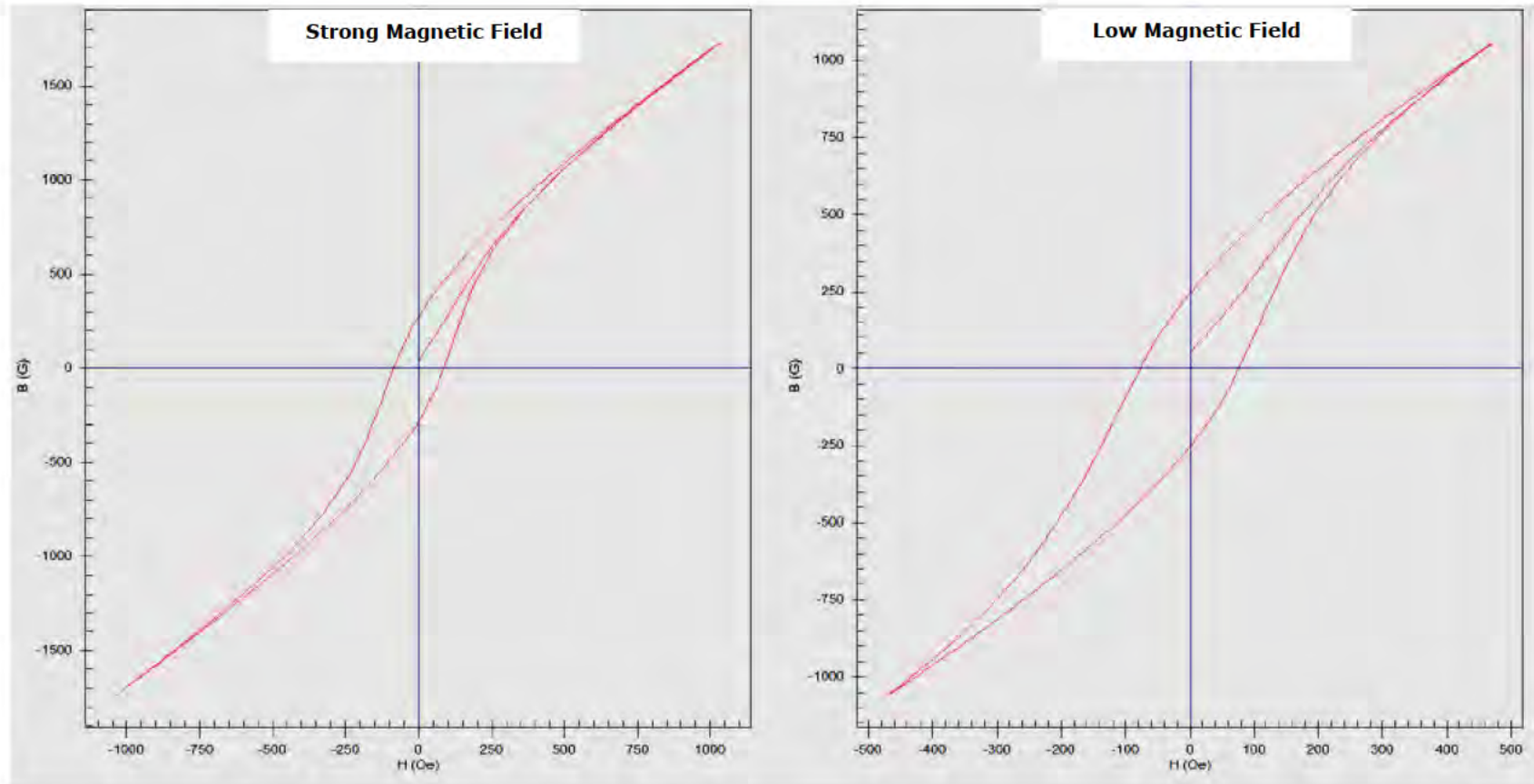


Figure E-13. Plots of magnetic induction (B, magnetic flux density) vs. magnetic field strength (H) for Corrosion Product Specimen 195318 – 3A: Strong magnetic field of 1000 Oe (Left) and Low magnetic field of 460 Oe (Right).

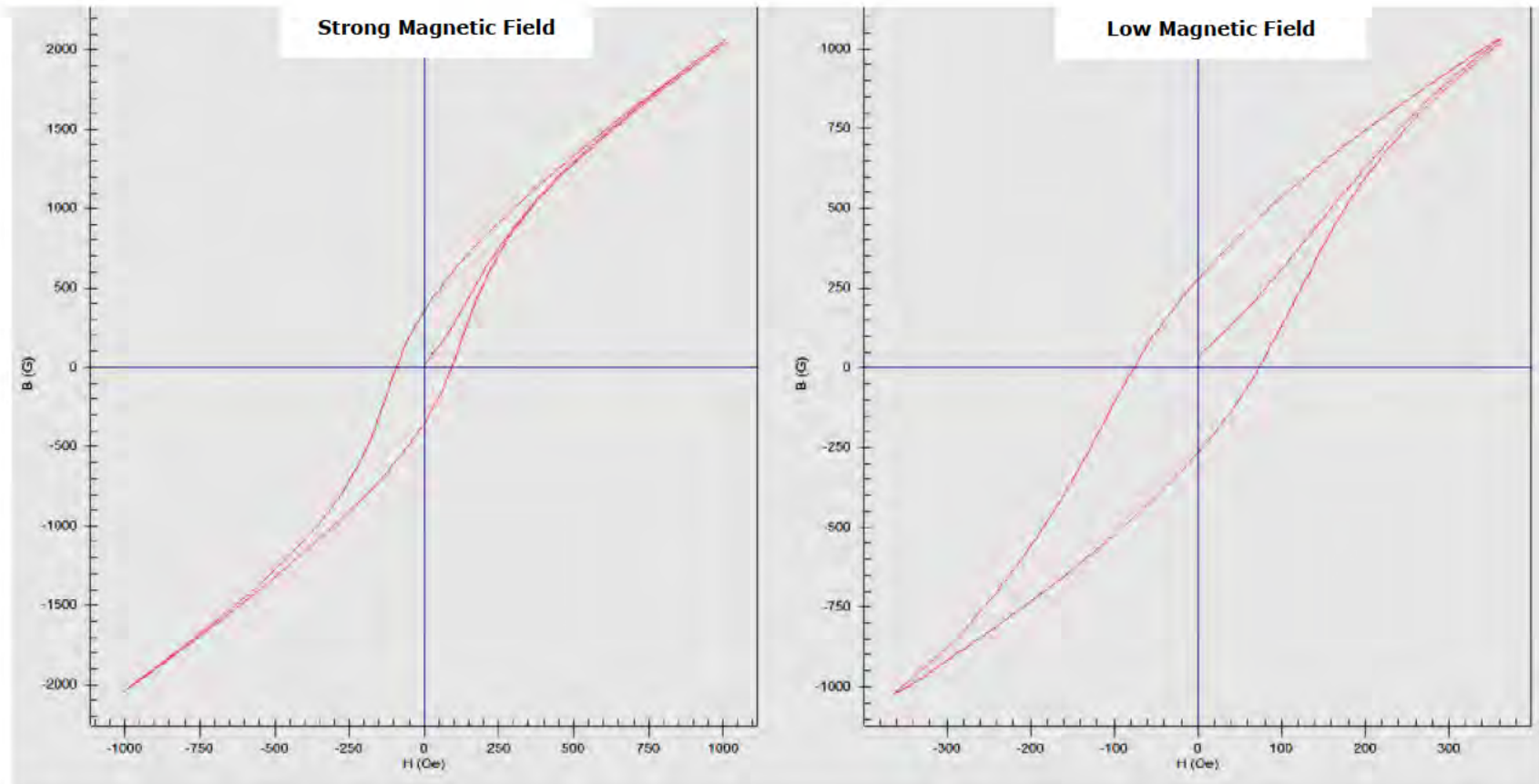


Figure E-14. Plots of magnetic induction (B, magnetic flux density) vs. magnetic field strength (H) for Corrosion Product Specimen 195318 – 3B: Strong magnetic field of 1000 Oe (Left) and Low magnetic field of 360 Oe (Right).

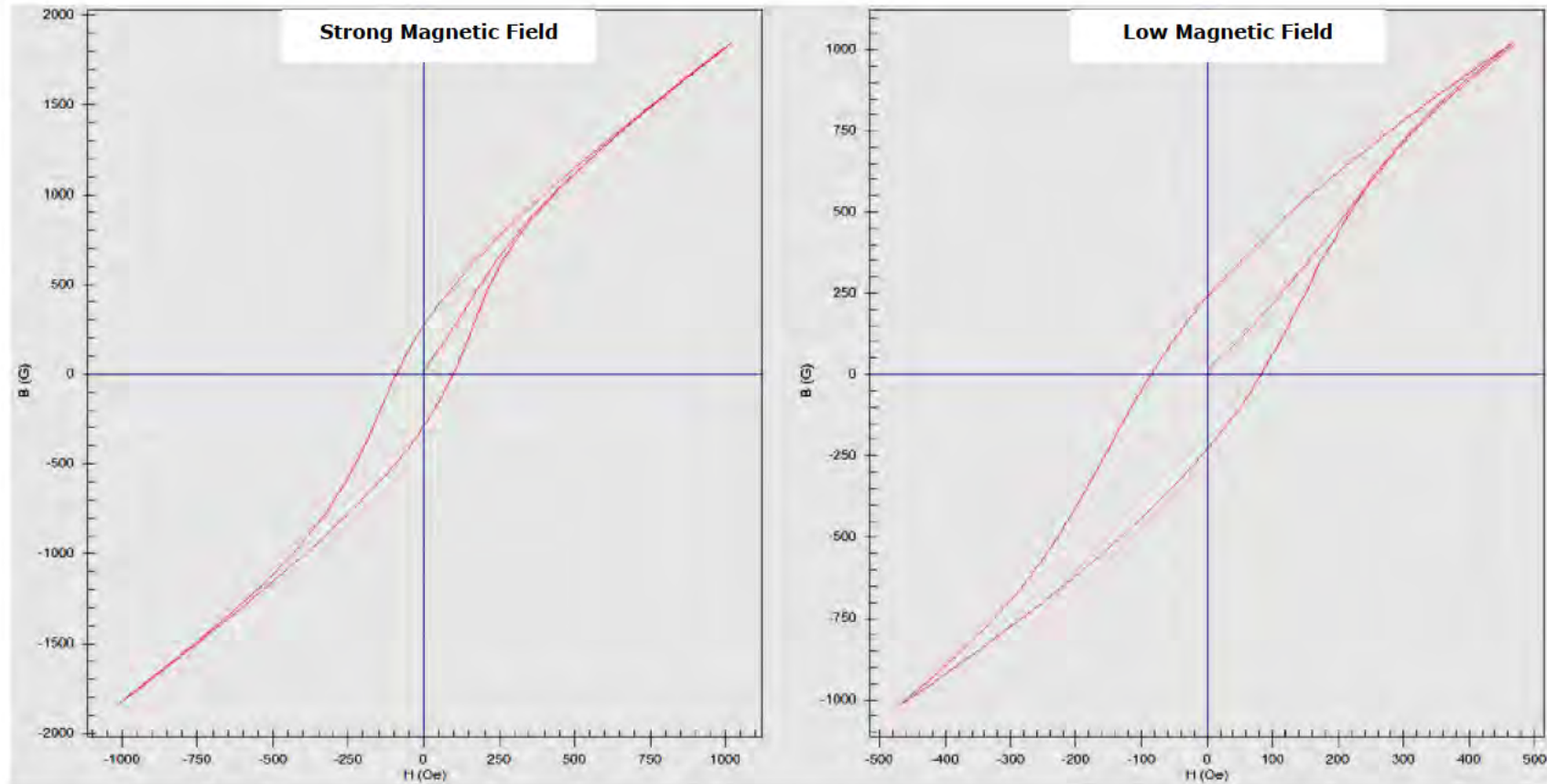


Figure E-15. Plots of magnetic induction (B, magnetic flux density) vs. magnetic field strength (H) for Corrosion Product Specimen 195331 - 2A: Strong magnetic field of 1000 Oe (Left) and Low magnetic field of 460 Oe (Right).

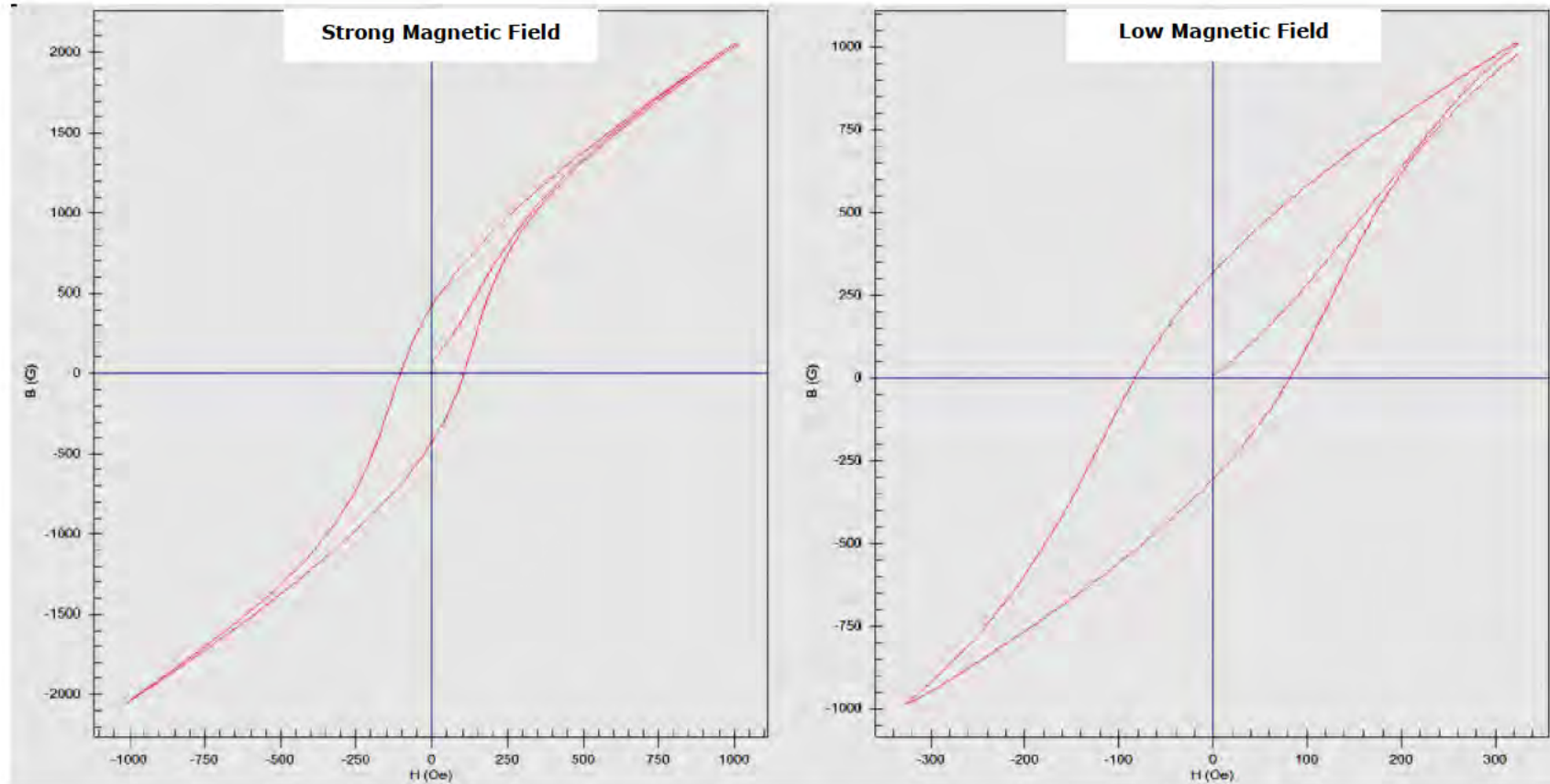


Figure E-16. Plots of magnetic induction (B, magnetic flux density) vs. magnetic field strength (H) for Corrosion Product Specimen 195331 - 2B: Strong magnetic field of 1000 Oe (Left) and Low magnetic field of 320 Oe (Right).

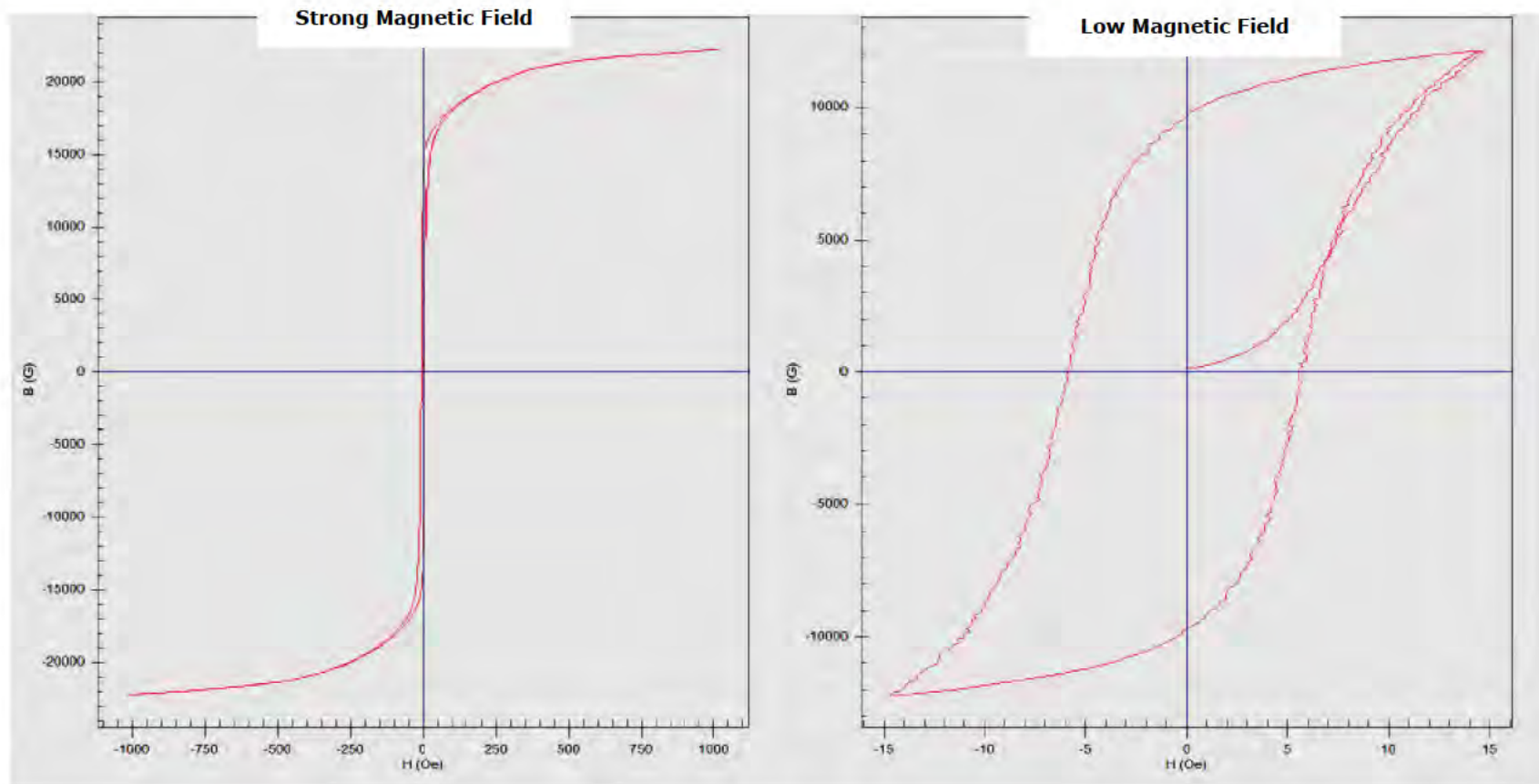


Figure E-17. Plots of magnetic induction (B , magnetic flux density) vs. magnetic field strength (H) for Steel Specimen 195363-2 (Longitudinal): Strong magnetic field of 1000 Oe (Left) and Low magnetic field of 15 Oe (Right).

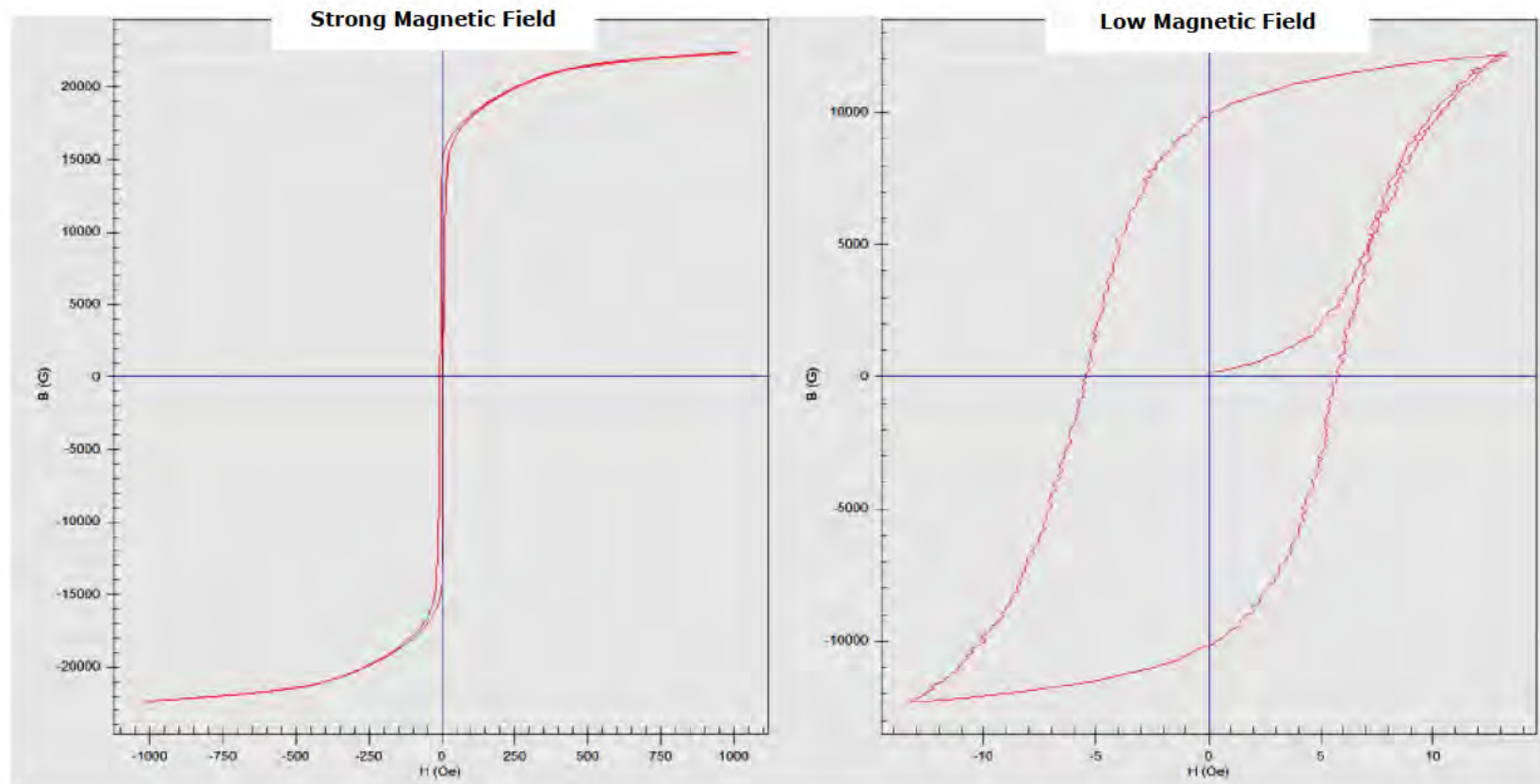


Figure E-18. Plots of magnetic induction (B, magnetic flux density) vs. magnetic field strength (H) for Steel Specimen 195363-3 (Transverse): Strong magnetic field of 1000 Oe (Left) and Low magnetic field of 13 Oe (Right).

APPENDIX F

Statistically Active Corrosion Assessment

STATISTICALLY ACTIVE CORROSION ASSESSMENT

1.0 BACKGROUND

This appendix provides a summary of the Statistically Active Corrosion (SAC) assessment completed on Line 901. The pipeline is comprised of 24-inch diameter by 0.344 inch wall thickness, API 5L Grade X65 line pipe steel that was manufactured by Nippon Steel and contains a high frequency (HF) electric resistance welded (ERW) longitudinal seam. It was installed in 1990 and is approximately 10.87 miles in length, spanning between Las Flores Station on the U/S end and Gaviota Station on the D/S end. The normal operating pressure and maximum discharge pressure (MDP) for the line are 616 psig and 1,025 psig, respectively. These pressures correspond to 33% and 55% of the specified minimum yield strength (SMYS), respectively.

The pipeline was inspected by Rosen with a magnetic flux leakage (MFL) in-line inspection (ILI) tool in June 2007, July 2012, and May of 2015.

1.1 Objective

The primary objective of the SAC assessment was to estimate the localized corrosion growth rates on Line 901 based on a comparison of the 2007 MFL and 2012 MFL ILI surveys.

1.2 Scope of Work

In order to determine corrosion growth rates, DNV GL conducted its SAC assessment of changes in reported metal loss between the un-clustered¹ metal loss reported in the 2007 MFL and 2012 MFL ILI surveys. Statistically (at a 95% confidence level) high growth areas were then reviewed in the ILI raw signal data sets to determine the actual hotspots of corrosion growth on the pipeline and the rates of that growth.

2.0 TECHNICAL APPROACH

The following tasks were conducted within the SAC assessment:

- Task 1: Data Alignment and Preparation of the Input Data
- Task 2: Comparison of ILI-Reported and Field-Measured Depths
- Task 3: Statistically Active Corrosion Assessment of the Inspection Data Sets
- Task 4: Compilation and Review of the Statistical Screening Results
- Task 5: Application of Corrosion Growth Rates

¹ Clustering is defined as combining multiple indications within a specific distance.

2.1 Task 1 – Data Alignment & Preparation of the Input Data

DNV GL aligned the 2007 MFL and 2012 MFL un-clustered metal loss inspection data sets prior to performing the statistical analysis on individual pipe joints.

The data sets were also matched in sensitivity to ensure that standard ILI survey instrument differences were considered during the screening process. The matching was conducted using unity plots based on pits reported in both inspections and by comparing raw signals (“boxed” data) from each ILI survey using the software provided by the ILI vendor. The unity plots were used to identify overall biases between the inspections. The box data were used to determine whether a sensitivity (depth) adjustment factor should be applied to either ILI data set.

2.2 Task 2 – Comparison of ILI-Reported and Field-Measured Depths

To aid in determining whether any adjustments were warranted for the most recent ILI inspection, the field-measured depths were compared with the ILI-reported depths. Axial and circumferential location information, as reported by the ILI for a given feature, was used to define the search area for a corresponding anomaly within the provided excavation results. Unity plots were produced to graphically review the results, which were then used within the SAC assessment.

2.3 Task 3 – Statistically Active Corrosion Assessment

DNV GL compared the two sets of ILI data (in this assessment, the 2007 MFL and 2012 MFL inspections) using its SAC assessment methodology. The SAC methodology identified pipeline locations for which the changes between the ILI data indicate a likelihood of active corrosion growth. Those locations that exceeded a desired level of confidence (95% confidence interval) were identified as statistically active locations. The SAC methodology is applied on a joint-by-joint basis.

Internal and external features were grouped together for the SAC assessment. This is typically done when the ID/OD discrimination is suspect, especially for deeper (more significant) features.

Potential locations of corrosion activity were identified from average depths, maximum depths, and metal loss anomaly frequency perspectives. If a joint exhibits a statistically significant increase in the average or maximum reported metal loss depth, it is identified as either a SAC Mean or SAC Max respectively:

- SAC Mean – identified locations and quantifies the corrosion growth where there is evidence of a statistically significant change between the average (mean) metal loss depths in each ILI survey.
- SAC Max – identified locations and quantifies the corrosion growth where there is evidence of a statistically significant change between the deepest metal loss calls in each ILI survey.

Estimated corrosion rates were calculated using the difference in the means or maximums and the time interval between inspections. To be conservative, DNV GL uses a default growth rate based on ILI tolerance, the nominal wall thickness, and the time frame between both inspections (see Equation (1)). Joints that were neither SAC Mean nor SAC Max were assigned this calculated minimum corrosion growth rate, CGR_{Min} .

$$CGR_{Min} = \frac{0.5 \times ILI_{Tolerance} \times nominal\ WT}{Date_{Recent} - Date_{Prev}} \quad (1)$$

2.4 Task 4 – Compilation and Review of Statistical Growth Results

Following the statistical assessment, DNV GL performed a manual review of the signal data on selected pipe joints to:

- Locate areas of growth that may not have been identified via the statistical analysis.
- Confirm areas identified as containing statistically significant growth.

Manually reviewed pipe joints were selected based on a number of characteristics determined from DNV GL's experience from similar projects. Characteristics used to select joints for manual review include joints with:

- The highest SAC Mean or SAC Max growth rates
- Statistically significant differences in the number of SAC counts
- The most unmatched metal loss features (Orphan and non-Orphan) in both 2012 and 2014
- The largest maximum depth in 2014, both with and without a corresponding 2012 feature
- The largest difference in maximum depths
- The largest difference in depth between matched (one-to-one) pits

Joints identified based on the characteristics above and the areas immediately upstream and downstream of these joints were reviewed for signs of growth by manually comparing the ILI signal data from each inspection. Each joint manually reviewed was classified per Table F-1.

Table F-1. Manual ILI Signal Review Classifications.

Classification	Description
Probable Significant Growth	The ILI signals appear to demonstrate a large difference between each tool survey for depth, length, or width.
Possible Growth	The ILI signals appear to demonstrate a difference between each tool survey, but this difference is not as pronounced as "Probable Significant Growth".
Unlikely Growth	The ILI signals do not appear to demonstrate a difference between each tool survey.

2.5 Task 5 – Application of Corrosion Growth Rates

The time to reach the scenarios, as defined below, was deterministically calculated for each metal loss indication from the 2012 ILI survey using the SAC growth rates. Internal and external indications were evaluated together in the SAC assessment and a single corrosion growth rate was calculated (see Section 2.3) for each pipe joint or the default growth rate was assigned. The estimated corrosion rate for each joint after the manual ILI signal review (i.e., after the estimated rate for joints identified as "Unlikely Growth" were adjusted to the determined minimum threshold rate) was applied to all metal loss indications reported within that joint. Metal loss indications that were reported to be repaired prior to the 2015 ILI were not included in the calculations.

The following scenarios were evaluated:

- Scenario 1
 - The reported depth plus the stated tool tolerance exceeds 80% WT
- Scenario 2
 - The reported length and depth lead to a predicted failure pressure of $1.39 \times \text{MOP}$ as calculated using modified (0.85 dL) B31G
 - (i.e. $P_{0.85dL} \leq 1.39 \times \text{MOP}$)
 - The growth is assumed to occur only in depth (i.e., the length remains constant)

DNV GL calculated a deterministic timeframe for each of the metal loss indications and identified the minimum predicted timeframe for each joint according to the two scenarios.

The estimated timeframe for features located on joints that were classified as “Unlikely Growth” via the manual review process were used as-is. To be as consistent as possible with Plains’ re-assessment interval approach, the estimated timeframe for features on joints that were found to exhibit growth or are on joints that were not manually reviewed were multiplied by a factor of 0.7². Those features that were predicted to meet any of the scenarios within five years of the 2012 inspection were identified.

3.0 RESULTS

The results from the assessment are presented in the following subsections.

3.1 Task 1 – Data Alignment and Preparation of Input Data

The joint listings for the 2007 MFL and 2012 MFL ILI surveys were aligned, and the joints successfully matched using the reported joint lengths and odometer locations.

Prior to the statistical review, the pit-to-pit matching algorithm was used to identify one-to-one matches between the 2007 and 2012 reported metal loss to aid in evaluating whether there is any bias in the ILI data. Figure F-1 shows a plot of the matched metal loss³. The 95% confidence interval between the ratio of the two data sets is [1.09,1.21], which indicates the 2012 MFL as-reported data, on average, is deeper than the as-reported 2007 MFL data.

DNV GL also compared raw signals from each ILI survey using the software provided by the ILI vendor in areas where the signal data did not show any evidence of change to identify any systematic differences between the sizing algorithms (sensitivities) used for each ILI. Results of the raw signal comparison are shown in Figure F-2.

No adjustment was made to either ILI data set based on either these comparisons.

2 Other factors of safety could also be employed to account for uncertainty.

3 A total of 167 one-to-one matches were identified. There were a total of 3618 un-clustered metal loss boxes reported by the 2007 MFL and 1705 un-clustered metal loss boxes reported by the 2012 MFL.

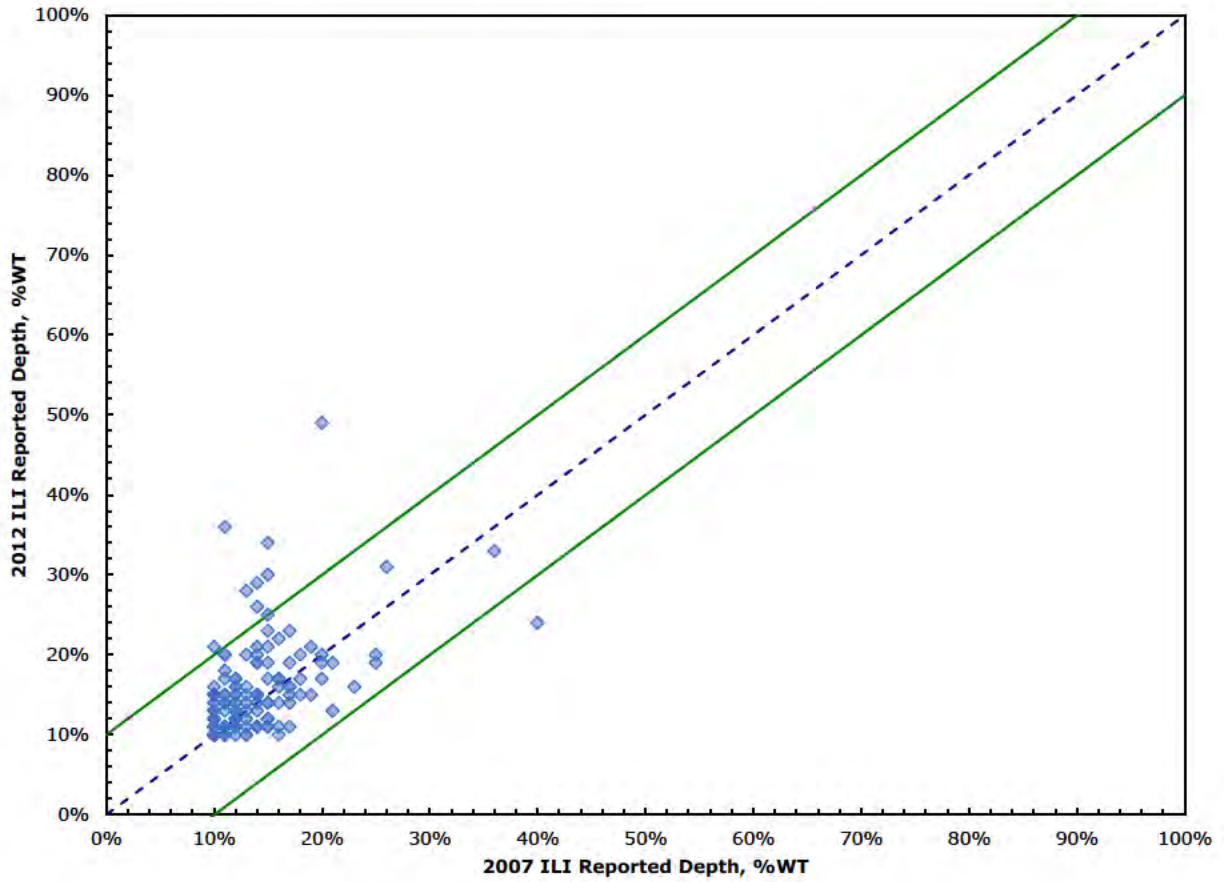


Figure F-1. Comparison of 2007 and 2012 Internal and External Metal Loss Non-Clustered ILI Depths.

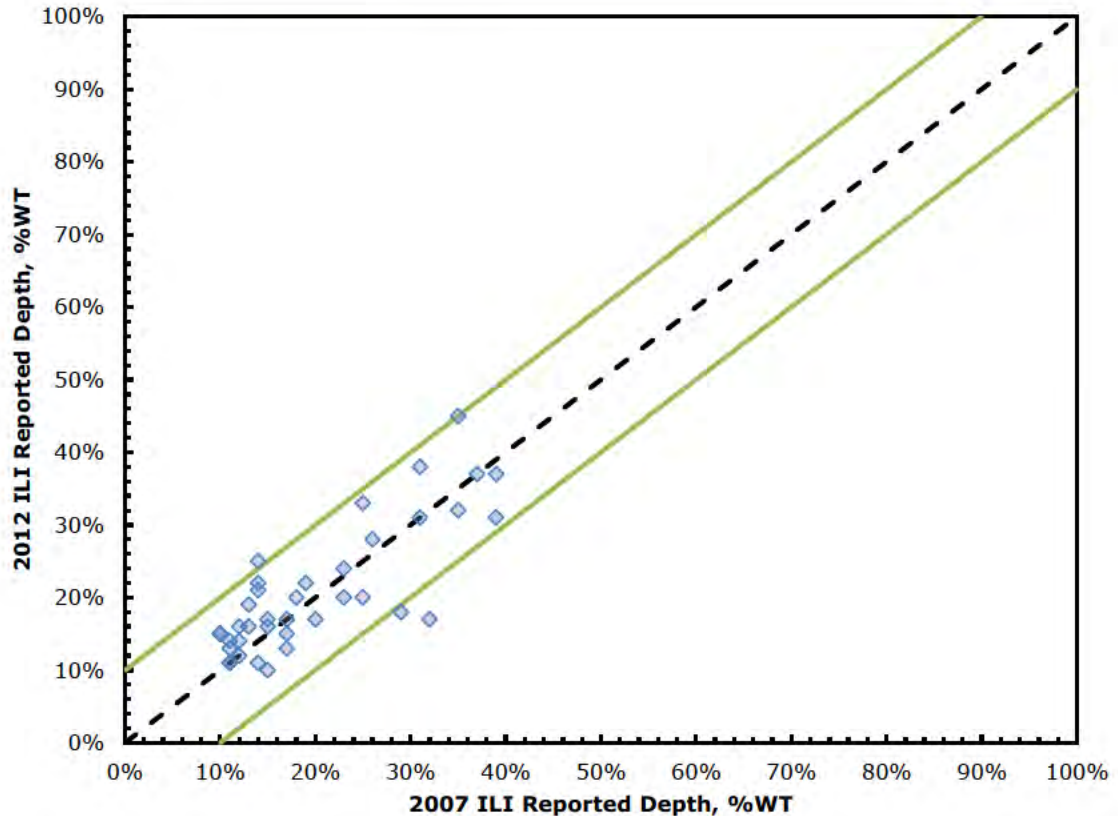


Figure F-2. Comparison of 2007 and 2012 Internal and External Metal Loss Non-Clustered ILI Depths in Areas of Unlikely Growth.

3.2 Task 2 – Comparison of ILI-Reported and Field-Measured Depths

Excavation records from the 2007 MFL and the 2012 MFL response program were provided to DNV GL and were used to gauge tool performance and determine whether an additional sensitivity adjustment factor was warranted. Based on records provided to DNV GL, 15 field-measured depths were matched to metal loss reported in the 2007 MFL and 52 field-measured depths were matched to metal loss reported in the 2012 MFL (see Figure F-3 and Figure F-4, respectively). Further discussion of the comparison between the field and ILI are in the main report.

No adjustment was made to either ILI data set based on these comparisons.

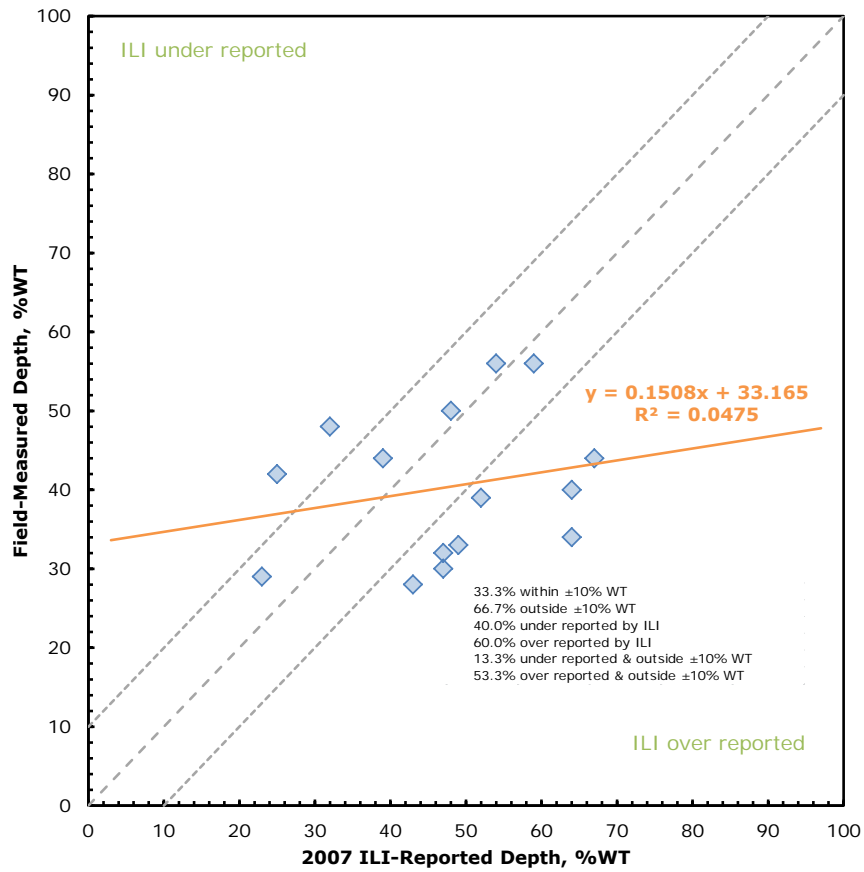


Figure F-3. Comparison of Field-Measured (following 2007 ILI) to 2007 ILI-Reported Depths.

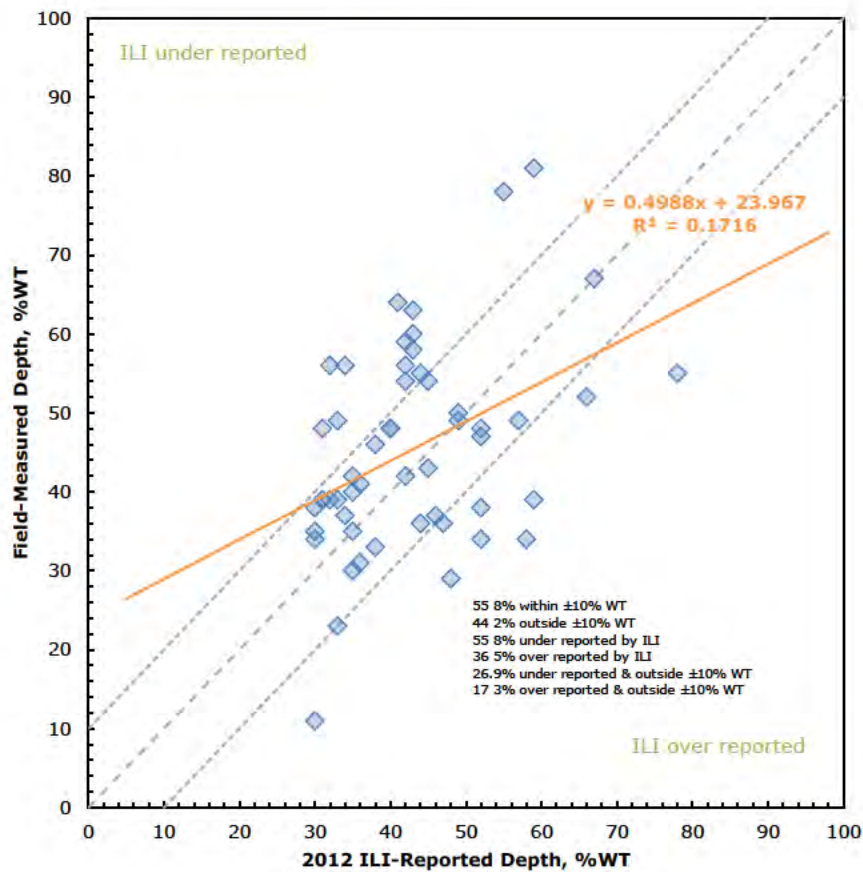


Figure F-4. Comparison of Field-Measured (following 2012 ILI) to 2012 ILI-Reported Depths.

3.3 Task 3 – Statistically Active Corrosion Assessment

As noted earlier, a corrosion growth rate was calculated for each pipe joint based on the results of the statistical assessment using either the differences in the ILI reported mean (average) or maximum depths between inspections. There were 11 identified joints that had SAC and the highest estimated corrosion growth rate prior to the manual signal review was 29.1 mpy.

Calculated corrosion rates of joints were adjusted to the minimum threshold rate determined using Equation (1) if the calculated corrosion rates were less than the minimum rate. The nominal wall thicknesses taken into consideration for Equation (1) were 0.344-

inch and 0.500-inch, resulting in minimum threshold rates of 3.5 and 5.0 mpy, respectively.⁴

3.4 Task 4 – Compilation and Review of Statistical Screening Results

A total of 169 pipe joints were selected for manual ILI signal review based on the characteristics described previously. The 169 manually reviewed joints included a single SAC Max joint and ten SAC Mean joints. The other 158 manually reviewed joints were selected based on criteria listed in Section 2.4.

Of the 169 joints manually reviewed, 87 joints (51%) were classified as “Unlikely Growth”, 53 joints (31%) were classified as “Possible Growth”, and 29 joints (17%) were classified as “Probable Significant Growth”.

In general, the manual review confirmed that the screening process (including the statistical analysis and selection criteria) identified joints with the potential for growth, but it also identified joints where little change was evident. This is not uncommon as differences in analysis algorithms can lead to what appears to be growth based on reported depths where none is observed in the signal data. The complete manual review results are tabulated in Section 5.0 of this appendix.

The results of the manual ILI signal review were superimposed on the calculated corrosion growth rates, which are displayed in Figure F-5. Estimated rates for joints identified as “Unlikely Growth” were adjusted down to the determined minimum growth rate calculated using Equation (1) for the applicable WT. The estimated rates for “Possible Growth” joints were adjusted to the rate based on the differences of the mean depths. “Probable Significant Growth” joints were adjusted to the rate based on the difference of the means or maximums with the highest confidence level.

4 Minimum corrosion growth rates were calculated based on the ILI survey dates (June 1, 2007 and July 3, 2012) and were rounded up to the nearest 0.5 mpy.

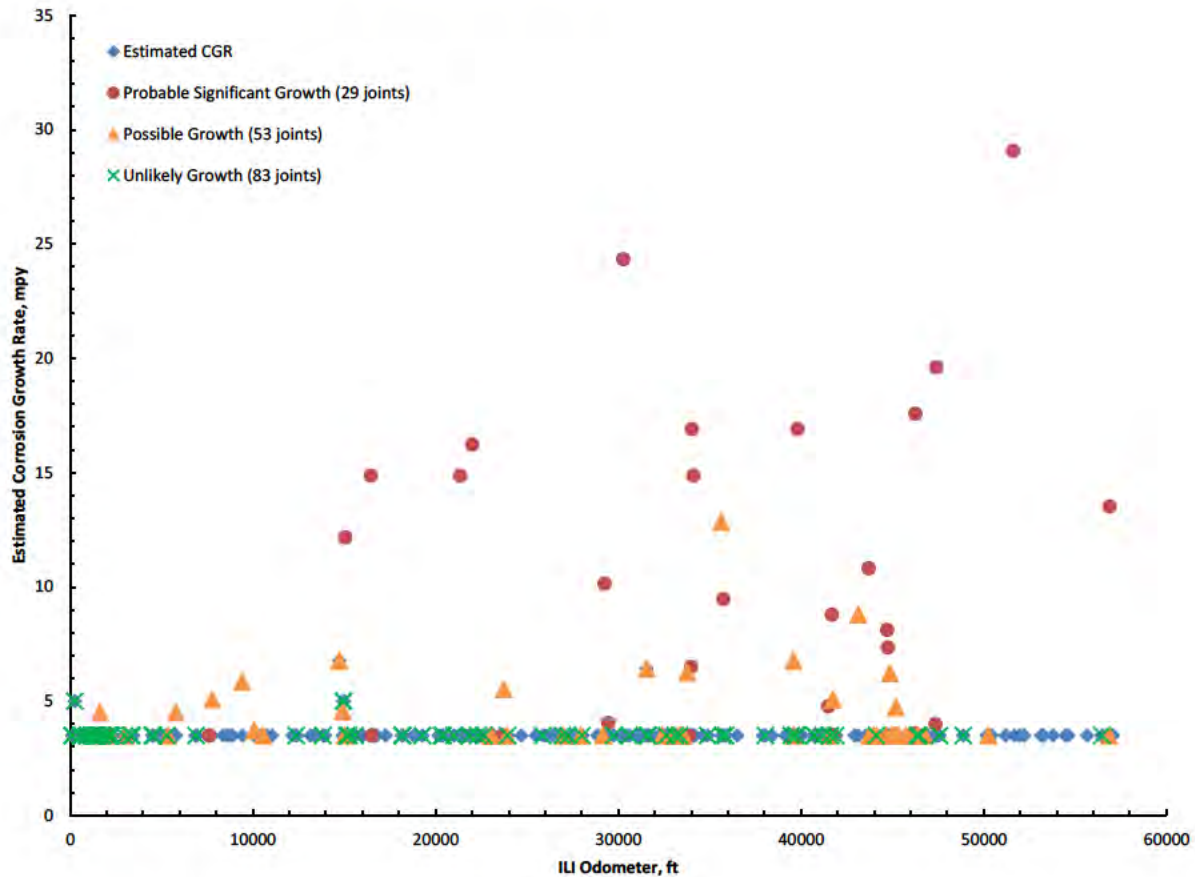


Figure F-5. Estimated Corrosion Growth Rate per Joint after Manual Review.

After incorporating the manual signal review results, the highest estimated corrosion growth rate for joints occurs at a “Probable Significant Growth” joint and is 29.1 mpy.

3.5 Task 5 – Application of Corrosion Growth Rates

There are eight joints with a predicted 70% minimum timeframe to scenario less than or equal to five years (the maximum allowed by 49 CFR 195.452(j)(3)) using the approach described in Section 2.5 when metal loss indications repaired prior to the 2015 ILI are taken into account. Three of these joints have a 70% timeframe less than three years (the specified reassessment interval); one was excavated after the 2015 ILI. A list of all joints with minimum timeframes less than or equal to five years is included in Table F-2.

Table F-2. Joints with 70% of the Predicted Timeframes Less Than or Equal to Five Years.

Joint ID	Odometer, ft	Manual Review †	Rate, mpy	Max. Depth, % WT	Scenario	Min. Time to Scenario, yrs	70% Time, yrs
4220	15065.38	PS	12.2	47	80% WT	6.5	4.6
5930	21351.11	PS	14.9	45	80% WT	5.8	4.0
8280	30276.76	PS	24.3	46	80% WT	3.4	2.4
9430	34027.19	PS	16.9	35	80% WT	7.1	5.0
11060	39808.08	PS	16.9	36	80% WT	6.9	4.8
12850	46264.57	PS	17.6	37	80% WT	6.5	4.5
13210	47401.55	PS	19.6	49	80% WT	3.7	2.6
14470‡	51618.37	PS	29.1	53	80% WT	2.0	1.4

† P = P, PS = Probable Significant Growth

‡ Features at 2015 ILI odometer 51640.00 and 51640.27 ft were repaired with a composite sleeve on June 4, 2015 [Ref 200]; the features on this joint in the 2012 ILI are between 51640.14 and 51642.68. The maximum depth in the field was measured at 65% WT.

4.0 SUMMARY REMARKS

The statistically active corrosion (SAC) methodology was developed with the objective to identify pipeline locations for which ILI data indicate a likelihood of corrosion growth. For selected joints with the potential for significant growth, a manual review of the ILI signal data was performed to determine whether the likely growth is evident in the ILI signal or a result of ILI sensitivity differences.

Based on the results of the corrosion growth screening and probabilistic assessment, DNV GL has developed the following conclusions:

- There does not appear to be a systematic bias between the 2007 and 2012 ILI reported depths; no adjustments to reported depths were applied prior to the statistical analysis.
- Based on the SAC analysis, when repairs prior to the 2015 ILI are accounted for, 11 joints out of 314 joints with metal loss indications (3.5% of joints with metal loss) were identified as potential growth locations. These are referred to as SAC joints.
- One hundred and sixty nine pipe joints were subjected to manual ILI signal review.

- Of the 169 joints, 87 joints (51%) were classified as “Unlikely Growth”, 53 joints (31%) were classified as “Possible Growth”, and 29 joints (17%) were classified as “Probable Significant Growth”.
- The highest estimated corrosion growth rate after adjusting the rates based on the manual signal review is 29.1 mpy.
 - This rate occurs on a joint repaired with a composite sleeve on June 4, 2015
- There are eight joints with a predicted 70% minimum timeframe less than or equal to five years.
 - Features identified to have been repaired prior to the 2015 ILI were not included in the growth projections.
- The joint that failed in 2015 (Joint 5930) is predicted to:
 - Have a SAC rate (15 mpy); a value between the rate used in the CGAR process (8 mpy) and the rate obtained via pit-to-pit matching (18 mpy)
 - Reach 80% WT in 5.8 years (70% of that time is 4.0 years)
- The SAC process predicts a reassessment interval on the order of the reassessment interval utilized by Plains for Line 901

5.0 TABULATED MANUAL REVIEW RESULTS

Joint ID	Odometer, ft	Review Selection Criteria	Manual Review †	Review Comments	Original Rate, mpy	Adjusted Rate, mpy
70.01	111.52	Estimated Corrosion Growth Rate	U		3.5	3.5
80	128.88	Estimated Corrosion Growth Rate	U		3.5	3.5
120	255.86	Estimated Corrosion Growth Rate	U		5.0	5.0
250	566.12	Estimated Corrosion Growth Rate	U		3.5	3.5
260	606.11	Estimated Corrosion Growth Rate	U		3.5	3.5
290	654.88	Deepest Features from 2012 Survey that were Matched	U	Located near GW.	3.5	3.5
420	954.76	Deepest Features from 2012 Survey that were Matched	U		3.5	3.5
480	1158.59	2012 Joints with Most Unmatched Metal Loss (non-Orphan)	U		3.5	3.5
490	1198.74	2007 Joints with Most Unmatched Metal Loss (non-Orphan)	U		3.5	3.5
500	1238.87	Estimated Corrosion Growth Rate	U		3.5	3.5
510	1279.00	2007 Joints with Most Unmatched Metal Loss (non-Orphan)	U		3.5	3.5
520	1319.13	2012 Joints with Most Unmatched Metal Loss (non-Orphan)	U		3.5	3.5
530	1359.26	2012 Joints with Most Unmatched Metal Loss (non-Orphan)	U		3.5	3.5
540	1399.33	2012 Joints with Most Unmatched Metal Loss (non-Orphan)	U		3.5	3.5
550	1439.41	2007 Joints with Most Unmatched Metal Loss (non-Orphan)	U		3.5	3.5
560	1474.52	2012 Joints with Most Unmatched Metal Loss (non-Orphan)	U		3.5	3.5
570	1514.60	2012 Joints with Most Unmatched Metal Loss (non-Orphan)	U		3.5	3.5
580	1554.67	2012 Joints with Most Unmatched Metal Loss (non-Orphan)	U	Located near GW.	3.5	3.5
590	1594.69	Deepest Features from 2012 Survey that were Matched	P	Located near GW.	3.5	3.5

Joint ID	Odometer, ft	Review Selection Criteria	Manual Review †	Review Comments	Original Rate, mpy	Adjusted Rate, mpy
600	1634.65	2007 Joints with Most Unmatched Metal Loss (non-Orphan)	P	Located near GW.	3.5	4.5
610	1674.68	2012 Joints with Most Unmatched Metal Loss (non-Orphan)	U		3.5	3.5
620	1714.66	2012 Joints with Most Unmatched Metal Loss (Orphan)	U		3.5	3.5
650	1821.71	2012 Joints with Most Unmatched Metal Loss (Orphan)	U		3.5	3.5
710	2060.81	2012 Orphan (no ML reported 2011) Joints with Largest Maximum Depth	U		3.5	3.5
720	2100.91	Largest Difference Between Matched Pits (1:1 matches ONLY)	U		3.5	3.5
730	2140.90	Largest Difference Between Matched Pits (1:1 matches ONLY)	U		3.5	3.5
740	2180.93	Largest Difference Between Matched Pits (1:1 matches ONLY)	U		3.5	3.5
750	2220.99	Largest Difference Between Matched Pits (1:1 matches ONLY)	P	Located near GW.	3.5	3.5
760	2260.83	Deepest Features from 2012 Survey that were Matched	U	Located near GW.	3.5	3.5
770	2300.87	Deepest Features from 2012 Survey that were Matched	U	Located near GW.	3.5	3.5
970	2989.81	2012 Joints with Most Unmatched Metal Loss (non-Orphan)	U		3.5	3.5
980	3029.58	2012 Joints with Most Unmatched Metal Loss (non-Orphan)	P	New growth not visible in the previous inspection.	3.5	3.5
1050	3308.39	Largest Difference Between Matched Pits (1:1 matches ONLY)	U	Located near GW.	3.5	3.5
1070	3388.53	Deepest Features from 2012 Survey that were Matched	U		3.5	3.5
1350	4491.84	2012 Joints with Most Unmatched Metal Loss (Orphan)	U	Located near GW.	3.5	3.5
1360	4531.86	Largest Difference Between Matched Pits (1:1 matches ONLY)	U	Located near GW.	3.5	3.5
1370	4571.90	Deepest Features from 2012 Survey that were Matched	U		3.5	3.5
1560	5305.93	2012 Orphan (no ML reported 2011) Joints with Largest Maximum Depth	U		3.5	3.5

Joint ID	Odometer, ft	Review Selection Criteria	Manual Review †	Review Comments	Original Rate, mpy	Adjusted Rate, mpy
1570	5346.04	Deepest Features from 2012 Survey that were Matched	P	Located outside of repaired area.	3.5	3.5
1700	5794.37	Deepest Features from 2012 Survey that were Matched	P	Located near GW.	3.5	4.5
1990	6903.85	Deepest Features from 2012 Survey that were Matched	U		3.5	3.5
2020	7016.64	2007 Joints with Most Unmatched Metal Loss (Orphan)	U	Located near GW.	3.5	3.5
2170	7617.42	Deepest Features from 2012 Survey that were Matched	PS	New growth not visible in the previous inspection.	3.5	3.5
2210	7777.78	2012 Orphan (no ML reported 2011) Joints with Largest Maximum Depth	P	Located near GW. Feature appears to be growing wider.	3.5	5.1
2640	9423.94	2012 Orphan (no ML reported 2011) Joints with Largest Maximum Depth	P	New growth not visible in the previous inspection.	3.5	5.9
2830	10080.65	2012 Joints with Most Unmatched Metal Loss (Orphan)	P	New growth not visible in the previous inspection. Located near GW.	3.5	3.7
2860	10174.60	2007 Joints with Most Unmatched Metal Loss (Orphan)	U		3.5	3.5
2960	10556.14	Deepest Features from 2012 Survey that were Matched	P		3.5	3.5
3420	12376.08	2012 Joints with Most Unmatched Metal Loss (non-Orphan)	U		3.5	3.5
3810	13831.31	2012 Joints with Most Unmatched Metal Loss (non-Orphan)	U		3.5	3.5
4080	14741.05	Estimated Corrosion Growth Rate	P		6.8	6.8
4150	14921.60	Deepest Features from 2012 Survey that were Matched	P		3.5	4.6
4160.01	14960.84	Deepest Features from 2012 Survey that were Matched	U		5.0	5.0
4160.02	14968.27	Deepest Features from 2012 Survey that were Matched	U		5.0	5.0
4210	15025.35	Deepest Features from 2012 Survey that were Matched	P		3.5	3.5

Joint ID	Odometer, ft	Review Selection Criteria	Manual Review †	Review Comments	Original Rate, mpy	Adjusted Rate, mpy
4220	15065.38	Deepest Features from 2012 Survey that were Matched	PS	New growth not visible in the previous inspection.	3.5	12.2
4240	15145.46	2012 Joints with Most Unmatched Metal Loss (Orphan)	U	Located near GW.	3.5	3.5
4270	15264.67	2012 Orphan (no ML reported 2011) Joints with Largest Maximum Depth	U	Located on GW.	3.5	3.5
4430	15584.42	Deepest Features from 2012 Survey that were Matched	U	Located near GW.	3.5	3.5
4650	16459.45	2012 Orphan (no ML reported 2011) Joints with Largest Maximum Depth	PS	Located near GW.	3.5	14.9
4660	16499.44	Deepest Features from 2012 Survey that were Matched	PS	Located near GW. Feature appears to be growing wider.	3.5	3.5
5100	18164.55	Deepest Features from 2012 Survey that were Matched	U	Located near GW.	3.5	3.5
5120	18212.77	Largest Difference Between Matched Pits (1:1 matches ONLY)	U	Located near GW.	3.5	3.5
5400	19284.44	Largest Difference Between Matched Pits (1:1 matches ONLY)	U	Located near GW.	3.5	3.5
5660	20324.54	Deepest Features from 2012 Survey that were Matched	U	Located near GW.	3.5	3.5
5680	20404.89	Largest Difference Between Matched Pits (1:1 matches ONLY)	U	Located near GW.	3.5	3.5
5840	21009.74	Deepest Features from 2012 Survey that were Matched	U	Located near GW.	3.5	3.5
5930	21351.11	Deepest Features from 2012 Survey that were Matched	PS	Located outside of repaired area.	3.5	14.9
6060	21834.30	Largest Difference Between Matched Pits (1:1 matches ONLY)	U	Located near GW.	3.5	3.5
6070	21874.41	Estimated Corrosion Growth Rate	U		3.5	3.5
6100	21994.61	2012 Orphan (no ML reported 2011) Joints with Largest Maximum Depth	PS	New growth not visible in the previous inspection. Located near GW.	3.5	16.2
6180	22315.00	2012 Joints with Most Unmatched Metal Loss (Orphan)	U	Located near GW.	3.5	3.5
6270	22652.08	2012 Joints with Most Unmatched Metal Loss (non-Orphan)	U		3.5	3.5

Joint ID	Odometer, ft	Review Selection Criteria	Manual Review †	Review Comments	Original Rate, mpy	Adjusted Rate, mpy
6350	22972.10	2012 Joints with Most Unmatched Metal Loss (non-Orphan)	P	New growth not visible in the previous inspection. Located near GW.	3.5	3.5
6360	23012.16	Estimated Corrosion Growth Rate	P		3.5	3.5
6370	23052.31	Largest Difference Between Matched Pits (1:1 matches ONLY)	P	Located near GW.	3.5	3.5
6520	23639.09	Deepest Features from 2012 Survey that were Matched	PS		3.5	3.5
6550	23746.71	Deepest Features from 2012 Survey that were Matched	P	Located near GW.	3.5	5.5
6590	23906.73	2012 Joints with Most Unmatched Metal Loss (Orphan)	P	New growth not visible in the previous inspection. Located near GW.	3.5	3.5
6600	23946.77	2012 Joints with Most Unmatched Metal Loss (Orphan)	U	Located near GW.	3.5	3.5
7120	25874.03	2012 Joints with Most Unmatched Metal Loss (non-Orphan)	U		3.5	3.5
7400	26930.83	2012 Joints with Most Unmatched Metal Loss (non-Orphan)	U	Located near GW.	3.5	3.5
7420	26984.21	2012 Joints with Most Unmatched Metal Loss (non-Orphan)	P	New growth not visible in the previous inspection.	3.5	3.5
7490	27246.37	2012 Joints with Most Unmatched Metal Loss (Orphan)	U	Located near GW.	3.5	3.5
7580	27595.59	2007 Joints with Most Unmatched Metal Loss (Orphan)	U		3.5	3.5
7670	27956.49	Deepest Features from 2012 Survey that were Matched	P		3.5	3.5
7690	28009.13	2012 Joints with Most Unmatched Metal Loss (Orphan)	U	Located near GW.	3.5	3.5
7990	29170.51	Deepest Features from 2012 Survey that were Matched	P	Located near GW. Feature appears to be growing wider.	3.5	3.5

Joint ID	Odometer, ft	Review Selection Criteria	Manual Review †	Review Comments	Original Rate, mpy	Adjusted Rate, mpy
8010	29250.55	2012 Orphan (no ML reported 2011) Joints with Largest Maximum Depth	PS	New growth not visible in the previous inspection. Located outside of repaired area.	3.5	10.1
8060	29451.25	Largest Difference Between Matched Pits (1:1 matches ONLY)	PS	New growth not visible in the previous inspection.	3.5	4.1
8140	29741.31	2012 Orphan (no ML reported 2011) Joints with Largest Maximum Depth	U		3.5	3.5
8280	30276.76	Deepest Features from 2012 Survey that were Matched	PS		3.5	24.3
8360	30596.93	2007 Joints with Most Unmatched Metal Loss (non-Orphan)	U		3.5	3.5
8640	31550.78	Estimated Corrosion Growth Rate	P	Located near GW.	6.4	6.4
8660	31597.28	2012 Joints with Most Unmatched Metal Loss (non-Orphan)	U		3.5	3.5
8680	31622.71	Deepest Features from 2012 Survey that were Matched	U	Located near GW. Previously repaired.	3.5	3.5
8690	31633.87	Largest Difference Between Matched Pits (1:1 matches ONLY)	U	Located near GW.	3.5	3.5
8980	32410.90	Estimated Corrosion Growth Rate	P	Located on GW.	3.5	3.5
9060	32644.07	Largest Difference Between Matched Pits (1:1 matches ONLY)	U	Located near GW.	3.5	3.5
9160	32962.17	Deepest Features from 2012 Survey that were Matched	P		3.5	3.5
9200	33122.06	2012 Joints with Most Unmatched Metal Loss (Orphan)	U	Located near GW.	3.5	3.5
9250	33322.18	Deepest Features from 2012 Survey that were Matched	P		3.5	3.5
9260	33362.23	2012 Joints with Most Unmatched Metal Loss (Orphan)	U	Located near GW.	3.5	3.5
9270	33401.66	Deepest Features from 2012 Survey that were Matched	P		3.5	3.5
9280	33441.67	2012 Joints with Most Unmatched Metal Loss (non-Orphan)	P	New growth not visible in the previous inspection.	3.5	3.5

Joint ID	Odometer, ft	Review Selection Criteria	Manual Review †	Review Comments	Original Rate, mpy	Adjusted Rate, mpy
9300	33521.75	Deepest Features from 2012 Survey that were Matched	P	New growth not visible in the previous inspection.	3.5	3.5
9310	33561.84	Deepest Features from 2012 Survey that were Matched	P	Located near GW.	3.5	3.5
9360	33761.78	2012 Orphan (no ML reported 2011) Joints with Largest Maximum Depth	P	New growth not visible in the previous inspection.	3.5	6.3
9390	33866.72	Deepest Features from 2012 Survey that were Matched	PS	Located near GW.	3.5	3.5
9420	33987.05	Deepest Features from 2012 Survey that were Matched	PS	New growth not visible in the previous inspection.	3.5	6.5
9430	34027.19	2012 Orphan (no ML reported 2011) Joints with Largest Maximum Depth	PS	Feature appears to be growing wider.	3.5	16.9
9450	34107.43	2012 Orphan (no ML reported 2011) Joints with Largest Maximum Depth	PS	Located outside of repaired area.	3.5	14.9
9650	34890.95	Largest Difference Between Matched Pits (1:1 matches ONLY)	U		3.5	3.5
9860	35634.99	Largest Difference Between Matched Pits (1:1 matches ONLY)	P		3.5	12.8
9880	35715.04	2012 Joints with Most Unmatched Metal Loss (Orphan)	U	Located near GW.	3.5	3.5
9890	35755.13	2012 Orphan (no ML reported 2011) Joints with Largest Maximum Depth	PS	Located near GW.	3.5	9.5
9920	35875.25	Deepest Features from 2012 Survey that were Matched	U		3.5	3.5
10540	38046.21	2012 Orphan (no ML reported 2011) Joints with Largest Maximum Depth	U	Located near GW.	3.5	3.5
10950	39466.11	2012 Joints with Most Unmatched Metal Loss (non-Orphan)	U		3.5	3.5
10990	39592.06	Largest Difference Between Matched Pits (1:1 matches ONLY)	P	Additional pit near GW in both inspections not called.	3.5	6.8
11000	39614.43	Deepest Features from 2012 Survey that were Matched	P		3.5	3.5
11030	39701.69	Deepest Features from 2012 Survey that were Matched	U	Located near GW.	3.5	3.5

Joint ID	Odometer, ft	Review Selection Criteria	Manual Review †	Review Comments	Original Rate, mpy	Adjusted Rate, mpy
11050	39768.01	2012 Orphan (no ML reported 2011) Joints with Largest Maximum Depth	U		3.5	3.5
11060	39808.08	Largest Difference Between Matched Pits (1:1 matches ONLY)	PS		3.5	16.9
11310	40693.57	Deepest Features from 2012 Survey that were Matched	U	Located near GW.	3.5	3.5
11330	40741.62	2012 Orphan (no ML reported 2011) Joints with Largest Maximum Depth	U	Located on GW.	3.5	3.5
11470	41210.73	2007 Joints with Most Unmatched Metal Loss (non-Orphan)	U		3.5	3.5
11540	41490.60	Estimated Corrosion Growth Rate	PS	New growth not visible in the previous inspection.	4.8	4.8
11550	41530.68	2012 Joints with Most Unmatched Metal Loss (non-Orphan)	P	New growth not visible in the previous inspection. Located near GW.	3.5	3.5
11570	41610.83	2007 Joints with Most Unmatched Metal Loss (non-Orphan)	U		3.5	3.5
11590	41690.92	Deepest Features from 2012 Survey that were Matched	PS	New growth not visible in the previous inspection.	3.5	8.8
11600	41730.90	Deepest Features from 2012 Survey that were Matched	PS	Located near GW. Feature appears to be growing wider.	3.5	3.5
11610	41744.11	2012 Orphan (no ML reported 2011) Joints with Largest Maximum Depth	P	Located near GW.	3.5	5.1
11650	41891.05	2012 Orphan (no ML reported 2011) Joints with Largest Maximum Depth	U	Located near GW.	3.5	3.5
11990	43143.07	2012 Orphan (no ML reported 2011) Joints with Largest Maximum Depth	P		3.5	8.8
12160	43705.68	Deepest Features from 2012 Survey that were Matched	PS	Feature appears to be growing wider and in length.	3.5	10.8

Joint ID	Odometer, ft	Review Selection Criteria	Manual Review †	Review Comments	Original Rate, mpy	Adjusted Rate, mpy
12170	43745.88	2012 Joints with Most Unmatched Metal Loss (non-Orphan)	P	There is growth on adjacent joint upstream. Feature appears to be growing wider.	3.5	3.5
12230	43974.21	Deepest Features from 2012 Survey that were Matched	P	Feature appears to be growing wider.	3.5	3.5
12240	44014.10	Estimated Corrosion Growth Rate	PS		3.5	3.5
12270	44125.63	Deepest Features from 2012 Survey that were Matched	U	Located near GW.	3.5	3.5
12280	44165.64	Deepest Features from 2012 Survey that were Matched	P	New growth not visible in the previous inspection.	3.5	3.5
12300	44245.65	2007 Joints with Most Unmatched Metal Loss (Orphan)	U		3.5	3.5
12410	44669.66	2012 Joints with Most Unmatched Metal Loss (Orphan)	P	New growth not visible in the previous inspection.	3.5	3.5
12420	44709.74	Deepest Features from 2012 Survey that were Matched	PS		3.5	8.1
12430	44748.75	Largest Difference Between Matched Pits (1:1 matches ONLY)	PS		3.5	7.3
12460	44868.95	2012 Orphan (no ML reported 2011) Joints with Largest Maximum Depth	P		3.5	6.2
12490	44988.84	Deepest Features from 2012 Survey that were Matched	P	Located near GW. Feature appears to be growing wider.	3.5	3.5
12510	45069.09	2012 Joints with Most Unmatched Metal Loss (non-Orphan)	P	Feature appears to be growing wider.	3.5	3.5
12540	45182.34	2012 Orphan (no ML reported 2011) Joints with Largest Maximum Depth	P	Located outside of repaired area.	3.5	4.7
12550	45204.55	Largest Difference Between Matched Pits (1:1 matches ONLY)	P	New growth not visible in the previous inspection.	3.5	3.5
12590	45331.80	2012 Joints with Most Unmatched Metal Loss (Orphan)	P	New growth not visible in the previous inspection.	3.5	3.5

Joint ID	Odometer, ft	Review Selection Criteria	Manual Review †	Review Comments	Original Rate, mpy	Adjusted Rate, mpy
12710	45747.80	Deepest Features from 2012 Survey that were Matched	P	New growth not visible in the previous inspection. Located near GW.	3.5	3.5
12800	46063.76	Estimated Corrosion Growth Rate	P		3.5	3.5
12820	46144.13	Deepest Features from 2012 Survey that were Matched	P	Located near GW. Feature appears to be growing wider.	3.5	3.5
12840	46224.40	Estimated Corrosion Growth Rate	PS	New growth not visible in the previous inspection.	3.6	3.6
12850	46264.57	Deepest Features from 2012 Survey that were Matched	PS	New growth not visible in the previous inspection. Located outside of repaired area.	3.5	17.6
12870	46344.80	Deepest Features from 2012 Survey that were Matched	U	Located near GW.	3.5	3.5
12880	46384.73	2012 Joints with Most Unmatched Metal Loss (non-Orphan)	P	Feature appears to be growing wider.	3.5	3.5
12900	46465.03	Deepest Features from 2012 Survey that were Matched	U	Located near GW.	3.5	3.5
13000	46781.15	2012 Joints with Most Unmatched Metal Loss (non-Orphan)	P		3.5	3.5
13200	47361.45	Deepest Features from 2012 Survey that were Matched	PS		3.5	4.0
13210	47401.55	2012 Joints with Most Unmatched Metal Loss (non-Orphan)	PS	New growth not visible in the previous inspection.	3.5	19.6
13260	47584.55	Deepest Features from 2012 Survey that were Matched	U	Located near GW.	3.5	3.5
13700	48881.37	Deepest Features from 2012 Survey that were Matched	U	Located near GW.	3.5	3.5
14060	50258.72	2012 Joints with Most Unmatched Metal Loss (non-Orphan)	P	New growth not visible in the previous inspection. Located outside of repaired area.	3.5	3.5

Plains All American Pipeline, L.P.
 Line 901 Release (5/19/15) Technical Root Cause Analysis

Joint ID	Odometer, ft	Review Selection Criteria	Manual Review †	Review Comments	Original Rate, mpy	Adjusted Rate, mpy
14470	51618.37	Estimated Corrosion Growth Rate	PS	Estimated Corrosion Growth Rate Joint.	29.1	29.1
15770	56459.87	Deepest Features from 2012 Survey that were Matched	U		3.5	3.5
15900	56849.78	2012 Joints with Most Unmatched Metal Loss (Orphan)	P	New growth not visible in the previous inspection.	3.5	3.5
15910	56889.91	2012 Orphan (no ML reported 2011) Joints with Largest Maximum Depth	PS		3.5	13.5

† P = P, PS = Probable Significant Growth



ABOUT DNV GL

Driven by our purpose of safeguarding life, property, and the environment, DNV GL enables organizations to advance the safety and sustainability of their business. We provide classification and technical assurance along with software and independent expert advisory services to the maritime, oil and gas, and energy industries. We also provide certification services to customers across a wide range of industries. Operating in more than 100 countries, our 16,000 professionals are dedicated to helping our customers make the world safer, smarter and greener.

Appendix O

NACE International: Effectiveness of Cathodic Protection on Thermally Insulated Underground Metallic Structures

PSK-2

Item No. 24156
NACE International Publication 10A392 (2006 Edition)



*This Technical Committee Report has been prepared
By NACE International Specific Technology Group 35* on
Pipelines, Tanks, and Well Casings*

Effectiveness of Cathodic Protection on Thermally Insulated Underground Metallic Structures

© September 2006, NACE International

This NACE International technical committee report represents a consensus of those individual members who have reviewed this document, its scope, and provisions. Its acceptance does not in any respect preclude anyone from manufacturing, marketing, purchasing, or using products, processes, or procedures not included in this report. Nothing contained in this NACE report is to be construed as granting any right, by implication or otherwise, to manufacture, sell, or use in connection with any method, apparatus, or product covered by Letters Patent, or as indemnifying or protecting anyone against liability for infringement of Letters Patent. This report should in no way be interpreted as a restriction on the use of better procedures or materials not discussed herein. Neither is this report intended to apply in all cases relating to the subject. Unpredictable circumstances may negate the usefulness of this report in specific instances. NACE assumes no responsibility for the interpretation or use of this report by other parties.

Users of this NACE report are responsible for reviewing appropriate health, safety, environmental, and regulatory documents and for determining their applicability in relation to this report prior to its use. This NACE report may not necessarily address all potential health and safety problems or environmental hazards associated with the use of materials, equipment, and/or operations detailed or referred to within this report. Users of this NACE report are also responsible for establishing appropriate health, safety, and environmental protection practices, in consultation with appropriate regulatory authorities if necessary, to achieve compliance with any existing applicable regulatory requirements prior to the use of this report.

CAUTIONARY NOTICE: The user is cautioned to obtain the latest edition of this report. NACE reports are subject to periodic review, and may be revised or withdrawn at any time without prior notice. NACE reports are automatically withdrawn if more than 10 years old. Purchasers of NACE reports may receive current information on all NACE International publications by contacting the NACE FirstService Department, 1440 South Creek Drive, Houston, Texas 77084-4906 (telephone +1 281/228-6200).

Foreword

The present trend in establishing an effective level of external metallic surface corrosion control is the application of a barrier coating or adhesive on the metallic surface prior to the application of a thermal insulating material. Experience has shown that there is generally a limited beneficial effect from the application of cathodic protection (CP) to a bare or ineffectively coated metallic surface under thermal insulation.

This NACE technical committee report was prepared as an information guide for external corrosion control of thermally insulated underground metallic surfaces and considerations

of the effectiveness of CP. This report is intended for those dealing with thermally insulated structures or pipelines.

Although pipelines are the primary focus of this report, the principles discussed would be applicable when a thermal insulating material has been applied on or in the immediate proximity of an underground metallic surface. This report was originally prepared in 1992 by NACE Task Group (TG) T-10A-19, a component of Unit Committee T-10A on Cathodic Protection and was reaffirmed with editorial changes in 2006 by Specific Technology Group (STG) 35 on Pipelines, Tanks, and Well Casings. It is published by NACE under the auspices of STG 35.

*Chair Paul R. Nichols, Shell Global Solutions, Houston, Texas.

PAA_PHMSA_000006

NACE International

NACE technical committee reports are intended to convey technical information or state-of-the-art knowledge regarding corrosion. In many cases, they discuss specific applications of corrosion mitigation technology, whether considered successful or not. Statements used to convey this information are factual and are provided to the reader as input and guidance for consideration when applying this technology in the future. However, these statements are not intended to be recommendations for general application of this technology, and must not be construed as such.

BACKGROUND

On most thermally insulated oil and gas transmission pipelines installed prior to 1980 to 1981, a shop mold-formed thermal insulation was placed directly over the bare steel pipe, with an outer jacket applied to moisture-proof the system. At the field joint, preformed insulation half shells were applied over the joint area to fit between the ends of the shop-applied insulation. After the insulation was fitted, a heat shrink sleeve or a tape wrap was applied over the insulation. When the integrity of the outer moisture barrier was compromised, the space, gap, or void between the edges of the preformed half shells and the shop-applied insulation allowed oxygenated water to diffuse to the bare steel beneath. Damage to the outer moisture barrier has also occurred remote from the joint, allowing oxygenated ground water ingress.

Thermally insulated pipelines have experienced relatively aggressive corrosion, with some failures occurring within three years of service, although acceptable industry standards of CP had been applied and maintained shortly after line construction. The most predominant failures have been those occurring at joints; however, moisture has migrated along the pipeline steel surface to create electrochemical corrosion cells remote from the field joint, culminating in extensive replacements of substantial lengths of line. An article titled "Corrosion of Underground Insulated Pipelines"¹ supports this committee's conclusions that sufficient CP current from an external source may not reach the insulated metallic surface in sufficient quantity to establish adequate corrosion control.

BASIC CORROSION MECHANISM

External failure of thermal insulated metallic surfaces has been primarily attributed to electrochemical corrosion cells generated from oxygenated ground waters, although some have found and concluded that failures are due to microbiologically influenced corrosion (MIC). When conventional CP is applied to a thermally insulated pipeline where an annular void exists, protection along the length of the void often does not occur. In a paper titled "Cathodic Protection Levels Under Disbonded Coatings,"² presented at CORROSION/82, the authors submitted experimental data that suggested a distance limitation of effective corrosion control by the use of externally applied CP. The amount of bare metallic surface under the thermal insulation (which can be equated to a severe condition of disbonded coating) would be the major factor limiting the area effectively protected by the externally applied CP.

Figures 1a, 1b, and 1c detail various metallic surface conditions and annular spaces where oxygenated water has migrated to a location remote or shielded from the external environment. Figure 1a shows a joint on which the joint wrap or sleeve, for some reason such as line movement, has become disbonded from the exterior coating and allows water to ingress to the pipe surface. The oxygenated water then migrates through the annulus, and active corrosion cells could be established if the foam or another barrier is not bonded to the pipe surface. Sufficient CP current generated externally cannot reach the metallic surface because of the shielding effect of the thermal insulation and the natural phenomenon of electrochemical reactions that result in active corrosion cells.

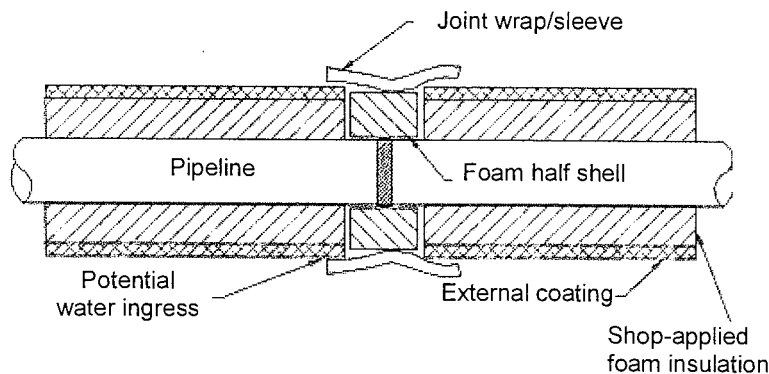


FIGURE 1a: Typical Joint with Damaged Wrap or Sleeve

Figure 1b details a close-up of a metallic surface on which a discontinuity (holiday) in the exterior coating and a void in the thermal insulation has been created. The externally applied CP current provides protection to the surface area at the void and for a limited distance beyond the void. Active corrosion cells result beyond the effective coverage of CP in which the insulating material affects or significantly inhibits current flow through the thermal material. It has been observed that when the rigid foam insulation adheres to the metallic surface, it forms an effective barrier and corrosion usually does not occur. Figure 1c is similar to 1b except a discontinuity also exists in a coating that was applied directly to the pipe surface.

Dye test experiments have indicated that impressed currents, such as those applied by CP systems, affect the water migration pattern once water has broken through the insulation. These impressed currents in fact cause the water to migrate further from the point of entry than it may otherwise have done.

The conditions described are not necessarily the worst- or best-case situations. When the metallic surface temperature has been maintained so that moisture is not allowed surface contact, the presence of active corrosion cells by oxygenated water is usually eliminated; however, elevated temperatures cannot be relied on as a corrosion control method.

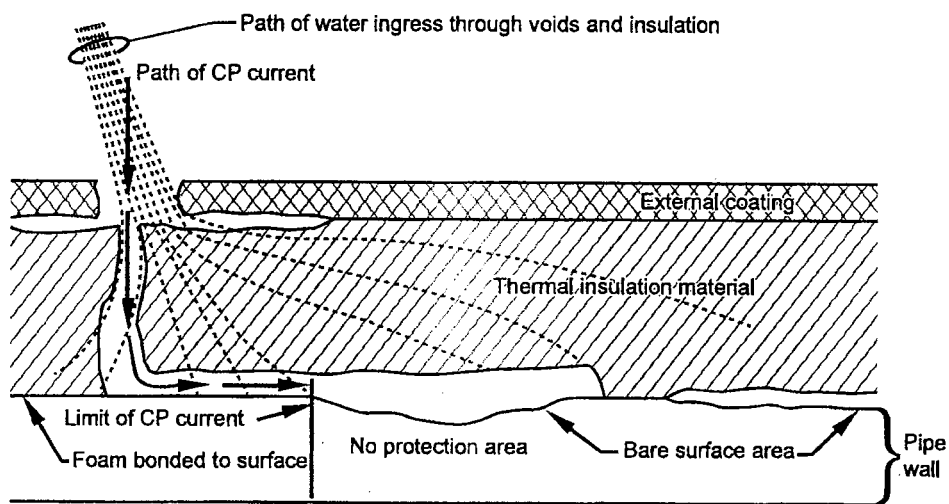


FIGURE 1b: Insulation Material Not Continuously Bonded to Metal

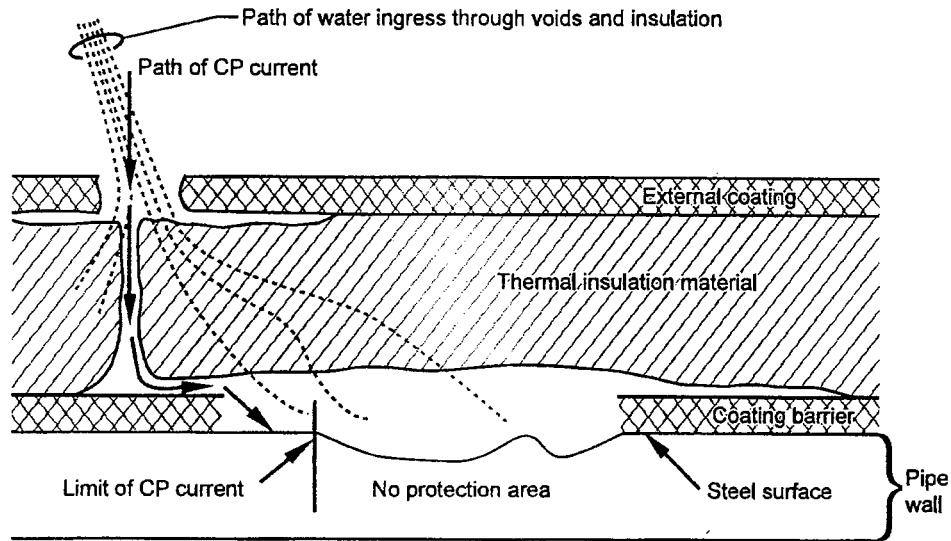


FIGURE 1c: Pipe with Discontinuity in the Barrier Coating on the Pipe Surface

TYPES OF THERMAL INSULATION

The most common thermal insulation utilized by the pipeline industry has been a polyurethane foam. Table 1 reviews some of the properties of materials that have been utilized

for thermal insulation and Table 1a reviews the water permeability of various types of thermal insulation.

TABLE 1—Properties of Thermal Insulation Materials

Type	Typical Use	Application Method	Feasible Operating Temperature	Heat Transfer Coeff. "K" W/m ² -K	Compression Strength kPa (psi)
Rigid Polyurethane	Pipelines	Shop Molding or Spray	to 93°C (200°F)	0.12	207-414 (30-60)
Isocyanurate	Pipelines	Shop Molding or Spray	to 150°C (302°F)	0.18	193 (28) (VERTICAL) 138 (20) (PARALLEL)
Polystyrene	Tank Bottoms	Board Stock Laid in Sheet Form	Cryogenic to 74°C (165°F)	0.26 at 4.4°C (40°F) 0.25 at -6.7°C (20°F)	241 (35) (VERTICAL) 138 (20) (PARALLEL)
Fiberglass	Pipe	Half Shells	to 316°C (600°F)	0.23	N/A
Cellular Glass	Pipe/Structures	Board Stock/Half Shells	-268° to 538°C (-450° to 1,000°F)	0.33 at 10°C (50°F)	689 (100) ³
Calcium Silicate	Geothermal Pipe High Temperature Hot Water Lines	Half Shells	to 593°C (1,100°F)	0.4	1379 (200) ^(A)

TABLE 1a—Water Permeability of Various Types of Thermal Insulation

Type	ASTM Methods	Typical Value
Rigid Polyurethane	D2842 ⁴	0.7 g/cm (0.05 lb/ft)
Isocyanurate	D2842 ⁴	0.7 g/cm (0.05 lb/ft)
Polystyrene	C2724 ⁵	0.3% by volume
Fiberglass	N/A	Less than 1% by volume
Cellular Glass	C240 ⁶	0.2% by volume
Calcium Silicate	Calcium silicate has a very high moisture absorption rate and may not be suitable for use on underground pipelines	

Cellular glass and calcium silicate insulations have been used underground in "pipe-within-a-pipe" systems. In these systems, the thermal insulation is placed as half or quarter shells in the annular space, and metallic spacers provide

concentricity. Protective coatings supplemented with CP are provided for the outer casing. This is necessary to ensure a dry environment within the annulus.

APPLICATION PROCESSES

Early methods of insulating steel line pipe intended for buried service copied the technology used for above-grade refinery piping. Preformed halves of polyurethane insulation were placed over the pipe and held in place with ties or bands of material and subsequently covered with an outer wrap, such as polyethylene tape or polyethylene heat shrinkable sleeves of the type commonly utilized in pipeline applications.

From this technique evolved a process of placing steel line pipe, one joint at a time, in a "dunk" tank or mold into which hot polyurethane was injected and allowed to form and set around the pipe. Mold tolerances of different dimensions are available to provide the desired thickness of insulation.

Subsequently, a patented process was developed for applying polyurethane insulation to a steel pipe that is rotating and travelling past a fixed point through a fixed nozzle or jet. This method represents a recent development for the application of insulation to steel pipes intended for buried service, permitting greater control of such variables as compressive strength and application temperature.

Variables in the polyurethane formulation, method of application, and physical conditions at the time of application determine the properties of the as-applied product. From a physical property point of view, end users are concerned with the integrity of the bond between the insulation and the steel pipe, the compressive strength of the insulation material, and maximum temperature at which the system can be operated without altering or damaging the properties of the insulation or its associated coating(s).

Traditionally, pipeline coatings have determined the temperature at which a pipeline can be operated. In order to realize maximum benefit and heat transfer efficiency from an insulated pipeline system, coating products that

maximize this feature are selected. In circumstances in which a coating or corrosion barrier is being applied to a bare steel pipe prior to application of insulation, a coating or barrier is selected to withstand the application temperature of the insulation. In other words, its effectiveness as a corrosion barrier remains intact after the insulation has been applied.

The principal change in the construction of thermally insulated line from what was practiced prior to 1980 to 1981 is the addition of a corrosion barrier coating on the steel pipe prior to applying the insulation materials. The typical shop preparation and application process listed below refers to the use of rigid polyurethane insulation that requires both an external vapor/moisture barrier to maintain the thermal integrity of the insulation system and a barrier at the steel surface to control corrosion:

1. Incoming pipe is inspected to ensure it is free of grease, oil, etc., that would impede proper coating application.
2. Pipe is preheated to specified temperature.
3. Pipe is blast cleaned to the specified finish.
4. Corrosion coating is applied to specification with proper cutback.
5. The polyurethane insulation is applied to specified properties and thickness.
6. The external moisture barrier jacket is applied according to specifications.
7. The specified quality control tests are conducted to confirm conformance to specifications.

NACE International

8. Half shells of the required size are manufactured for shipment to the field for joint completion.

9. Heat shrink sleeves or polyethylene tape are provided for joint completion of the pipeline coating and the external jacket. Some companies prefer to inject insulation on site after the joint has been made and properly prepared.

CONSTRUCTION PRACTICES

Buried pipeline designs incorporate pipe-soil resistance in restraint calculations. This characteristic works on the premise that the line pipe and any applied coatings or insulation are completely bonded and do not allow the pipe to move freely inside the outer protective layers. This relies on a good, long-lasting bond.

Coatings and insulation that are able to withstand the anticipated shipping, handling, and field bending employed during pipeline installation are chosen. A bending shoe or a hydraulic bender and an internal mandrel are usually used for field bending. Insulation with high compressive strength is used to resist pulverizing or breaking into numerous small pieces, and bending at low temperatures is avoided to minimize damage to the insulation.

Preformed insulation half shells have been most commonly used for the insulation of field joints at girthweld areas. These half shells are typically designed to be installed over the properly prepared and coated joint area and to fit between the ends of the shop-applied insulation. After the insulation halves are in place, a heat shrink sleeve or tape is applied to provide an external seal and to hold the insulation in place (see Figure 1a).

An alternative method of insulating field joints involves an injection molding at the job site followed by the application of shrink sleeves or tape wrap.

The main concern in field construction practice is the installation of the insulated pipe in a manner that ensures the integrity of both coating barriers. Moisture ingress causes a loss of thermal properties and may lead to pipe corrosion. Some of the typical field construction practices used to avoid coating damage are:

1. Padded supports (typically sandbags) are used for pipe handling and field stringing.
2. Properly trained field personnel are employed for the application and completion of joints to ensure the application is performed as specified and to adopt a specification that tests the joint integrity.
3. Properly padded bending shoes are used to minimize crushing of the thermal insulation and to avoid compromising the external coating.
4. Proper ditch padding and select backfill are used when appropriate to avoid external coating perforation.

EVALUATION OF EXTERNAL CORROSION MITIGATION

The use of internal pipeline corrosion inspection tools to locate/detect metal loss on external metallic surfaces has been relatively successful in evaluating corrosion control. Random excavation by personnel using sound engineering judgement has also been used to locate external corrosion. When a metal loss area on a metallic surface is located, the location is excavated, and the corrosion status is evaluated. The line section is then recoated, repaired, or replaced, depending on the severity of the metal loss. A schedule to reevaluate the condition on a regular basis is usually adopted.

Conventional CP electrical evaluation techniques have not been able to accurately determine the status of corrosion

control under thermal insulation. CP is only effective when there is direct contact with the surrounding soil/water electrolyte. Normal pipe-to-soil (pipe-electrolyte) measurements with current applied, or when compensating for voltage drop, result in a reading between the reference electrode on the ground/earth surface and the nearest conducting path to the metallic surface. The indicated potential is therefore only representative of the nearest metal/electrolyte interface. When sufficient bare steel exists remote from the void or holiday, the measurements of potential are not representative of the actual conditions at these remote locations.⁷ Figure 2 illustrates this situation.

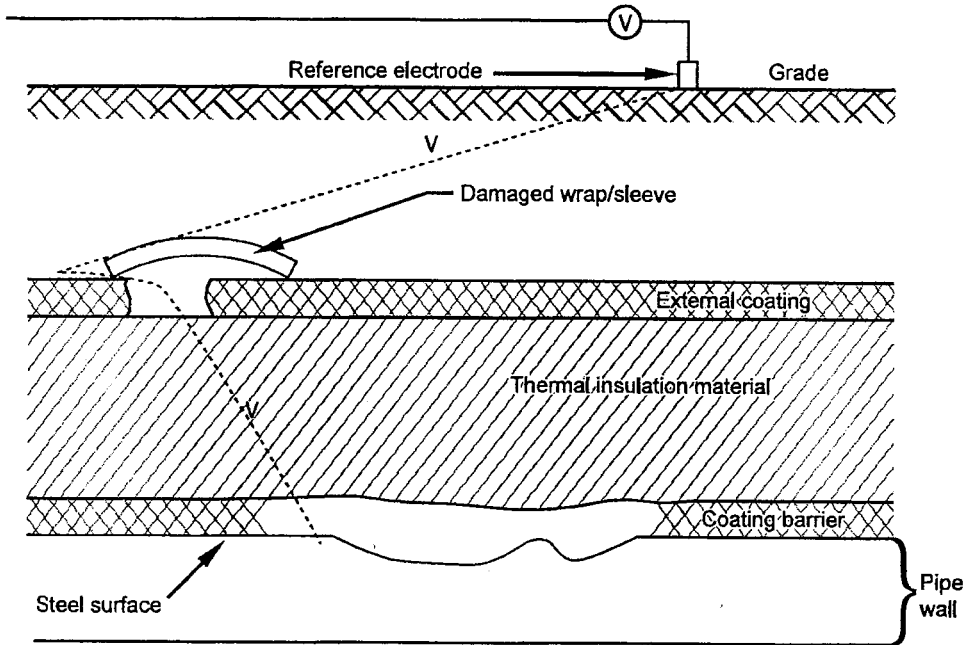


FIGURE 2: Representative Circuit of Potential Measurement

EXPERIENCES

Table 2 presents a partial overview of one North American operating company's experiences with corrosion of joints involving thermally insulated pipelines.⁸ A relatively

substantial amount of thermally insulated pipe has been installed in North America, with virtually every owner documenting similar situations.

TABLE 2—Experiences with Corrosion of Joints on Thermally Insulated Pipelines

Incident	Years in Service	Corrosion Barrier	Joint Coating	Comments
#1	10	No	Shrink sleeve	Poor shrink sleeve application
#2	6	No	Shrink sleeve	Poor shrink sleeve application; resulted in catastrophic failure
#3	17	No	Shrink sleeve	Poor shrink sleeve application
#4	17	No	Shrink sleeve	Poor shrink sleeve application
#5	3	Yes	Wraparound	Poor application of undercoat tape; also shop-damaged barrier
#6	6	No	Wraparound	Poor application; wrap too short; inner barrier specified but not installed

Another experience involves a pipeline with a primary coal tar epoxy coating of 400 µm (16 mil), with 50 mm (2.0 in.) of polyurethane foam and a polyethylene jacket exterior coating of 4.1 mm (160 mil). Field joints were primed, top coated with 300 µm (12 mil) of coal tar epoxy and 50 mm (2.0 in.) of foam, and finished with a shrink sleeve. After six

years, this 135-km (84.0-mile), 457-mm (18.0-in.) diameter line was checked with an instrumented and intelligent tool (smart pig) that indicated two locations with external corrosion.

NACE International

Investigations revealed the corrosion was caused by water migration through the shrink sleeves to the poorly coated pipeline at the joint. Both locations were also at test stations where adequate potentials had been recorded during annual CP surveys.

Five years later (1987), the second intelligent tool survey showed accelerated external corrosion with most anomalies at field joints and areas where the pipe was field-coated. At

many of these sites, close-interval surveys were taken before the defect was excavated in order to determine whether the corrosion cell could be located in this manner. In every test section, this method proved ineffective. Preliminary evaluation of a 1989 log indicated that some corrosion was beginning to develop on sections of factory-coated pipe. Of 266 anomalies identified, 168 were at or near field joints.

CONCLUSIONS

1. Generally, the application of external CP to thermally insulated metallic surfaces has been ineffective.
2. The principal or primary means of corrosion control of thermally insulated metallic surfaces is the application of an effective coating on the metallic surface.
3. Care is typically taken in the application of the external jacket and during pipe installation to minimize water ingress,

which causes corrosion at imperfections in the primary coating.

4. When practical, the thermally insulated metallic surfaces need to be inspected at routine time intervals for metal loss (e.g., an internal pipeline inspection tool could be used).

REFERENCES

1. J.F. Delahunt, "Corrosion of Underground Insulated Pipelines," *Journal of Protective Coatings and Linings* 3, 1 (1986): p. 36.
2. R.R. Fessler, A.J. Markworth, R.N. Parkins, "Cathodic Protection Levels Under Disbonded Coatings," *CORROSION/82*, paper no. 118 (Houston, TX: NACE, 1982).
3. ASTM C165 (latest revision), "Standard Method for Measuring Compressive Properties of Thermal Insulations" (West Conshohocken, PA: ASTM).
4. ASTM D2842 (latest revision), "Standard Test Method for Water Absorption of Rigid Cellular Plastics" (West Conshohocken, PA: ASTM).
5. ASTM C272 (latest revision), "Standard Test Method for Water Absorption of Core Materials for Structural Sandwich Constructions" (West Conshohocken, PA: ASTM).
6. ASTM C240 (latest revision), "Standard Test Methods of Testing Cellular Glass Insulation Block" (West Conshohocken, PA: ASTM).
7. W.B. Holtsbaum, "Potential Measurement Pitfalls with Thermally Insulated Pipes," NACE Canadian Region Eastern Conference, held November 18, 1991 (Houston, TX: NACE, 1991).
8. J.J. Baron, "Pipeline Field Joint Corrosion: Experiences and a Review of Materials," 39th Annual Technical Meeting, paper no. 88-39-114 (Calgary, Alberta, Canada: The Petroleum Society of CIM,⁽¹⁾ 1988).

⁽¹⁾ The Petroleum Society of CIM (CIM), 500-5th Avenue SW Suite 720, Calgary, Alberta, Canada, T2P 3L5.